Current Debates on Natural and Engineering Sciences

11

Editor
Hikmet Yeter ÇOĞUN

BİDGE

BIDGE Publications

Current Debates on Natural and Engineering Sciences 11

Editor: Hikmet Yeter ÇOĞUN

ISBN: 978-625-6488-21-2

Page Layout: Gözde YÜCEL

1st Edition:

BIDGE Publications, 2023

Certificate No: 71374

www.bidgeyayinlari.com.tr - bidgeyayin@gmail.com

Krc Bilişim Ticaret ve Organizasyon Ltd. Şti.
Güzeltepe Mahallesi Abidin Daver Sokak Sefer Apartmanı No: 7/9 Çankaya / Ankara

Contents

Prediction Score Measurements for Prognostic and Health Management Data Challenges

Oğuz BEKTAŞ[1]

Introduction

In the evolving field of Prognostics and Healthcare Management (PHM), the search for accurate and reliable data has been a long-standing challenge (Javed et al., 2017). Over the years, the field has witnessed remarkable developments in both technology and methodology and PHM data challenges have served as a major source for innovation and progress in the field. Particularly, the performance measurements introduced by these data challenges have a very significant realm in the field of PHM. These metrics serve as benchmarks to measure the accuracy, effectiveness, and overall performance of prognostic systems. They provide a structured framework for evaluating how well a system performs in terms of predicting health and anticipating potential problems. Performance metrics are, in essence, a critical bridge that connects the theoretical concepts of PHM to real-world applications.

This section discusses the importance of measuring performance through metrics and highlights the importance of these measurable indicators in assessing the effectiveness of prognostic systems. Through these metrics, PHM research can gain invaluable insight into how their systems are performing and whether they are on track to achieve predefined goals.

In the following sections, this work delves deeper into the field of Prediction Score Measurements, drawing on a comprehensive analysis of various datasets published in the PHM space. Through this research, it is aimed to provide a clearer understanding of the key metrics used to evaluate the predictive capabilities of PHM systems and their vital role in achieving overall business goals.

PHM 2014 Data Challenge

The specifics of the 2014 Data and domain are not disclosed due to proprietary concerns (Garvey, D., and Wigny R. 2014). The datasets include Train – Part Consumption, Train – Usage, Train – Failures, Test – Part Consumption, Test – Usage, and Test Instances.

For the submission, the result file's line should indicate the threshold value that separates assets into low and high-risk categories based on their health scores. Low-risk assets have scores below this limit, while high-risk assets have scores above it. Also, the file should contain three columns: asset ID, calculation time, and health score. A health score of 0 represents a healthy asset, with larger values indicating more severe degradation. The test assets and times are designed to include a balanced sample of instances where assets either did or did not fail in the immediate future (within 3 time units). The scoring of submissions is based on the following formula (Garvey, D., and Wigny R. 2014).

$$Score = \left(\frac{L}{N}\right) + \left(\frac{H}{N}\right)$$

[1] Öğretim Görevlisi Dr., İstanbul Medeniyet Üniversitesi

where:

- N is the number of samples for both types (with and without immediate failure, making a total of 2N).
- L is the number of samples without an immediate failure and classified as low risk.
- H is the number of samples with an immediate failure and classified as high risk.
- This score formula likely evaluates the performance of submissions in predicting asset failures based on the provided data.

This score formula likely evaluates the performance of submissions in predicting asset failures based on the provided data.

PHM 2015 Data Challenge

This challenge involves predicting plant failures in advance using sensor data and fault codes (Justinian et al., 2015). Data includes sensor measurements, control signals, zone data, and fault events for multiple plants. The goal is to predict future failures of types 1-5 from past data. Training data is provided for around 30 plants, and test data for approximately 10 plants with missing fault information. Teams can submit predictions once a week, and the scoring system evaluates the accuracy of fault detection with a one-hour tolerance.

The scoring system evaluates the performance of fault detection by giving credit for correctly identifying a fault within an hour of its occurrence (true positives, *tp*) while penalizing incorrect identifications (false positives *fp* and false negatives *fn*). The overall prediction score for a plant test file is determined using the following formula that takes into account a table of confusion scores for the first five fault codes (N=5) (Justinian et al., 2015).

$$Score = \frac{1}{N}\sum_{j=1}^{N}\left(4 * tp_j - 10 * fp_j - fn_j\right)$$

PHM 2016 Data Challenge

The PHM 2016 Data challenge (Propes and Rosca, 2016) focuses on predicting the removal rate of material during the Chemical-Mechanical Planarization (CMP) process. Participants can use physics-based or statistical approaches. The system involves a CMP tool with various components like a rotating table, polishing pad, wafer carrier, slurry dispenser, and dresser. The objective is to estimate the removal rate using provided data (Propes and Rosca, 2016). Training and test data sets are given, and submissions should include predicted removal rates for each wafer and stage.

In the scoring process, the final score for all submissions will be determined by considering two main factors. The majority of the score, 90%, is attributed to the Mean Squared Error (MSE) accuracy (Propes and Rosca, 2016). Additionally, there is a 10% weight assigned to evaluating the physics-based modeling approach based on specific criteria, which include estimating the impact of dresser condition on the polishing pad removal rate (3%), estimating the effect of polishing pad condition on the removal rate (3%), and assessing the influence of other parameters on the polishing pad removal rate (4%).

PHM 2017 Data Challenge

The PHM 2017 Data challenge focuses on combining physics-based modeling and statistics for predicting vibrations in a conventional bogie vehicle (Rosca et al., 2017). The

system consists of a vehicle body, bogies, and wheelsets with various sensors to measure accelerations. The goal is to connect physical aspects to the data, considering variations in track conditions, vehicle parameters, and sensor data, including vertical accelerations, speed, mass, and track information.

This challenge involves predicting faulty operation of a train car using sensor data. The data includes various sensor readings, vehicle parameters, and track information. The goal is to identify when the train car is faulty and, if so, determine which component is at fault. Training and testing data are provided for this task.

In the competition, participants have their scores calculated based on two objectives. The first objective assesses the accuracy of predicting healthy and faulty operation of a car. The scores are calculated using an accuracy rate measure, and the final score is the sum of scores from both objectives.

$$\frac{truePositives + trueNegatives}{truePositives + trueNegatives + falsePositives + falseNegatives}$$

The second objective aims to measure the sensitivity in detecting specific faults by calculating the proportion of accurate predictions for each fault type divided by the total number of faulty instances.

$$\frac{\sum_{i=1}^{n} truePositives(i)}{Total\ number\ of\ faults}$$

PHM 2018 Data Challenge

This data challenge focuses on analyzing the fault behavior of an ion mill etch tool used in wafer manufacturing (Bonatakis, 2018). The ion mill etching process involves steps such as wafer insertion, configuration, processing, and removal. It employs an ion source to generate ions, which are accelerated through electric grids, creating an ion beam that removes material from the wafer. A Particle Beam Neutralizer control system influences ion distribution. The wafer is cooled by a helium/water system, with various potential failure mechanisms, such as leaks and wear. The goal is to predict and schedule maintenance for these ion mills to prevent failures.

The data challenge aims to create a model using time series sensor data from ion mill etching tools (Bonatakis, 2018). It has two main goals:

- Detect and identify failures.
- Predict the remaining useful life until the next failure.

The predictions for time-to-failure should only rely on past and current time-series data, without trying to predict the exact failure point and then backtrack.

Scoring is done by comparing a submitted time-to-failure (TTF) prediction with a correct TTF. Each prediction is given a sub-score based on specific rules. These sub-scores are added up for each prediction, divided by the total number of cells, and then summed for the entire file. A lower score indicates a better prediction.

(GT) Ground Truth TTF	(SUB) Submission TTF	Score
Number	Number	exp(-0.001*GT)*abs(GT-SUB)
NaN	Number	exp(-0.001*SUB)*SUB
Number	NaN	exp(-0.001*GT)*GT
NaN	NaN	0

PHM 2019 Data Challenge

The data from PHM 2019 Data Challenge (Corbetta et al. 2019) is based on the work of Peng et al. (2015). Participants in this data challenge must estimate crack lengths in an aluminium structure subjected to dynamic tensile loading conditions. Data from piezo sensors and loading conditions were collected, and ground truth data for crack length is provided for testing. Participants must provide estimates for validation sets containing only sensor data and future load conditions. Model-based and data-driven approaches are encouraged. Validation data is released incrementally, and submissions are scored using a specified scoring function.

In the challenge, the scenario includes measurements from piezoelectric (PZT) sensors attached to aluminium specimens subjected to fatigue testing. Cracks develop in the specimens, and failure occurs when a specific crack length is reached. Ultrasonic waves are used to detect these cracks, and the distance between the actuator and receiver is 161 mm. The goal is to predict crack lengths in lap joint structures.

- Training Data: Six specimens (T1-T6) provide ultrasonic data, true crack length measurements, and loading profiles.
- Validation Data: Two specimens (T7 and T8) offer ultrasonic data, but crack lengths must be predicted as they are not provided.
- Performance Evaluation: Predicted crack lengths will be evaluated using an error function. Submissions are required for specific cycle numbers.

The data is organized into folders by specimen, with description files, loading profiles, and sensor signals. Specimen T8 has variable amplitude loading. Crack length is measured as a percentage of full crack length at failure. Normalization will be applied for scoring, as the full crack length is unknown during submission.

Time Penalty Function:

$$T(i) = a + bx_i,$$

$$a = 2,\ b = 10$$

This penalizes late-stage prediction errors more than early-stage ones in crack growth.

$$A(i) = \exp\left\{\frac{|\tilde{x_i} - x_i|}{a_1}\right\},\ \ if(\tilde{x_i} - x_i) \geq 0$$

This penalizes late-stage prediction errors more than early-stage ones in crack growth.

Asymmetric Penalty Function:

$$A(i) = \exp\left\{\frac{|\widetilde{x_i} - x_i|}{a_2}\right\}, \quad if(\widetilde{x_i} - x_i) \geq 0$$

$$a_1 > a_2 > 0,$$

$$a_1 = 0.5 \, and \, a_2 = 0.2$$

The penalty for underestimating crack length is higher than for overestimation due to more severe consequences.

Monotonicity Penalty Function:

$$M(i) = 1 + m * (|\widetilde{x_i} - \widetilde{x_{i-1}}|) \, ; \, if(\widetilde{x_i} - \widetilde{x_{i-1}}) < 0$$

$$M(i) = 1 \, ; \, if(\widetilde{x_i} - \widetilde{x_{i-1}}) \geq 0$$

$$m = 10$$

Penalizing non-monotonic crack length estimates is necessary, especially when data-driven methods produce results that don't align with the physics of crack growth.

Overall Penalty Function:

$$S(i) = T(i) * A(i) * M(i)$$

$$Cumulative \, Penalty \, Score = \sum_{i=1}^{L} S(i)$$

The score ranges from 0 to infinity, with a perfect score of 0 achieved when the prediction matches the ground truth.

PHM Society Data Challenge 2021

PHM Society Data Challenge 2021 focuses on predicting the remaining useful lifetime (RUL) of aircraft engines within a variable flight envelope and with multiple possible failure modes (Chao et al. 2021). Participants are tasked with creating a data-driven model using condition monitoring data to estimate RUL, using a subset of the N-CMAPSS dataset's (Arias Chao et al. 2021) run-to-failure degradation trajectories. The system under analysis is a commercial turbofan engine with six main components: fan, low-pressure compressor (LPC), high-pressure compressor (HPC), combustor, high-pressure turbine (HPT), and low-pressure turbine (LPT). The HPC and HPT are connected by the core shaft, while the fan, LPC, and LPT are connected by the fan shaft (May et al. 2010). The engine also includes various additional features like an inlet, rear nozzle, bypass duct, inter-stage bleed valve, guide vanes, and cooling bleeds.

Model performance will be assessed using an independent validation dataset. The evaluation metric combines root-mean-square error (RMSE) and NASA's scoring function, with the formula:

$$score = 0.5 \cdot RMSE + 0.5 \cdot s_c$$

$$RMSE = \sqrt{\frac{1}{m_{v*}}\sum_{j=1}^{m_{v*}}(\Delta^{(k)})^2}$$

$$s_c = \frac{1}{m_{v*}}\sum_{k=1}^{m_{v*}}\exp\left(\alpha\left|\Delta^{(k)}\right|\right) - 1$$

where:

- m_{v*} is the total number of validation dataset
- $\Delta^{(k)}$ denotes the difference between the estimated RUL and the true RUL of the k sample
- The value of α is 1/13 when RUL is underestimated and 1/10 otherwise. The s metric it produces is asymmetric and penalizes overestimation more than underestimation.

PHM Asia-Pacific 2023 dataset:

JAXA (The Japan Aerospace Exploration Agency) is working to enhance PHM technology for spacecraft propulsion systems (PHMAP, 2023). Limited telemetry was obtained in orbit due to sensor constraints and downlink capacity. They developed a numerical simulator to predict spacecraft propulsion system behaviour accurately under various conditions and fault scenarios.

Experimental Scenarios:

- A propulsion system using water pressurized to 2 MPa is employed with four solenoid valves (SV1-SV4) simulating thrusters.
- Pressure data is collected at a 1 kHz sampling rate for 1200 ms, and solenoid valves are opened and closed to induce pressure fluctuations.

Competition Goals:

- Determine whether test data is normal or abnormal.
- Identify the type of abnormality (bubble contamination, solenoid valve fault, or an unknown fault).
- For bubble contamination, pinpoint the bubble's location among eight possibilities.
- For solenoid valve faults, identify which of the four solenoid valves failed.
- Predict the opening ratio for faulty solenoid valves (0% <= Opening ratio < 100%).
- Scoring:
- Normal/abnormal classification: Up to 10 points.
- Correct classification of abnormality type: Up to 10 points.
- Correct identification of bubble location: Up to 10 points.

- Correct identification of the faulty solenoid valve: Up to 10 points.
- Accurate prediction of the opening ratio for faulty solenoid valves:

$$\max(-|truth - prediction| + 20, 0)$$

PHM North America 2023 Conference Data Challenge:

PHM North America 2023 Conference Data Challenge focuses on estimating gearbox degradation under various conditions, emphasizing trust, robustness, and explainability metrics, along with the requirement for confidence measures in submitted results (PHMNA, 2023). Participants were required develop a fault severity estimate using provided data, including healthy and faulty states. They needed to generalize their models to unseen conditions and express confidence in their predictions.

Various health states (ranging from 0 to 10), where 0 signifies a healthy state and 10 represents the most degraded state, were submitted for scoring metrics. These 11 health states are ordinal, meaning that each successive state reflects more degradation. Although each health state can be assigned a probability between 0 and 1, the sum of all health state probabilities must not exceed 1, constituting a discrete probability distribution.

The final part of the submission was reserved for indicating confidence in the discrete probability distribution, and it is a binary classification, with 0 denoting low confidence and 1 denoting high confidence. It's important to note that high-confidence submissions carry more weight in the final scoring, whereas low-confidence submissions have a lower weight. Likewise, incorrect predictions with a high confidence level incur a more substantial penalty. The exact rewards or penalties depend on the discrepancy between the predicted label and the true label, as specified by a formula that takes into account the confidence factor and health state scores.

$$Score_{total} = \sum Score_{observation}$$

where,

$$Score_{observation} = confidenceFactor * \sum predictionprobability * healthStateScore$$

The confidence factor here is 0.2 for a reported confidence of 0 and 1 for a reported confidence of 1.

Future of Metrics for Prognostic and Health Management

In conclusion, the field of Prognostics and Healthcare Management (PHM) has made significant progress in technology and methodology, driven in part by data challenges. Performance metrics have become essential in assessing the accuracy and effectiveness of prognostic systems, connecting theoretical concepts to real-world applications. Future developments in the role and future of scoring functions will continue to be crucial in advancing the field of PHM by providing valuable insights into system performance and its alignment with predefined goals.

REFERENCES

Arias Chao, M., Kulkarni, C., Goebel, K., & Fink, O. (2021). Aircraft engine run-to-failure dataset under real flight conditions for prognostics and diagnostics. *Data*, 6(1), 5.

Bonatakis J., Chokor A. and Propes N. (2018). The PHM Data Challenge 2018. In Annual Conference of the Prognostics and Health Management Society 2018

Chao, M. A., Kulkarni, C., Goebel, K., & Fink, O. (2021). PHM Society Data Challenge 2021. In *Annual Conference of the Prognostics and Health Management Society 2021*

Corbetta, M, Banerjee P., Doughty K. Clements S. & Goebel, K. (2019). The PHM Data Challenge 2018. In *Annual Conference of the Prognostics and Health Management Society 2019*

Garvey, D., and Wigny R. (2014). The PHM Data Challenge 2014. In Annual Conference of the Prognostics and Health Management Society 2014

Javed, K., Gouriveau, R., & Zerhouni, N. (2017). State of the art and taxonomy of prognostics approaches, trends of prognostics applications and open issues towards maturity at different technology readiness levels. *Mechanical Systems and Signal Processing*, *94*, 214-236.

Justinian R., Williard N., Eklund N. and Song Z. (2015). The PHM Data Challenge 2015. *In Annual Conference of the Prognostics and Health Management Society 2015*

May, R., Csank, J., Lavelle, T., Litt, J., & Guo, T. H. (2010, October). A high-fidelity simulation of a generic commercial aircraft engine and controller. In *46th AIAA/ASME/SAE/ASEE Joint Propulsion Conference & Exhibit* (p. 6630).

Peng, T., He, J., Xiang, Y., Liu, Y., Saxena, A., Celaya, J., & Goebel, K. (2015). Probabilistic fatigue damage prognosis of lap joint using Bayesian updating. *Journal of Intelligent Material Systems and Structures*, *26*(8), 965-979.

Propes N. and Rosca J., (2016). The PHM Data Challenge 2016. In Annual Conference of the Prognostics and Health Management Society 2016

PHMAP (2023). PHM Asia-Pacific 2023 Conference Data Challenge. In A Asia Pacific Conference of the Prognostics and Health Management Society 2023

PHMNA (2023). PHM North America 2023 Conference Data Challenge. In Annual Conference of the Prognostics and Health Management Society 2023

Rosca J., Propes N. and Girstmair B. (2017). The PHM Data Challenge 2017. In *Annual Conference of the Prognostics and Health Management Society 2017*

Major Oxıde And Trace Element Characterıstıcs Of The Bozdağ Formatıon Dolomıtes (Konya Northwest, Türkiye)

Ali Müjdat ÖZKAN[1]

Introduction

The aim of this study is to examine the dolostones (Middle Devonian-Lower Carboniferous) belonging to the Bozdağ Formation, located around the Söğütözü-Ladik district in the northwest of Konya (Figure 1), according to their major and trace element properties.

The study area is located in the Kütahya-Bolkardağı belt, in the Konya region (Figure 1). The Bozdağ Formation, which forms the basis of the study area, is defined as consisting of massive bedded limestone, dolomitic limestone, dolostone, and calcitic dolostone (Özkan, 2016). The Bozdağ Formation dolostone types are defined as (1) dolomicrite, (2) euhedral dolomite disseminated in the micritic matrix, (3) crack and void fill dolomite, and (4) stylolytic dolomite (Özkan, 2016).

The Sr content (20-123 ppm) of the Bozdağ Formation dolostones is consistent with the Sr values of the burial dolostones. The Na content of Bozdağ Formation dolostones (122-371 ppm) is also consistent with the Na content of burial dolostones. The Fe and Mn contents of Bozdağ Formation dolostones (0-4616 and 0-232 ppm, respectively) support the Fe and Mn contents of the burial dolostones. Major oxide and trace element properties of Bozdağ Formation dolostones indicate diagenetic alteration and insignificant terrigenous input.

The Bozdağ Formation dolostones must have been formed late diagenetically at elevated temperatures in a medium-deep burial environment from partially evaporative, altered sea water with some meteoric water effect.

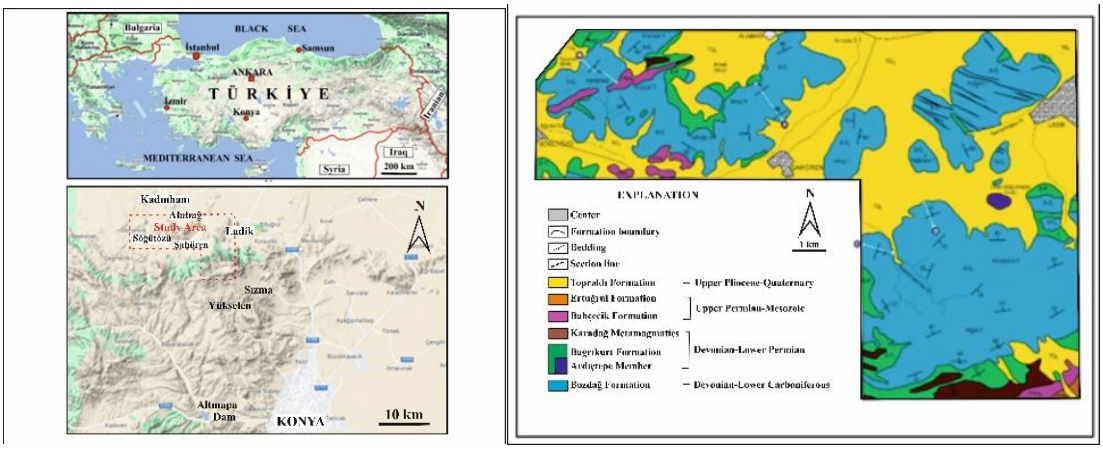

Figure 1. Location (GoogleMaps) and geological map of the study area (modified from Özkan 2016)

Four measured stratigraphic sections were taken from the Bozdağ Formation by Özkan (2016). Stromatoporoid bioherms are also encountered in the Bozdağ Formation dolostones, which contain abundant fossils (mostly *Amphipora*).

[1] Assoc. Prof. Dr. Ali Müjdat ÖZKAN; Konya Technical University Faculty of Engineering & Natural Sciences Department of Geological Engineering. amozkan@ktun.edu.tr ORCID ID: 0000-0001-6686-327X

Major Oxide and Trace Element Properties of the Bozdağ Formation Dolostones

Analysis results of 16 dolostone samples are given in Tables 1 and 2. Based on this analysis data, major oxide and trace element values and geochemical interpretation of the Bozdağ Formation dolostones were made.

Table 1. Major oxide contents of dolostones in the Bozdağ Formation

Sample	SiO_2	Al_2O_3	Fe_2O_3	MgO	CaO	Na_2O	K_2O	TiO_2	P_2O_5	MnO	LOI
A185	0.25	0.04	0.25	20.99	29.64	0.04	0.02	<0.01	<0.01	0.02	48.6
A115	0.54	0.26	0.30	21.32	30.17	0.03	0.08	<0.01	<0.01	0.02	46.7
A50	0.35	0.08	0.19	21.10	30.56	0.03	0.02	<0.01	<0.01	0.03	46.6
A1	0.17	<0.01	0.31	20.83	29.93	0.04	<0.01	<0.01	<0.01	0.02	48.2
B291	0.63	0.32	0.17	21.12	30.65	0.02	0.11	0.02	<0.01	<0.01	46.1
B234	0.86	0.47	0.05	20.89	30.04	0.02	0.16	0.02	<0.01	<0.01	46.4
B210	0.32	0.13	0.23	20.59	30.23	0.03	0.04	<0.01	0.01	0.01	47.0
B77	0.30	0.13	0.66	21.48	30.53	0.02	0.04	<0.01	<0.01	0.01	46.6
B6	0.17	0.05	<0.04	20.36	31.91	0.03	0.02	<0.01	0.01	<0.01	47.0
C153	0.52	0.26	0.16	20.94	30.70	0.02	0.09	0.01	<0.01	<0.01	46.6
C78	0.34	0.15	0.13	20.86	30.59	0.05	0.05	<0.01	<0.01	<0.01	46.9
C22	0.36	0.13	0.47	21.12	30.10	0.02	0.05	<0.01	0.02	0.03	47.3
D17	0.14	0.04	0.14	21.48	30.65	0.03	0.02	<0.01	<0.01	<0.01	47.2
D11	0.16	0.07	0.10	21.35	30.53	0.03	0.02	<0.01	<0.01	<0.01	47.2
D8	0.23	0.10	0.19	21.09	30.82	0.03	0.03	<0.01	<0.01	<0.01	47.0
D4	0.30	0.15	0.20	21.38	30.77	0.02	0.05	<0.01	<0.01	<0.01	46.7

Table 2. Trace element contents of dolostones in the Bozdağ Formation

Sample	Sr	Ba	Rb	Fe	Mn	Al	Na
A185	27.9	<1	0.3	1748	155	212	297
A115	28.1	2	1.7	2098	155	1376	222
A50	106.1	4	0.2	1329	232	423	222
A1	24.8	1	<0.1	2168	155	0	297
B291	55.8	5	2.1	1189	0	1693	148
B234	66.5	2	2.6	350	0	2487	148
B210	81.8	1	0.6	1609	77	688	222
B77	20.1	2	0.6	4616	77	688	148
B6	82.8	5	0.1	0	0	264	122
C153	73.3	3	1.9	1119	0	1376	148
C78	67.7	4	0.9	909	0	794	371
C22	30.1	1	0.6	3287	232	688	148
D17	54.7	2	0.1	979	0	212	297
D11	83.2	2	0.2	699	0	370	297
D8	66.4	2	0.5	1329	0	529	297
D4	122.5	3	0.9	1399	0	794	148

In the mole %$MgCO_3$-mol%$CaCO_3$ graph, it is observed that there is a strong positive relationship between the $MgCO_3$ content and the $CaCO_3$ content (Figure 2). A positive correlation is observed between SiO_2 and Al_2O_3 in the %SiO_2-%Al_2O_3 graph (Figure 3).

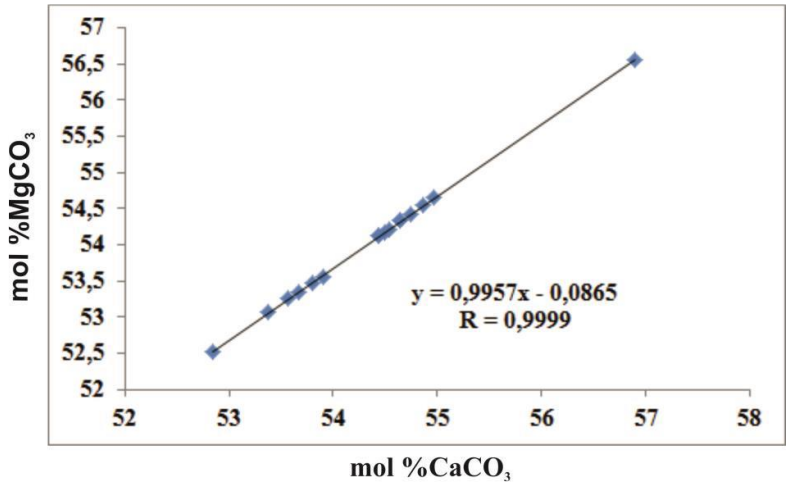

Figure 2. mol %$MgCO_3$-mol %$CaCO_3$ graph (from Özkan, 2016)

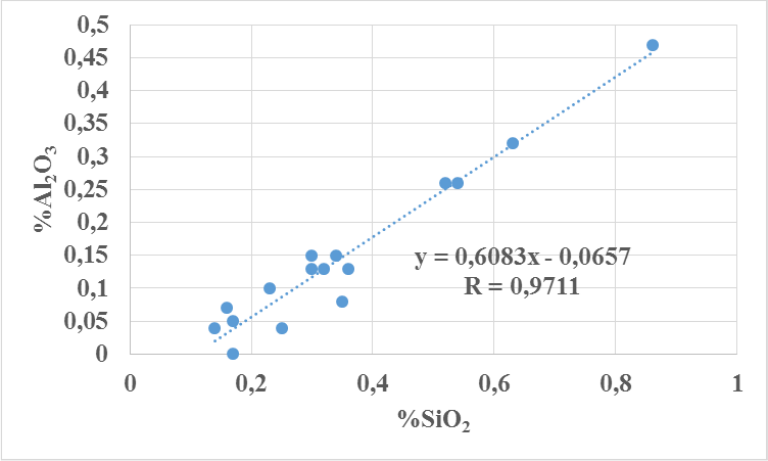

Figure 3. % SiO_2-% Al_2O_3 graph (from Özkan, 2016)

In the %K_2O-Rb graph, a positive correlation is observed between Rb content and %K_2O (Figure 4). In the Fe-Mn graph, a positive relationship is observed between Mn and Fe content in dolomites, that is, as the Fe content increases, so does the Mn content (Figure 5).

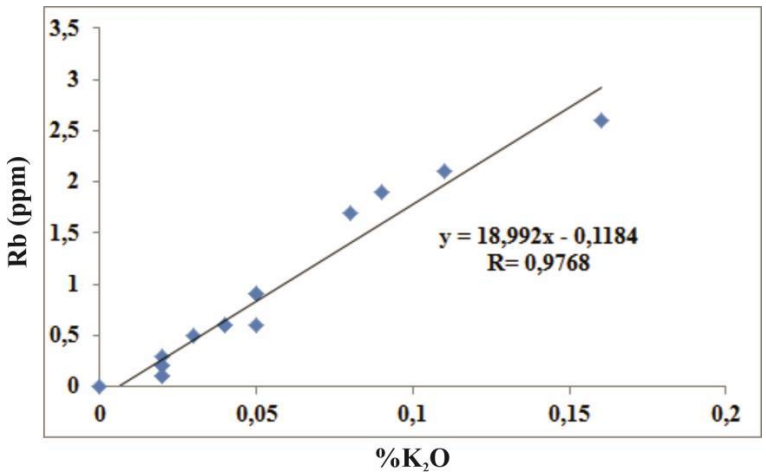

Figure 4. %K_2O-Rb graph (from Özkan, 2016)

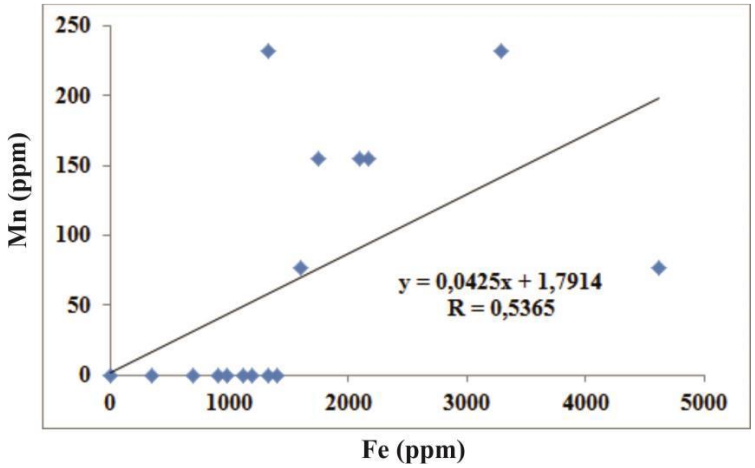

Figure 5. %Fe-Mn graph (from Özkan, 2016)

In the Fe-Al graph, a negative relationship is observed between the Al content and the Fe content in the dolostones (Figure 6). A positive correlation is observed between the Sr content and the $CaCO_3$ content in the dolostones in the Sr-$CaCO_3$ graph (Figure 7). In the Sr-$MgCO_3$ graph, a positive correlation is observed between Sr content and $MgCO_3$ content in dolostones (Figure 8). In the Sr-Mn graph, a negative correlation is observed between Sr content and Mn content in dolostones (Figure 9). In the Sr-Fe graph, a negative correlation is observed between the Sr content and the Fe content in the dolostones (Figure 10). In the Fe-$MgCO_3$ graph, a negative correlation is observed between the Fe content and $MgCO_3$ content in the dolostones (Figure 11). In the Fe-$CaCO_3$ graph, a negative correlation is observed between the Fe content and the $CaCO_3$ content in the dolostones (Figure 12).

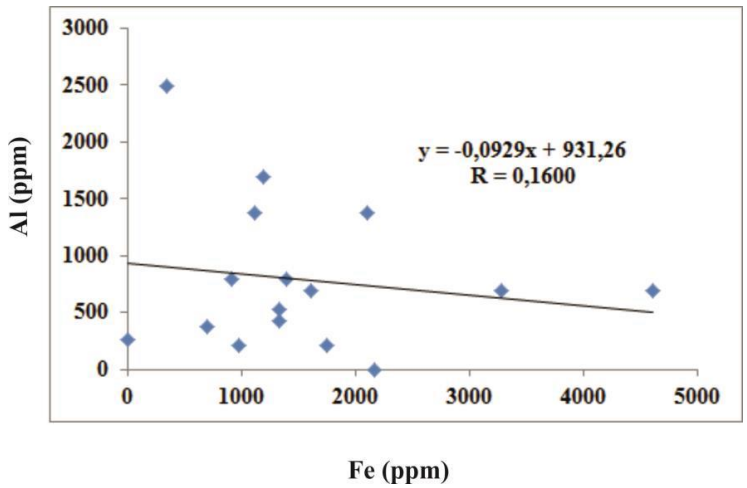

Figure 6. %Fe-Al graph (from Özkan, 2016)

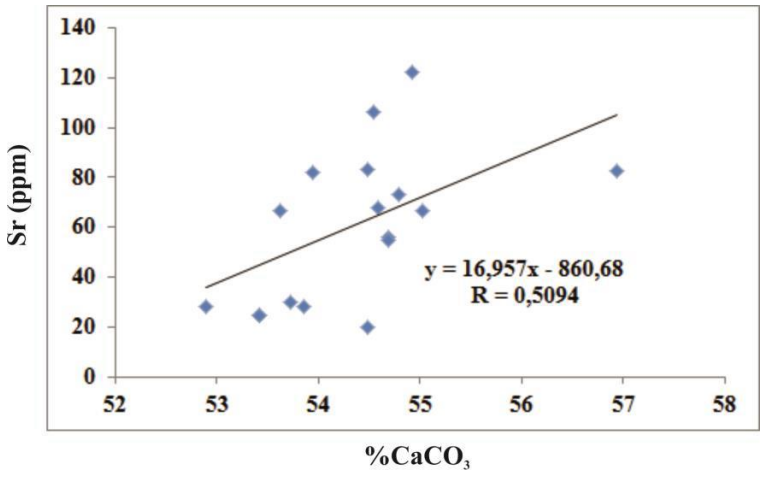

Figure 7. %$CaCO_3$-Sr (ppm) graph (from Özkan, 2016)

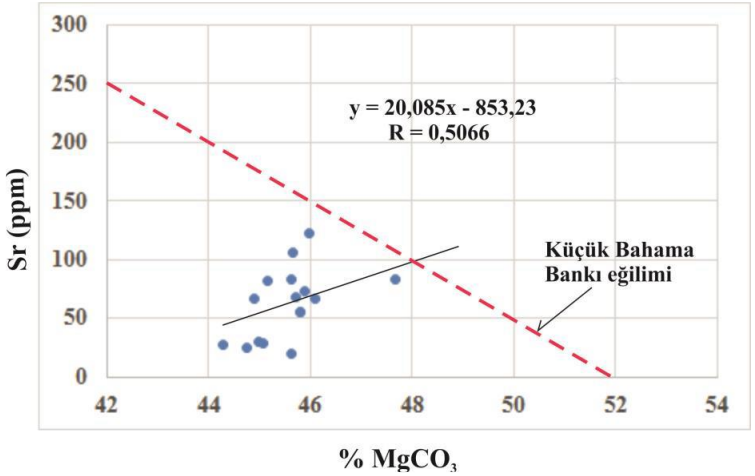

Figure 8. %$MgCO_3$-Sr (ppm) graph. Sr/Ca seawater: 0.0195, Sr/Ca the Bozdağ Formation dolostones: 0.0001-0.0006 (from Özkan, 2016)

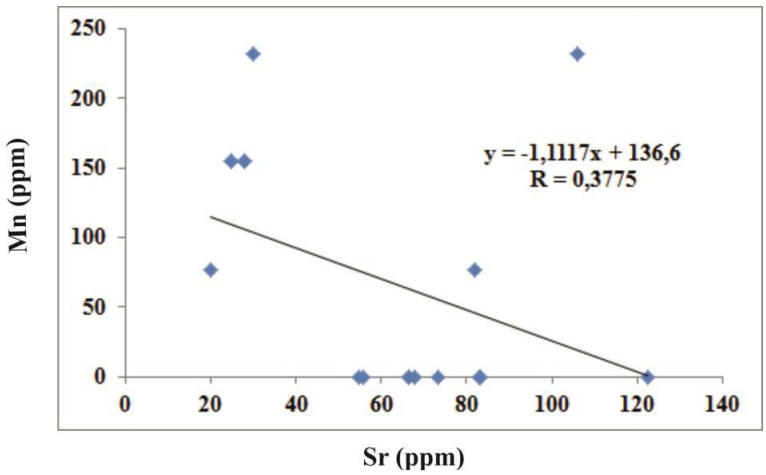

Figure 9. Sr (ppm)-Mn (ppm) graph (from Özkan, 2016)

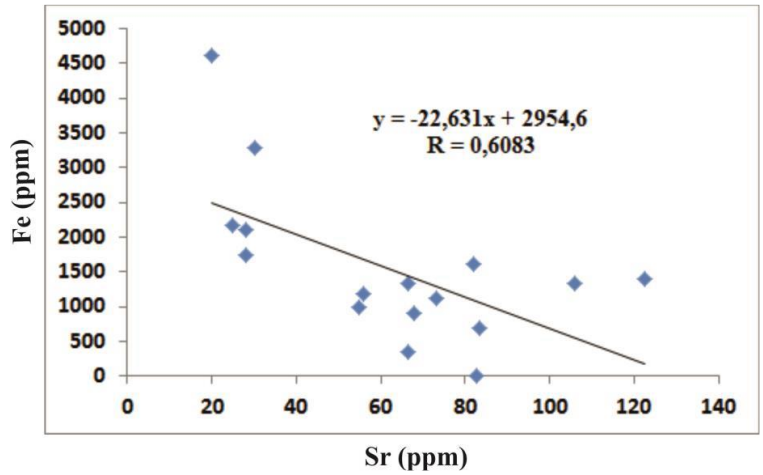

Figure 10. Sr (ppm)-Fe (ppm) graph (from Özkan, 2016)

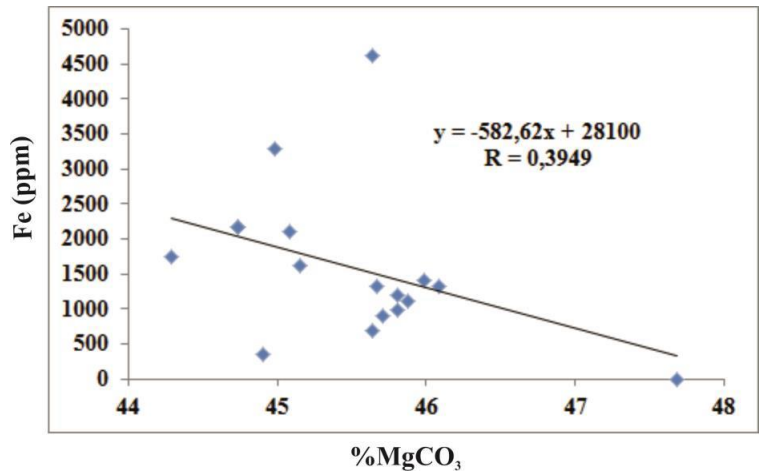

Figure 11. %$MgCO_3$-Fe (ppm) graph (from Özkan, 2016)

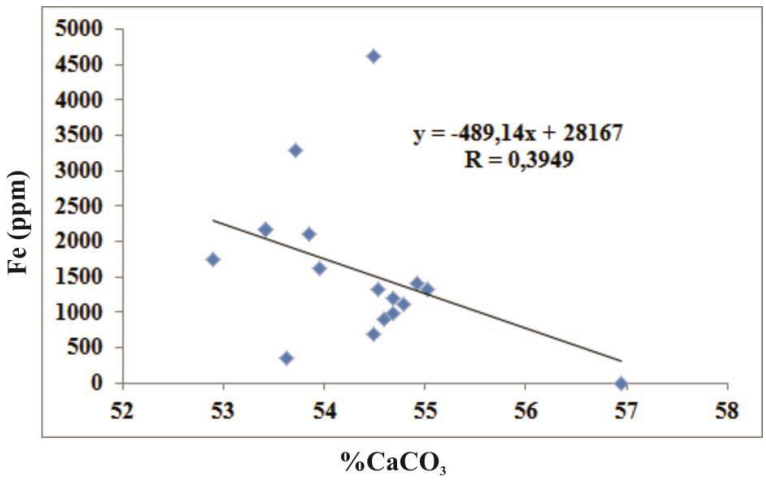

Figure 12. %$CaCO_3$-Fe (ppm) graph (from Özkan, 2016)

Geochemical Comments

The positive correlation between mol% $CaCO_3$ and mol% $MgCO_3$ observed in the Bozdağ Formation dolostones (Figure 2) indicates dolomitization developed from evaporative waters. During dolomitization, as the Ca ions in the dolomite minerals move away from the environment, the ratio of Mg ions increases. Thus, the composition of the dolomite formed approximates that of the ideal dolomite (stoichiometric dolomite). However, the dolomites in our samples are in Ca-rich non-stoichiometric dolomite composition (Figure 2). Due to the semi-stable nature of the dolomites, they are expected to become more stoichiometric during progressive recrystallization (Gao and Land 1991; Malone et al. 1994, 1996; Kırmacı and Akdağ 2005). However, some researchers have suggested that Ca-rich dolomites may remain stable for long periods of time (Lumsden and Chimahusky 1980; Reinhold 1998; Kırmacı and Akdağ 2005). Ca-rich non-stoichiometric dolomite is generally expressed as a function of the Mg/Ca ratio of the dolomitized solution and the liquid/rock ratio during dolomitization. As these ratios decrease, non-stoichiometric dolomite rich in Ca is formed. The presence of calcian dolomites indicates that it is composed of a solution with a low Mg/Ca ratio. Non-stoichiometric calcian dolomite can easily form in a partially closed system under rock control (Sperber et al. 1984; Török 2000; Kırmacı and Akdağ 2005).

The Mg/Ca ratio in the Bozdağ Formation dolomites is 0.6, which refers to the non-stoichiometric calcium-rich dolomites attributed to the basinal salty formation waters, which shows that the formation waters are enriched in calcium and depleted in magnesium with increasing temperature during burial.

Concentrations of trace elements in dolostones; can be determined by the concentrations of these elements in the pore fluids, the degree of openness of the diagenetic system, and the effective distribution coefficient of trace elements between dolomite and water (Suzuki et al. 2006).

Although Fe^{2+} and Mn^{2+} are in lower concentrations than Na^{+} and K^{+} in meteoric waters, if Fe and Mn increase while Na decreases in samples, this is probably related to the continuous reduction of abundant organic matter (Mahboubi et al., 2002). In addition, reducing forms of Fe^{2+} and Mn^{2+} are found in carbonate minerals; therefore, an increase in Fe and Mn concentrations indicates that carbonates precipitate under reducing conditions (Land, 1986; Mahboubi et al., 2002; Adabi, 2009). The reducing conditions increase with increasing burial depth (Adabi, 2009).

Barnaby and Read (1992) emphasized that the positive correlation between Fe and Mn is a commonly observed feature in burial dolomites. The positive correlation between Fe and Mn observed in Bozdağ formation dolomites (Figure 5) indicates burial dolomitization.

Primary oxic marine carbonates have been estimated to have <100 ppm Fe and <10 ppm Mn (Veizer 1983; Satterley et al. 1994), where levels of these elements reflect the degree of diagenetic enrichment. Fe (0-4616 ppm, average 1551.7 ppm) and Mn (0-232 ppm, average 67.7 ppm) contents in the Bozdağ Formation dolostone samples also indicate diagenetic enrichment.

It is difficult to determine whether Mg, Fe, and Mn are obtained from previous carbonates (Srinivasan et al., 1994). Rich Fe concentrations may be the result of primary formation from Fe-rich fluids (Srinivasan et al., 1994). Iron oxide incrustations are likely to form on detrital grains during atmospheric exposure (Srinivasan and Walker, 1993; Srinivasan et al., 1994), so they can be preserved as local sources of Fe under reducing diagenesis conditions. Alternatively, recrystallization of early fine-grained dolomites (poorly ordered and very low stoichiometric) during burial in the presence of compaction from basinal fluids (Mazzullo, 1992) may contribute to increasing Fe^{2+} concentrations (Srinivasan et al., 1994).

The infiltration of near-surface oxidized liquids into dolomites may explain dolomite dissolution and subsequent oxy/hydroxide precipitation (Nader et al., 2007). Near-surface waters, such as meteoric water, are generally oxidized and promote rapid precipitation of insoluble Fe-oxy/hydroxide and Mn-oxy/hydroxide (Lohmann, 1988; Nader et al., 2007). It is believed that the oxidation-reduction system results in the evacuation of Mn and Fe within the matrix dissolution porosity and subsequently controls their proper incorporation into and/or subsequent cement phases (Brand and Veizer 1980; Lohmann, 1988; Nader et al., 2007).

Moss and Tucker (1995) stated that the low Sr (average 127 ppm) concentrations of the Cretaceous-aged shallow burial dolomites of southeast France may be due to the replacement of low strontium stabilized marine carbonates or the subsequent crystallization of dolomites. Therefore, we can say that the low Sr concentration (25-122 ppm, average 62 ppm) in the Bozdağ Formation dolostones developed as a result of burial recrystallization.

Rao (1996) stated that the Na content in current dolomites varies between 100-2500 ppm; with low values of mixed zone dolomites, and high values of hypersaline dolomites. The Na content in old dolomites ranges between 114-982 ppm (Baum et al. 1985). Veizer (1983) stated that Na concentrations in old dolomites are expected to be above 600 ppm for hypersaline dolomites. A marine source without significant evaporation effects shows values much lower than 600 ppm (110-380 ppm; average 226 ppm). Marine burial dolomites contain about 300-500 ppm Na (Holail et al. 1988). The Na content of Bozdağ formation dolomites (148-371 ppm, average 227 ppm) also indicates that there is no significant evaporation effect and that they are formed from seawater changed at high temperatures in the burial environment.

The Fe/Al ratio in marine sediments depends on the geochemistry of the source rock and the absolute values of Fe and Al affected by the total amount of terrigenous material associated with the biogenic fraction (Lamy et al., 2000). The negative correlation, albeit weak, between Fe and Al in the Bozdağ Formation dolostones indicates that the dolomitization developed in a reducing environment. Therefore, this situation also indicates that terrigenous material input is low in the Bozdağ Formation dolomites.

A strong positive correlation is observed between SiO_2 and Al_2O_3 in the Bozdağ Formation dolomites. This shows a variable mixture of marine carbonates and clay minerals. Therefore, it indicates clay input to the basin during the deposition of the Bozdağ carbonates.

The strong positive correlation observed between Rb and K_2O in the Bozdağ Formation dolostones indicates that the clays in the carbonates are of marine origin (Rao, 1989). Therefore, this feature supports that the Bozdağ Formation is of marine origin.

The low Sr content and low Sr/Ca ratio of the Bozdağ Formation dolostones suggest altered sea water rather than meteoric water or evaporative concentrated brine. The low Sr content in the Bozdağ Formation dolomites and the positive correlation between Sr and $CaCO_3$ and $MgCO_3$ indicate recrystallization.

The negative correlation observed between Sr and Fe and Mn in the Bozdağ Formation dolostones, low Sr content, and high Fe and Mn content indicates a diagenetic alteration in the reducing burial environment. The negative correlation between Fe and Mn and $CaCO_3$ and $MgCO_3$ in the Bozdağ Formation dolomites also indicates the diagenetic alteration in the reducing burial environment.

Most diagenetic brines are meteoric and marine mixed waters modified by burial processes, and they are usually unsaturated with calcite but supersaturated with dolomite (Lapponi, 2007). The dolomite-calcite balance changes towards higher Ca/Mg ratios at higher temperatures (Lapponi, 2007). The temperature increase during burial in sedimentary basins will increase the saturation level of dolomite relative to calcite in solution with constant Ca/Mg ratios (Lapponi, 2007).

Mattes and Mountjoy (1980), Zenger (1983), and Mountjoy and Amthor (1994) have shown widespread replacement of limestones with an estimated depth of at least 1000 m. The most recommended fluid sources for burial dolomitization are magnesium-rich residual evaporitic brines, altered seawater, and shale compaction waters. Fluids can be transmitted to the dolomitization environment via porous aquifers or along faults by a series of transport mechanisms brought to the dolomitization environment by sediment compaction, thermal convection, and topographically or tectonically.

Trace element (especially Na and Sr) contents of carbonate rocks are important in determining the salinity of the original fluids that formed the carbonates (Wanas, 2002). This is a view based on the fact that both hypersaline and marine carbonates are enriched in Na and Sr relative to their freshwater origin (Kinsman, 1969; Land and Hoops, 1973; Land, 1980; Morrow, 1988) (Wanas 2002). It is also known that the Na and Sr contents of carbonate rocks are also reduced by meteoric waters during their diagenesis (Land et al., 1975; El-Hinnawi and Loukina, 1993; Wanas, 2002).

Wanas (2002) stated that the Na content of 1030-5120 ppm (mean=3008 ppm) is very similar to that of hypersaline or evaporitic dolostones (Land and Hoops, 1973; Mitchell et al., 1987); He stated that the Na content of 520-890 ppm (mean=656 ppm) corresponds to the concentrations of marine and marine-meteoric water mix dolomites (Land et al. 1975; Holail 1989).

Wanas (2002) found that the Sr content of 387-610 ppm (mean=508 ppm) was close to the Sr content of marine-hypersaline dolomites (Land and Hoops 1973; Land 1980); He stated that 64-140 ppm (average=108 ppm) Sr content reached the content of old marine and marine-meteoric water mix dolomites (Land 1980; Brand and Veizer 1980; Mitchell et al. 1987).

Low Sr concentrations (<300 ppm) confirm an origin from seawater (Budd, 1997; Suzuki et al., 2006). Veizer (1977) stated that the approximate average of the Sr content of pre-Quaternary limestones was around 320 ppm (Rao, 1989). The Sr ratios in the Bozdağ Formation dolostone samples are 20 ppm-122 ppm (mean=62 ppm), which is far below the rate stated by Veizer (1977). Therefore, he states that this loss is the result of meteoric diagenesis and/or recrystallization (diagenetic alteration during burial).

Milliman (1974) stated that aragonite in current marine carbonate deposits contains about 2500 ppm Na and calcite contains about 250 ppm Na. During diagenesis, Na is gradually lost due to the increasing influence of meteoric waters (Rao, 1989). Therefore, the high (148-371 ppm; mean=227 ppm) Na ratios observed in the Bozdağ formation dolomite samples indicate that the original rock is aragonite rather than calcite, as 6 out of 16 samples are higher than the current value despite diagenetic alteration.

Milliman (1974) and Rao (1989) stated that <20 ppm Mn is present in recent aragonitic marine sediments. Oxidation conditions greatly inhibit the association of Mn in CaCO3, whereas under reducing conditions calcite may have several percentages of Mn (Shanmugam and Benedict, 1983; Rao, 1989). The Bozdağ Formation dolostone samples (7 out of 16 samples) have Mn content of 77-232 ppm (average = 155 ppm for seven samples; mean = 68 ppm for sixteen samples) and originally defined aragonite mineralogy, oxidation conditions during shallow marine deposition (in most samples). Mn was not observed) and was interpreted as reflecting enrichment under reduced conditions during burial.

Acknowledgment

This study was supported by the project numbered 11201124 by the Scientific Research Projects Coordinators of Selçuk University. The author would like to thank Selçuk University Scientific Research Projects Coordinators.

REFERENCES

Adabi, M. H. (2009). Multistage dolomitization of Upper Jurassic Mozduran formation, Kopet-Dagh Basin, N.E. Iran, *Carbonates and Evaporites, 24* (1), 16-32.

Barnaby, G. J. & Read, J. F. (1992). Dolomitization of a Carbonate Platform During Late Burial: Lower to Middle Cambrian Shady Dolomite, Virginia Appalachians. *Journal of Sedimentary Petrology, 62* (6), 1023-1043.

Baum, G. R., Harris, W. B. & Drez, P. E. (1985). Origin of Dolomite in the Eocene Castle Hayne Limestone, North Carolina. *Journal of Sedimentary Petrology, 55*, 506-517.

Brand, V. & Veizer, J. (1980). Chemical Diagenesis of Multicomponent Carbonate Systems: Trace Elements. *Jour. Sedim. Petrol., 50*, 1219-1236.

Budd, D. A. (1997). Cenozoic Dolomite of Carbonate Islands: Their Attributes and the Origin. *Earth Sci. Rev., 42*, 1-47.

El-Hinnawi, E. & Loukina, S. (1993). Isotopic Composition of Egyptian Cenozoic Limestones. *Sediment., Egypt, 1*, 35-42.

Gao, G. & Land, L. S. (1991). Early Ordovician Cool CNTEk Dolomite, Middle Arbuckle Group, slick Hills, SW Oklahoma, USA: Origin and Modification. *Jour. Sediment. Petrol. 61*, 161-173.

GoogleMaps: https://www.google.com/maps/@40.079773,32.794561,12.21z

Holail, H. M., Lohmann, K. C. & Sanderson, I. (1988). Dolomitization and Dedolomitization of Upper Cretaceous Carbonates, Bahariya Oasis, Egypt. In Shukla, V., Baker, P. (eds.), Sedimentology and Geochemistry of Dolostones. *Soc. Econ. Paleont. Mineral. Spec. Publ., 43*, 191-207.

Holail, H. M. (1989). Carbon and Oxygen Isotopic Ratio of Dolomites from Gebal Ataqa, Abstract, *1st International Conference of Geochemistry, Alexandria University*, Egypt, p. 262.

Kırmacı, M. Z. & Akdağ, K. (2005). Origin of Dolomite in The Late Cretaceous-Paleocene Limestone Turbidites, eastern Pontides, Turkey. *Sedimentary Geology, 181*, 39-57.

Kinsman, D. J. J. (1969). Interpretation of Sr^{2+} Concentrations in Carbonate Minerals and Rocks. *Jour. Sedim. Petrol., 39*, 486-508.

Lamy, F., Klump, J., Hebbeln, D. & Wefer, G. (2000). Late Quaternary Rapid Climate Change in Northern Chile. *Terra Nova, 12* (1), 8-13.

Land, L. S. & Hoops, G. K. (1973). Sodium in Carbonate Sediments and Rocks: A Possible Index to Salinity of Diagenetic Solution. *Jour. Sedim. Petrol., 43*, 614- 616.

Land, L. S., Salem, M. R. & Morrow, D. W. (1975). Paleohydrology of Ancient Dolomites: Geochemical Significance. *Amer. Assoc. Petrol. Geol. Bull., 59*, 1602-1625.

Land, L. S. (1980). The Isotopic and Trace Element Geochemistry of Dolomite: the State of the Art. *SEPM Spec. Publ., 28*, 87-110.

Land, L. S. (1986). Limestone diagenesis--some geochemical considerations, in F. A. Mumpton, Ed., Studies in Diagenesis. *U.S. Geol. Survey Bull. 1578*, 129-137.

Lapponi, F. (2007) Late Burial, Hydrothermal Dolomitization of the Cambrian Lancara Formation, Cantabrian Zone (NW Spain): Origin of the Dolomitizing Fluid and Relation to the Geodynamic Setting, Ph.D. Thesis, *Geological Institute of the University of Heidelberg*, 174 p.

Lohmann, K. C. (1988). Stable Isotopes and Limestone Lithification. *Jour. Geol. Soc. Lond., 133*, 637-660.

Lumsden, D. N. & Chimahusky, J. S. (1980). Relationship Between Dolomite Nonstoichiometry and Carbonate Facies Parameters. In: Zenger, D. H., Dunham, J. B., Ethington, R. L. (Eds.), Concepts and Models of Dolomitization. *Soc. Econ. Paleontol. Mineral. Spec. Publ., 28*, 123-137.

Mahboubi, A., Moussavi-Harami, R., Brenner, R. L. & Gonzalez, L. A. (2002). Diagenetic History of Late Paleocene Potential Carbonate Reservoir Rocks, Kopet-Dagh Basin, NE Iran. *Jour. Petrol. Geol., 25*, 465-484.

Malone, M. J., Baker, P. A. & Burns, S. J. (1994). Recrystallization of Dolomite: Evidence from the Monterey Formation (Miocene), California. *Sedimentology, 41*, 1223- 1239.

Malone, M. J., Baker, P. A. & Burns, S. J. (1996). Hydrothermal Dolomitization and Recrystallization of Dolomite Breccias from the Miocene Monterey Formation, Tepuquet Area, California. *Jour. Sediment. Res., 66*, 976-990.

Mattes B. W. & Mountjoy, E. W. (1980). Burial Dolomitization of the Upper Devonian Miette Build-up, Jasper National Park, Alberta. In: Concepts and Models of Dolomitization (ed. by D. H. Zenger, J. B. Dunham, and R. L. Ethington), Spec. Publs. Soci. Econ. Paleont. Miner., 28, 259-297.

Mazzullo, S. J. (1992). Geochemical and Neomorphic Alteration of Dolomite: a review. *Carbonates Evaporites, 7*, 21-37.

Milliman, J. D. (1974). Marine Carbonates, Recent Sedimentary Carbonates, Part I, *Springer-Verlag, New York*, 375 p.

Mitchell, H. G., Land, L. S. & Miser, D. N. (1987). Modern Marine Dolomite Cement in a North Jamaican Fringing NTEf. *Geology, 15*, 557-560.

Morrow, D. W. (1988). Diagenesis. Dolomite-Part I: The Chemistry of Dolomitization and Dolomite Precipitation. *Geosci. Can. Rep. Ser., 4*, 113-123.

Moss, S. & Tucker, M. E. (1995). Diagenesis of Barremian-Aptian Platform Carbonates (the Urgonian Limestone Formation of SE France): Near-Surface and Shallow-Burial Diagenesis. *Sedimentology, 42* (6), 853-874.

Mountjoy, E. W. & Amthor, J. E. (1994). Has burial dolomitization come of age? Some answers from the Western Canada sedimentary basin. *Dolomites: A volume in honour of Dolomieu*, 203-229.

Nader, F. H., Swennen, R. & Ellam, R. M. (2007). Field Geometry, Petrography and Geochemistry of a Dolomitization Front (Late Jurassic, Central Lebanon). *Sedimentology, 54*, 1093-1119.

Özkan, A. M. (2016). Söğütözü-Ladik (Konya) Çevresindeki Bozdağ Formasyonu (Silüriyen-Alt Karbonifer) Dolomitlerinin Sedimantolojik ve Jeokimyasal İncelenmesi. *Selçuk Üniversitesi Bilimsel Araştırmalar Projesi*, Proje no: 11201124.

Rao, C. P. (1989). Geochemistry of the Gordon Limestone (Ordovician), Mole CNTEk, Tasmania. *Australian Jour. Earth Sci., 36*, 65-71.

Rao, C.P. (1996). Elemental composition of marine calcite modern temperate shelf brachiopods, bryozoans, and bulk carbonates, eastern Tasmania, Australia. *Carbonates and Evaporites, 11*, 1-18.

Reinhold, C. (1998). Multiple Episodes of Dolomitization and Dolomite Recrystallization During Shallow Burial in Upper Jurassic Shelf Carbonates, Eastern Swabian, South Germany. *Sediment. Geol., 121*, 71-95.

Satterley, A. K., Marshall, J. D. & Fairchild, I. J. (1994). Diagenesis of an Upper Triassic reef complex, Wilde Kirche, Northern Calcareous Alps, Austria. *Sedimentology, 41*, 935-950.

Shanmugam, G. & Benedict, G. L. III. (1983). Manganese Distribution in the Carbonate Fraction of Shallow and Deep Marine Lithofacies, Middle Ordovician, Eastern Tennessee. *Sedimentary Geology, 35*, 159-175.

Sperber, C. M., Wilkinson, B. H. & Peacor, D. R. (1984). Rock Composition, Dolomite Stoichiometry and Rock/Water Reactions in Dolomitic Carbonate Rocks. *Jour. Geol., 92*, 609-692.

Srinivasan, K. & Walker, K. R. (1993). Sequence Stratigraphy of an Intrashelf Basin Carbonate Ramp to Rimmed Platform Transitions of the Maryville Limestone (Middle Cambrian) Southern Appalachians. *Bull. Geol. Soc. Amer., 105*, 883-896.

Srinivasan, K., Walker, K. R. & Goldberg, S. A. (1994). Determining Fluid Source and Possible Pathways During Burial Dolomitization of Maryville Limestone (Cambrian), Southern Appalachians, USA. *Sedimentology, 41*, 293-308.

Suzuki, Y., Iryu, Y., Inagaki, S., Yamada, T., Aizawa, S. & Budd, D. A. (2006). Origin of Atol Dolomites Distinguished by Geochemistry and Crystal Chemistry: Kita-Daito-Jima, Northern Philippine Sea. *Sedimentary Geology, 183*, 181-202.

Török, A. (2000). Formation of Dolomite Mottling in Middle Triassic Ramp Carbonates (Southern Hungary). *Sediment. Geol., 131*, 131-145.

Veizer, J. (1977). Diagenesis of Pre-Qaternary Carbonates as Indicated by Tracer Studies. *Jour. Sedim. Petrol., 46*, 565-581.

Veizer, J. (1983). Chemical Diagenesis of Carbonates: Theory and Application of Trace Element Technique. In: Arthur, M.A., Anderson, T.F., Kaplan, I.R., Veizer, J., Land, L.S. (Eds.), Stable Isotopes in Sedimentary Geology. *Soc. Econ. Paleont. Miner. Short Course, 10* (3), 1-100.

Wanas, H. A. (2002). Petrography, Geochemistry and Primary Origin of Spheroidal Dolomite from the Upper Cretaceous/Lower Tertiary Maghra El-Bahari Formation at Gabal Ataqa, Northwest Gulf of Suez, Egypt. *Sediment. Geol., 151*, 211-224.

Zenger, D. H. (1983). Burial Dolomitization in the Lost Burro Formation (Devonian), East-Central California, and the Significance of Late Diagenetic Dolomitization. *Geology, 11*, 519-522.

Sedımentary Structures Observed In The Flysch Featured Dikmende Formatıon (Upper Cretaceous)

Ali Müjdat ÖZKAN[1]
Ayla BOZDAĞ[2]

Introduction

Flysch are sedimentary units that are deposited in the deep marine environment, consisting of detritus carried and deposited by turbid currents, a type of density current. Turbid currents and turbidites can develop in any environment from deep marine to shallow marine and aquatic terrestrial environments. Every flysch is a turbidite, but not every turbidite is a flysch. For sediment to be flysch, it must be deposited in a deep marine environment.

The study area is located in Orhaniye (Kazan) and its surroundings, located in the northwest of Ankara province (Figure 1).

The Dikmendede Formation, which typically has flysch features, is mainly composed of sandstone-shale intercalation and also includes siltstone and lenticular conglomerates at some levels. Conglomerates in intermediate levels are green-gray colored, polygenic pebbly, medium-thick bedded, poorly sorted, tightly carbonate cemented, and gradually transitioning to sandstones.

Green-greenish-gray-colored sandstones are thin-thick bedded, coarse-grained at conglomerate-sandstone transitions, and fine-grained at sandstone-shale transitions. Sandstones contain abundant sedimentary structures. Grey-green colored shales are alternated with siltstones at some levels, with good fissility. It is common to encounter plant fragments and coaled fragments in the siltstones.

The Dikmendede Formation is intermediate turbidite in the Ta-Te interval of the Bouma sequence and forms the middle part of the deep sea fan. In other words, in terms of facies characteristics, it was developed in a deep sea fan system between the upper slope and the abyssal plain. The Dikmendede Formation was deposited in the back-arc trough of the Neotethys, which began to close in the Late Cretaceous, and volcanic inputs were occasionally added to the deposition (Sagular and Toker, 1990).

Dikmendede Formation Sedimentary Structures

Although there is no consensus among researchers, sedimentary structures are generally divided into four groups (1) Erosional, (2) Depositional, (3) Post-depositional/deformational, and (4) Biogenic.

Erosional, depositional, deformational, and biogenic sedimentary structures were all observed in Dikmendede Formation. Quite large flute casts were observed at the base of the sandstones (Figure 2).

[1] Assoc. Prof. Dr. Ali Müjdat ÖZKAN; Konya Technical University Faculty of Engineering & Natural Sciences Department of Geological Engineering. amozkan@ktun.edu.tr **Corresponding author* ORCID ID: 0000-0001-6686-327X
[2] Prof. Dr. Ayla BOZDAĞ; Konya Technical University Faculty of Engineering & Natural Sciences Department of Geological Engineering. aybozdag@ktun.edu.tr ORCID ID: 0000-0002-6114-0678

The flute casts are round/elliptical or pear-shaped. It is asymmetrical, deep, and rounded in cross-section, with the current upstream. They are generally 5-10 cm wide and 10-20 cm long and are found in groups directed in the same direction (Reading, 1996). The formation of flute casts occurs as a result of the sediment-laden streams forming small eddies as they pass over the settled mud and these small eddies prevent deposition in their location. Due to the formation of sedimentation on the edges of the eddies, the regions where the eddies remain as deep pits (Reading, 1996). The flute casts are seen at the base of the upper layer as a result of remaining as pits during the formation of the structure and these pits are subsequently filled with sand in the upper layer, and naturally, they indicate the substratum (Reading, 1996).

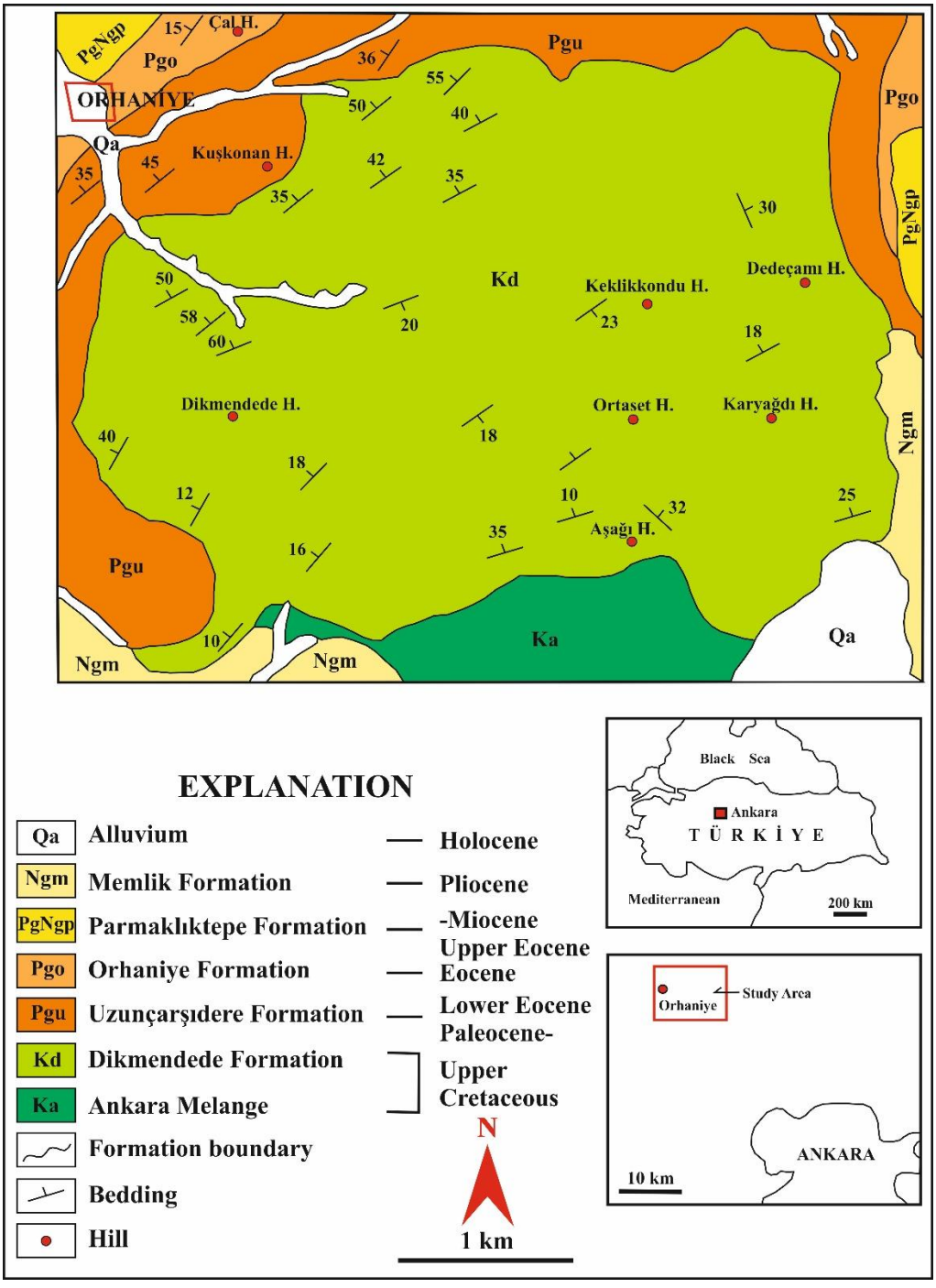

Figure1. Location & geological map of the study area (modified from Özkan ve Ayaz, 2004)

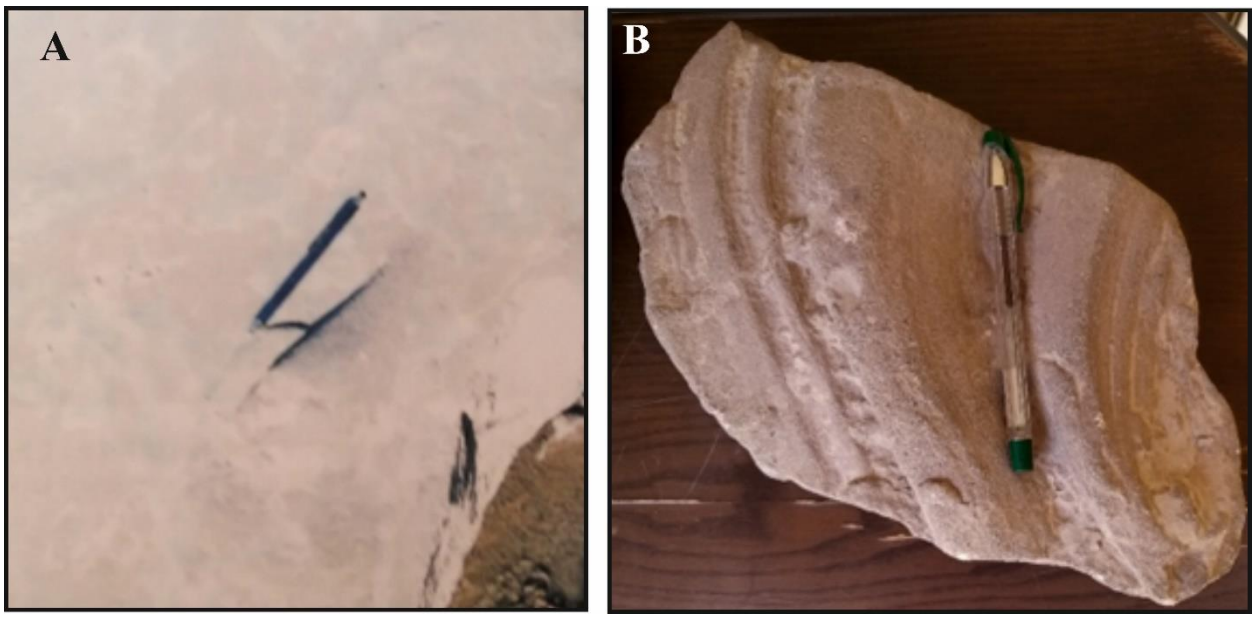

Figure 2. Flute cast in turbiditic sandstones. A) The length of the flute cast is 20 cm and its diameter is 3.5 cm. (Inside Uzunçarşı Creek). Scale, pencil: 14 cm. b) The length of the flute cast is 24 cm and its diameter is 6.5 cm.

Again, bounce marks from the structures observed under the layer were also observed in the Dikmendede Formation (Figure 3). Impact structures develop as a result of the material carried by the stream hitting the underlying layer and creating pits by bouncing during the flow (Reading, 1996). If the impinging particle gets stuck in the layer, it is called the tool structure or the plug structure. The formed depression is drop-shaped and the thin edge of the drop points upstream (Reading, 1996).

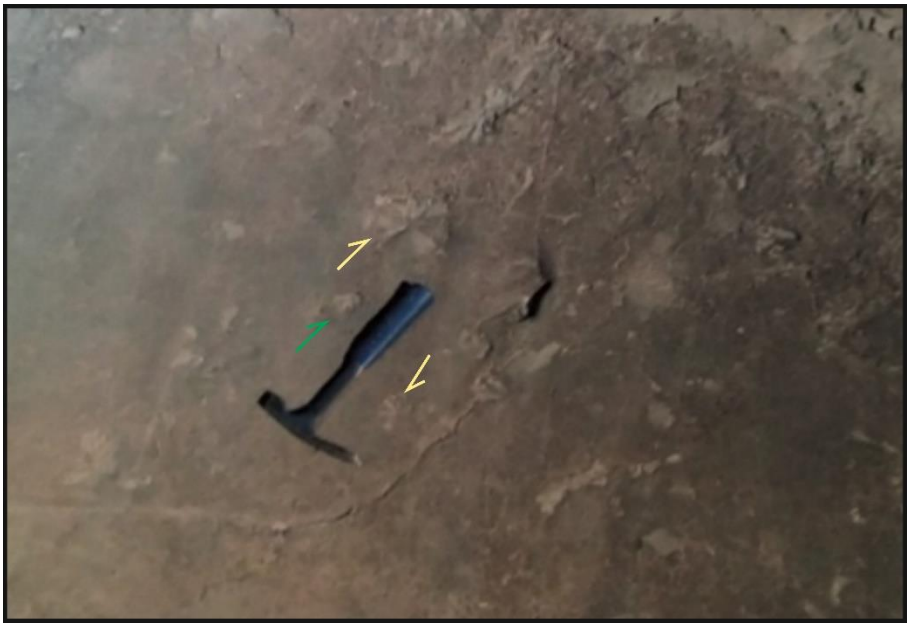

Figure 3. Bounce structures (green arrow) and rest traces (yellow arrow) were observed in the sandstones of Dikmende (Uzunçarşı Creek interior). Scale, hammer length: 28 cm.

Bedding and lamination structures were also observed in Dikmendede Formation (Figure 4-7). The layer or lamination, which is the most characteristic feature of sedimentary rocks, is formed due to changes in the sedimentation pattern. These changes are generally sediment transport and/or grain size changes (Reading, 1996). A layer is called a layer thicker than 1 cm.

The thinner layers are on the millimeter scale and are called the lamina. In fact, the internal structure of a layer consists of laminae (Reading, 1996). Many layers form within hours or days, sometimes during turbid or storm currents, and in other cases over decades or even longer (Reading, 1996). After the layer is formed, the erosional structures on it are formed in the period before the next layer is deposited. In this period, tectonic events may also affect and deform the layers (Reading, 1996). Lamination mostly occurs as a result of the change in grain size or the change of grain composition between the laminae. In many cases, the lamina is the product of a single deposition and is geologically formed momentarily or over longer periods of time (Reading, 1996). It is formed in fine sands, silt, and clays by precipitation directly from suspension, slow-moving sediment clouds, or less dense suspension streams (Reading, 1996).

Figure 4. Stratification, fissilite/lamination observed in the shales of the Dikmendede Formation (south of Uzunçarşı Creek). Scale, hammer length: 28 cm.

Figure 5. Bedding, fissilite/lamination (south of Uzunçarşı Creek) observed in the shales of the Dikmendede Formation (shale-flysch: although the shale is very thick, the sandstone is very thin). Scale, hammer length: 28 cm.

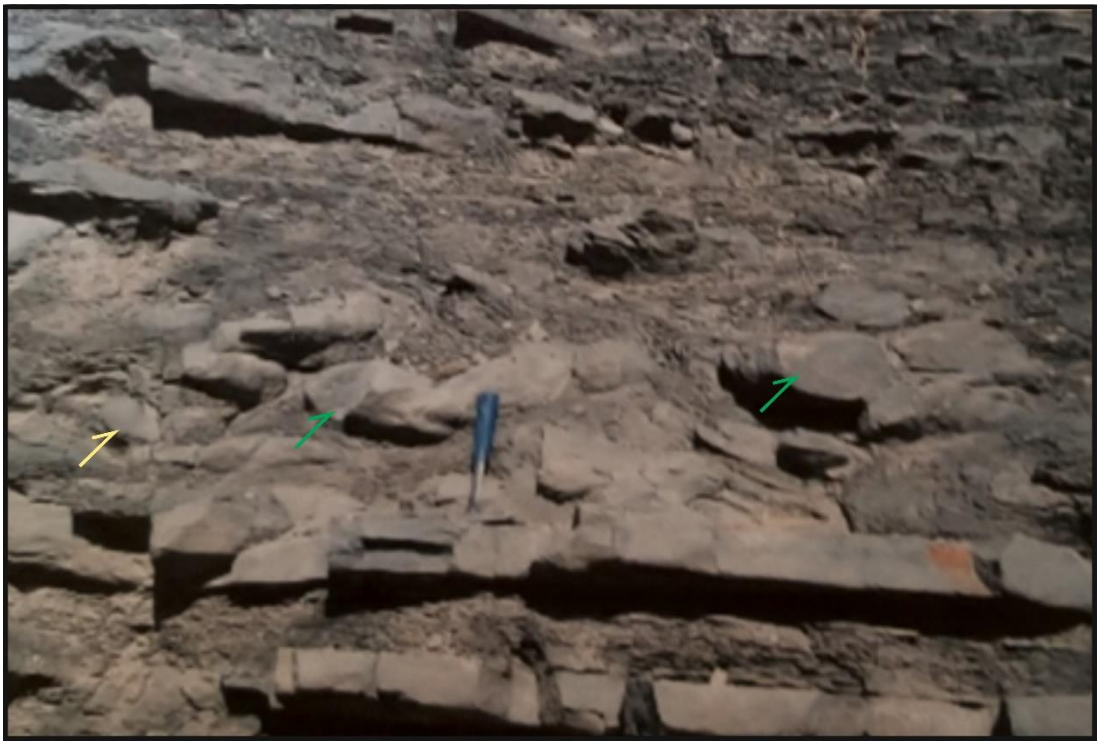

Figure 6. The bedding, fissilite/lamination observed in the flysch (normal-flysch: sandstone and shale in approximately equal proportion) of the Dikmendede Formation. In addition, at this level, the deformation structure, the ball (yellow arrow), and the pillow (green arrow) structure were also observed. (south of Kuşkonan Hill). Scale, hammer length: 28 cm.

Figure 7. Bedding and lamination were observed in the flysch of the Dikmendede Formation (southeast of Kuşkonan Hill). Scale, hammer length: 28 cm.

Another sedimentary structure observed in Dikmendede Formation is channel structures (Figure 8-10). Channels are much more organized structures than digging structures. They are usually waterways where the sediment is transported (Reading, 1996). They may have formed over long periods of time. Some large channels may be large enough to be mapped. Channels are generally filled with coarser material than the material in which they are formed or above and below (Reading, 1996). It may have residual pebbles or intraformational (derived from the same environment) pebbles at its base. Channels are formed in many environments, although they are well known to occur in the fluvial environment, they are frequently seen in glaciers, deltas, tidal plains, shelf margins, continental slopes, and submarine fans (Reading, 1996).

Figure 8. The turbiditic channel fill (southeastern of Kuşkonan Hill) developed in a median fan environment consisting of a conglomerate-sandstone alternation of the Dikmendede Formation. Scale, human height: 180 cm.

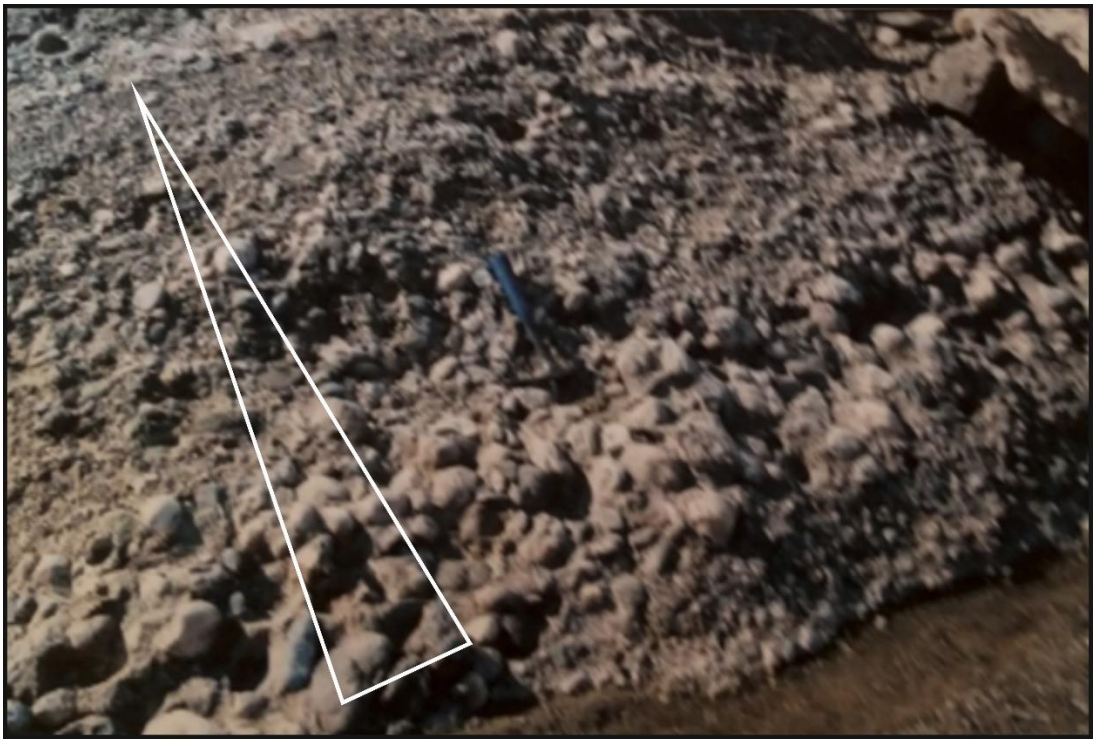

Figure 9. Normal grading was observed in the turbiditic channel fill developed in a median fan environment consisting of a conglomerate-sandstone alternation of the Dikmendede Formation (southeast of Gelinbattı Ridge). Scale, hammer length: 28 cm.

Figure 10. The imbricated structure observed in the turbiditic channel fill (south of Uzunçarşı Creek) developed in a median fan environment consisting of a conglomerate-sandstone alternation of the Dikmendede Formation. The direction of the paleocurrent was measured from west to east at the lower level and from N25W to S25E at the upper level. Scale, hammer length: 28 cm.

In addition, ball and pillow structures, which are deformation structures in Dikmendede Formation, were also encountered (Figure 6). Ball and pillow structures develop when the relatively coarser-grained sand-sized material overlying the fine-grained and not yet consolidated shale/mudstone sinks into the mudstone, and the load pattern first breaks away from the sand layer with the progression of the submersion and sinks completely into the mud (Reading, 1996). The spherical-shaped structures are called ball structures, and the ellipsoidal ones are called pillow structures (Figure 6).

Another structure observed in Dikmendede Formation is biogenic structures formed by organisms (Figures 11 and 12). Sedimentary structures formed by organisms are fossil traces and are also called ichnofossils (Reading, 1996). Fossil traces are so specific to each type of organism that it can be understood which fossil left them. These traces disrupt the original sedimentary structures and even are bioturbation structures that can completely destroy the primary structure, bedding, or lamination (Reading, 1996). However, although it is not known exactly by which organisms many traces were made, we can at least understand the way of life, since creatures with similar life forms leave similar traces. The most important feature of these fossils is that they give us information about the depositional environment in which the sediment was formed (Reading, 1996). Because certain fossil traces are only found in certain sedimentary environments or at a certain water depth. Ichnofossils are divided into five basic groups; (1) feeding structures, (2) nesting structures, (3) crawl marks, (4) resting structures (5) scraping marks.

Figure 11. Trace fossil (Paleodictyon) (Dam Creek) representing the deep marine environment observed in the turbiditic sandstones of the Dikmendede Formation. Scale, pen length: 14 cm.

Figure 12. Trace fossil (Dam Creek) observed in the turbiditic sandstones of the Dikmendede Formation. Scale, pen length: 14 cm.

The model showing the sedimentation environment of turbidites belonging to the Dikmendede Formation is shown in Figure 13. This figure is taken from Shanmugam (2016) article.

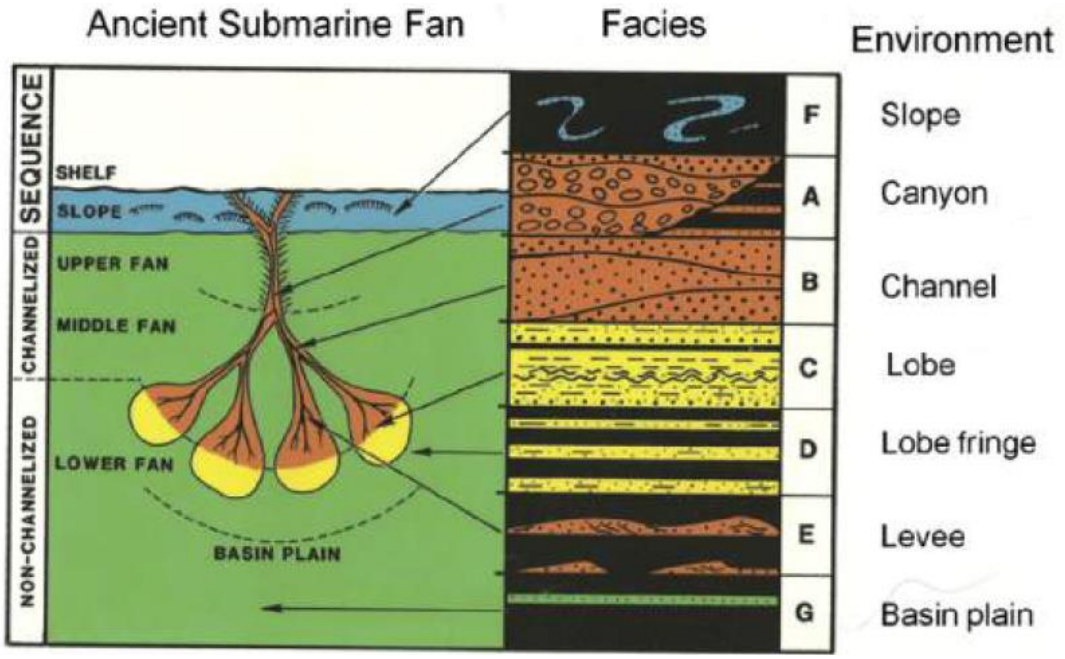

Figure 13. Possible deposition model of Dikmendede Formation (from Mutti & Ricci Lucchi, 1972; Shanmugam, 1985a & 1985b; Shanmugam, 2016).

Acknowledgment

This study was supported by the project numbered 2003/024 by the Scientific Research Projects Coordinators of Selçuk University. The authors would like to thank Selçuk University Scientific Research Projects, Coordinators.

KAYNAKÇA

Mutti, E. & Ricci Lucchi, F. (1972). Turbidites of the northern Apennines, introduction to facies analysis (English translation by T.H. Nilsen, 1978). *International Geology Review 20*, 125-166.

Özkan, A. M. & Bozdağ, A. (2004). Güvenç-Memlik (Kazan-Ankara) Yöresinin Stratigrafisi ve Sedimantolojisi; S. Ü. Bilimsel Araştırma Projeleri, Proje No: 2003/024, 112 s, Konya (unpublished).

Reading, H. G. (1996). Sedimentary Environments. Processes, Facies and Stratigraphy, 3rd edition. Blackwell, 688 p.

Sagular, E. K. ve Toker, V. (1990). Orhaniye (KB Ankara) yöresinin nannoplanktonlarla Kretase biyostratigrafisi. *Türkiye Jeoloji Bülteni, 33*, 57-78.

Shanmugam, G., Damuth, J.E., Moiola, R.J., 1985a. Is the turbidite facies association scheme valid for interpreting ancient submarine fan environments? *Geology 13*, 234-237.

Shanmugam, G., Moiola, R.J., Damuth, J.E., 1985b. Eustatic control of submarine fan development. In: Bouma, A.H., Normark, W.R., Barnes, N.E. (Eds.), Submarine Fans and Related Turbidite Systems. Springer-Verlag, New York, pp. 23-28.

Shanmugam, G. (2016). Submarine fans: A critical retrospective (1950-2015). *Journal of Paleogeography, 5* (2), 110-184.

Miniaturization of Photobioreactors (Micro Photobioreactors) For Bioprocess Development

Başar UYAR[1]

Introduction

A bioreactor is a device or system that supports a biologically active environment under controlled conditions (Tredici, 2004). They are usually closed vessels containing a nutrient solution to support growth of microorganisms or enzymes to carry out biochemical reactions. Bioreactors are a necessary part of any biotechnology based production process whether it is for producing biomass or metabolites, biotransforming one compound into another or degrading unwanted wastes (Chisti, 2006). Design of bioreactors is a complex process that incorporates biological and engineering principles (van't Riet & Tramper, 1991).

A photobioreactor is a specific type of bioreactor that can be defined as a culture system in which light has to pass through the transparent bioreactor's wall to reach the cultivated cells that carry out a light-dependent biological process (Tredici, 2004). They are mainly employed for photosynthetic culture of microalgae and cyanobacteria. Photobioreactors require sunlight or articial illumination to operate.

A bioproduction facility has a train of bioreactors ranging from 20 liters to 250 m^3, or even more in certain processes. The most common operational practice starts with culturing microorganisms in the smallest bioreactor. After pre-determined batch time the content of this bioreactor is transferred to a larger bioreactor and this process is repeated until the largest bioreactor in the train, the production bioreactor, is reached (Chisti, 2006).

Conventional laboratory bioreactors are mechanically complex systems of between 1 and 15 liter volume. Early stage development of new bioproducts is usually limited by the number of processes that can be run in a short time due to availability of laboratory scale bioreactors. To overcome this bottleneck, smaller volume bioreactors have been developed. The microbioreactor is (arbitrarily) defined as a bioreactor with a volume of less than 10 ml (Applikon, 2015). Micro photobioreactor (also called miniature photobioreactor or mini photobioreactor) can similarly be defined as a photobioreactor with a very small (i.e. less than 10 mL) volume. Those very small sized bioreactors are rapidly gaining market share in R&D laboratories due to many benefits they provide.

This chapter is a guide to the central aspects of micro photobioreactors, with a focus on design, properties and applications for bioprocess development. A coverage of the literature was presented as a concise summary. The areas examined include: principles of bioreactor scaling down, motivation and requirement for development of these devices, challenges and limitations encountered during miniaturization process, critical review of available publications on the subject, and finally concluding remarks as well as a future scope for these systems.

[1] Assoc. Prof. Dr., Kocaeli University

Scaling Down Photobioreactors

Scaling is the procedure to determine the design of a reactor from experimental data gained from a reactor operating at a different capacity. In scaling, the engineering objective is usually to maintain dimensional similarity as size is changed (McDuffie, 1991).

For industrial bioreactor design, operation, control and optimization, the scale-down approach is often advocated to efficiently generate data on a small scale, and effectively apply suggested improvements to the industrial scale. In all cases it is important to ensure that the scale-down conditions are representative of the real large-scale bioprocess (Noorman, 2011).

Ideally, an environment in which the production organism displays the same productivity and physiology as in the other (large or small) scale process should be established. To obtain such an environment, many different aspects (including physical properties, fluid dynamics, concentration gradients, used raw materials, process control strategy, etc.) need to match. However, in practice, it is impossible to keep all relevant scaling aspects constant at the same time. Furthermore, there is only a limited number of process operating conditions (stirrer speed, aeration rate, and volume) that may be manipulated to achieve the desired outcome. Therefore, scaling process typically narrows down to selecting one scale up/down parameter (e.g. volumetric power input, oxygen mass transfer coefficient, impeller tip speed) and adjusting the operating conditions to keep that parameter constant across scales (Tajsoleiman et al., 2019).

In many cases for bioreactors, the objective must be to maintain mass-transfer coefficients for oxygen and carbon dioxide (McDuffie, 1991).

On the other hand, in photobioreactor design, efficient light supply to the culture represents a major challenge. Therefore, scale transfer cannot be done using classical concepts. Instead, efficient delivery of light to the cells must be the central dogma. The ultimate goal is that light supply to the individual cells needs to be kept as equal as possible across different scales (Morschett et al., 2018).

Additionally, cell growth, pH, and metabolites should also display similar profiles compared to larger scales photobioreactors to ensure micro photobioreactors could successfully mimic larger scale photobioreactors and give good predictive results (Delouvroy et al., 2015). Scaling up or down of a bioreactor is a process that involves trial-and-error, the amount depending on the type of bioreactor involved. To develop the most cost efficient industrial sized process, extensive scale-up data must be collected by repeating experiments at the lab and pilot scale level. Unfortunately, the collection is far more difficult than it would be in the chemical and petrochemical industries. The nature of working with living material makes contamination commonplace and reproducibility of data difficult to achieve (Harada et al., 1996).

Microbioreactors are gaining popularity as a cost-effective approach to scale-down experimentation. However, realizing conditions that reflect the large-scale process accurately can be challenging. The scale-down factor between an industrial-size fermenter and a microbioreactor is extreme, which inevitably creates physical differences and limitations that complicate the recreation of large-scale conditions. The effect of this deviation on the process becomes apparent in different aspects. To be able to draw the correct conclusions from scale-down experiments and to improve the experimental design of microbioreactor trials, it is important to be aware of these differences and to make a thorough characterization of the process, with mass balances, on-line monitoring, and off-line analysis of the strain morphology and metabolites (Tajsoleiman et al., 2019).

The Need For Microbioreactor Systems

The development of a biotechnological production process can be simply described as a sequential workflow, starting from screening and selection of microbial strain which is further investigated under lab-scale bioreactor conditions, in which high level of process control can be enabled. Finally, the developed bioprocess is transferred to pilot and industrial scale. The need for increased experimental throughput under well controlled conditions gave rise to the development of microbioreactor systems (Hemmerich et al., 2018).

The main motives to scale down bioreactors to obtain microbioreactors thus can be listed as:

1) Increasing timeline pressures for research and development of bioprocesses which leads to rapidly screen and optimize cell culture process parameters

2) Decrease use of consumables by avoiding resource intensive approaches such as the use of shake flasks and bench-top bioreactors

3) Limited physical space for experimentation.

4) The need to conduct large numbers of experiments (i.e. screening and optimizing studies).

Those motives in turn have resulted in the scale down of bioreactors to obtain miniaturized versions that mimic regular sized microbioreactors to efficiently reduce bioprocess development time and costs (Tajsoleiman et al., 2019).

Ultimately, the aim of microbioreactors is to replace shake flasks and lab-scale bioreactor systems for early and mid-stages of biotechnological bioprocess development (Hemmerich et al., 2018).

Similarly, micro photobioreactors represent a potential platform technology for the high-throughput, phototrophic cultivation of photosynthetic microorganisms (Ojo et al., 2015).

It is also important to underline that working at such small scales allows using microorganisms from the same batch, at the same passage, thus increasing homogeneity and consistency in the results by reducing the intrinsic sample-to-sample variability which is a major drawback of biological systems (Perin et al., 2016).

Ultimately, micro photobioreactors, or microbioreactors in general must satisfy two essential requirements to be actually useful:

1) Reproducible culture performance across individual microbioreactors under identical operating conditions to prove that parallel work is possible.

2) Ability to mimic culture conditions in larger scale photobioreactor designs to address scale-translation, that is, cross-system transferability of obtained data among micro photobioreactors and larger photobioreactors.

Challenges and Limitations of Miniaturization Process

Unlike chemical reactors in which chemical reactions take place, bioreactors contain living cells. Living things are more sensitive, fragile and unstable than chemicals. Therefore, in order to achieve the desired biological activity and to prevent unwanted biological activities, the process conditions should be controlled in a better and narrower range than the chemical reactors.

The deviation in conditions results in more serious consequences than chemical reactors; deactivation of biomass may not be reversed.

Overall, designing a bioreactor is a complex engineering task, and requires attention to several aspects irrespective of the specific reactor configuration demanded by a given application (Chisti, 2006):

1) The need to maintain monoseptic operation,

2) Mixing to ensure suspension of the biocatalyst and attain a relatively homogenous envireonment in the bioreactor,

3) Suppy of oxygen and removal of carbon dioxide,

4) Supply of various other nutrients in such a way that the rate of supply does not limit the performance of the biocatalyst,

5) Heat transfer for temperature control,

6) Control of the shear stress levels in the bioreactor so that the biocatalyst is not damaged by various hydrodynamic forces.

Unfortunately, there are further limitations to the design parameters that need to be addressed in case of photobioreactors (Uyar, 2016):

1) The photobioreactor should be made of a highly transparent material to allow light inside (i.e. common bioreactor construction materials such as stainless steel cannot be used). Additionally, materials which promote cellular adhesion should be avoided to prevent biofilm formation on light receiving surfaces. Materials that can satisfy these requirements such as glass, polymethyl methacrylate, polycarbonate and low-density polyethylene have poor strength which causes the photobioreactor to be fragile, decreases its durability, and limits the maximum photobioreactor size.

2) The photosynthetic microorganisms employed create a self-shading effect, which limits the light penetration into the depths of the photobioreactor. Consequently, maximum photobioreactor depth becomes limited and large areas are required for the photobioreactors.

3) Solar illumination should be preferred since artificial illumination increases cost dramatically due to the electric consumption. Therefore, harsh outdoor conditions (i.e. wind, rain, temperature and pressure fluctuations) should be taken into account when designing photobioreactors to prevent premature failures.

4) Due to the limited depth of the bioreactor and the nature of the construction material, mixing options are limited. Mechanical agitation cannot usually be used; possible mixing methods are either recycling the medium or air bubbling through culture medium.

Finally, challenges introduced in the scale down of these systems to micro scale include:

1) Accurate measurement and control of basic process parameters (pH, temperature and dissolved oxygen)

2) Mimicking the fluid dynamics (mass transfer and mixing time) of the larger volume bioreactors (Applikon, 2015).

3) Increased impact of wall growth due to the larger surface to volume ratio at small scale (Tajsoleiman et al., 2019).

4) Taking samples is also increasingly challenging when reducing the scale of the experiments. In miniaturized reactors, fewer samples can be taken, with less volume per sample, compared with larger reactors (Rowland-Jones et al., 2017). The lower the sampling volume, the higher the probability that sampling errors (e.g., variation of the sample volume) might influence the result, and therefore the use of automatic sampling systems becomes increasingly

relevant when decreasing reactor volume (Tajsoleiman et al., 2019). Low volume also prohibits continuous sampling, which is another drawback of these systems (Benner et al., 2022).

5) Evaporation. When applying aeration to a bioreactor, there is a significant rate of evaporation from liquid systems. This is especially relevant for fermentation processes that are typically operated above environmental air temperatures and run for days or weeks. This leads to considerable loss of water in the off-gas, and this affects the volume dynamics (Tajsoleiman et al., 2019). Even though that is a common operational problem in all aerated bioreactors, larger bioreactors can be equipped with a condenser to recycle water vapor to minimize water evaporation. The condenser is a simple heat exchanger through which cool water passes and allows water vapor in the exit air stream of bioreactor to condense on the inner condenser surface. Unfortunately, condensers are not practical to use in microbioreactors. On the other hand, evaporation is more prominent in case of micro photobioreactors, due to additional heat input by illumination, and more importantly, longer duration of the bioprocess, and therefore should be given serious consideration (Morschett et al., 2017, Ojo et al., 2015). Photosynthetic microorganisms growth modes are photoautotrophy, photoheterotrophy, or a mixture of those (mixotrophy). All those modes result in lower growth rates than that in pure fermentative mode, which means longer bioprocess durations. Evaporation which may not be significant for short fermentations in bioreactors thus becomes considerable in photobioreactors. Evaporation results in liquid volume decrease, which may affect sensor readings, mixing and hydrodynamics, light distribution and cause osmotic stress on the microorganisms due to increasing culture osmolarity. On the other hand, evaporation also results in the increase of concentrations of the culture medium components which may cause inhibition / toxicity on the cells. Due to these consequences, evaporation rate should be monitored and controlled in micro photobioreactors. There are several effective methods suggested to decrease / eliminate evaporation in micro photobioreactors. Those are lowering aeration rate to the required minimum, using humidified air for aeration, or using semipermeable membranes at air exits to trap water vapor inside. Finally, adding distilled water to compensate lost liquid can also be considered (Silk et al., 2010). One or a combination of those methods can be employed to control evaporation effectively. Morschett et al (2017) managed to decrease evaporation rate in micro photobioreactors down to 0.56% per day, which can be regarded as non-interfering and liquid loss can be neglected, enabling long term phototrophic cultivation in micro photobioreactors (Morschett et al., 2017). Similarly, Ojo et al (2015), reported that under typical culture conditions only 8–10% of liquid in the micro photobioreactor was lost over 3.5 days of cultivation and claimed that this level of evaporation is considered to have minimal impact on the growth of microalgae (Ojo et al., 2015). Finally, Toulope (2019) reported that when humidified air was used for aeration instead of dry air, there was noticeable 72% reduction in the evaporation rate at similar conditions. He also reported a minimum of 3.2% loss of culture medium per day due to evaporation (Tolulope Victor, 2019).

6) Illumination. The main difference between microbioreactors and micro photobioreactors is the illumination of the latter and placement of lamps is a key design factor. Commercial microbiorectors are usually stacked on a plate in a form of cassette, which allows high density stacking of those microbioreactors and the overall equipment can be very compact to use on a bench or desk. Top of microbioreactors are usually crowded with measurement and control equipment such as pH, temperature sensors, air inlets outlets, mixing shaft, sampling ports etc. Therefore illumination of micro photobioreactors from the top is not practically possible. Side illumination is preferred in available commercial units, however this configuration limits stacking of micro photobioreactors, as all the micro photobioreactors need to receive ample light, resulting in lower bioreactor density in the overall system. This bottleneck persists and needs more attention. Illumination from below may be the most suitable

solution here, considering that the micro photobioreactors are not heavy and have limited height (Morschett et al., 2017).

Micro Photobioreactor Systems

According to the web of science database, the first publication to use the term microbioreactor date back to 1992. The interest grew exponentially until around 2010, and then stabilized at an average of 40 publications per year from then onwards. This is a reflection of the enormous progress made in the field of microbioreactor systems recently. As a result, a variety of different microbioreactor systems covering a broad technological range and a wide field of application became available commercially (Hemmerich et al., 2018). Their superior experimental throughput initiated a rapid spread and they are nowadays routinely applied in upstream process development and were proven to be valuable tools (Morschett et al., 2018). Another survey of about 500 publications revealed that, of the various cultivation techniques; 19% used a volume below 100 ml, 5% a volume below 10 ml and 3% below 1 ml. Among the small-scale devices are shake-flasks, test-tubes, microtiter plates, miniaturized bioreactors and specific devices for animal cells such as spinner-flasks, roller bottles, T-flasks etc (Kumar, Wittmann & Heinzle, 2004). It should also be noted that all necessary specifications and desired properties have not yet been realized and great efforts in fundamental and applied research are still ongoing.

The first article to use the term micro photobioreactor was published in 2015, and since then, only a handful followed, which indicates novelty and potential of the field. Commercial availability of micro photobioreactors still lacking although recently several prototype systems have been developed mainly relying on microfluidic chips or microtiter plates (Morschett et al., 2018).

Notable studies were summarized below:

Morschett et al (2016, 2017) employed micro photobioreactors in microalgae cultivation to overcome the laborious and slow early-stage parameter optimization which they saw as a major drawback. A micro photobioreactor system supported by a liquid-handling robot for automated medium preparation and product quantification was used to enable highly efficient execution of screening applications. The resulting platform was used for medium optimization of a lipid production process using microalgae toward maximum volumetric productivity. Within only four experimental rounds, lipid production was increased approximately threefold. They concluded that the integration of parallelized microscale cultivation supported by laboratory automation proved to be a fruitful tool for the accelerated development of phototrophic bioprocesses in a very timely and material efficient manner. Micro photobioreactor system used had 48 independent wells of 1 mL volume each. They were sealed with an gas-permeable seal for evaporation reduction. Micro photobioreactors were placed in a closed incubation chamber for indirect temperature control. The system relied on bottomside illumination with a set LEDs. Mixing was provided by continuous shaking. Cultivation processes can be monitored quasionline applying non-invasive optical measurements during continuous shaking. Regarding growth homogeneity, strict control of the process conditions enabled a high comparability between the distinct micro photobioreactors (5.2% fluctuation in biomass formation) (Morschett et al., 2017, Morschett et al., 2017). Micro photobioreactor cultivation showed a very good comparability to the laboratory-scale photobioreactors (80-1000 mL flask/tubular/panel photobioreactors) especially during the exponential growth phase, while the small scale helped prolonging this phase due to superior light supply and mixing characteristics. Overall, photo microbioreactors may be regarded as a proper replacement for phototrophic cultivation in shake flasks or test tubes (Morschett et al., 2017).

In another study, Ojo et al (2015) described the development and characterisation of a novel orbitally shaken micro photobioreactor system consisting of 24 parallel wells, suitable for the batch cultivation of microalgae. Obtained results demonstrated the application of the micro photobioreactor for rapid optimisation of phototrophic culture conditions and establishment of high cell density cultures. Each micro photobioreactor unit had a working volume of 4 mL and was illuminated by a cool white LED from the side. Mixing was achieved using an incubator shaker equipped with temperature, humidity and CO_2 sensors coupled to a control unit. The micro photobioreactor platform allowed 20-fold reduction in material requirements compared to current shake flask systems. The authors claimed that generally, evaluation of biomass concentration at the tested conditions showed good reproducibility across the 24-micro photobioreactors and in essence, use of the micro photobioreactor for parallel microalgae cultivation showed consistent and reproducible results. However, the ability to mimic culture conditions in larger scale photobioreactor designs has yet to be shown (Ojo et al., 2015).

More recently, Busnel et al (2021) developed a miniaturized, small-scale photobioreactor to characterize microalgal growth under controlled conditions. The system consisted of 6 mini flat photobioreactors operated independently in parallel, with a volume of 75 mL each, thus cannot exactly be classified as micro photobioreactor as defined here but more of a transition between lab scale photobioreactors and micro photobioreactors. The system permitted screening of (i) microalgae species performance; (ii) medium composition; (iii) growth temperature; (iv) illumination conditions (continuous or day/night cycles) in reliable conditions. Under the same operating conditions, the difference between biomass productivity and the pigment contents of microalgae in different micro photobioreactor units did not exceed 5%; confirming the reliability of the micro photobioreactor system by conducting parallel experiments in each photobioreactor cell. Moreover, continuous cultures of microalgae were run in both this system and 1 L Airlift flat-panel photobioreactor under the same culture conditions to confirm reliability in the determination of areal biomass productivity. Similar results were obtained in the two photobioreactors with a variance of less than 5% (Busnel et al., 2021).

Perin et al (2016) constructed a micro photobioreactor system of very small scale (75 × 50 mm), composed of 45 wells (40 µl of working volume each) linked in columns by a network of microfluidic channels to grown microalgae cells. The wells were covered with a thin (~1.5 mm) PDMS layer to turn them into real independent growth chambers. The design of the micro photobioreactor followed specific criteria such as: (i) support of cultures of microalgae in a no-shear environment, (ii) high-throughput studies with biologically relevant numbers of replicates, (iii) compatibility with on-line imaging, (iv) ease of retrieval of the cell samples for eventual post-processing analyses, and (v) capability to generate stable concentration gradients over the culture area in case fluid flow is applied. When compared to traditional methodologies (i.e. flask culture), the data generation capability of this platform is dramatically increased which demonstrate its suitability for high-throughput studies. Algae consistently show faster growth rates, thus cutting the duration of the experiments of about 30 %. In addition, the capability of simultaneously testing multiple variables (i.e. cell density and light intensity), on 9 levels and with 5 replicas each was possible. The authors stated that reproducing the same experimental campaign using standard techniques would dramatically lengthen the timespan, increase the risk of operator-related errors, increase nutrients and chemicals usage by several orders of magnitude (Perin et al., 2016).

Tolulope (2019) claimed that the shaken well-type micro photobioreactors might not be truly representative of the large scale pneumatic photobioreactors due to the different engineering environment thus making scale-up difficult. Thus, he performed the design,

fabrication and engineering evaluation of a miniature pneumatic photobioreactors which mimics conventional large scale pneumatic photobioreactors such as airlift and bubble column devices, for heterotrophic and phototrophic microalgae cultivation. The prototype 6-well micro photobioreactor consisted of four bubble columns and two airlift columns, with 15 mL working volume for each. Comparison of the different configurations showed that the bubble column micro photobioreactor had the highest mass transfer coefficient and the best performance in microalgae culture frowth compared to air lift micro photobioreactor. Overall, the micro photobioreactor was established as a tool for phototrophic, heterotrophic, and mixotrophic culture of microalgae for rapid and early stage evaluation at small scale (Tolulope Victor, 2019).

Concluding Remarks and Future Scope

In recent years, micro photobioreactors have evolved as promising tools to accelerate phototrophic bioprocess development and the acquisition of physiological data of microorganisms. They are especially useful for tasks such as microbial strain or media screening. However, significant technological advances are still needed and no commercial systems are available as of yet.

Micro photobioreactors allow production of large experimental datasets easily in comparably short times compared to traditional bench scale systems, shifting the bottleneck of bioprocess development to the processing of relevant information.

The up/down scaling of photobioreactors has additional light-based challenges such as light availability, self-shading, photoinhibition, and light-emitted heat in addition to the ones that exist for conventional bioreactors.

Ideally, the micro photobioreactor should be able to exactly simulate the cultivation conditions of the projected industrial-scale photobioreactor. Thus, the design depends on the geometry of the larger scale photobioreactor to help minimize deviations between scales. Shake flasks, micro channels, microtiter plates, miniaturized bubble columns, and small-scale stirred tanks belong to the established examples to micro photobioreactors.

Mathematical modeling and computer simulation can be used as practical tools for the analysis and design of mPBRs at different scales. They can complement experimental information where quantitative measurements are challenging.

The current trend is towards automation of these systems and integration of more relevant hardware for process monitoring and control. These developments will reinforce the use of micro phorobioreactor systems for bioprocess development.

REFERENCES

Applikon. Generating scalable results in micro-bioreactors. 2015; Available from: https://www.biopharma-reporter.com/Library/Generating-scalable-results-in-micro-bioreactors.

Benner P, Meier L, Pfeffer A, Krüger K, Oropeza Vargas JE, Weuster-Botz D. (2022) Lab-scale photobioreactor systems: principles, applications, and scalability. *Bioprocess and Biosystems Engineering*,*45*(5),791-813.

Busnel A, Samhat K, Gérard E, Kazbar A, Marec H, Dechandol E, Le Gouic B, et al. (2021) Development and validation of a screening system for characterizing and modeling biomass production from cyanobacteria and microalgae: Application to Arthrospira platensis and Haematococcus pluvialis. *Algal Research*,*58*,102386.

Chisti Y. (2006) Bioreactor design. In: Kristiansen B, Ratledge C, editors. Basic Biotechnology. 3 ed. Cambridge: Cambridge University Press. p. 181-200.

Delouvroy F, Siriez G, Tran A-V, Mukankurayija L, Kochanowski N, Malphettes L. (2015) ambr™ Mini-bioreactor as a high-throughput tool for culture process development to accelerate transfer to stainless steel manufacturing scale: comparability study from process performance to product quality attributes. *BMC Proceedings*,*9*(9),P78.

Harada Y, Sakata K, Sato S, Takayama S. (1996) 1 - Fermentation Pilot Plant. In: Vogel HC, Todaro CL, editors. Fermentation and Biochemical Engineering Handbook (Second Edition). Westwood, NJ: William Andrew Publishing. p. 1-66.

Hemmerich J, Noack S, Wiechert W, Oldiges M. (2018) Microbioreactor Systems for Accelerated Bioprocess Development. *Biotechnology Journal*,*13*(4),1700141.

Kumar S, Wittmann C, Heinzle E. (2004) Review: Minibioreactors. *Biotechnology Letters*,*26*(1),1-10.

McDuffie NG. (1991) Chapter 7 - Cell Culture Bioreactors. In: McDuffie NG, editor. Bioreactor Design Fundamentals: Butterworth-Heinemann. p. 93-119.

Morschett H, Freier L, Rohde J, Wiechert W, von Lieres E, Oldiges M. (2017) A framework for accelerated phototrophic bioprocess development: integration of parallelized microscale cultivation, laboratory automation and Kriging-assisted experimental design. *Biotechnology for Biofuels*,*10*(1),26.

Morschett H, Loomba V, Huber G, Wiechert W, von Lieres E, Oldiges M. (2018) Laboratory-scale photobiotechnology—current trends and future perspectives. *FEMS Microbiology Letters*,*365*(1),fnx238.

Morschett H, Schiprowski D, Müller C, Mertens K, Felden P, Meyer J, Wiechert W, et al. (2017) Design and validation of a parallelized micro-photobioreactor enabling phototrophic bioprocess development at elevated throughput. *Biotechnology and Bioengineering*,*114*(1),122-31.

Morschett H, Schiprowski D, Rohde J, Wiechert W, Oldiges M. (2017) Comparative evaluation of phototrophic microtiter plate cultivation against laboratory-scale photobioreactors. *Bioprocess and Biosystems Engineering*,*40*(5),663-73.

Noorman H. (2011) An industrial perspective on bioreactor scale-down: What we can learn from combined large-scale bioprocess and model fluid studies. *Biotechnology Journal*,*6*(8),934-43.

Ojo EO, Auta H, Baganz F, Lye GJ. (2015) Design and parallelisation of a miniature photobioreactor platform for microalgal culture evaluation and optimisation. *Biochemical Engineering Journal*,*103*,93-102.

Perin G, Cimetta E, Monetti F, Morosinotto T, Bezzo F. (2016) Novel micro-photobioreactor design and monitoring method for assessing microalgae response to light intensity. *Algal Research*,*19*,69-76.

Rowland-Jones RC, van den Berg F, Racher AJ, Martin EB, Jaques C. (2017) Comparison of spectroscopy technologies for improved monitoring of cell culture processes in miniature bioreactors. *Biotechnology Progress*,*33*(2),337-46.

Silk NJ, Denby S, Lewis G, Kuiper M, Hatton D, Field R, Baganz F, et al. (2010) Fed-batch operation of an industrial cell culture process in shaken microwells. *Biotechnology Letters*,*32*(1),73-8.

Tajsoleiman T, Mears L, Krühne U, Gernaey KV, Cornelissen S. (2019) An Industrial Perspective on Scale-Down Challenges Using Miniaturized Bioreactors. *Trends in Biotechnology*,*37*(7),697-706.

Tolulope Victor A. Design and Characterization of a Miniature Photobioreactor for Microalgae Culture [Ms.C]: University College London; 2019.

Tredici MR. (2004) Mass production of microalgae: Photobioreactors. In: Richmond A, editor. Handbook of Microalgal Culture, Biotechnology and Applied Phycology. London: Blackwell Scientific. p. 178-214.

Uyar B. (2016) Bioreactor design for photofermentative hydrogen production. *Bioprocess and Biosystems Engineering*,*39*(9),1331-40.

van't Riet K, Tramper J. (1991) Basic Bioreactor Design: CRC Press.

Quantum Chemical, Molecular Docking, and Hirshfeld Surface Analysis Studies of 8-Bromo-9-hydroxy-7,7-dimethyl-11-methylenespiro[5.5]undec-1-en-3-one Molecule Isolated from Algae

Cem Cüneyt ERSANLI[1]

Introduction

The term algae, derived from the Latin word for seaweed, refers to living organisms that can be found in fresh, salty, and even bitter waters, as well as on animals or plants, in moist and illuminated caves, and even on snow. Algae are found in various regions around the world. They are categorized into five primary groups according to their colors: brown algae, diatoms, blue-green algae, green algae, and red algae. There are studies in the literature related to the algae flora in aquatic environments (Gönülol, Tezel Ersanli & Baytut, 2009; Tezel Ersanli & Hasirci Mustak, 2013; Tezel Ersanli & Gönülol, 2014; Hasirci Mustak & Tezel Ersanli, 2015; Tezel Ersanlı & Hasırcı Mustak, 2017; Tezel Ersanlı & Öztürk, 2017; Baytut, Gümüş & Ersanlı, 2018; Gümüş, Gümüş & Tezel Ersanlı, 2023). In recent years, algae have been used as promising biosorbent materials in research related to biosorption and bioremediation (Deniz & Tezel Ersanli, 2016a, 2018b, 2018c) for their potential use as a source of nutrition (Serrano et al., 1998). Furthermore, studies in the literature have explored the potential of natural macroalgae consortia as biyosorbents (Deniz & Tezel Ersanli, 2016b, 2018a, 2020a, 2020b, 2020c, 2021, 2022, 2023). *Laurencia dendroidea* J. Agardh (synonym, *Laurencia scoparia* J. Agardh) is a marine species and is belonging to Florideophyceae, Rhodophyta. Taylor (1960) presented their distribution in Atlantic Islands, N. America, Central America, Caribbean Islands and S. America. John et al. (2004) also recorded it in Africa, Senegal (Taylor, 1960; John et al., 2004; Guiry & Guiry, 2012). *Laurencia dendroidea* is a red algae species belonging to the Rhodomelaceae family. Red algae predominantly comprise seaweed species, but also include genera of free-living unicellular microalgae. They are predominantly found in marine ecosystems but can also thrive in freshwater and terrestrial environments. Unique characteristics of these algae encompass the lack of flagellate stages, the absence of centrioles, and the presence of accessory phycobiliproteins arranged in phycobilisomes. Chlorophyll a is the special type of chlorophyll found in these algae. The primary storage compound is floridean starch, an α-1,4-glucan polysaccharide, stored in the cytoplasm. Unlike Chlorophyta, where starch grains are located within chloroplasts, in red algae, starch grains are exclusively found in the cytoplasm. Most rhodophytes primarily undergo photoautotrophy. The class Florideophyceae encompasses all multicellular genera, both in marine and freshwater habitats. The cell wall in Florideophyceae is composed of over 70% water-soluble sulfated galactans such as agars and carrageenans. These substances hold significant commercial value in the food and pharmaceutical sectors owing to their capacity to create gels (Barsanti & Gualtieri P., 2006).

In this study, the structure of a chamigrene-type metabolite (spiro[5.5]undecane derivative) isolated from *Laurencia scoparia* has been identified. A non-sesquiterpene named mailione, $C_{14}H_{19}BrO_2$, was detected previously in *Laurencia cartilaginea* (Suescon et al., 2001). Quantum chemical calculations provide useful information on the electronic, spectroscopic and

[1] Prof.Dr., Sinop Üniversitesi

optical properties of molecular systems, including structural properties such as bond lengths, bond angles and torsion angles, primarily to supplement experimental data. They offer insights into chemical processes that are difficult, time-consuming, and/or expensive to determine experimentally. In fact, some studies indicate that theoretical methods can yield more precise data than experimental methods. Theoretical calculation data always serve as guiding, supporting, and illuminating information for experimental data. Therefore, in order to support the experimental data of the BHDMU (Suescon et al., 2001) available in the literature, the BHDMU was optimized using the Density Functional Theory (DFT) method and the 6-311G(d,p) basis set with the Gaussian 03W program (Frisch et al., 2004). The BHDMU's three-dimensional structure was visualized using the GaussView 4.1.2 program (Dennington, Keith & Millam, 2007) to validate experimental data. The optimized structure was then compared with X-ray diffraction results, analyzing geometric properties such as bond lengths, bond angles, and torsion angles. Furthermore, a comparative study was conducted by overlaying the BHDMU's X-ray and optimized geometries. Electronic properties such as ionization potential (I), chemical hardness-softness, electronegativity (χ), electron affinity (A), electrophilic and nucleophilic indices, HOMO (highest occupied molecular orbital) and LUMO (lowest unoccupied molecular orbital) energies and the energy gap (ΔE) between these orbitals were studied. Additionally, total energy, dipole moment, Mulliken atomic charge values, and thermodynamic properties were calculated in the gas-phase and five varied solvents (benzene, dichloromethane, acetone, dimethyl sulfoxide, water). Molecular electrostatic potential (MEP) maps were generated to identify electrophilic and nucleophilic regions in the structure. Finally, molecular docking and Hirshfeld surface analysis were performed for the investigated BHDMU.

Results and Discussion

Crystal Structure

The elucidation of the crystal structure of the spiro[5.5]undecane derivative, 8-bromo-9-hydroxy-7,7-dimethyl-11-methylenespiro[5.5]undec-1-en-3-one molecule (BHDMU), separated from the red algae *Laurencia scoparia*, was carried out by Suescon and colleagues using X-ray diffraction (Suescon et al., 2001). The chemical diagram, experimental, and crystal structures of the BHDMU are illustrated in Figure 1.

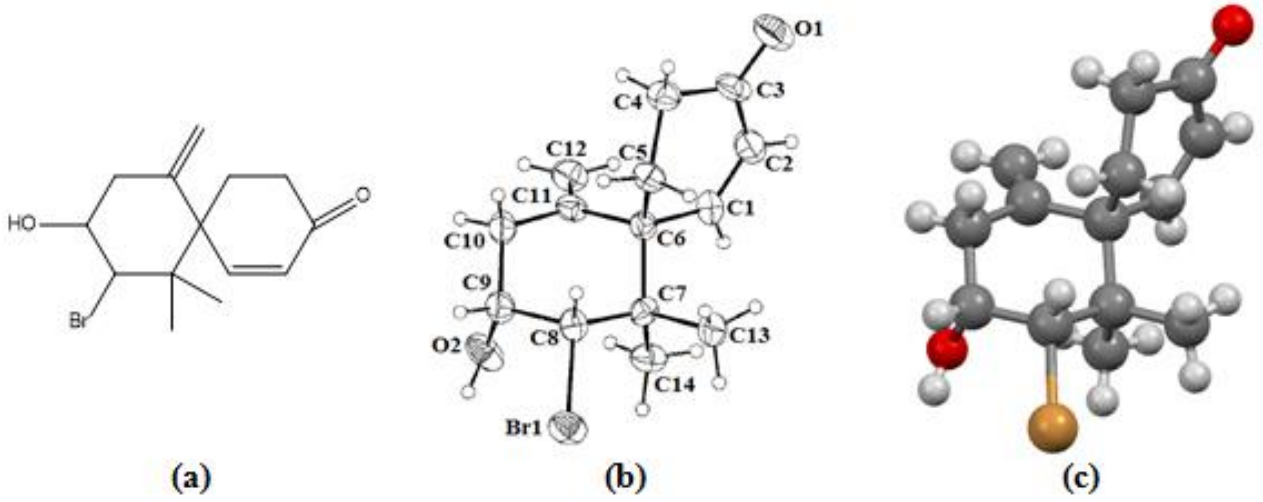

Figure 1. a) Chemical Diagram, b) Experimental (X-Ray) Structure, c) Crystal Structure

The experimental X-ray single crystal structure of the studied BHDMU is available at the Cambridge Crystallographic Data Center under the code CCDC 162566. It has a closed formula

of $C_{14}H_{19}BrO_2$, a molecular formula weight of 299.20 g/mol, and an orthorhombic unit cell in the $P2_12_12_1$ crystal structure. The presence of intermolecular O2-H2O…O1 interactions was observed (Suescon et al., 2001).

Geometric Optimization

The BHDMU, acquired from the Cambridge Crystallographic Data Centre with the code CCDC 162566, was subjected to theoretical computations in the gas-phase at its ground state. The B3LYP method (Becke, 1993; Lee, Yang & Parr, 1988) and DFT using the 6-311G(d,p) basis set (Foresman & Frisch, 1996) implemented through the Gaussian 03W software package. The optimized geometry of the BHDMU was visualized using GaussView 4.1.2 (see Figure 2).

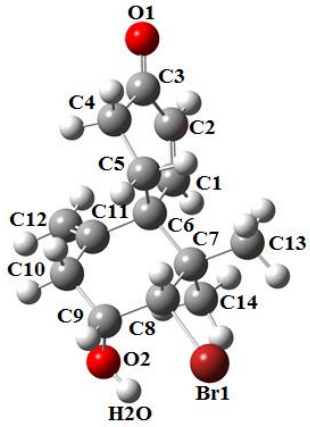

Figure 2. Optimized Geometry of the BHDMU

Through geometrical optimization, the spatial configurations of atoms and molecular structure were elucidated and theoretical calculations were used to determine bond lengths, bond angles, and torsion angles. These calculated parameters, along with specific experimental values, are detailed in Table 1.

Table 1. Selected Variables

	Experimental	**Theoretical**
Bond Length (Å)		
Br1-C8	1.975 (7)	1.9878
O1-C3	1.231 (7)	1.22540
O2-C9	1.409 (8)	1.41763
C9-C10	1.522 (9)	1.53433
C10-C11	1.495 (9)	1.50148
Bond Angle **(º)**		
O1-C3-C2	122.1 (8)	121.894
O1-C3-C4	121.9 (8)	122.771
C1-C6-C11	111.0 (5)	110.652
C11-C6-C5	109.9 (5)	108.663
C11-C6-C7	108.1 (5)	108.310
C9-C8-Br1	107.8 (4)	107.098
C7-C8-Br1	112.5 (4)	112.788
O2-C9-C10	107.8 (5)	107.160
O2-C9-C8	114.0 (6)	113.920
Torsion Angle **(º)**		
O1-C3-C4-C5	-146.7 (6)	-148.177
C1-C2-C3-O1	176.3 (6)	179.586
C1-C6-C7-C14	-54.4 (7)	-54.786
C14-C7-C8-Br1	63.7 (6)	61.923

C13-C7-C8-Br1	-56.5 (6)	-57.834
C6-C7-C8-Br1	-175.3 (4)	-177.270
C7-C8-C9-O2	65.6 (7)	66.855
Br1-C8-C9-O2	-62.2 (6)	-60.785
Br1-C8-C9-C10	177.7 (5)	178.143
O2-C9-C10-C11	-75.4 (8)	-77.001

Another method for comprehensive comparison involved overlaying the molecular skeleton obtained from theoretical calculations onto the X-ray diffraction structure, resulting in a root mean square error (RMSE) of 0.046 Å for the theoretical calculation (Figure 3). This discovery shows that the DFT/B3LYP/6-311G(d,p) calculation faithfully reproduces the geometry of BHDMU in question. It is very important to emphasize that the experimental results were obtained in the solid phase, while the theoretical calculations were performed in the gas-phase. The RMSE value can be attributed to the lack of intermolecular coulombic interactions with neighboring molecules in the gas phase, a factor present in the crystal lattice observed in the experimental results.

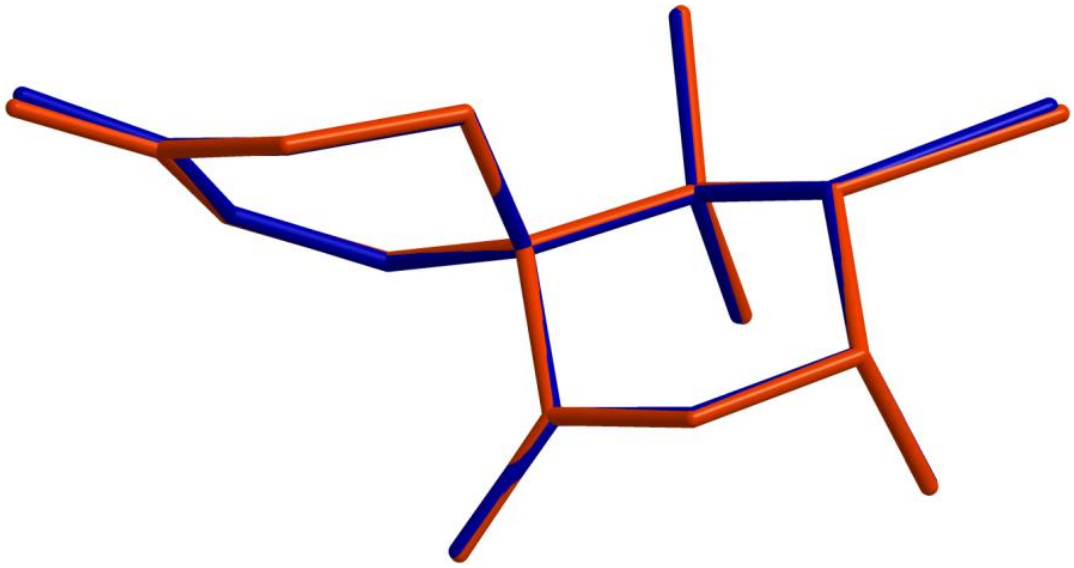

Figure 3. Atom-Atom Alignment: Calculated Structure (Shown in Red) Superimposed on X-Ray Structure (Shown in Blue). Hydrogen Atoms Excluded for Clarity

The molecular structure of the BHDMU exhibits C_1 point group symmetry. It comprises 36 atoms and is anticipated to have 77 normal modes of vibrations within the same a species under C_1 symmetry.

HOMO-LUMO Energies and Electronic Properties

Frontier Molecular Orbitals (FMOs), namely HOMO-LUMO kinetic stability, elucidate electron transitions as well as electrical and optical properties. Analyzing the electron density distribution of a structure provides valuable insights into ionization potential, electron affinity, chemical hardness/softness parameters, electrostatic potential, and the shapes of molecular orbitals. The molecular orbitals are referred to as HOMO-LUMO. Here, HOMO represents the molecule's tendency to donate electrons and is the highest energy occupied orbital. LUMO, on the other hand, signifies the molecule's tendency to accept electrons and is the lowest unoccupied orbital. In this study, Gaussian 03W program was used to calculate the E_{HOMO} and E_{LUMO} energy values for BHDMU using the same method and basis set. By examining the electron density distribution based on the calculated E_{HOMO} and E_{LUMO} energies, ΔE, I, A, χ, η, μ, S, and w parameters were calculated in both gas-phase and five varied solvents, as presented in Table 2. The formulas for these parameters are as follows: $\chi=(I+A)/2$, $\mu=-(I+A)/2$, $\eta=(I-A)/2$,

S=1/2η, w= μ^2/2η, (where: I and A represent ionization potential, electron affinity, respectively); I=-E_{HOMO}, A=-E_{LUMO}, respectively (Koopmans, 1933; Perdew et al., 1982; Parr & Pearson, 1983; Senet, 1997; Geerlings, Proft & Langenaeker, 2003; Schüürmann, 2004). Upon investigating the BHDMU in the gas-phase and five varied solvents, the dielectric constant value correlated with an increase in the negativity of E_{total}, E_{HOMO}, and chemical potential values, as well as an expansion of the ΔE, chemical hardness, electrophilicity index, electronegativity, and dipole moment parameters, while E_{LUMO} and chemical softness parameters exhibited a decrease.

Table 2. Theoretically Calculated Electronic Structure Variables

B3LYP/6-311G(d,p)			
	In gas-phase (ε =1)	In solution-phase	
		Benzene (ε =	Dichloromethane (ε = 8.93)
E_{total} (Hartree)	-3269.66849377	-3269.6732607	-3269.67770589
E_{HOMO} (eV)	-7.0992	-7.2555	-7.3781
E_{LUMO} (eV)	0.5853	0.5108	0.4392
$\Delta E_{HOMO-LUMO}$	7.6845	7.7658	7.8173
Chemical hardness (η)	3.8422	3.8829	3.9086
Chemical potential (μ)	-3.2569	-3.3721	-3.4695
Electronegativity (χ)	3.2559	3.3721	3.4695
Chemical softness (S)	0.1301	0.1288	0.1279
Electrophilicity index (w)	1.3804	1.4643	1.5398
Dipole moment (Debye)	2.2978	2.5824	2.8345
	In solution-phase		
	Acetone (ε = 20.49)	DMSO (ε = 46.7)	Water (ε = 78.39)
E_{total} (Hartree)	-3269.67882090	-3269.67934272	-3269.67951133
E_{HOMO} (eV)	-7.4015	-7.5060	-7.5849
E_{LUMO} (eV)	0.4218	0.4120	0.4117
$\Delta E_{HOMO-LUMO}$	7.8233	7.9180	7.9966
Chemical hardness (η)	3.9116	3.9590	3.9983
Chemical potential (μ)	-3.4899	-3.5470	-3.5866
Electronegativity (χ)	3.4899	3.5470	3.5866
Chemical softness (S)	0.1278	0.1263	0.1251
Electrophilicity index (w)	1.5568	1.5889	1.6086
Dipole moment (Debye)	2.8970	2.9264	2.9359

When the energy gap (ΔE) of a BHDMU is large, the electron distribution undergoes minimal changes, resulting in low polarization. A small ΔE indicates significant changes in the electron distribution and high polarization. In Table 2, if the ΔE is greater than 1.5 eV, it signifies that the BHDMU is thermodynamically stable and robust. Furthermore, the BHDMU does not undergo self-reactions, dimerization, or polymerization. The ΔE in the gas-phase is 7.6845 eV. This substantial energy range indicates the molecule's stable structure. The HOMO and LUMO distributions obtained theoretically with the B3LYP method are depicted in Figure 4.

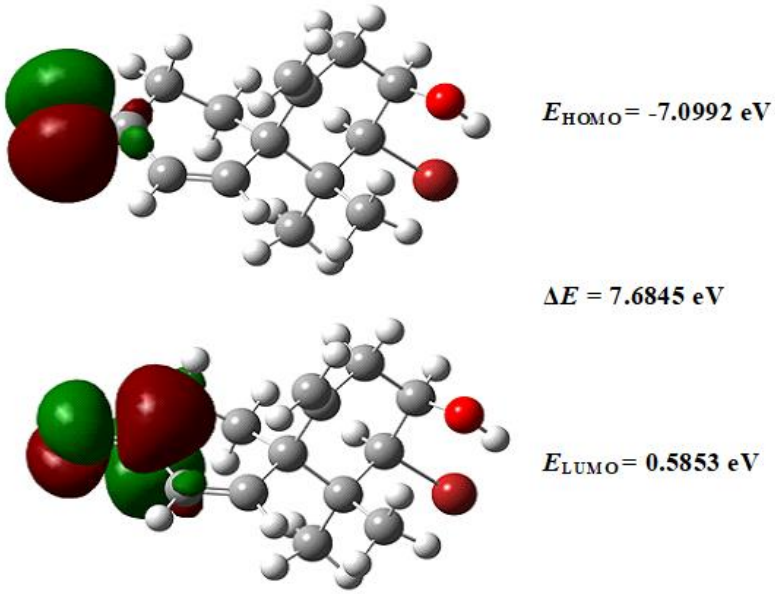

Figure 4. HOMO and LUMO Distributions

Mulliken Charge Distribution

The Mulliken charge distribution method is widely used due to its ability to provide extensive information about the molecule's polarity, electronic structure, dipole moments of atomic structures, charge distribution on atoms, donor and acceptor pairs facilitating electron transfer in the molecule, and various properties of molecular structures (Mulliken, 1955). This method is based on obtaining molecular orbitals through linear combinations of atomic orbitals. However, this distribution does not precisely reflect the electronegativity of each element (Reed & Weinhold, 1985; Reed, Curtiss & Weinhold, 1988). In some extreme cases, it can assign negative electron population to an orbital or calculate more than two electrons in a single orbital. Consequently, Mulliken charges are used not only for quantitatively predicting experimental results but also for making qualitative predictions. To calculate the atomic charges of the BHDMU, Mulliken density analysis was performed using the same method (Table 3). According to these results, negative charges are mainly concentrated on oxygen (O) and carbon (C) atoms, which have the highest electronegativity in the studied BHDMU.

Table 3. Atomic Charges of BHDMU in Gas-Phase and Various Solvent Media (e)

Atom	In gas-phase (ε = 1)	In solution-phase B3LYP/6-311G(d,p)				
		Benzene (ε=2.27)	Dichloromethane (ε = 8.93)	Acetone (ε = 20.49)	DMSO (ε = 46.7)	Water (ε = 78.39)
Br1	-0.094522	-0.111683	-0.122704	-0.125441	-0.126717	-0.127128
O1	**-0.303344**	**-0.332207**	**-0.354866**	**-0.360231**	**-0.362693**	**-0.363482**
O2	**-0.383193**	**-0.389412**	**-0.400021**	**-0.402852**	**-0.404203**	**-0.404643**
C1	-0.035841	-0.031194	-0.026813	-0.025683	-0.025150	-0.024977
C2	-0.101486	-0.107345	-0.112273	-0.113522	-0.114107	-0.114296
C3	0.206631	0.211832	0.217079	0.218392	0.219004	0.219201
C4	-0.213121	-0.213769	-0.214631	-0.214816	-0.214898	-0.214924
C5	-0.188413	-0.187357	-0.187190	-0.187089	-0.187033	-0.187014
C6	-0.236929	-0.239385	-0.242541	-0.243395	-0.243803	-0.243936
C7	-0.179671	-0.180220	-0.180842	-0.180994	-0.181066	-0.181090
C8	**-0.255357**	**-0.253932**	**-0.253682**	**-0.253602**	**-0.253560**	**-0.253546**
C9	0.095357	0.096907	0.098491	0.099040	0.099322	0.099417
C10	-0.163410	-0.164527	-0.166426	-0.167000	-0.167285	-0.167380
C11	-0.019590	-0.024263	-0.024633	-0.024675	-0.024687	-0.024690
C12	-0.149194	-0.154580	-0.163976	-0.166647	-0.167946	-0.168373

C13	-0.218750	-0.221639	-0.224662	-0.225514	-0.225925	-0.226060
C14	-0.238333	-0.237526	-0.237019	-0.236795	-0.236673	-0.236632
H1	0.122601	0.134058	0.141263	0.143058	0.143892	0.144160
H2	0.109049	0.113557	0.114922	0.115119	0.115190	0.115210
H4A	0.139517	0.146412	0.149894	0.150723	0.151105	0.151228
H4B	0.133005	0.126609	0.125896	0.125662	0.125548	0.125510
H5A	0.113141	0.117675	0.125739	0.128029	0.129141	0.129506
H5B	0.134417	0.132385	0.134661	0.135188	0.135427	0.135503
H8	0.179235	0.182312	0.190758	0.193143	0.194299	0.194679
H9	0.132660	0.135200	0.139725	0.140907	0.141468	0.141651
H10A	0.133936	0.139545	0.139305	0.139009	0.138835	0.138774
H10B	0.126416	0.129412	0.137270	0.139563	0.140686	0.141055
H12A	0.099349	0.110158	0.114261	0.115173	0.115583	0.115713
H12B	0.105324	0.111144	0.113838	0.114538	0.114869	0.114976
H13A	0.131945	0.130209	0.128176	0.127511	0.127178	0.127067
H13B	0.106994	0.104818	0.108394	0.109379	0.109853	0.110008
H13C	0.115253	0.116122	0.117694	0.118141	0.118358	0.118429
H14A	0.116453	0.117685	0.117530	0.117455	0.117414	0.117400
H14B	0.098999	0.104720	0.109752	0.111110	0.111757	0.111968
H14C	0.135500	0.135895	0.129740	0.127820	0.126862	0.126544
H2O	**0.245374**	**0.252385**	**0.257892**	**0.259296**	**0.259955**	**0.260169**

The Mulliken atomic charge value of carbon atom C8 was calculated to be higher compared to other carbon atoms, mainly due to the significant electronegative properties of its neighboring atoms. All hydrogen atoms exhibit a clear positive atomic charge. The H2O atom has the highest positive atomic charge, calculated as 0.245374 e in the gas-phase. Negative charges are concentrated on the oxygen atoms, which have the highest electronegativity. As seen in Table 3, oxygen atoms O1 and O2 have higher negative values compared to other atoms, indicating the presence of hydrogen bonding between O2-H2O…O1 molecules. Upon investigation in the gas-phase and varied solvents, it was observed that as the solvent polarity increases, the negativity of atomic charge values for atoms in the molecule's structure becomes more negative, and the positivity becomes more positive (Table 3).

Thermodynamic Properties

Due to the complexity of studying heat effects in thermodynamics, many compounds lack known values for heat formation. This situation emphasizes the importance of quantum chemical methods in theoretical calculations. By examining quantum chemical results for heat effects, decisions can be made regarding the occurrence of chemical reactions. Thermodynamic quantum chemical data are widely used in studying the reaction mechanisms of compounds. The thermodynamic characteristics of the studied BHDMU were calculated under gas-phase conditions at 298.15 K and 1 atmosphere pressure. Gaussian 03W program using the same method and the same basis set. The results are presented in Table 4.

Table 4. Thermodynamic Properties Calculated at 298.15 K in Gas-Phase

Parameter		**B3LYP/6-311G(d,p)**
Zero-point		
Vibrational energy, E_{vib} (kCal/Mol)		190.69655
Rotational constants (GHz)	X	0.75543
	Y	0.22555
	Z	0.20481
Thermal energy, E_{total} (kCal/Mol)		
Total		201.134
Vibrational		199.356
Rotational		0.889
Translational		0.889
Heat capacity (C_v) (Cal/Mol.K)		
Total		66.702
Vibrational		60.740
Rotational		2.981
Translational		2.980
Entropy (*S*) (Cal/Mol.K)		
Total		128.209
Vibrational		51.748
Rotational		33.487
Translational		42.973

The same calculations were performed in the temperature range 100-1000 K. The results are presented in Table 5. As shown in Table 5, these parameters increase with increasing temperature, indicating that the thermal energies of molecular vibrations increase with temperature.

Table 5. Thermodynamic Characteristics at Various Temperatures Using the B3LYP/6-311G(d,p) Method

T (K)	C_v (Cal/Mol.K)	*S* (Cal/Mol.K)	*H* (kCal/Mol)
100.00	24.417	80.139	1.566
200.00	46.022	105.190	5.305
298.15	66.702	128.209	11.030
400.00	87.172	151.309	19.087
500.00	104.442	173.119	28.893
600.00	118.633	193.821	40.270
700.00	130.274	213.318	52.932
800.00	139.950	231.630	66.657
900.00	148.103	248.832	81.269
1000.00	155.040	265.014	96.634

Quadratic equations were used to establish correlation relationships between heat capacities, entropies, enthalpy changes and temperatures as shown in the following equations.

The factors of agreement (R^2) for thermodynamic properties were 0.99976, 1 and 0.99953, respectively. The corresponding temperature dependent correlation plots are shown in Figure 5.

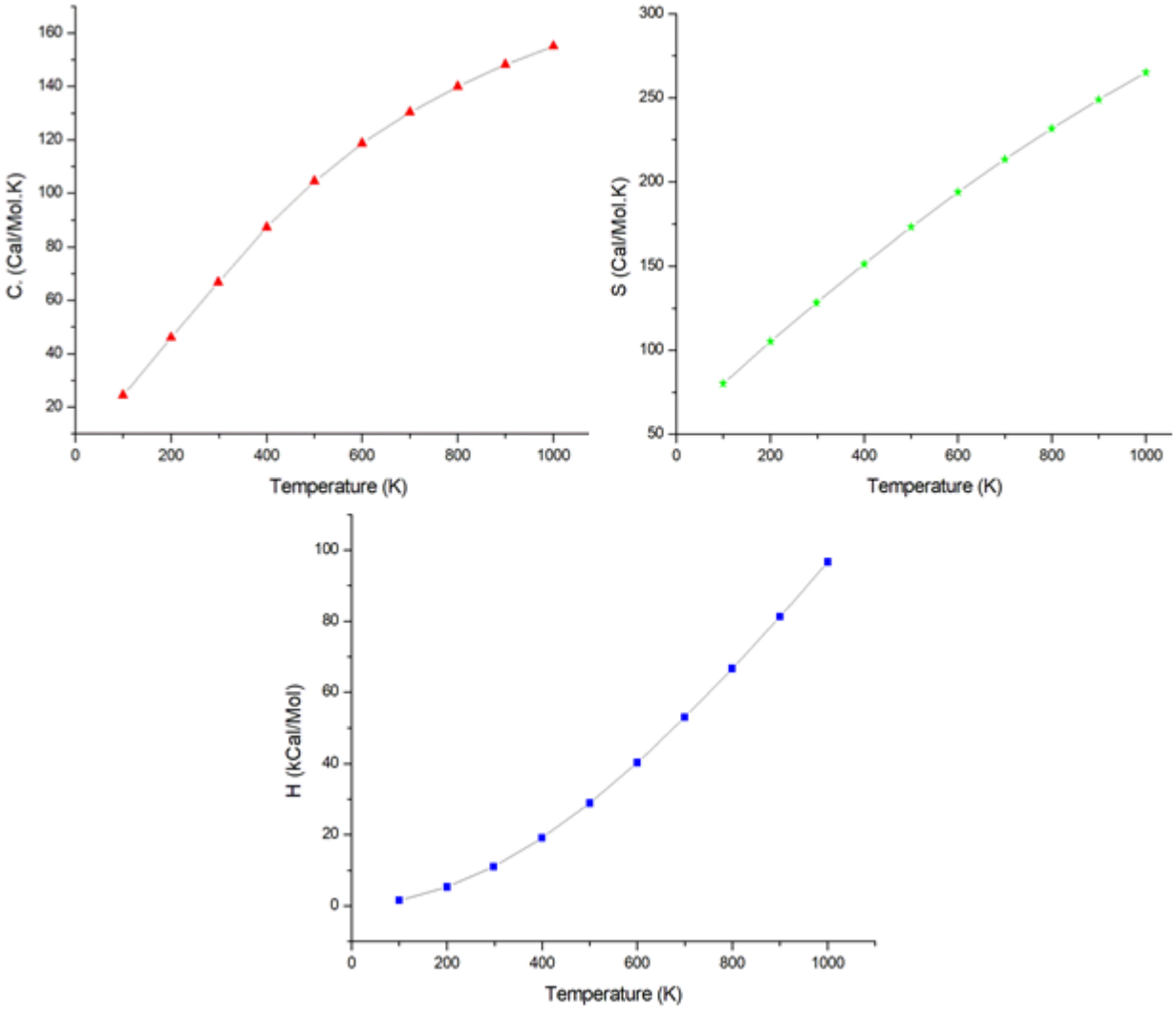

Figure 5. Temperature Variation of Theoretically Calculated Thermodynamic Properties for the BHDMU

C_v (T) = -1.7164+0.2648T-1.08602x$10^{-4}$$T^2$ R^2 = 0.99976 (1)

S (T) = 54.15291+0.26508T-5.41501x$10^{-5}$$T^2$ R^2 = 1 (2)

H (T) = -2.89997+0.02784T+7.26446x$10^{-5}$$T^2$ R^2 = 0.99953 (3)

These equations can be utilized in subsequent studies involving the BHDMU. For example, when investigating the interaction of the BHDMU with another substance, these thermodynamic properties can be derived from the aforementioned equations. These properties can be used in further studies to determine the change in the Gibbs free energy for the reaction.

Molecular Electrostatic Potential (MEP) Surface Analysis

MEP provides insights into the local polarity of a molecule (Pearson, 1989). MEP surfaces serve as a valuable tool for explaining the reactivity, structural activity, and hydrogen bonding of molecules. MEP is described using a color-coding system. Red regions (-) represent negatively charged electrostatic potential areas, indicating the pull of protons (due to lone pairs, π bonds) by the high electron density of the molecules. The blue regions represent areas of electrostatic potential with (+) positive charges, indicating that protons are repelled by the

atomic nucleus in areas where the electron density and nuclear charge are not perfectly balanced. The MEP surface map of the structure optimized with the B3LYP method is shown in Figure 6.

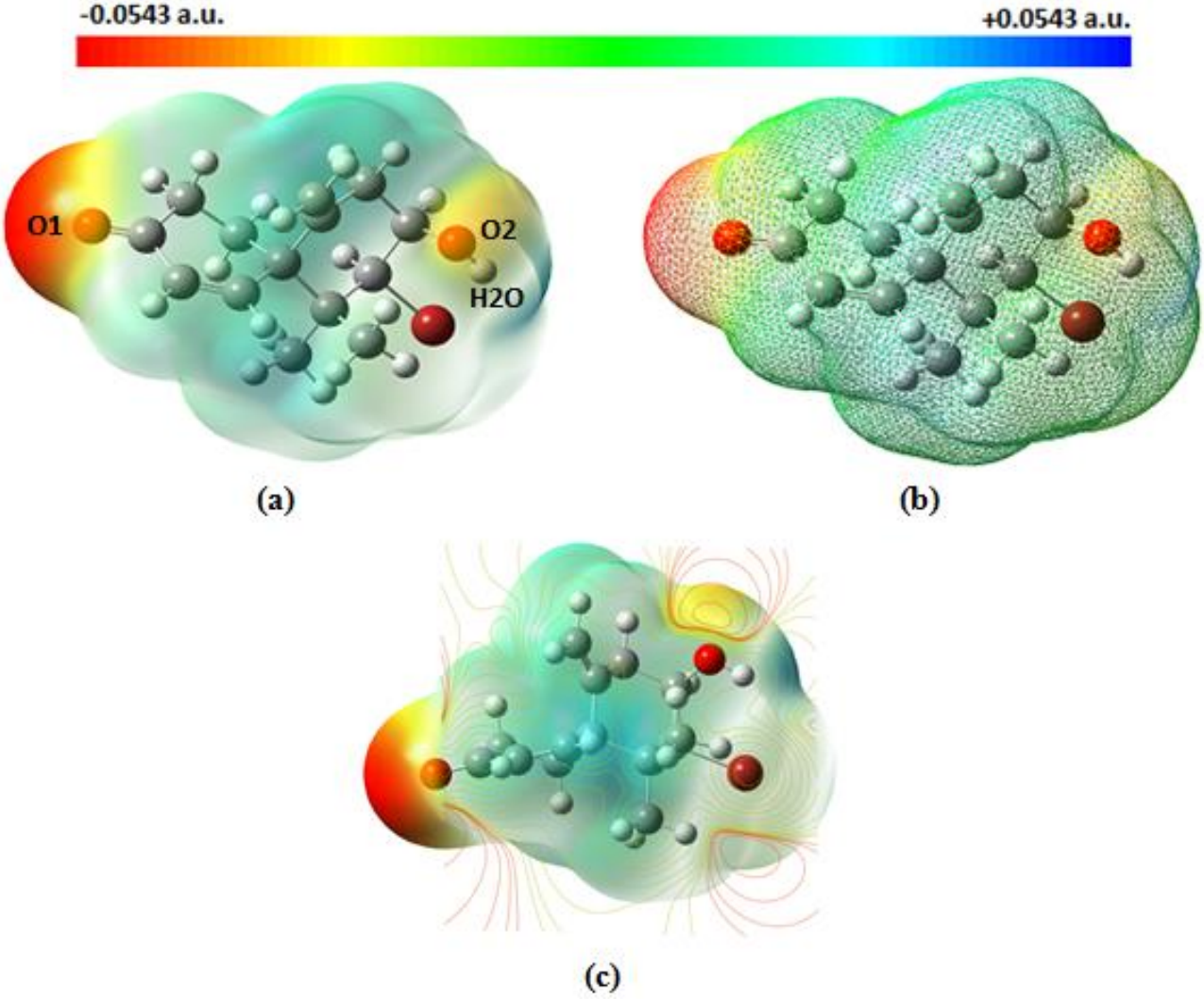

Figure 6. (a) MEP, (b) MESH, and (c) MEP Contour View of the BHDMU

Negative regions are observed around the oxygen atoms in the BHDMU compound (O1 and O2; -0.05388, -0.03245 a.u., respectively), indicating the presence of hydrogen bonding between the O2-H2O...O1 molecules. Electron-rich red lines are localized around the oxygen atoms, whereas regions with high hydrogen density are shown by greenish-yellow lines.

Molecular Docking (MD) Studies

The significance of MD methods in molecular structure analysis has become increasingly evident, reflected in the rising number of research studies in the literature. MD stands out as one of the most useful techniques for deciphering the binding geometry between macro molecules and small molecules. In these studies, particularly in protein-ligand binding simulations, MD proves uniquely advantageous, accelerating biochemical and pharmacological research. It facilitates the calculation of crucial data such as binding affinity, binding pose, and binding geometry. The surge in computer-aided drug design's popularity has driven the demand for innovative software, making the MD method applicable across diverse disciplines.

Schiff bases find versatile applications spanning biology, physics, chemistry, pharmacology, and more. Their imine structure endows them with a wide array of properties.

Literature studies undeniably confirm the anticancer and antitumor properties of Schiff bases, evident since their synthesis. Furthermore, Schiff base complexes with metals emerge as promising ligand candidates. An MD analysis was performed on the complex containing Kelch-like ECH-associated protein 1 (KEAP1) and nuclear factor erythroid 2-associated factor 2 (NRF2) (PDB ID: 2flu). The Keap1-Nrf2 signaling pathway plays an important role in both systems, providing insights into oxidative stress and cancer pathogenesis. (Cheng et al., 2021). Oxidative stress refers to the imbalance in a biological system's ability to neutralize reactive oxygen species and by-products generated during reactions or repair processes (Preddy & Watson, 2010). This imbalance can result in various biological damages, including DNA base damage and strand breaks, potentially causing significant disruptions in organisms' vital processes. Keap1 functions as a negative regulator of the Nrf2 protein, which in turn governs the expression of protective proteins against oxidative damage induced by injury or inflammation in cells. Absence of oxidative stress, Keap1 inhibits Nrf2 activation, keeping Nrf2 in the cytoplasm. However, when Keap1 is subjected to stress or mutations, this inhibition is disrupted. Consequently, Nrf2 relocates to the nucleus, activating cytoprotective genes. Literature studies have substantiated Keap1 mutations in certain lung cancer patients (Padmanabhan et al., 2006). The MD study involving BHDMU and the Keap1-Nrf2 complex was done using Autodock Vina 1.5.6 software (Trott & Olson, 2010). The findings from this analysis are detailed in Table 6.

Table 6. MD Results between BHDMU and Keap1-Nrf2 Complex

MODE	AFFINITY (kCal/Mol)	RMSD l.b.	RMSD u.b.
1	-7.9	0.000	0.000
2	-7.8	3.504	6.451
3	-7.7	2.993	6.007
4	-7.5	2.235	4.832
5	-7.3	2.284	5.174
6	-6.9	5.477	8.402
7	-6.8	5.651	8.566
8	-6.7	5.245	6.937
9	-6.7	5.705	7.703

According to Table 6, the MD process resulted in 9 different binding modes for the BHDMU. Among these binding modes, the best binding mode was observed to be mode 2, with a binding affinity of -7.8 kCal/Mol. Considering the interaction of Schiff base ligands with proteins, this score appears to be a sufficiently good value. According to Table 6, the MD process resulted in 9 different binding modes for BHDMU. Among these binding modes, the best binding mode was observed to be mode 2, with a binding affinity of -7.8 kCal/Mol. Considering the interaction of Schiff base ligands with proteins, this score appears to be a sufficiently good value.

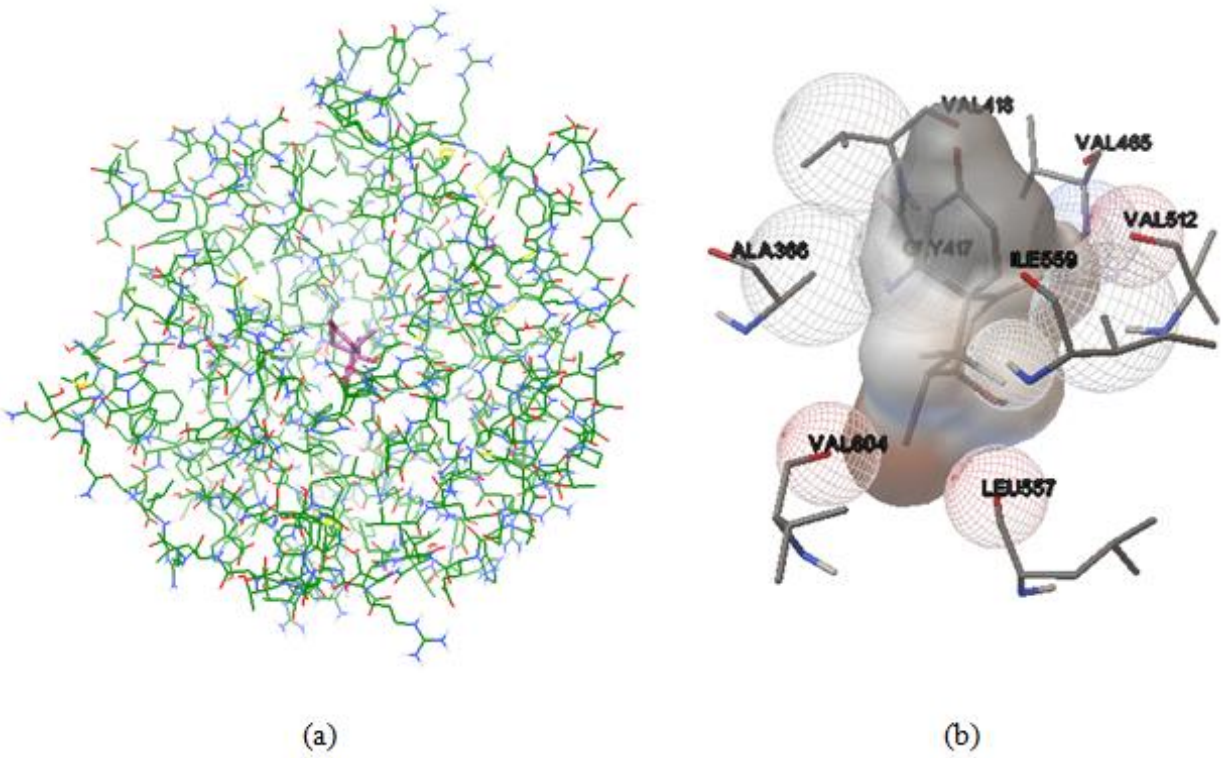

Figure 7. MD Results for the BHDMU and Keap1-Nrf2 Complex

Figure 7 depicts the outcomes of the MD analysis between the BHDMU and the Keap1-Nrf2 complex, highlighting the optimal binding mode and amino acid interactions. The binding mode shown in Figure 7.a illustrates the precise localization of the compound within the active site of the Keap1-Nrf2 protein. Figure 7.b provides insights into the specific interactions occurring between the BHDMU and adjacent amino acid residues in the macromolecular structure. In particular, a hydrogen bond is observed between the oxygen atom of BHDMU and the amino acid residue ILE:559. Upon closer examination of the docking results, it becomes apparent that the distinctive -C=N (imine) structure in the BHDMU significantly contributes to its remarkable physical and chemical properties. Existing literature supports the notion that Schiff base ligands engage with the active regions of proteins, leveraging their superior conformational features to enhance the physical and chemical characteristics of the resulting structure.

Hirshfeld Surface (HS) Analysis

HS analysis is a novel approach for the graphical exploration of all intra- and intermolecular contacts within a crystal structure, providing detailed quantitative insights (McKinnon, Jayatilaka & Spackman, 2007; Spackman & Jayatilaka, 2009). In this study, the crystallographic information file (.cif file) of the crystal lattice of the BHDMU molecule, whose structure was elucidated by Suescon et al. in 2001, was used as an input file in CrystalExplorer17.5 (Turner et al. 2017) to perform HS analysis of the structure. The aim was to understand the packing nature of molecules within the crystal lattice and confirm all interactions within the BHDMU. This analysis visualized all intermolecular and intramolecular interactions (Spackman & McKinnon, 2002; McKinnon, Jayatilaka & Spackman, 2007; Spackman & Jayatilaka, 2009; Spackman et al. 2021) and provided insights into the normalized contact distance (d_{norm}), distance to the nearest nucleus outside the HS (d_e), distance corresponding to the nearest nucleus inside the surface (d_i), shape index, curvedness, and fragment patch maps related to the studied BHDMU, as shown in Figure 8.

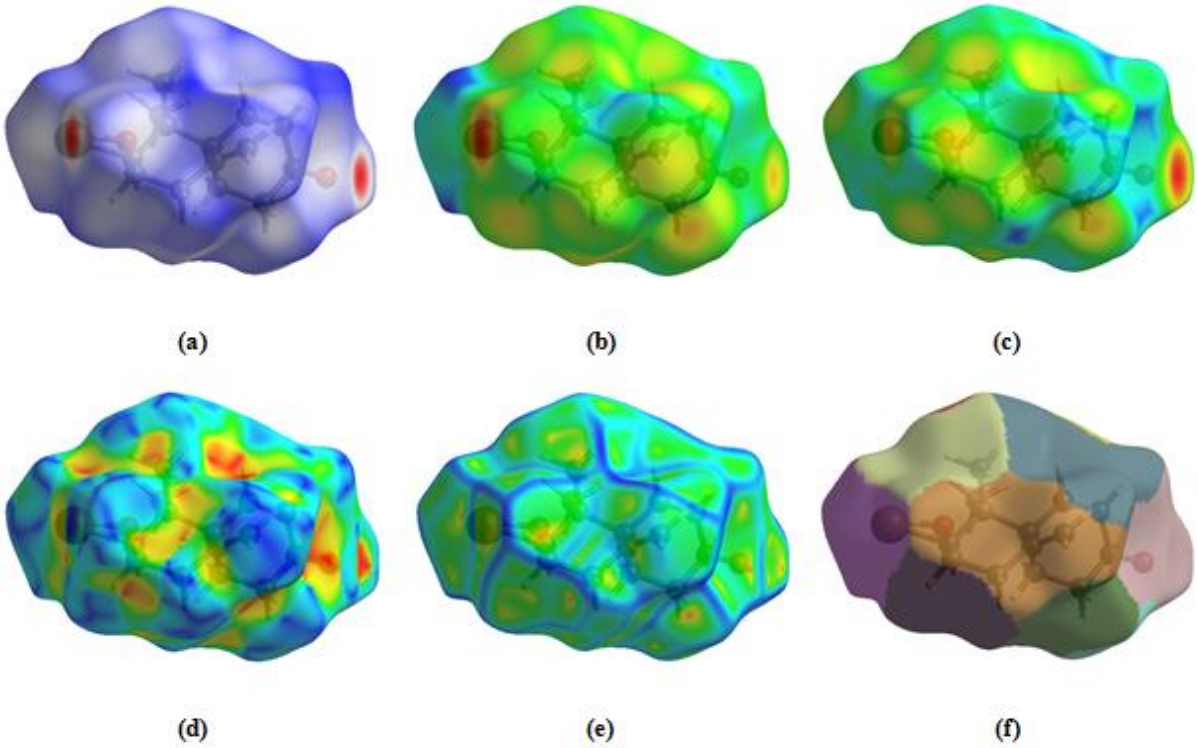

Figure 8. HS Maps for the Investigated BHDMU, Including (a) d_{norm}, (b) d_i, (c) d_e, (d) Shape Index, (e) Curvedness, and (f) Fragment Patch

For the BHDMU, the indices corresponding to d_{norm}, d_i, and d_e surfaces were obtained within the ranges of -0.5083 to 1.3017, 0.8027 to 2.5360, and 0.8015 to 2.4529 Å, respectively. Shape index, curvedness and fragment patch were observed in the ranges -1 to 1, -4 to 4 and 0 to 13, respectively (Figure 8). The shape index indicates planar $\pi...\pi$ interactions between molecules. These interactions are represented in HS by adjacent blue and red triangles in the shape index. The red points observed on the HS (d_{norm}) provide information about bond strengths based on color concentration, with darker red points indicating stronger hydrogen bonds compared to lighter red points. When examining the red regions on the dnorm map in Figure 9, illustrating intermolecular contact regions of the studied BHDMU, it is noted that the oxygen atom involved in the O-H···O contact is prominently featured.

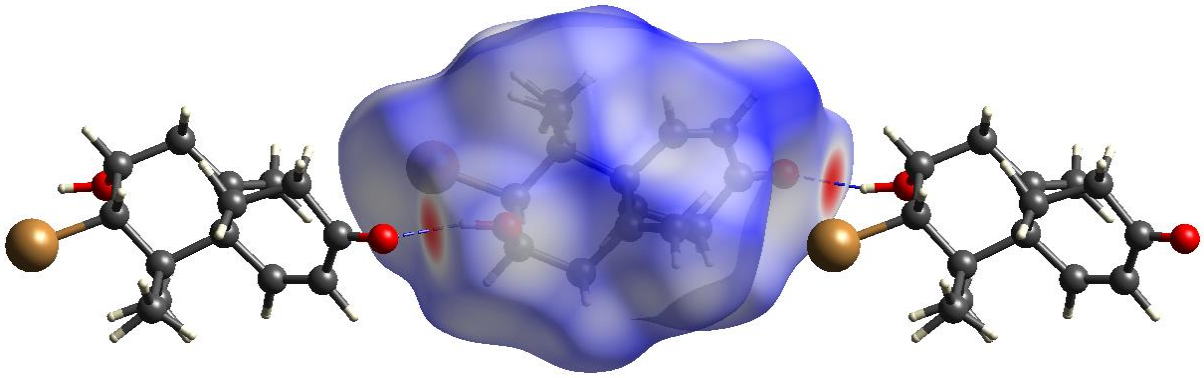

Figure 9. d_{norm} HS Map Illustrating the Intermolecular Contact Regions of the Investigated Molecule

Figure 9 displays the packing arrangement of the investigated molecule on the d_{norm} HS. Two-dimensional (2D) fingerprint plots based on HS analysis represent a way to characterize and summarize the contact types of all interactions between molecules (Spackman &

McKinnon, 2002). The two-dimensional representation of the Hirshfeld surface, resembling a fingerprint and composed of blue dots, is drawn with d_i values given on the y-axis and d_e values on the x-axis. All interactions are depicted through separate 2D fingerprint plots for each interaction, along with their relative contributions to the HS, as shown in Figure 10. The dominant interaction, accounting for 64.0% of the fingerprint plot, was found to involve H---H interactions as a result of the high abundance of hydrogen atoms on the molecular surface. Contributions on the HS are primarily attributed to H…H/H…H (64.0%), O…H/H…O (18.3%), Br…H/H…Br (12.8%), C…H/H…C (2.4%), C…Br/Br…C (1.3%), and Br…O/O…Br (1.2%) interactions.

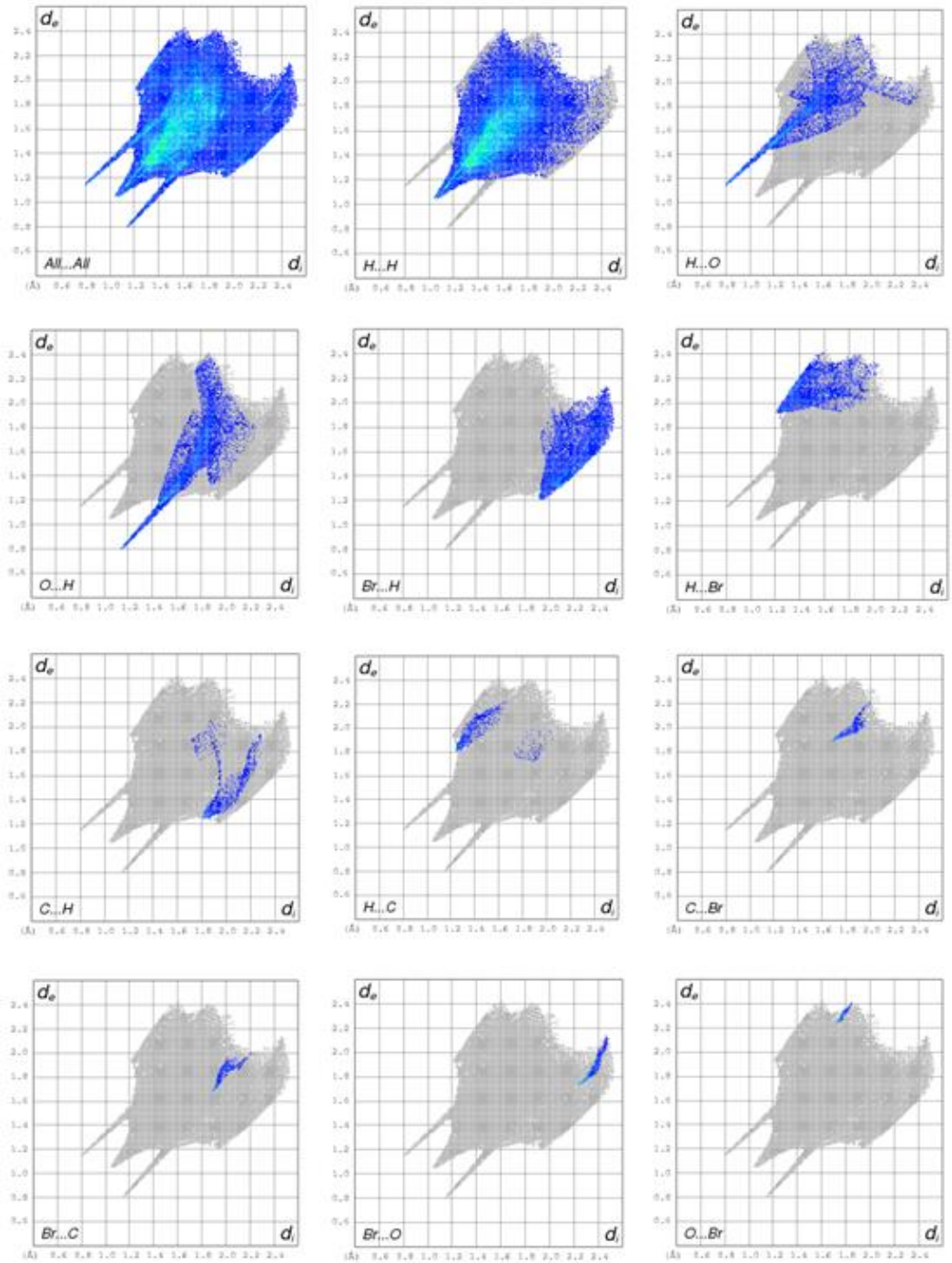

Figure 10. Two-Dimensional Fingerprint Plot Illustrating the Main Intermolecular Interactions of the Investigated Molecule

Conclusion

In this study, quantum chemical calculations were performed using the Gaussian 03W program to elucidate the structural, electrical, and electronic properties of the BHDMU. The geometrical, electrical, and electronic properties of the molecule were theoretically investigated using the DFT/B3LYP/6-311G(d,p). The obtained minimum energy structures were compared with the experimental values obtained using the X-ray method available in the literature, and it was found that the geometric parameters of the molecules are in good agreement with the experimental values. To determine the stable structure, geometry optimization was performed first. As a result of this optimization, bond lengths, bond angles and torsion angles of the molecule were determined. The experimental values obtained were compared with the calculated geometric parameters since the structure of the investigated molecule had previously been determined by the X-ray diffraction method. It is important to emphasize that the experimental results correspond to the solid phase, while the theoretical calculations are based on the gas-phase. In the solid state, the effect of the crystal field, coupled with intermolecular interactions, leads to molecular interconnections, resulting in differences in bond parameters between calculated and experimental values. Consequently, the molecule's FMO energies and total energies were computed. The ΔE and the molecular parameters including I, A, χ, η, μ, S, and w were calculated both in the gas-phase and in five varied solvents. According to Mulliken charge analysis, it was observed that O1 and O2 atoms have higher negative values compared to other atoms, indicating the presence of hydrogen bonding between O2-H2O…O1 molecules. Mulliken charge analysis in the gas-phase and varied solvents revealed that as the solvent polarity increases, the negativity of atomic charges in the molecule's structure increases if they are negative and decreases if they are positive. Correlations between statistical thermodynamics and temperature were also established. The thermodynamic parameters were found to increase with rising temperature due to the intensification of molecular vibrations. The MEP map confirmed the presence of intramolecular O-H...O interactions. MD studies were carried out for BHDMU. HS analysis was performed to examine the intermolecular interactions of the BHDMU under investigation. Additionally, 2D fingerprint plots were generated to determine contributions to the HS area. It was found that the most significant contribution to the HS area was due to hydrogen abundance in the BHDMU, indicating H···H interactions (64.0%).

References

Barsanti, L. & Gualtieri, P. (2006). *Algae: anatomy, biochemistry, and biotechnology*, CRC Press, Taylor & Francis Group., 301p

Baytut, Ö., Gümüş, F. & Ersanlı, E. (2018) Molecular phylogeny of a thycoplanktonic naviculoid diatom, *Haslea howeana*, from the Black Sea: a new record for the Turkish Algal Flora. *Genetics of Aquatic Organisms*, *2* (2), 49-52. Doi: 10.4194/2459-1831-v2_2_04

Becke, A. D. (1993) Density-functional thermochemistry. III. The role of exact exchange. *The Journal of Chemical Physics*, *98*, 5648-5652. Doi: 10.1063/1.464913

Cheng, L., Wang, H., Li, S., Liu, Z. & Wang, C. (2021) New insights into the mechanism of Keap1-Nrf2 interaction based on cancer-associated mutations. *Life Sciences, 282* (119791),. 1-11. Doi: 10.1016/j.lfs.2021.119791

Deniz, F. & Tezel Ersanli, E. (2016a) Removal of colorant from simulated wastewater by phyco-composite material: Equilibrium, kinetic and mechanism studies in a lab-scale application. *Journal of Molecular Liquids*, *220*, 120-128. Doi: 10.1016/j.molliq.2016.04.081

Deniz, F. & Tezel Ersanli, E. (2016b) Simultaneous bioremoval of two unsafe dyes from aqueous solution using a novel green composite biosorbent. *Microchemical Journal*, 128, 312-319. 10.1016/j.microc.2016.05.012

Deniz, F. & Tezel Ersanli, E. (2018a) Application of a novel phyco-composite biosorbent for the biotreatment of aqueous medium polluted with manganese ions. *International Journal of Phytoremediation, 20* (2), 138-144. Doi: 10.1080/15226514.2017.1337074

Deniz, F. & Tezel Ersanli, E. (2018b) An ecofriendly approach for bioremediation of contaminated water environment: Potential contribution of a coastal seaweed community to environmental improvement. *International Journal of Phytoremediation, 20* (3), 256-263. Doi: 10.1080/15226514.2017.1374335

Deniz, F., Tezel Ersanli, E. (2018c) A natural macroalgae consortium for biosorption of copper from aqueous solution: Optimization, modeling and design studies. *International Journal of Phytoremediation*, *20* (4), 362-368. Doi: 10.1080/15226514.2017.1393387

Deniz, F. & Tezel Ersanli, E. (2020a) A low-cost and eco-friendly biosorbent material for effective synthetic dyeremoval from aquatic environment: characterization, optimization, kinetic, isotherm and thermodynamic studies. *International Journal of Phytoremediation*, *22* (4), 353-362. Doi: 10.1080/15226514.2019.1663485

Deniz, F. & Tezel Ersanli, E. (2020b) Purification of malachite green as a model biocidal agent from aqueous system by using a natural widespread coastal biowaste (*Zostera marina*). *International Journal of Phytoremediation*, *23* (7), 772-779. Doi: 10.1080/15226514.2020.1857684

Deniz, F. & Tezel Ersanli, E. (2020c) An effectual biosorbent substance for removal of manganese ions from aquatic environment a promising environmental remediation study with activated coastal waste of *Zostera marina* plant. *Hindawi Limited, 7806154*, 1-8. Doi: 10.1155/2020/7806154

Deniz, F. & Tezel Ersanli, E. (2021) A renewable biosorbent material for green decontamination of heavy metal pollution from aquatic medium: a case study on manganese removal, *International Journal of Phytoremediation*, *23* (3), 231-237. Doi: 10.1080/15226514.2020.1807905

Deniz, F. & Tezel Ersanli, E. (2022) A novel biowaste-based biosorbent material for effective purification of methylene blue from water environment. *International Journal of Phytoremediation*, *24* (12), 1243-1250. Doi: 10.1080/15226514.2021.2025039

Deniz, F. & Tezel Ersanli, E. (2023) An efficient biosorbent material for green remediation of contaminated water medium, *International Journal of Phytoremediation*, Doi: 10.1080/15226514.2023.2191742

Dennington, R., Keith, T. & Millam, J. (2007). *Gauss View*, Version *4.1.2*. Semichem Inc., Shawnee Mission

Foresman, J. B. & Frisch, Æ. (1996). *Exploring Chemistry with electronic structure methods* (2nd ed.), Pittsburgh, PA: Gaussian Inc., 266, 278-283

Frisch, M. J., Trucks ,G. W., Schlegel, H. B., Scuseria, G. E., Robb, M. A., Cheeseman, J. R., Montgomery, J. A. Jr., Vreven, T., Kudin, K. N., Burant, J. C., Millam, J. M., Iyengar, S. S., Tomasi, J., Barone, V., Mennucci, B., Cossi, M., Scalmani, G., Rega, N., Petersson, G. A., Nakatsuji, H., Hada, M., Ehara, M., Toyota, K., Fukuda, R., Hasegawa, J., Ishida, M., Nakajima, T., Honda, Y., Kitao, O., Nakai, H., Klene, M., Li , X., Knox, J. E., Hratchian, H. P., Cross, J. B., Bakken, V., Adamo, C., Jaramillo, J., Gomperts, R., Stratmann, R. E., Yazyev, O., Austin, A. J., Cammi, R., Pomelli, C., Ochterski, J. W., Ayala, P. Y., Morokuma, K., Voth, G. A., Salvador, P., Dannenberg, J. J., Zakrzewski, V. G., Dapprich, S., Daniels, A. D., Strain, M. C., Farkas, O., Malick, D. K., Rabuck, A. D., Raghavachari, K., Foresman, J. B., Ortiz, J. V., Cui, Q., Baboul, A. G., Clifford, S., Cioslowski, J., Stefanov, B. B., Liu, G., Liashenko, A., Piskorz, P., Komaromi, I., Martin, R. L., Fox, D. J., Keith, T., Al-Laham, M. A., Peng, C. Y., Nanayakkara, A., Challacombe, M., Gill, P. M. W., Johnson, B., Chen, W., Wong, M. W., Gonzalez, C. & Pople, J. A. (2004). *Gaussian 03W*, Revision C. 02. Gaussian, Inc, Wallingford CT

Geerlings, P., Proft, F. De & Langenaeker, W. (2003) Conceptual density functional theory. *Chemical Review, 103* (5), 1793-1873. Doi: 10.1021/cr990029p

Gönülol, A., Tezel Ersanli, E. & Baytut, Ö. (2009) Taxonomical and numerical comparison of epipelic algae from Balik and Uzun lagoon. *Journal of Environmental Biology, 30* (5), 777-784. Doi: 10.4194/2459-1831-v2_2_04

Guiry, G. M. & Guiry, M. D. (2012). *AlgaeBase*. World-wide electronic publication, National University of Ireland, Galway. https://www.algaebase.org; searched on 01 September 2023

Gümüş, F., Gümüş, D. & Tezel Ersanli, E. (2023) *Cystoseira* (Ocrophyta) *sensu lato*'nın Sinop kıyılarında biyoçeşitliliğinin moleküler ve morfolojik olarak tanımlanması ve biyokütlesinin atıksu arıtımında biyosorbent olarak kullanımının araştırılması. *Acta Aquatica Turcica, 19* (2), 109-124. Doi: 10.22392/actaquatr.1211893

Hasirci Mustak, S. & Tezel Ersanli, E. (2015) Spatial and temporal characterization of the physicochemical parameters and phytoplankton assemblages in Dodurga Reservoir Sinop Turkey. *Turkish Journal of Botany, 39*, 547-554. Doi: 10.3906/bot-1407-32

John, D. M., Prud'homme van Reine, W. F., Lawson, G. W., Kostermans, T. B. & Price, J. H. (2004) A taxonomic and geographical catalogue of the seaweeds of the western coast of Africa and adjacent islands. *Beihefte zur Nova Hedwigia, 127*, 1-339

Koopmans, T. (1933) Ordering of wave functions and eigenenergies to the individual electrons of an atom. *Physica, 1*, 104-113. Doi: 10.1016/S0031-8914(34)90011-2

Lee, C., Yang, W. & Parr, R. G. (1988) Development of the Colle-Salvetti correlation-energy formula into a functional of the electron density. *Physical Review*, *37*, 785-789. Doi: 10.1103/PhysRevB.37.785

McKinnon, J.J., Jayatilaka, D. & Spackman, M. A. (2007) Towards quantitative analysis of intermolecular interactions with Hirshfeld surfaces. *Chemical Communications Journal*; *37*: 3814-3816. Doi: 10.1039/b704980c

Mulliken, R. S. (1955) Electronic population analysis on LCAO-MO molecular wave functions. I. *The Journal of Chemical Physics*, *23* (10), 1833-1840. Doi: 10.1063/1.1740588

Padmanabhan, B., Tong, K. I., Ohta, T., Nakamura, Y., Scharlock, M., Ohtsuji, M., Kang, M., Kobayashi, A., Yokoyama, S. & Yamamoto, M. (2006) Structural basis for defects of Keap1 activity provoked by its point mutations in lung cancer. *Molecular cell*, *21* (5), 689-700. Doi: 10.1016/j.molcel.2006.01.013

Parr, R. G. & Pearson, R. G. (1983) Absolute hardness: Companion parameter to absolute electronegativity. *Journal of the* ***American Chemical Society***, *105*, 7512-7516. Doi: 10.1021/ja00364a005

Pearson, R. (1989) Absolute electronegativity and hardness: applications to organic chemistry. *Journal of Organic Chemistry*, *54*, 1423-1430. Doi: 10.1021/jo00267a034

Perdew, J. P., Parr, R. G., Levy, M. & Balduz, J. L. (1982) Density-functional theory for fractional particle number: Derivative discontinuities of the energy. *Physical Review Letters*, *49*, 1691-1694. Doi: 10.1103/PhysRevLett.49.1691

Preddy, V. R. & Watson, R. R. (2010). Oxidative Stress: Handbook of disease burdens and quality of life measures, Springer, p. 4278-4278

Reed, A. E., Curtiss, L. A. & Weinhold, F. (1988) Intermolecular interactions from a natural bond orbital, donor-acceptor viewpoint. *Chemical Reviews*, *88* (6), 899-926. Doi: 10.1021/cr00088a005

Reed, A. E. & Weinhold, F. (1985) Natural localized molecular orbitals. *The Journal of Chemical Physics*, *83* (4), 1736-1740. Doi: 10.1063/1.449360

Schüürmann, G. (2004) Quantum chemical descriptors in structure-activity relationships-calculation, interpretation and comparison of methods. *In Predicting Chemical Toxicity and Fate*, Doi: 10.1201/9780203642627.ch6

Senet, P. (1997) Chemical hardnesses of atoms and molecules from frontier orbitals. *Chemical Physics Letters*, *275*, 527-532. Doi:10.1016/S0009-2614(97)00799-9

Serrano, A., Palacios, C., Roy, G., Cespón, C., Villar, M. L., Nocito, M., González-Porqué, P. (1998) Derivatives of gallic acid induce apoptosis in tumoral cell lines and inhibit lymphocyte proliferation. *Archives of Biochemistry and Biophysics*, *350* (1), 49-54. Doi: 10.1006/abbi.1997.0474

Spackman, M. A. & Jayatilaka, D. (2009) Hirshfeld surface analysis. *CrystEngComm*, *11* (1), 19-32. Doi: 10.1039/B818330A

Spackman, M. A. & McKinnon, J. J. (2002) Fingerprinting intermolecular interactions in molecular crystals. *CrystEngComm*, *4* (66), 378-392. Doi: 10.1039/B203191B

Spackman, P. R., Turner, M. J., McKinnon, J. J., Wolff, S. K., Grimwood, D. J., Jayatilaka, D., Spackman, M. A. (2021) CrystalExplorer: A program for Hirshfeld surface analysis, visualization and quantitative analysis of molecular crystals. *Journal of Applied Crystallography*; *54* (3): 1006-1011. Doi: 10.1107/S1600576721002910

Suescun, L., Alvaro, W. M., RauÂl, A. M., Danilo, D., Rafael, F. & Eduardo, M. (2001) Two natural products from the algae *Laurencia scoparia*. *Acta Crystallographica Section C, 57*, 286-288. Doi: 10.1107/S0108270100017935

Taylor, W. R. (1960). *Marine algae of the eastern tropical and subtropical coasts of the Americas*. pp. [i]-xi, 1-870, 14 figs, 80 pls. Ann Arbor: The University of Michigan Press

Tezel Ersanlı, E., Hasırcı Mustak, S. (2017) Distribution dynamics of vegetative cells and cyst of *Ceratium hirundinella* in two reservoirs, Turkey. *Süleyman Demirel University Journal of Natural and Applied Sciences, 21* (1), 247-253. Doi: 10.19113/sdufbed.99878

Tezel Ersanlı, E. & Öztürk, R. (2017) Ecological and statistical evaluation of algal flora and water quality of Karasu stream. *Kahramanmaraş Sütçü İmam Üniversitesi Doğa Bilimleri Dergisi, 20* (3), 193-200. Doi: 10.18016/ksudobil.264177

Tezel Ersanli, E. & Gönülol, A. (2014) phytoplankton dynamics and some physicochemical variables in cakmak reservoir Samsun Turkey. *MANAS Journal of Agriculture and Life Sciences, 4* (1), 17-25

Tezel Ersanli, E. & Hasirci Mustak, S. (2013) The relationship between environmental variables and the vertical and horizontal assemblages of phytoplankton in Erfelek Reservoir in Sinop Turkey. *Fundamental and Applied Limnology / Archiv Für Hydrobiologie, 183* (3), 177-188. Doi: 10.1127/1863-9135/2013/0516

Trott, O. & Olson, A. J. (2010) AutoDock Vina: improving the speed and accuracy of docking with a new scoring function, efficient optimization and multithreading. *Journal of Computational Chemistry, 31* (2), 455-461. Doi: 10.1002/jcc.21334

Turner, M. J., MacKinnon, J. J., Wolff, S. K., Grimwood, D. J., Spackman, P. R., Jayatilaka, D. & Spackman, M. A. (2017). *Crystal Explorer Ver. 17.5*, University of Western Australia, Pert

Investigation of the Sense of Belonging Among University Students Using Statistical Methods

Cengiz GAZELOĞLU[1]
Tunahan TURHAN[2]

Introduction

Belonging, primarily a concept related to understanding human relationships, refers to the sense of "relatedness," "affiliation," and "belongingness." It is fundamentally a concept understood through association and represents an individual's effort to integrate with what they desire to belong to (Karip et al., 2020).

Bowlby argues that establishing close relationships with one's environment is a fundamental necessity for development in order to sustain one's life. Bowlby emphasizes that emotional bonds form the foundation of development, and initially, the individual has a primary need to establish close relationships with their family (Karip et al., 2020, Erşanlı & Koçyiğit, 2013).

In the literature, it is expressed that individuals living with a functional/healthy family have no difficulty in expressing themselves, are open to communication, and demonstrate a more respectful attitude towards themselves and others (Muyibi at al., 2010).

In terms of an individual's psychological well-being, feeling loved, respected, and having a sense of belonging play a significant role. However, the absence of a sense of belonging can negatively impact an individual's mental health, leading to behavioral and adjustment problems (Duru, 2007).

In this context, it does not seem feasible to expect that the work and interpersonal relationships of individuals who lack a sense of belonging to the environment they find themselves in would be the same as those who possess a sense of belonging. Insufficient sense of belonging can adversely affect an individual's life circumstances.

When individuals cannot fulfill their need for belonging adequately, they may experience emotional problems such as depression, anxiety, and loneliness (Uysal at al., 2015).

For example, Beyer (2008) found that students experiencing a lack of belongingness have a higher risk of rejection, alcohol/substance use, school absenteeism, a tendency towards violence in the school environment, and depression (Özgök, 2013).

Also, Melor et al. (2008) aimed to examine the subjective states of loneliness and the need to belong with a sample of 436 volunteer participants selected from the Australian Unity Wellbeing database. In this study, the authors collected data from participants through a questionnaire that included the Personal Well-Being Index, the UCLA Loneliness Scale, the life satisfaction measure, and the satisfaction with personal relationships measure included in the Need to Belonging Scale. They then talked in detail about the implications for these subjective situations.

[1] Assoc. Dr. Süleyman Demirel University, Department of Statistics, cengizgazeloglu@sdu.edu.tr
[2] Assoc. Dr. Süleyman Demirel University, Faculty of Education, Department of Elementary Mathematics Education, tunahanturhan@sdu.edu.tr

According to Maslow's hierarchy of needs theory, with the onset of adolescence, important needs such as belonging, status, commitment, and a high sense of self emerge for individuals (Alptekin, 2011).

Maslow (1987) defines the sense of belonging as a need for being accepted, recognized, valued, and significant by others (Karip et al., 2020).

Similarly, Frey and Wilhite (2005) define the environment where a sense of belonging is felt as an interactive network of relationships characterized by intense interest, love, and respect (Alptekin, 2011). This definition emphasizes the importance of interactive relationships in the development of a sense of belonging. According to Frey and Wilhite, for an individual to feel a sense of belonging to a group, community, or environment, there needs to be intense experience of interest, love, and respect in that environment. This collective of relationships allows individuals to feel accepted, valued, and significant.

Mavili et al. (2014) developed a measurement tool to determine the belonging of individuals to their families in their study. At the end of the study, a five-point Likert-type scale consisting of a total of 17 items thought to represent family belonging was obtained. Later, this scale was applied to 1579 university students studying at different universities in Konya and the results were analyzed.

The environment where emotions are expressed significantly influences an individual's style of emotional expression. When people perceive their environment as healthy and peaceful, they can express their emotions more freely. This environment helps individuals relax psychologically (Karip et al., 2020).

Individuals know that in order to express their emotions, they need to feel safe and be met with understanding by the people around them. In a healthy environment, individuals are encouraged and supported to express their emotions. This occurs in an environment where emotional burdens can be shared and emotional expressions are accepted.

With an increase in the sense of belonging, individuals can achieve better emotion regulation. They can make sense of their emotional experiences, express them, and manage them appropriately. This helps individuals control their emotional states more effectively.

The strengthening of a sense of belonging makes an individual's daily life more productive. It enables maintaining emotional balance, establishing positive relationships, seeking and providing support, and coping with emotional challenges. This improves the individual's quality of life and helps them cope with stress.

The sense of belonging can also play an important role in coping with problems. Feeling a sense of belonging to a community or environment provides support and assistance to the individual. Connecting with others, working together, and being in solidarity enable access to more resources and support for problem-solving. The sense of belonging enhances the individual's problem-solving skills and helps them find more effective solutions.

In conclusion, it is believed that an increased sense of belonging enhances emotional and situational control and makes an individual's daily life more productive. Similarly, it can be said that a sense of belonging can contribute to coping with problems.

Literature Review

Concept of Belonging

The sense of belonging is an inherent emotion that emerges with human existence and is intertwined with human identity. From primitive societies to modern developed societies, the

need for individuals to feel a sense of belonging has always been present. In primitive societies, the need to be a member of a group and to belong to that group arose due to reasons such as establishing a settled order, meeting housing needs, and ensuring defense and security (Levett at al., 2007).

Need for Belonging

The need for belonging has been described as a fundamental requirement by various theories and theorists. Bowlby argued that establishing close relationships is a fundamental prerequisite for human development to ensure survival, and emphasized the crucial role of close emotional bonds in development. According to Bowlby, the individual has a primary need to establish a relationship with the family. The need for belonging expresses the desire of individuals to form social connections, be accepted, and participate in relationships. This need influences the formation of identity and self-esteem. The family is where individuals establish their first and most fundamental social relationships, shaping their sense of belonging and social connections (Ecke at al., 2006).

Human Needs and Theoretical Approach to Belonging (Maslow's Theory)

Maslow developed a theory that explains human needs in a hierarchical structure, and within this theory, the sense of belonging and the need for it also hold an important place. Maslow's hierarchy of needs theory has gained broad acceptance in the literature and has been used in numerous studies (Yusufoğlu & Cerev, 2019).

Figure 1. Maslow's Hierarchy of Needs

When examining Maslow's Hierarchy of Needs Pyramid theory, developed by Maslow in 1943, it can be seen in the literature review that the introduction story refers to the research findings conducted by a psychologist in a clinical setting (Walsh, 2011). Clinical studies have shown that individuals set specific goals in their lives and shape their lives accordingly. The self-actualization stage in Maslow's theory encompasses the fulfillment of goals in one's life and the needs that arise in pursuit of these goals (Kula & Çakar, 2015).

It is known that individuals have ongoing needs throughout their lives and set goals based on these needs, which establishes the theoretical order of the hierarchy. Within Maslow's Hierarchy of Needs Pyramid, needs are divided into specific categories and levels. For an individual to move to the upper level of the hierarchy, it is expected that their needs in the lower level have been met to a sufficient extent (Çoban, 2021).

When examining Figure 1, it is noteworthy that the first two levels of the theory primarily focus on physiological needs, while the subsequent levels focus more on sociological and psychological needs. Since humans are social beings and need to fulfill their basic physical

needs in order to socialize, it is not possible for them to concentrate on the higher levels without prioritizing these lower levels (Çoban, 2021).

A study conducted by Sirgy (1986) focuses on life satisfaction and human development perspectives. This study was conducted by incorporating factors that balance individual development and life satisfaction into Maslow's hierarchy of needs theory (Kula & Çakar, 2015).

Material and Method

This research was conducted using data obtained through surveys filled out by students actively enrolled at Süleyman Demirel University during the 2022-2023 academic year. The "Sense of Belonging Scale" was used in the study and administered to participants selected through simple random sampling. The sample size was n=180, with a confidence level of 95% and a margin of error of 5%. The scale consisted of two parts: the first part collected participants' demographic information, followed by an 18-item questionnaire. Data processing and analysis were performed using the Statistical Packages for the Social Sciences (SPSS) software. Independent Samples t-test was employed for variables with two groups, and One-Way Analysis of Variance (ANOVA) was used for variables with more than two groups. When examining the results of the variance analysis, groups showing significant differences were identified, and in cases where the variances were homogeneous, Tukey's test was used for interpretation, while Tamhane's test was utilized in cases of heterogeneous variances.

Findings and Discussion

The descriptive statistics table of the participants based on the administration of the Sense of Belonging Scale to Süleyman Demirel University students is presented in Table 1.

Table 1. *Descriptive Statistics*

Variable	Group	Frequency	%
Gender	Female	99	55.0
	Male	81	45.0
Age	18-22	106	58.9
	23+	74	41.1
Place of Residence	Apartment	34	18.9
	House	126	70.0
	Dormitory	20	11.1
Educational Status	Undergraduate	144	80.0
	Graduate	36	20.0
Level of Education	Bachelor's Degree	101	56.1
	Master's Degree	29	16.1
	Associate's Degree	50	27.8
Class Level	1	25	13.9
	2	75	41.7
	3	37	20.6
	4+	43	23.9
Monthly Income Level	2000-2500	39	21.7
	2501-3000	18	10.0
	3001-3500	20	11.1
	3501+	103	57.2

Table 2. *Gender Analysis Results*

Variable	Factor	Group	n	$\bar{x}$	Std.	(p)
Gender	Sense of Belonging	Female	99	2,47	0,75	0,166
		Male	81	2,56	0,70	

H_0: There is no statistically significant difference in the sense of belonging among the gender groups of the participants.

H_1: There is a statistically significant difference in the sense of belonging among the gender groups of the participants.

The calculated significance (p) value from the analysis is determined as 0.166. Therefore, the H_0 hypothesis is accepted. Based on the findings, it is concluded that there is no statistically significant difference in the sense of belonging between females and males at a 95% confidence level. Detailed result are given in table 2.

In addition, the results obtained when Table 2 is examined can be summarized as follows: While the average of the sense of belonging among women is 2.47, this value is 2.56 among men. We can say that men have a slightly higher sense of belonging than women. However, the p value was found to be 0.166. This is higher than the 5% (0.05) threshold. Therefore, we can conclude that this difference between gender groups is not statistically significant. Standard deviation values show the distribution of participants' answers. The distribution of answers on the sense of belonging among women (0.75) is slightly higher than that of men (0.70). That is, the answers to the sense of belonging among women are somewhat more variable. In conclusion, based on these data, it was concluded that there was no statistically significant difference in sense of belonging between men and women. This means that gender does not have a determining effect on the sense of belonging on this scale. However, there is a small difference between the averages in both gender groups.***Table 3.*** *Age Analysis Results*

Variable	Factor	Group	n	$\bar{x}$	Std.	(p)
Age	Sense of Belonging	18-22	106	2,56	0,72	0,979
		23+	74	2,43	0,74	

H_0: There is no statistically significant difference in the sense of belonging among the age groups of the participants.

H_1: There is a statistically significant difference in the sense of belonging among the age groups of the participants.

The calculated significance (p) value from the analysis is determined as 0.979. Therefore, the H_0 hypothesis is accepted. Based on the findings, it is concluded that there is no statistically significant difference in the sense of belonging among the age groups at a 95% confidence level. Detailed result are given in table 3.

In Table 3, the results obtained regarding the sense of belonging of the participants according to their age groups are given. Considering Table 3, while the average sense of belonging is 2.56 among the participants aged 18-22, this value is 2.43 among the participants aged 23 and over. We can say that participants aged 18-22 have a slightly higher sense of belonging than participants aged 23 and over. However, the p value was found to be 0.979. This value is much higher than the 5% (0.05) threshold value generally used in scientific studies. This means that the difference between age groups is not statistically significant. That is, the

H0 hypothesis was accepted. On the other hand, the standard deviation values show the distribution of the participants' answers. The distribution of responses on sense of belonging was similar between both age groups, but the 23 and older group was slightly more variable (0.74 vs 0.72).

In conclusion, based on these data, it was concluded that there was no statistically significant difference in sense of belonging between age groups. This means that age has no decisive influence on the sense of belonging on this scale. However, there is a small difference between the averages between the two age groups.

Table 4. *Place of Residence Analysis Results*

Variable	Factor	Group	n	$\bar{x}$	Std.	(p)
Place of Residence	Sense of Belonging	House	126	2,55	0,77	0,531
		Apartment	34	2,40	0,63	
		Dormitory	20	2,43	0,60	

H_0: There is no statistically significant difference in the sense of belonging among the locations where the participants reside.

H_1: There is a statistically significant difference in the sense of belonging among the locations where the participants reside.

The calculated significance (p) value from the analysis is determined as 0.531. Therefore, the H_0 hypothesis is accepted. Based on the findings, it is concluded that there is no statistically significant difference in the sense of belonging among the locations where the participants reside at a 95% confidence level. Detailed result are given in table 4.

Table 4 presents the analysis of the results obtained regarding the sense of belonging of the participants by place of residence (housing type). According to this table, the average of the sense of belonging among the participants residing at home is 2.55, 2.40 for those living in flats and 2.43 for those living in dormitories. We can say that the participants living in the house have a slightly higher sense of belonging compared to other types of housing. In addition, when the standard deviation values are taken into account, the distribution of the answers in the sense of belonging of the participants living at home (0.77) is slightly more variable than the other types of housing.

As a result, based on these data, it was concluded that there was no statistically significant difference in sense of belonging according to residence (housing types). This means that the place of residence does not have a decisive influence on the sense of belonging at this scale. However, there are small differences in the averages between the three housing types.

Table 5. *Education Level Analysis Results*

Variable	Factor	Group	n	$\bar{x}$	Std.	(p)
Educational Status	Sense of Belonging	Undergraduate	144	2,51	0,71	0,176
		Graduate	36	2,49	0,81	

H_0: There is no statistically significant difference in the sense of belonging among the educational statuses of the participants.

H_1: There is a statistically significant difference in the sense of belonging among the educational statuses of the participants.

The calculated significance (p) value from the analysis is determined as 0.176. Therefore, the H_0 hypothesis is accepted. Based on the findings, it is concluded that there is no statistically significant difference in the sense of belonging among the educational statuses of the participants at a 95% confidence level. Detailed result are given in table 5.

Table 5 includes the results obtained regarding the sense of belonging according to the educational status of the participants. Here, while the average sense of belonging is 2.51 among the participants who have received education at the undergraduate level, it is seen that this value is 2.49 for those who are at the graduate level. Accordingly, it can be said that there is a very small difference between the averages and this shows that the participants at the undergraduate and graduate levels have a similar sense of belonging. When the standard deviation values were examined, it was observed that the distribution of the answers in the sense of belonging of the graduate level participants (0.81) was slightly more variable than the undergraduate level participants (0.71).

As a result, based on these data, it was concluded that there was no statistically significant difference in sense of belonging according to educational status. This means that education level does not have a decisive influence on the sense of belonging on this scale. However, there is a very small difference between the averages between the two education levels.

Table 6. *Education Level Analysis Results*

Variable	Factor	Group	n	$\bar{x}$	Std.	(p)
Level of Education	Sense of Belonging	Associate's Degree	50	2,64	0,69	0,006
		Bachelor's Degree	101	2,56	0,74	
		Master's Degree	29	2,12	0,64	

H_0: There is no statistically significant difference in the sense of belonging among the educational statuses of the participants.

H_1: There is a statistically significant difference in the sense of belonging among the educational statuses of the participants.

The calculated significance (p) value from the analysis is determined as 0.006. Therefore, the H0 hypothesis is rejected. Based on the findings, it is concluded that there is a statistically significant difference in the sense of belonging among the educational statuses of the participants at a 95% confidence level. Specifically, there is a difference observed between individuals with Associate's and Bachelor's degrees compared to those with Master's degrees. Information regarding the means of the relevant groups is provided explicitly in Table 6.

Table 6 shows the results regarding the sense of belonging according to the education level of the participants. The average of the sense of belonging of the participants at the associate degree level is 2.64, the average of those at the undergraduate level is 2.56, and the average of the participants at the graduate level is 2.12. This shows that especially the graduate level participants have a lower sense of belonging compared to other education levels. Here, the p value was found to be 0.006. This value is above the 1% (0.01) threshold but below the 5% (0.05) threshold. This means that there is a statistically significant difference in sense of belonging by education level. So the H0 hypothesis cannot be accepted. This analysis shows that the sense of belonging of the graduate level participants is statistically significantly lower than the associate and undergraduate level participants. However, the difference between associate and undergraduate level is less clear. This finding may suggest that individuals at the graduate level may have different experiences or expectations compared to those at other levels

of education. In addition, these results may reveal the necessity of conducting further analyzes in order to examine the effect of education level on individuals' sense of belonging.

Table 7. *Class Level Analysis Results*

Variable	Factor	Group	n	$\bar{x}$	Std.	(p)
Class Level	Sense of Belonging	1	25	2,35	0,75	0,425
		2	75	2,46	0,66	
		3	37	2,59	0,59	
		4+	43	2,61	0,91	

H_0: There is no statistically significant difference in the sense of belonging among the class levels of the participants.

H_1: There is a statistically significant difference in the sense of belonging among the class levels of the participants.

The calculated significance (p) value from the analysis is determined as 0.425. Therefore, the H_0 hypothesis is accepted. Based on the findings, it is concluded that there is no statistically significant difference in the sense of belonging among the class levels of the participants at a 95% confidence level. Detailed result are given in table 7.

Table 7 shows the data obtained regarding the sense of belonging of the participants according to their class levels. Considering the averages, we can see that as the grade level increases, the mean sense of belonging also increases: while the average sense of belonging is 2.35 for 1st grade students, this value increases to 2.46 for 2nd grade, 2.59 for 3rd grade students, and 2.35 for 1st grade students. It increases to 2.61 for 4th grade and above. This increasing trend may suggest that the sense of belonging may increase with the time students spend at university or college. However, we must examine the p-value to see if this trend is statistically significant. On the other hand, the p value was found to be 0.425. This value is higher than the 5% (0.05) threshold. This means that there is no statistically significant difference in sense of belonging by grade level.

In conclusion, based on these data, it was concluded that there was no statistically significant difference in sense of belonging between grade levels. However, it was observed that the sense of belonging showed an increasing trend as the grade level increased. This may indicate that students' sense of belonging may evolve during their time at school. In addition, these results reveal that class level does not have a determining effect on the sense of belonging.

Table 8. *Monthly Income Level Analysis Results*

Variable	Factor	Group	n	$\bar{x}$	Std.	(p)
Monthly Income Level	Sense of Belonging	2000-2500	39	2,63	0,80	0,504
		2501-3000	18	2,47	0,78	
		3001-3500	20	2,32	0,59	
		3501+	103	2,51	0,71	

H_0: There is no statistically significant difference in the sense of belonging among the monthly income levels of the participants.

H_1: There is a statistically significant difference in the sense of belonging among the monthly income levels of the participants.

The calculated significance (p) value from the analysis is determined as 0.504. Therefore, the H_0 hypothesis is accepted. Based on the findings, it is concluded that there is no statistically

significant difference in the sense of belonging among the monthly income levels of the participants at a 95% confidence level. Detailed result are given in table 8.

Table 8 shows the results obtained for the sense of belonging according to monthly income levels. From this point of view, it is seen that there is a slight fluctuation in the sense of belonging according to monthly income levels. When the averages are examined; It is seen that the average sense of belonging of those in 2000-2500 income brackets is 2.63, this average is 2.47 with a slight decrease for those who earn 2501-3000, and the average of sense of belonging drops to 2.32 for those who earn 3001-3500. Finally, it can be said that this value increases to 2.51 for those with a monthly income of 3501 and above. Although there is a small trend between the means, the p-value (0.504) indicates that these differences are not statistically significant at the 95% confidence level. Simply put, there may be some variation in the sense of belonging between different income groups, but it is concluded that these differences are not statistically significant and may be coincidental.

As a result, the monthly income level of the participants does not have a statistically significant effect on their sense of belonging, according to the data provided.

CONCLUSION

In this study, the potential effects of different demographic characteristics (gender, age, place of residence, education level, class level, monthly income level) on the sense of belonging were discussed. When we examine each feature in detail, the following conclusions are reached:

Gender: There was no statistically significant difference between men and women in terms of sense of belonging. This shows that gender is not a determining factor in this context.

Age: No significant variance in sense of belonging was observed between different age groups. This indicates that age does not have a dominant effect on this emotional process.

Place of Residence: There was no significant effect of living in a house, apartment or dormitory on the sense of belonging. This indicates that other factors, rather than the type of place where individuals live, may affect their sense of belonging more.

Educational Status: Educational level is the only factor that shows a significant difference in the sense of belonging among the demographic characteristics examined. Individuals at the graduate level may have a lower sense of belonging compared to other levels of education. This may suggest that academic and social pressures brought about by higher education levels may negatively affect individuals' sense of belonging.

Grade Level and Monthly Income: Both grade level and monthly income level do not have a significant effect on the sense of belonging.

In conclusion, it can be said that most demographic factors do not have a dominant effect on this emotional process. However, it has been observed that some factors such as education level can create differences in the sense of belonging. Such findings are important for educational institutions, policy makers, and counselors, as a sense of belonging can have significant effects on individuals' academic success, mental health, and overall quality of life. Therefore, it may be necessary to develop supportive strategies and programs, especially for individuals at higher education levels.

REFERENCES

Alptekin, D. (2011). Toplumsal Aidiyet ve Gençlik: Üniversite Gençliğinin Aidiyeti Üzerine Sosyolojik Bir Araştırma. Doktora Tezi. Selçuk Üniversitesi, Sosyal Bilimler Enstitüsü, Konya.

Çoban, G. S. (2021). Maslow'un İhtiyaçlar Hiyerarşisi kendini gerçekleştirme basamağında gizil yetenekler. European Journal of Educational and Social Sciences, 6 (1), 111 – 118.

Duru, E. (2007). Sosyal Bağlılık Ölçeği'nin Türk Kültürüne Uyarlanması.Eurasian Journal of Educational Research, (26), 85-94.

Ecke, Y.V., Chope, R. C. & Emmelkaamp, P. M. (2006). Bowlby and Bowen: Attachment Theory. Counselling and Clinical Psychology Journal, 3(2).81- 108.

Erşanlı, K., Koçyiğit, M. (2013). Ait Olma Ölçeği'nin Psikometrik Özellikleri. International Periodical For The Languages, Literature and History of Turkish or Turkic 8:751-764

Karip, S., Kesen, N.F. ve Daşbaş, S. (2020). Genç yetişkinlerin kullandıkları duygu stilleri ile aile aidiyetinin ilişkisi üzerine bir araştırma. Toplum ve Sosyal Hizmet, 31(3), 823-848.

Kula, S. & Çakar, B. (2015). Maslow ihtiyaçlar hiyerarşisi bağlamında toplumda bireylerin güvenlik algısı ve yaşam doyumu arasındaki ilişki, Bartın Üniversitesi İ.İ.B.F. Dergisi, 6(12), 191-210.

Levett J T., Lathlean, J., Maguire, J., Mcmillan, M., (2007), "Belongingness: A Critique of The Concept and Implications for Nursing Education", Nurse Education Today, Elsevier Ltd., Vol. 27, s. 210-218.

Mavili, A., Kesen, NF., Daşbaş, S. (2014). Aile Aidiyeti Ölçeği: Bir Ölçek Geliştirme Çalışması, Sosyal Politika Çalışmaları Dergisi (33), 29-45.

Melor,D., Stokes, M., Firth, L., Hayashi, Y., & Commins, R. (2008). Need for belonging, relationship satisfaction, loneliness and life satisfaction. Personality and İndividual Differences, 45, 213–218.

Muyibi AS, Ajayi IO, Irabor AE, Ladipo MA (2010). Relationship between adolescents family function with socio-demographic characteristics and behaviour risk factors in a primary care facility. PHCFM; 2(1):2-7

Uysal M.S, Alıcıoğlu Ö., Tosun, U. (2015). Depresyon Etiyolojisinde Etnik Köken ve Arkadaşlık Örüntülerinin Etkisi. Eleştirel Psikoloji Bülteni. Sayı:6 145-147.

Özgök, A. (2013). Ortaokul Öğrencilerinde Okula Aidiyet Duygusunun Arkadaşlara Bağlılık Düzeyinin ve Empatik Sınıf Atmosferi Algısının İncelenmesi. Yüksek Lisans Tezi. Çukurova Üniversitesi, Sosyal Bilimler Enstitüsü, Adana.

Yusufoğlu Ş. Ö., Cerev G., (2019) Fırat Üniversitesi Sosyal Bilimler Dergisi The Journal of International Social Sciences, cilt: 29 sayı:2, 289-302.

Walsh, P. R (2011), Creating a "values" chain for sustainable development in developing nations: where Maslow meets Porter. Environment, Development and Sustainability, 13(4): 789- 805.

An Insight into Deposition & Processing of High-Resistivity Large-Area Amorphous Selenium Alloy Film Devices for Medical Imaging and High Energy Detection Applications

Cihan ÖNER[1]

Introduction

Amorphous selenium (a-Se) alloys, as a material for high resolution flat panel x-ray detectors, are in high demand for medical imaging applications (Rowlands & Kasap, 1997; Kasap, 2002; Tanaka & Shimakawa, 2011; Frey et al., 2012; Gruner, 2012) such as real-time digital mammography and digital chest radiography (Kasap et al., 2009; Kasap et al., 2011). This is because it can operate at extremely high biasing voltages without undergoing breakdown, while simultaneously maintaining a very low level of dark leakage current due to its high resistive capabilities. Additionally, it is viable to scale up this technology for use in large area detection applications (Kabir & Imam, 2013; Walornyj & Kasap, 2013; Mandal et al., 2013; Fogal & Kasap, 2014; Kabir & Imam, 2014; Kabir & Hijazi, 2014; Kasap et al., 2015; Kabir, 2015).

Amorphous selenium, which is a material sensitive to impurities in the parts per million (ppm) range, cannot be utilized in radiation detection applications due to the fact that commercially available selenium material with 5N (99.999%) purity is not suitable for this purpose. During high electric field operation, the presence of impurities can lead to the formation of detrimental native point defects. These defects can act as trapping or recombination centers, reducing charge carrier collection efficiency. These point defects may also result in charge build up, so impeding the uniformity of the electric response across the detector (Song et al., 1999; Emelianova et al., 2003; Benkhedir et al., 2006). In order to use commercially available Se for radiation detection, it is necessary to perform a purification procedure known as zone refining (ZR) to achieve improved material purities, typically ~7N (Chowdhury, 2019).

Unalloyed a-Se is susceptible to crystallization. To utilize this material for commercial purposes in medical imaging and high energy detector applications, it is imperative to alloy it with different materials to enhance its stability. An effective method for retarding the crystallization of a-Se is to alloying the material with arsenic (As) in the concentration range of 0.3% to 0.6%. By maintaining this range of arsenic quantity, the p-type properties of a-Se are preserved and the crystallization process is prevented. However, as a drawback, this also leads to a reduction in hole lifetime, resulting in a drop in the material's hole properties. In order to address this limitation, a-Se is also combined with chlorine (Cl) in the parts-per-million (ppm) range (Mehta, 2013).

While developing high resolution detectors, it is essential to ensure that the dark current levels remain low, typically about 10^{-11} to 10^{-12} A, even when the detectors are subjected to high bias conditions. The selection of the metal for the top contact in metal/a-Se/metal sandwich structures is crucial in determining the outcome. Although it may be challenging to achieve high Schottky barrier heights on p-type semiconductors, the relatively high work function of a-Se (~5.9 eV) complicates the task of using metals with low φm values to accomplish this goal.

[1] Dr. Öğr. Üyesi, Nevşehir Hacı Bektaş Veli Üniversitesi, Orcid: 0000-0003-4967-9598, cihanoner@nevsehir.edu.tr

Nevertheless, the complex physical properties of a-Se and the uncertain mechanisms of metal/a-Se junctions provide significant challenges in managing the leakage current through the exclusive adjustment of the barrier height (Pak, 2016).

Although the main interest for a-Se is in the areas of medical imaging, primarily in chest radiography and mammographic systems, there are conducted research in pursuit to attract attention to the material in neutron detection applications. The concept primarily depends on lithium and boron doping of a-Se alloys to detect alpha particles that are proxy for thermal neutrons. a-Se in this regard would offer compact, and lightweight detectors compared to the mainstream counterparts (Oner et al., 2015a; Oner et al., 2015b; Pak, 2016; Chowdhury; 2019).

Material Properties

The material choice for nuclear detector depends on how well the material can absorb the incoming ionizing radiation. The process basically follows as the absorption of the ionizing radiation, electron-hole pair generation due to the energy absorbed from the radiation, and transportation of the generated charge carriers to the electrodes from where the nuclear detection measurement systems collect and amplify the pulses. The amplified pulses whose energy level corresponds to the incident radiation then shown in a pulse height spectrum with a gaussian peak that shows the incident radiation interactions.

Hence, the choice of semiconductor material for nuclear detectors must have a large energy bandgap that is higher than 1.5 eV. The reasoning is to tackle the thermal noise in room temperature and elevated temperature applications where a larger bandgap corresponds to a lower thermal noise. While having a large enough energy bandgap is crucial, at the same time a small enough electron-hole pair generation energy is needed for the energy deposited by the incident radiation can generate as much as charge carriers possible. Another must have property is the high resistivity of the material to assure low leakage current levels that will provide low noise as a result. The resistivity levels for the material of choice should be at least 10^{10} Ω-cm.

For the detector to have the ability to stop high energy x-ray and gamma-rays, a material with high density and high atomic number is also peripheral. High thermal conductivity is an important material property which would allow operation at elevated temperatures in return. The material of choice should also be resistant to damage and possess a good level of radiation hardness for which a high atomic displacement energy is needed. Finally, a mobility lifetime product higher than 10^{-3} cm^2/V is expected for low recombination, and high charge collection.

In this regard a-Se offers very low thermal noise due to very high resistivity ~10^{13} Ω-cm. a-Se alloys have an energy bandgap ~2.22 eV at 300K (Kasap et al., 2000) which provides a big electron-hole pair energy for the detector to have low thermal noise at elevated temperature operations while still being able to generate sufficient charge carriers due to the incident radiation. Alloying the a-Se improves the material energy bandgap from 1.74 eV levels to 2.22 eV at room temperature (300K). Even though the electron-hole pair creation energy allows for sufficient charge carriers, it is far less from the ideal case as it is extremely high compared to the bandgap energy (~50 eV). This results in poor charge transport properties in the material such as $\mu\tau_e$ = 1.4 x 10^{-5} cm^2/V (Pak, 2016).

Amorphous selenium has an atomic number of Z = 34 and a density of 4.29 g/cm^3. As the atomic number is not ideal, it has sufficient x-ray stopping ability. Large area films from thin to thick layers up to ~500-micron levels could be deposited with thermal evaporation technique under low growth temperatures (365 – 485) ℃ where the substrate temperatures do not exceed 70 ℃ (Pak, 2016). In overall thermal evaporation technique provides a low-cost deposition capability. Low temperature growth capability of a-Se gives the material a huge advantage over

crystalline semiconductors which usually requires higher temperature profiles for the crystallization happen.

Amorphous structure of a-Se offers high radiation tolerance that renders the material suitable for thermal neutron detection applications. Other properties of the material such as low effective atomic number, and high thermal neutron cross-section also supports this suitability. ^{6}Li and ^{10}B doping on a-Se are being demonstrated to improve the thermal neutron capturing capabilities of a-Se. This doping favors the material with a larger thermal neutron cross-section (940 barns, where 1 barn = 10^{-24} cm^2 for ^{6}Li nucleus, whereas 3840 barns for ^{10}B nucleus). The probability of making small and lightweight handheld detectors using a-Se semiconductors makes this material highly desirable compared to big- bulky gas and scintillator-based neutron detectors (Mitchell, 1936).

Material Purification

Selenium materials that is commercially available are in the range of 4N (99.99%)-5N (99.999%) purity. a-Se is a semiconductor that is highly sensitive to material impurity. The presence of impurities in the crystal reduces the charge transport properties of the semiconductors especially if the semiconductor device made from the material is used under high bias conditions. Under these conditions additional steps for the further purification of the a-Se material is required in order to use it for radiation detection applications.

Zone refining (ZR) method is a technique that is being utilized for semiconductor material purification since 1950's. This technique utilizes the distribution of the impurities differently in liquid and solid phases at equilibrium. This is dependent to the larger solubility of impurities in the liquid phase rather than the solid phase. When one side of the solid in ZR is melted and this molten zone is passed through the other side by moving the heater, the impurities present in the feed material is also passed through by this molten zone. As this process is repeated multiple times, one side of the feed material ends up with clusters of impurities while leaving the rest of the crystal with very high purity. The schematic of the ZR method can be seen in Fig. 1 where a single-zone horizontal furnace is used.

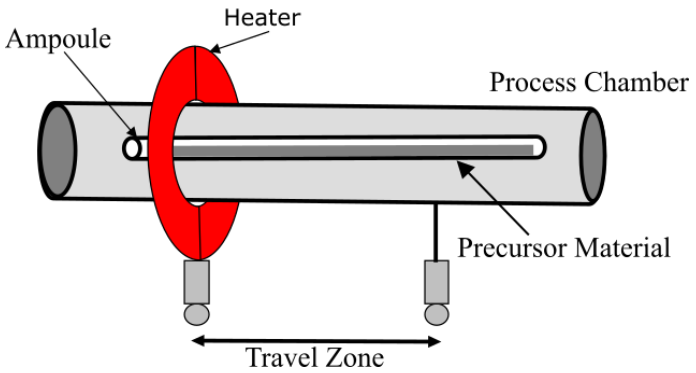

Fig. 1. *The schematic of a generic zone refining setup*

The preparation of the ampoule that is used for the ZR system is also an important step to keep further contamination of the precursor materials. This involves a series of procedure sequentially cleaning of the ampoule to remove any possible contaminants before the refining process. The consequent step is vacuuming and sealing of the ampoule. The temperature of the heater should be above the melting point of selenium (221 ℃), usually in the range of 255 ℃ to 310 ℃. To reach the 7N purity levels, a purification process involving very slow heater movement of ~4-5 cm/hr and multiple passes which corresponds to a total of 30-35 days is required (Oner, 2015b). After the ZR process, a yield of 80% or more with ~7N purity can be obtained where the impurities end up being segregated at one side while extremely high purity

precursor material on the other side of the ampoule. Fig. 2. shows an example of zone refined Se ingots with ~7N purity after the multi-pass ZR process.

Fig. 2. *Zone refined Se ingots (Oner, 2015a)*

Alloying of a-Se

The reason behind choosing amorphous selenium over crystallized selenium for imaging and detection applications lies in the low resistive nature of crystallized selenium which leads to high leakage current in the material. This leads to undesirable background noise in the pulse height spectra. On the other hand, unalloyed a-Se has crystallization proneness. For this specific reason alloying a-Se is a must to stabilize the material. A very effective way of retarding the crystallization of a-Se is to alloy the semiconductor with arsenic (As) which also improve the electron mobility lifetime product. One side effect of alloying with As is that the process reduces the hole mobility lifetime product of the material. To balance the negative effects, further alloying with Chlorine (Cl) is necessary in parts-per-million (ppm) ranges. As a result, Cl alloying compensates the hampering hole mobility lifetime product reduction due to As, in return Cl reduces that of electrons. As a result, a golden ratio of ~0.5% As and ~5 ppm Cl addition is found to improve and optimize the physical and optoelectronic properties of the a-Se alloys (Chowdhury, 2019). Fig. 3. shows a generic schematic of an a-Se alloying reactor.

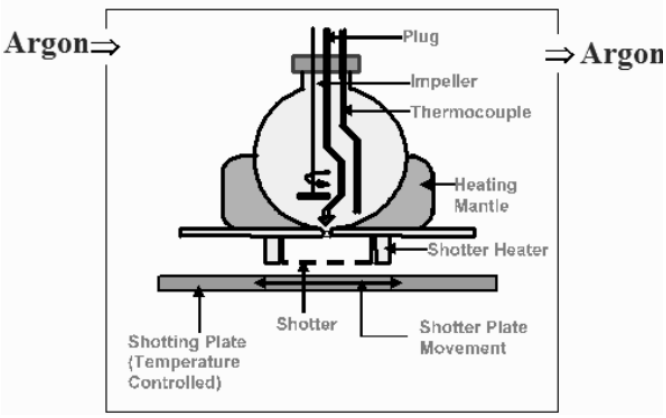

Fig. 3. *Schematic of a generic a-Se alloying reactor (Chowdhury, Oner & Mandal, 2017)*

The alloying reactor needs to operate in an inert argon environment to prevent any kind of contaminations and reactions during the high temperature alloying procedure. The synthesis of Se-As master alloy involves a melt temperature of ~700 ℃ while Se-Cl master alloy melt temperature is ~350 ℃. To synthesize the final alloy mixture, the master alloys are melted in the alloy reactor whose temperature generally raised to ~470 ℃ in about 5 hours of a period. A rotating impeller ensures the homogeneity of the mixed material during the heating periods. After the heating period is complete, the melt is cooled to the temperature levels of ~350 ℃ while the shutter usually kept ~5 ℃ higher than the cooled melt temperatures with a shutter plate temperature of 5-6 ℃. During this procedure when the melt reaches the shutting plate, the

rapid decrease of the temperature results in quenching of the melt and as a result an amorphous phase is formed (Mehta, 2013; Pak, 2016). Fig. 4. Shows an example of a-Se dry pellets with As, and Cl doping.

Fig. 4. *A-Se alloy pellets (Oner et al., 2015a)*

Further ^{6}Li and ^{10}B doping can be added on a-Se alloys using the same alloying reactor process to further render the material for thermal neutron detection. With the high thermal neutron capture cross section of the a-Se alloy as a result of ^{10}B doping, thermal neutrons can be captured by the ^{10}B nucleus. As a result, thermal neutrons undergo a reaction where the reaction produces ^{7}Li and ^{4}He (α) with a combined emitted energy of 2.79 MeV. This kinetic energy is then partially deposited into the crystal lattice and creates electron-hole pairs. A similar reaction is observed when thermal neutrons are captured by the ^{6}Li nucleus. $^{3}H_1$ (tritium) and ^{4}He (α) is produced as a result of this reaction with a combined deposited energy of 4.78 MeV (Pak, 2016; Chowdhury, 2019).

Film Deposition

Thermal Evaporation technique has always been the go-to method for a-Se photoconductive layer deposition. This is a well-studied technique for coating thin layers under vacuum conditions. In this technique the material inside the heated boats is evaporated under vacuum environment. After the opening of the shutter, the evaporated material reaches and condenses on the cold substrates. In order to avoid the oxidation of the grown films, high vacuum to the levels ~10^{-6} torr is necessary inside the deposition chamber. The typical deposition rates of thermal evaporation method are roughly around 1-5 μm/min (Kasap et al., 2009).

Another procedure is increasing the deposition chamber temperatures to ~100 ℃ to avoid any residual gasses or moisture in the chamber environment after the evacuation. The deposition temperatures of the chamber to grow amorphous selenium structure is in between 60 to 65 ℃ (Pak, 2016). The low glass transition temperature (~50 ℃) and the poor thermal conductivity selenium possess makes the grown film prone to crystallization. This results in the requirement of precise substrate temperature control during deposition. A generic schematic of Thermal Evaporation System can be seen in Fig. 5.

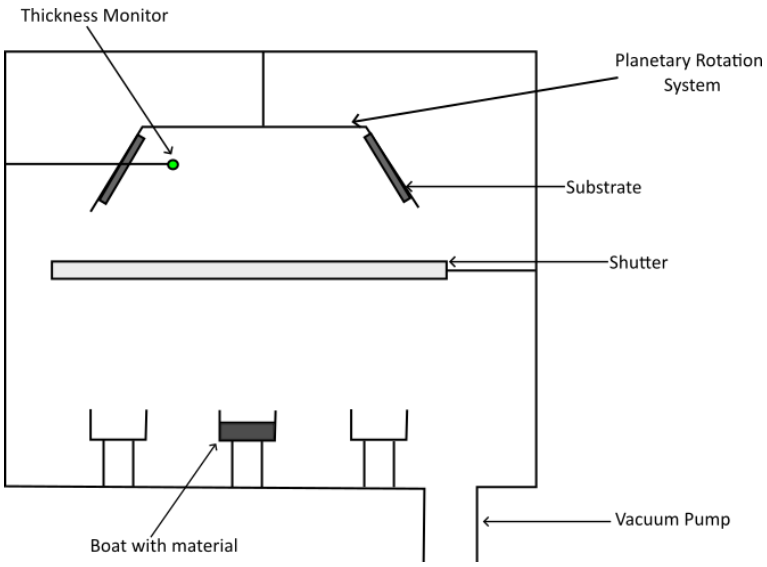

Fig. 5. *Schematic of a generic Thermal Evaporation System*

The system consists of a planetary rotation system that is used for as a substrate holder with rotation capabilities, multiple boats to give system the ability to melt different materials one at a time in case of multiple thin layer growth. In this case only one boat is needed to grown the films. Also, a quartz crystal thickness monitor to keep an eye on the grown film thickness. The working principle of this monitor is either monitoring the thickness or the change in mass of the adhering layers to the surface of a quartz crystal. As last a shutter that is present in the system which ensures the precise control of the deposition by blocking the evaporated material before all the intended conditions meet throughout the system.

The choice of substrate for thermally evaporated a-Se deposition is usually ITO (indium tin oxide) coated glass substrate or oxidized aluminum (Al) substrates. The coated ITO layer in the former substrate acts as the back contact as the sides of the substrate is covered during the growth. This way the a-Se film would not be coated on the sides of the glass, which would be used as the side/back contact. The latter acts as a p-like layer which blocks the injection of electrons from the negative biased electrode, basically acting as an electron blocking layer. As a result, reduce the leakage current. As in the former substrate the front side of the substrate is conducting Al where only the back side is Al2O3 which ensures the use of the sides of the substrate as the side/back contact.

Even though Thermal evaporation is the mostly used deposition technique for a-Se film deposition, there are other methods being employed to deposit the material. One of the techniques is called cathode sputtering where a selenium target is used for the deposition. Vacuum levels of ~10^{-5} torr is at least required for this method. Following the vacuum procedure, an inert gas as argon is introduced to the chamber. The argon plasma is used to bombard the target layer and as a result amorphous selenium starts forming layer by layer on the substrate (Tan, 2006).

Another method used to deposit amorphous selenium films is chemical bath deposition technique. This is a simple technique that can be used to deposit large area films at low cost which does not require high growth temperatures. Chemical bath deposition method uses the process of substrates that are immersed in the dilute solutions which contains the ions of the growth material. As alternative methods are seen to be utilized, commercially available a-Se films for various applications are mostly deposited via thermal evaporation systems (Bindu et al., 2002).

The e-beam evaporation (eBE) technique is another alternative method to thermal evaporation where this method offers a more controllable process as a result of the controlled substrate temperature in this method. In thermal evaporation precise control of chamber temperature and boat temperature is imperative as an event of substrate temperature rise due to source temperature, the a-Se would result in crystallization fairly easily. On the other hand, the eBE technique only heats up the source material during the deposition process which ensures precise control over the substrate and the grown film (Sun et al., 2016).

Device Fabrication

The final step in the making of an a-Se based detector is the contact deposition. The a-Se films have p-type properties with a high work function (φm) of ~5.9 eV. As a result, obtaining high Schottky barrier heights to be able to maintain low dark current under high biasing conditions might become a big issue. On top of this issue, a-Se have unpredictable metal/semiconductor junction mechanisms which results in hardship of controlling the leakage current levels by engineering the barrier height by itself.

Table. 1. *Work Functions of suitable metals for a-Se contact formation*

Metal	**Symbol**	**φm (eV)**	**Metal**	**Symbol**	**φm (eV)**
Gold	Au	5.10 eV	Aluminum	Al	4.28 eV
Silver	Ag	4.26 eV	Molybdenum	Mo	4.37 eV
Nickel	Ni	5.15 eV	Chromium	Cr	4.50 eV
Indium	In	4.12 eV	Tin	Sn	4.42 eV
Tungsten	W	4.55 eV	Zinc	Zn	4.33 eV
Palladium	Pd	5.12 eV	Copper	Cu	4.65 eV

Even though gold (Au) with a work function of 5.1 eV which would result in a relatively lower barrier height compared to metals with lower work functions as can be seen from Table. 1. above, in general Au supplies one of the best diode characteristics with high rectification with ~nA leakage levels up to 1000 V levels of reverse bias conditions for a-Se devices (Pak, 2016). Fig. 6. shows a schematic of a-Se alloy detector with planar contact formation. X-ray imaging applications on the other hand prefer array formation which offer high resolution and high sensitivity in return.

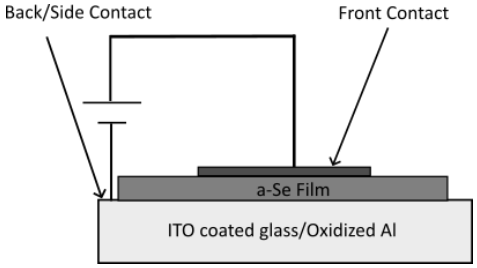

Fig. 6. *A planar a-Se alloy detector*

Applications

Stabilized a-Se alloys have served the mankind for over 20 years as a photoconductor material for photocopy machines, a process known as xerography, until the organic photoconductors replaced the material with their low-cost advantage. More importantly a-Se alloy films are being used as photoreceptors in x-ray imaging that is called xeroradiography.

Modern x-ray imaging systems combine amorphous silicon thin film transistor based active-matrix arrays (AMAs) with a-se technology which changed the flow of xeroradiography into flat panel x-ray imaging. Imaging systems based on a-Se materials is especially highly used in mammography and chest radiology (Brody, 1996; Kasap et al., 2009; Kasap et al., 2011; Huang & Abbaszadeh, 2020).

Apart from commercial imaging and medical imaging, a-Se shows real promise as a high energy radiation detector material. The technology may be preferred for thermal neutron detection, nuclear waste management, and homeland security applications as well due to its favorable material properties.

Conclusion

Amorphous selenium has many advantages over most of the materials preferred in various ionizing radiation detection devices such as very high resistivity 10^{13} Ω-cm, atomic number Z (34) which is high enough to stop x-rays, high thermal neutron cross sections with B-10 and Li-6 doping, low temperature growth with possibility of large area detector films with low-cost. On the other hand, the material shows some disadvantages over its opponents namely, radiation damage at high gamma dosses, low mobility, high electron-hole pair creation energy. Most of the disadvantage could be tackled by engineering some modifications which renders the material as a very high potential detector candidate.

Amorphous selenium possesses the ability to operate at high biasing voltages without succumbing to breakdown, while maintaining minimal dark leakage current, making them indispensable in medical imaging, especially in mammography and chest radiology. Material purification, accomplished through the meticulous zone refining (ZR) process, elevates the purity of commercially available selenium materials to levels suitable for radiation detection. Alloying a-Se with arsenic and chlorine further enhances its stability and properties, ensuring it to retain amorphous structure.

In film deposition, thermal evaporation stands as the go-to method, offering precise control and low crystallization susceptibility. Nevertheless, alternative deposition methods, such as cathode sputtering and chemical bath deposition, e-beam evaporation techniques show promise. The choice of contact metals, notably gold (Au), plays a pivotal role in achieving low leakage current and desirable diode characteristics in a-Se devices. As a result, a-Se alloys have not only revolutionized x-ray imaging but also hold promise in fields like thermal neutron detection, nuclear waste management, and homeland security, thanks to their exceptional material properties.

References

Benkhedir, M., Brinza, M., Qamhieh, N., & Adriaenssens, G. (2006, June). Discrete defect levels in the amorphous selenium bandgap. *Journal of Non-Crystalline Solids*, *352*(9–20), 1543–1546. https://doi.org/10.1016/j.jnoncrysol.2005.10.048

Bindu, K., Lakshmi, M., Bini, S., Kartha, C. S., Vijayakumar, K. P., Abe, T., & Kashiwaba, Y. (2002, February 18). Amorphous selenium thin films prepared using chemical bath deposition: optimization of the deposition process and characterization. *Semiconductor Science and Technology*, *17*(3), 270–274. https://doi.org/10.1088/0268-1242/17/3/316

Brody, T. P. (1996). The birth and early childhood of active matrix — A personal memoir. *Journal of the Society for Information Display*, *4*(3), 113. https://doi.org/10.1889/1.1985000

Chowdhury, T. A. (2019). Fabrication and Characterization of Thin Films for Heterojunction Solar Cells and Radiation Detectors. (Doctoral dissertation). Retrieved from https://scholarcommons.sc.edu/etd/5141

Chowdhury, T. A., Oner, C., & Mandal, K. C. (2017). Synthesis and Characterization of Amorphous Selenium Alloys Radiation Detectors. *IEEE Nuclear Science Symposium and Medical Imaging Conference (NSS/MIC 2017)*, 21-28 Oct 2017, Atlanta, GA, USA, 2017, (pp. 1-5).

Emelianova, E., Qamhieh, N., Brinza, M., Adriaenssens, G., Kasap, S., Johanson, R., & Arkhipov, V. (2003, October). Defect levels and charge carrier photogeneration in amorphous selenium layers. *Journal of Non-Crystalline Solids*, *326–327*, 215–219. https://doi.org/10.1016/s0022-3093(03)00426-5

Fogal, B., & Kasap, S. (2014). Temperature dependence of charge carrier ranges in stabilized a-Se photoconductors. *Canadian Journal of Physics*, *92*(7/8), 634–640. https://doi.org/10.1139/cjp-2013-0524

Frey, J. B., Belev, G., Tousignant, O., Mani, H., Laperriere, L., & Kasap, S. O. (2012). Dark current in multilayer stabilized amorphous selenium based photoconductive x-ray detectors. *Journal of Applied Physics*, *112*(1). https://doi.org/10.1063/1.4730135

Gruner, S. M. (2012). X-ray imaging detectors. *Physics Today*, *65*(12), 29–34. https://doi.org/10.1063/pt.3.1819

Kabir, M. Z. (2015). Dark current mechanisms in amorphous selenium-based photoconductive detectors: an overview and re-examination. *Journal of Materials Science: Materials in Electronics*, *26*(7), 4659–4667. https://doi.org/10.1007/s10854-015-2675-2

Kabir, M. Z., & Hijazi, N. (2014). Temperature and field dependent effective hole mobility and impact ionization at extremely high fields in amorphous selenium. *Applied Physics Letters*, *104*(19). https://doi.org/10.1063/1.4876239

Kabir, M. Z., & Imam, S. A. (2013). Transient and steady-state dark current mechanisms in amorphous selenium avalanche radiation detectors. *Applied Physics Letters*, *102*(15). https://doi.org/10.1063/1.4802840

Kabir, M., & Imam, S. A. (2014). Determination of deep trapping states of the hole blocking layer in multilayer amorphous selenium X-ray detectors using transient dark current analysis. *Canadian Journal of Physics*, *92*(7/8), 641–644. https://doi.org/10.1139/cjp-2013-0536

Kasap, S. O. (2002). Photoreceptors: *The Chalcogenides* Diamond, A., Dekker, M. (Eds.), *The Handbook of Imaging Materials* (2nd ed., 40 pages). New York: CRC Press

Kasap, S. O., Haugen, C., Nesdoly, M., & Rowlands, J. A. (2000, May). Properties of a-Se for use in flat panel X-ray image detectors. *Journal of Non-Crystalline Solids*, *266–269*, 1163–1167. https://doi.org/10.1016/s0022-3093(99)00954-0

Kasap, S., Frey, J. B., Belev, G., Tousignant, O., Mani, H., Greenspan, J., . . . Rowlands, J. A. (2011). Amorphous and Polycrystalline Photoconductors for Direct Conversion Flat Panel X-Ray Image Sensors. *Sensors*, *11*(5), 5112–5157. https://doi.org/10.3390/s110505112

Kasap, S., Frey, J. B., Belev, G., Tousignant, O., Mani, H., Laperriere, L., . . . Rowlands, J. A. (2009). Amorphous selenium and its alloys from early xeroradiography to high resolution X-ray image detectors and ultrasensitive imaging tubes. *Physica Status Solidi (B)*, *246*(8), 1794–1805. https://doi.org/10.1002/pssb.200982007

Kasap, S., Koughia, C., Berashevich, J., Johanson, R., & Reznik, A. (2015). Charge transport in pure and stabilized amorphous selenium: re-examination of the density of states distribution in the mobility gap and the role of defects. *Journal of Materials Science: Materials in Electronics*, *26*(7), 4644–4658. https://doi.org/10.1007/s10854-015-3069-1

Mandal, K. C., Mehta, A., Chaudhuri, S. K., Cui, Y., Groza, M. & Burger, A. "Characterization of amorphous selenium alloy detectors for xrays and high energy nuclear radiation detection," Proc. SPIE 8852, Hard X-Ray, Gamma-Ray, and Neutron Detector Physics XV, 88521O (26 September 2013); https://doi.org/10.1117/12.2027139

Mehta, A. (2013). High Resistivity Amorphous Selenium Alloy Semiconductors For Radiation Detection Applications. (Master's thesis). Retrieved from https://scholarcommons.sc.edu/etd/2412

Mitchell, D. P. (1936, March 15). The Absorption of Neutrons Detected by Boron and Lithium. *Physical Review*, *49*(6), 453–458. https://doi.org/10.1103/physrev.49.453

Oner, C., Nguyen, K. V., Pak, R. O., Chowdhury, T., & Mandal, K. C. (2015b). Investigation of metal contacts on high-resistivity large-area amorphous selenium alloy films. *IEEE Nuclear Science Symposium and Medical Imaging Conference (NSS/MIC 2015)*, 31 Oct-07 Nov 2015, San Diego, CA, USA, 2015b, (pp. 1-6).

Oner, C., Nguyen, K. V., Pak, R. O., Mannan, M. A., Mandal, K. C. (2015a). Investigation of thermally evaporated high resistive B-doped amorphous selenium alloy films and metal contact studies. *SPIE Optical Engineering + Applications*, 13-15 Aug 2015, San Diego, CA, USA, 2015a, (pp. 1-11).

Pak, R. O. (2016). Investigation Of Wide Bandgap Semiconductor Devices For Radiation Detection Applications. (Doctoral dissertation). Retrieved from https://scholarcommons.sc.edu/etd/3930

Rowlands, J., & Kasap, S. (1997). Amorphous Semiconductors Usher in Digital X-Ray Imaging. *Physics Today*, *50*(11), 24–30. https://doi.org/10.1063/1.881994

Song, H. Z., Adriaenssens, G. J., Emelianova, E. V., & Arkhipov, V. I. (1999, April 15). Distribution of gap states in amorphous selenium thin films. *Physical Review B*, *59*(16), 10607–10613. https://doi.org/10.1103/physrevb.59.10607

Sun, H., Zhu, X., Yang, D., Wangyang, P., Gao, X., & Tian, H. (2016, November). An economical method for amorphous selenium thick films preparation: e-beam evaporation. *Materials Letters*, *183*, 94–96. https://doi.org/10.1016/j.matlet.2016.07.084

Tan, W. C. (2006). Optical properties of amorphous selenium films. (Master's thesis). Retrieved from https://harvest.usask.ca/handle/10388/etd-07032006-182757

Tanaka, K., & Shimakawa, K. (2011). *Amorphous Chalcogenide Semiconductors and Related Materials*. Springer Science & Business Media.

Walornyj, M., & Kasap, S. O. (2013). X-ray irradiation induced changes in electron transport in stabilized a-Se photoconductors. *Journal of Applied Physics*, *114*(21). https://doi.org/10.1063/1.4839935

Correlation of Albedo, EVI, NDVI, NDSI and NDBI as indicators of surface urban heat island effect in MODIS imagery

Duygu ARIKAN[1]
Ferruh YILDIZ[2]

1.Introduction

One of the most important environmental problems of the present time is climate change. The increase in greenhouse gases in the atmosphere and the excessive use of natural resources lead to global temperature rise, rising sea levels, and changes in weather patterns (Şekertekin & Marangoz, 2019). Efforts to understand the climate system and identify influencing factors are rapidly continuing in order to address this critical issue (Akdeniz, 2023; Durak & Ayyıldız, 2022).

In this context, surface temperature and urban heat islands constitute a significant focus of climate change research (Akdeniz, 2023). Urban areas house a large portion of the world's population and are rapidly expanding. The development of cities significantly influences local climate, often explained by the phenomenon known as urban heat islands (Durak & Ayyıldız, 2022).

Urban heat islands allude to the idea that cities have hotter temperatures than their rural neighbors. (Elhabodi et al., 2023; Oke, 1982; Yüksel & Yılmaz, 2008). The causes of this temperature increase are complex and result from a combination of factors. The warming effect of concrete and asphalt surfaces, reduced surface reflectivity of buildings, leads to heat gains (Akdeniz, 2023; Yücer, 2023). Factors such as traffic and industrial activities also play a role in the formation of urban heat islands (Elhabodi et al., 2023).

There are many factors that cause Land Surface Temperature (LST) to change both spatially and temporally. This is because land surface comprises vegetation, impervious surfaces, water, and soil composition. Various studies have been conducted using MODIS and Landsat satellite images to determine LST. Researchers have specifically looked at the correlation or relationship between LST and several vegetation indicators. For example, Rasul, Balzter, and Smith (2017) established a strong negative linear correlation with the NDVI index, while Singh, Verma, Chaudhuri, Singh, and Rai (2023) and Schwarz, Schlink, Franck, and Großmann (2012) found relationships with NDVI, NDBI, and air temperature, respectively. Different studies in different regions and times have reported varying results regarding the relationship between LST and NDVI.

Accurately monitoring and analyzing environmental variables and land surface characteristics is of great importance to various scientific and applied disciplines, including geography, environmental science, agriculture, forestry management, climate science, and urban planning. In this context, the indices and indicators developed for measuring and monitoring land surface characteristics and variables provide critical information to researchers and decision-makers. Land surface temperature is important for understanding a region's

[1] Araştırma Görevlisi, Konya Teknik Üniversitesi, Mühendislik ve Doğa Bilimleri Fakültesi, Harita Mühendisliği Bölümü
[2] Profesör, Konya Teknik Üniversitesi, Mühendislik ve Doğa Bilimleri Fakültesi, Harita Mühendisliği Bölümü

microclimate and assessing the impacts of climate change. LST measurements are obtained through thermal remote sensing technologies and meteorological stations.

This study examines the relationship between LST and Albedo, EVI, NDVI, NDBI, and NDSI (Normalized Difference Soil Index). MODIS satellite images were downloaded using the Google Earth Engine platform. Provinces from two different regions of Turkey were selected for the study: Karabük, with the highest forested area in terms of land area, and Iğdır, with the lowest forested area. Data from the years 2013 and 2023 were used to understand temperature differences on the Earth's surface, while data from the year 2023 were used to interpret the relationship between Albedo, EVI, NDVI, NDBI, and NDSI. These indices play a significant role in identifying different features and environmental variables The goal of this investigation is to focus on monitoring and analyzing natural and human-induced processes in both regions through various land surface indices.

The continuation of the article will discuss information related to the selected cities of Karabük and Iğdır for the application, the fundamental principles of each index used in the study, how they are calculated, what type of information they provide, and how data are obtained using which satellite systems.

2.MATERIAL-METHOD

2.1.Study Area

The study area includes two different regions located in different parts of Turkey: Karabük and Iğdır provinces. Karabük is situated in the Black Sea Region of Turkey, while Iğdır is located in the Eastern Anatolia Region. With a land area of 4,074 km², Karabük has the highest forested area among the provinces of Turkey. On the other hand, Iğdır, which is slightly smaller than Karabük with an area that is 0.487 km² less, is one of the provinces in Turkey with the least forested area. The selection of these provinces for the study was primarily based on the number of forested areas in these regions.

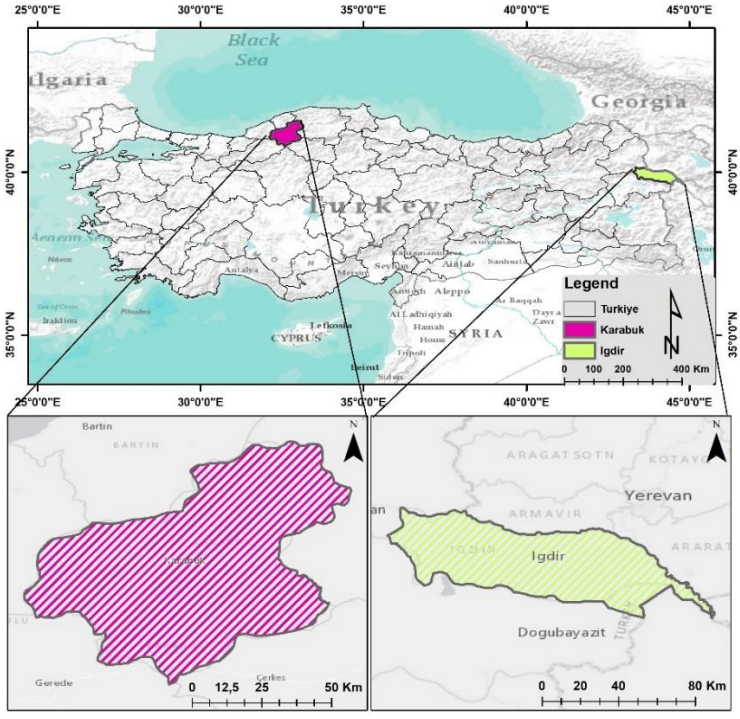

Figure 1. Study Area

2.2.The data used in the study

In this study, data from MODIS satellite imagery have been used. Table 1 contains information for each data point retrieved from the Google Earth Engine (GEE) library. MODIS, a remote sensing device developed by NASA and the United States Geological Survey (USGS), is used to examine the temperature distribution and variations on the Earth's surface in terrestrial regions. The product used in this study, MODIS/006/MYD11A2, is a part of MODIS' Land Surface Temperature (LST) product. This product scans an area of 1200 x 1200 kilometers approximately every 8 days, using data acquired by the Terra and Aqua satellites. The mentioned 8-day period is expressed as the average value for each pixel (Xu et al., 2022).

Table 1. Information about the data used in the research.

Data	Spatial Resolution	Temporal Resolution	Data ID in GEE	Selected Band
LST	1 km	8 days	MODIS/006/MYD11A2	LST_Day_1km
Albedo	500 m	1 day	MODIS/006/MCD43A3	Albedo_BSA_Band1
NDVI	500 m	16 days	MODIS/006/MYD13A1	NDVI
EVI	500 m	16 days	MODIS/006/MYD13A1	EVI
NDBI	500 m	1 day	MODIS/006/MCD43A3	Nadir_Reflectanece_Band2, Nadir_Reflectanece_Band6
NDSI	500 m	1 day	MODIS/006/MCD43A3	Nadir_Reflectanece_Band1, Nadir_Reflectanece_Band4

DVI and EVI vegetation indices from the MYD13A1 V6 product were utilized. These goods are produced using surface reflectance that has been adjusted for the atmosphere. With the use of GEE, the selection of the relevant band automates this process. Alternatively, NDVI and EVI can be calculated using satellite bands separately. Formulas for indices developed by Rouse Jr, Haas, Deering, Schell, and Harlan (1974) and H. Q. Liu and Huete (1995) to reflect the spectral signature of vegetation are provided in Equation 1 and Equation 2.

NDVI and EVI are two distinct vegetation indices used to monitor plant health and determine vegetation density. Both indices fall within the range of -1 to +1.

$$NDVI = \frac{NIR-RED}{NIR+RED} \quad \text{(Equation 1)}$$

$$EVI = G \times \frac{NIR-RED}{NIR+(C_1 \times RED)-(C_2 \times BLUE)+L} \quad \text{(Equation 2)}$$

The variables NIR, representing reflectance in the near-infrared portion (841–876 nm), RED, representing reflectance in the red portion (620–670 nm), and BLUE, representing reflectance in the blue portion (459–759 nm) are present in the equations. The scale factor G, correction constant C1 for red reflectance, and correction constant C2 for blue reflectance are denoted in the equations. Typically, in studies, values of 2.5 for G, 6 for C1, and 7.5 for C2 are used. The value of L is used to enhance observation and is generally set to 1.

Albedo, NDBI, and NDSI indices were calculated from the MCD43A3 V6 product, and corresponding maps were generated. Albedo represents the distribution of solar radiation between the surface and the atmosphere (Sarafanov, Kazakov, Nikitin, & Kalyuzhnaya, 2020; Yücer, 2023). Albedo takes values between 0 and 1 and varies depending on the surface characteristics. It is dimensionless (Yücer, 2023). The Albedo map is produced using Albedo_BSA_Band1, while NDBI and NDSI are calculated using Equations 3 and 4, respectively. The NDBI index is employed for mapping urban or built-up areas using satellite imagery (Ali, Hasim, & Abidin, 2019; Zha, Gao, & Ni, 2003). Both NDBI and NDSI indices

range between -1 and +1. NDSI is utilized to analyze the spectral reflectance of the soil (Liu, Meng, Zhang, & Wu, 2022).

$$NDBI = \frac{B6-B2}{B6+B2} \quad \text{(Equation 3)}$$

$$NDSI = \frac{B1-B4}{B1+B4} \quad \text{(Equation 4)}$$

3.RESULTS

In this study, changes in land surface temperature were monitored, and the factors contributing to these changes were examined. To achieve this goal, two distinct study areas in different regions of Turkey (Karabük and Iğdır) were selected. The LST maps created for the Karabük and Iğdır regions in the years 2013 and 2023 are shown in Figure 2 and Figure 3.

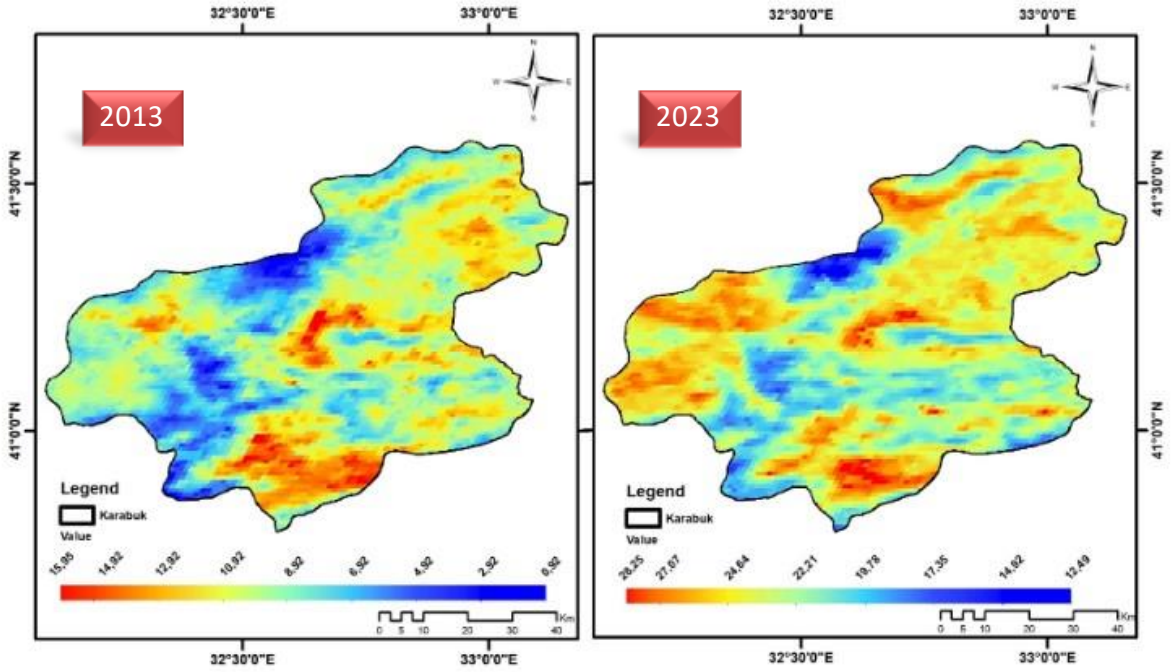

Figure 2. 2013 and 2023 LST maps of Karabük.

As depicted in Figure 2 and Figure 3, It has been determined that the highest temperature in the study area is 28.25°C for Karabük and 41.21°C for Iğdır. In Figure 2, the average temperature in 2013 is approximately 8.92°C, while it is observed to have increased to around 13.5°C in 2023.

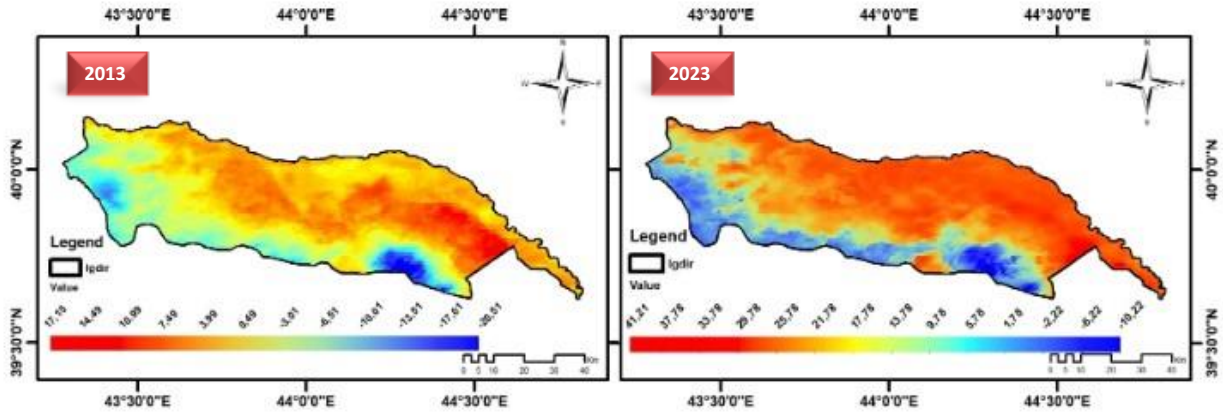

Figure 3. 2013 and 2023 LST maps of Iğdır

When examining the maps for Karabük in the year 2023, it is observed that the average temperature in 2013 was approximately 0.49°C, whereas in 2023, this value increased to around 18.5°C. It can be noted that in a significant portion of the region, the land surface temperature is relatively high.

The relationship between LST, NDVI, EVI, NDBI, NDSI, and Albedo in the year 2023 was investigated. NDVI, EVI, and Albedo maps were directly obtained from satellite imagery, while NDBI and NDSI maps were produced using Equations a and b. The NDVI, EVI, NDBI, NDSI, and Albedo maps generated for the Karabük region are shown in Figure 4, and maps produced for the Iğdır region using the same indices are displayed in Figure 5. After that, correlation analysis was used to look into how the indexes and LST related to one another. A total of 1000 random points were distributed homogeneously across both study areas, and the analysis process was conducted from these points.

When examining the maps for Karabük in the year 2023, it is observed that EVI values range from -0.1038 to 0.6559, NDSI values range from -0.5977 to 0.4762, NDVI values range from -0.2090 to 0.8856, and NDBI values range from -0.8231 to 0.4528. It was found that the albedo values are higher in areas with sparse vegetation and bare soil cover. It can be stated that there is a positive relationship between albedo and LST. Similar results are observed in the NDBI map, as there is an increase in LST in areas covered by soil. This is also applicable to the NDBI map, as higher temperatures are observed in areas with buildings.

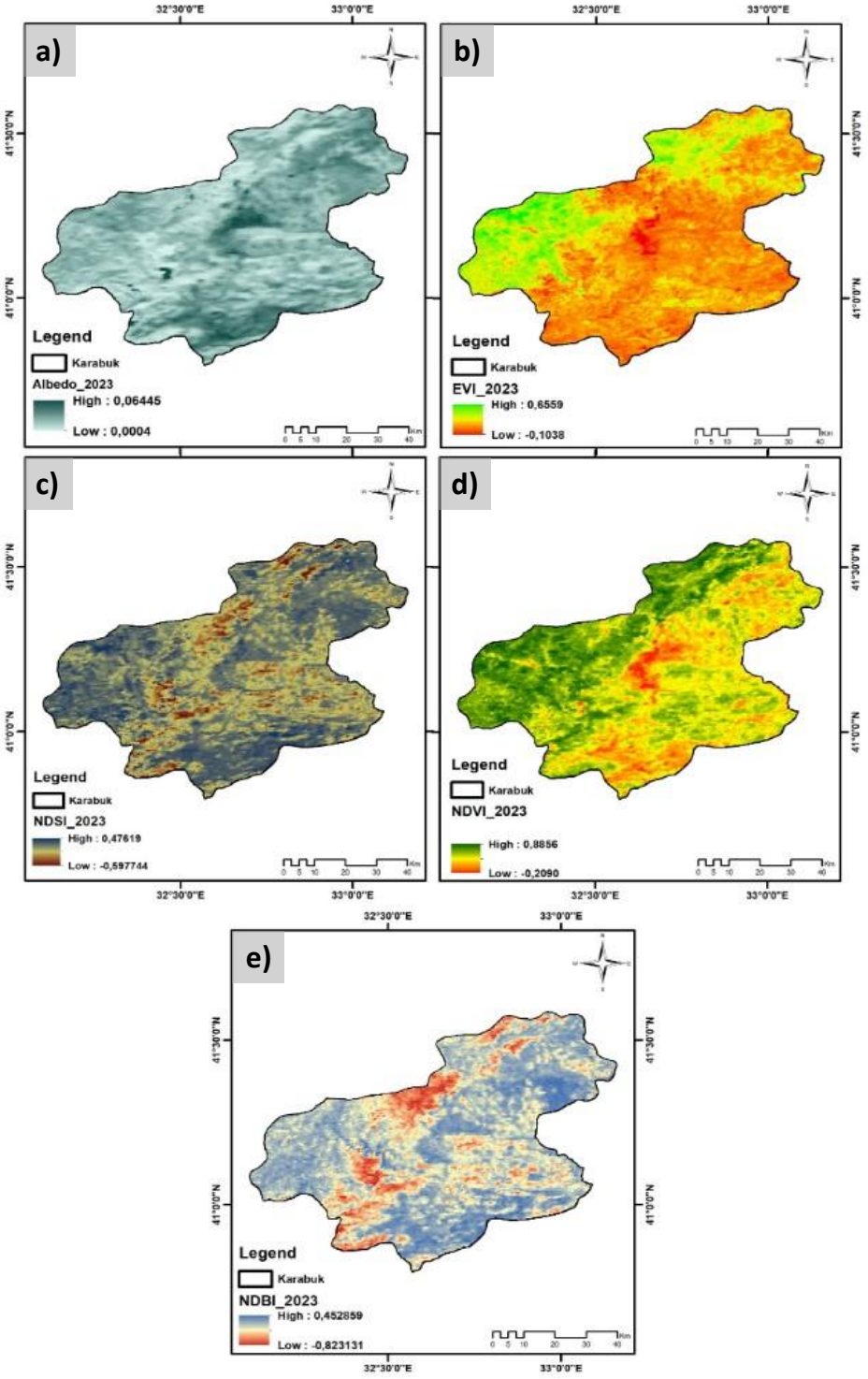

Figure 4. 2023 Albedo (a), EVI (b), NDSI (c), NDVI (d), and NDBI (e) maps of Karabuk

When examining the maps for Iğdır in the year 2023, it is observed that EVI values range from -0.3080 to 0.5014, NDSI values range from -0.4688 to 0.4467, NDVI values range from -0.3450 to 0.6918, and NDBI values range from -0.9475 to 0.5851. It has been determined that in a significant portion of both regions, NDVI and EVI values are below 0.

In Iğdır, vegetation cover is observed at very low levels. This can be understood from Figure 5b and Figure 5d, as areas in red in the EVI and NDVI maps indicate low or unhealthy vegetation cover. While there is a negative relationship between NDVI and EVI with albedo,

there is a positive relationship between NDBI and NDSI. It is observed that NDBI and NDSI maps yield nearly similar results.

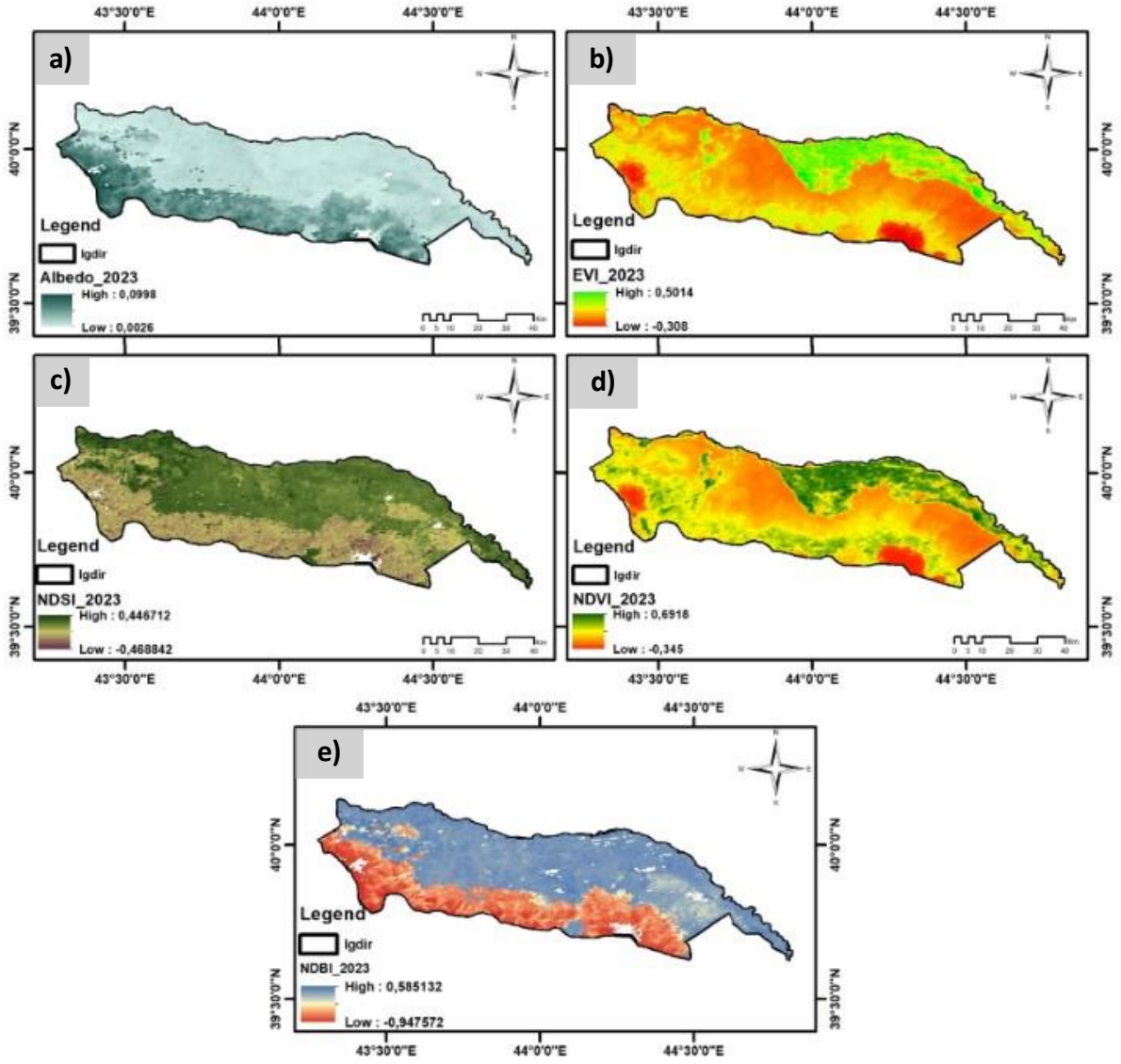

Figure 5. 2023 Albedo (a), EVI (b), NDSI (c), NDVI (d), and NDBI (e) maps of Igdir

Based on the findings obtained from Figure 4 and Figure 5, when comparing the NDVI and EVI maps with the LST map, it is observed that they exhibit a negative correlation. In other words, areas where NDVI and EVI values are negative tend to have higher land surface temperatures, and the opposite is also observed. Additionally, it has been determined that in areas where Albedo, NDBI, and NDSI values are high, LST is also high.

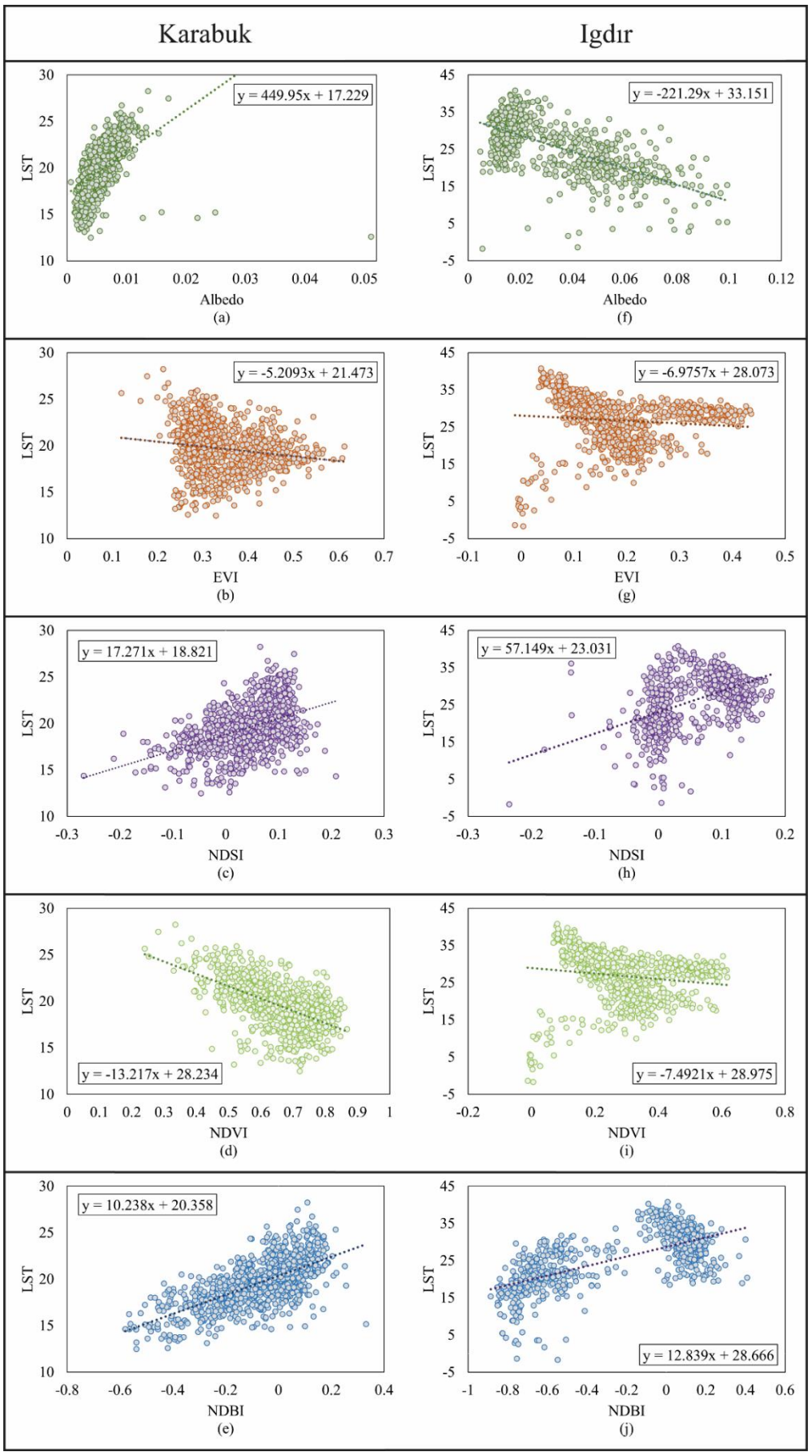

Figure 6. The correlation between LST and another indexes

The correlation analysis results among LST and the other indices (Albedo, EVI, NDSI, NDVI, NDBI) are shown in Figure 6. In Figure 6, a, b, c, d, e represents the values for the Karabük province, while f, g, h, i, j visuals represent the values for Iğdır. The results obtained from the maps are confirmed by correlation coefficients. LST exhibits a negative correlation with NDVI and EVI, while it has a positive correlation with NDSI and NDBI. For Karabük, there is a positive relationship between LST and Albedo, while for Iğdır, a negative relationship is observed. This is primarily attributed to factors such as radiation type, temperature, and precipitation, influenced by seasonal effects in the region. The dominance of higher temperatures in Iğdır compared to Karabük has resulted in the negative relationship.

4.DISCUSSION and CONCLUSIONS

The primary indication of the urban heat island phenomenon is LST, a reflection of surface temperatures. In this study, two different regions with distinct geographical locations, land areas, and forest coverage were selected. Firstly, the temporal changes in land surface temperature were addressed. Secondly, the impact of environmental factors and climate variations on land surface temperature was investigated for the same regions. To achieve this, various indices such as Albedo, EVI, NDVI, NDBI, and NDSI for the year 2023 were downloaded.

The primary feedback in this study revealed that land surface temperature increases over time and is higher in areas with a high building density and limited green spaces in urban centers. According to Yücer (2023), who established a positive correlation between LST and albedo and a negative correlation between albedo and NDVI, dry vegetation and bare soil often have higher albedo than biologically active vegetation. Similarly, it was observed that in areas with low vegetation indices and high levels of urbanization and industrialization, land surface temperatures are high. These relationships are explanatory in terms of the impact of vegetation cover on LST in urban areas.

A strong relationship between LST and NDBI was identified. In areas with buildings, asphalt, and pavement, high NDBI and LST ratios were observed, while in areas with green vegetation, temperature and NDBI indices were lower. Dimoudi et al. (2014) obtained similar results in their study, noting that surface temperatures in urban centers are generally higher than in other areas due to traditional materials (buildings, asphalt, and pavement stones), reaching approximately 50-56°C.

Different results were obtained for the Albedo map in the two regions. While a positive correlation was found between LST and Albedo for Karabük province, a negative correlation was found for Iğdır. Zolotokrylin, Brito-Castillo, and Titkova (2020) stated in their study that seasonal variations, radiation type, temperature, and precipitation affect albedo values. Therefore, proposed solutions in LST studies may vary from region to region due to these factors influenced by the unique geographical characteristics of each region.

In conclusion, the increase in land surface temperature is attributed to factors such as concrete, asphalt, high-rise buildings, increased vehicle numbers, and industrial activities. This leads to a decrease in green areas in cities, resulting in the loss of shade and cooling vegetation. All of these factors contribute to the increase in land surface temperature, exacerbating the effects of climate change and global warming.

To mitigate the effects of LST, collaboration among individuals, communities, and governments is essential. In this regard, activities such as environmental education, energy efficiency incentives, and the development of environmental protection policies are recommended. For example, increasing the number of trees and creating parks in urban and suburban areas can help increase the amount of green space. Reflective materials or vegetation

can be used on building rooftops to reflect sunlight. Practices such as recycling and waste reduction can be adopted to reduce energy consumption, and solar panels can be installed and encouraged in homes and businesses. Infrastructure design can incorporate materials that reduce land surface temperatures.

REFERENCES

Akdeniz, H. (2023). Spatio-Temporal Analysis of the Effects of Urban Growth on Urban Heat Island: Case of Konya, Turkiye. The International Archives of the Photogrammetry, Remote Sensing and Spatial Information Sciences, 48, 441-448.

Ali, M. I., Hasim, A. H., & Abidin, M. R. (2019). Monitoring the built-up area transformation using urban index and normalized difference built-up index analysis. International Journal of Engineering Transactions B: Applications, 32(5), 647-653.

Arıkan, D., & Yıldız, F. (2023). Investigation of urban heat island and carbon monoxide change using Google Earth engine in Konya. Niğde Ömer Halisdemir Üniversitesi Mühendislik Bilimleri Dergisi, 12(4), 1-1.

Dimoudi, A., Zoras, S., Kantzioura, A., Stogiannou, X., Kosmopoulos, P., & Pallas, C. (2014). Use of cool materials and other bioclimatic interventions in outdoor places in order to mitigate the urban heat island in a medium size city in Greece. Sustainable Cities and Society, 13, 89-96.

Durak, Ş., & Ayyıldız, S. (2022). Geleneksel kırsal konutların ekolojik açıdan değerlendirilmesinde bir model denemesi: Yalova örneği. Gazi Üniversitesi Mühendislik Mimarlık Fakültesi Dergisi, 38(1), 85-102.

Elhabodi, T. S., Yang, S., Parker, J., Khattak, S., He, B.-J., & Attia, S. (2023). A review on BIPV-induced temperature effects on urban heat islands. Urban Climate, 50, 101592.

Liang, S., & Shi, P. (2009). Analysis of the relationship between urban heat island and vegetation cover through Landsat ETM+: A case study of Shenyang. Paper presented at the 2009 Joint Urban Remote Sensing Event.

Liu, H. Q., & Huete, A. (1995). A feedback based modification of the NDVI to minimize canopy background and atmospheric noise. IEEE Transactions on Geoscience and Remote Sensing, 33(2), 457-465.

Liu, Y., Meng, Q., Zhang, L., & Wu, C. (2022). NDBSI: A normalized difference bare soil index for remote sensing to improve bare soil mapping accuracy in urban and rural areas. Catena, 214, 106265.

Oke, T. R. (1982). The energetic basis of the urban heat island. Quarterly Journal of the Royal Meteorological Society, 108(455), 1-24.

Rasul, A., Balzter, H., & Smith, C. (2017). Applying a normalized ratio scale technique to assess influences of urban expansion on land surface temperature of the semi-arid city of Erbil. International journal of remote sensing, 38(13), 3960-3980.

Rouse Jr, J., Haas, R. H., Deering, D., Schell, J., & Harlan, J. C. (1974). Monitoring the vernal advancement and retrogradation (green wave effect) of natural vegetation. Retrieved from

Sarafanov, M., Kazakov, E., Nikitin, N. O., & Kalyuzhnaya, A. V. (2020). A machine learning approach for remote sensing data gap-filling with open-source implementation: An example regarding land surface temperature, surface albedo and NDVI. Remote Sensing, 12(23), 3865.

Schwarz, N., Schlink, U., Franck, U., & Großmann, K. (2012). Relationship of land surface and air temperatures and its implications for quantifying urban heat island indicators—An application for the city of Leipzig (Germany). Ecological indicators, 18, 693-704.

Singh, P., Verma, P., Chaudhuri, A., Singh, V., & Rai, P. (2023). Evaluating the relationship between Urban Heat Island and temporal change in land use, NDVI and NDBI: a case study of Bhopal city, India. International Journal of Environmental Science and Technology, 1-12.

Şekertekin, A., & Marangoz, A. M. (2019). Zonguldak metropolitan alanındaki arazi kullanımı arazi örtüsünün yer yüzey sıcaklığına etkisi. Geomatik, 4(2), 101-111.

Xu, X., Zhang, X., Riley, W. J., Xue, Y., Nobre, C. A., Lovejoy, T. E., & Jia, G. (2022). Deforestation triggering irreversible transition in Amazon hydrological cycle. Environmental research letters, 17(3), 034037.

Yücer, E. (2023). Albedo, Yer Yüzey Sıcaklığı ve NDVI Arasındaki İlişkinin Landsat-7 ve Landsat-8 Uydu Verileri Kullanılarak İncelenmesi: Safranbolu Örneği. Kahramanmaraş Sütçü İmam Üniversitesi Mühendislik Bilimleri Dergisi, 26(1), 177-190.

Yüksel, Ü. D., & Yılmaz, O. (2008). Ankara kentinde kentsel isi adasi etkisinin yaz aylarinda uzaktan algilama ve meteorolojik gözlemlere dayali olarak saptanmasi ve değerlendirilmesi. Gazi Üniversitesi Mühendislik Mimarlık Fakültesi Dergisi, 23(4).

Zha, Y., Gao, J., & Ni, S. (2003). Use of normalized difference built-up index in automatically mapping urban areas from TM imagery. International journal of remote sensing, 24(3), 583-594.

Zhang, Z., Ji, M., Shu, J., Deng, Z., & Wu, Y. (2008). Surface urban heat island in Shanghai, China: Examining the relationship between land surface temperature and impervious surface fractions derived from Landsat ETM+ imagery. Int. Arch. Photogramm. Remote Sens. Spat. Inf. Sci, 37, 601-606.

Zolotokrylin, A. N., Brito-Castillo, L., & Titkova, T. B. (2020). Local climatically-driven changes of albedo and surface temperatures in the Sonoran Desert. Journal of Arid Environments, 178, 104147.

Some Convergence Results of Iteratıon Scheme For $G-$ Asymptotically Nonexpansiveness

Esra YOLAÇAN[1]

Introduction and Preliminaries

Let $\eta \neq \emptyset$ be a subset of a Banach space X. A digraph is a pair: $G = (V(G), E(G))$, here $V(G)$ is the set of vertices of graph and $E(G)$ is the set of its edges which encapsules all the loops, i.e. $(p,p) \in E(G)$ for $\forall p \in V(G)$. Supposing G has no parallel edges. If p and q be vertices of G, then a path on G from p through q of length N is $\{p_i\}_{i=0}^{N}$ of $N+1$ vertices such that $p_0 = p$, $p_N = p$ and $(p_{i-1}, p_i) \in E(G)$ for $i = 1, \cdots, N$. A digraph G is called to be transitive if, for any $p, h, l \in V(G)$ such that $(p,h), (h,l) \in E(G)$, we have $(p,l) \in E(G)$.

The map $f: \eta \to \eta$ is called to be

- $G-$*nonexpansive* if it provides (i) $(p,l) \in E(G) \Rightarrow (fp, fl) \in E(G)$ (f preserves edges of G), (ii) $(p,l) \in E(G) \Rightarrow \|fp - fl\| \leq \|p - l\|$ (Alfuraidan&Khamsi, 2015);
- $G-$continuous if for any given $\tau \in X, \{\tau_n\} \subseteq X$, $\tau_n \longrightarrow \tau$ and $(\tau_n, \tau_{n+1}) \in E(G)$ imply $f\tau_n \to f\tau$ (Jachymski, 2008);
- $semicompact$ if for $\{x_n\} \subseteq \eta$ with $\|x_n - fx_n\| \to 0$ as $n \to \infty$, there exists a subsequence $\{x_{n_i}\}$ of $\{x_n\}$ such that $x_{n_i} \to \sigma_* \in \eta$ (Shahzad&Al-Dubiban, 2006);
- $G-$ *asymptotically nonexpansive* if it provides (i) f preserves edges of G, (ii) there exists a sequence $\phi_n \subset [1, \infty), \phi_n \to 1$ as $n \to \infty$ such that $\|f^n p - f^n l\| \leq \phi_n \|p - l\|$, whenever $(p,l) \in E(G)$ for any $p, l \in \eta$ and $n \geq 1$ (Sangago & et al., 2018).

Fixed point (brief, *FP*) iterative process for $G-$nonexpansiveness maps in Banach spaces with a graph (brief, *BSWG*) including Ishikawa, $S-$iteration, explicit iteration, $SP-$iteration schemes have been intensively investigated by various researchers (Tripak, 2016), (Suparatulatorn& et al., 2018), (Hunde& et al., 2017), (Sridarat& et al., 2018). The authors established the class of $G-$asymptotically nonexpansiveness maps, who verified some convergence results in *BSWG* (Sangago & et al., 2018).

The mapping $f: \eta \to \eta$ is called to yield *Condition (A)* if there is a nondecreasing function $g: [0, \infty) \to [0, \infty)$ with $g(t) > 0$ for $\forall t \in (0, \infty)$, $g(0) = 0$ such that $\|x - fx\| \geq g\left(d\left(x, F(f)\right)\right)$. Two mappings $f_1, f_2: \eta \to \eta$ are called to yield *Condition (B)* if there is a nondecreasing function $g: [0, \infty) \to [0, \infty)$ with $g(t) > 0$ for $\forall t \in (0, \infty)$, $g(0) = 0$ such that $max\{\|x - f_1 x\|, \|x - f_2 x\|\} \geq g\left(d\left(x, Fix(F)\right)\right)$, where $Fix(F) = F(f_1) \cap F(f_2)$. The mappings $f_1, f_2, f_3: \eta \to \eta$ are called to yield *Condition (C)* if there is a nondecreasing function $g: [0, \infty) \to [0, \infty)$ with $g(t) > 0$ for $\forall t \in (0, \infty)$, $g(0) = 0$ such that $max\{\|x - f_1 x\|, \|x - f_2 x\|, \|x - f_3 x\|\} \geq g\left(d\left(x, Fix(F)\right)\right)$, where $Fix(F) = F(f_1) \cap F(f_2) \cap F(f_3)$.

Let $p_0 \in V(G)$ and $V(G) \supseteq \Gamma$. We call that (i) Γ is dominated by p_0 if $(p_0, p) \in E(G)$ for $\forall p \in \Gamma$, (ii) Γ dominates p_0 if for each $p \in \Gamma$, $(p_0, p) \in E(G)$ (Suparatulatorn& et al., 2018).

[1] Assistant Professor Doctor, Cappadocia University, School of Applied Sciences, Department of Airframe and Powerplant Maintenence, Mustafapasa Campus, Ürgüp, Nevşehir, Türkiye yolacanesra@gmail.com , ORCID: 0000-0002-1655-0993

Let $\eta \neq \emptyset \subseteq X$, $f: \eta \longrightarrow X$ be a map. Then is called to be $G - demiclosed$ at $q^* \in X$ [14] if, for any $\{x_n\} \subseteq \eta$ such that $\{x_n\} \rightharpoonup p^* \in \eta$, $\{fx_n\} \to q^*$ and $(x_n, x_{n+1}) \in E(G)$ imply $fp^* = q^*$.

Let $\eta \neq \emptyset \subseteq X$, $G = (V(G), E(G))$ be digraph such that $V(G) = \eta$. Here η is called to own *Property P* if for each $\{p_n\} \subseteq \eta$ such that $\{p_n\} \rightharpoonup p \in \eta$, $(p_n, p_{n+1}) \in E(G)$, there is a subsequence $\{p_{n_l}\}$ of $\{p_n\}$ such that $(p_{n_l}, p) \in E(G)$ for $\forall l \in N$ (Alfuraidan, 2015).

Remark 1. If G is transitive, then *Property P* is equivalence to the feature:

- If $\{p_n\} \subseteq \eta$ with $(p_n, p_{n+1}) \in E(G)$ such that for any subsequence $\{p_{n_l}\}$ of $\{p_n\}$ converging weakly to p in X, then $(p_n, p) \in E(G)$ for $\forall n \in N$ (Sridarat& et al., 2018).

The authors considered the following modified Ishikawa process, for arbitrary $x_0 \in \eta$,

$$x_{n+1} = (1 - a_n)fx_n + a_n f\big((1 - b_n)x_n + b_n fx_n\big), n \geq 1,$$

where $\{a_n\}, \{b_n\} \subset (0,1)$ (Agarwal & et al., 2007).

The authors introduced the following iteration scheme, for arbitrary $x_0 \in \eta$,

$$\begin{aligned} x_{n+1} &= (1 - a_n)fy_n + a_n fz_n, \\ y_n &= (1 - b_n)fx_n + b_n fz_n, \\ z_n &= (1 - c_n)x_n + c_n fx_n \; n \geq 1, \end{aligned}$$

where $\{a_n\}, \{b_n\}, \{c_n\} \subset (0,1)$ (Abbas&Nazir, 2014).

The authors studied an iterative process, for arbitrary $x_0 \in \eta$,

$$\begin{aligned} x_{n+1} &= (1 - a_n)fx_n + a_n fy_n, \\ y_n &= (1 - b_n)z_n + b_n fz_n, \\ z_n &= (1 - c_n)x_n + c_n fx_n \, , n \geq 1, \end{aligned}$$

where $\{a_n\}, \{b_n\}, \{c_n\} \subset (0,1)$ (Thakur& et al, 2014).

Motivated by above studies, in this writing we consider an iterative procedure for providing a common fixed point of three $G -$ asymptotically nonexpansive maps as follows:

For arbitrary $x_0 \in \eta$, $\{x_n\}$ defined by

$$\begin{aligned} x_{n+1} &= (1 - a_n)f_2^n x_n + a_n f_3^n y_n \\ y_n &= (1 - b_n)z_n + b_n f_2^n z_n, \\ z_n &= (1 - c_n)x_n + c_n f_1^n x_n \; n \geq 1, \end{aligned} \tag{1.1}$$

where $\{a_n\}, \{b_n\}, \{c_n\} \subset (0,1)$.

Lemma 1. Let $\{\tau_n\}$, $\{\upsilon_n\}, \{\varrho_n\}$ be sequences of nonnegative real numbers supplying the inequality

$$\tau_{n+1} \leq (1 + \varrho_n)\tau_n + \upsilon_n, n \geq 1$$

if $\sum_{n=1}^{\infty} \upsilon_n < \infty$ and $\sum_{n=1}^{\infty} \varrho_n < \infty$, then

(i) $\lim_{n\to\infty} \tau_n$ exists;

(ii) Notedly, if $\{\tau_n\}$ hold a subsequence $\{\tau_{n_k}\} \to 0$, then $\lim_{n\to\infty} \tau_n = 0$ (Tan&Xu,1993).

Lemma 2. Let X be a uniformly convex Banach space. Supposing $n \geq 1$, $1 > c \geq t_n \geq b > 0$. Let $\{e_n\}, \{h_n\} \subseteq X$ be such that $limsup_{n\to\infty}\|e_n\| \leq a$, $limsup_{n\to\infty}\|h_n\| \leq a$, $\|(1 - t_n)h_n + t_n e_n\| \to a \geq 0$ as $n \to \infty$. Then $\|e_n - h_n\| \to 0$ as $n \to \infty$ (Sahu, 1991).

Lemma 3. Let f be a $G-$asymptotically nonexpansiveness map in η with asymptotic coefficient ϕ_n such that $\sum_{n=1}^{\infty}(\phi_n - 1) < \infty$. Assume that η has the Property P, then $I - f$ if $G-$demiclosed at 0 (Sangago & et al., 2018).

Lemma 4. Let $\{x_n\}$ be a bounded sequence in reflexive Banacah space X. If for any weakly convergent subsequence $\{x_{n_j}\}$ of $\{x_n\}$, both $\{x_{n_j}\}$ and $\{x_{n_{j+1}}\}$ converge weakly to the same point in X, then $\{x_n\}$ is weakly convergent (Shahzad&Al-Dubiban, 2006).

The goal of this writing is to furnish a three step iterative procedure to approach of *FP* of the $G-$ asymptotically nonexpansiveness in *BSWG* and to demonstrate weak and strong convergence results for the proposed maps.

Main Results

Note that $\eta \neq \emptyset \subset X$ is a closed subset of Banach space via $(V(G), E(G)) = G$ such that $V(G) = \eta$, convex of $E(G)$ and transitive of G. The mappings $f_1, f_2, f_3 : \eta \to \eta$ are $G-$ asymptotically nonexpansiveness maps via $\{\phi_n^{(i)}\} \subset [1, \infty)$ satisfying $\sum_{n=1}^{\infty}(\phi_n^{(i)} - 1) < \infty$ for $i = 1,2,3$, resp. Take $\phi_n = max\{\phi_n^{(1)}, \phi_n^{(2)}, \phi_n^{(3)}\}$ then clearly $\sum_{n=1}^{\infty}(\phi_n - 1) < \infty$. Henceforward we will get the sequence $\{\phi_n\}$ for $\{f_1, f_2, f_3\}$ and $Fix(F) = F(f_1) \cap F(f_2) \cap F(f_3) \neq \emptyset$. For $x_0 \in \eta$, let the sequence $\{x_n\}$ identified by (1.1).

Proposition 1. Let $s^* \in Fix(F)$ be such that $(x_0, s^*), (s^*, x_0) \in E(G)$. Then (x_n, s^*), (s^*, x_n), $(x_n, z_n), (z_n, x_n)$, (s^*, z_n), (z_n, s^*), $(x_n, y_n), (y_n, x_n), (s^*, y_n)$, $(y_n, s^*), (x_n, x_{n+1}) \in E(G)$ for $\forall n \in N$.

Proof. Let $(x_0, s^*) \in E(G)$. We have $(f_1 x_0, s^*) \in E(G)$ in connection with edge preserving of f_1. Since $E(G)$ is convex, we get

$$\begin{aligned}(1 - c_0)(x_0, s^*) + c_0(f_1 x_0, s^*) &= \big((1 - c_0)x_0 + c_0 f_1 x_0, s^*\big) \\ &= (z_0, s^*) \in E(G).\end{aligned}$$

We hold $(f_2 z_0, s^*) \in E(G)$ on the score of edge-preserving f_2. As $(z_0, s^*), (f_2 z_0, s^*) \in E(G)$, $E(G)$ is convex, we have

$$\begin{aligned}(1 - b_0)(z_0, s^*) + b_0(f_2 z_0, s^*) &= \big((1 - b_0)z_0 + b_0 f_2 z_0, s^*\big) \\ &= (y_0, s^*) \in E(G).\end{aligned}$$

By edge-preserving f_2 and f_3, we own $(f_2 x_0, s^*), (f_3 y_0, s^*) \in E(G)$, resp. Due to the convexity of $E(G)$, we obtain

$$\begin{aligned}(1 - a_0)(f_2 x_0, s^*) + a_0(f_3 y_0, s^*) &= \big((1 - a_0)f_2 x_0 + a_0 f_3 y_0, s^*\big) \\ &= (x_1, s^*) \in E(G).\end{aligned}$$

Because of the $\{f_1, f_2, f_3\}$ are edge preserving, we enjoy edge preserving of $\{f_1^2, f_2^2, f_3^2\}$. Thereof, changing (x_1, s^*) in lieu of (x_0, s^*) and $\{f_1^2, f_2^2, f_3^2\}$ in lieu of $\{f_1, f_2, f_3\}$ in above procedure, we get

$$(z_1, s^*), (y_1, s^*) \in E(G) \text{ and } (x_2, s^*) \in E(G).$$

Assume that $(x_u, s^*) \in E(G)$ for $u \in N$. By virtue of the fact that $\{f_1, f_2, f_3\}$ are edge preserving, we acquire edge preserving of $\{f_1^u, f_2^u, f_3^u\}$, and thus $(f_1^u x_u, s^*) \in E(G)$, from the convexity of $E(G)$, we have

$$\begin{aligned}(1 - c_u)(x_u, s^*) + c_u(f_1^u x_u, s^*) &= \big((1 - c_u)x_u + c_u f_1^u x_u, s^*\big) \\ &= (z_u, s^*) \in E(G).\end{aligned}$$

We possess $(f_2^u z_u, s^*) \in E(G)$ in view of edge-preserving f_2^u. Since $(z_u, s^*), (f_2^u z_u, s^*) \in E(G)$, $E(G)$ is convex, we get

$$\begin{aligned}(1-b_u)(z_u, s^*) + b_u(f_2^u z_u, s^*) &= \left((1-b_u)z_u + b_u f_2^u z_u, s^*\right)\\ &= (y_u, s^*) \in E(G).\end{aligned}$$

On account of edge-preserving f_2^u and f_3^u, we own $(f_2^u x_u, s^*), (f_3^u y_u, s^*) \in E(G)$, resp. As $E(G)$ is convex, we obtain

$$\begin{aligned}(1-a_u)(f_2^u x_u, s^*) + a_u(f_3^u y_u, s^*) &= \left((1-a_u)f_2^u x_u + a_u f_3^u y_u, s^*\right)\\ &= (x_{u+1}, s^*) \in E(G).\end{aligned}$$

Resuming the process for $(x_{u+1}, s^*) \in E(G)$, we conclude that

$$(z_{u+1}, s^*), (y_{u+1}, s^*) \in E(G).$$

Hence, by mathematical induction, we obtain that

$$(y_n, s^*), (x_n, s^*), (z_n, s^*) \in E(G) \text{ for } n \in N.$$

Handling an analogue assertion, we could indicate that $(s^*, x_n), (s^*, z_n), (s^*, y_n) \in E(G)$ for $n \in N$, under the supposition that $(s^*, x_0) \in E(G)$. Owing to transitivity of G, we have (x_n, z_n), (z_n, x_n), (x_n, y_n), (y_n, x_n) and $(x_n, x_{n+1}) \in E(G)$ for $n \geq 1$.

Lemma 5. Let X and G be as above. Let $\eta \neq \emptyset$ is a closed convex subset of a real uniformly convex Banach space X. Let $f_1, f_2, f_3 : \eta \to \eta$ are $G-$ asymptotically nonexpansive mappings with $\{\phi_n\} \subset [1, \infty)$ providing $\sum_{n=1}^{\infty}(\phi_n - 1) < \infty$. Assume that $\{x_n\}$ given by (1.1), here $\{a_n\}$, $\{b_n\}, \{c_n\} \subset [\xi, 1-\xi]$ for some $\xi \in (0,1)$ and $(x_0, s^*), (s^*, x_0) \in E(G)$ for $x_0 \in \eta$ and $s^* \in Fix(F)$, then

(i) $\lim_{n\to\infty} \|x_n - s^*\|$ exists;
(ii) $\lim_{n\to\infty} \|x_n - f_i x_n\| = 0$ for $i = 1,2,3$.

Proof. (i) Let $s^* \in Fix(F)$. By Proposition 1, (x_n, s^*), (s^*, x_n), $(x_n, z_n), (z_n, x_n)$, (s^*, z_n), (z_n, s^*), $(x_n, y_n), (y_n, x_n), (s^*, y_n)$, $(y_n, s^*)(x_n, x_{n+1})$ are in $E(G)$ for $\forall n \in N$.
From (1.1) and $G-$ asymptotically nonexpansiveness of f_1, we have

$$\begin{aligned}\|z_n - s^*\| &\leq (1-c_n)\|x_n - s^*\| + c_n\|f_1^n x_n - s^*\| \\ &\leq (1-c_n)\|x_n - s^*\| + c_n\phi_n\|x_n - s^*\| \\ &= \{1 + c_n(\phi_n - 1)\|x_n - s^*\|\} \\ &\leq \phi_n\|x_n - s^*\|.\end{aligned} \tag{2.1}$$

It follows from (1.1)&(2.1), $G-$ asymptotically nonexpansiveness of f_2 that we get

$$\begin{aligned}\|y_n - s^*\| &\leq (1-b_n)\|z_n - s^*\| + b_n\|f_2^n z_n - s^*\| \\ &\leq \phi_n\|z_n - s^*\| \leq \phi_n^2\|x_n - s^*\|.\end{aligned} \tag{2.2}$$

Using (1.1)&(2.2), $G-$ asymptotically nonexpansiveness of f_2 and f_3, we have

$$\begin{aligned}\|x_{n+1} - s^*\| &\leq (1-a_n)\|f_2^n x_n - s^*\| + a_n\|f_3^n y_n - s^*\| \\ &\leq \phi_n^3\|x_n - s^*\| \\ &= \{1 + (\phi_n^3 - 1)\}\|x_n - s^*\|.\end{aligned} \tag{2.3}$$

By virtue of $0 \leq \alpha^t - 1 \leq t\alpha^{t-1}(\alpha - 1)$ for all $\alpha \geq 1$, the hypothesis $\sum_{n=1}^{\infty}(\phi_n - 1) < \infty$ implies that $\{\phi_n\}$ is bounded, then $\phi_n \in [1, Q]$ for some Q and $\forall n \geq 1$. Thus, $\phi_n^3 - 1 \leq 3Q^2(\phi_n - 1)$ for $\forall n \geq 1$. Hereat, $\sum_{n=1}^{\infty}(\phi_n^3 - 1) < \infty$. Due to Lemma 1, we find out that $\lim_{n\to\infty} \|x_n - s^*\|$ exists.

(ii) From hypothesis (i), $\lim_{n\to\infty}\|x_n - s^*\|$ exists. Assume that $\lim_{n\to\infty}\|x_n - s^*\| = w$. If $w = 0$, the conclusion is apparent. Suppose $w > 0$. By (2.1)&(2.2), we get

$$limsup_{n\to\infty}\|z_n - s^*\| \le w, \tag{2.4}$$
$$limsup_{n\to\infty}\|y_n - s^*\| \le w. \tag{2.5}$$

Hence,

$$\begin{aligned}\|f_1^n x_n - s^*\| &\le \phi_n\|x_n - s^*\|,\\ \|f_2^n z_n - s^*\| &\le \phi_n\|z_n - s^*\|,\\ \|f_2^n x_n - s^*\| &\le \phi_n\|x_n - s^*\|,\\ \|f_3^n y_n - s^*\| &\le \phi_n\|y_n - s^*\|,\end{aligned}$$

for $\forall n \ge 1$ implies that

$$limsup_{n\to\infty}\|f_1^n x_n - s^*\| \le w, \tag{2.6}$$
$$limsup_{n\to\infty}\|f_2^n z_n - s^*\| \le w. \tag{2.7}$$
$$limsup_{n\to\infty}\|f_2^n x_n - s^*\| \le w, \tag{2.8}$$
$$limsup_{n\to\infty}\|f_3^n y_n - s^*\| \le w. \tag{2.9}$$

On account of

$$w = \lim_{n\to\infty}\|x_{n+1} - s^*\| = \lim_{n\to\infty}\|(1-a_n)(f_2^n x_n - s^*) + a_n(f_3^n y_n - s^*)\|$$

by Lemma 2, we have

$$\lim_{n\to\infty}\|f_2^n x_n - f_3^n y_n\| = 0. \tag{2.10}$$

Noting that

$$\begin{aligned}\|x_{n+1} - s^*\| &= \|(1-a_n)f_2^n x_n + a_n f_3^n y_n - s^*\|\\ &\le \|f_2^n x_n - s^*\| + a_n\|f_3^n y_n - f_2^n x_n\|\\ &\le \|f_2^n x_n - s^*\| + [1-\xi]\|f_3^n y_n - f_2^n x_n\|\end{aligned}$$

which yields that

$$w \le liminf_{n\to\infty}\|f_2^n x_n - s^*\|. \tag{2.11}$$

By (2.8)&(2.11), we obtain

$$\lim_{n\to\infty}\|f_2^n x_n - s^*\| = w \tag{2.12}$$

Furthermore, from (2.10)&(2.12) and, $G-$ asymptotically nonexpansiveness of f_3

$$\begin{aligned}\|f_2^n x_n - s^*\| &\le \|f_2^n x_n - f_3^n y_n\| + \|f_3^n y_n - s^*\|\\ &\le \|f_2^n x_n - f_3^n y_n\| + \phi_n\|y_n - s^*\|\end{aligned}$$

implies that

$$w \le liminf_{n\to\infty}\|y_n - s^*\|. \tag{2.13}$$

By (2.5)&(2.13), we get

$$\lim_{n\to\infty}\|y_n - s^*\| = w \tag{2.14}$$

Since

$$w = \lim_{n\to\infty}\|y_n - s^*\| = \lim_{n\to\infty}\|(1-a_n)(z_n - s^*) + a_n(f_2^n z_n - s^*)\|.$$

By (2.4)&(2.7) and Lemma 2, we get

$$\lim_{n\to\infty}\|z_n - f_2^n z_n\| = 0. \tag{2.15}$$

Noting that

$$\begin{aligned}\|y_n - s^*\| &= \|(1-b_n)z_n + b_n f_2^n z_n - s^*\| \\ &\le \|z_n - s^*\| + b_n\|f_2^n z_n - z_n\| \\ &\le \|z_n - s^*\| + [1-\xi]\|f_2^n z_n - z_n\|\end{aligned}$$

which yields that

$$w \le liminf_{n\to\infty}\|z_n - s^*\|. \tag{2.16}$$

Using (2.4)&(2.16), we obtain

$$\lim_{n\to\infty}\|z_n - s^*\| = w \tag{2.17}$$

Because of

$$w = \lim_{n\to\infty}\|z_n - s^*\| = \lim_{n\to\infty}\|(1-c_n)(x_n - s^*) + c_n(f_1^n x_n - s^*)\|$$

from Lemma 2, we get

$$\lim_{n\to\infty}\|x_n - f_1^n x_n\| = 0. \tag{2.18}$$

On the other hand, by (2.18)

$$\begin{aligned}\|z_n - x_n\| &= \|(1-c_n)x_n + c_n f_1^n x_n - x_n\| \\ &\le c_n\|f_1^n x_n - x_n\| \\ &\le [1-\xi]\|f_1^n x_n - x_n\| \\ &\to 0 \; as \; n \to \infty,\end{aligned} \tag{2.19}$$

and, from (2.15)&(2.19), we have

$$\begin{aligned}\|y_n - x_n\| &= \|(1-b_n)z_n + b_n f_2^n z_n - x_n\| \\ &\le \|z_n - x_n\| + b_n\|f_2^n z_n - z_n\| \\ &\le \|z_n - x_n\| + [1-\xi]\|f_2^n z_n - z_n\| \\ &\to 0 \; as \; n \to \infty,\end{aligned} \tag{2.20}$$

Using (2.15)&(2.19), we obtain

$$\begin{aligned}\|x_n - f_2^n x_n\| &\le \|z_n - x_n\| + \|f_2^n z_n - z_n\| + \|f_2^n z_n - f_2^n x_n\| \\ &\le \|z_n - x_n\| + \|f_2^n z_n - z_n\| + \phi_n\|z_n - x_n\|\end{aligned}$$

so that

$$\|x_n - f_2^n x_n\| \to 0 \; as \; n \to \infty. \tag{2.21}$$

Also

$$\begin{aligned}\|x_n - f_3^n x_n\| &\le \|x_n - f_2^n x_n\| + \|f_2^n x_n - f_3^n y_n\| + \|f_3^n y_n - f_3^n x_n\| \\ &\le \|x_n - f_2^n x_n\| + \|f_2^n x_n - f_3^n y_n\| + \phi_n\|y_n - x_n\|\end{aligned}$$

implies by (2.10), (2.20)&(2.21) that

$$\|x_n - f_3^n x_n\| \to 0 \; as \; n \to \infty. \tag{2.22}$$

It follows from (2.10)&(2.21) that we get

$$\begin{aligned}\|x_{n+1} - x_n\| &= \|(1-a_n)f_2^n x_n + a_n f_3^n y_n - x_n\| \\ &\le \|f_2^n x_n - x_n\| + a_n\|f_3^n y_n - f_2^n x_n\| \\ &\le \|f_2^n x_n - x_n\| + [1-\xi]\|f_3^n y_n - f_2^n x_n\|\end{aligned} \tag{2.23}$$

$$\to 0 \; as \; n \to \infty.$$

Then, for $l = 1,2,3$

$$\begin{aligned}\|x_n - f_l x_n\| &\le \|x_{n+1} - x_n\| + \|x_{n+1} - f_l^{n+1} x_{n+1}\| + \|f_l^{n+1} x_{n+1} - f_l^{n+1} x_n\| \\ &\quad + \|f_l^{n+1} x_n - f_l x_n\| \\ &\le \|x_{n+1} - x_n\| + \|x_{n+1} - f_l^{n+1} x_{n+1}\| + \phi_{n+1}\|x_{n+1} - x_n\| \\ &\quad + \phi_1 \|f_l^n x_n - x_n\|\end{aligned}$$

by (2.18), (2.21), (2.22)&(2.23) gives that for $l = 1,2,3$

$$\lim_{n\to\infty} \|x_n - f_l x_n\| = 0. \tag{2.24}$$

Theorem 1. Let X, η, G and f_l for $l = 1,2,3$ be as above. Suppose that η has the Property P, f_l for $l = 1,2,3$ satisfy the *Condition (C)*, $\{x_n\}$ defined by (1.1), where $\{a_n\}$, $\{b_n\}, \{c_n\} \subset [\xi, 1-\xi]$ for some $\xi \in (0,1)$ and $(x_0, s^*), (s^*, x_0) \in E(G)$ for $x_0 \in \eta$, then $\{x_n\} \to s^* \in Fix(F)$.

Proof. Let $s^* \in Fix(F)$ such that (x_n, s^*), (s^*, x_n), $(x_n, z_n), (z_n, x_n)$, (s^*, z_n), (z_n, s^*), $(x_n, y_n), (y_n, x_n), (s^*, y_n)$, $(y_n, s^*)(x_n, x_{n+1})$ are in $E(G)$ for $\forall n \in N$. From Lemma 5 (i), $\lim_{n\to\infty} \|x_n - s^*\|$ exists, and thus $\lim_{n\to\infty} d(x_n, Fix(F))$ exists for all $s^* \in Fix(F)$. Again, by Lemma 5 (ii) $\lim_{n\to\infty} \|x_n - f_l x_n\| = 0$ for $l = 1,2,3$. Using the Condition (C), there is a nondecreasing function $g: [0,\infty) \to [0,\infty)$ with $g(t) > 0$ for $\forall t \in (0,\infty)$, $g(0) = 0$ such that $max\{\|x - f_1 x\|, \|x - f_2 x\|, \|x - f_3 x\|\} \ge g\left(d\big(x, Fix(F)\big)\right)$, that is to say

$$\lim_{n\to\infty} g\left(d\big(x, Fix(F)\big)\right) = 0. \tag{2.25}$$

Hereby, we can receive a subsequence $\{x_{n_s}\}$ and $\{x_n\}$ and sequence $\{\alpha_s\} \subset Fix(F)$ such that $\|x_{n_s} - \alpha_s\| < 2^{-s}$ for $\forall s \ge 1$. Because of the fact that strong convergence stand for weak convergence and by Remark 1, we hold $(x_{n_s}, \alpha_s) \in E(G)$. By the proof of [23], we have $\|x_{n_{s+1}} - \alpha_s\| < \|x_{n_s} - \alpha_s\| < 2^{-s}$, and so $\|\alpha_{s+1} - \alpha_s\| < {}^{2}/_{2^s}$. We infer that $\{\alpha_s\}$ is a Cauchy sequence in $Fix(F)$, thus it converges. Let $\alpha_s \to \alpha$. As $Fix(F)$ is closed, and thus $\alpha \in Fix(F)$ and then $x_{n_s} \to \alpha$. From Lemma 5 (i), $x_n \to s^* \in Fix(F)$.

In an analog way to Theorem 1, when $c_n \equiv 0$ in (1.1), we show convergence result of a modified $S-$iterative procedure as shown below.

Theorem 2. Let X, η, G and f_2, f_3 be as above. Suppose that η has the Property P, f_2, f_3 satisfy the *Condition (B)*, $\{x_n\}$ defined by (1.1), where $\{a_n\}, \{b_n\} \subset [\xi, 1-\xi]$ for some $\xi \in (0,1)$ and $(x_0, s^*), (s^*, x_0) \in E(G)$ for $x_0 \in \eta$, then $\{x_n\} \to s^* \in F(f_2) \cap F(f_3)$.

In line with the Theorem 1, if $f_2 = I$ and $b_n = c_n \equiv 0$ in (1.1), then obtain Mann-type convergence results for $G-$asymptotically nonexpansive mappings with *BSWG* as noted below.

Theorem 3. Let X, η, G and f_3 be as above. Suppose that η has the Property P, f_3 satisfy the *Condition (A)*, $\{x_n\}$ defined by (1.1), where $\{a_n\} \subset [\xi, 1-\xi]$ for some $\xi \in (0,1)$ and $(x_0, s^*), (s^*, x_0) \in E(G)$ for $x_0 \in \eta$, then $\{x_n\} \to s^* \in F(f_3)$.

In the next theorem, we express the strong convergence of $\{x_n\}$ defined by (1.1) under semi-compact.

Theorem 4. Let X, η, G and f_l for $l = 1,2,3$ be as above. Suppose that η has the Property P, one of f_l for $l = 1,2,3$ is *semi-compact*, $\{x_n\}$ defined by (1.1), where $\{a_n\}, \{b_n\}, \{c_n\} \subset [\xi, 1-\xi]$ for some $\xi \in (0,1)$ and $(x_0, s^*), (s^*, x_0) \in E(G)$ for $x_0 \in \eta$, then $\{x_n\} \to s^* \in Fix(F)$.

Proof. Let $s^* \in Fix(F)$ such that (x_n, s^*), (s^*, x_n), $(x_n, z_n), (z_n, x_n)$, (s^*, z_n), (z_n, s^*), $(x_n, y_n), (y_n, x_n), (s^*, y_n)$, $(y_n, s^*)(x_n, x_{n+1})$ are in $E(G)$ for $\forall n \in N$. By virtue of the fact that one of f_l for $l = 1,2,3$ is semi-compact, $\{x_n\}$ is bounded and by (2.24), and then

$$there\ exists\ subsequence\ \left\{x_{n_p}\right\}\ of\ \{x_n\}\ such\ that\ x_{n_p} \to s^*. \tag{2.26}$$

Owing to the fact that strong convergence state weak convergence and by Remark 1, we enjoy $\left(x_{n_p}, s^*\right) \in E(G)$. We get that $s^* \in Fix(F)$. Hereby, $\lim_{n\to\infty} \|x_n - s^*\|$ exists from Lemma 5 (i). On the score of (2.26), then $\{x_n\} \to s^* \in Fix(F)$.

For $c_n \equiv 0$ in (1.1), then Theorem 4, reduces to the following convergence result of a modified $S-$iterative procedure for $G-$asymptotically nonexpansiveness in *BSWG*.

Theorem 5. Let X, η, G and f_l for $l = 2,3$ be as above. Suppose that η has the Property P, one of f_l for $l = 2,3$ is *semi-compact*, $\{x_n\}$ defined by (1.1), where $\{a_n\}, \{b_n\} \subset [\xi, 1-\xi]$ for some $\xi \in (0,1)$ and $(x_0, s^*), (s^*, x_0) \in E(G)$ for $x_0 \in \eta$, then $\{x_n\} \to s^* \in F(f_2) \cap F(f_3)$.

Similarly, taking $f_2 = I$ and $b_n = c_n \equiv 0$ in Theorem 4, then we attain Mann-type convergence results for $G-$asymptotically nonexpansive mappings with *BSWG* as follows.

Theorem 6. Let X, η, G and f_3 be as above. Suppose that η has the Property P, f_3 is semi-compact, $\{x_n\}$ defined by (1.1), where $\{a_n\} \subset [\xi, 1-\xi]$ for some $\xi \in (0,1)$ and $(x_0, s^*), (s^*, x_0) \in E(G)$ for $x_0 \in \eta$, then $\{x_n\} \to s^* \in F(f_3)$.

In the subsequent result, we testify the weak convergence of iteration (1.1) for $G-$asymptotically nonexpansiveness with *BSWG* without assuming the Opial's condition of X.

Theorem 7. Let X, η, G and f_l for $l = 1,2,3$ be as above. Suppose that η has the Property P, $\{x_n\}$ defined by (1.1), where $\{a_n\}$, $\{b_n\}, \{c_n\} \subset [\xi, 1-\xi]$ for some $\xi \in (0,1)$ and $(x_0, s^*), (s^*, x_0) \in E(G)$ for $x_0 \in \eta$, then $\{x_n\} \rightharpoonup u_* \in Fix(F)$.

Proof. Let $s^* \in Fix(F)$ such that (x_n, s^*), (s^*, x_n), $(x_n, z_n), (z_n, x_n)$, (s^*, z_n), (z_n, s^*), $(x_n, y_n), (y_n, x_n), (s^*, y_n)$, $(y_n, s^*)(x_n, x_{n+1})$ are in $E(G)$ for $\forall n \in N$. $\{x_n\}$ is bounded from Lemma 5 (i). Because of that $\eta \neq \emptyset$ is a closed convex subset of a real uniformly convex Banach space X, it is weakly compact, and thus there exists subsequence $\left\{x_{n_p}\right\}$ of $\{x_n\}$ such that $x_{n_p} \to u_*$. We know that for $l = 1,2,3$ $\lim_{p\to\infty} \left\|x_{n_p} - f_l x_{n_p}\right\| = 0$ by (2.24). Using Lemma 3, $I - f_l$ for $l = 1,2,3$ is $G-$ demiclosed at 0 so that $u_* \in Fix(F)$.

Now, we show that $x_n \rightharpoonup u_*$. Let $\left\{x_{n_p}\right\}$ be a subsequence of $\{x_n\}$ that converges weakly to $w_* \in K$. On the lines similar to above, we also have $w_* \in Fix(F)$. Next, for each $p \geq 1$, we get

$$\begin{aligned} x_{n_p+1} &= \left(1 - a_{n_p}\right) f_2^{n_p} x_{n_p} + a_{n_p} f_3^{n_p} y_{n_p} - x_{n_p} + x_{n_p} \\ &= x_{n_p} + \left(f_2^{n_p} x_{n_p} - x_{n_p}\right) + a_{n_p}\left(f_3^{n_p} y_{n_p} - f_2^{n_p} x_{n_p}\right). \end{aligned} \tag{2.27}$$

It follows from (2.10) and (2.21) that

$$\lim_{p\to\infty} \left\|f_3^{n_p} y_{n_p} - f_2^{n_p} x_{n_p}\right\| = 0 \ and \ \lim_{p\to\infty} \left\|f_2^{n_p} x_{n_p} - x_{n_p}\right\| = 0. \tag{2.28}$$

Due to $a_{n_p} \in [\xi, 1-\xi]$ for some $\xi \in (0,1)$, we obtain

$$\lim_{p\to\infty} a_{n_p} \left\| f_3^{n_p} y_{n_p} - f_2^{n_p} x_{n_p} \right\| = 0; \tag{2.29}$$

vincelet, using (2.28) and (2.29), we deduce that $x_{n_p+1} \rightharpoonup w_*$. By Lemma 4, $\{x_n\} \rightharpoonup w_*$ so that $w_* = u_*$.

Putting $c_n \equiv 0$ in (1.1), then Theorem 7 reduces to the following convergence result of a modified $S-$iterative procedure for $G-$asymptotically nonexpansiveness in *BSWG*.

Theorem 8. Let X, η, G and f_l for $l = 2,3$ be as above. Suppose that η has the Property P, $\{x_n\}$ defined by (1.1), where $\{a_n\}$, $\{b_n\}, \{c_n\} \subset [\xi, 1-\xi]$ for some $\xi \in (0,1)$ and $(x_0, s^*), (s^*, x_0) \in E(G)$ for $x_0 \in \eta$, then $\{x_n\} \rightharpoonup u_* \in F(f_2) \cap F(f_3)$.

In a similar manner, when $f_2 = I$ and $b_n = c_n \equiv 0$ in Theorem 7, then we get Mann-type convergence results for $G-$asymptotically nonexpansiveness in *BSWG* as follows.

Theorem 9. Let X, η, G and f_3 be as above. Suppose that η has the Property P, $\{x_n\}$ defined by (1.1), where $\{a_n\}, \{b_n\}, \{c_n\} \subset [\xi, 1-\xi]$ for some $\xi \in (0,1)$ and $(x_0, s^*), (s^*, x_0) \in E(G)$ for $x_0 \in \eta$, then $\{x_n\} \rightharpoonup u_* \in F(f_2) \cap F(f_3)$.

Remark 2. If $\phi_n \equiv 0$ for $\forall n \geq 1$, then the class of $G-$asymptotically nonexpansiveness coincide with $G-$nonexpansiveness. Because of this reason, Theorem 1-7 widen and enhance the results of Theorem 2-3 in Suparatulatorn& et al. and Theorem 3.12-3.15 in Thakur& et al ((Suparatulatorn& et al., 2018), (Thakur& et al., 2014)).

Now, we consider the numerical instance which is inspired by Example 3.1 in Razani&Moradi (Razani&Moradi, 2015).

Example 1. Let X is the real line with the usual norm $|.|$, $\eta = [0,2]$ and $G = (V(G), E(G))$ such that $(V(G) = \eta$ and $(x, y) \in E(G)$ iff $0.30 \leq x, y \leq 1.20$ or $x = y$. Define $f_l: \eta \to \eta$ for $l = 1,2,3$ as

$$f_1 x = \begin{cases} \dfrac{3\sin x}{10 + 10x}, x = 0.5 \\ 0, \quad x \neq 0.5 \end{cases},$$

$$f_2 x = \begin{cases} \dfrac{2\sin x}{5 + 5x}, x = 0.5 \\ 0, \quad x \neq 0.5 \end{cases}$$

$$f_3 x = \begin{cases} \dfrac{\sin x}{10 + 10x}, x = 0.5 \\ 0, \quad x \neq 0.5 \end{cases}$$

for any $x \in \eta$. It is easy to see that f_l for $l = 1,2,3$ are $G-$asymptotically nonexpansive mappings. Set

$$a_n = b_n = c_n = {}^1\!/_2, for\ n \geq 1.$$

Let $\{x_n\}$ be the sequence defined by (1.1). Thereof,

$$x_{n+1} = {}^1\!/_2 f_2^n x_n + {}^1\!/_2 f_3^n y_n,$$
$$y_n = {}^1\!/_2 z_n + {}^1\!/_2 f_2^n z_n,$$
$$z_n = {}^1\!/_2 x_n + {}^1\!/_2 f_1^n x_n, n \geq 1,$$

and $Fix(F) = \{0\}$. As $x_1 = 0.5$, we know that $x_2 = 7.2003 \times 10^{-2}$, $x_3 = 5.3372 \times 10^{-3}$, $x_4 = 1.7011 \times 10^{-4}$, $x_5 = 2.179 \times 10^{-6}$, $x_6 = 1.1159 \times 10^{-8}$ and $x_7 = 2.2855 \times 10^{-11}$ (see Figure 1). This example reveals that the algorithm is efficient to approach common fixed points of G −asymptotically nonexpansiveness on *BSWG*.

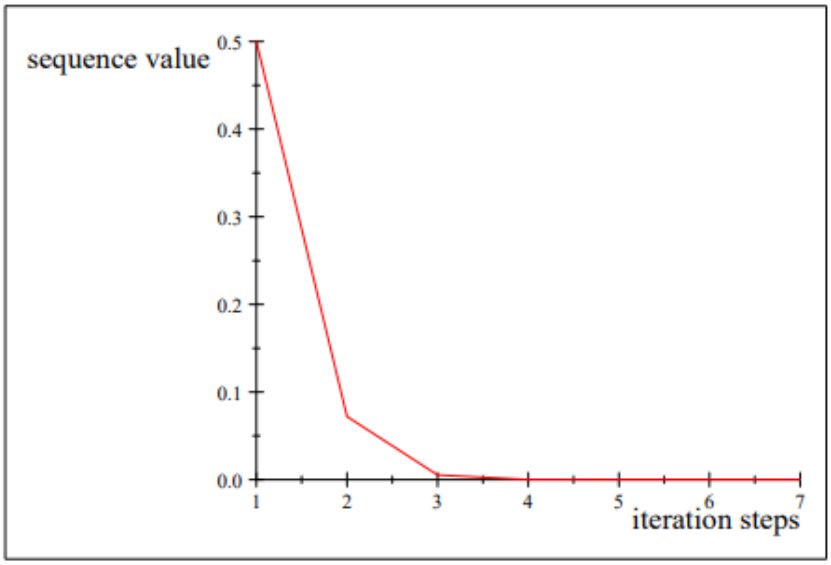

Figure 1. The values in the first seven steps of $\{x_n\}$ *in Example 1.*

REFERENCES

Abbas, M., Nazir T. (2014). A new faster iteration process applied to constrained minimization and feasibility problems. *Mathematic Vesnik*. 66 (2), 223--234.

Agarwal, P.R., O'Regan D., Sahu D.R. (2007). Iterative construction of fixed points of nearly asymptotically nonexpansive mappings. *J. Nonlinear Convex Anal.* 8 (1), 61-79.

Alfuraidan, M. (2015). Fixed points of monotone nonexpansive mappings with a graph. *Fixed Point Theory and Applications.* 49. https://doi.org/10.1186/s13663-015-0299-0.

Alfuraidan, M.R., Khamsi, M.A. (2015). Fixed points of monotone nonexpansive mappings on a hyperbolic metric space with a graph. *Fixed Point Theory Appl.* Doi: 10.1186/s13663-015-0294-5.

Hunde, T.W., Sangago, M.G., Zegeye, H. (2017). Approximation of a common fixed point of a family of G-nonexpansive mappings in Banach spaces with a graph. *International journal of Advances in Mathematics*. Vol. 2017, No:6, 137-152.

Jachymski J. (2008). The contraction principle for mappings on a metric space with a graph. *Proc. Amer. Math. Soc*. 136, 1359-1373.

Razani A., Moradi R. (2015). On the iterates of asymptotically k-strict pseudocontractive mappings in Hilbert space with convergence analysis. *Fixed Point Theory and Applications* 21 Doi:10.1186/s13663-015-0270-0.

Sahu J., (1991). Weak and strong convergence to fixed points of asymptotically nonexpansive mappings. *Bull. Aust. Math. Soc.* 43 153-159.

Sangago M.G. (2011). Convergence of iterative schemes for nonexpansive mappings. *Asian-European Journal of Math.* 4(4), 671-682.

Sangago M.G., Hunde T.W., Hailu H.Z. (2018). Demiclodeness and fixed points of G-asymptotically nonexpansive mappings in Banach spaces with a graph. *Adv. Fixed Point Theory*. 8(3), 313-340.

Shahzad N., Al-Dubiban P. (2006). Approximating common fixed points of nonexpansive mappings in Banach spaces. *Georgian Mathematical Journal*, 13(3), 529-537.

Sridarat P., Suparatulatorn R., Suantai S., Cho Y.J., (2018). Convergence analysis of SP-iteration for G-nonexpansive mappings with directed graphs. *Bulletin of the Malaysian Mathematical Sciences Society*. 1-20. https://doi.org/10.1007/s40840-018-0606-0.

Suparatulatorn R., Cholamjiak W., Suantai S. (2018). A modified S-iteration process for G-nonexpansive mappings in Banach spaces with a graph. *Numer Algor*. 77, 479-490. Doi: 10.1007/s11075-017-0324-y.

Tan K.K., Xu H.K. (1993). Approximating fixed points of nonexpansive mappings by the Ishikawa iteration process. *J. Math. Anal. Appl*. 178, 301-308.

Thakur D., Thakur B.S., Postolache M. (2014). New iteration scheme for numerical reckoning fixed points of nonexpansive mappings. *Journal of inequalities and applications*. 328, Doi:10.1186/1029-242X-2014-328.

Tripak O. (2016). Common fixed points of G-nonexpansive mappings on Banach spaces with a graph. *Fixed Point Theory Appl*. Doi: 10.1186/s13663-016-0578-4.

Morphological and Microstructure Analysis of the Shells of *Dreissena polymorpha, Unio pictorum* and *Viviparus contectus*

Filiz KUTLUYER KOCABAŞ[1]
Mehmet KOCABAŞ[2]

Introduction

As a biologically controlled process, biomineralization is complex and controls biological activity (de Paula and Silveira, 2005). Living organisms are synthesized carbonaceous biominerals in consequence of biomineralization. In a biological matrix, shells are formed by process of biomineralization in Molluscs via biodeposition of the ingredient minerals (Chakraborty et al., 2020). The mantle controls biomineralization for shell formation through ion pumps and channels (Sakalauskaite et al., 2020). In Mollusc, shells are consisted of the calcium carbonate (CaCO3) in different forms (crystal, calcite and aragonite) and organic components [chitin (C8H13NO5)n, acidic polysaccharides and largely proteins] (Chakraborty et al., 2020; Yarra et al., 2021). Additionally, vaterite as a polymorph of $CaCO_3$ is present in gastropod molluscs shell (Medakovic et al., 2003; de Paula and Silveira, 2005).

In Molluscs, the soft tissues are protected by shells from abiotic and biotic stress (Li et al., 2017). A calcified leathery hinge is joined two symmetrical calcareous valves at their dorsal margins in Bivalvia (Lakshmanna et al., 2018; Chakraborty et al., 2020). Gastropods have organic or calcified plate on the dorsal surface of the met podium of the foot (Lakshmanna et al., 2018). *Viviparus contectus* is a Gastropod species and it has thin thick and concentrically lined dextral shell. Their dimensions are varied 25-40 mm long. The univalve shells of *V. contectus* are 6–7 whorled as rising-spiral. *Unio pictorum* is freshwater mussel belonging to Bivalvia and it has elongate elliptical and relatively thin shell. Their dimensions are varied 30-40 x 70-100 x 23-28 (height) mm, exceptionally up to 140 mm long. The color of shell varied yellow and greenish to dark brown. *Dreissena polymorpha* is an invasive freshwater mussel species and it has triagonal or triangular shell with stripes. Their dimensions are varied 20-50 mm long. Thus far, microstructure and the mineralogy of shells have been poorly assessed at micro-nano scale. The existing studies have been performed about physical and structural properties and, chemical compositions in mussels and gastropods shells (Chateigner et al., 2000; Medakovic et al., 2003; de Paula and Silveira, 2005; Li et al., 2017; Lakshmanna et al., 2018; Chakraborty et al., 2020; Parveen et al., 2020; Ravi et al., 2021; Yarra et al., 2021). To our best knowledge, the microstructural details of shells have not yet to be assessed in *D. polymorpha* and *V. contectus*. Dauphin et al. (2017) have been investigated structure and composition of *U. pictorum* shell.

The synthesis of alternative materials has been increasingly interested in cement industry (Ravi et al., 2021). Therefore, clarification of structuring of biomaterials is important for new resource of construction materials and prospective use in industry (Parveen et al., 2020). Moreover, the stratigraphic age of geological formations and phylogenetic evolution are assessed by geologist in fossils (Chateigner et al., 2000). In addition, shell microstructures are realized for precise description using scanning electron microscopy in Palaeontology (Taylor et al., 1973; Carter, 1980; Carter and Clark, 1985; Hedegaard, 1990; Hedegaard, 1997; Chateigner et al., 2000). According to the briefly mentioned reasons, the current study aimed to assess the elemental analyses on D. polymorpha, U. pictorum and V. contectus shells by Energy Dispersive X-ray

[1] Assoc. Prof. Dr., Munzur University, Fisheries Faculty, 62000, Tunceli, Turkey.
[2] Prof. Dr., Karadeniz Technical University Faculty of Forestry, Department of Wildlife Ecology and Management 61080, Trabzon, Turkey.

spectroscopy coupled to Scanning Electron Microscopy (SEM-EDX). XRD and FTIR analyses were also applied for assessing the structure in shells of freshwater mussels (*D. polymorpha* and *U. pictorum*) and freshwater snail (*V. contectus*).

Material and Methods

Animals and Sample preparation

Freshwater mussels (*D. polymorpha* and *U. pictorum*) and freshwater snail (*V. contectus*) were obtained from Demirköprü Dam Lake (Manisa, Turkey) by diving in summer (August). The flesh of the mussels was removed. Shells were cleaned and washed under running water as previously described by de Paula and Silveira (2005). After washing, shells were dried in air.

Scanning Electron Microscopy (SEM) Analysis

Shells of freshwater snail and mussels were crushed to powder using a mortar and pestle. For accessing the inner layers, shells were immersed in 0.1 N HCl for10 min, or 2% EDTA for 2 min as previously described by Silvia et al. (2005). Samples were carefully rinsed with ultrapure water and dried in air. Gold and Palladium were covered samples after chemical treatment. Some sections were observed without any further treatment. Hitachi SU3500 scanning electron microscope were used for SEM observations.

Energy-dispersive X-ray Spectroscopy (EDS)

Energy-dispersive X-ray spectroscopy (EDS, Oxford INCA X-ray spectrometer) was used with AZtec and INCA software (EDS). The prepared samples were gold-coated for EDS measurements. An acceleration voltage for elemental distribution maps was 20 kV and count rates were between 1,000 and 2,000 $s^{-1.}$

XRD (X-ray Diffraction) Analysis

XRD analysis was realized in powdered shells by a Rigaku miniflex600 X-ray diffractometer (0.02º at scattering angles (2θ) ranging from 10 to 90º by using monochromatic Cu-Ka radiation [1.5406 (λ)] at 40 kV and 15 mA). To assess the aragonite transformation, CaCO3 (ref JCPDS 9000226, 4001361, 9013801 Rigaku) peaks were used as a reference.

FTIR (Fourier transform infrared spectroscopy) Analysis

Infrared spectra (IR) were recorded by direct ATR transmission on powdered samples as previously described by Silvia et al. (2005). The spectra were recorded by Bruker (Vector 22) in the range 4000–400 wave numbers (cm^{-1}), 4 cm−1 resolutions, 32 scans.

Results

External views of *D. polymorpha*, *U. pictorum* and *V. contectus* shells are presented in Figure 1.

Figure 1. External views of shells, A) D. polymorpha. B) U. pictorum, and C) V. contectus.

SEM micrographs of cross-sectional view of shells and structural aspect of the organic matrix of *U. pictorum*, *D. polymorpha*, and *V. contectus* shells (SEM) after surface treatment by HCl (surface decalcification) are given Figure 2, 3 and 4. In SEM micrographs of cross-sectional view of *U. pictorum*, aragonite sheets horizontally overlapped with one another to make continuous superimposed sheets in the area indicated in Figure 2A-B. The thick inner nacreous layer and the outer prismatic layer were indicated in vertical section. Nacreous layer was composed of CaCO3 crystals. Plate and needle-like and polygonal-shaped crystals were irregular size and shape in the area indicated in Figure 2C. Figure 2D-F showed polygonal prisms surrounded by a thick organic envelope. The area indicated in Figure 2G-I correspond to a cauliflower and flake like granules region. Figure 3A-C demonstrated concentric layers. Figure 3D-F showed presence of fibers. Figure 4A-F showed irregular grains at micrometric scale.

Energy Dispersive X-ray Spectroscopy (EDS) images indicating the distribution of some elements on part of a shell cross-section are given in Figure 5. O, C, Ca, Mg, Sc, Si, Al and Fe were obtained from analysis. The elemental composition of mineralized layer was confirmed by the EDS spectra. The polymorphs of calcium carbonate in *D. polymorpha* and *V. contectus* demonstrated strong O peaks as well as C peaks with the incidence of Al and Si peaks while the polymorphs of calcium carbonate in *U. pictorum* exhibit strong C peaks as well as Ca and O peaks with the incidence of Si, Sc, Mg, Fe and Al peaks.

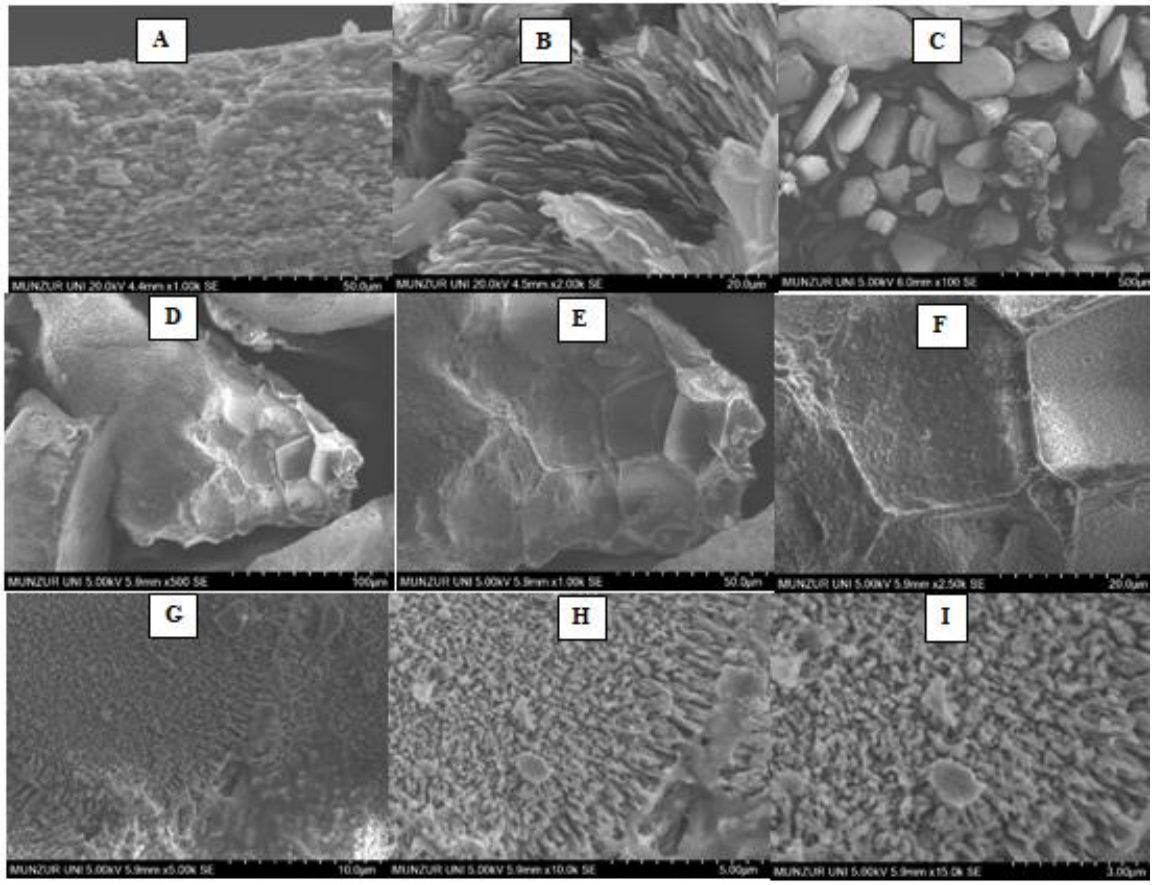

Figure 2. SEM micrographs of cross-sectional view and structural aspect of the organic matrix of U. pictorum shells (SEM). A–B: SEM micrographs of cross-sectional view of shells at different magnifications. C–I: organic matrix fibers forming parallel layers of different widths and densities observed after surface treatment by HCl (surface decalcification

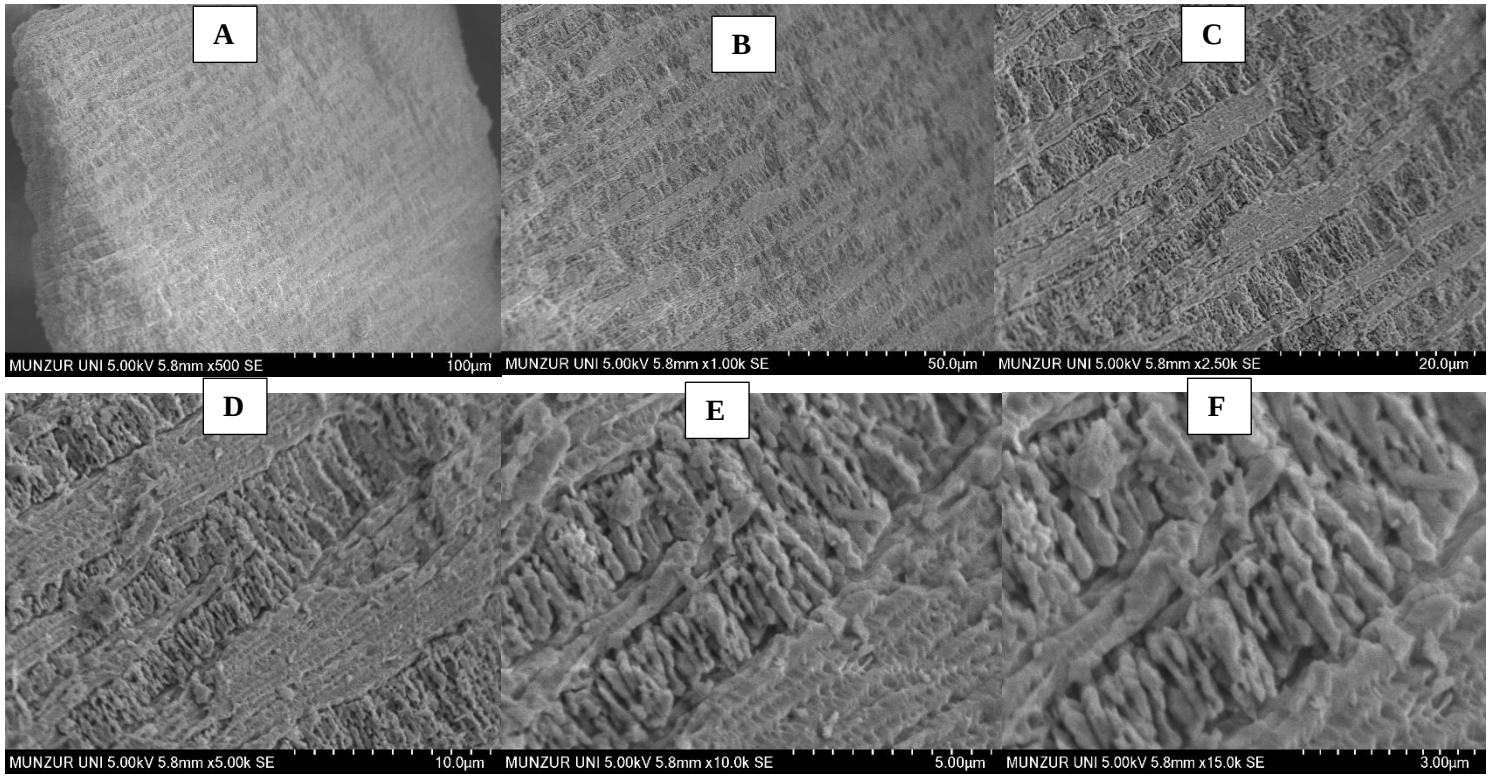

Figure 3. Structural aspect of the organic matrix of D. polymorpha shells (SEM) at different magnifications. A-F: organic matrix fibers forming parallel layers of different widths and densities observed after surface treatment by HCl (surface decalcification).

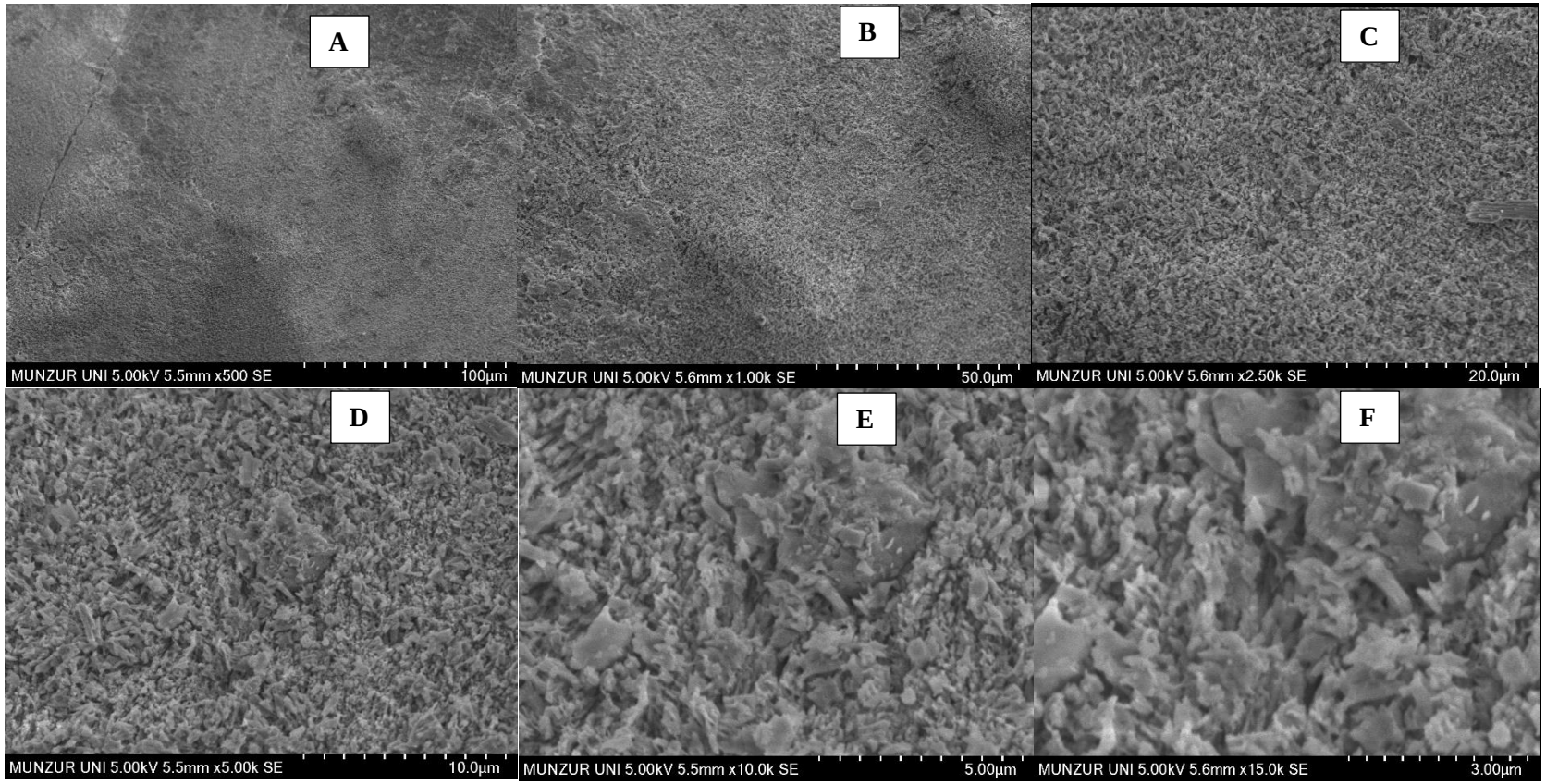

Figure 4. Structural aspect of the organic matrix of V. contectus shells (SEM) at different magnifications. A-F: organic matrix fibers forming parallel layers of different widths and densities observed after surface treatment by HCl (surface decalcification).

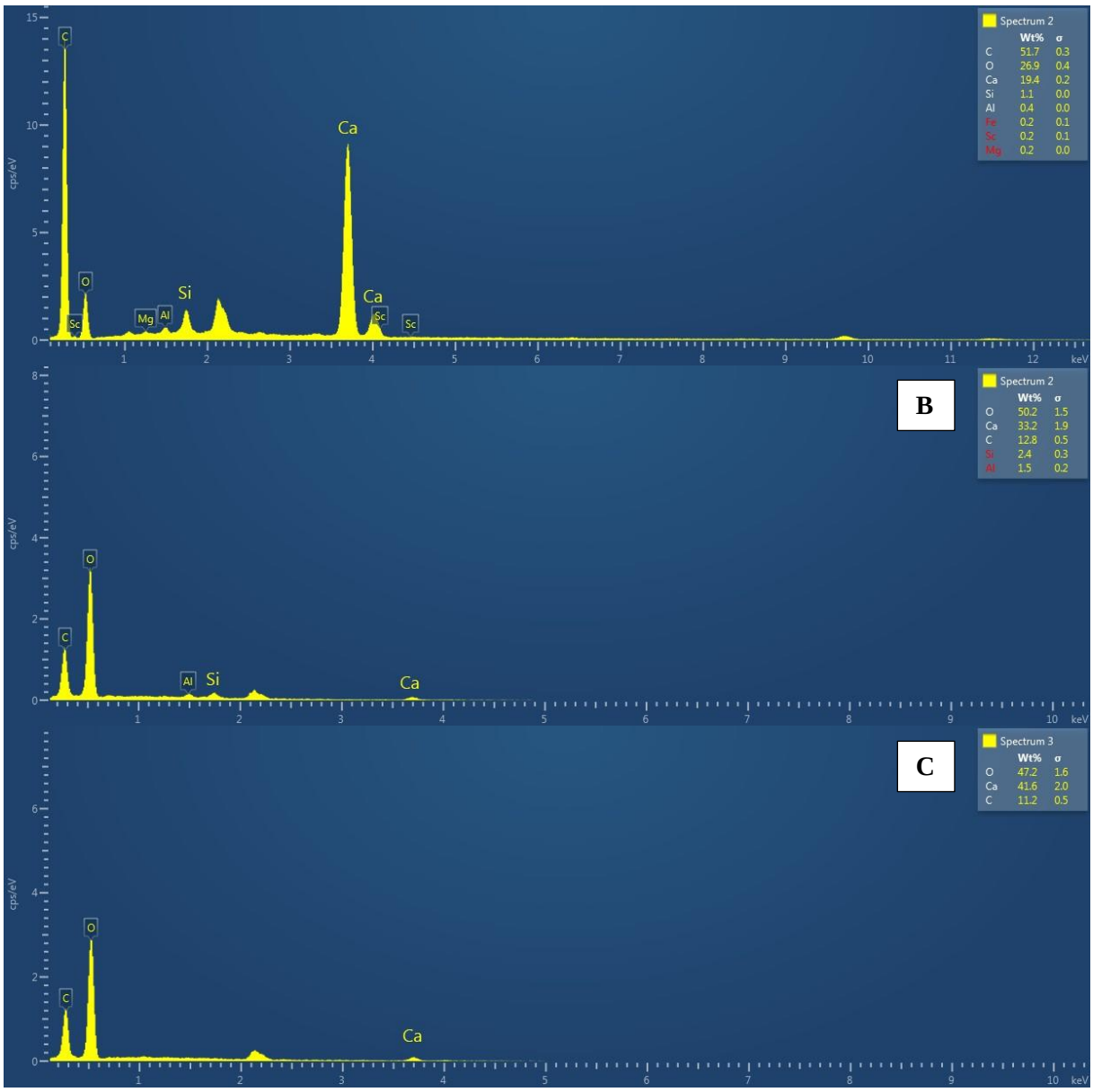

Figure 5. The SEM-EDS of cross sectioned surface of shells A) U. pictorum, B) V. contectus and C) D. polymorpha.

XRD patterns of shells of two freshwater mussels (*D. polymorpha, V. contectus* and *U. pictorum*) showed similarities in crystalline peaks with the existence aragonite forms of calcium carbonate. The existence of orthorhombic aragonite phase in the XRD pattern was revealed with the intense peaks at (111) and (012) planes (Figure 6).

Figure 7 shows the FTIR spectra of shells *D. polymorpha, V. contectus* and *U. pictorum*. FTIR spectra analysis showed similar features in the shell of *D. polymorpha, V. contectus* and *U. pictorum*. All three aragonite samples exhibited v1 and v2 bands at 1083 and 854 cm-1 respectively in their FTIR.

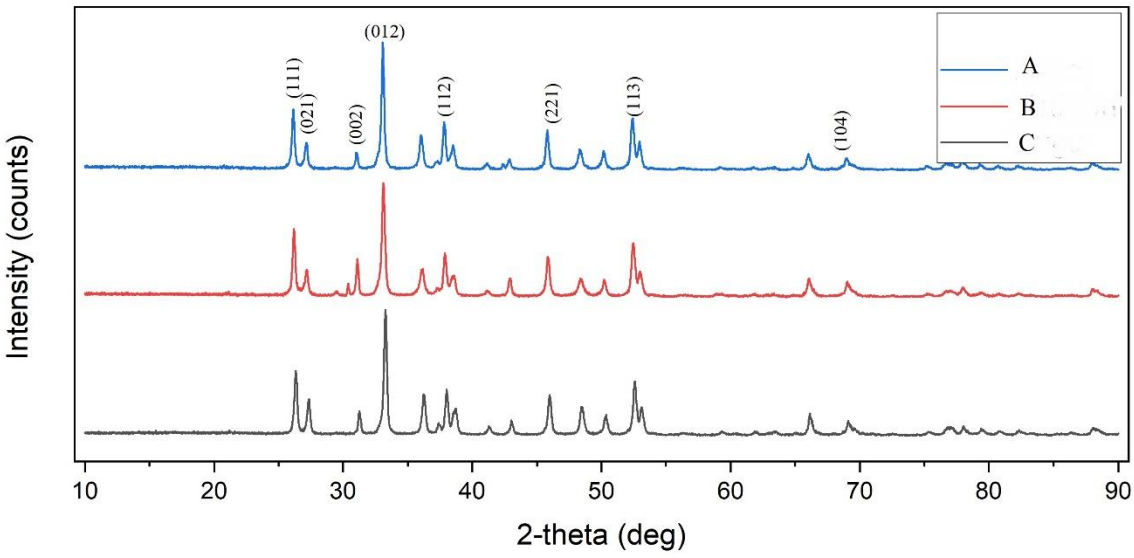

Figure 6. XRD pattern of A) D. polymorpha. B) V. contectus and C) U. pictorum,

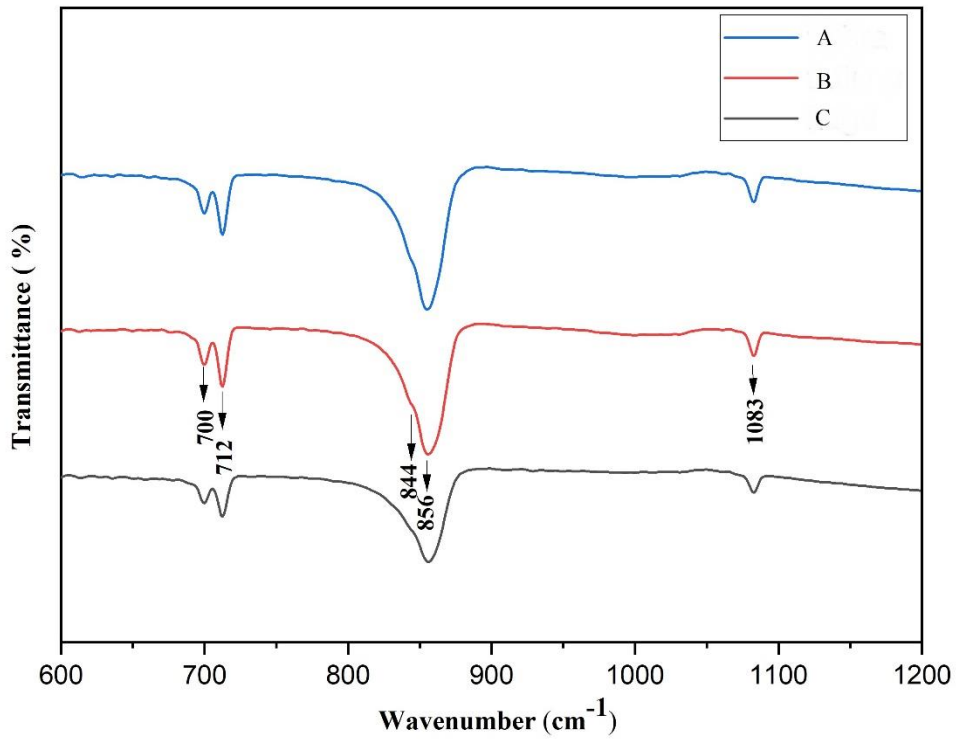

Figure 5. The representative FTIR spectra of the prepared shells of A) D. polymorpha. B) V. contectus and C) U. pictorum,

Discussion

In aquatic life, the freshwater mussels and snails have an important role in sustenance of the environmental quality through biofiltration, biodeposition and bioremediation (Binelli et al., 2014; Hossain et al., 2015; Voudanta et al., 2016; Vaughn, 2018; Bergström et al., 2019; Chakraborty et al., 2020). As a protecting exoskeleton, Molluscan shells defend against predators with rigid, stronger, tensile, and resistant to breakage structure and biomass of shells increases during growth (West and Cohen, 1996; Preston, 2007; Lind et al., 2009; Covich, 2010; Mukai et al., 2010; Adak and Purohit, 2011; Suzuki et al., 2011; Gosselin, 2015; Vermeij, 2015; Chakraborty et al., 2020; Parveen et al., 2020). The inorganic and organic components aggregate in shells. The layer of the shells formed crossed lamellar, foliated, and prismatic structures as the essential building blocks (Parveen et al., 2020). Mainly shells composed of calcium carbonate are consisted of different forms such as crystal, calcite, aragonite and vaterite. In particular, aragonite crystals have an unique crystalline property and shells can be used constructional flexibility as an alternative biological material (Willinger et al., 2015; Parveen et al., 2020). Shells of marine bivalves and gastropods have been used in multiple applications (soil amelioration, biodiesel production, waste water treatment, bone materials, fillers and alternative to mortars, biosorbent for dye and heavy metal) as a waste (Lee et al., 2010; Hu et al., 2011; Jones et al., 2011; Alvarez et al., 2012; Hossain et al., 2015; Perea et al., 2016; Gonzalez-Chang et al., 2017; Papadimitriou et al., 2017; Delali et al., 2019; Ji et al., 2019; Meski et al., 2019; Chakraborty et al., 2020). In this regard, structures and features of different Molluscan species is important for multiple applications.

The species-specific differences cause the variations in the mechanical properties and organic matter and minerals contents of the shells (Parveen et al., 2020). Previous studies by Jacob et al. (2008) and Lakshmanna et al. (2018) reported that the structure of bivalve and Gastropoda shells composed of carbon and oxygen and on the surface of the material of Cardita also adsorbed to elements Ca, Na, Si and Al. Our data obtained EDS spectra indicated that the shell in freshwater *U. pictorum*, *V. contectus* and *D. polymorpha* shells composed of atomic elements C 51.7%, 12.8% and 11.2%, O 26.9%, 50.2% and 47.2%, Ca 19.4%, 33.2% and 41.6%, Si 1.1%, and 2.4%, Al 0.4% and 1.5%, Fe 0.2% and 0.7%, Sc 0.2%, Mg 0.2%. The presence of C, O, and Ca is not surprising due to commonly found in most of the carbonated biominerals. Interestingly, the presence of Scandium (Sc) was assessed by EDS in shells of *U. pictorum*. As a metallic element, Sc is one of rare earth elements and widespread in the earth crust (Encyclopaedia Britannica, 1965). Scandium can be in the sediment. The elemental form of Sc can be obtained by chemical synthesis although its ratio is low in the shell.

Regarding to the sheet-like arrangement, the nacreous layer in U. pictorum was composed of CaCO3 crystals and the row stacking structure in nacreous layers was determined similar to previous reports in Molluscan species (Carter et al., 2012; Debruyne et al., 2014; Parveen et al., 2020). Aragonitic or sometimes calcitic prisms are most prominent in the outer crystalline layer bivalves (Carter et al., 2012; Agbaje et al., 2017; Chakraborty et al., 2020). In contrast to other forms of CaCO3 crystals (e.g. vaterite and calcite), the aragonite polymorph of CaCO3 is more stable, rigid and relatively fragile (Chakraborty et al., 2020). Concerning mineralogy of shells analyzed in this study, aragonite mineralogy was dominant in an inorganic layer of shells of three Molluscan species. Consistent with our results, Medakovic et al. (2003) reported form of crystal in an outer inorganic layer of two freshwater snails (*Belgrandiella fontinalis* and *B. kuesteri*). Dauphin et al. (2017) demonstrated aragonite crystals in the prismatic layer of *U. pictorum*. Nearly pure biogenic aragonite (98% $CaCO_3$) in freshwater snail

shell has been reported by Vu et al. (2019). The mineralogy of in the inner inorganic layer are influenced by the environmental conditions, locality and species (Medakovic et al., 2003).

In conclusion, microstructure and mineral composition of *U. pictorum*, *V. contectus* and *D. polymorpha* shells were assessed with different analytical techniques in this study. Our data clearly indicated that aragonite crystals by confirmed with XRD and FTIR. FTIR showed the diverse arrangement pattern in shells of freshwater snail and two freshwater mussels. Mineral content obtained by EDS showed that shells can be used as an eco-friendly construction material due to good mechanical performance. Further studies are required to assess characterization of different Molluscan species for green concrete material.

REFERENCES

Adak, M.D., & Purohit, K.M. (2011). Synthesis of nano-crystalline hydroxyapatite from dead snail shells for biological implantation. *Trends in Biomaterials and Artificial Organs*, 25, 101−106.

Agbaje, O.B.A., Wirth, R., Morales, L.F.G., Shirai, K., Kosnik, M., Watanabe, T., & Jacob, D.E. (2017). Architecture of crossed lamellar bivalve shells: the southern giant clam (*Tridacna derasa*, Röding, 1798). *Royal Society Open Science*, 4, 170622.

Alvarez, E.M.J., Fern´andez and Sanjurjon, N., Seco, S., & Nunez, S. (2012). *Pedosphere*. 22(2), 152–164.

Bergström, P.N., Hallmark, K.J., & Larsson, M. (2019). Biodeposits from Mytilus edulis: A potentially high-quality food source for the polychaete, *Hediste diversicolor*. Lindegarth, *Aquaculture International*, 27, 89–104.

Binelli, A.S., Magni, C., Soave, F., Marazzi, E., Zuccato, S., Castiglioni, M., & Parolini, V. (2014). The biofiltration process by the bivalve *D. polymorpha* for the removal of some pharmaceuticals and drugs of abuse from civil wastewaters. *Ecological engineering*, 71, 710–721.

Carter, J.G. (1990). Skeletal Biomineralisation: Patterns, Processes and Evolutionary Trends. Van Nostrand Reinhold, New York.

Carter, J.G., & Clark, II., G.R. (1985). Classi®cation and phylogenetic signi®cance of molluscan shell microstructure. In: Bottjer, D.J., Hickman, C.S., Ward, P.D., Broadhead, T.W. (Eds.), Molluscs, Notes for a Short Course. University of Tenessee, Department of Geological Sciences Studies in Geology. pp. 50-71.

Carter, J.G., Harries, P.J., Malchus, N., Sartori, A.F., Anderson, L.C., Bieler, R., Bogan, A.E., Coan, E.V., Cope, J.C.W., Cragg, S.M., & García-March, J.R. (2012). Illustrated glossary of the Bivalvia. *Treatise Online*, 1−209.

Chakraborty, A., Parveen, S., Chanda, D.K., & Aditya, G. (2020). An insight into the structure, composition and hardness of a biological material: the shell of freshwater mussels. *RSC Advances*, 10(49), 29543–29554.

Chateigner, D., Hedegaard, C., & Wenk, H.R. (2000). Mollusc shell microstructures and crystallographic textures. *Journal of Structural Geology*, 22(11-12), 1723–1735.

Covich, A.P. (2010). Winning the biodiversity arms race among freshwater gastropods: competition and coexistence through shell variability and predator avoidance. *Hydrobiologia*, 653, 191−215.

Dauphin, Y., Luquet, G., Salome, M., Bellot-Gurlet, L., & Cuif, J.P. (2017). Structure and composition of *Unio pictorum* shell: arguments for the diversity of the nacroprismatic arrangement in molluscs. *Journal of Microscopy*, 270(2), 156–169.

Debruyne, S. (2014). Stacks and sheets: The microstructure of nacreous shell and its merit in the field of archaeology. *Environmental Archaeology*, 19, 153−165.

Delali, H.D.R., Merouani, H., Aguedal, M., Belhakem, A., Iddou B., & Ouddane, B. (2019). *Key Engineering Materials*, 800, 187–192.

De Paula, S.M., & Silveira, M. (2005). Microstructural characterization of shell components in the Mollusc *Physa* sp. *Scanning*, 27, 120–125.

Encyclopaedia, B., I.N.C., William, B., Publisher: Chicago, London, Toronto, Geneva, Sydney and Tokyo. vol.20, p. 49, 1965.

Gonzalez-Chang, M.S., Boyer, G.L., Creasy, M.C., & Lefort, S.D. (2017). Mussel shell mulch can increase vineyard sustainability by changing scarab pest behavior. *Agronomy for Sustainable Development*, 37, 42.

Gosselin, M.P. (2015). Conservation of the freshwater pearl mussel (*Margaritifera margaritifera*) in the river Rede, UK: Identification of instream indicators for catchment-scale issues. *Limnologica*, 50, 58–66.

Hedegaard, C. (1990). Shell Structures of the Recent Archaeogastropoda. PhD Thesis, University of Aarhus, Denmark. Vols. 1 and 2.

Hedegaard, C. (1997). Shell Structures of the recent Vetigastropoda. *Journal of Molluscan Studies,* 63, 369-377.

Hossain, A.S.R., Bhattacharyya, H., & Aditya, G. (2015). Biosorption of Cadmium by waste shell dust of fresh water mussel *Lamellidens marginalis*: Implications for metal bioremediation. *ACS Sustainable Chemistry and Engineering*, 3, 1–8.

Hu, S.Y., Wang, H., & Han, H. (2011). Utilization of waste freshwater mussel shell as an economic catalyst for biodiesel production. *Biomass Bioenergy*, 35, 3627–3635.

Jacob, D.E., Soldati, R., Wirth, J., Huth, U., & Wehrmeister, W. (2008). Hofmeister, Nanostructure, composition, and mechanisms of bivalve shell growth, *Geochimica Geochimica et Cosmochimica Acta,* 72, 5401–5415.

Ji, L., Song, W., We, D., Jiang, D., Cai, L., Wang, Y., & Guo, J. (2019). Modified mussel shell powder for microalgae immobilization to remove N and P from eutrophic wastewater. Zhang, *Bioresource Technology*, 284, 36–42.

Jones, M., Wang, L., Abeynaike, A., & Darrell, P. (2011). Utilisation of waste material for environmental applications: calcination of mussel shells for waste water treatment. *Advances in Applied Ceramics*, 110, 280–286.

Lee, Y.H., Islam, S.J., Hong, K.M., Cho, R.K., Math, J.Y., Heo, H., Kim, H., & Yun, H.D. (2010). Composted oyster shell as lime fertilizer ıs more effective than fresh oyster shell. *Bioscience, Biotechnology, and Biochemistry*, 74(8), 1517–1521.

Li, L., Zhang, X., Yun, H., & Li, G. (2017). Complex hierarchical microstructures of Cambrian mollusk Pelagiella: insight into early biomineralization and evolution. *Scientific Reports,* 7(1), doi:10.1038/s41598-017-02235-9.

Lind, C.E., Evans, B.S., Knauer, J.J.U., Taylor, D.R., & Jerry, D.R. (2009). *Aquaculture,* 286, 12–19.

Medaković, D., Slapnik, R., Popović, S., & Gržeta, B. (2003). Mineralogy of shells from two freshwater snails *Belgrandiella fontinalis* and *B. kuesteri*. *Comparative Biochemistry and Physiology Part A: Molecular & Integrative Physiology*, 134(1), 121–127.

Meski, S., Tazibt, N., Khireddine, H., Ziani, S., Biba, W., Yala, S., Sidane, D., Boudjouan, F., & Moussaoui, N. (2019). Synthesis of hydroxyapatite from mussel shells for effective adsorption of aqueous Cd(II). *Water Science & Technology*, 80(7), 1226–1237.

Mukai, H., Saruwatari, K., Nagasawa, H., & Kogure, T. (2010). Aragonite twinning in gastropod nacre. *Journal of Crystal Growth*, 312, 3014−3019.

Papadimitriou, C.A., Krey, N., Stamatis, A., & Kallianiotis, J. (2017). The use of waste mussel shells for the adsorption of dyes and heavy metals. *Journal of Chemical Technology & Biotechnology*, 92(8), 1943–1947.

Parveen, S., Chakraborty, A., & Chanda, D.K. (2020). Microstructure analysis and chemical and mechanical characterization of the shells of three freshwater snails. *ACS Omega*, 5, 25757–25771.

Perea, A., Kelly, T., & Hangun-Balkir, Y. (2016). Utilization of waste seashells and Camelina sativa oil for biodiesel synthesis. *Green Chemistry Letters and Reviews*, 9(1), 27–32.

Preston, S.J., Keys A., & Roberts, D. (2007). Culturing freshwater pearl mussel *Margaritifera margaritifera*: a breakthrough in the conservation of an endangered species. *Aquatic Conservation*, 17(5), 539–549.

Ravi, M., Balasubramanian, M., Jeyakumar, A., & Kiranmayi, R. (2021). A review on utilizing the marine biorefinery waste in construction raw materials to reduce land pollution and enhance green environment. *Advanced Functional Materials*. 21(3), 43-62.

Sakalauskaite, J., Plasseraud, L., Thomas, J., Albéric, M., Thoury, M., Perrin, J., & Marin, F. (2020). The shell matrix of the European thorny oyster, *Spondylus gaederopus*: microstructural and molecular characterization. *Journal of Structural Biology*, doi:10.1016/j.jsb, 107497.

Suzuki, M., Kogure, T., Weiner, S., & Addadi, L. (2011). Formation of aragonite crystals in the crossed lamellar microstructure of limpet shells. *Crystal Growth and Design*, 11, 4850−4859.

Taylor, J.D., Kennedy, W.J., & Hall, A. (1973). The shell structure and mineralogy of the Bivalvia, Part II, Lucinacea±Clavagellacea. *Bulletin of the British Museum (Natural History) Zoology*. 22(9), 253-294.

Vaughn C. C. (2018). Ecosystem services provided by freshwater mussels. *Hydrobiologia*, 810, 15–27.

Vermeij, G.J. (2015). Gastropod skeletal defences: land, freshwater, and sea compared. *Vita Malacology*. 13, 1−25.

Voudanta, E., Kormas, K.A., Monchy, S., Delegrange, A., Vincent, D., Genitsaris, S., & Christaki, U. (2016). Mussel biofiltration effects on attached bacteria and unicellular eukaryotes in fish-rearing seawater. *PeerJ*, 4, 829.

Vu, X.H., Nguyen, L.H., Van, H.T., Nguyen, D.V., Nguyen, T.H., Nguyen, Q.T., & Ha, L.T. (2019). Adsorption of Chromium(VI) onto freshwater snail shell-derived biosorbent from aqueous solutions: Equilibrium, kinetics, and thermodynamics. *Journal of Chemistry*, 1–11.

West, K., & Cohen, A. (1996). Shell microstructure of gastropods from Lake Tanganyika, Africa: adaptation, convergent evolution, and escalation. *Evolution*, 50:672−681.

Willinger, M., G., Checa, A., G., Bonarski, J., T., Faryna, M., & Berent, K. (2015). Biogenic crystallographically continuous aragonite helices: the microstructure of the planktonic gastropod. Cuvierina. *Advanced Functional Materials*. 26, 553−561.

Yarra, T., Ramesh, K., & Blaxter, M. (2021). Transcriptomic analysis of shell repair and biomineralization in the blue mussel, *Mytilus edulis*. *BMC Genomics*, 22:437.

Investigation of Tribological Properties of Aluminum Alloy Materials Under Lubricants of Different Viscosities: Etial 171 Example

İbrahim YAVUZ[1]
Ercan ŞİMŞİR[2]
Soner Tayfun ŞIRAHANE[3]

Introduction

Material loss from surfaces in contact with each other due to mechanical and chemical effects is one of the most important mechanical problems encountered in mechanisms. Considering that 1/3 of the mechanical energy in the world is spent on mechanical losses, the importance of friction and wear will emerge (Kaplan, 2019).

Friction losses are one of the most studied topics in machine parts and mechanisms. Among the main factors affecting friction, material stands out (Cui et al., 2020). Aluminum alloy is one of the leading materials in terms of both its lightness and wear resistance (Khelge et al., 2022, Reddy et al., 2020, Ferraris et al., 2022). Aluminum alloys have found use in every field, especially in the automotive industry, in many sectors from food to machinery and space aviation (Gialanella & Malandruccolo, 2020, Doan et al., 2021, Işık et al., 2020, Omiyale, 2022). The reason for the use of aluminum is that its density is generally lower than steel (Sharma et al., 2020, Kotadia et al., 2021). Safety, comfort and fuel consumption are important elements in the manufacturing of vehicles (Hu et al., 2021, Cheng et al., 2020, Payalan & Guvensan, 2019). At this point, aluminum and aluminum alloys; They are one of the most suitable materials that can meet these elements due to their lightness, high thermal conductivity and increased strength (Sharma et al., 2020, Ferraris et al., 2022, Zhang & Li, 2023).

Aluminum is used by enriching it with various elements according to the desired properties. Elements such as copper, magnesium, titanium, iron, nickel, boron, and silicon are some of the elements used in this enrichment (Zhang et al., 2023, Sathish et al., 2023, Dhas et al., 2023).

Wear losses become very important in mechanisms that come into contact with each other. For this reason, studies examining the wear resistance of machine elements under wear conditions of aluminum are of great importance.

Tribology

Friction, which is accepted as a branch of science, is referred to as Tribology (Yavuz et al., 2021, Minami, 2009). Tribology is derived from the Greek word Tribos (Friction). Tribology is the branch of science that studies wear and friction between surfaces that are in contact with each other and have relative motion (Yüksel & Şahin, 2014).

Friction

The reaction force resulting from the relative motion of two or more materials in contact is called friction. There is constant friction, even if it is small, in objects that move relative to each other (Ru et al., 2020). The friction force, denoted Fs, tends to oppose motion. Depending on

[1] Assistant Professor, Afyon Kocatepe University, Faculty of Technology, Department of Automotive Engineering
[2] Lecturer Dr, Afyon Kocatepe University, Faculty of Technology, Department of Automotive Engineering
[3] Engineer, Medikalpark Mersin Biomedical Manager

the operating systems, there are mechanisms and situations where friction is desired to be high and friction is desired to be low.

When a moving object is wanted to be stopped or slowed down, friction is a desired situation (brake systems), and if the object is wanted to be moved or accelerated, friction becomes an undesirable situation (gear systems, bearings). The free body diagram of a relatively moving object is given in Figure 1.

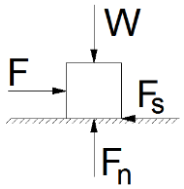

Figure 1. Free body diagram.

Calculation of friction force according to the diagram is given in Equation 1.

$$Fs=\mu \times Fn \quad (1)$$

Dry friction

It is the situation where objects move without lubricants on surfaces that are in immediate contact with their relative motion. It is friction where a lot of heat is released and energy and material losses occur (Jabbar et al., 2021, Adly & Attouch, 2020). In the automotive industry, dry friction is used in brake and clutch systems. It is shown together with the free body diagram in the diagram given in Figure 2.

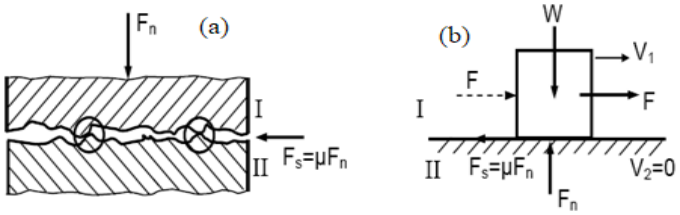

Figure 2. (a) Dry friction model and (b) free body diagram (Hatice et al., 2020).

As can be seen in Figure 2, heat is generated when particles and surface roughnesses come into contact with each other, and material loss occurs as the surface roughnesses erode each other.

Liquid friction

The friction that occurs when a thin oil film is formed between two relatively moving solid objects so that their surface roughness does not come into contact with each other is liquid friction (Dhanola et al., 2022, Zhang et al., 2019) (Figure 3). In this case, friction occurs between the layers of the lubricating fluid.

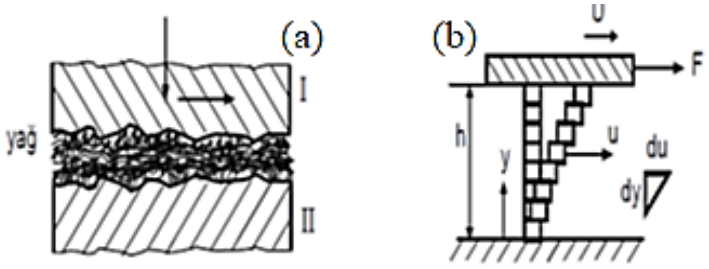

Figure 3. (a) Liquid Friction model and (b) liquid friction diagram (Hatice et al., 2020).

Wear

It is the involuntary detachment of particles from surfaces subject to friction. In this case, the materials lose their shape and voids occur. In case of wear, it is possible to talk about five factors in general. These; wear material, abrasive material, intermediate materials, movement and loads. Temperature value can also be considered a sixth factor. Wear causes the machine's sensitivity to decrease and noise to increase. Main types of wear: It is classified as adhesion, abrasion, fatigue wear (pitting) and mechanical corrosion wear (Öztürk, 2018).

Adhesion wear

Strong boiling occurs between materials that are close to each other and can be mixed. Surface asperities undergo plastic deformation when the flow limit is exceeded under the influence of external force, and the liquid or gas molecules and oxide layers absorbed on the surface disintegrate. Micro weld bonds form at the contact points. If the contact surfaces move relative to each other, these bonds break and material loss occurs (Ölmez, 2016).

Adhesive wear is a type of wear that occurs due to local adhesion of two solid bodies in contact, causing material transfer or material loss between two surfaces. If no abrasive particles are present, the magnitude of slip is greater than friction, and the rate of material loss is not controlled by oxidation principles, adhesive wear is said to occur (Erdem, 2006).

Abrasion wear

It is the wear that occurs as a result of the roughness or grains on the surface of one of the hard objects rubbing due to movement and loads, scratching the other and removing micro chips from it. Particles such as sawdust and dust entering between the surfaces from the working environment can be corrosive. Surface hardening should be applied to the surfaces to prevent abrasion wear. Sealing must be ensured to prevent any external substance from entering the contact areas of the surfaces. Systems must be constantly cleaned (Ölmez, 2016).

According to ASTM's definition, abrasive wear occurs when hard particles or protrusions are pressed against a solid surface and move forward. Wear is solid surface damage that generally involves progressive material loss due to relative movements between the object or objects in contact with the surface (Li et al., 2023).

Abrasive wear occurs when a force is applied to a solid object by materials with equal or higher hardness. The cost of abrasive wear is high, accounting for between 1% and 4% of the gross national product of an industrial society. The effect of abrasive wear is evident in mining, mineral processing, agriculture, earth moving and generally wherever sand, stone and minerals are found. Basic examples are: ore loading/carrying buckets, crushers, truck dumpers and plows (Rodríguez et al., 2023).

Corrosion wear

It can be defined as the chemical dissolution of metals. It is a chemical reaction and starts especially on the material surface. From an economic point of view, the corrosion problem is an important factor. It is estimated that 5% of national income is spent in industrialized countries in terms of material losses and maintenance costs as a result of corrosion. Corrosion problems, which are so common that everyone knows them, are examples of rusting of door panels and exhaust in the automotive industry. This is the situation where materials lose mass due to wear (Callister & Retwisch, 2014).

Pitting (fatigue wear)

Fatigue wear begins in the surface area, but microscopic cracks form on the surface during vibratory loading or when the material is subjected to repeated stresses. This situation is

generally encountered in systems operating with roller bearings and systems with cam mechanisms (Akkurt, 1990).

Erosion wear

Erosion wear is the type of wear that occurs when the relative speed between the superficial parts of the materials and the environment is high and occurs when solid or liquid particles hit the superficial part of the object rapidly (Ölmez, 2016).

Etial 177, Etial 171 and Etial 140 aluminum alloy samples, which are widely used in the automotive industry, were examined as samples in the experiments. The ratios of the chemical compositions in the standard are shown in Table 1, and the production properties of the samples are shown in Table 2.

Table 1. Chemical composition limits (weight%) of the alloy samples used (ETI Alüminyum, 2023).

Material	Fe	Si	Cu	Mn	Mg	Zn	Ni	Ti	Pb	Sn
ETİAL-171	0.5	9.00-10.00	0.1	0.40-0.60	0.30-0.45	0.1	0.1	0.15	0.05	0.05

Table 2 Typical properties of the samples used (ETI Alüminyum, 2023).

Material	Specific Weight (gr/cm^3)	Melting Range (℃)	Thermal Conductivity (cal/cm.s℃)	Corrosion Strength	Castability	Processability	Anodic Oxidation
ETİAL-171	2,64	575-595	0,27	Very good	Perfect	Middle	Surface Protection Only

Lubricants

Lubricants are substances used to minimize the friction force and provide easy movement by separating two solid objects from contact with each other and are called 'oil'. They perform lubrication with the logic of reducing the high friction between objects with their own friction values. Duties of lubricants,

1) Reduce wear

2) Protection from corrosion

3) Cooling

4) Cleaning surface dirt, are listed as.

In general terms, it is possible to examine oils in three classes; These are mineral and synthetic oils. Oils obtained by adding some synthetic substances to mineral oils are called semi-synthetic oils.

Mineral oils are standard oils that are used conventionally. After the distillation of underground oil, it is produced by adding additives that improve viscosity and affect wear. It has low cost and average performance.

Synthetic oils are oils produced by chemical processes in a laboratory environment. Its cost is higher than mineral oils. It has higher performance and longer lifespan. It also has higher temperature resistance.

Semi-synthetic oils are oils obtained as a result of the mixture of these two oils. It shows a performance between mineral and synthetic oils in terms of performance and cost. It is generally produced by mixing 20 to 30% synthetic oil and 70 to 80% mineral oil.

The most important feature used to distinguish oils is viscosity. Viscosity is the resistance of fluids to flow. It varies inversely with temperature. Centistoke (cs) is used as the unit of measurement.

The most used viscosity classification is The Society of Automotive Engineers (SAE). The difference in SAE classification compared to other classifications is that it is classified according to viscosity at low and high temperatures. In this classification, degrees consist of values separated by the letter "W". It is the abbreviation of the English word Winter and indicates the viscosity of the oil at low temperatures. The lower the first degree, the more fluid, i.e. thinner, the oil is. The second number shows the fluidity at high temperature.

The oils used in these experiments are 10W40 and 20W50 viscosity oils, which are frequently used in the automotive industry. Technical specifications of the oils used are given in Table 3 below.

Table 3. Typical property values of lubricants within normal manufacturing tolerances.

Lubricant Viscosity	Intensity 15°C (g/ml)	Viscosity 100°C (mm^2/s)	Viscosity 40°C (mm^2/s)	Viscosity Index	Pour Point (°C)	Sulfate Ash (weight%)
10W40	0,868	14,6	101	150	-42	1,2
20W50	0,885	19,8	186,9	122	-30	1,3

Abrasion tester

The wear test device used in the analysis is a wear device designed as a prototype and works with the principle of pin friction on the disc. It can be seen in Figure 4. The samples are fixed to the loading arm with a holder, and the load is transmitted to the sample with weights placed on the load arm. The tests were repeated with oils of different viscosities by changing the load and speed. The lubrication mechanism is provided with the help of a felt that is immersed in oil and removed.

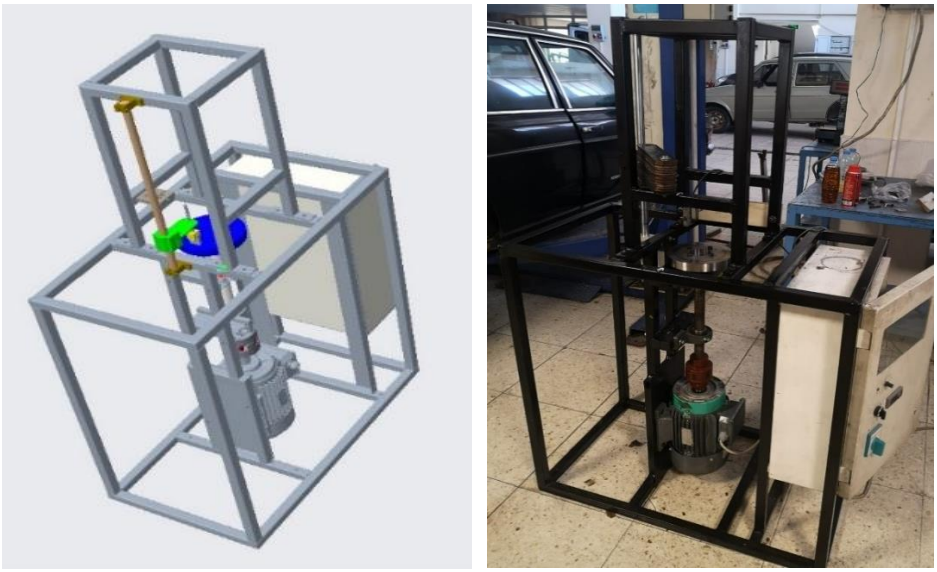

Figure 4. Design view of the device and its picture after manufacturing.

The design of the device is entirely my own, and the part module, assembly module and technical drawings were designed with the Creo Parametric program. Figure 4 shows the welded connection assembly and post-manufacturing picture. Device calibration and tare operation is done via software while the load cell is in empty position.

Findings

Friction tests performed at different revolutions

In the tests under this heading, tests performed at speeds of 800 rpm and 1200 rpm are given. All tests using oil were carried out with a load of 5000 N. Graphic 1 shows the friction coefficient change of the Etial 171 sample with 10W40 oil at 800 and 1200 rpm.

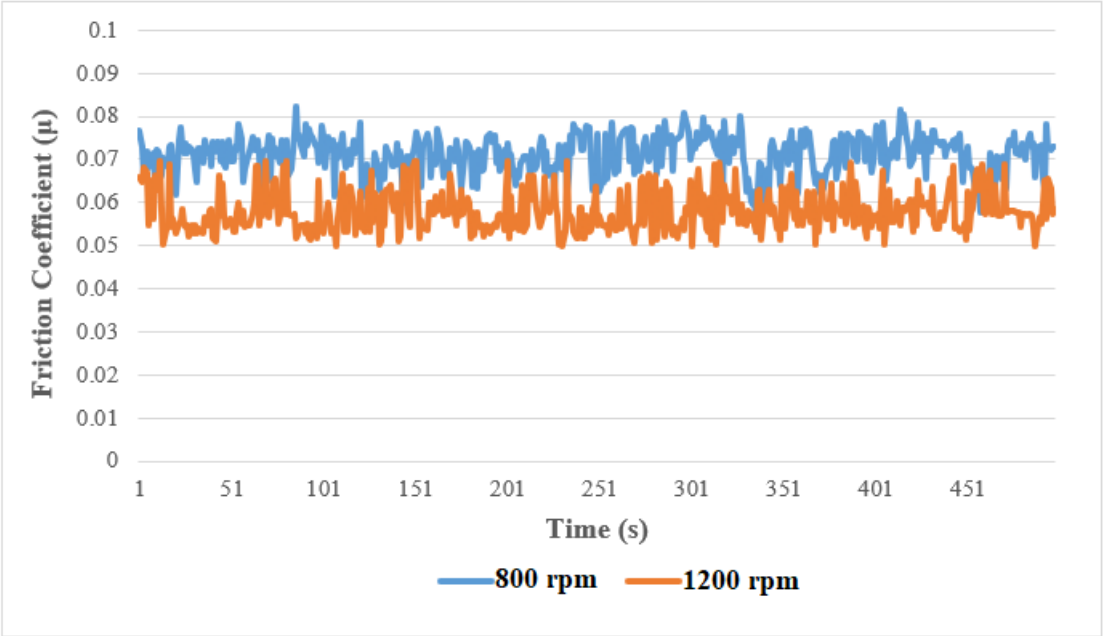

Graphic 1. Friction coefficient change of Etial 171 sample with 10W40 oil at 800 and 1200 rpm.

The average friction coefficients were measured as 0.0712 for 800 revolutions and 0.0580 for 1200 revolutions. As can be seen in this experiment, friction increases at 800 rpm.

Table 4. Temperature change of ETİAL 171 sample with 10W40 oil at different cycles over time.

RPM	1 min	2 min	3 min	4 min	5 min	6 min	7 min	8 min
800	21,9	22,4	22,8	22,9	23,2	23,4	23,5	23,8
1200	22,3	23,2	23,3	23,4	24	24,1	24,2	24,4

As can be seen in Table 4, the maximum temperature increase occurred at 1200 rpm. Weight changes were measured as 0.001 g for 800 rpm, and no weight change was observed for 1200 rpm. The changes in the friction coefficients of the ETİAL 171 sample with 20W50 lubricant at different speeds are shown in Graphic 2.

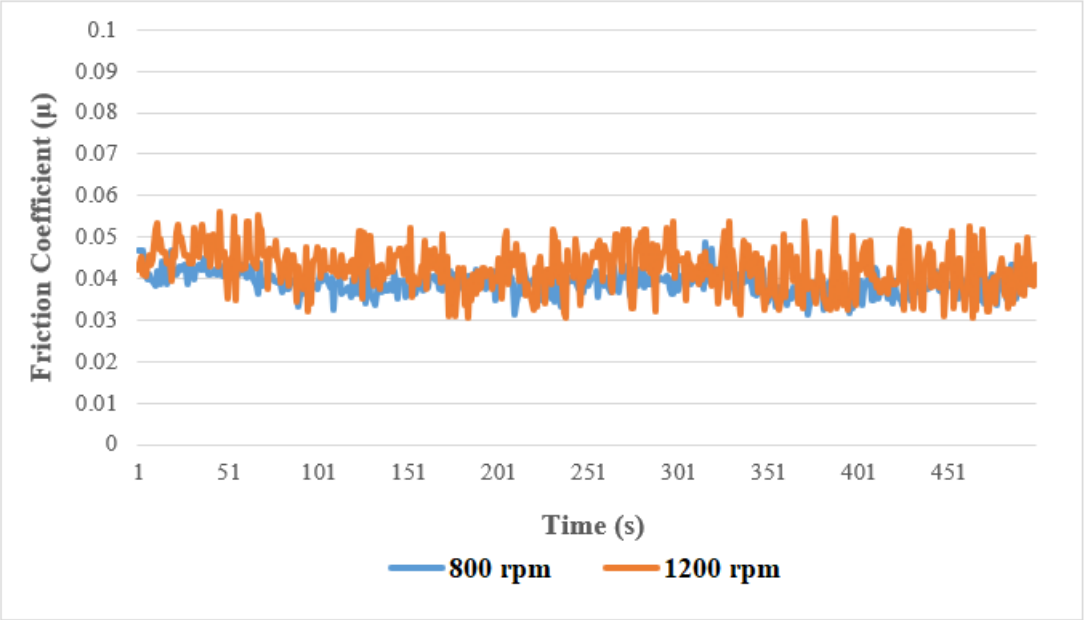

Graphic 2. Friction coefficient change of ETİAL 171 sample with 20W50 oil at 800 and 1200 rpm.

In the graph shown in Graphic 2, friction coefficients were measured as 0.0390 for 800 rpm and 0.0424 for 1200 rpm. As can be seen in this experiment, the average friction coefficient increases at 1200 rpm. Accordingly, as the speed increases, the distance traveled increases and as a result, the friction coefficient may increase.

Table 5. Temperature change over time of ETİAL 171 sample with 20W50 oil at different cycles.

RPM	1 min	2 min	3 min	4 min	5 min	6 min	7 min	8 min
800	22	22,2	22,4	22,4	22,4	22,4	22,4	22,6
1200	21,6	22,5	22,9	23,1	23,2	23,9	24	24,3

As seen in Table 5, the maximum temperature increase occurred at 1200 rpm. Weight changes were measured as 0.003 g for 800 rpm and 0.001 g for 1200 rpm.

Friction tests with oils of different viscosities

The tests performed with 10W40 and 20W50 lubricants were examined by dividing them into cycles under this heading.

Tests performed at 800 rpm speed

Friction coefficient changes are shown in Graphic 3 by applying friction tests with 10W40 and 20W50 oil at 800 rpm on the ETİAL 171 sample.

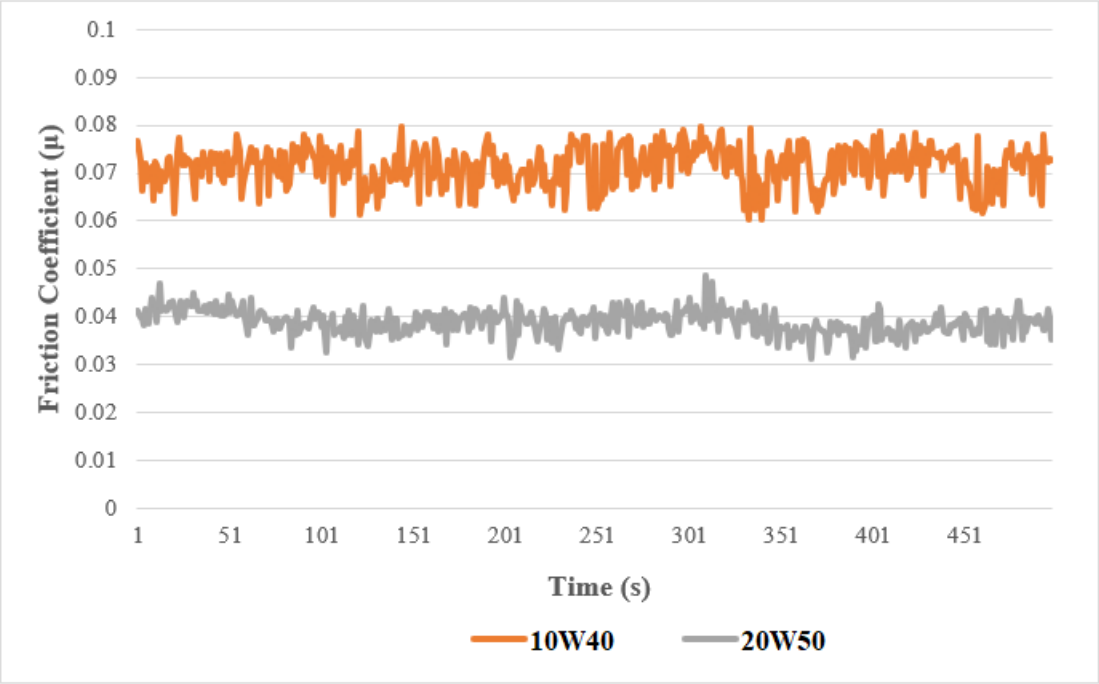

Graphic 3. Friction coefficient change of ETİAL 171 sample with variable oils at 800 rpm.

The average friction coefficient was determined as 0.0713 for 10W40 oil and 0.0389 for 20W50 oil. It can be said that 10W40 oil causes more wear for the ETIAL 171 sample alloy. Table 6 shows the time-dependent temperature changes of the ETİAL 171 sample with different oils at 800 rpm.

Table 6. Temperature change over time of ETİAL 171 sample with different oils at 800 rpm.

Lubricants	**1 min**	**2 min**	**3 min**	**4 min**	**5 min**	**6 min**	**7 min**	**8 min**
10W40	21,9	22,4	22,9	23	23,2	23,4	23,5	23,8
20W50	21,5	22	22,4	22,4	22,4	22,4	22,4	22,5

The friction coefficient change of ETİAL 171 sample was performed at 1200 rpm with 10W40 and 20W50 oil and the change in friction coefficient is shown in Graphic 4.

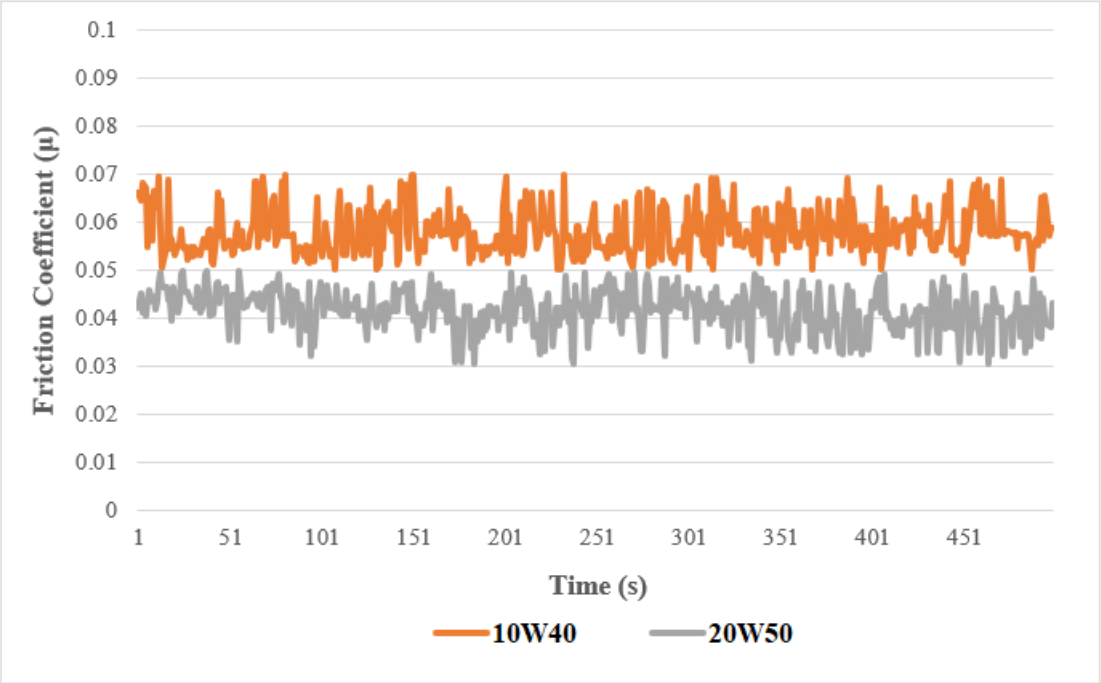

Graphic 4. Friction coefficient change of ETİAL 171 sample with variable oils at 1200 rpm.

The average friction coefficient was determined as 0.0579 for 10W40 oil and 0.0420 for 20W50 oil. The oil that reduces wear on the alloy structure of the ETİAL 171 sample is 20W50 oil.

Table 7. Temperature change of ETİAL 171 sample over time with different oils at 1200 rpm.

Lubricant	1 min	2 min	3 min	4 min	5 min	6 min	7 min	8 min
10W40	22,3	23,2	23,3	23,4	23,8	24,1	24,2	24,4
20W50	21,6	22,5	22,7	23	23,2	23,9	24	24,3

As shown in Table 7, the maximum temperature increase occurred in 10W40 oil for ETİAL 171. The weight change was 0.001 g in 20W50 oil and there was no weight loss in 10W40 oil.

Results

The alloy ratios of silicon and copper, which are alloying elements that directly affect the coefficient of friction, change the coefficient of friction on the material surface. According to this information, the amount of silicon must be increased to reduce the friction coefficient.

It was observed that the sample mass decreased with the increase in temperature, and thus it was determined that the temperature had an effect on wear.

The increase in friction coefficients is clearly seen at 1200 rpm. Accordingly, it has been determined that when the number of revolutions is increased, wear will increase depending on the distance traveled.

When the experiments were examined, it was concluded that the change factor in wear depends on temperature, alloy aluminum, speed and friction lubricant viscosity. In the light of this information and tests, it has been concluded that oil types should be selected according to the alloy structure of each material and the load.

REFERENCES

Adly, S. & Attouch, H. (2020). Finite convergence of proximal-gradient inertial algorithms combining dry friction with Hessian-driven damping. *SIAM Journal on Optimization*, *30*(3), 2134-2162.

Akkurt M. (1990). Makine Elemanları. Cilt 1, Birsen Yayınevi, 280-281, İstanbul.

Callister W. D. & Retwisch D. G. (2014). Materials and engineering 9th edition. New York: Jonh Wiley and Sons Inc.

Cheng, S., Li, L., Chen, X., Fang, S. N., Wang, X. Y., Wu, X. H. & Li, W. B. (2020). Longitudinal autonomous driving based on game theory for intelligent hybrid electric vehicles with connectivity. *Applied energy*, *268*, 115030.

Cui, Y., Ding, M., Sui, T., Zheng, W., Qiao, G., Yan, S. & Liu, X. (2020). Role of nanoparticle materials as water-based lubricant additives for ceramics. *Tribology International*, *142*, 105978.

Dhanola, A., Khanna, N. & Gajrani, K. K. (2022). A critical review on liquid superlubricitive technology for attaining ultra-low friction. *Renewable and Sustainable Energy Reviews*, *165*, 112626.

Dhas, D. S. E. J., Raja, R., Jannet, S., Wins, K. L. D., Thomas, J. M. & Kandavalli, S. R. (2023). Effect of carbide ceramics and coke on the properties of dispersion strengthened aluminium-silicon7-magnesium hybrid composites. *Materialwissenschaft und Werkstofftechnik*, *54*(2), 147-157.

Doan, B. Q., Nguyen, D. T., Nguyen, M. N., Le, T. H. & Hao, T. M. (2021). A review on properties and casting technologies of aluminum alloy in the machinery manufacturing. *Journal of Mechanical Engineering Research and Developments*, *44*(8), 204-217.

Erdem, V. E. (2006). AISI 1060 Çeliğinin Erozif Aşınma Özelliklerinin İncelenmesi ve Geliştirilmesi (Doctoral dissertation, Fen Bilimleri Enstitüsü).

ETİ Alüminyum (2023). Alaşımlı Külçelerin Kimyasal Bileşim Limitleri. (19.10.2023 on https://www.etialuminyum.com/urunler/ham-aluminyum-urunler/dokumhane-urunleri/#1518777754160-ea84cb9f-55e1 accessed from)

Ferraris, M., Gili, F., Lizarralde, X., Igartua, A., Mendoza, G., Blugan, G. & Casalegno, V. (2022). SiC particle reinforced Al matrix composites brazed on aluminum body for lightweight wear resistant brakes. *Ceramics International*, *48*(8), 10941-10951.

Gialanella, S. & Malandruccolo, A. (2020). *Aerospace alloys* (pp. 129-189). Cham, Switzerland: Springer.

Ferraris, M., Gili, F., Lizarralde, X., Igartua, A., Mendoza, G., Blugan, G. & Casalegno, V. (2022). SiC particle reinforced Al matrix composites brazed on aluminum body for lightweight wear resistant brakes. *Ceramics International*, *48*(8), 10941-10951.

Hatice, A. K. Ç. A., İyibilgin, O. & Gepek, E. (2020). Biyomalzemeler ile İmplant Üretimi Sürecinin Biyotriboloji Yönünden Değerlendirilmesi. *Düzce Üniversitesi Bilim ve Teknoloji Dergisi*, *8*(1), 667-692.

Hu, L., Zhou, X., Zhang, X., Wang, F., Li, Q. & Wu, W. (2021). A review on key challenges in intelligent vehicles: Safety and driver-oriented features. *IET Intelligent Transport Systems*, *15*(9), 1093-1105.

Işık, Y., Tekin, B., Yılmaz, A., Tatoğlu, F. & Öztürk, D. (2020). Weight Optimization of Aluminum Alloys Used in Vehicles. *International Journal of Mechanical Engineering*, *7*(11).

Jabbar, N. A., Hussain, I. Y. & Abdullah, O. I. (2021). Thermal and thermoelastic problems in dry friction clutch: A comprehensive review. *Heat Transfer*, *50*(8), 7855-7878.

McCracken K. E. & Yoon J. Y. (2016). Recent approaches for optical smartphone sensing in resourcelimited settings: A brief review. Analytical Methods, c. 8, s. 36, ss. 6591–6601.

Kaplan, A. U., Duysak, L., Gulaboğlu, M., Dogru, U. & Çetin, M. (2019). Determination of antioxidant capacity of methanol and aqueous extracts of Inula graveolens. In *4th Internatıonal Conference On Advances In Natural & Applıed Scıences* (p. 690).

Khelge, S., Kumar, V., Shetty, V. & Kumaraswamy, J. (2022). Effect of reinforcement particles on the mechanical and wear properties of aluminium alloy composites. *Materials Today: Proceedings*, *52*, 571-576.

Kotadia, H. R., Gibbons, G., Das, A. & Howes, P. D. (2021). A review of Laser Powder Bed Fusion Additive Manufacturing of aluminium alloys: Microstructure and properties. *Additive Manufacturing*, *46*, 102155.

Li, Y., Schreiber, P., Schneider, J. & Greiner, C. (2023). Tribological mechanisms of slurry abrasive wear. *Friction*, *11*(6), 1079-1093.

Minami, D. (2009). Ionic liquids in tribology. Molecules (Basel, Switzerland), c. 14, s. 6, ss. 2286– 2305.

Ölmez S. (2016). Alüminyum Alaşımlı Malzemelerin Yüksek Sicaklık Aşınma Davranışlarının İncelenmesi, Yıldız Teknik Üniversitesi, Fen Bilimleri Enstitüsü, Yüksek Lisans Tezi, İstanbul.

Omiyale, B. O., Olugbade, T. O., Abioye, T. E. & Farayibi, P. K. (2022). Wire arc additive manufacturing of aluminium alloys for aerospace and automotive applications: A review. *Materials Science and Technology*, *38*(7), 391-408.

Öztürk M. (2018). Bor Minerali Atığı Katkılı Polipropilen Kompozit Malzemelerin Mekanik Ve Tribolojik Özelliklerinin İncelenmesi, Sakarya Üniversitesi, Fen Bilimleri Enstitüsü, Yüksek Lisans Tezi, Sakarya.

Payalan, Y. F. & Guvensan, M. A. (2019). Towards next-generation vehicles featuring the vehicle intelligence. *IEEE Transactions on Intelligent Transportation Systems*, *21*(1), 30-47.

Reddy, P. V., Kumar, G. S., Krishnudu, D. M. & Rao, H. R. (2020). Mechanical and wear performances of aluminium-based metal matrix composites: a review. *Journal of Bio-and Tribo-Corrosion*, *6*(3), 83.

Rodríguez, J. S., Duran, J. F., Aguilar, Y., Alcazar, G. P., Toro, A. & Zambrano, O. A. (2023). Effect of Al content on the low-stress abrasive wear behaviour of Fe-18Mn-xAl-0.7 C alloys. *Tribology International*, *180*, 108286.

Ru, G., Qi, W., Tang, K., Wei, Y. & Xue, T. (2020). Interlayer friction and superlubricity in bilayer graphene and MoS2/MoSe2 van der Waals heterostructures. Tribology International, 151, 106483.

Sathish, T., Saravanan, R., Kumar, A., Prakash, C., Shahazad, M., Gupta, M. & Smirnov, V. A. (2023). Influence of Synthesizing Parameters on Surface Qualities of Aluminium Alloy AA5083/CNT/MoS2 Nanocomposite in Powder Metallurgy Technique. *Journal of Materials Research and Technology*.

Sharma, A. K., Bhandari, R., Aherwar, A., Rimašauskienė, R. & Pinca-Bretotean, C. (2020). A study of advancement in application opportunities of aluminum metal matrix composites. *Materials Today: Proceedings*, *26*, 2419-2424.

Sharma, A. K., Bhandari, R., Aherwar, A., Rimašauskienė, R. & Pinca-Bretotean, C. (2020). A study of advancement in application opportunities of aluminum metal matrix composites. *Materials Today: Proceedings*, *26*, 2419-2424.

Yavuz İ., Mutlu İ., Çetkin A. & İşel B. (2021). Effect of The Operating Temperature of Oil On Gear Teeth Surface Damages, El-Cezeri Fen ve Mühendislik Dergisi, 8(1); 495-503.

Yüksel, N. ve Şahin, S. (2014). Fe-Cr-C ve Fe-Cr-C-B bazlı sert dolgu alaşımlarının aşınma davranışı-sertlik-mikroyapı ilişkisi. *Malzemeler ve tasarım* , *58* , 491-498.

Zhang, A. & Li, Y. (2023). Effect of alloying elements on thermal conductivity of aluminum. *Journal of Materials Research*, *38*(8), 2049-2058.

Zhang, M., Tian, Y., Zheng, X., Zhang, Y., Chen, L. & Wang, J. (2023). Research Progress on Multi-Component Alloying and Heat Treatment of High Strength and Toughness Al–Si–Cu–Mg Cast Aluminum Alloys. *Materials*, *16*(3), 1065.

Zhang, S., Qiao, Y., Liu, Y., Ma, L. & Luo, J. (2019). Molecular behaviors in thin film lubrication—Part one: Film formation for different polarities of molecules. *Friction*, *7*, 372-387.

An Improved Deep Multi-Layered GMDH-Type Neural Network for Pharmaceutical Sales Forecasting

Kenan KARAGUL[1]
Sezai TOKAT[2]
Yusuf SAHIN[3]
Erdal AYDEMIR[4]

1. Introduction

Sales forecasting entails the process of predicting a company's future sales. This prediction relies on the analysis of historical sales data, market trends, and other relevant information to estimate a company's likely sales in the upcoming months or years. Sales forecasting and prediction provide crucial insights for managing a company's workforce, including labor, cash flow, and resources (Kohli et al., 2021). These forecasts empower businesses to plan for the future and make informed decisions regarding areas such as inventory management, marketing strategies, and resource allocation. Additionally, they assist in identifying potential challenges or opportunities, allowing for adjustments in business strategies.

Common methods employed in sales forecasting include time series analysis, regression analysis, and artificial intelligence techniques. The Group Method of Data Handling (GMDH) is an approach used for automating the creation of predictive models. GMDH belongs to the category of self-organizing artificial intelligence algorithms that build models based on input data (Nyugen et al., 2019). These algorithms find application in various domains, encompassing predictive analytics, optimization, data mining, complex system modeling, physiological experiments, cybernetics, medical science, pattern recognition, and machine learning (Alizamir et al., 2020; Tsai and Yen, 2017). They prove particularly valuable when dealing with a substantial number of input variables where determining their significance in predicting outcomes is not immediately evident (Nariman-Zadeh et al., 2003).

GMDH algorithms initiate with a set of input variables. The traditional GMDH algorithm generates models for all possible combinations of input variables. These models are subsequently tested and evaluated. If they do not meet the required accuracy, the algorithm repeats the process using different input variables, refining the model iteratively. This iteration continues until a satisfactory model capable of accurately predicting outcomes based on the input data is achieved (Anastasakis and Mort, 2001). GMDH-type neural networks refer to neural networks that can autonomously organize their architecture through a heuristic self-organization method (Farloow, 1984; Ivakhenko, 1970), a form of evolutionary computation. Deep GMDH-type neural networks, on the other hand, can self-organize deep neural network architectures with numerous hidden layers to accommodate the complexity of medical images. Furthermore, these deep GMDH-type neural networks can self-select the best neural network

[1] Assoc. Prof. Dr., Pamukkale University, Honaz MYO, Dept. of Logistics, Denizli, Turkiye
[2] Prof. Dr., Pamukkale University, Faculty of Engineering, Dept. of Computer Engineering, Denizli, Turkiye
[3] Assoc. Prof. Dr., Burdur Mehmet Akif Ersoy University, Faculty of Economics and Administrative Sciences, Dept. of Business Administration, Burdur, Turkiye
[4] Assoc. Prof. Dr., Suleyman Demirel University, Faculty of Engineering and Natural Sciences, Dept. of Industrial Engineering, Isparta, Turkiye

architecture from three types: sigmoid function neural networks, radial basis function (RBF) neural networks, and polynomial neural networks (Takao et al., 2018).

This study's primary contribution lies in exploring the capability of a deep multi-layered Group Method of Data Handling (GMDH)-type artificial neural network model for sales forecasting in the pharmaceutical dataset. Nevertheless, it's worth noting that the reliance on a single dataset can be considered a limitation of this research. Additionally, the study uses and enhances forecasting performance indicators, such as MAPE and RMSE values, to evaluate the performance.

The rest of this paper is organized as follows. A highly related literature review is given in Sect. 2. Then, the deep multi-layered GMDH-type neural network and its extensions with Hampel filter and moving average smoothing approaches are given in detail in Sect. 3. Moreover, Sect. 4 provides the experimental study with computational solutions considering the proposed methodology by applying monthly pharmaceutical sales data and the conclusion with future directions are given in Sect. 5.

2. Background

The Group Method of Data Handling (GMDH), also known as Polynomial Neural Networks, is an alternative neural network modeling algorithm. GMDH operates on an inductive self-organizing approach to establish black box models when relationships between variables are unknown (Vissikirsky and Stepashko, 2005). Unlike extensively studied multi-layer network structures, the GMDH network structure has received relatively less attention. This concept and the GMDH networks were introduced by Professor Alexey G. Ivakhnenko in 1966 during his studies at the Ukrainian Institute of Cybernetics in Kyiv (Madala and Ivankhnenko, 1994). These networks automatically determine essential input variables, the number of layers, neurons in hidden layers, and the optimal model structure. Consequently, GMDH networks consist of active neurons that self-organize. They learn inductively, striving to build a polynomial model with minimal error between predicted and expected outputs (Farlow, 1981). In 1984, the self-organizing approach was further developed for the GMDH method (Farlow, 1984).

After the expansion of GMDH studies in the English language, Ivakhnenko and Ivakhnenko (1995) presented GMDH algorithms for research fields such as physical, multidimensional processes, stepwise forecasting, data sampling and clustering, pattern recognition, complexity, and more. Steiger (1997) subsequently utilized the GMDH method to determine key model parameters with a simplified polynomial metamodel, enhancing decision makers' understanding. Nikolaev and Iba (2003) proposed a polynomial harmonic GMDH learning model for time-series forecasting, achieving superior polynomial network performance compared to previous GMDH, Neuro-fuzzy GMDH, and traditional MLP neural networks. Huang (2006) introduced an adaptive learning network, known as the neural-fuzzy GMDH, which was compared with traditional MLP GMDH models. In another study, a fuzzy-GMDH network model was applied to forecast container demand under fuzzy demand uncertainties (Huang, Bae, and Cho, 2006).

As a result, there was a rapid increase in time series forecasting studies using the GMDH methodology. GMDH-based abductive network models were used to forecast mean hourly wind speed time series in Dhahran, Saudi Arabia, showing an 8.2% reduction in Mean Absolute Error (MAE) compared to hourly persistence (Abdel-Aal, Elhadidy, and Shaahid, 2009). In a different study, monthly cigarette sales with long-term upward and seasonal fluctuations were modeled using ARIMA and GMDH network models, both linear and nonlinear, to improve forecasting accuracy (Zheng, Liu, and Zhao, 2010). Samsudin, Saad, and Shabri (2011)

proposed a new forecasting model that combined GMDH and least squares support vector machine (LSSVM) for three well-known time series datasets. Shaverdi, Fallahi, and Bashiri (2012) achieved high performance in predicting the stock price of petrochemical companies using a GMDH-type neural network. In another study, GMDH, along with other methods, was applied to improve ATMs' cash demand forecasts, with the general regression neural network (GRNN) method yielding the best result (Venkatesh et al., 2014).

In the context of short-term electric load forecasting, the GMDH-type neural network model outperformed the regression analysis model for Gidan Kwano campus, Federal University of Technology Minna, Nigeria, in terms of root mean square error (RMSE) and mean absolute percentage error (MAPE) (Jacob et al., 2015). Additionally, an R package for GMDH was introduced for short-term forecasting of the cancer death rate in Pennsylvania from 1930 to 2000, demonstrating greater effectiveness compared to ARIMA and exponential smoothing models (Dag and Yozgatligil, 2016).

In this paper, a deep multi-layered Group Method of Data Handling (GMDH)-type artificial neural network model is developed for pharmaceutical sales forecasting data (Web-1). This section summarizes studies using GMDH and its applications as related literature.

3. Proposed Methodology

In this section, the details of the GMDH type artificial neural network used for demand forecasting and the new methods added to this structure are explained. GMDH was the first model used for forecasting (Model 1). Model 2 was created by adding the Hampel Filter to this model, and Model 3 was created by adding the moving average to Model 2.

3.1. GMDH-type Polynomial Neural Networks: A self-organizing machine learning algorithm (Model 1)

Artificial Neural Networks (ANN) are robust tools for modeling systems, estimating time series data, and making predictions. Unlike traditional time series analysis and prediction methods, ANNs require minimal information about time series data and have a broad range of applications (Srinivasan, 2008). Today, various neural network models are employed for handling time-series data, including demand and inventory forecasting. The multi-layer feed-forward neural network structure is the most commonly used and well-documented in the literature, showing its effectiveness in prediction and estimation through numerous research studies. Although methods have been developed to determine the optimal number of hidden layers and hidden neurons, these values are often determined through trial and error.

In contrast, the Group Method of Data Handling (GMDH) network structure, which is another option, has received comparatively less attention in the realm of neural networks than the multi-layer structure. This concept and GMDH networks were first introduced by Professor Alexey G. Ivakhnenko in 1968 during his studies at the Ukrainian Institute of Cybernetics in Kyiv. It gained widespread recognition only after being translated into English. GMDH networks automatically determine critical input variables, the number of layers, neurons in the hidden layers, and the optimal model structure. Consequently, these networks are composed of active neurons that organize themselves. The GMDH network operates in an inductive manner, striving to create a function (referred to as the polynomial model) that minimizes the error between predicted values and expected outputs.

Group Method of Data Handling (GMDH) polynomial neural networks are a specialized form of "self-organizing" artificial neural networks. GMDH networks begin with input neurons, and during the training process, neurons are selected from a candidate pool and added to hidden layers in each step. GMDH methods have found their place in both the literature and practical

applications across various domains, encompassing deep learning, information extraction, forecasting, estimation, data mining, optimization, and pattern recognition (Kasaeian et al., 2017). GMDH algorithms enable the automatic discovery of data relationships to select an optimal model or network structure and enhance the accuracy of existing algorithms. The structure and components of the GMDH network are explained in the following section.

3.1.1.Structure of the GMDH network

GMDH networks are self-organizing. The self-organization of this network means that the connections and layer numbers between neurons in the network are not constant but instead are chosen to optimize the network during training. GMDH networks traditionally use regression analysis to solve the problem. The first step is to decide the type of polynomial the regression must find. The aim is to make the error between the throughput $\hat{f}$ and the target output f the smallest. A target function for M observations defined with multiple-input-single-output data pairs can be expressed as shown in Equation (1) (Kasaeian vd., 2017):

$$y_i = f(x_{i1}, x_{i2}, \dots, x_{iM})(i = 1,2, \dots, M) \tag{1}$$

In a GMDH type artificial neural network, any specified input vector $X = (x_{i1}, x_{i2}, \dots, x_{iM})$ is used to calculate the network output:

$$\hat{y}_i = \hat{f}(x_{i1}, x_{i2}, \dots, x_{iM})(i = 1,2, \dots, M) \tag{2}$$

The next step is to define a GMDH-type neural network model to minimize the square of the difference between the actual target y_i and the predicted $\hat{y}_i$:

$$min \left\{ \sum_{i=1}^{M} [\hat{f}(x_{i1}, x_{i2}, \dots, x_{iM}) - y_i^2] \right\} \tag{3}$$

Using a complex discrete form of the Volterra functional series (Srinivasan, 2008), the general relationship between input and output parameters can be formulated as Equation (4):

$$\hat{y} = a_0 + \sum_{i=1}^{n} a_i x_i + \sum_{i=1}^{n} \sum_{j=1}^{n} a_{ij}\, x_i x_j + \sum_{i=1}^{n} \sum_{j=1}^{n} \sum_{k=1}^{n} a_{ijk}\, x_i\, x_j x_{k+\cdots} \tag{4}$$

This formulation is known as the Kolmogorov-Gabor polynomial (Srinivasan, 2008). For example, if we want to express the above equation for a partial quadratic polynomial system consisting of only two parameters (i.e. neuron for network structure), it is possible to express it with the following total algebraic equation (Equation 5):

$$\hat{y} = a_0 + a_1 x_i + a_2 x_j + a_3 x_i^2 + a_4 x_j^2 + a_5 x_i x_j \tag{5}$$

To establish the general mathematical correlation of input-output parameters a_{ij} presented in the general relationship formulation between input and output parameters, a partial quadratic plot is performed in the opposite direction through a common neuron network. Regression methods are used for this purpose to minimize the difference between the actual output y and the calculated network output $\hat{y}$ for each input parameter x_i, x_j pair. Learning of the network is

carried out on this structure. For detailed information, Farlow (1984) and Rezai et al. (2018) can be examined. GMDH network structure is given in Figure 1 (Zor et al., 2020).

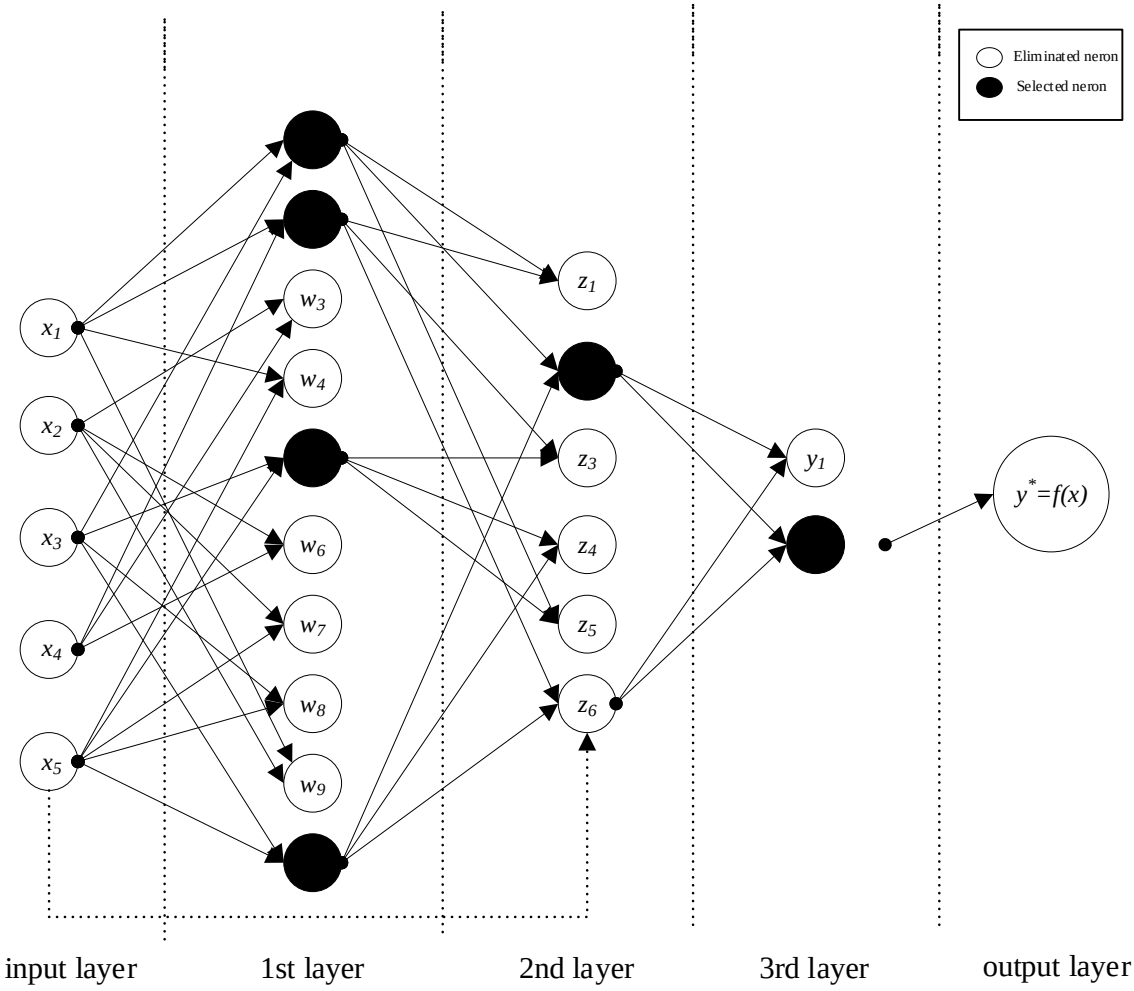

Figure 1. GDMH Network Structure (Zor et al. 2020)

3.1.2.Training Algorithm of GMDH

Two sets of input data are used in the training process: (1) primary training data and (2) control data used to halt the construction process when overfitting occurs. Control data are typically chosen to be about 20% of the training data. GMDH network training steps can be listed as follows:

Step 1. The first layer is created using each of the input prediction variable values.

Step 2. Using the input combinations from the previous layer and the allowed set of functions, all possible functions are obtained. If specifically, only bivariate polynomials are enabled, for example, then $n\ x\ \frac{(n-1)}{2}$ candidate neurons are created, where the parameter *n* is the number of neurons in the previous layer. If inputs from the previous layer and input layer are allowed, then *n* will be the sum of the number of neurons in the previous layer and the input layer. If input from any layer is allowed, the parameter *n* will be the sum of the number of input variables plus the number of neurons in all previous layers.

Step 3. Use least squares regression to calculate optimal parameters for the function in each candidate neuron to best fit the training data. Singular value decomposition (SVD) is used to avoid problems with singular matrices. If nonlinear functions such as logistics or asymptotic are selected, a nonlinear fitting routine based on the Levenberg-Marquardt method is used.

Step 4. The mean square error for each neuron is calculated by applying it to the control data.

Step 5. The candidate neurons are listed in order of increasing error.

Step 6. For the next layer, the best (smallest error) neurons are selected from the candidate cluster. The modeling parameter specifies how many neurons are used in each layer.

Step 7. If the error of the best neuron in the layer measured by the control data is better than the error of the best neuron in the previous layer and the maximum number of layers is not reached, go back to step 2 and build the next layer. Otherwise, the target has been achieved and the training process will be stopped. When overfitting starts, the training is stopped because the error measured by the control data will increase.

3.2. Model 2: Model 1 + Hampel Filter

Step 1. Storage of data from Excel file

Step 2. Detecting extremes and bringing them to average values (outlier detection). This should be done to reduce the effect of temporary leaps in sales on the learning process. Otherwise, since these leaps will be learned, it will not be possible to obtain the desired general sales model. Hampel filter was used for this purpose (Pearson, 2005). The pseudo code of the Hampel filter is given in Algorithm-1. If $t = 0$ in the Hampel filter, a median filter is obtained (Web-2, Web-3).

```
HampelFilter <---- function (x, k, t0=3)
{
        n <---- length(x)
        y <---- x
        ind<---- c( )
        L <---- 1.4826
        for (i in (k + 1):(n - k))
        {
        x0 <---- median(x[(i - k):(i + k)])
        S0 <---- L * median(abs(x[(i - k):(i + k)] - x0))
        if (abs(x[i] - x0) > t0 * S0)
        {
        y[i] <---- x0
        ind<---- c(ind, i)
        }
        }
        list(y = y, ind = ind)
}
```

Figure 2. Hampel Filter Pseudo Code (Algorithm 1)

3.3.Model 3: Model 2 + Moving Average

Step 3. Data smoothing with moving smoothing filter.

Step 4. Separating the data set into training and test data sets.

Step 5. Creating the GMDH Network with the training set.

Step 6. Testing the results with test data independent of the training set used in modeling the GMDH Network.

Step 7. Obtaining the estimated stock value for the next month at a certain moment

4. Experimental Results

4.1. Test Instances and Solution Procedure

Monthly and weekly data were emphasized in the analysis studies. Successful estimation results were obtained on both monthly and weekly data. The process flow diagram discussed in the study is given in Figure 3. Since the ABC Analysis in Figure 2 is a very common and known approach in inventory management systems and the literature, details about ABC Analysis are not given here. However, for those who are interested, it is recommended to consult the article of Zenkova and Kabanova (2018).

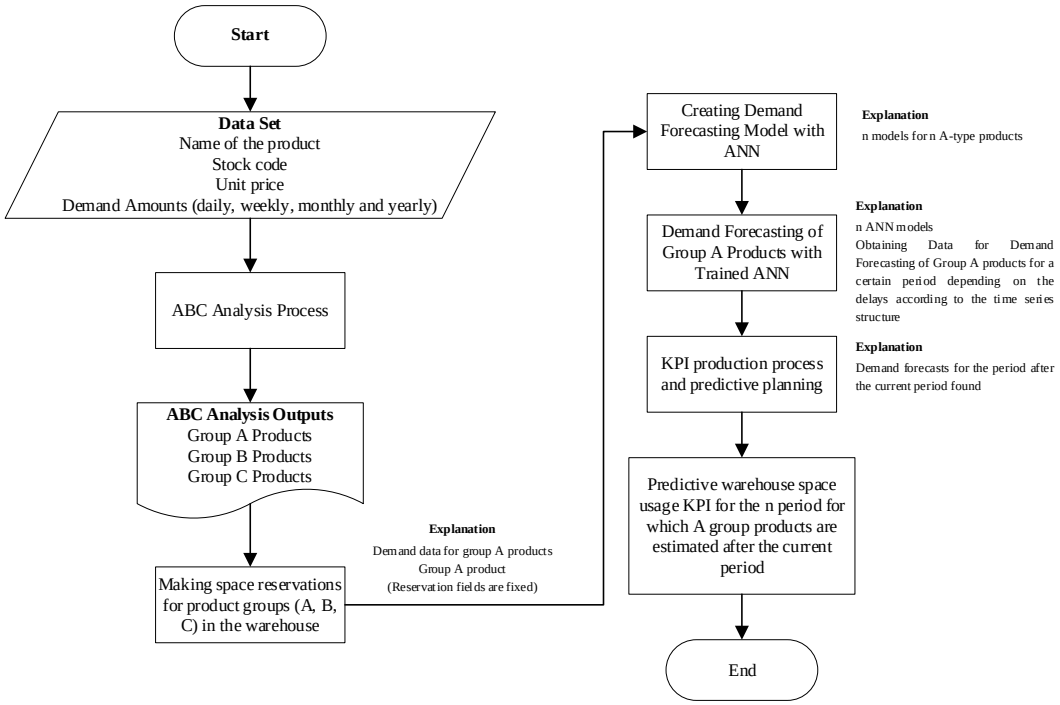

Figure 3. Flow process of the method

4.2. Computational Results

In this section, the dataset is performed on i7 CPU and 16 Gb Ram computer with MATLAB® software on the reasonable times. The computational analysis is given eight dataset such as M01AB, M01AE, N02BA, N02BE, N05B, N05C, R03 and R06 respectively (Web-1). So, the successful forecasting results are obtained on both monthly and weekly data. MAPE and RMSE performance indicators are used here for forecasting success. The all results are shown in Table 1.

According to the results obtained from Model1 to the proposed Model3, the change in R value for dataset M01AB is 160.86% and for dataset M01AE 112.21% improvement is observed. Similarly, 77.69%, 18.46%, 60.87% were observed for dataset 3-5. A dramatic improvement of 1520.43% was observed for dataset 6 (N05C). In dataset 7 and 8, these rates are 68.26% and 24.92% respectively.

Furthermore, in Figure 4, the RMSE deviation is shown for all datasets for both the training process, the testing process and the solution approach respectively, and then in Figure 5, the correlation coefficient (R) values are similarly shown.

Table 1. All results

Dataset	Analysis	Model 1		Model 2		Model 3	
		RMSE	**MAPE**	**RMSE**	**MAPE**	**RMSE**	**MAPE**
#01 M01AB	Train	8.1111	3.25E-04	7.4663	1.82E-04	3.1613	4.31E-05
	Test	8.0739	6.62E-04	6.3459	3.17E-04	2.7704	7.92E-05
	All	8.1000	2.19E-04	7.1487	1.18E-04	3.0493	2.82E-05
	R	**0.3270**		**0.3830**		**0.8530**	
#02 M01AE	Train	6.0427	1.59E-04	5.3695	1.64E-04	2.4105	3.69E-05
	Test	7.1133	2.86E-04	6.7270	3.77E-04	3.4621	7.44E-05
	All	6.3828	1.04E-04	5.8101	1.14E-04	2.7683	1.20E-05
	R	**0.4037**		**0.4726**		**0.8567**	
#03 N02BA	Train	7.3280	1.34E-04	6.7473	2.01E-04	2.9167	3.71E-05
	Test	7.3022	1.80E-03	5.4743	1.20E-03	2.5430	7.76E-04
	All	7.3203	2.31E-05	6.3921	4.80E-05	2.8099	2.23E-05
	R	**0.5075**		**0.5707**		**0.9018**	
#04 N02BE	Train	43.4468	1.47E-04	36.5255	9.54E-05	16.1227	4.59E-05
	Test	45.9360	2.87E-04	44.6881	2.00E-04	21.4680	4.07E-05
	All	44.2083	9.82E-05	39.1533	6.48E-05	17.8947	2.63E-05
	R	**0.8151**		**0.8438**		**0.9656**	
#05 N05B	Train	19.6380	4.08E-04	17.3227	3.03E-04	7.6722	5.76E-05
	Test	15.6128	5.03E-04	15.5414	9.17E-04	7.3283	2.43E-05
	All	18.5225	2.48E-04	16.8081	2.30E-04	7.5707	3.08E-05
	R	**0.5660**		**0.6164**		**0.9105**	
#06 N05C	Train	2.8931	1.80E-03	2.4400	1.40E-03	1.0134	1.92E-04
	Test	3.9482	5.40E-03	2.8163	3.90E-03	1.3021	6.89E-04
	All	3.2459	1.40E-03	2.5587	1.10E-03	1.1080	1.61E-04
	R	**0.0509**		**0.304**		**0.8248**	
#07 R03	Train	17.2869	8.17E-04	15.3128	7.58E-04	6.5949	1.92E-04
	Test	23.4612	3.10E-03	23.2956	3.40E-03	10.0584	6.89E-04
	All	19.3472	7.37E-04	18.0816	7.68E-04	7.7972	1.61E-04
	R	**0.5416**		**0.5706**		**0.9113**	
#08 R06	Train	6.3728	4.71E-04	6.1124	3.22E-04	2.6104	1.23E-04
	Test	9.1584	1.20E-03	7.9616	1.00E-03	3.6696	4.70E-04
	All	7.3206	3.39E-04	6.7208	2.58E-04	2.9681	1.10E-04
	R	**0.7668**		**0.7949**		**0.9579**	

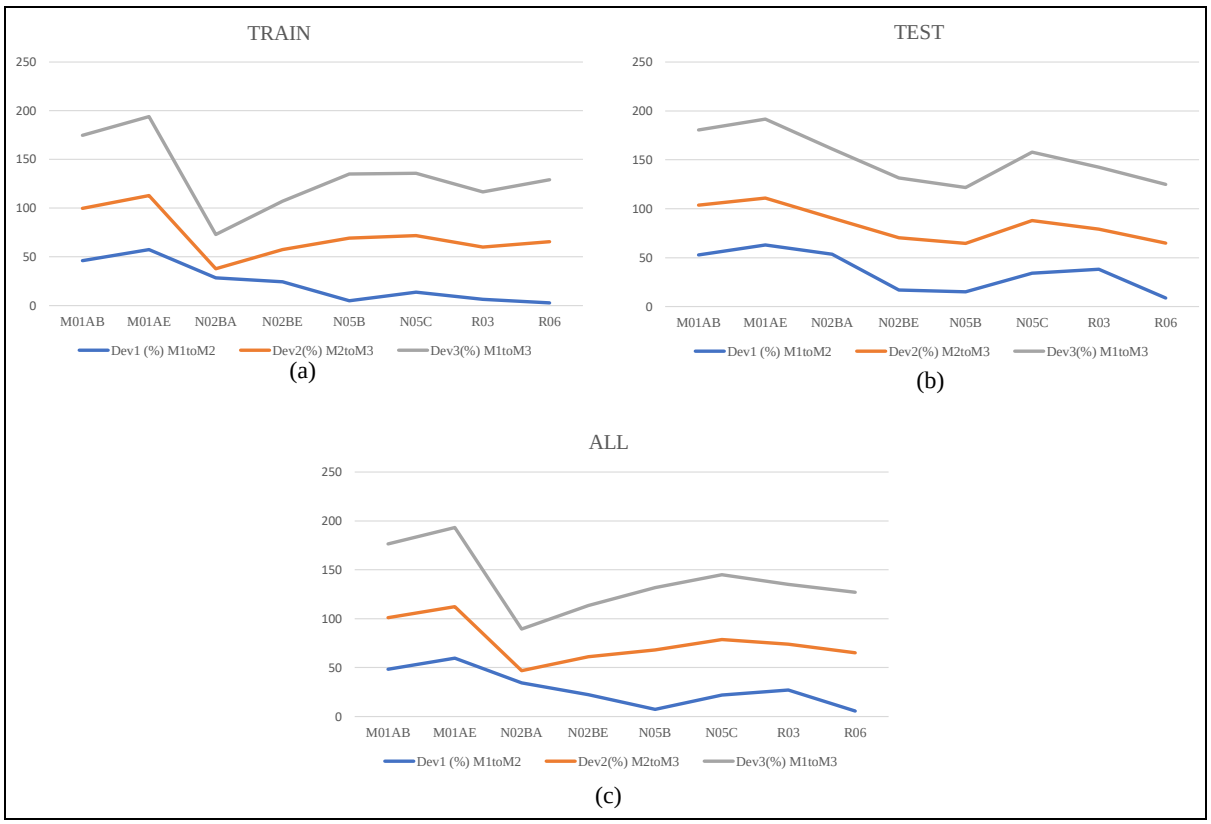

Figure 4. RMSE deviation analysis for the models

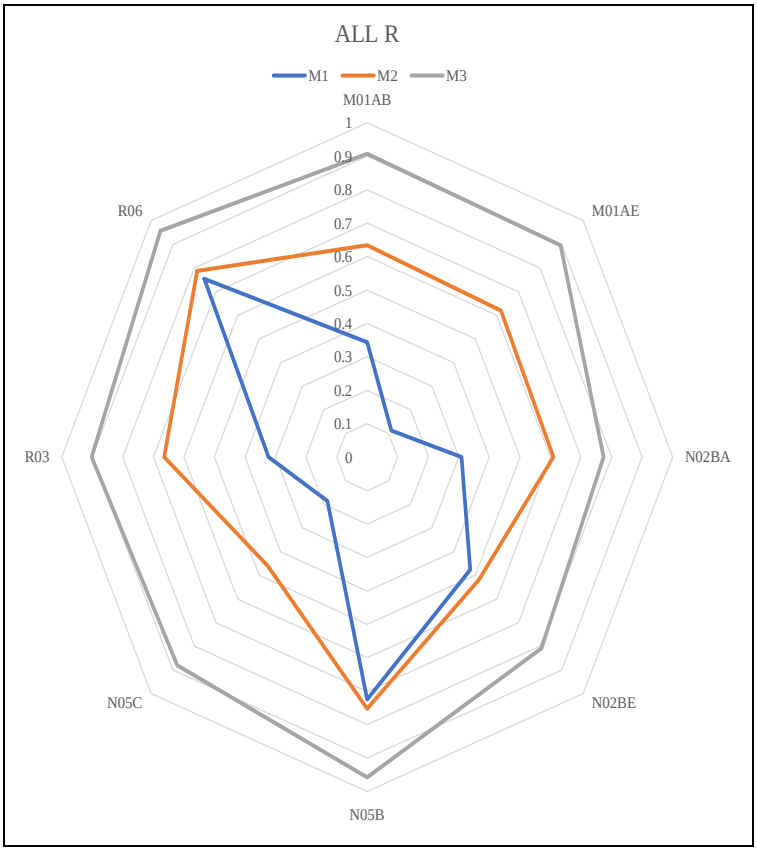

Figure 5. R deviation analysis for the models

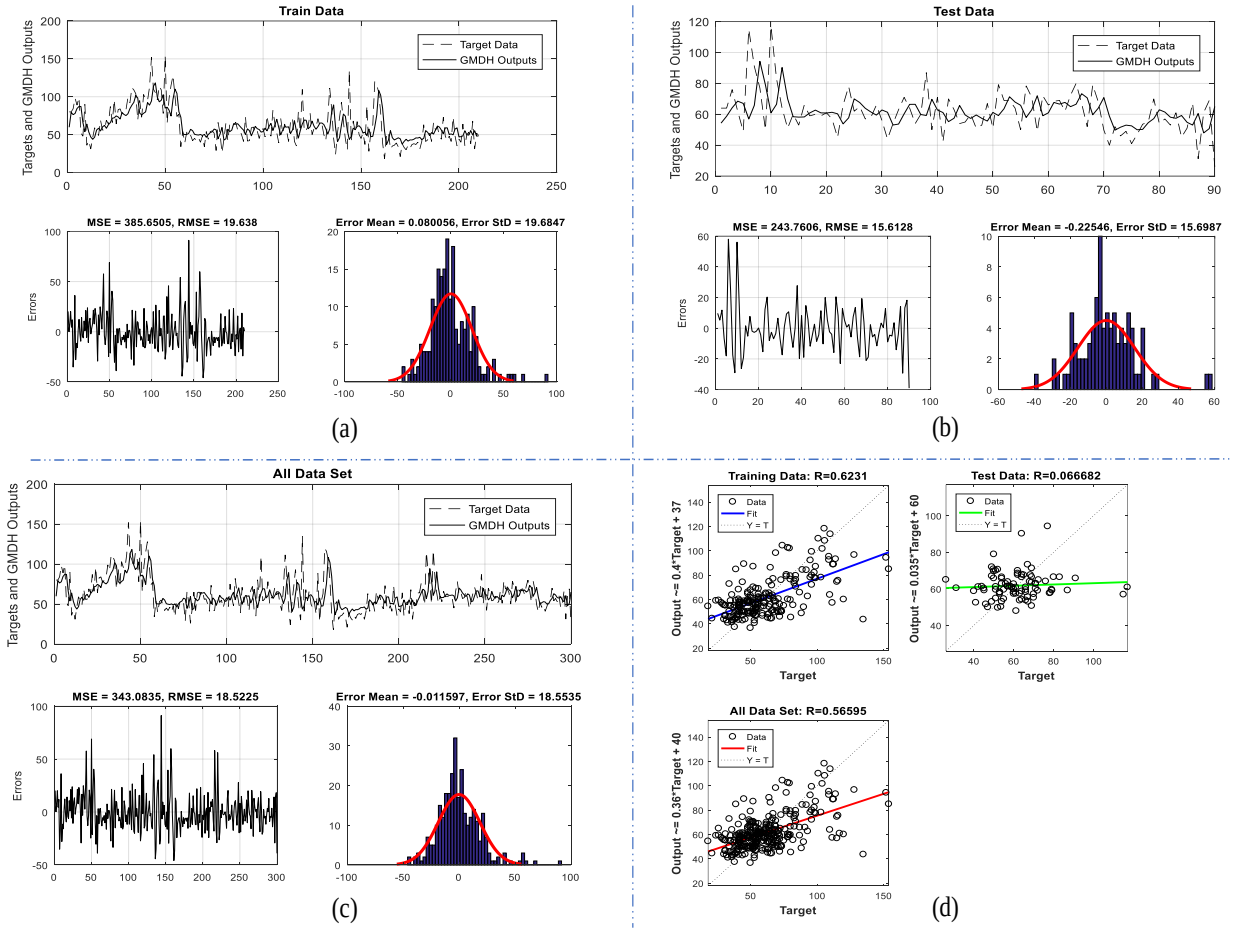

Figure 6. The results for Test 5 (NO5B)

The comparison of target and GMDH network outputs for the training set on weekly data, error amount, and error histogram are shown in Figure 6. The ratio of the variation that can be explained in the regression analysis given to the unexplained variation is defined as the correlation coefficient (R) for the N05B dataset. If the linear curve passes through all points on the graph, then R=1. In this case, the variation that can be explained is equal to the variation that cannot be explained. If the points on the graph deviate along the linear curve, this time the unexplained variation will be greater and R<1. If the value of R is greater than 0.8, it is understood that there is a good relationship between the 2 variables, whereas if it is less than 0.5, it is understood that there is a weak relationship. If Figure 6 is examined within the scope of these explanations, it is seen that there is a high correlation between the target and network output for both training and test data, and the network model can acceptably model data points. Consequently, this study aims to improve the accuracy and error minimization of the forecasting equation as well as the forecasting power.

5. Conclusion and Further Research

The Group Method of Data Handling (GMDH) is a mathematical modeling approach used to create predictive models based on data. It operates through an iterative process, where a set of input variables is chosen to predict the output variable. There are several potential avenues for advancing GMDH. One direction involves enhancing the algorithm's efficiency and scalability, enabling it to handle larger and more complex datasets. Another possibility is to explore different methods for selecting input variables and determining model structures to

enhance the accuracy and robustness of the models produced. Furthermore, researchers may investigate ways to incorporate various types of data, such as time series or unstructured data, into the GMDH modeling process. Also, there may be opportunities to apply GMDH in a broader range of applications, including fields like finance, healthcare, or marketing.

Conflict of Interest

The authors declare no conflict of interest.

Funding Sources

This research did not receive any specific grant from funding agencies in the public, commercial, or not-for-profit sectors.

REFERENCES

Abdel-Aal, R. E., Elhadidy, M. A., & Shaahid, S. M. (2009). Modeling and forecasting the mean hourly wind speed time series using GMDH-based abductive networks. Renewable Energy, 34(7), 1686-1699.

Alizamir, M., Kisi, O., Ahmed, A. N., Mert, C., Fai, C. M., Kim, S., ... & El-Shafie, A. (2020). Advanced machine learning model for better prediction accuracy of soil temperature at different depths. *PLoS One*, *15*(4), e0231055.

Anastasakis, L., & Mort, N. (2001). The development of self-organization techniques in modelling: a review of the group method of data handling (GMDH). *Research Report-University of Sheffield Department of Automatic Control and Systems Engineering*.

Dag, O., & Yozgatligil, C. (2016). GMDH: An R Package for Short Term Forecasting via GMDH-Type Neural Network Algorithms. R J., 8(1), 379.

Farlow SJ (ed) (1984) Self-organizing methods in modeling, GMDH-type algorithm. Marcel Dekker Inc., New York

Farlow, S. J. (1981). The GMDH algorithm of Ivakhnenko. The American Statistician, 35(4), 210-215.

Farlow, S. J. (1984). Self-Organizing Methods in Modeling: GMDH Type Algorithms. Vol 54, CRC Press.

Hwang, H. S. (2006). Fuzzy GMDH-type neural network model and its application to forecasting of mobile communication. Computers & Industrial Engineering, 50(4), 450-457.

Hwang, H. S., Bae, S. T., & Cho, G. S. (2007, September). Container terminal demand forecasting framework using fuzzy-GMDH and neural network method. In Second International Conference on Innovative Computing, Informatio and Control (ICICIC 2007) (pp. 119-119). IEEE.

Ivakhnenko AG (1970) Heuristic self-organization in problems of engineering cybernetics. Automatica 6(2):207–219

Ivakhnenko, A. G., & Ivakhnenko, G. A. (1995). The review of problems solvable by algorithms of the group method of data handling (GMDH). Pattern recognition and image analysis c/c of raspoznavaniye obrazov i analiz izobrazhenii, 5, 527-535.

Jacob, T., Usman, U. A., Bemdoo, S., & Susan, A. A. (2015). Short-term electrical energy consumption forecasting using GMDH-type neural network. Journal of Electrical and Electronic Engineering, 3(3), 42-47.

Kohli, S., Godwin, G. T., & Urolagin, S. (2021). Sales prediction using linear and KNN regression. In *Advances in machine learning and computational intelligence* (pp. 321-329). Springer, Singapore.

Kondo T (1998) GMDH neural network algorithm using the heuristic self-organization method and its application to the pattern identification problem. In: Proceedings of the 37th SICE annual conference, pp 1143–1148

Kondo T, Ueno J, Takao S (2012) Feedback GMDH-type neural network and its application to medical image analysis of liver cancer. Int J Innov Comput Inform Control 8(3):2285–2300

Kondo T, Ueno J, Takao S (2014) Medical image recognition of abdominal multi-organs by hybrid multi-layered GMDH-type neural network using principal component-regression

analysis. In: Proceedings of 2014 second international symposium on computing and networking, pp 157–163

Kondo T, Ueno J, Takao S (2015) Logistic GMDH-type neural network using principal component-regression analysis and its application to medical image diagnosis of lung cancer. Artif Life Robot 20(2):137–144

Kondo T, Ueno J, Takao S (2015) Medical image diagnosis of liver cancer by hybrid feedback GMDH-type neural network using principal component-regression analysis. Artif Life Robot 20(2):145–151

Madala, H. R. & Ivakhnenko, A.G., (2019). Inductive learning algorithms for complex systems modeling. CRC press.

Nariman-Zadeh, N., Darvizeh, A., & Ahmad-Zadeh, G. R. (2003). Hybrid genetic design of GMDH-type neural networks using singular value decomposition for modelling and prediction of the explosive cutting process. *Proceedings of the Institution of Mechanical Engineers, Part B: Journal of Engineering Manufacture*, *217*(6), 779-790.Nikolaev, N. Y., & Iba, H. (2003). Polynomial harmonic GMDH learning networks for time series modeling. Neural Networks, 16(10), 1527-1540.

Nguyen, T. N., Lee, S., Nguyen-Xuan, H., & Lee, J. (2019). A novel analysis-prediction approach for geometrically nonlinear problems using group method of data handling. *Computer Methods in Applied Mechanics and Engineering*, *354*, 506-526.

Rezaei, M. H., Sadeghzadeh, M., Nazari M. A., Ahmadi, M. H., & Astaraei, F. R., (2018) Applying GMDH artificial neural network in modeling CO2 emissions in four nordic countries, *International Journal of Low-Carbon Technologies*, Volume 13, Issue 3, Pages 266–271, https://doi.org/10.1093/ijlct/cty026

Samsudin, R., Saad, P., & Shabri, A. (2011). A hybrid GMDH and least squares support vector machines in time series forecasting. Neural Network World, 21(3), 251-268.

Shaverdi, M., Fallahi, S., & Bashiri, V. (2012). Prediction of stock price of Iranian petrochemical industry using GMDH-type neural network and genetic algorithm. Applied mathematical sciences, 6(7), 319-332.

Steiger, D. M. (1997). Using non-traditional approaches to statistical classification and regression in DSS model analysis. Annals of Operations Research, 74, 269-276.

Takao, S., Kondo, S., Ueno, J., & Kondo, T. (2018). Medical image analysis of abdominal X-ray CT images by deep multi-layered GMDH-type neural network. *Artificial Life and Robotics*, *23*(2), 271-278.

Tsai, T. M., & Yen, P. H. (2017). GMDH algorithms applied to turbidity forecasting. *Applied Water Science*, *7*(3), 1151-1160.

Venkatesh, K., Ravi, V., Prinzie, A., & Van den Poel, D. (2014). Cash demand forecasting in ATMs by clustering and neural networks. European Journal of Operational Research, 232(2), 383-392.

Vissikirsky, V. A., Stepashko, V. S., Kalavrouziotis, I. K., & Drakatos, P. A. (2005). Growth dynamics of trees irrigated with wastewater: GMDH modeling, assessment, and control issues. *Instrumentation Science and Technology*, *33*(2), 229-249.

Web-1, Link: https://www.kaggle.com/milanzdravkovic/pharma-sales-data, Accessed date:26 Sept 2019.

Web-2, Lewinson, E., “Outlier Detection with Hampel Filter”, Link: https://towardsdatascience. com/outlier- detection- with-hampel-filter-85ddf523c73d, Accessed date: 26 Sept 2019.

Web-3, Link: http://exploringdatablog.blogspot.com/2012/01/moving-window-filters-and- pracma.html, Accessed date: 26 Sept 2019.

Zheng, A., Liu, W., & Zhao, F. (2010). Double trends time series forecasting using a combined ARIMA and GMDH model. In 2010 Chinese Control and Decision Conference (pp. 1820-1824). IEEE.

Underground Engineering Education for Subterranean Spaces

Mehmet Kemal GOKAY[1]

Introduction

Rock masses are the main solid materials of the earth crust, in more general they may be the main solid constituent of crustal features of planets and meteoroids. Different forms of rocks in different compositions which have been explored in the earth crust might be enriched as the exploration in the other planets will be enhanced. Natural underground spaces (porosities in microscales & caves in macroscales) are common features of rock masses. Man-made subterranean spaces have mostly been excavated to handle Urban Underground Spaces, (UUSs), mine openings, passages, tunnelsand military/defence purposes. When the time spent underground is under consideration for the current human population, rapid trends of increases have been observed. Subterranean facilities, *(roads, tunnels, metro-lines, car parks, shopping centres, pedestrian passageways with shopping activities, cultural & social activity, sport facilities, etc.)* have gradually been used more frequently. These underground spaces are engineered in different rock masses through diverse projected concepts. Diverse targets aimed to be reached by projected UUSs have mostly come across limitations due to; land ownership rights, archaeological remains, urban city plans, earlier UUSs and mine openings, engineering technology levels, States' legislation Acts, etc. As the requirements of UUSs have become efficient and unavoidable, opportunities and limitations of UUSs have to be rearranged in more engineering touches. UUSs have their special considerations which should be handled by "underground engineers". This new branch of engineering has its academic position in undergraduate/graduate level programs in countries like the US, China, Germany, Czech Republic, Turkey. Urban Underground Space, (UUS), topics in modern urbanisations have been studied here together with "underground engineering" education options to provide necessities of this new branch of engineering.

Underground Spaces Usages

"Urban Spaces" as protected volumes in/on earth crust have been required to supply protection for humans against; climatic features (wind, dust, rain, snow, high/low temperatures etc.) and dangerous influences of sun (radioactivity and other harmful effects of sunlight) including other radioactivity sources (due to the earth crust or outer space sources). Caves had been used for many years for protected spaces together with man-made underground cavities in later years. Cave research has still been important for current space exploration studies for the Moon and Mars. North Arizona University (US) presented their research at caves in earth crusts to understand the other caves which are most probably expected to be located at the other planets, moons of them, and large asteroids in space. Caves have evidence related to rock masses' caving procedures, and they might have hints of ancient (geological era related) and current life (if there was/is any opportunity to be realised) due their sheltering advantages against space related radiations, temperature differences, etc. The researchers here noted words which display significance of the subterranean spaces; "*it's not just finding life - these same*

[1] Prof. Dr., Konya Technical University, Mining Engineering Department, Konya-Turkey.

factors make caves good locations for astronaut shelters on Mars and the Moon when crewed missions are able to explore", (NAU, 2023).

Humans societies have gradually shown cultures in time to form small urban settlements in/on earth crust. Underground spaces which were excavated in ancient times (archaeological eras) show clues that the people excavating them have enough experiences about rock strength, cuttability of rock masses and rock supports. Ancient underground cities and tunnels which have been discovered in Turkey are generally in tuffitic rock masses. In order to present the size of their efforts, it should be mentioned that, there are many known (already explored) underground city type urbanisation activities in Central Anatolia in Turkey. However, the new discoveries of ancient archaeological underground tunnels have shown that there are some extra underground spaces still waiting for their exploration & discoveries. Like the ancient Derinkuyu (Nevsehir-Turkey) underground city, some of them had been excavated to accommodate more than 10K-20K habitants. Urban settlements have progressively been developed on different continents for the last 10K-15K years. They are mostly on the earth crust but there are also settlements in the crust as well. In these years, underground spaces are used for sheltering spaces. Even more, in modern times underground shelters had also been excavated for the state's main commanders and presidents together with their urban people in order to supply protection for an atomic bomb attack.

In the last century, subterranean metro lines have gradually been excavated at crowded cities to handle traffic jams on the city-roads. Metro-lines and big-scale metro stations (including shopping activities) have sparked the usage of underground spaces (Seequent, 2019; Seng, 2023). Actually, underground openings excavated and abandoned by mine operations in the world have histories starting from the early human settlements, but they are always accepted as "underground mining sites". Due to the mining activities (dusty, noisy, dangerous etc.), abandoned but stable underground spaces had not usually been thought of as urban living activity spaces. Coal mining related methane explosions and related disastrous situations might have also led to those negative considerations about abandoned mine openings. However, in the last decades, underground metro-lines and underground shopping centres & car parks have forced the engineers to think about the economic usages of underground spaces in comprehensive manners. Currently three is no common procedure followed by countries for underground spaces. Each new underground space excavation is generally projected individually to obtain permission to start its excavations. However, certain circumstances have illustrated that underground spaces have to be projected according to states' national urban master plans (by following procedures dealing with actual 2 Dimensional, 2D, land ownership rights). Recently, some countries have provided their "Legislative Acts" for their 3 Dimensional, 3D, volumetric space ownership procedures to coordinate rights & responsibilities among "underground spaces" and "surface land ownerships" rights. Gravitational force influences solid materials/rock masses surrounding all volumetric spaces in/on the earth crust. Therefore, stability considerations of all engineered volumes (living & working spaces) should be analysed according to stresses-strains (primary and induced) distributions in those solid materials (i.e.; concrete, rock masses) around these volumes. Rock masses include underground spaces or rock masses engineered as surface structures' foundations; they all have to provide stable deformation behaviours under their induced stresses circumstances. Rock mass behaviours under 3D induced stress conditions directly influence deformations of all the man-made engineered structures in/on rock masses. When the logical background is under focus of the UUSs' usages, there are many alternatives that might be arising due to the purposes of related UUS projects.

Kshirsagar etal., (2021) performed a "*bibliometric review of the literature related to underground construction"*. The analysis covered the time period from 1975 to 2020 and the

underground construction subjects are reviewed under the considerations of energy and land optimisation issues. In this study, 166 materials were reviewed and it was concluded that the concepts of the literature and their ratios in total materials were listed as follows; engineering (33.0%), earth and planetary sciences (30.7%), environmental science (13.3%), energy (5.4%), social sciences (5.4%), computer science (2.4%), art & humanities (1.2%), and the other subjects (business-management-accounting, decision sciences, material sciences, multidisciplinary, physics-astronomy, psychology; where each of them has the ratio, 0.6%). Besner (2016) as an urban planner stated that, "*planning underground spaces hasn't the same meaning even today for an engineer as compared to an urban planner*". Planning and design activities for particular man-made engineered structures have their influencing parameters and different professionals in urban planning, architecture designs, human related (social-culture-art- aesthetic etc.) planning efforts, and different engineering fields have their own approaches to the content according to their point of professional views. Starting points which should be selected among these professional efforts must include importantly the stability and safety related concerns of structures. This is the same concern which has been considered in the mining industry since at the beginning with the word phrase; "safety first". Therefore, all the design efforts performed by different professionals could be considered step by step after ensuring the "all conditions" influencing the man-made underground structures' safety. When the concept is UUS, safety of commuters in them starts through the considerations; "Is it safe to go down? What are the dangerous conditions and related precautions?". These contexts mainly include; Roof & sidewall collapses of UUSs, natural gases discharge through the surrounding rock masses, explosions of natural gasses (or by-product gasses & liquids of used equipment and machineries), flooding, fire dangers, poisonous smokes, human related accidents & actions (individual/crowd related social behaviours which influence the safety of underground spaces). Besner (2016) wrote also that, *"during a very long period of time, civil engineers have been the sole experts of the underground space"*. Actually, a limited number of man-made UUSs' structures which were constructed as adjoining parts of the surface constructions and subterranean metro line projects realized by civil engineering consultants and companies have formed this situation. However, even the planned structures are surface structures with basement floors, their design works push the urban planners, surveyors, architects and civil engineers into the same working- group while urbanisations have been developed without thinking of large scale UUSs like tunnels. Actually, in most of the countries, underground spaces (originated due to; small caves, labyrinth cave systems, abandoned small mine openings, abandoned historic underground tunnels, etc.) used for civil urbanisation purposes are not totally mapped and officially regulated like the basement floors of surface structures. However, underground metro systems which are used in different cities since the last century have started to change understanding related to UUSs. Length of subterranean metro lines in cities are mentioned in several kilometres, km, or a few "hundred" km in distances. Total time which each commuter spent underground per day has already reached a meaningful level. In addition, the number of people using subterranean systems in big cities is more than about 100K which is a huge amount when the safety of them is under engineered considerations. Safety rules and related precautions have to be very strictly followed in order to ensure smooth operations of engineered systems at UUSs. Stability and safety facts of UUSs have forced the engineers & professionals to avoid handling UUSs in sole responsibility of planning-designing-operation actions. In case of accidents, legal court related procedures are ready to follow the written legislative Acts and Rules. Projects, land ownership rights, contractors, consultants, engineers, foremen, workers, work-force education documents, professionalism, expertise, diploma of graduations, knowledge in the field of applications, certificate documentations, transcripts presenting ECST credits of courses taken by individuals in certain area of professions (urban planning, architecture, engineering, etc.), responsibilities, duties, controlling operations, monitoring

actions & systems, etc. have all to be considered and evaluated in detail. Therefore, professionals should not accept any responsibility which is not in their area of diploma of graduations. New understanding in man-made structures in/on earth crust are then planned-designed-executed-monitored through multidisciplinary manners by professional work-party groups. In this point, information supplied by Besner (2016) helps to visualise organisational efforts in tunnelling and underground spaces to collaborate related professionals under societies dedicated to underground spaces in general.

Underground space requirements

Underground spaces below the surface could be formed in two manners. First one is natural procedures, which have started from the point where the rock masses first solidified/formed in geological eras. Solid magmatic rocks even have porosities due to their crystallisations features. When porous rock masses are under consideration their porosity values could be as high as 40-45%. Liquid and gas reserves like; groundwater, oil, natural carbonic gasses, other volcanic gasses etc. have their settling volumes in rock masses through these porosities. For example, North Sea chalk rock masses which have porosity values as much as 40%, constitute reservoir rock masses for North Sea oils. Actually, porosities supplied by deep underground rock masses could still have economic value in future, if they do not be even occupied by any liquids and gasses. Carbon-zero policies followed by countries have forced the governments to collect their discarded carbons (solids, liquids, gasses) to deposit safely in underground spaces in rock masses instead of releasing them to the atmosphere. In this context, reservoir capacities of certain rock masses have their economic future potentials to accommodate liquid and gaseous state of carbon compounds.

Other than deep micro spaces in underground rock masses, man-made, excavated, underground spaces have gradually gathered enough consideration among the countries, (Bresnahan, 2022). Especially mine related galleries, stopes, shafts, and all the other underground activity related spaces have their own histories in those countries' mining pasts. Second usage of these spaces in addition to opening the new UUSs are main activities in current underground businesses in urban environments. In big cities, people have preferred underground transportations systems to avoid traffic jams. Each modern urban settler then spent at least certain time underground for travelling, shopping, driving their car through road tunnels, etc. Underground road tunnels have their positions in modern urban city plans (Samsung C&T Global, 2018; Paddison, 2022). With the climate conditions under consideration for human comfort, cities which have hot and cold weather conditions, have gradually confronted construction of UUSs as shopping centres, pedestrian passageways, depots, etc., (because they have their controlled air conditioning systems). Moreover, galleries related to underground metro stations have extended below the surface to form pedestrian passages including shopping facilities as well. Belanger (2007) wrote about the extent of the Toronto's (Canada) subterranean pedestrian system and he noted that, *"beneath the surface of the streets of Toronto lies a sprawling labyrinth that serves over 100,000 people every day and countless tourists and visitors".* This subterranean system is reported to be 3 km long and includes 1200 stores with 2500 employees. Its map circulated publicly, so commuters can direct themselves there accordingly (PATH, 2023). Experiences and knowledge gained during the design-excavation-construction-operation stages of these UUSs by workers, engineers, architects, city planners, contractors, project holders, and other professionals are very valuable assets for the consideration of similar new UUS cases. When similar UUS projects are in focus, these assets then have to be coordinated according to urban master plans by considering other structures in/on earth crust. Zhao, etal., (2016) noted rapid extension of city limits have accelerated the requirements of urban development plans which include subterranean facilities as well.

According to them, UUS developments have their master planning efforts in China since 1997 through the "Management Regulations on Urban Underground Space Development and Utilization". Zhao, etal., (2016) pointed also that, UUSs *"should be planned as a whole, so as to ensure that space beneath city can be developed orderly and systematically. Problems such as unchecked and scattered development, unbalanced function, limited overall benefits and low efficiency can be avoided*". Actually, the rule related with the mentioned Regulation in China has prepared to coordinate the actions related with UUSs. These researchers also wrote that, this Regulation has a rule (Article-5 in Section-2), which regulates the UUS development and utilisation by supplying following steps: *i) UUS development planning forms an integral part of urban planning. ii) While conducting urban master planning, governments at all levels should compile master plans of UUS development based on local development needs. iii) Regulations concerning UUS development and utilization subject to UUS master plan should be integrated into urban detailed plans.*

Safaee and Nematipour (2021) pointed out key aspects of modern cities in their work. Most of the cities have had ample land resources in the last centuries. This can be perceived through historical pictures of them. Some of them have been extended through new settlements in time according to their urban master plans. But, some others have not followed such plans. Even the cities which have their urban planning have encountered complications when the population pressure is under consideration. Living spaces, official buildings, social & cultural activity centres, sport areas have their land requirements to be constructed. Planned or not, when the reserved land parcels have gradually been used for different city requirements, there are comparably less parcels for green areas for city people. These researchers mentioned progressive settlement expansion of Tehran (Iran) in history. Requirement of land parcels even for further necessities of public services at certain city locations, have decreased the reserved areas of the cities into very critical levels. Safaee and Nematipour (2021) explained the requirement of public areas in cities especially when the quality of life is under consideration. In modern times for crowded cities, underground spaces have step by step become solutions to keep certain public constructions underground. In this way, green areas, parks and other open-land facilities at ground level will be protected. While listing advantages of UUSs, they mentioned; i) combined urban planning to connect UUSs and surface structures to improve quality of life in cities, ii) UUSs have influences also on the control of city land parcel prices, besides pedestrian pathways, and other UUS usages help to improve quality of life of their commuters. Taxes and fees related with surface structures and UUSs are dependent on the policies of central government bodies in countries, so it may differentiate in time. Thus, shareholders of possible UUS facilities should think about all the possible design, technology, engineering, investment scenarios and parameters before their attempt to start UUSs excavations. In addition, when the rock mechanics contents under considerations, (induced stresses-strains conditions, rock types, strength of rock materials and rock masses, discontinuities in the rock masses, deformations characteristics of rocks around UUSs, etc.), some design limitations could be involved for UUSs. Actually, 3D-dimensions and depth of UUSs might also have some defined restrictions in future due to re-organisation of 3D land ownership right descriptions in countries. Legislative Acts and procedures attempts in this content might have possible long discussions in National Parliaments when the actual rights of surface land ownerships and possible definition of 3D UUSs ownership rights and their rules are under consideration.

Ramlakhan, etal., (2021) wrote that, 2D land ownership rights' registration system could not represent subterranean spaces adequately. In general countries have their urban and countryside maps in parcelled manners, formats. Some countries have continued mapping of their ground surface to define actual (detail) situations of urbanisations and other types of land

parcel usages with their related information & documentations. Some countries have their regional and local urban development plans also to follow their future settlements including land usage policies. Digitalisation of these maps and projected master plans bring extra loads on the continued planning activities. In most countries digitisation efforts of actual land ownership conditions are continued on the bases of defined land parcel numbers (which were defined land surface parcelled areas, 2D in characters) according to predefined urban master plans. As the number of UUSs are increasing, their rights & responsibilities should also be defined, (Gokay, 2023), through legislative Acts. When the UUSs and any other volumes, objects, located underground are under consideration for their stable & safe usages, there are concerns related to rock mechanics as well. According to Ramlakhan, etal., (2021) by using a 2D registration system, "*it is not easy to identify the owners of these objects and the relations between objects below and above the surface are not explicitly provided".* In their paper, they presented their literature review "*to develop a standardised workflow to model the legal spaces of BIM/IFC models of 3D underground objects according to the LADM in 3D LASs*", (Where: IFC is a model file in the form of "Industry Foundation Classes", IFC file format is an open file format used by Building Information Modelling, BIM, programs. LADM is The Land Administration Domain Model, and LASs is Land administration systems).

Registering the UUS in formal systems has gradually been considered by countries which have enough UUSs to register for their official rights, related responsibilities and states' taxation purposes. When UUS registration is under consideration, Singapore is the first country to be reviewed. Due to its population and limited land opportunities, this state has started to survey & map all the subterranean facilities and UUSs through a digitisation project to have documentary-data related to underground spaces (Singapore - ETH Centre, 2022; Schrotter & Van Son, 2019). Similar workout was reported earlier for the UK through "Project Iceberg", (BGS Research, 2017). New understanding and new conditions, (economic, social, environment, technology, engineering etc.) which have already appeared in certain countries (like; Singapore, Netherland, Finland, Canada), related to UUSs have important hints which other countries might have also experienced, if they are not put forward urgent legislative Acts to regulate UUSs including their ownerships' rights and DECOM (design-excavate-construct-operate-monitor) procedures to define official order to distribute rights and responsibilities. Forming additional space volumes might be seeming to governments as additional economic values and issues of taxations. But, in cases of stabilities and work & workplace safety-health procedures, there are issues to be evaluated under the rock mechanic contexts. These issues need to be regulated firmly for safe UUSs operations as well. It should be bear in mind that, there will always be underground spaces (in micro/macro scale) which hinders the rights and intactness of any other UUS and ground surface structures around. In cases of ownership rights, Ramlakhan, etal., (2021) pointed out that, Poland registers underground objects in a separate manner since their rights could be held by different owners with respect to the surface structures. Registration of UUS in Poland has been reported to be realised by using a concept called "object-oriented spatial plot". Ramlakhan etal., (2021) mentioned also about the UUS registration efforts followed in Korea and Serbia as well. Countries, in general, have their 2D cadastral systems, defining UUS in these systems provides additional coverages of their legal land ownership rights. Defining all UUSs (natural and man-made) will become necessary in the near future for all countries. So they need to evaluate their UUS potentials and best possible registration system definition to coordinate UUSs and natural resources in/on rock masses. Excavating UUSs in rock mass influences the rock masses surrounding them. These influences cannot be withdrawn after the excavations are realised due to secondary (induced) stress fields & related deformations. Thus, all the decisions related to UUS and surface structure developments should be taken carefully and there should always be an urban master plan and

legislative Acts to follow. Otherwise, individuals can disturb natural rock masses' intactness which might prohibit further developments of UUSs and surface structures later on.

Most of the cities in the modern world have their 2D spatial parcelled maps including actual situations of roads, houses, parks, pedestrian ways, car parks etc. These maps usually coincide with the countries' land ownership parcels and regulations. Commonly, when "3D" phrases are used for these urban plans, these generally include topographical Cartesian Coordinate System's "x, y, z" value differences of ground surface. That means, they don't generally have underground related information. It is also very common in civil engineering plans that; all surface structures have their foundation structures (and basement floors whenever available). When high-rise apartments are in concern (height; 50-600 metres or more), their foundation might have piles which might extend down to 10-50 (or more) metres below, (depending on the height of building and ground load-bearing characteristics). Recent construction works have started to include more apartment floors below cities' main ground surface datum. Thus, deeper construction activities of high-rise surface structures can easily be seen as the future trends at certain locations of the cities as the urban populations increased in similar manners. Therefore, regulations for land uses in urban and countryside should be re-settled carefully. These regulations must coordinate urban master plans which include; man-made structures and natural features (by referencing cities main surface ground datum). In order to provide comprehensive actual-situation lay-outs, 3D digital maps which should include all the natural features & man-made structures at below-surface-above the main surface ground datum should be prepared. Then, regional master plans including countryside and urban settlements can be considered and evaluated through groups of professionals including; city-planners, architects, historians, archaeologists, artists, engineers (geological, civil, mining, environmental, chemical, mechanical, electrical, etc.), technicians, workers and local people. Due to the rapid development of underground facilities all over the world in recent years, "underground engineering" concept should also be included to the above professionals, in case of;

a) Planning; (designing subterranean man-made structures according to regulated regional & local urban master plans),

b) Engineering; (following the standards and rules to coordinate underground space construction efforts. Scheduling the daily operations according to supplied designs. Be sure to have minimum disturbances on surrounding rock masses intactness of UUSs),

c) Controlling; (monitoring underground construction efforts to be ensure about the stability of the underground spaces),

d) Analysing & Directing; (ensure the minimum possible harassment to surrounding rock masses of underground spaces),

e) Instrumentation; (procedures related with the measurements of surrounding rock masses stresses and deformation during and after the construction stages, these instruments are supposed to be in operation for many years after the completion of underground construction activities. Therefore, their selection, positioning and recording the data obtained from them in predefined time periods are the concerns to be followed. Additionally, field data evaluations should be closely monitored and analysed to be ensure about the stability of the subterranean spaces),

f) Monitoring; (UUSs should be monitored according to regulated safety rules, including stability, ventilation, transportation, etc., covering all the concerns related to safety and health protection rules),

g) Reporting; (official reporting of all excavation and operation steps. All features, events and circumstances encountered during UUS's DECOM stages, (design-excavation- construction-operation-monitoring), should be recorded and filed in official manners).

When 3D mappings are gradually under consideration due to UUS facilities, historic underground cities, tunnels, chambers, caves etc., and their features should be included in a common database where urban planners and engineers could understand their features & conditions when they would like to build new UUSs or surface structures. At this point, BIM attempts on different platforms have their advantages. BIM applications have been developed to combine all possible information related to buildings. When we think about urban planning, land parcel groups cover parks, houses, industrial sites etc. which are all documented including roads and their available infrastructures. Information collected for buildings can be extended further away from the legal documentations to provide a wide range of information for further engineering modelling. BIM could be used not only for surface structure documentations; it can also supply documentation methodology for cities' infrastructures (from their design stage to their usages). At this point the words of Kontothanasis, etal., (2020) should be revealed; *"the created intelligent 3D model enables document management, coordination, and simulation during the entire life cycle of a project (plan, design, construction, maintenance, and operation)*" for 3D objects in/on rock masses. When BIM related information is collected for subterranean metro line projects, the model formed in the BIM software should cover topographic interactive coordinated maps to compare surface and underground coordinates including underground rock formations' data supplied through boreholes. Officially, engineering evaluations and engineers' decisions could also be reachable for different surface and underground locations including projects' locations, (the data may cover; geology, geotechnical descriptions, and available rock mechanics field & laboratory test results). The project details in different engineering sectors of construction and their engineering steps should all be documented for further controlling actions. Project realisations in daily bases together with engineering reports and photos of development in tunnel excavation and its supports form a detailed data-bank for any further engineering analyses in later years. Engineering activities covering excavation operations, hauling of the excavated rocks, transportations of workforces, ventilations, groundwater pumping etc. should be recorded in this data-bank for further official control whenever required. After the UUSs' construction works, they should also be monitored during their operation years. The data collected from UUSs-related instrumentations must be securely saved in the BIM data bank system. The monitoring data ought to include operational activities of UUSs like, induced stress-strain monitoring, ventilation & controlled climate data, work & workplace safety and health related data, etc. In order to combine all the aspects related to engineered structure in/on rock masses documentation, Kontothanasis, etal., (2020) wrote that BIM documentation have additional "levels" on 3D considerations as follows: a) "*3D aspect: geometry, semantics, physical visualization, clash analysis"; b) "4D aspect: time scheduling, project phasing simulations, activity progress, virtual construction"; c) "5D aspect: Cost-budget tracking, cost analysis scheduling, estimations for materials, equipment, man power"; d) "6D aspect: Sustainability, energy consumption analyses, infrastructure performance"; e) "7D aspect: Facility management, operation, maintenance, scheduling, project phasing simulations, activity progress, life cycle". These aspects summarise engineering usage of BIM for UUS documentation purposes. BIM software data could officially be reachable in cases of any further engineering design activity or any other legal procedures coincided in the excavation-construction-operation-monitoring periods of UUSs.*

Underground facilities have provided solutions to urban transportation and other requirements, but their legislative usages should be well planned and strictly controlled for their

positions with respect to other UUSs and surface structures to prevent further disputes and stability problems. Actually, UUSs like; existing metro-lines, roads, and railway tunnels still have their problems related to their influences on existing structures in/on earth crusts. Countries realizing the future problems and solution possibilities of UUSs have organised special government offices to handle their urban & countryside master plans including underground, surface and over-surface engineered activities to coordinate ownership rights, taxes and responsibilities. At this position the procedures supplied for Helsinki (Finland) can be an example and Vahaaho (2014) wrote that, "*There are 10,000,000 m^3 underground spaces in Helsinki (parking, sports, oil and coal storages, the metro, etc.), more than 400 premises, 220 km of technical tunnels, 24 km of raw water tunnels and 60 km of 'all-in-one' utility tunnels (district heating and cooling, electrical and telecommunications cables, and water)*". In the paper, there is information also about a subterranean swimming pool in Itakeskus (Helsinki, Finland) which is reported to suitable 1000 customers and in case of emergency, it can be used as underground shelter for 3800 people. At this point, engineering considerations should be remembered to follow in planning and construction of 3D urban settlements. In the modern world, information storage through high-performance main computer systems have become essential assets of countries for their official data-banks. In general, UUSs provide required cold, stable and secure spaces for these types of computer data systems. Data storage hardware through computer cloud-data-systems are also suitable for UUSs where these spaces supply a certain degree of privacy and protected volumes, (Datwyler, 2023). Large scale retailers which supply foods and everyday goods for local people have required large scale storage depots which should be protected from influences of climate. Secure UUSs have provided such conditions in different parts of the world. One of the big ones had been redeveloped from an abandoned underground limestone mine (Subtropolis, Kansas, US). This is the example of the secondary usage of stable and secure abandoned underground mine openings as UUSs. The analyses and evaluations which are required during rehabilitations of already existing underground spaces, (secondary usages of abandoned mine openings, caves, historic underground chambers & tunnels, etc.), underground engineering activities have been required.

Underground engineering concept in engineering fields

It is important to notify that engineers, architects and city planners who currently provide activities for underground spaces through preliminary reports, tests, designs, shift engineering, stability control, rock engineering, etc. could be handled by a group of engineers and professions who have education in different aspects of underground space developments. Assuming UUSs' engineering operations are some kind of verification in civil purpose construction works, and handling the UUSs projects accordingly might push decision makers (engineers, investors, directors etc.) into grey-zone about their works which should be handled by "adequate engineering" operations and reporting procedures. In the cases of underground spaces and coincided constructions, engineers and professionals who graduated for ground surface structures, might have been asked to provide designs, reports, evaluations for underground spaces. Actually, these engineers should be watchful about their interpretations, decisions in different stages of UUSs development and utilisations. Thus, underground spaces have their specialities covered by rock masses & behaviours, ventilations, design strategies, safety & health protection rules. Therefore, engineers without context related background (education, practices and experiences in official documentation) are advised to be careful in their engineering decisions. Municipalities or local government bodies supplying contracts for underground tunnels and spaces should also be aware about the complexity of the UUSs developments. In recent years, requirements of metro lines have increased and these bodies all over the world have pushed municipalities to supply new contracts related to new UUSs like; metro tunnels & stations, car parks, and pedestrian passages. Actually, the central government

and local municipalities should follow urban master plans which should also be prepared for 3D land development and utilisation purposes. Transportation in crowded cities are becoming problems due to traffic jams, and underground metro lines are one of the solutions to handle this problem. But, decisions provided for the underground metro line should be taken after detailed research including; city plans, archaeology, architecture, engineering factors, social cultural influences, etc. Otherwise these decisions will provide further problems after the realisations of the lines. For example; municipalities or central government who may supply UUSs development contract (i.e. underground road/metro tunnels etc.) will most probably have disputes in Law-Courts in future about their decisions if they have supplied UUSs contracts without researching and handling official evaluation reports about the influences of projected UUSs on surrounding underground and surface structures. Because at the beginning of any UUSs project, it is already obvious that; planned subterranean space will definitely influence the surrounding rock masses through induced stress fields. Surrounding UUSs and surface structures above the ground are also affected from these stresses-strains differentiations. Thus, existing UUSs and projected UUSs have to be analysed and evaluated for their influences on existing and planned city structures. Urban city plans therefore play an important role here to coordinate the surface and underground structures for their influences. These influences should be kept in minimum engineered levels to provide safe spaces for further urban structures in/on earth crust. That means central governments, municipalities and companies which handle UUSs should have enough graduates, especially for underground space engineering activities. It was explained already that, underground engineering activities should cover all stages of UUSs development and utilisations including; a) Regional and local urban plans; b) Monitoring local areas for their surface subsidence and sliding evidences; c) Determining requirements of new UUSs; d) Preliminary reports including engineering, environmental, architectural, social, archaeological, art-history, etc. features of planned UUSs (covering parameters; influenced by UUSs and influences on the planned UUSs); e) Preliminary field and laboratory testing, reports should include official data and their evaluations; f) Designing-construction stages of UUSs; g) Instrumentation of UUSs locations "before-during-after" the excavation & constructions stages of them; h) Monitoring stability of UUSs while they are in service and supplying official files to report collected data; i) Monitoring and directing operational parameters of UUSs' safety-health conditions (ventilation, crowd control, gasses emission controls, flooding-fire-explosion protections & controls of their prevention procedures, accident protection including electricity-machinery, etc.).

The issues presented here have tendency to be enhanced as the UUSs usages are increased in urban areas. The main concerning points related to UUSs development cases have been seen on the distributions of "ownership rights" and "responsibilities". UUSs developments have advantages by supplying extra spaces underground which have economic values to be defined and distributed according to ownership right procedures. But there are also influences due to excavation of UUSs which should be analysed and minimised according to rock mechanics rules. Designing and predicting these influences before the UUS project's realisation, and monitoring them during & after the UUS's excavations & constructions supply responsibilities to the professionals (who are working for government offices, project holders, consultants, contractors, design offices, etc.) and UUSs' ownership holders. Central governments must provide Acts and legislative rules for fair and safe usages of UUSs in urban areas. Otherwise, underground spaces are continued to be excavated without full-scale engineering considerations, b) existing underground spaces, (natural or man-made ones) are continued to be used without proper safety & engineering reports, c) these types of UUSs usages have not even defined practices of instrumentations & monitoring procedures for their service life periods. The questions should always bear in mind that; stable underground metro tunnels were handed out to the companies operating metro-line systems at municipalities after their excavations &

utilisations. Then; What can be the stability conditions of these metro tunnels after a certain time period of usage? Are they still stable enough? Do they require additional supporting features? What can be the effects of earthquakes on these tunnels? All the factors provided above are some considerations, cases, which should be handled under the "underground engineering" concept in a multidisciplinary manner. When UUSs are the issue; accidents, failures or disastrous events might cause loss of many lives due to their usage in congested manners. Therefore, UUSs usage in countries should be well engineered and strictly monitored, otherwise societies cannot eliminate the accidental cases which will be remembered with the words in the news; *"Unseen circumstances. New precautions will be added to the system to prevent further events in future"*.

Lavagno, (2016) analysed the underground space development, and he stressed on multidisciplinary approach. He stated that "the underground development involves several multidisciplinary actors such as technicians, architects, engineers, urban planners, etc. that have different expertise and learning patterns among each other". He reported about the survey performed among the members of "Associated Research Centres for the Urban Underground Space", ACUUS. This association is a non-governmental, international organisation to combine partnership among experts dealing (design, analyse, decide etc.) with UUSs, (ACUUS, 2023). The purpose of the survey was stated as; recognising & analysing the educational background parameters which are linked to the specialization developed to handle UUSs. Main concerning facts considered for UUSs were listed briefly by Lavagno as; a) for urban design, city planning, topics: (architecture, indoor space design, commercial functions, mass transit issues, behavioural studies, economics/feasibility studies, fiscal and legal studies); b) for security topics: (user safety, construction engineering, geology, rock mechanics, tunnelling, geographic information system, GIS). The survey presented that survey attendees felt positive, "quite good", about their technical & scientific background about underground related topics, but not for the topics related to "commercial functions", and "rock mechanics". Survey attendees have feelings that, good background knowledge is necessary to become a true underground expert. According to the findings of the survey, present knowledge related to UUSs which have been provided in universities is considered not sufficient for future experts of UUSs. Engineering branches dealing with different issues of human related subjects already have their definitions in Engineering Departments of Universities. "Underground engineering" has not been defined yet in most of the universities, but in the near future it will be one of the preferable engineering branches, as the number of UUS have increased in the urban areas. As (Martin, 2022) reported, UUSs cannot be an avoidable phenomenon for the next generations in future. Thus, city planners, architects, engineers (in mining, civil environment, geology, geophysics, geotechnics), and rock mechanics experts have to describe coordination methodologies for "underground engineering" concepts.

Actually, certain pioneering universities in the world have their BSc and MSc departments to supply graduation degrees in underground engineering. Guo, etal., (2021) reported that *"in light of the rapid development of underground spaces in China and the intense demands of professionals for underground space, the Ministry of Education of the People's Republic of China has permitted the offering of the urban underground space engineering professional degree program in universities since 2001".* According to these researchers, in 2021 there are more than 80 universities in China which have offered "underground engineering" degree programs. After analysing the courses provided in these university departments in China, they presented some differentiations that occurred due to the departmental curriculums. In point of fact, underground engineering departments in China are new branches, and departments (civil engineering, mining engineering and railroad engineering) existing in the adjoining university faculties have supplied educational support &

assistance for them. These supports have delivered with the existing departmental experiences on UUSs which resulted in those diversities. Subjects especially forwarded have issues on; a) underground engineering organisation, b) UUS excavation and related machinery usages, c) Rock engineering and underground space stability concerns. Lei, etal., (2022) described circumstances at the beginning of "underground engineering" education in China which were related to courses and textbooks involved. They also mentioned significant expansion in tunnelling and underground engineering concepts in recent years in China. They wrote that Chinese universities *"invested a lot of manpower and material resources in the construction of main courses"*. According to them, Tongji University, Beijing Jiaotong University, and Southwest Jiaotong University (and other "Tunnel and underground engineering" majors) have their textbooks published related to tunnelling and underground engineering. In their paper, they presented standardization efforts on undergraduate graduation of tunnel designing and underground engineering as well. Conferring their statistical study on the graduation study topics, (selected by students in between 2018-2022), at "Tunnel and underground engineering" of Central South University, (Changsha, Hunan, China), the trend which students preferred in their graduation works was comprehended. The study topics (with their % ratios in total number of 449 graduation thesis subjects) were given in this statistical study as follows; Mountain tunnels (44.5%), Subway tunnels (52.6%), Pipe jacking tunnels (0.2%) and Science class (2.7%). These ratios presented the students' intimations where the engineering employments and projects will be led in the near future in China. It may be a logical consideration; similar expectations will arise in the other universities concentrated on UUSs.

One of the opportunities in the educational field of underground engineering is supplied by Purdue University (Indiana, US). A course; "Development of underground space" has been provided here. Purdue University has supplied a special education "program" at its Construction engineering and management (CEM) division under the name of "Future underground construction leaders (FUCL) development program". This program's website has the following words; "*During the past few years, Purdue CEM has made a dedicated effort to get engineering students more aware, excited and committed to careers related to underground construction"*, (Purdue-FUCL, 2023). One of the other US based universities which has education activities on underground constructions and tunnels is Colorado School of Mines. This University has a mining engineering department, and underground mining operations still have their important positions in mining sectors, (Fields, 2023). However, this university has also presented its awareness about the potential activities of UUSs by supplying the following words; *"The job market is promising for underground construction and tunnelling engineers"*, (MINES, 2023a). Therefore "Underground construction and tunnel engineering program" is offered in the graduate level at Colorado of Mines. Its targets and supporting university departments are defined as; *"on the design, construction, rehabilitation and management of underground spaces. This interdisciplinary program, offered jointly by the departments of Civil and Environmental Engineering, Geology and Geological Engineering and Mining Engineering",* (MINES, 2023b). When the educational activities on underground engineering have been under focus, the program offered by University of Delft (Netherland) also needs to be mentioned. DeepNL program of the Dutch Research Council, NOW, is a research program about the deep subsurface rock masses which are under the influence of natural gas extraction, (TUDelft, 2023). Underground spaces as rock mass porosities have constituted a large number of volumes which depended on the rock masses physical-mechanical characteristics. When huge amounts of oil (or natural gas, groundwater) have discharged through boreholes and if there are no new charges (gaseous and/or liquids) to these deep emptied (depleted) rock porosities, reservoir rock masses may provide deformations due to the induced stresses formed around these voids. The deformations occurring in microscale (surrounding the porosities) may cause subsidence on earth ground surface which can be harmful for surface lands and urban settlements. When the

options are searched for the secondary usage of these emptied microscale rock porosities, discarded & harmful CO^2 gas depositions in them might be the future trends in engineering projects.

One of the studentship announcements at University of Cambridge has a statement presenting the importance of the UUSs in UK's engineering education. It covered the words; "a *substantial amount of underground construction, much of it in urban environments, is planned in the UK for the coming decades*". There is another statement here which is important to realise the future conditions around modern urban areas, and that is; "g*iven the current economic climate and the UK's current progress on the Net-Zero agenda, we urgently need new ways to deliver this infrastructure in a way that is low-cost, efficient and sustainable"*, (Univ-Cambridge, 2023). Some universities in the world have realised the trends & conditions and they have already supplied university education in BSc, and/or Graduate degrees in underground engineering. Geotechnics and underground engineering at VSB-Technical University of Ostrava (Czech Rep.) is one of them in Europe, (VSB TU-Ostrava, 2023). As the number of underground metro lines and other UUSs have increased, requirements for underground engineers have also been felt in real-world industry but there are limited graduates in this branch of engineering in western world. Actually the requirements & procedures of education in underground engineering have seemed to be more earlier evaluated in China because China already has more than 80 underground engineering related departments, (Guo, etal., 2021). Yet, the following universities are also examples which have supplied degrees, programs and courses related to underground engineering education; a) The programs offered at RWTH-Aachen University (Germany) are; Underground engineering (BSc, M.Ed) vocational school teacher, Google cartographer in underground robotic mapping, Test and evaluation of 3D mapping / localization / SLAM algorithm for underground robotics, Field experiments / evaluation for underground robotics, Enhance underground vision by thermal image processing, (RWTH-Aechen, 2023). b) Institute for Geotechnical Engineering at ETH Zurich has an academic program; "Chair of Underground Construction" which includes courses on "Planning of underground spaces" and "Tunnelling". This chair has supplied thesis in BSc and MSc education, (ETH-Zurich, 2023). c) Atilim University, (Ankara, Turkey) has a program on "Tunnelling and underground construction" reported on its webpages (Atilim, 2023). d) The CEE-Online certificate program which is supplied by University of Illinois Urbana-Champaign, US, (Univ-Illinois, 2023), and e) The course, "Tunnelling and underground engineering", is being provided by The University of British Columbia, Canada, (UBC, 2023).

Due to the increase in requirements of UUSs in China, Singapore, HongKong, Malaysia, etc., some of the countries have already provided legislative procedures for UUS development and utilisations. Underground engineering education departments have already been included in the main university education system in China for instance. China University of Geoscience has a Civil Engineering Department which has course contents especially about underground construction (including mine construction) of roads and tunnels, (CUG, 2023). Another university in China which has a major degree in UUS is Wenzhou University. This university internet website has an announcement in 2023 about a Major degree on "New urban underground space engineering". This department was approved and put in the list of "Undergraduate Majors in Regular Institutions of Higher Learning" in 2021 by the Ministry of Education in China. The statement given in the university website about this department as follows; "*the Urban Underground Space Engineering major of Wenzhou University is the first major of the kind of undergraduate colleges and universities in Zhejiang Province, which will be set up in the College of Civil Engineering and Architecture of our university*", (WU, 2023). Similarly, Shenyang University of Technology (China) has a School of Architecture & Civil Engineering and one of the departments here is "Urban underground space engineering". The

department website has the following words; *"urban underground space engineering is a major of full-time undergraduate with a wide range of obtaining employment and strong comprehensiveness, which is established for urban underground space resources development and utilization*", (SUT, 2023). Moreover, The Chinese University of Hong Kong - Shenzhen organised a ceremony on Nov, 23th 2020 for the establishment of an institute related to the UUS. It was named as "Institute of Urban Underground Space and Energy Studies, IUSE". One statement supplied through the related website (CUHK, 2023), defined the purpose of this institution briefly which all the other countries should also think about. The statement is; *"In general, the Institute will make full use of the regional advantages of the Guangdong - Hong Kong - Macao Greater Bay Area to carry out comprehensive research on the prevention and control of urban underground space security, urban strategic energy reserves, exploration and development of strategic materials…"*. At this point seminars and special lectures which were supplied to enhance the views (in societies) related to UUSs are also important educational approaches. One of them was given in Nov. 2022 at UC- San Diego, Jacobs School of Engineering. It was related to structural Engineering and it was titled; "Building big underground - Modern challenges in meeting the demands of expanding the urban environment.", The statement covered in this seminar website points to the facts which most of the UUS related experts and engineers have also stressed. The subjects include the world population increase and adjacent high rise in population of cities and their land coverages. These living conditions in future eventually will force the municipalities of cities to facilitate underground transportation and UUS related living activities. The statement here includes words; *"city municipalities are expanding their subterranean networks, requiring longer, larger, and more extensive underground networks",* (UCSD, 2023). Another special lecture given at University of Singapore in Nov. 2018 was titled as "uncovering the underground". One statement forwarded on the website of the lecture showed where the directions of UUSs development and utilisations lead to; *"from an engineering perspective, there's really no limit to underground space (construction), including areas under the seabed. The limit often lies in the economic and commercial viability of the projects"*, (Yong, 2018).

Conclusions

Knowledge and experiences related to UUSs have been enhanced together with the regulated underground spaces in modern urban areas. Underground engineering concept has gradually appeared to be new branches of engineering other than mining engineering in which underground work & workplaces are also main parts of their engineering issues. Numbers of university departments, programs, and courses related to underground engineering are expected to increase more in the near future as the popularity and effectiveness of UUSs are augmented. The UUSs concept has been a historical issue which some countries are familiar with. However, new requirements and developments have aroused mainly due to population increase in the world. Population & environmental issues, and economic & technological developments push the societies to decide over efficient usage of "energy-land-natural" resources. They have gradually redefined their potentials in agriculture, livestock, natural resources, groundwater, industrial productions, constructions, daily lifestyles, etc. according to carbon-zero waste production procedures. For instance, there is tendency to work out on deposition of the excess amounts of carbonic gases underground rock masses' porosities instead of releasing them into the atmosphere. Energy efficiency supplied through underground; metro lines, road tunnels, and railway tunnels have already been known by societies living in big urban cities. However, it may not be well known by people that deep underground hot rock resources of some countries have recently been researched dynamically to handle their energy potentials in electricity production. Porosity and permeability properties of these deep hot rock bodies have been studied together with their rock masses behaviours to be answered for future energy

requirements. It is also important to point that, UUSs like, *hotels, cultural-social-sport centres, carparks, shopping centres, pedestrian passageways, metro lines, etc*, are also considered with their opportunities in energy prevention circumstances. Underground engineering concepts including the energy, transportation, and urban settlement cases have provided new "work-decision-responsibility" areas which certain branches of engineers should be handled. Available engineering branches have provided partial solutions in the decisions but, the requirements of underground engineering for UUSs have realised vigorously where the usage of UUSs have already reached huge volumetric amounts in total. Their design, excavations, constructions and monitoring stages have involved many engineering decisions which should be handled by underground engineers who have to be equipped with good knowledge and experiences in underground engineering operations and rock mass behaviour & stability contexts.

REFERENCES

ACUUS, (2023) *Associated Research Centres for the Urban Underground Space*, Website, www.acuus.org/index.php/what-is-acuus, Retrieved in Aug. 2023.

Atilim, (2023) Department of tunnelling and underground construction, Atilim University, Website, www.atilim.edu.tr/en/tunelcilik, Retrieved in Aug. 2023.

Belanger, P. (2007) Underground landscape: The urbanism and infrastructure of Toronto's downtown pedestrian network, *Tunnelling and Underground Space Tech.*, 22, pp272-292.

Besner, J. (2016) Underground space needs an interdisciplinary approach, *Tunnelling and Underground Space Technology*, 55, pp224–228.

BGS Research, (2017) *Project Iceberg: Breaking new ground for future cities*, BGS, British Geological Survey, Natural Environment Research Council, Website; http://os.uk/ projecticeberg, Retrieved in Aug. 2023.

Bresnahan, S. (2022) *Why the future of our cities might be headed underground*, CNN Com, Website, https://edition.cnn.com/2022/12/21/world/underground-development-singapore-dtss-tnf-spc-intl/index.html, Retrieved in Aug. 2023.

CUG, (2023) *Undergraduate Major: Civil Engineering*, China University of Geoscience, Website; https://en.cugb.edu.cn/SET/40970.jhtml, Retrieved in Aug. 2023.

CUHK, (2023) *CHUK-Shenzhen-Establishes "Institute of urban underground space and energy studies",* The Chinese University of Honk Kong, Shennzhen, Website; CUHK-Shenzhen Establishes Institute of Urban Underground Space and Energy Studies CUHK-Shenzhen, Retrieved in Aug. 2023.

Datwyler, (2023) *Underground data centres for the urban spaces of the future,* Website; https:// itinfra.datwyler.com/company-press/digital-training-platform-copy-copy-2/, Retrieved in July 2023.

Fields, J. (2020) The future is (still) underground, *Mines Magazine*, Colorado School Mines, Website; https://minesmagazine.com/16070/, Retrieved in July 2023.

ETH-Zurich, (2023) Chair of Underground Construction, Institute for Geotechnical Engineering, Eidgenössische Technische Hochschule, ETZ, Zurich, Website; https:// wtunnel.ethz.ch/en/ about-us/wie-finden-sie-uns.html, Retrieved in Aug. 2023.

Gokay, M.K. (2023) Interactions in subterranean and surface structures, *International Journal of Environmental Trends*, 7, (1), pp27-37.

Guo, D., Zhu, X., Xie, J., Zhang, C., Zhao, Z. and Zheng, L. (2021) Undergraduate program for Urban Underground Space Engineering in China: Exploration and practice, *Tunnelling and Underground Space Technology*, 116, 104084.

Kontothanasis, P., Krommyda, V., and Roussos, N. (2020) *BIM and advanced computer-based tools for the design and construction of underground structures and tunnels,* (Chapter in), Tunnel Engineering- Selected Topics, (Ed.: Sakellariou, M.), ISBN 978-1-78985-466-4.

Kshirsagar, M.P., Kulkarni, S.K., Arora, N.V., Maheshwari, D.D., and Meena, A.K. (2021) Underground construction and space utilisation: A Bibliometric analysis, *Library Philosophy and Practice (e-journal),* 5416, p21, https://digitalcommons.unl.edu/libphilprac/5416.

Lei, M., Wang, W., Shi, C., Jia, C. and Gong, C. (2022) Practice research on standardization of undergraduate graduation design of tunnel and underground engineering, *Journal of educational theory and management*. 6, (1), pp46-50.

Lavagno, E. (2016) Underground Education: attitudes towards more underground oriented educational programs, *Procedia Engineering*, 165, pp114-118.

Martin, N. (2022) *The only way is… down! Why underground urban development is on the rise*, UNSW-Sydney Website, https://www.unsw.edu.au/news/2022/01/the-only-way-is----down--why-underground-urban-development-is-on, Retrieved in July 2023.

MINES, (2023a) *The job market is promising for underground construction and tunnelling engineers*, Colorado School Mines, Website; https://gradprograms.mines.edu/blog/the-job-market-is-promising-for-underground-construction-and-tunneling-engineers/ 4/12, Retrieved in July 2023.

MINES, (2023b) *Underground construction and tunnel engineering*, Website; Underground Construction and Tunnel Engineering (mines.edu), Retrieved in Aug. 2023.

NAU, (2023) *Space exploration goes underground: Is there life in Martian caves?* The NAU Review, NAU Communication, Northern Arizona University, Website; https://news.nau.edu/space-exploration-goes-underground/, Retrieved in July 2023.

Paddison, L. (2022) *What if all roads went underground?* BBC-Future Website, Planet, https://www.bbc.com/future/article/20220621-what-if-roads-went-underground, Retrieved in July 2023.

PATH, (2023) *Toronto (Canada) Underground pedestrian pathway map (PATH) for public information*, https://www.theicecondos.com/path_brochure.pdf, Retrieved in July 2023.

Purdue-FUCL, (2023) *Future underground construction leaders (FUCL) development program*, Website; https://bami-i.com/future-underground-construction-leadersfucl-development-program/, Retrieved in July 2023.

Ramlakhan, R.J.K., Kalogianni, E., and Van Oosterom, P.J.M. (2021) *Modelling 3D underground legal spaces in 3D Land Administration Systems*, Proceedings of the 7th International FIG Workshop on 3D Cadastres (Virtual/online event), pp37-52.

RWTH-Aechen, (2023) *Underground engineering related programs*, TWTH-Aachen University, Website; https://www.rwth-aachen.de/cms/root/~hx/search-aaaaaaaaaaaaaa/lidx/1/?search=underground+engineering+program&institution=RWTH%20Aachen%20University&page=2, Retrieved in July 2023.

Safaee, M.M. and Nematipour, N. (2021) Development of urban public spaces using urban underground spaces: A new method to improve quality of life (QOL) in Tehran metropolis, (17th World Conference, ACUUS, 2020, Helsinki, Finland), *IOP Conf. Series: Earth and Environmental Science*, 703, 012025.

Samsung C&T Global, (2018) *Underground roads - The future of urban transportation*, Website; https://news.samsungcnt.com/features/engineering-construction/2018-09-underground-roads-future-urban-transportation/, Retrieved in Aug. 2023.

Schrotter, G. and Van Son, R. (2019) *Digital Underground: Towards a reliable map of subsurface utilities in Singapore*, Published by Digital Underground, Digital-Underground-1.pdf (ethz.ch), p60.

Seequent, (2019) *Five of the World's most surprising underground developments*, Seequent-The Bentley Subsurface Company, Website, https://www.seequent.com/five-of-the-worlds-most-surprising-underground-developments/, Retrieved in July 2023.

Seng, L.T. (2023) *Subterranean Singapore: A deep dive into manmade tunnels and caverns underground in the city state*, Website; https://biblioasia.nlb.gov.sg/vol-18/issue-2/jul-sep-2022/underground-space-singapore/, Retrieved in July 2023.

Singapore - ETH Centre, (2022) *Digital Underground*, Website; https://sec.ethz.ch/research/digital-underground.html, Retrieved in Aug. 2023.

SUT, (2023) *Urban underground space engineering department*, Shenyang University of Technology, Website; htttps://tmgc.sut.edu.cn/info/1017/1061.htm, Retrieved in July 2023.

TUDelft, (2023) *Consequences of underground engineering*, TUDelft University, Civil engineering and geosciences, Website; Consequences of underground engineering (tudelft.nl), Retrieved in Aug. 2023.

UBC, (2023) *EOSC 547-Tunneling and underground engineering*, Courses, The University of British Columbia, Vancouver, Canada, Faculty of Science, Department of Earth, Ocean and Atmospheric Sciences, Website, https://www.eoas.ubc.ca/academics/courses/eosc547, Retrieved in Aug. 2023.

UCSD, (2023) *Building big underground - Modern challenges in meeting the demands of expanding the urban environment*, UC-San Diego, Jacobs School of Engineering, Website, https://se.ucsd.edu/seminars/building-big-underground-modern-challenges-meeting-demands-expanding-urban-environment, Retrieved in Aug. 2023.

Univ-Cambridge, (2023) *EPSRS-DTP Studentship-Underground digital twins for future tunnelling*, Website; https://www.c2d3.cam.ac.uk/opportunities/epsrc-dtp-studentship-underground-digital-twins- future-tunnelling, Retrieved in July 2023.

Univ-Illinois, (2023) *CEE Online Certificate Program*, Underground engineering certificate, University Illinois Urbana-Champaign, The Grainger College of Engineering, Civil & Environmental Engineering, Website, https://cee.illinois.edu/academics/graduate-programs/cee-online/cee-online-certificate-program, Retrieved in July 2023.

Vahaaho, I. (2014) Underground space planning in Helsinki, *Journal of Rock Mechanics and Geotechnical Engineering*, 6, pp387-398.

VSB TU-Ostrava, (2023) *Civil Engineering, Geotechnics and Underground Engineering*, VSB- Technical University of Ostrava, Website, https://www.vsb.cz/en/search?query=Geotechnics %20and%20Underground%20Engineering, Retrieved in July 2023.

WU, (2023) *Urban Underground Space Engineering*, Wenzhou University, Website; www.wzu.edu.cn/info/1505/38370.htm, Retrieved in July 2023.

Yong, K.Y. (2023) Uncovering the Underground, CLC-Lecture series, Centre for Liveable Cities - Singapore, National University of Singapore, Website; clc-lecture-uncovering-the-underground.pdf, Retrieved in July 2023.

Zhao, J.W., Peng, F.L., Wang, T.Q., Zhang, X.Y. and Jiang, B.N. (2016) Advances in master planning of urban underground space (UUS) in China, *Tunnelling and Underground Space Technology*, 55, pp290–307.

Current Outlook On Clean Coal Technologıes: A Comprehensıve Revıew

Mesut YAZICI[1]

Introduction

Among fossil fuels, coal reserves are more evenly distributed around the world, unlike oil and natural gas reserves. This situation offers an important advantage, especially for countries with coal reserves, in ensuring energy supply security. Bringing coal reserves into the economy of a country can provide versatile benefits. Its impact on employment is undeniable, especially in regions where reserves are located, and mass consumption occurs. On the other hand, there is a widespread belief in the public that coal is a non-environmental energy source. On the other hand, important steps are being taken to eliminate the polluting effects of coal by using renewable energy sources.

Renewable energy sources provide many advantages such as reducing carbon emissions, getting rid of political pressures, reducing the cost of providing energy resources, etc. However, it will take many years to fully adapt renewable energy sources to areas of continuous and intense energy consumption such as transportation, heating, and industry. So much so that electricity cannot be produced continuously from wind and solar energy sources, which have the most installed capacity and investment among renewable energy sources. The energy produced at the maximum level from these sources during the hours when demand is low has a problem of being evaluated. To overcome this problem, a solution to direct this excess energy to hydrogen production by electrolysis is proposed. However, the high cost of hydrogen production by electrolysis is a challenge to overcome. In addition, it is an important question mark whether renewable energy sources can provide the energy needed by heavy industries such as iron-steel, cement, and petrochemical industries.

To ensure uninterrupted energy production, coal resources have been used intensively in many places around the world for many years. Coal is more polluting than other hydrocarbons, oil, and natural gas. In order to pollute the atmosphere less, a century-long transition from coal to oil and from oil to natural gas has been observed in the world. On the other hand, difficulties experienced in the supply of oil and natural gas as a result of international political conflicts and regional conflicts around the world bring the evaluation of existing coal reserves to the agenda.

Coal is used as fuel in energy facilities, heating applications, iron steel, cement, etc. in many industries. Coal occupies an important place in the economy with its extraction, processing, and transportation processes and then putting it into use. At these stages, coal extraction is quite laborious and difficult. Worldwide, coal is mined by underground and open-surface mining methods. Depending on the characteristics of the coalfield, one of these two methods is preferred. However, some coal fields are not suitable for the use of both methods. Coal reserves in such areas have no economic value. However, with the spread of more environmentally friendly technologies, the consumption areas of coal are decreasing every year. In particular, in line with the zero-carbon targets that have been discussed in the last few years, governments are trying to reduce carbon emissions with heavy environmental legislation. In this context, the use of coal in some heavy industry branches is being replaced by natural gas.

[1] Dr., Kutahya Dumlupinar University, Faculty of Simav Technology, Mechanical Engineering, Kutahya, Turkiye, mesut.yazici@dpu.edu.tr, ORCID ID: 0000-0001-6379-8396

For developing countries, coal reserves become strategic in ensuring energy supply security. In order to bring these resources into the economy, on-site transformation of coal has been a subject of research for many years. In this context, clean coal technologies applications are encountered more frequently. Newly built thermal power plants are equipped with innovative and efficient combustion technologies. In addition, flue gas treatment systems are being put into operation. In particular, coal gasification methods and coal liquefaction methods, which have a long history, aim to make coal more functional. In addition to the benefit of bringing these reserves into the economy, such applications also enable the production of higher-value products from coal. In addition to such applications, carbon capture, use, and storage technologies are being developed to eliminate the carbon emissions released into the atmosphere when coal is burned. In this chapter, firstly, the current situation of coal on a global and Turkish scale is discussed. Afterward, clean coal technologies and the latest developments about them were shared.

Global Coal Reserves and Outlook

Many countries around the world have coal reserves, albeit in small quantities. On the other hand, some countries differ from others by having very high amounts of reserves. Table 1 shows the countries with significant coal reserves in the world. The US alone owns 23.2% of global coal reserves. Of the total 248,941 million tons of reserves this country has, 218,938 million tons are in the anthracite and bituminous coal category, while the remaining amount is in the sub-bituminous and lignite category. The second largest reserve is the Russian Federation, which has significant oil and natural gas reserves. Russia has 15.1% (162,166 million tons) of total global reserves. Russia is followed by Australia with 14%, China with 13.3% and India with 10.3%. The countries that come after have a share below 4%. The total proven coal reserves in the world are 1,074,108 million tons. Of this, 753,639 million tons are anthracite and bituminous coal, while 320,469 million tons are sub-bituminous and lignite. All of Germany's coal, which has 3.3% of the world's coal reserves, is in the al-bituminous and lignite category. Although China has 143.197 million tons of coal reserves, the lifespan (R/P) of this reserve is calculated as 37 years. On the other hand, Turkey, which has a reserve of 11.525 million tons, has a reserve of 168 years.

Table 1. According to the BP 2021 Statistical Review of World Energy Report, the total proved coal reserves at the end of 2020 (BP, 2021)

Billion Tonnes	Anthracite & bituminous	Sub-bituminous & lignite	Total	Share of Total	R/P Ratio
US	218.938	30.003	248.941	23.2%	-
Russian Federation	71.719	90.447	162.166	15.1%	407
Australia	73.719	76.508	150.227	14.0%	315
China	135.069	8.128	143.197	13.3%	37
India	105.979	5.073	111.052	10.3%	147
Germany	-	35.900	35.900	3.3%	334
Ukraine	32.039	2.336	34.375	3.2%	-
Indonesia	23.141	11.728	34.869	3.2%	62
Poland	22.530	5.865	28.395	2.6%	282
Kazakhstan	25.605	-	25.605	2.4%	226
Türkiye	0.550	10.975	11.525	1.1%	168
Others	44.395	43.506	87.901	8.3	-
Total	753.639	320.469	1074.108	100	139

Table 2 shows the coal production and consumption shares of countries with significant coal reserves in the world. While China has the highest production share with 50.7%, it has the highest consumption share with 54.3%. As can be understood from here, China, which has one of the highest coal reserves in the world, is a net importer despite producing the highest amount of coal in the world. Although Taiwan does not produce coal, it has a share of 1.1% of total global coal consumption. In addition, Japan, South Korea, and Vietnam, whose production amounts are very low, have a total share of 6.4% in consumption. Namely, this share is less than India, which has the highest consumption in the world after China, with a share of 11.6%, and more than the US, which ranks third with a share of 6.1%. The US, Russia, Australia, Indonesia, and South Africa, which produce more than they consume, are in a net exporter position. South Africa, which has less than 1% of global coal reserves, has a 3.7% share in production. Its share in consumption is 2.3%.

Table 2. Shares of major coal producing and consuming countries in the world in 2021 (BP, 2021

Exajoules	**Production**	**Share of Total**	**Consumption**	**Share of Total**
US	10.71	6.7%	9.20	6.1%
Russian Federation	8.37	5.2%	3.27	2.2%
Australia	12.42	7.8%	1.69	1.1%
China	80.91	50.7%	82.27	54.3%
India	12.68	7.9%	17.54	11.6%
Germany	0.98	0.6%	1.84	1.2%
Ukraine	0.54	0.3%	0.98	0.6%
Indonesia	13.88	8.7%	3.26	2.2%
Poland	1.68	1.1%	1.67	1.1%
Kazakhstan	2.04	1.3%	1.64	1.1%
Türkiye	0.60	0.4%	1.66	1.1%
South Africa	5.97	3.7%	3.48	2.3%
Japan	0.02	-	4.57	3.0%
South Korea	0.02	-	3.03	2.0%
Taiwan	-	-	1.63	1.1%
Vietnam	1.14	0.7%	2.10	1.4%
Others	7.65	4.9%	11.59	7.6%
Total	**159.61**	**100**	**151.42**	**100**

Approximately 3/4 of coal consumption in 2022 took place in the countries of Asia and Oceania. According to the IEA (International Energy Agency), despite the decline in US and European coal consumption in 2022, strong growth in both industrial applications and energy production in Asia has driven global coal consumption to an all-time high (IEA, 2023). In 2022, coal consumption increased by 3.3%, reaching 8.3 billion tons.

Turkey's Coal Reserves

Türkiye has an important geopolitics in terms of world energy trade. Namely, it is a bridge between the Middle East and Caspian region countries, which are the world's major oil and natural gas producers, and European countries, which are important consumption points. Although Turkey neighbors a geography (Middle East) with 47.6% of the world's oil reserves and 40.9% of its natural gas reserves, it does not have a significant amount of reserves in terms of both resources. However, it has discovered significant amounts of oil and natural gas reserves

in the last few years. As a result, Türkiye is overwhelmingly dependent on foreign oil and natural gas.

Unlike oil and natural gas, Türkiye has significant coal reserves. According to the latest data, it has a total coal reserve of over 21 billion tons, including 1.5 billion tons of hard coal and 19.3 billion tons of lignite + asphaltite. Hard coal reserves are located only within the borders of Zonguldak and Bartın provinces in the northwestern part of the country. On the other hand, lignite reserves are more evenly distributed throughout the country. Asphaltite is located within the borders of Şırnak province in the southeastern part of the country. While the lower calorific value of Turkish hard coal varies between 6200-7250 kcal/kg, that of lignite varies between 100-4200 kcal/kg (MENR, 2023).

Since the hard coal reserves in the Zonguldak and Bartın regions show a certain degree of coking feature, most of the coal produced from this region is used in the iron and steel industry. Table 3 shows the amount of Türkiye's hard coal reserves by field (TTK, 2023). The reserves with the highest lower calorific value are located in the Armutçuk field, with a range ranging from 6050 to 7050 kcal/kg. Additionally, in general, coals in the Zonguldak basin have a moisture content ranging from 2% to 14% and ash content ranging from 9% to 15%. There are six important coal fields in the Zonguldak coal basin: Amasra-A, Amasra-B, Armutçuk, Karadon, Kozlu, and Üzülmez. Among these, the highest total coal reserve is located in the Amasra-B field. The proven reserve of this field, which has a total reserve of 549.3 million tons, is 395.9 million tons. Less than half (0.7 billion tons) of the basin's total 1.5 billion tons of reserves have been proven. Production in this basin is generally based on labor-intensive methods (Ozturk, 2014). For this and many other reasons, production remains limited. While the coals in the Amasra field do not show coking properties, those in the Armutçuk field show semi-coking properties and those in the remaining fields show coking properties. For this reason, the coal produced can be utilized in the iron and steel industry in the region. The annual coal need of this sector in Turkey is around 5.5 million tons (Mishra, Panda, & Akcil, 2021). However, the production to meet such demand in the basin was only 5 million tons in 1974 (Kasap, Şensöğüt, & Ören, 2020).

Table 3. Turkey's hard coal reserves according to fields in the Zonguldak coal basin (Million tons) (TTK, 2023)

Reserve Type	Amasra-A	Amasra-B	Armutçuk	Karadon	Kozlu	Üzülmez	TTK
Ready	0.22	-	2.17	3.06	2.46	0.48	8.4
Proven	4.75	395.95	6.34	127.64	62.35	131.93	728.5
Probable	7.69	151.16	14.40	159.16	40.54	94.34	467.3
Possible	56.62	2.19	7.88	117.03	47.97	74.02	305.7
Total	69.28	549.31	30.80	406.89	153.33	300.77	1509.9

Table 4 shows Turkey's most important lignite reserve areas. The largest reserve is the Afşin-Elbistan lignite field (4642.34 million tonnes) located within the borders of Kahramanmaraş. There are five lignite basins in Turkey with reserves of over 1 billion tons. Apart from Afşin-Elbistan, these are Konya-Karapınar, Tekirdağ-Malkara, Eskişehir-Alpu and Istanbul-Silivri basins. In addition to these, Afyon-Dinar, Manisa-Soma, Muğla-Milas, and Tekirdağ-Çerkezköy basins have reserves between 0.5-1 billion tons. Others have reserves below 0.5 billion tons. Turkish lignites have high ash, moisture, and sulfur values despite their low calorific value. For this reason, the extracted lignite is utilized in thermal power plants. Although Turkey has significant hard coal and lignite reserves, production in coal fields has

remained very limited due to multiple fatal coal mine accidents, especially in the last decade. This situation causes the reserves not to be utilized at the desired level.

Table 4. Turkey's important lignite basins and reserve amounts (MTA,2023)

Lignite fields	Reserves (Million tons)	Lignite fields	Reserves (Million tons)
Afşin-Elbistan	4642,34	Beypazarı	498
Afşin-Elbistan (MTA)	515	Tufanbeyli	429,55
Karapınar	1832	Muş	400
Malkara	1533,3	Beyşehir-Seydişehir	348
Alpu	1453	Tunçbilek	317,73
Silivri	1100	Kangal	202,6
Dinar-Dombayova	941,5	Seyitömer	198,66
Soma	861,45	Mengen	142,76
Milas	750,21	Saray	141,2
Çerkezköy	573,6	Orta	123

The Position Of Coal In Turkiye's General Energy Outlook

According to the 2021 energy balance tables published by the Ministry of Energy and Natural Resources of Turkey, the primary energy supply is as given in Table 5 (MENR,2022). Accordingly, the total primary energy supply was 159,687 million TOE (Tonne of Oil Equivalent). While the share of renewable energy resources in this total amount is 15.59%, the share of fossil-based energy resources is 84.41%. As can be understood from these ratios, the country's energy profile is overwhelmingly dependent on foreign sources and fossil-based resources are the overwhelming majority. The total share of coal in the primary energy supply is 26.03%. The share of lignite supply is 10.44%, and the share of hard coal is 14.68%. The total share of asphaltite and coke is below 1%. It should be taken into consideration that a large portion of hard coal is imported coal.

Table 5. Turkey's primary energy supply according to sources in 2021 (MENR,2022)

Sources	Supply (MTOE)	Rate (%)
Hydro	4.810	3,01
Wind	2.704	1,69
Solar	2.059	1,29
Biomass	4.099	2,57
Geothermal	11.234	7,03
Total Renewables	24.906	15,59
Hard Coal	23.444	14,68
Lignite	16.672	10,44
Asphaltit	0.707	0,44
Coke	0.744	0,47
Total Coal	41.567	26,03
Oil Products	7.742	4,85
Crude Oil	36.241	22,70
Total oil	43.983	27,55
Natural Gas	49.231	30,83
Total Conventional	134.781	84,41
Total	**159.687**	**100**

Table 6 shows Turkey's electrical energy installed capacity and production according to sources as of the end of June 2023. As of this date, Turkey's total electrical energy installed capacity is 104.9 GW. On the other hand, the total electrical energy produced is 84,497.3 GWh. The total share of coal resources in the total installed power is 20.8%. It should be said that this share is the third highest share after hydro energy and natural gas. Installed power for imported coal is 10.4 GW (9.89%), for lignite 10.2 GW (9.72%), for hard coal 0.8 GW (0.8%), and for alsphaltite 0.405 GW (0.39%) Its share in total production is 34.97%. The share of coal (imported coal+hard coal+lignite+asphaltit) in total electricity production is much higher than other energy sources. Namely, hydro energy has the second highest share with 21.86%, and natural gas has the third share with 20.19%. Here, special attention should be paid to imported coal. Although the installed powers based on imported coal and lignite are almost the same in terms of installed capacity, imported coal has a significant advantage over lignite in electrical energy production. From this situation, it can be understood that thermal power plants based on imported coal are operated more efficiently than those based on lignite. However, even this indicator may encourage investors to establish thermal power plants based on imported coal. As a result, this situation may have an increasing effect on Turkey's dependence on foreign energy.

Table 6. Turkey's electrical energy installed capacity and electrical energy production distribution according to sources as of the end of June 2023 (PetroTurk, 2023)

Sources	Installed Power (GW)	Rate (%)	Production (MWh)	Rate (%)
Hydro	31.58	30,11	33.367.800,35	21,86
Wind	11.56	11,03	15.822.658,36	10,37
Solar	10.19	9,72	8.671.051,31	5,68
Biomass	2.031	1,94	4.709.695,94	3,09
Geothermal	1.69	1,61	5.564.050,66	3,65
Total Renewables	57.05	54,40	68.135.256,62	44,64
Naturalgas	25.75	24,55	30.813.349,27	20,19
İmported Coal	10.37	9,89	31.518.477,50	20,65
Lignite	10.19	9,72	19.560.601,15	12,82
Hard Coal	0.84	0,80	1.530.722,39	1,00
Asphaltit	0.40	0,39	760.281,02	0,50
Fuel-oil	0.26	0,25	313.884,96	0,21
Naphtha	0.004	0,00	0,00	0,00
LNG	0.001	0,00	0,00	0,00
Diesel	0.001	0,00	0,00	0,00
Total Thermal	47.82	45,60	84.497.316,29	55,36
Total	104.87	100	152.632.572,92	100

Clean Coal Technologies

With the Paris Climate Agreement in 2015, the trend towards renewable energy sources has gained momentum in line with the 2050 net zero carbon target. Turkey became a party to this goal by signing this agreement in 2021. However, many reasons such as the high cost of renewable energy power plants and their equipment, the fact that they are imported to a certain extent, and the inability to produce continuous energy in terms of resources, pose an important challenge to developing countries such as Turkey. In addition, the current technology in storing

electrical energy still needs development, and the costs are high, making the increase in solar and wind energy installed capacity risky. On the other hand, the war between Russia and Ukraine, which started in 2022, has caused significant increases in the prices of fossil resources. Such reasons have made coal a strategic energy source for countries such as Turkey, which are poor in terms of oil and natural gas reserves but have coal reserves.

If coal, which is a national wealth for countries with little or no oil and natural gas reserves, is burned with old burning technologies, it releases high amounts of harmful emissions into the atmosphere, which poses a problem in meeting environmental regulations. Not only the burning of coal but also the extraction and cleaning processes of coal cause damage to surface and underground water resources by creating pollution such as coal gangue and sludge (Vejahati et al., 2010; Yuan et al., 2015). Clean coal technologies are needed to bring coal reserves into the economy. Namely, it is important to transform coal into value-added products that can compete with oil and natural gas. Efforts to substitute coal for oil, natural gas, and their derivative products are not a new initiative. The history of clean coal technology research goes back many years. For example, in the 1940s, the Germans used coal liquefaction to fuel their military units. Before the use and widespread use of natural gas in Turkey, gases obtained by the gasification of coal were used as fuel in some large populated settlements as a precaution against the pollution of the atmosphere by burning coal for heating purposes. However, the studies did not continue with the same concentration and motivation. Especially in periods of major energy crises, work intensified, and in non-crisis conditions, work slowed down as oil and natural gas became cheaper.

The energy content of raw coal decreases both when it is gasified and when it is liquefied. However, the current use of coal, especially in solid form, is rarely preferred in the transportation, industry, heating, electricity, and service sectors where energy demand is intense. Particularly noteworthy are the liquefaction and gasification mechanisms that enable the transformation of coal into value-added fuels, semi- and final products with properties close to oil and natural gas. In addition, there are important lignite reserves that have been discovered in Turkey but cannot be extracted with current technologies. Since these reserves cannot be mined, they cannot contribute to the country's economy. For such situations, these reserves can be evaluated and brought into the economy, especially by underground gasification method.

The general opinion on clean coal technologies is combustion technologies and cleaning of flue gas after combustion. It is widely known that emissions can be kept under control to a certain extent during combustion, especially with fluidized bed combustion systems. In addition, releasing the flue gas into the atmosphere after being passed through electrostatic filters and desulfurization units after combustion is one of the practices encountered in coal-fired thermal power plants. Before these, the coal is washed after being removed from the mine.

One of these technologies that should be mentioned here is carbon capture, use, and storage technologies. However, this technology is still in need of development. In addition, this technology can be integrated into coal gasification and liquefaction processes to provide functionality. As a result, coal can be re-functionalized with clean coal technologies in order to fulfill environmental regulations and ensure energy supply security. Clean coal technologies can generally be classified as coal liquefaction, gasification, and carbon capture. In addition, making combustion technologies more environmentally friendly and efficient can also be added to this category. Turkish Coal Enterprise divides clean coal technologies into four main groups (TKİ, 2023). These;

- Coal preparation, improvement, enrichment, and liquefaction technologies
- Coal gasification, integrated gasification combined cycle technologies (IGCC), advanced technologies such as underground gasification, etc.

- Efficiency improvement and emission control technologies in power plants
- Carbon capture, utilization, and storage technologies (CCS/CCUS)

Coal Liquefaction

Liquefaction of coal is one of the clean coal technologies. This method contributes to energy supply security by increasing coal use efficiency (Li et al., 2023). Liquefaction of coal can be expressed as subjecting coal pieces to a number of processes and obtaining products close to the properties of liquid hydrocarbons. In this process, the aim is to remove carbon or increase the share of hydrogen by breaking the bonds in aromatic structures. Coal liquefaction processes are classified as direct coal liquefaction, indirect coal liquefaction, and hybrid coal liquefaction. (Höök, & Aleklett, 2010).

In addition to obtaining more useful liquid fuel with the direct coal liquefaction (DCL) method, residues, and light hydrocarbons are also produced (Li et al., 2008). The efficiency of this method products largely depends on the structure and composition of coals with high H/C ratio and volatile content (Liang et al., 2021; Li et al., 2022). The DCL method can be an effective option for countries such as Turkey, which have very high amounts of lignite and sub-bituminous coal reserves with high ash and moisture content and low calorific value. Namely, clean liquid fuels, value-added chemicals, and carbon-based materials can be obtained from these types of coals using the DCL method (Mochida et al., 2014; Li et al., 2015; Gündüz et al., 2023).

This method converts coal into liquid hydrocarbon fuels through catalytic hydrogenation with higher energy conversion efficiency and under high pressure and temperature conditions. Thus, it is highly preferred because it provides a high-level final product without sulfur, nitrogen, and oxygen (Kong et al., 2019). In other words, DCL turns coal into liquid by increasing the H/C ratio without damaging its molecular structure. A DCL process operates in the range of 400 to 470°C at a hydrogen pressure of 70 to 200 bar in the hydrogen donor solvent when appropriate catalysts are selected (Xu et al., 2021). In the DCL process, if the breaking rate of the weak bridge bonds of the coals and the hydrogenation rate of the free radical fragments produced from the breaking of the bonds are maximized, a high oil yield is obtained (Shen et al., 2023).

Figure 1 schematizes a typical direct coal liquefaction process (Ali & Zhao, 2020). This process aims to produce synthesis gases, liquid fuel, chemical raw materials, and solid fuel. For this purpose, heteroatoms and mineral substances in the structure of the coal must be removed. First, in the slurry preparation section, coal is turned into a slurry with hydrogen-enriched recycling oil. Afterward, it is heated in the liquefaction section. In this section, coal is dissolved and separated from its inorganic components. Technologies developed for direct coal liquefaction either use catalysts or do not. The products coming out of the liquefaction section are sent to the distillation and vacuum distillation sections. While gas and oil are obtained in the distillation section, residue is obtained in vacuum distillation. Additionally, liquefied recycling oil is obtained from both distillation processes. Afterward, in the solvent hydrogenation section, light oil and hydrogenated recycling oil are obtained in the hydrogen ambient. NEDOL, SRC-II, BCL, EDS, IGOR+, Shenhua, HTI, and H-coal are some of the developed DCL technologies (Vasireddy et al., 2011; Bai et al., 2023; Wang et al. 2024). For many years, many researchers have focused on NEDOL (Hirano, 2000; Onazaki et al., 2000) and Shenhua (Li et al., 2019; Wang et al. 2024) technologies.

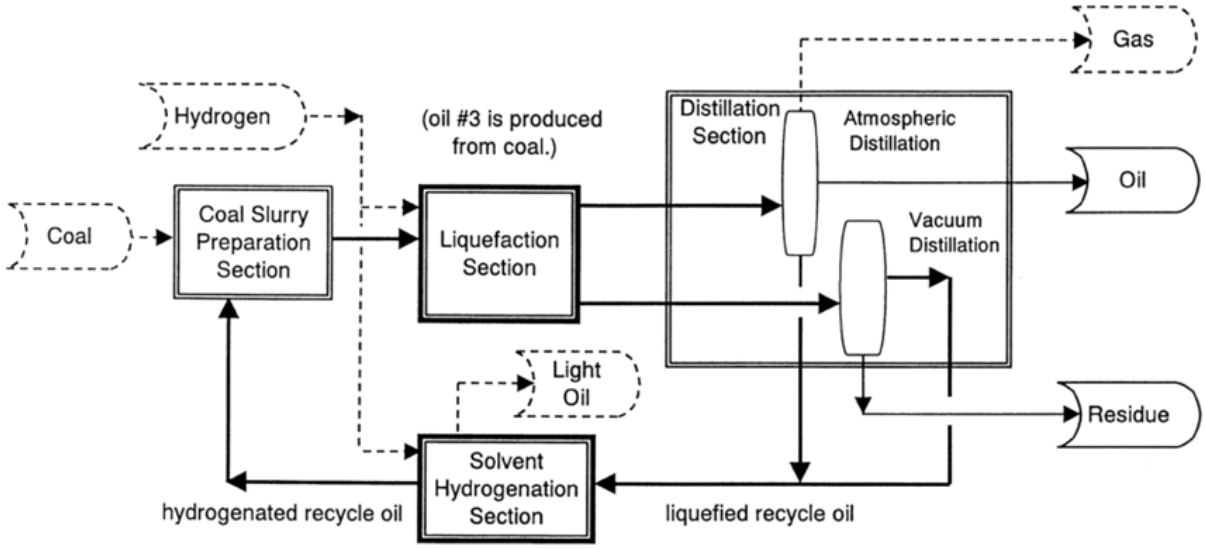

Figure 7. Schematic diagram of a typical direct coal liquefaction process (Ali & Zhao, 2020)

Qin et al. (2024), investigated the residue formation in the direct coal liquefaction process and its relationship with the vitrinite structure structure and product yield. For this reason, Naomaohu, a low-grade coal with high vitrinite, was examined at 380-460°C in the presence of tetrahydrinphthalene and in the absence of a catalyst. Xiu et al. (2023), developed a method for both resource upgrading and waste treatment by synergistic co-liquefaction of low-grade coal and waste plastic express bags in a supercritical water-ethanol system.

The indirect coal liquefaction method is based on first obtaining synthesis gas from coal and then converting this gas into liquid with the help of catalysts. Indirect liquefaction is based on two main categories: conversion of synthesis gas into light hydrocarbon fuels by the Fischer-Tropsch method and conversion into oxygenates such as methanol, dimethyl ether, ethylene glycol, etc. (Jin et al., 2014). In the production of synthetic oil through the indirect coal liquefaction process, a residue that constitutes approximately 30% of the coal is formed (Xu, 2015).

Figure 2 shows the flowchart of a typical Fischer-Tropsch indirect coal liquefaction process (Ra et al., 2021). Coal is first gasified in an oxygen or steam environment in a gasifier. The resulting products are subjected to a cleaning process. Here, sulfur, carbon dioxide, and ash are separated from the products. Synthesis gas consisting of H_2+CO turns into liquid hydrocarbons and wax by the Fischer-Tropsch Synthesis method in the presence of a suitable catalyst. In addition, waste gas and steam are used to produce electricity in the electricity generation plant. In recent years, many researchers have carried out important studies on the subject of indirect coal liquefaction (Chen et al., 2022; Wang, Zhang, Gao, 2022; Zhang, et al., 2022). Some researchers have compared direct and indirect coal liquefaction processes (Williams, R.H., Larson, E.D., 2003; Gao et al., 2018).

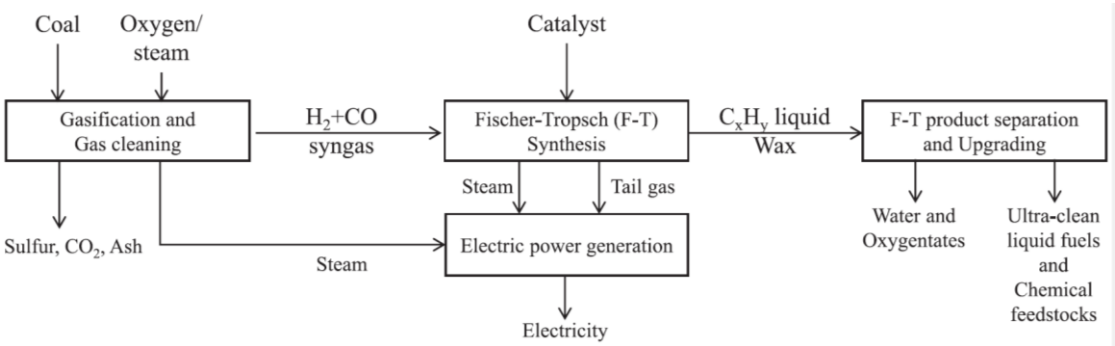

Figure 2. Indirect coal liquefaction system flowchart (Ra et al., 2021)

Coal Gasification

Gasification is defined as the conversion of carbon-rich coal such as petro-coke and biomass into synthesis gas by chemical reactions without combustion, using air, oxygen, and steam at temperatures above 700°C and below 10 MPa (Breault, 2010; Erik 2022). As a result of the gasification process, different amounts of carbon monoxide, hydrogen, methane, carbon dioxide, water vapor, sulfur, hydrogen sulfate, and ammonia are generally obtained. The gasification process is also known as incomplete combustion. Coal is converted into a usable gas by gasification technology, which is essential for oil refining, chemical industry, power generation, metallurgy, and other industries (Xu et al., 2015).

The first study on coal gasification was the coal gasification process carried out by K W Siemens in 1860. In 1909, A G Betts received the first patent in this field in Great Britain. The first field test was carried out by Williams Ramsey in England in 1912. Noteworthy studies after the First World War were the underground tests carried out in the Donetsk and Moscow coal basins in 1928-1939. After the Second World War, underground coal gasification tests were carried out in France, Belgium, England, the USA, and Italy between 1947 and 1950. However, Russia carried its pioneering initiatives to an industrial scale and illuminated the cities of Shatsky, Angren, and Yuzhno-Abinsk with electricity obtained by underground gasification.

The coal gasification process is divided into two: underground and surface gasification. The underground coal gasification process generally allows the evaluation of coal reserves in areas where coal production is difficult or not possible. The surface coal gasification method is applied to coal extracted from underground and open-surface mines, where there is no problem in extracting the coal.

Underground coal gasification (UCG) is a complex process. UCG depends on many factors such as geological and geo-hydrological analysis of layers, physical and chemical properties of coal, operational process parameters, seismic events, and real-time analysis of produced gases (Mandal, & Maity, 2023). Figure 3 depicts an underground coal gasification process. Two wells are being drilled in the detected coal seam, one for injection and one for production. A section of the seam is burned in a controlled manner to produce the necessary heat for the gasification and pyrolysis reactions to occur. This heat allows the volatile components of the coal to be separated from the coal. Air, oxygen, or water vapor is introduced into the seam from the injection well. The resulting carbon monoxide, methane, hydrogen, and synthesis gas are withdrawn from the production well (Bhutto et al., 2013). Afterward, the final products are sent to the gas cleaning and CO_2 separation facility. The final products are delivered to electricity generation facilities, the iron and steel industry, liquefaction facilities, and chemical production facilities as final products.

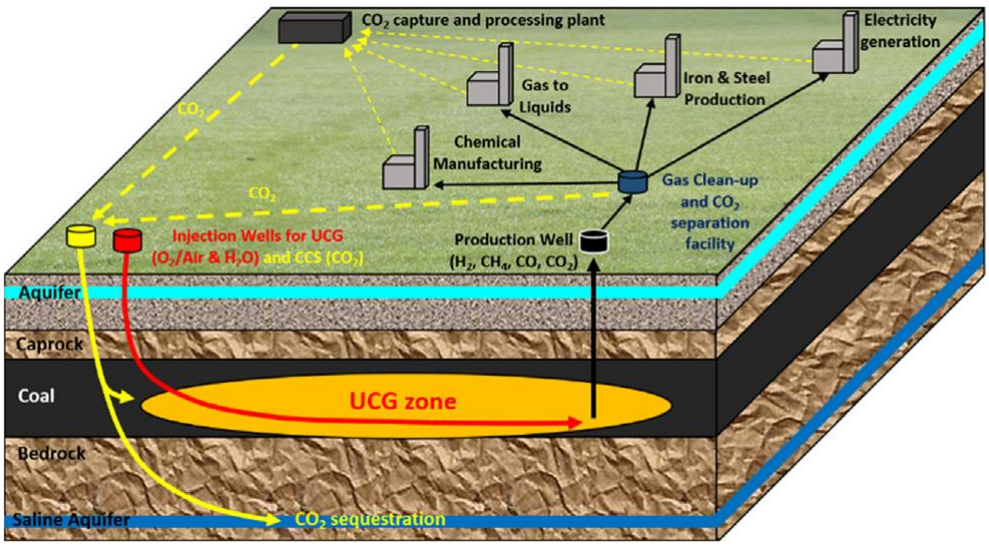

Figure 3. Underground coal gasification proces (Zagorščak et al. 2019)

The success of the UCG system depends on the permeability of the coal seam or the permeability of the channel formed within the seam to transmit gases to and from the combustion zone (Friedmann et al., 2009). Many researchers have focused on the effects of coal rank and chemical composition on the underground gasification process (Kapuska, & Stanczyk, 2015; Sadasivam et al., 2020). In addition, studies on operational parameters have made significant contributions to the literature (Zagorščak et al., 2020; Huang, et al., 2021; Feng et al., 2023). Su et al. (2023) investigated the effect of different oxygen flows on the cavity volume in the gasification zone. Ahmed et al. (2023) used the machine learning method in the multivariate modeling of UCG. Feng et al. (2022) used the analytical hierarchy process and ex-situ experiment methods to determine the order of importance of the criteria affecting the UCG process.

In the surface gasification method, coal must first be extracted from underground or open-surface coal mines. Afterward, the coal is subjected to preliminary processes such as sorting, washing, shredding, and drying. It is then transported to the gasification plant. This method also includes the transportation and storage costs of coal. Additionally, unlike the underground coal gasification method, a gasification plant is established in this gasification method. Thus, this method is more complicated, complex, and more costly than the underground gasification method.

The most important component in gasification plants is the gasifier. Gasifiers are divided into four groups according to various specifications: plasma, entrained bed, fixed bed, and fluidized bed gasifier (Midilli et al., 2021). For many years, many studies have been conducted on gasification processes using supercritical water (Tian et al., 2023; Mu, Liu, & Yan, 2023), plasma (Pan et al., 2022; Okati et al., 2023), entrained bed (Li et al. 2023), fixed bed (Chen, et al., 2021; Li, & Song, 2022), and fluidized bed (Ramakrishnan et al., 2023; Shao et al. 2023) gasifiers. These gasifiers have operating characteristics with different parameters. As in coal-burning systems, the size of the coals to be used, operating temperatures, and pressures are decisive. Apart from this, using air, pure oxygen, and steam is also effective.

Ramakrishnan et al. (2023), performed a CFD investigation of the coal gasification process in a fluidized bed gasifier. The stability of the reactor was verified through different design parameters. In order to obtain maximum syngas efficiency, the effect of oxygen/carbon ratio on coal gasification was investigated. One of the products of the coal gasification process is slag. Slag contains heavy metals. Storage of this product poses a risk of contamination of soil

and water resources and therefore a dangerous situation for human health may arise (Han, et al., 2018; Yu et al., 2021). For this reason, slag has become one of the important research areas in studies on gasification processes (Zhao et al., 2023; Wang, et al. 2023). Yan et al. (2023) presented a comprehensive review study on the sustainable use of coal gasification slag. Lv et al. (2023) conducted a review study on the use and enrichment of waste carbon as a result of the process. Some researchers have compared underground and surface coal gasification methods (Feng et al., 2021; Liu, & Liu, 2021; Liu, Guo, & Liu, 2022).

Developments on Increasing Efficiency in Thermal Power Plants

Developing countries such as Türkiye generally use their coal reserves in electrical energy production. Coal is burned in boilers of many different specifications in thermal power plants. Thermal power plants are generally complex facilities consisting of coal preparation, coal-burning electricity production, and other parts. These units are kept under constant surveillance, malfunctions are eliminated and efficiency-increasing measures are taken at points where efficiency decreases. In this context, the condition of boilers, which are coal-burning systems that are considered the heart of a thermal power plant, becomes important. Preventing a decrease in the efficiency of a combustion system or increasing the efficiency will make the business meet economic expectations. In addition, they must meet legal regulations in terms of carbon emission values to be released into the atmosphere from these facilities. Increasing efficiency will naturally reduce carbon emissions released into the atmosphere.

In a thermal power plant, processes are carried out before, during, and after burning coal to produce the desired type of energy by burning coal efficiently. Before coal is burned, it is subjected to several different processes such as sorting, washing, and drying. By performing the washing process, combustion efficiency and calorific value can be increased, while boiler ash load and ash content can be reduced. Additionally, the slag accumulation period in boilers is prolonged. In addition to affecting the calorific value, the moisture content of coal affects many parameters such as ash resistance in electrostatic filters, heat transfer in boilers, flame temperature, primary air temperature requirement, fuel burning rate, etc. Positive improvements can be achieved in these parameters with the drying process. With the drying process, the moisture content in the coal is also reduced.

Combustion systems that have completed their economic life are being replaced with combustion systems based on clean combustion technologies. In this way, both efficiency is increased and emissions released into the atmosphere are reduced. For this purpose, many studies have been conducted for many years (Leckner, & Gómez-Barea, 2021; Çam et al., 2023). In particular, many researchers have focused on combustion technologies such as, sub-critical (Zhu et al., 2015; Panday et al., 2021), supercritical (Deng et al., 2019; Zhou et al., 2021; Zhu et al., 2022;), ultra-supercritical (Hasti et al., 2015; Zhang et al., 2018; Esmaeili & Moradi, 2023), oxy-combustion (Szuhanszki et al., 2013; Li, Zeng, & Luo, 2020; Kim et al., 2021;), co-combustion (Vekemans, Laviolette, & Chaouki, 2016; Rahimipetroudi et al., 2021; Wei et al., 2023). Fluidized bed boilers, one of these technologies, allow the efficient burning of low calorific value fuels. For many researchers, this combustion technology has been a popular research topic. Hong et al. (2021), evaluated the performance of a CFB (Circulated Fluidized Bed Boiler) at low loads. In order to sustain these operations for long periods of time, a control strategy has been developed to keep the primary air volume under control. Ke et al. (2021) modeled the axial distribution of volatile species in coals in this type of boiler. In the last few years, infrastructures such as machine learning, artificial neural networks, etc. have been extensively used to increase the efficiency of boilers. Blackburn et al. (2022) used machine learning to increase the efficiency of a boiler. Combustion optimization in boilers is an important application to increase energy efficiency and achieve low emission values cheaply

(Jing et al., 2022). Xu et al. (2023) conducted an optimization study for an ultra-supercritical boiler to reduce emission values, increase boiler efficiency, and ensure safe operation limits.

In facilities with old combustion systems that have not completed their economic life, electrostatic filters are used to purify the flue gas, and desulfurization systems are used to purify it from sulfur emissions. There are many desulfurization processes such as hydro, oxidative, adsorptive, bio, extractive, and bio-adsorptive (Zaidi et al., 2023). In general, the desulfurization process cleans the flue gas from sulfur emissions as much as possible by washing it with various chemicals. Many studies have been conducted by researchers on the methods mentioned above (Jha, et al., 2023; Kompanijec, & Swierk, 2023; Lee, Yun, Min, Byun, & Yim, 2023).

Carbon Capture

Increasing the efficiency of combustion systems and eliminating the produced CO_2 with carbon capture technology are the two main strategies implemented to reduce CO_2 emissions released by coal-fired thermal power plants (Petrescu, & Cormos, 2017). In addition to thermal power plants, oil refineries, cement, ethylene oxide, iron and steel, ammonia production facilities and biogas conditioning facilities are other industrial sources that cause CO_2 formation (Markewitz et al., 2012).

Carbon capture technology or process can be simply expressed as capturing carbon dioxide emissions. Looking at the literature, this technology is referred to as carbon capture and storage. In addition, if these captured and stored emissions are also used, this can be expanded to carbon capture, use, and storage. The most important known carbon capture process occurs spontaneously in nature. Environmental factors such as trees, plants, forests, etc. are effective in this process. Apart from this method, carbon emissions are captured at the source as a result of a series of technical processes. Figure 4 shows the stages of carbon capture methods (Lau et al. 2021; Davoodi et al. 2023). Pre-combustion, oxyfuel combustion, and post-combustion methods are generally used in carbon capture, use, and storage (Osman et al., 2021; Krishnan et al., 2023). In a review study, Dziejarski et al. (2023) subjected these methods to a comprehensive technical evaluation and revealed their advantages and disadvantages.

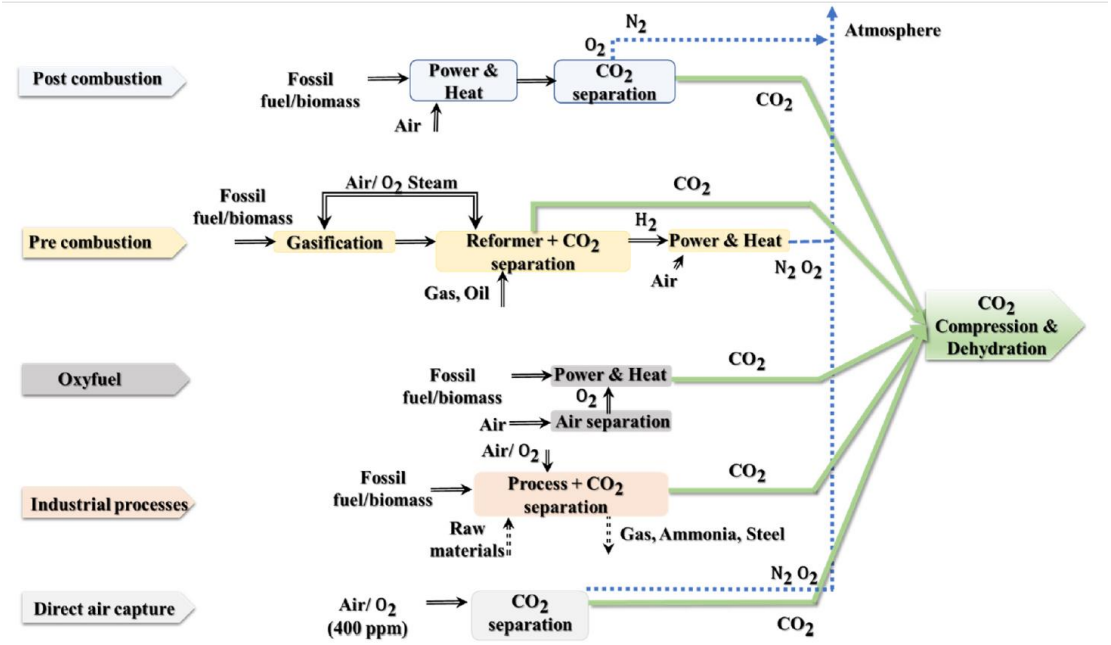

Figure 4. The stages of carbon capture methods (Lau et al. 2021; Davoodi et al. 2023)

In addition to capturing carbon emissions, it is also important how this captured material will be evaluated. Figure 5 provides a framework for carbon capture, transport, and storage processes. Once carbon is captured, it can be used in a process where it is needed. Carbon dioxide is used in carbonated beverages, dry ice manufacturing, agricultural activities, carbon-based material production, and many different applications. Apart from this, it can be stored for later use. Storage is generally done in oil and natural gas wells that have completed their economic and reserve life. Here, transporting the captured emissions becomes important. Because generally, the environments where carbon capture and storage are carried out may be in different locations. For this reason, captured emissions are transported by trucks, ships, and pipelines.

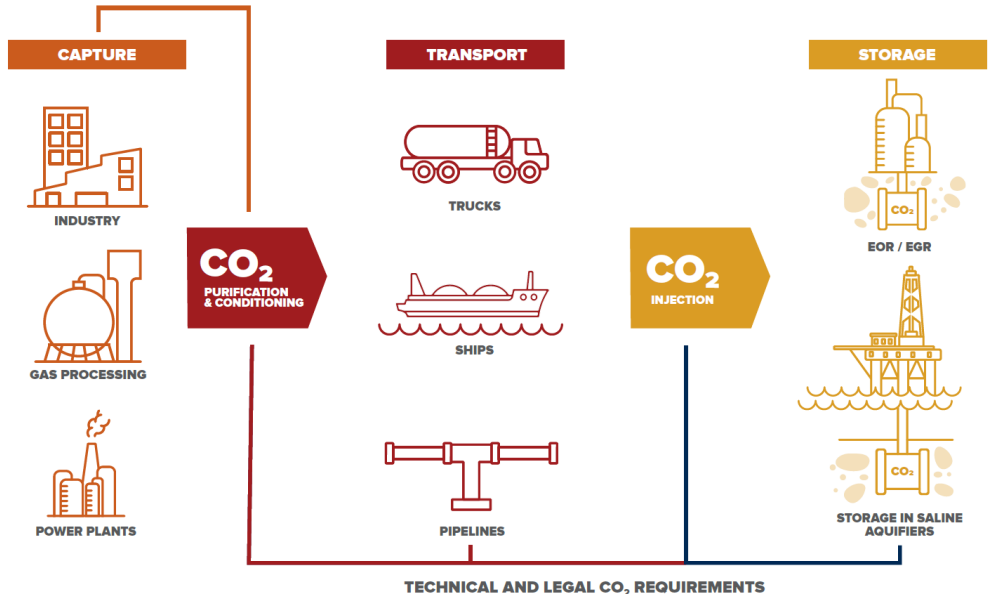

Figure 5. A framework for carbon capture, transport and storage processes (Kearns et al., 2021)

Actually, pre-combustion carbon capture uses a coal gasification process. In this carbon capture method, coal is first gasified under high pressure in the presence of oxygen or air. As a result of this process, hydrogen-rich gas containing carbon dioxide is obtained. Afterwards, carbon dioxide is separated from this gas. Carbon dioxide separation and compression processes require lower amounts of energy than other methods (Wang, & Song, 2020). This method also has lower costs than the other two methods (Portillo et al. 2019; Omodolor et al., 2020).

The Oxyfuel combustion method, it is aimed to have a high carbon dioxide concentration in the flue gas resulting from combustion. Unlike air used in traditional combustion processes, this innovative approach uses pure oxygen. As a result of the combustion reaction, carbon dioxide, and water vapor are formed in the flue gas. Water vapor is separated from carbon dioxide by condensing water vapor (Kok, & Vural, 2012). Carbon dioxide is then captured. Providing very high amounts of pure oxygen for this method increases costs (Anwar et al., 2018). Very high oxygen concentration causes changes in ash chemistry, corrosion, contamination, and possible leaks into the facility, resulting in high maintenance costs (Toftegaard).

Post combustion process is the process of absorbing carbon emissions in the flue gas at the end of combustion using chemical solvents or different methods and separating them from the flue gas. Post-combustion carbon capture methods are classified in Figure 6 (Osman et al.,

2020). These methods are divided into four: absorption, adsorption, membrane separation, and micro-algae. Absorption and adsorption methods are each divided into two: physical and chemical techniques. Amines, blends, and ionic liquids are used in the absorption method. Absorbent-based amines, amine-grafted, metal oxides, metal salts, and double salts are used in chemical adsorption. Carbonaceous materials, zeolites, and silica materials are used in physical adsorption. Techniques such as high temperature and perm selective polymers, liquid and gas contactors, and blend membrane materials are used in the membrane separation method. Finally, in the microalgae method, enzyme catalytic hydrolysis and carbon anhydrase techniques are used. Chao et al. (2021) presented a very comprehensive review of post-combustion carbon capture technology methods. In this method, low carbon dioxide concentration at ambient pressures causes high costs (Olajire, 2010; Elhenawy et al. 2020).

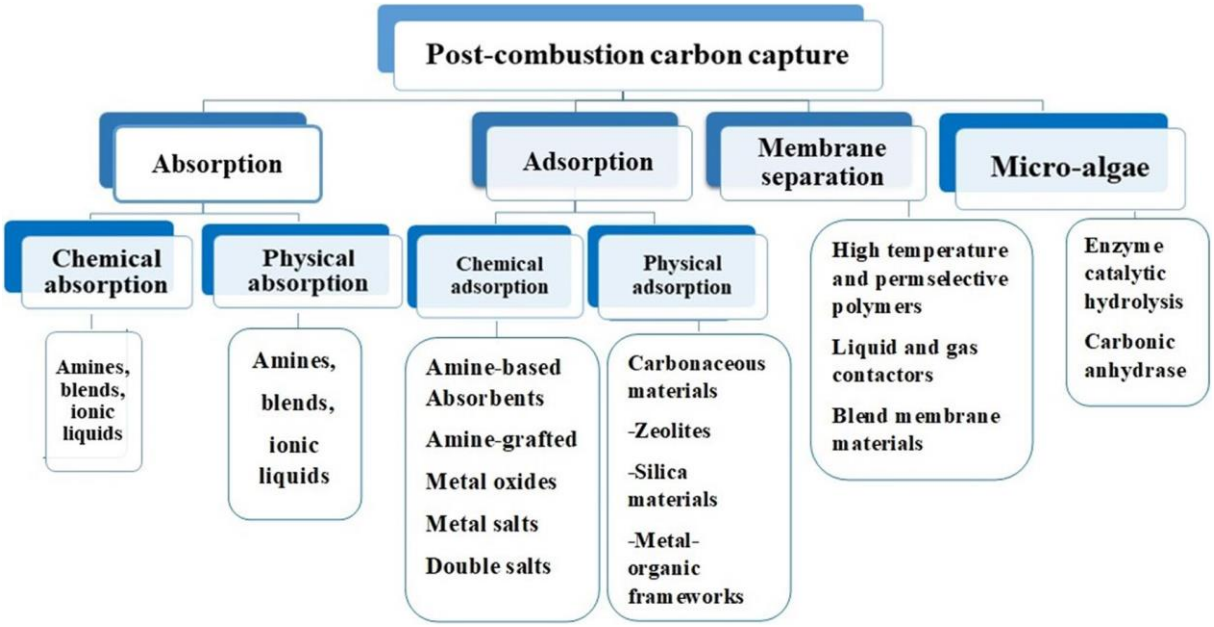

Figure 6. Post-combustion carbon capture methods (Osman et al., 2020)

Studies on carbon capture have been carried out for many years. Carbon capture processes first began to be used in the 1970s to inject carbon dioxide into oil wells to increase oil production. Nowadays, with the developing technology, many researchers have focused on this subject. (Okonkwo et al., 2023; Shen et al., 2023; Zhang et al., 2023;). Li et al. (2023) aimed to achieve high efficiency in a thermal power plant by combining a chemical recuperator, cascade coal gasification system, and carbon dioxide capture systems. Adhikari et al (2023) conducted a techno-economic analysis of the poly MEEP membrane they developed in the process of capturing carbon dioxide from low-concentration sources. Like many researchers, Olabi et al. (2023) and Xue et al. (2023) contributed to the literature on membrane carbon capture technologies. Ashraf ve Dua (2023), presented the modeling and optimization of the carbon capture process with a post-combustion method using machine learning. Al-Sakkari et al. (2023) used machine learning to select adsorbents with high capture properties for carbon capture methods. In recent years, many comprehensive studies have been conducted that contribute to the literature on the post-combustion method in carbon capture technology (Kev et al., 2023; Zhao et al., 2023; Weimann et al., 2023). Likewise, many studies have been conducted on pre-combustion (Theo et al., 2016; Zhou et al., 2021;Meng et al., 2023) and oxyfuel combustion (Bouillon, Hennes, & Mahieux, 2009; Roeder, Hasenbein, & Kather, 2013; Magli et al., 2022) carbon capture methods for many years.

Hydrogen, which is shown as an alternative fuel in line with the 2050 zero carbon target, can be produced using electricity obtained from renewable energy sources. However, it can be said that current electrolysis costs in such production are still very high. On the other hand, in the case of hydrogen production from fossil-based sources, the produced carbon dioxide must be captured, transported, and stored. The carbon capture process itself carries question marks. In particular, since it is an energy-intensive process, more energy will need to be produced to capture carbon in coal-consuming industrial establishments such as thermal power plants, cement factories, etc. More coal will need to be burned to meet this energy production.

Conclusions And Future Prospects

Although Turkey has very low amounts of oil and natural gas resources, it has around 21 billion tons of coal reserves. 1.5 billion tons of these are hard coal (bituminous coal). However, only 0.5 billion tons of this reserve is visible reserve. In addition, since Turkey's lignite reserves have low calorific value, they are mostly used for electricity generation in thermal power plants. The lignites have low calorific value and high ash and moisture content. This makes it difficult for existing conventional combustion technologies to meet environmental regulations. In addition, bringing existing reserves into the economy is important for the country's energy supply security. For this reason, these resources need to be made more usable with clean coal technologies.

It is thought that clean coal technologies have just emerged because coal is known by the public as an energy source that pollutes the environment. In contrast, coal gasification technologies date back a century and coal liquefaction technologies date back just as long. These technologies and the research on them were put in the background when oil and natural gas resources were cheap and easily accessible. However, it comes to the agenda again in times of abnormal increases in oil and natural gas prices. Over the last few decades, these technologies have become a popular research topic to reduce carbon emissions. However, with each passing day, these technologies are being implemented with industrial applications. However, it must be stated that the speed of implementation of these technologies is not at the desired level.

Intensive studies on carbon capture technologies are continuing. However, at this point, the installation amount of these technologies is not at the desired level. However, it is a matter of curiosity how much of the captured carbon dioxide will be utilized in another process and how much will be stored. Currently, the cost of carbon capture is high, while transportation and storage processes require separate effort, initial investment, and operating costs. What needs to be considered here is how much carbon is captured annually in the world, how much of it is consumed, and how much of it is stored. Discussions need to be made on whether this method is a sustainable process with the world's total carbon storage capacity.

References

Hampden-Thompson, G. & Galindo, C. (2017) School–family relationships, school satisfaction and the academic achievement of young people. *Educational Review, 69* (2), 248-265. Doi: 10.1080/00131911.2016.1207613

Adhikari, B., Orme, C.J., Stetson, C., & Klaehn, J.R. (2023). Techno-economic analysis of carbon dioxide capture from low concentration sources using membranes. *Chemical Engineering Journal*, 474, 145876. https://doi.org/10.1016/j.cej.2023.145876

Ahmed, A., Uppal, A.A., % Javed, S.B. (2023). Nonlinear-control-oriented modeling of the multi-variable underground coal gasification process for UCG project thar: a machine learning perspective. *Journal of Process Control*, 131, 103090. doi:10.1016/j.jprocont.2023.103090

Ali, A., & Zhao, C. (2020). Direct liquefaction techniques on lignite coal: a review. *Chinese Journal of Catalysis*, 41, 375-389. https://doi.org/10.1016/S1872-2067(19)63492-3

Al-Sakkari, E.G., Ragab, A., So, T.M.Y., Shokrollahi, M., Dagdougui, H., Navarri, P., Elkamel, A., & Amazouz, M. (2023). Machine learning-assisted selection of adsorption-based carbon dioxide capture materials. *Journal of Environmental Chemical Engineering*, 11, 110732. https://doi.org/10.1016/j.jece.2023.110732

Anwar, M.N., Fayyaz, A., Sohail, N.F., Khokhar, M.F., Baqar, M., Khan, W.D., Rasool, K., Rehan, M., & Nizami, A.S. (2018). CO_2 capture and storage: a way forward for sustainable environment. *Journal of Environmental Management,* 226, 131-144.

Ashraf, W.M., & Dua, V. (2023). Machine learning based modelling and optimization of post-combustion carbon capture process using MEA supporting carbon neutrality. *Digital Chemical Engineering*, 8, 100115. https://doi.org/10.1016/j.dche.2023.100115

Bai, Y., Feng, F., Tian, L., Xiong, Y., Yang, Y., Guo, Q., & Liu, Y. (2023). The impact of nitrogen-containing compounds on the S-vacancies over the iron-based catalysts for direct coal liquefaction during the pre-sulfurization process. *Fuel*, 337, 126880. doi:10.1016/j.fuel.2022.126880

BP (British Petroleum Company). (2021). Statistical Review of World Energy. https://www.bp.com/content/dam/bp/business-sites/en/global/corporate/pdfs/energy-economics/statistical-review/bp-stats-review-2021-coal.pdf

Bhutto, A.W., Bazmi, A.A., & Zahedi, G. (2013). Underground coal gasification: From fundamentals to applications. *Progress in Energy and Combustion Science*, 39(1), 189-214.

Blackburn, L.D., Tuttle, J.F., Andersson, K., Hedengren, J.D., Powell, & K.M. (2022). Dynamic machine learning-based optimization algorithm to improve boiler efficiency. *Journal of Process Control*, 120, 129-149. https://doi.org/10.1016/j.jprocont.2022.11.002

Bouillon, P.A., Hennes, S., & Mahieux, C. (2009). ECO_2: post-combustion or oxyfuel a comparison between coal power plants with integrated CO_2 capture. *Energy Procedia*, 1 (1), 4015-4022. https://doi.org/10.1016/j.egypro.2009.02.207

Breault, R.W., (2010). Gasification Processes Old and New: A Basic Review of the Major Technologies. *Energies*, 3(2), 216-240. https://doi.org/10.3390/en3020216

Chao, C., Deng, Y., Dewil, R., Baeyens, J., & Fan, X. (2021). Post-combustion carbon capture. *Renewable and Sustainable Energy Reviews*, 138, 110490. doi:10.1016/j.rser.2020.110490

Chen, C., Jia, P., Chen, Y., Tu, Z., Deng, B., Liu, H., & Huang, H. (2022). A multi-component surrogate mechanism of diesel from indirect coal liquefaction for diesel engine combustion and emission simulations. *Fuel*, 320, 123928. https://doi.org/10.1016/j.fuel.2022.123928

Chen, X., Wang, C., Jiang, L., Li, H., Wang, J., & He, X. (2021). Pilot-scale catalytic ozonation pretreatment for improving the biodegradability of fixed-bed coal gasification wastewater. *Process Safety and Environmental Protection*, 148, 13-19. https://doi.org/10.1016/j.psep.2020.09.056

Çam, M.M., Soyhan, H.S., Al Qubeissi, M., & Çelik, C. (2023). Designing a new bell-type primary air nozzle for large-scale circulating fluidized bed boilers. *Fuel*, 335, 127065. https://doi.org/10.1016/j.fuel.2022.127065

Deng, B., Zhang, M., Lyu, J., Li, S., & Yang, H. (2019). Safety analysis on the water wall in the 350 MW supercritical CFB boiler under sudden electricity failure. *Energy*, 189, 116364. https://doi.org/10.1016/j.energy.2019.116364

Davoodi, S., Al-Shargabi, M., Wood, D.A., Rukavishnikov, V.S., & Minaev, K.M. (2023). Review of technological progress in carbon dioxide capture, storage, and utilization. *Gas Science and Engineering*, 117, 205070. https://doi.org/10.1016/j.jgsce.2023.205070

Dziejarski, B., Krzyżyńska, R., & Andersson, K. (2023). Current status of carbon capture, utilization, and storage technologies in the global economy: A survey of technical assessment. *Fuel*, 342, 127776. https://doi.org/10.1016/j.fuel.2023.127776

Elhenawy, S.E.M., Khraisheh, M., AlMomani, F., & Walker, G. (2020). Metal-organic frameworks as a platform for CO2 capture and chemical processes: adsorption, membrane seperation, catalytic-conversion, and electrochemical reduction of CO2. *Catalysts*, 10 (11), 1293. https://doi.org/10.3390/catal10111293

Erik, N.Y. (2022). Kömür özellikleirnin temiz kömür teknolojilerine (gazlaştırma, sıvılaştırma, karbon elyaf ve kok üretimi) etkisi: derleme. *UMUFED International Journal of Western Black Sea Engineering and Science*, 4 (2), 22-56.

Esmaeili, M., & Moradi, H. (2023). Robust & nonlinear control of an ultra-supercritical coal fired once-through boiler-turbine unit in order to optimize the uncertain problem. *Energy*, 282, 128312. https://doi.org/10.1016/j.energy.2023.128312

Feng, L., Dong, M., Wang, B., & Qin, B. (2023). Gas production performance of underground coal gasification with continuously moving injection: effect of direction and speed. *Fuel*, 347, 128425. https://doi.org/10.1016/j.fuel.2023.128425

Feng, Y., Yang, B., Hou, Y., Duan, T-H., Yang, L., & Wang, Y. (2021). Comparative environmental benefits of power generation from underground and surface coal gasification with carbon capture and storage. *Journal of Cleaner Production*, 310, 127383. https://doi.org/10.1016/j.jclepro.2021.127383

Feng, L., Zhou, S., Xu, X., & Qin, B. (2022). Importance evaluation for influencing factors of underground coal gasification through ex-situ experiment and analytic hierarchy process. *Energy*, 261 (Part A), 125116. https://doi.org/10.1016/j.energy.2022.125116

Friedmann, S.J., Upadhye, R., & Kong F.M. (2009). Prospects for underground coal gasification in carbon-constrained world. *Energy Procedia*, 1 (1), 4551-4557.

Gao, D., Ye, C., Ren, X., & Zhang, Y. (2003). Life cycle analysis of direct and indirect coal liquefaction for vehicle power in China. *Fuel Processing Technology*, 169, 42-49. https://doi.org/10.1016/j.fuproc.2017.09.007

Gündüz, F., Olam, M., & Karaca, H. (2023). Direct liquefaction of low rank lignite with peach seed kernel and waste polpropylene for alternative fuel production. *Process Safety and Environmental Protection*, 170, 1208-1216. https://doi.org/10.1016/j.psep.2022.12.048

Han, F., Gao, Y., Huo, Q., Han, L., Wang, J., Bao, W., & Chang, L. (2018). Characteristics of vanadium-based coal gasification slag and the NH3-selective catalytic reductionof NO. *Catalysts*, 8 (8), 327. https://doi.org/10.3390/catal8080327

Hasti, S., Aroonwilas, A., & Veawab, A. (2013). Exergy analysis of ultra super-critical power plant. *Energy Procedia*, 37, 2544-2551. doi: 10.1016/j.egypro.2013.06.137

Hirano, K. (2000). Outline of NEDOL coal liquefaction process development (pilot plant program). *Fuel Processing Technology*, 62 (2-3), 109-118. https://doi.org/10.1016/S0378-3820(99)00121-6

Hong, F., Chen, J., Wang, R., Long, D., Yu, H., & Gao, M. (2021). Realization and performance evaluation for long-term low-load operation of a CFB boiler unit. *Energy*, 214, 118877. https://doi.org/10.1016/j.energy.2020.118877

Höök, M., & Aleklett, K. (2010). A review on coal-to-liquid fuels and its coal consumption. *International Journal of Energy Research*, 34, 848-864. DOI: 10.1002/er.1596

Huang, W-G., Wang, Z-T., Duan, T-H., & Xin, L. (2021). Effect of oxygen and steam on gasification and power generation in industrial tests of underground coal gasification. *Fuel*, 289, 119855. https://doi.org/10.1016/j.fuel.2020.119855

Jha, D., Maheshwari, P., Singh, Y., Haider, M.B., Kumar, R., & Balathanigaimani, M.S. (2023). A comparative review of extractive desulfurization using designer solvents: ionic liquids & deep eutectic solvents. *Journal of the Energy Institute*, 110, 101313. https://doi.org/10.1016/j.joei.2023.101313

Jin, E., Zhang, Y., He, L., Harris, H.G., Teng, B., & Fan, M. (2014). Indirect coal to liquid technologies. *Applied Catalysis A: General*, 476, 158-174. doi:10.1016/j.apcata.2014.02.035

Jing, R., Hua, W., Lin, J., Zhao, Y., Zhou, Y., & Wu, J. (2022). Cost-efficient decarbonization of local energy systems by whole-systems by whole-system based design optimization. *Applied Energy*, 326,119921. https://doi.org/10.1016/j.apenergy.2022.119921

IEA (Internatioal Energy Agency). (2023). Global coal demand set to remain at record levels in 2023. (in 09/10/2023 https://www.iea.org/news/global-coal-demand-set-to-remain-at-record-levels-in-2023)

Kapusta, K., & Stanczyk, K. (2015). Chemical and toxicological evaluaiton of underground coal gasification (UCG) effluents. The coal rank effect. *Ecotoxicology and Environmental Safety*, 112, 105-113. https://doi.org/10.1016/j.ecoenv.2014.10.038

Kasap, Y., Şensöğüt, C., & Ören, Ö. (2020). Efficiency change of coal used for energy production in Turkey. *Resources Policy*, 65, 101577. https://doi.org/10.1016/j.resourpol.2019.101577

Kearns, D., Liu, H., & Consoli, C. (2021). Technology readiness and costs of CCS. *Global CCS Institute*, 2021. https://www.globalccsinstitute.com/wp-content/uploads/2022/03/CCE-CCS-Technology-Readiness-and-Costs-22-1.pdf

Ke, X., Engblom, M., Zhang, M., Da Silva, P.S.P., Hupa, L., Lyu, J., Yang, H., 6 Wei, G. (2021). Modeling of the axial distributions of volatile species in a circulating fluidized bed boiler. *Chemical Engineering Science*, 233, 116436. https://doi.org/10.1016/j.ces.2021.116436

Kev, K., Modi, N., Milani, D., Luu, M.T., Nelson, S., Manaf, N.A., Wang, X., Negnevitsky, M., & Abbas, A. (2023). A comparative life cycle impact assessment for solar heat integration in post-combustion carbon capture. *Energy Conversion and Management*, 297, 117745. https://doi.org/10.1016/j.enconman.2023.117745

Kim, T., Park, S.D., Lee, U.D., Park, B.C., Park, K.I., & Hong, J. (2021). Thermodynamic analysis of the 2nd generation pressurized fluidized-bed combustion cycle utilizing an oxy-coal boiler and a gasifier. *Energy*, 236, 121471. https://doi.org/10.1016/j.energy.2021.121471

Kok, M.V., & Vural, A. (2012). The clean coal and carbon capture and storage technology of Turkey. *Energy Sources Part A Recovery Utilization and Environmental Effects*, 34, (5-8), 531-539.

Kompanijec, V., & Swierk, J.R. (2023). Evaluation of anodic materials in electrocatalytic oxidative desulfurization. *Cell Reports Physical Science*, 4 (6), 101425.

Kong, H., Kong, X., Wang, J., & Zhang, J. (2019). Thermodynamic analysis of a solar thermochemical cycle-based direct coal liquefaction system for oil production. *Energy*, 179, 1279-1287. https://doi.org/10.1016/j.energy.2019.05.019

Krishnan, A., Nighojkar, A., & Kandasubramanian, B. (2023). Emerging towards zero carbon footprint via carbon dioxide capturing and sequestration. *Carbon Capture Science & Technology*, 9, 100137. https://doi.org/10.1016/j.ccst.2023.100137

Lau, H.C., Ramakrishna, S., Zhang, K., & Radhamani, A.V. (2021). The role carbon capture and storage in the energy transition. *Energy Fuels*, 35, 9, 7364-7386. https://doi.org/10.1021/acs.energyfuels.1c00032

Leckner, B., Gómez-Barea, A. (2021). Change of existing circulating fluidized bed boilers to oxy-firing conditions for CO2 capture. *Applications in Energy and Combustion Science*, 8, 100042. https://doi.org/10.1016/j.jaecs.2021.100042

Lee, D., Yun, T.H., Min, J.G., Byun, Y., & Yim, C. (2023). Regeneration of sodium bicarbonate from industrial Na-based desulfurization waste using ammonium hydroxide. *Journal of Industrial and Engineering Chemistry*, 122, 500-510. doi:10.1016/j.jiec.2023.03.012

Liang, S., Hou, Y., Wu, W., Li, H., He, Z, & Ren, S. (2021). Residues characteristics and structural evolution of Naomaohu coal during a mild direct liquefaction process. *Fuel Process*. Technol., 215, 106753. https://doi.org/10.1016/j.fuproc.2021.106753

Li, J., Yang, J., & Liu, Z. (2008). Hydro-treatment of a direct coal liquefaction residue and its components. *Catalysis Today*, 130, 389-94. https://doi.org/10.1016/j.cattod.2007.10.069

Li, K, Ma, X., He, R., & Li, Z. (2019). Co-pyrolysis characteristics and interaction route between low-rank coals and Shenhua coal direct liquefaction residue. *Chinese Journal of Chemical Engineering*, 27 (11), 2815-2824. https://doi.org/10.1016/j.cjche.2019.03.032

Li, P., Zong, Z-M., Liu, F-J, Wang, Y-G., Wei, X-Y., Fan, X., Zhao, Y-P., & Zhao, W. (2015). Sequential extraction and characterization of liquefaction residue from Shenmu-Fugu subbituminous coal. *Fuel Process Technolgy*, 136, 1-7. doi:10.1016/j.fuproc.2014.04.013

Li, H., Liang, Y., Hou, Y., Wang, Y., Ren, S., & Wu, W. (2022). A study on the structure of Naomaohu coal and its suitability for direct coal liquefaction. *Fuel Process Technology*, 227, 107135. https://doi.org/10.1016/j.fuproc.2021.107135

Li, K., Zeng, Y., & Luo, J-L. (2020). Corrosion performance of candidate boiler tube alloys under advanced pressurized oxy-fuel combustion conditions. *Energy*, 215 (Part B), 119178. https://doi.org/10.1016/j.energy.2020.119178

Li, T., Choi, C., Fukomoto, K., Machida, H., & Norinaga, K. (2023). Polycyclic aromatic hydrocarbons (PAHs) and soot formations under different gasifying agents: detailed chemical kinetic analysis of a two-stage entrained flow coal gasifier. *Fuel*, 343, 127876. https://doi.org/10.1016/j.fuel.2023.127876

Li, Y.M., Khursid, A., & Khan, K. (2023). Optimization of coal-to-liquid processes; a way forward towards carbon neutrality, high economic returns and effective resource utilization. Evidences from China. *Fuel*, 2344, 128082. https://doi.org/10.1016/j.fuel.2023.128082

Li, W., & Song, Y. (2022). Artificial neural network model of catalytic coal gasificaiton in fixed bed. *Journal of the Energy Institute*, 105, 176-183. https://doi.org/10.1016/j.joei.2022.08.012

Lv, B., Deng, X., Jiao, F., Dong, B., Fang, C., & Xing, B. (2023). Enrichment and utilization of residual carbon from coal gasification slag: A review. *Process Safety and Environmental Protection*, 171, 859-873. https://doi.org/10.1016/j.psep.2023.01.079

Liu, H., Guo, W., & Liu, S. (2022). Comparative techno-economic performance analysis of underground coal gasification and surface coal gasification based coal-to-hydrogen process. *Energy*, 258, 125001. https://doi.org/10.1016/j.energy.2022.125001

Liu, H., & Liu, S. (2021). Life cycle energy consumption and GHG emissions of hydrogen production from underground coal gasification in comparison with surface coal gasification. *International Journal of Hydrogen Energy*, 46 (14), 9630-9643. doi:10.1016/j.ijhydene.2020.12.096

Magli, F., Spinelli, M., Fantini, M., Romano, M.C., & Gatti, M. (2022). Techno-economic optimization and off-design analysis of CO_2 purification units for cement plants with oxyfuel-based CO_2 capture. *International Journal of Greenhouse Gas Control*, 115, 103591. https://doi.org/10.1016/j.ijggc.2022.103591

Mandal, R., & Maity, T. (2023). Operational process parameters of underground coal gasification technique and its control. *Journal of Process Control*, 129, 103031.

Markewitz, P., Kuckshinrichs, W., Leitner, W., Linssen, J., Zapp, P., Bongartz, R., Schreiber, A., & Muller, T.E. (2012). Worldwide innovations in the development of carbon capture technologies and the utilization of CO_2. *Energy Environmental Science*, 5, (6), 7281–7305.

Meng, L., Kai, T., Nakao, S.I., & Yogo, K. (2023). Modeling of pre-combustion carbon capture with CO_2-selective polymer membranes. *International Journal of Greenhouse Gas Control*, 123, 103830. https://doi.org/10.1016/j.ijggc.2022.103830

MENR (Ministry of Energy and Natural Resources). (2022). 2021 2021 national energy balance table. (in 15/10/2023 https://enerji.gov.tr/eigm-raporlari)

MENR (Ministry of Energy and Natural Resources). (2023). Coal. (in 15/10/2023 https://enerji.gov.tr/bilgimerkezi-tabiikaynaklar-komur)

Midilli, A., Kucuk, H., Topal, M.E., Akbulut, U., & Dincer, I. (2021). A comprehensive review on hydrogen production from coal gasification: challenges and opportunities. *International Journal of Hydrogen Energy*, 46, 25385-25412. doi:10.1016/j.ijhydene.2021.05.088

Mishra, S., Panda, S., & Akcil, A. (2021). Indispensable role of coal as an energy source in Turkey with focus on biodesulphurization studies and advances. *Case Studies in Chemical and Environmental Engineering*, 4, 100139. https://doi.org/10.1016/j.cscee.2021.100139

Mochida, I., Okuma, O., & Yoon, S. (2014). Chemicals from direct coal liquefaction. *Chemical Reviews*, 114 (3), 1637-1672. https://doi.org/10.1021/cr4002885

Mu, R., Liu, M., & Yan, J. (2023). Advanced exergy analysis on supercritical water gasification of coal compared with conventioanl O_2-H_2O and chemical looping coal gasification. *Fuel Processing Technology*, 245, 107742. https://doi.org/10.1016/j.fuproc.2023.107742

MTA (Maden Tetkik ve Arama). (2023). Kömür Arama Araştırmaları. (in 09/10/2023 https://www.mta.gov.tr/v3.0/arastirmalar/komur-arama-arastirmalari)

Okati, A., Khani, M.R., Shokri, B., Monteiro, E., & Rouboa, A. (2023). Parametric studies over a plasma co-gasification process of biomass and coal through a restricted model in Aspen plus. *Fuel*, 331, (Part 2), 125952. https://doi.org/10.1016/j.fuel.2022.125952

Okonkwo, E.C., AlNouss, A., Shahbaz, M., & Al-Ansari, T. (2023). Developing integrated direct air capture and bioenergy with carbon capture and storage systems: progress towards 2℃ and 1.5℃ climate goals. *Energy Conversion and Management*, 296, 117687. https://doi.org/10.1016/j.enconman.2023.117687

Olabi, A.G., Alami, A.H., Ayoub, M., Aljaghoub, H., Alasad, S., Inayat, A., Abdelkareem, M.A., Chae, K-J., & Sayed, E.T. (2023). Membrane-based carbon capture: recent progress, challenges, and their role in achieving the sustainable development goals. *Chemosphere*, 320, 137996. https://doi.org/10.1016/j.chemosphere.2023.137996

Olajaire, A.A. (2010). CO2 capture and seperation technologies for end-of-pipe applications-a review. *Energy*, 35 (6), 2610-28. https://doi.org/10.1016/jenergy.2010.02.030

Omodolor, I.S., Otor, H.O., Andonegui, J.A., Allen, B.J., & Alba-Rubio, A.C. (2020). Dual-function materials for CO2 capture and conversion: a review. *Industrial & Engineering Chemistry Research*, 59 840), 17612-17631. https://doi.org/10.1021/acs.iecr.0c02218

Onazaki, M., Namiki, Y., Ishibashi, H., Kobayashi, M., Itoh, H., Hiraide, M., & Morooka, S. (2000). A process simulation of the NEDOL coal liquefaction process. *Fuel Processing Technology*, 64 (1-3), 253-269. https://doi.org/10.1016/S0378-3820(00)00069-2

Osman, A.I., Deka, T.J., Baruah, D.C., & Rooney, D.W. (2020) Critical challenges in biohydrogen production processes from the organic feedstocks. *Biomass Convers Biorefinery*. ISSN 2190-6823.

Osman, A.I., Hefny, M., Maksoud, M.I.A.A., Elgarahy, A.M., & Rooney, D.W. (2021). Recent advances in carbon capture storage and utilisation technologies: a review. *Environmental Chemistry Letters*, 19, 797-849. DOI: 10.1007/s10311-020-01133-3

Ozturk, M. (2014). Studies of gas content determination of the coal seams in Zonguldak, vol. 71. *TTK Health, Safety and Education Directorate*, Zonguldak (in Turkish).

Pan, P., Peng, W., Li, J., Chen, H., Xu, G., & Liu, T. (2022). Design and evaluation of a conceptual waste-to-energy approach integrating plasma waste gasificaition with coal-fired power generation. *Energy*, 238 (Part C), 121947. https://doi.org/10.1016/j.energy.2021.121947

Panday, R., Indrawan, N., Shadle, L.J., & Vesel, R.W. (2021). Leak detection in a subcritical boiler. *Applied Thermal Engineering*, 185, 116371. doi:10.1016/j.applthermaleng.2020.116371

Petrescu, L., & Cormos, C-C. (2017). Environmental assessment of IGCC power plants with pre-combustion CO2 capture by chemical & calcium looping methods. *Journal Cleaner Production*, 158, 233-244.

PetroTurk. (2023). EPİAŞ announced the installed power statistics for June 2023. (in 17/10/2023 https://www.petroturk.com/elektrik-haberleri/epias-2023-haziran-ayi-kurulu-guc-istatistiklerini-acikladi)

Portillo, E., Alonso-Farinas, B., Vega, F., Cano, M., & Navarrete, B. (2019). Alternatives for oxygen-selective membrane systems and their integration into the oxy-fuel combustion process: a review. *Separation and Purification Technology*, 229, 115708. https://doi.org/10.1016/j.seppur.2019.115708

Qin, Z., Shen, T., Pan, Y., Yang, H., Liu, Z., & Liu, Q. (2024). Condensation of residue during direct liquefaction of a high-vitrinite coal. *Fuel*, 357, 129721. doi:10.1016/j.fuel.2023.129721

Ra, H.W., Mun, T-Y., Hong, S.J., Chun, D.H., Lee, H.T., Yoon, S.M., Moon, J.H., Park, S.J., Lee, S.H., Yang, J.H., Kim, J.K., Jung, H., & Seo, M.W. (2021). Indirect coal liquefacion by integrated entrained flow gasification and Rectisol/Fischer-Tropsch processes for producing automobile diesel substitutes. *Energy*, 219,119597. doi:10.1016/j.energy.2020.119597

Rahimipetroudi, I., Rashid, K., Yang, J.B., & Dong, S.K. (2021). Development of environment-friendly dual fuel pulveried coal-natural gas combustion technology for the co-firing power plant boiler: experimental and numerical analysis. *Energy*, 228, 120550. doi:10.1016/j.energy.2021.120550

Ramakrishnan, P., Singh, J.K., Sahoo, A., & Mohapatra, S.S. (2023). CFD simulation for coal gasificaition in fluidized bed gasifier. *Energy*, 281, 128272. doi:10.1016/j.energy.2023.128272

Roeder, V., Hasenbein, C., & Kather, A. (2013). Evaluation and comparison of the part load behaviour of the CO_2 capture technologies oxyfuel and post-combustion. *Energy Procedia*, 37, 2420-2431. https://doi.org/10.1016/j.egypro.2013.06.123

Sadavisam, S., Zagorščak, R., Thomas, H.R., Kapusta, K., & Stanczyk, K. (2020). Experimental study of methane-oriented gasification of semi-anthracite and bituminous coals using oxygen and steam in the context of underground coal gasification (UCG): Effects of pressure, temperature, gasification reactant supply rates and coal rank. *Fuel*, 268, 117330. https://doi.org/10.1016/j.fuel.2020.117330

Shao, R., Zhu, J., Wei, X., Shao, Y., & Peng, M. (2023). Gasificaiton of a bituminous coal in 15 MWth KEDA@circulating fluidized-bed gasifier with high-temperature preheating. *Applied Thermal Engineering*, 230, (Part A), 120693. doi:10.1016/j.applthermaleng.2023.120693

Shen, K., Cheng, D., Reyes-Lopez, E., Jang, J., Sautet, P., & Morales-Guio, C.G. (2023). On the origin of carbon sources in the electrochemical upgrade of CO2 from carbon capture solutions. *Joul*e, 7 (6), 1260-1276. https://doi.org/10.1016/j.joule.2023.05.010

Shen, T., Liu, Q., & Liu, Z. (2023). Comparison of two stage and single-stage liquefaction schemes for their effect on conversion and liquid yield of two low rank coals. *Journal of Analytical and Applied Pyrolsis*, 172, 106018. https://doi.org/10.1016/j.jaap.2023.106018

Szuhanszki, J., Black, S., Pranzitelli, A., Ma, L., Stanger, P.J., Ingham, D.B., & Pourkashanian, M. (2013). Evaluation of the performance of a power plant boiler firing coal, biomass and a blend under oxy-fuel conditions as a CO2 capture technique. *Energy Procedia*, 37, 1413-1422. https://doi.org/10.1016/j.egypro.2013.06.017

Su, F-Q., He, X-L., Dai, M-J., Yang, J-N., Hamanaka, A., Yu, Y-H., Li, W., & Li, J-Y. (2023). Estimation of the cavity volume in the gasificaiton zone for underground coal

gasification under different oxygen flow conditions. *Energy*, 7, 129309. doi:10.1016/j.energy.2023.129309

Theo, W.L., Lim, J.S., Hashim, H., Mustaffa, A.A., & Ho, W.S. (2016). Review of pre-combustion capture and ionic liquid in carbon capture and storage. *Applied Energy*, 183, 1633-1663. https://doi.org/10.1016/j.apenergy.2016.09.103

Tian, Y., Feng, H., Zhang, Y., Li, Q., & Liu, D. (2023). New insight into allam cycle combined with coal gasification in supercritical water. *Energy Conversion and Management*, 292, 117432. https://doi.org/10.1016/j.enconman.2023.117432

TKİ (Türkiye Kömür İşletmeleri). (2023). Temiz Kömür Teknolojileri. (in 09/10/2023 https://www.tki.gov.tr/temiz-komur-teknolojileri)

TTK (Türkiye Taş Kömürü Kurumu). (2023). 2022 yılı taşkömürü sektör raporu. (in 09/10/2023 http://www.taskomuru.gov.tr/)

Vasireddy, S., Morreale, B., Cugini, A., Song, C., & Spivey, J.J. (2011). Clean liquid fuels from direct coal liquefaction: chemistry, catalysis, technological status and challenges. *Energy & Environmental Science*, 4 (2), 311-345. https://doi.org/10.1039/c0ee00097c

Vejahati, F., Xu, Z., & Gupa, R. (2010). Trace elements in coal: associations with coal and minerals and their behavior during coal utilization a review. *Fuel*, 89 (4), 904-911.

Vekemans, O., Laviolette, J-P., & Chaouki, J. (2016). Co-combustion of coal and waste in pulverized coal boiler. *Energy*, 94, 742-754. https://doi.org/10.1016/j.energy.2015.11.026

Wang, J., Xie, L., Peng, Y., Yin, T., Jiang, H., Wang, Z., Wang, Y., Zhou, Q., Xu, C., & Shi, Q. (2024). Molecular composition of direct coal liquefaction products obtanied from the Shenhua industrial plant. *Fuel*, 357, Part B, 129735. https://doi.org/10.1016/j.fuel.2023.129735

Wang, Y., Zhang, Z., Li, L., Guo, X., Wei, D., Kong, J., Du, H., Wang, H., Zhuang, Y., & Xing, P. (2023). A novel process to recycle coal gasification fine slag by preparing Si-Fe-Al-Ca alloy. *Journal of Environmental Management*, 337, 117681. doi:10.1016/j.jenvman.2023.117681

Wang, Z., Zhang, B., Gao, D. (2022). A novel knowledge graph development for industry design: a case study on indirect coal liquefaction process. *Computers in Industry*, 139, 103647.

Wang, X., & Song, C. (2020). Carbon capture from flue gas and the atmosphere: A perspective. *Front Energy Research*, 8, 560849. https://doi.org/10.3389/fenrg.2020.560849

Wei, D., An, D., Wang, T., Zhang, H., Guo, Y., & Sun, B. (2023). Influence of fuel distribution on co-combustion of sludge and coal in a 660 MW tangetially fired boiler. *Applied Thermal Engineering*, 227, 120344. https://doi.org/10.1016/j.applthermaleng.2023.120344

Weimann, L., Dubbink, G., Van Der Ham, L., & Gazzani, M. (2023). A thermodynamic-based mixed-integer linear model of post-combustion carbon capture for reliable use in energy system optimisation. *Applied Energy*, 336, 120738. doi:10.1016/j.apenergy.2023.120738

Willams, R.H., & Larson, E.D. (2003). A comparison of direct and indirect liquefaction technologies for amking fluid fuels from coal. *Energy for Sustainable Development*, 7 (49, 103-129. https://doi.org/10.1016/S0973-0826(08)60382-8

Xiu, F-R., Wang, J., Song, Z., Qi, Y., Bai, Q., Wang, S., Lei, X., Yang, R., & Gao, Z. (2023). Synergistic co-liquefaction of waste plastic express bags and low-rank coal based on supercritical water-ethanol system: Waste treatment and resource upgrading. *Journal of Cleaner Production*, 425, 138957. https://doi.org/10.1016/j.jclepro.2023.138957

Xu, Y. (2015). Development of indirect coal liquefaction: expanding product structure (in Chinese). *Large Scale Nitrogenous Fertilizer Ind.* 38 (3), 145-150.

Xu, J., Yang, Y., & Li, Y.W. (2015). Recent development in converting coal to clean fuels in China. *Fuel*, 152, 122-130. https://doi.org/10.1016/j.fuel.2014.11.059

Xu, Y.Y., Sun, Z-Q., Fan, X., Ma, F-Y., Kuznetsov, P.N., Chen, B., & Wang, J-F. (2021). Building methodology for evaluating the effects of direct coal liquefaction using coal structure-chemical index. *Fuel*, 305, 121568. https://doi.org/10.1016/j.fuel.2021.121568

Xu, W., Huang, Y., Song, S., Yue, J., Chen, B., Liu, Y., & Zou, Y. (2023). A new on-line combustion optimization approach for ultra-supercritical coal-fired boiler to improve boiler efficicency, reduce NOX emission and enhance operating safety. *Energy*, 282, 128748. https://doi.org/10.1016/j.energy.2023.128748

Xue, K., Zhan, G., Wu, X., Zhang, H., Chen, Z., Chen, H., & Li, J. (2023). Integration of membrane contactors and catalytic solvent regeneration for efficient carbon dioxide capture. *Journal of Membrane Science*, 684, 21870. https://doi.org/10.1016/j.memsci.2023.121870

Yan, S., Xuan, W., Cao, C., & Zhang, J. (2023). A review of sustainable utilization and prospect of coal gasification slag. *Environmental Research*, 238, Part 2, 117186.

Yuan, B., Ren, S., & Chen, X. (2015). The effects of urbanization, consumption ratio and consumption structure on residential indirect CO_2 emissions in china: a regional comparative analysis. *Applied Energy*, 140, 94-106. https://doi.org/10.1016/j.apenergy.2014.11.047

Yu, C., Cai, L., Jiang, G., Shao, J., Wei, W., Wang, R., Jin, Z., Jing, Y., & Wang, Q. (2021). Mineral carbonation of CO2 with utilization of coal gasification slags based on chemical looping, *Asia-Pacisific Journal of Chemical Engineering*, 16 (4), e2636. doi:10.1002/apj.2636

Zaidi, Z., Gupta, Y., Gayatri, S.L., & Singh, A. (2023). A comprehensive discussion on fuel combustion and desulfurization technologies. *Inorganic Chemistry Communications*, 154, 110964. https://doi.org/10.1016/j.inoche.2023.110964

Zagorščak, R., An, N., Palange, R., Green, M., Krishnan, M., & Thomas, H.R. (2019). Underground coal gasification-A numerical approach to study the formation of syngas and its reactive transport in the surrounding strata. *Fuel*, 253, 349-360. doi:10.1016/j.fuel.2019.04.164

Zagorščak, R., Sadasivam, A., Thomas, H.R., Stanczyk, K., & Kapusta, K. (2020). Experimental study of underground coal gasification (UCG) of a high-rank coal using atmospheric and high-pressure conditions in an ex-situ reactor. *Fuel*, 270, 117490. doi:10.1016/j.fuel.2020.117490

Zhang, F., Xue, Y., Li, D., Shen, J., Wu, X., Wu, Z., & He, T. (2018). Multiobjective operation of ultra-supercritical boiler-turbine unit. *IFAC PapersOnLine*, 51-28, 592-597. https://doi.org/10.1016/j.ifacol.2018.11.768

Zhang, K., Ding, L., Chai, M., Fu, Z., Chen, J., Hou, C., & Lv, H. (2023). Kinetic investigations of coal gasification for high-purity H_2 production with carbon capture and storage potential. *Journal of he Energy Institute*, 111, 101411. https://doi.org/10.1016/j.joei.2023.101411

Zhang, L., Wei, J., Bai, Y., Song, X., Wang, J., Su, W., Lv, P., Zhou, Y., Nai, G., & Yu, G. (2022). Correlation study between microstructure and fluidity of molten slag during co-gasification of coal and indirect coal liquefaction residue: molecular dynamics simulation. *Fuel*, 326, 125031. https://doi.org/10.1016/j.fuel.2022.125031

Zhao, F., Cui, C., Dong, S., Xu, X., & Liu, H. (2023). An overview on the corrosion mechanisms and inhibition techniques for amine-based post-combustion carbon capture process. *Seperation and Purification Technology*, 304, 122091. doi:10.1016/j.seppur.2022.12209

Zhao, J., Zhang, X., Sheng, J., Wang, Y., He, G., & Liu, Q. (2023). Utilization of coal gasificaiton fine ash for construction material: from physical and chemical properties to the hydration activity of thermally modified CGFA. *Journal of Environmental Chemical Engineering*, 11 (6), 111137. https://doi.org/10.1016/j.jece.2023.111137

Zhou, T., Shi, H., Ding, X., & Zhou, Y. (2021). Thermodynamic modeling and rational design of ionic liquids for pre-combustion carbon capture. *Chemical Engineering Science*, 229, 116076. https://doi.org/10.1016/j.ces.2020.116076

Zhou, X., Niu, T., Xin, Y., Li, Y., & Yang, D. (2021). Experimental and numerical investigation on heat transfer in the vertical upward flow water wall of a 660 MW ultra-spercritical CFB boiler. *Applied Thermal Engineering*, 188, 116664. doi:10.1016/j.applthermaleng.2021.116664

Zhu, X., Wang, W., & Xu, W. (2015). A study of the hydrodynamic characteristics of a vertical water wall in a 2953 t/h ultra-supercritical pressure boiler. *International Journal of Heat and Mass Transfer*, 86, 404-414. https://doi.org/10.1016/j.ijheatmasstransfer.2015.03.010

Zhu, M., Zhou, J., Chen, L., Su, S., Hu, S., Qing, H., Li, A., Wang, Y., Zhong, W., & Xiang, J. (2022). Economic analysis and cost modeling of supercritical CO2 coal-fired boiler based on global optimization. *Energy*, 239 (Part D), 122311. doi:10.1016/j.energy.2021.122311

A Review on 4th Generation Nuclear Reactor Technologies and Some Recent Developments

Murat MAKARACI[1]

Introduction:

According to data published by the United Nations, On 15 November 2022, the world's population surpassed 8 billion people (1), and in 2023 it was declared as 8,045,000,000 (2). According to World Bank data from 2014, the average energy consumption per capita in the world is calculated as 3,133 kWh/person/year (3). As of 2019, more than 10% of the total electricity produced in the world, which is 2,657 TWh, was provided through 442 nuclear power plants (NPPs) located in 30 countries. The production ranking of countries that produce nuclear electricity is given in Table 1. In the list, the United States, which meets 18% of its energy of 772 TWh from 93 nuclear power plants, is by far the leader, followed by China and France. It should be noted that France, Slovakia, and Ukraine are heavily dependent on nuclear energy, which is above 50% of its energy. Nuclear energy is also used in neighboring vicinity countries close to Türkiye, such as Armenia, Bulgaria, and Iran, as well as some countries such as Slovenia, Ukraine, and Pakistan to meet their energy needs.

Table 2 The world nuclear power generation data (4)

	NUCLEAR ELECTRICITY GENERATION		OPERABLE		UNDER CONSTRUCTION		PLANNED		PROPOSED		URANIUM REQUIRED
Country	2022		August 2023		August 2023		August 2023		August 2023		2023
	TWh		% e		No.		MWe net		No.		MWe gross
Argentina	7.5	5.4	3	1641	1	29	1	1150	2	1350	169
Armenia	2.6	31.0	1	416	0	0	0	0	1	1060	55
Bangladesh	0	0	0	0	2	2400	0	0	2	2400	371
Belarus	4.4	11.9	2	2220	0	0	0	0	2	2400	357
Belgium	41.7	46.4	5	3928	0	0	0	0	0	0	516
Brazil	13.7	2.5	2	1884	1	1405	0	0	4	4000	339
Bulgaria	15.8	32.6	2	2006	0	0	1	1000	3	3000	334
Canada	81.7	12.9	19	13,624	0	0	11	6100	0	0	1482
China	395.4	5.0	55	53,286	24	27,231	44	48,61	154	175,25	11,303
Czech Republic	29.3	36.7	6	4212	0	0	1	1200	3	3600	715
Egypt	0	0	0	0	3	3600	1	1200	0	0	0
Finland	24.2	35.0	5	4394	0	0	0	0	0	0	616
France	282.1	62.5	56	61,37	1	1650	0	0	6	9900	8783
Germany	31.9	5.8	0	0	0	0	0	0	0	0	0

[1] Asc.Prof.Dr. Department of Mechanical Engineering, Kocaeli University, Türkiye, 41001, E-mail: mmakaraci@kocaeli.edu.tr ORCID ID: 0000-0002-7952-1989

Hungary	15.0	47.0	4	1916	0	0	2	2400	0	0	320
India	42.0	3.1	22	6795	8	6700	12	8400	28	32	1408
Iran	6.0	1.7	1	915	1	1057	1	1057	5	2760	153
Japan	51.9	6.1	33	31,679	2	2756	1	1385	8	11,562	1785
Jordan	0	0	0	0	0	0	0	0	1	100	0
Kazakhstan	0	0	0	0	0	0	0	0	2	600	0
Korea RO (South)	167.5	30.4	25	24,489	3	4200	0	0	6	8400	4105
Lithuania	0	0	0	0	0	0	0	0	2	2700	0
Mexico	10.5	4.5	2	1552	0	0	0	0	3	3000	237
Netherlands	3.9	3.3	1	482	0	0	0	0	2	2000	69
Pakistan	22.2	16.2	6	3262	0	0	1	1170	0	0	558
Poland	0	0	0	0	0	0	0	0	6	6000	0
Romania	10.2	19.4	2	1300	0	0	2	1440	1	720	185
Russia	209.5	19.6	37	27,727	3	2810	25	23,525	21	20,1	6284
Saudi Arabia	0	0	0	0	0	0	0	0	2	2900	0
Slovakia	14.8	59.2	5	2308	1	471	0	0	1	1200	443
Slovenia	5.3	42.6	1	688	0	0	0	0	1	1000	127
South Africa	10.1	4.9	2	1854	0	0	0	0	8	9600	277
Spain	56.0	20.3	7	7123	0	0	0	0	0	0	1218
Sweden	50.0	29.4	6	6937	0	0	0	0	0	0	932
Switzerland	23.2	36.4	4	2973	0	0	0	0	0	0	412
Türkiye	0	0	0	0	4	4800	0	0	8	9600	441
Ukraine	58.7	-	15	13,107	2	1900	0	0	9	11,25	1567
UAE	19.3	6.8	3	4019	1	1400	0	0	0	0	853
United Kingdom	43.5	14.2	9	5883	2	3440	2	3340	10	17	908
USA	772.2	18.2	93	95,835	1	1250	3	2550	18	8000	18,045
Uzbekistan	0	0	0	0	0	0	2	2400	2	2400	0
WORLD	**2545**	**c 10.0**	**436**	**391,699**	**60**	**67,099**	**110**	**106,927**	**321**	**355,852**	**65,651**
	TWh	**% e**	**No.**	**MWe**	**No.**	**MWe**	**No**	**MWe**	**No.**	**MWe**	**tonnes U**
	NUCLEAR ELECTRICITY GENERATION		**OPERABLE**		**UNDER CONSTRUCTION**		**PLANNED**		**PROPOSED**		**URANIUM REQUIRED**

Reactor and electricity data are taken from International Atomic Energy Agency Power Reactor Information System (PRIS) (5) and World Nuclear Association estimates (6) (*The Nuclear Fuel Report*, published September 2023) for uranium requirements. Here, the equivalent Uranium conversion is given by 65,651 tU = 77,419 t U_3O_8. Nuclear power plants are classified as:

Operable = Connected to the grid.
Under Construction = First concrete for reactor poured.
Planned = Approvals, funding, or commitment in place, mostly expected to be in operation within the next 15 years.
Proposed = Specific program or site proposals; timing very uncertain.

As of today, 41 countries can be said under the nuclear power country club of which 9 of them have zero operating NPP but planned/in construction to build nuclear power plants. These countries are **Bangladesh, Egypt, Jordan, Kazakhstan, Lithuania, Poland, Saudi Arabia**, **Türkiye**, and **Uzbekistan**.

New plants coming online are largely balanced by old plants being retired. Over the past 20 years (2003-2022), 108 reactors were retired and 97 started operations. However, the reactor grid connected during this period was larger, on average, than that shut down, so capacity increased by about 10 GW. The Reference Scenario in the 2023 edition of *The Nuclear Fuel Report* (Table 2.5) has 66 reactors closing by 2040, and 308 new ones coming online (figures include 31 Japanese reactors online by 2040).

TWh = terawatt hour (billion-kilowatt hours); kWh = kilowatt hour; MWe = megawatt (electrical as distinct from thermal).

The nuclear share of electricity by country is given in Table 2 (7).

Table 3 Nuclear share of electricity by country (7)

Country	**NUCLEAR SHARE OF ELECTRICITY (%)**											**Nuclear electricity production (billion kWh)**	
	2012	2013	2014	2015	2016	2017	2018	2019	2020	2021	2022	2021	2022
Argentina	4.7	4.4	4.0	4.8	5.6	4.5	4.7	5.9	7.5	7.2	5.4	**10.2**	**7.5**
Armenia	26.6	29.2	30.7	34.5	31.4	32.5	25.6	27.8	34.5	25.3	31.0	**1.9**	**2.6**
Belarus	0.1	0.1	0.1	0.1	0.1	0.1	0.1	0.1	1.0	14.1	11.9	**5.4**	**4.4**
Belgium	51.0	52.1	47.5	37.5	51.7	49.9	39.0	47.6	39.1	50.8	46.4	**48.0**	**41.7**
Brazil	3.1	2.8	2.9	2.8	2.9	2.7	2.7	2.7	2.1	2.4	2.5	**13.9**	**13.7**
Bulgaria	31.6	30.7	31.8	31.3	35.0	34.3	34.7	37.5	40.8	34.6	32.6	**15.8**	**15.8**
Canada	15.3	16.0	16.8	16.6	15.6	14.6	14.9	14.9	14.6	14.3	12.9	**86.8**	**81.7**
China	2.0	2.1	2.4	3.0	3.6	3.9	4.2	4.9	4.9	5.0	5.0	**383.2**	**395.4**
Czech Rep	35.3	35.9	35.8	32.5	29.4	33.1	34.5	35.2	37.3	36.6	36.7	**29.0**	**29.3**
Finland	32.6	33.3	34.6	33.7	33.7	33.2	32.4	34.7	33.9	32.8	35.0	**22.6**	**24.2**
France	74.8	73.3	76.9	76.3	72.3	71.6	71.7	70.6	70.6	69.0	62.5	**363.4**	**282.1**
Germany	16.1	15.5	15.8	14.1	13.1	11.6	11.7	12.4	11.3	11.9	5.8	**65.4**	**31.9**
Hungary	45.9	50.7	53.6	52.7	51.3	50.0	50.6	49.2	48.0	46.8	47.0	**15.1**	**15.0**
India	3.6	3.5	3.5	3.5	3.4	3.2	3.1	3.2	3.3	3.2	3.1	**39.8**	**42.0**
Iran	0.6	1.5	1.5	1.3	2.1	2.1	2.1	1.8	1.7	1.0	1.7	**3.2**	**6.0**
Japan	2.1	1.7	0.1	0.5	2.2	3.6	6.2	7.5	5.1	7.2	6.1	**61.3**	**51.9**
Korea, S	30.4	27.6	30.4	31.7	30.3	27.1	23.7	26.2	29.6	28.0	30.4	**150.5**	**167.5**
Mexico	4.7	4.6	5.6	6.8	6.2	6.0	5.3	4.5	4.9	5.3	4.5	**11.6**	**10.5**
Netherlands	4.4	2.8	4.0	3.7	3.4	2.9	3.0	3.2	3.3	3.1	3.3	**3.6**	**3.9**

Pakistan	5.3	4.4	4.3	4.4	4.4	6.2	6.8	6.6	7.1	10.6	16.2	**15.8**	**22.2**
Romania	19.4	19.8	18.5	17.3	17.1	17.7	17.2	18.5	19.9	18.5	19.4	**10.4**	**10.2**
Russia	17.8	17.5	18.6	18.6	17.1	17.8	17.9	19.7	20.6	20.0	19.6	**208.4**	**209.5**
Slovakia	53.8	51.7	56.8	55.9	54.1	54.0	55.0	53.9	53.1	52.3	59.2	**14.6**	**14.8**
Slovenia	36.0	33.6	37.2	38.0	35.2	39.1	35.9	37.0	37.8	36.9	42.6	**5.4**	**5.3**
South Africa	5.1	5.7	6.2	4.7	6.6	6.7	4.7	6.7	5.9	6.0	4.9	**12.2**	**10.1**
Spain	20.5	19.7	20.4	20.3	21.4	21.2	20.4	21.4	22.2	20.8	20.3	**54.2**	**56.0**
Sweden	38.1	42.7	41.5	34.3	40.0	39.6	40.3	34.0	29.8	30.8	29.4	**51.4**	**50.0**
Switzerland	35.9	36.4	37.9	33.5	34.4	33.4	37.7	23.9	32.9	28.8	36.4	**18.6**	**23.2**
- Taiwan	18.4	19.1	18.9	16.3	13.7	9.2	11.4	13.4	12.7	10.8	9.1	**26.8**	**22.9**
United Arab Emirates	0.1	0.1	0.1	0.1	0.1	0.1	0.1	0.1	1.1	7.0	6.8	**10.1**	**19.3**
UK	18.1	18.3	17.2	18.9	21.2	19.3	17.7	15.6	14.5	14.8	14.2	**41.8**	**43.5**
Ukraine	46.2	43.6	49.4	56.5	52.3	55.0	53.0	53.9	51.2	55.0	-	**81.1**	-
USA	19.0	19.4	19.5	19.5	19.7	20.0	19.3	19.7	19.7	19.6	18.2	**771.6**	**772.2**
TOTAL												**2653**	**2545**

The heat value of a fuel is the amount of heat released during its combustion. Also referred to as energy or calorific value, heat value is a measure of a fuel's energy density, and is expressed in energy (joules) per specified amount (*e.g.* kilograms). A typical heat value table of fuels is given in Table 3 (8). Uranium figures are based on 45,000 MWd/t burn-up of 3.5% enriched U in LWR. 1 MJ = 10^6 Joule, GJ = 10^9 J and MJ to kWh @ 33% efficiency: x 0.0926. One tonne of oil equivalent (toe) is equal to 41.868 GJ.

Natural uranium, in LWR (normal reactor), has 500 GJ which is superior to natural gas, coal, and petroleum in the order of 10,000 (ten thousand fold) per the same amount of mass (of a kilogram). Thus, uranium-fueled power generation is not only a green energy classification but also significantly efficient.

Table 4 Heat Values of Various Fuels (8)

FUEL	HEAT VALUE (MJ/kg)
Hydrogen (H_2)	120-142
Methane (CH_4)	50-55
Methanol (CH_3OH)	22.7
Dimethyl ether - DME (CH_3OCH_3)	29
Petrol/gasoline	44-46
Diesel fuel	42-46
Crude oil	42-47
Liquefied petroleum gas (LPG)	46-51
Natural gas	42-55
Hard black coal (IEA definition)	>23.9
Hard black coal (Australia & Canada)	c. 25

Sub-bituminous coal (IEA definition)	17.4-23.9
Sub-bituminous coal (Australia & Canada)	c. 18
Lignite/brown coal (IEA definition)	<17.4
Lignite/brown coal (Australia, electricity)	c. 10
Firewood (dry)	16
Natural uranium, in LWR (normal reactor)	500
Natural uranium, in LWR with U & Pu, recycle	6,50E+05
Natural uranium, in FNR	2,80E+07
Uranium enriched to 3.5%, in LWR	3,90E+06

Global electricity consumption is declared to be on the rise trend (9). In 2021, net electricity consumption worldwide amounted to over 25,300 terawatt-hours, an increase of more than 30 percent in comparison to a decade earlier. When compared to 1980, global electricity consumption more than tripled. On the generation side, the world is still strongly dependent on fossil fuels. Despite the world's renewable energy capacity quintupling in the last decade, coal and gas combined still accounted for almost 60 percent of global electricity generation in 2022. For example, In Türkiye, it was published as 3,821 kWh/person/year for the year 2022 while it is 28,095 for Norway, 12,072 for the USA, 7,799 for Japan, 7,704 for Russia, 4i813 for the UK, 1,297 for India, and just 147 for Nigeria (9).

When countries that have produced electricity from nuclear power have been listed in the order for 2022, the USA tops the list with 772.2 TWh and Armenia finishes at the last by only 2.6 TWh. When nuclear share within the energy pool is taken into account, France leads the world by 62.5 % and Iran takes place at the very end by 1.7 %. The ranking of nuclear energy production of countries and their national share is presented in Table 4 where colored cells indicate maximum and minimum values.

Table 5 Ranking of nuclear energy production of countries and their national share.

COUNTRY	ELECTRICITY PRODUCTION FROM NUCLEAR ENERGY (2022)	
	Nuclear Electricity Production TWh	Nuclear share of electricity (%)
USA	772.2	18.2
China	395.4	5.0
France	282.1	62.5
Russia	209.5	19.6
South Korea	167.5	30.4
Canada	81.7	12.9
Ukraine (2021)	81.1	55.0
Spain	56.0	20.3
Japan	51.9	6.1
Sweden	50.0	29.4
United Kingdom	43.5	14.2
India	42.0	3.1
Belgium	41.7	46.4

Germany	31.9	5.8
Czech Rep	28,6	35,2
Finland	24.2	35.0
Switzerland	23.2	36.4
Pakistan	22.2	16.2
UnitedArabEmirates	19.3	6.8
Bulgaria	15.8	32.6
Hungary	15.0	47.0
Slovakia	14.8	59.2
Brazil	13.7	2.5
Mexico	10.5	4,5
Romania	10.2	19.4
South Africa	10.1	4.9
Argentina	7.5	5.4
Iran	6.0	1.7
Slovenia	5.3	42.6
Netherlands	3.9	3.3
Armenia	2.6	31.0
WORLD TOTAL	**2545 TWh**	**10.0 (% e)** (Estimated)

Based on the current data as of 2022, 60 nuclear power plants are under construction, 110 are planned, and 321 are in the proposal stage, including Türkiye. It is understood that the use of nuclear energy will continue to increase globally, and 16 countries are going to expand nuclear energy in their energy portfolios.

Table 5 provides the ranking of various countries in terms of the share of nuclear energy in the total energy produced. According to this table, all of the top 13 countries that generate more than one-third to over half of their energy from nuclear power are European countries (shown in orange color). Countries whose share is above the world average of 10 % are marked in gray color, including countries such as the USA, United Kingdom, Canada, Russia, Spain, Pakistan, and Romania. BRICS countries all have a share of 5-2.5 % which is half of the world average, except Russia which has a 19% share of nuclear energy concerning its total production.

Table 6 Ranking of countries by nuclear share of their national electricity production

COUNTRY	ELECTRICITY PRODUCTION FROM NUCLEAR ENERGY (2022)	
	Nuclear share of electricity (%)	Nuclear Electricity Production TWh
France	62.5	282.1
Slovakia	59.2	14.8
Ukraine (2021)	55.0	81.1
Hungary	47.0	15.0
Belgium	46.4	41.7
Slovenia	42.6	5.3
Switzerland	36.4	23.2
Czech Rep	35,2	28,6
Finland	35.0	24.2
Bulgaria	32.6	15.8
Armenia	31.0	2.6
South Korea	30.4	167.5
Sweden	29.4	50.0
Spain	20.3	56.0
Russia	19.6	209.5
Romania	19.4	10.2
USA	18.2	772.2
Pakistan	16.2	22.2
United Kingdom	14.2	43.5
Canada	12.9	81.7
United Arab Emirates	6.8	19.3
Japan	6.1	51.9
Germany	5.8	31.9
Argentina	5.4	7.5
China	5.0	395.4
South Africa	4.9	10.1
Mexico	4,5	10.5
Netherlands	3.3	3.9
India	3.1	42.0
Brazil	2.5	13.7
Iran	1.7	6.0
WORLD TOTAL	**10.0 (% e)** (Estimated)	**2545 TWh**

When Group20 countries are put into their nuclear capacity analysis, the picture parallels their economies. The G20 is composed of most of the world's largest economies' finance ministries, including both industrialized and developing countries; it accounts for around 80% of gross world product (GWP), 75% of international trade, two-thirds of the global population,[and 60% of the world's land area (10).

As of 2020 values, looking at the annual per capita distribution of energy produced using nuclear technology in the 30 countries that make up 60% of the world's population, Sweden stands at the forefront with 6,376 kWh per person per year. The top 5 countries in this distribution are predominantly from Northern European nations. The average for these countries with nuclear technology is found to be 568 kWh per person per year. If the current nuclear energy were to be shared among the entire world population, it would result in an average of 341 kWh per person per year.

Taking into account the average annual energy consumption per person worldwide across all energy sources, which is 3,133 kWh, and in Türkiye, which is 3,821 kWh, it becomes evident that transitioning to nuclear energy could make a significant contribution to addressing energy-related challenges.

4 th GENERATION NUCLEAR REACTOR DEVELOPMENT EFFORTS

Since the 1950s, nuclear technology has become a part of the energy portfolio, and first, second, and third-generation nuclear power plants have continued to develop over time with advancements in materials and computational technologies. Efforts to develop fourth-generation nuclear reactors began as an international task force in 2001 under the Generation IV International Forum (GIF), consisting of 9 countries (Argentina, Brazil, Canada, France, Japan, South Korea, South Africa, the United Kingdom, and the United States). In subsequent years, Australia, China, Switzerland, Russia, and Euratom (the European Atomic Energy Community) also joined this initiative. GIF leads international collaborative efforts to develop new-generation nuclear energy systems that could help meet the world's future energy needs. Fourth-generation designs are expected to use fuel more efficiently, reduce waste production, be economically competitive, and meet stringent safety standards while preventing the proliferation of nuclear weapons (11).

Over 100 GIF experts have identified six fourth-generation nuclear reactor technologies from among 130 candidate technologies for joint research and development, with plans to deploy them between 2020 and 2030. Four of these are fast neutron reactors, all designed to operate at higher temperatures than today's reactors, with four of them particularly chosen for hydrogen production. All six systems represent advancements in sustainability, economics, safety, reliability, and non-proliferation of nuclear weapons. Europe is advancing with designs for three fast reactors. This article will examine the six fourth-generation reactor designs identified by GIF. The following sections are mainly referred to GIF by Reference 11.

Generation IV designs, driven by international collaborations, aim to respond to the energy needs of the future with efficient fuel utilization, reduced waste production, economic competitiveness, and strict safety and security standards. The six different R&D designs selected for this purpose are as follows:

1. Gas-Cooled Fast Reactor (GFR)
2. Lead-Cooled Fast Reactor (LFR)
3. Molten Salt Reactor (MSR)
4. Super-Critical Water-Cooled Reactor (SCWR)
5. Sodium-Cooled Fast Reactor (SFR)
6. Very High-Temperature Reactor (VHTR)

Over the next decade, plans for licensing and commissioning these reactors are visible primarily in China, Russia, and France, as well as in official institutions and commercial companies located in the United States, Canada, and the United Kingdom.

I. Gas-Cooled Fast Reactor (GFR) (11)

The GFR system is a closed fuel cycle, high-temperature helium-cooled, fast-spectrum reactor. It combines the advantages of fast-spectrum systems (such as multiple reprocessing and the transmutation of long-lived actinides for the long-term sustainability of uranium resources and waste reduction) with high-temperature systems (high thermal cycle efficiency and industrial applications, e.g., heat production for hydrogen generation).

GFR employs the same fuel recycling processes as SFR and the same reactor technology as VHTR. Therefore, the development approach is based on technologies developed for VHTR as much as possible, including structures, materials, components, and power conversion systems. However, GFR requires specific R&D beyond the existing and anticipated work on the VHTR system, particularly in terms of basic design and safety approach.

The reference design for GFR is based on a 2400 MWth reactor core contained within a pressure vessel made of steel. The core consists of a group of hexagonal fuel elements, each containing mixed carbide fuel pins coated with ceramic, enclosed in ceramic-coated hexagonal tubes. Currently, the preferred material for the pin cladding and hexagonal tubes is silicon carbide fiber-reinforced silicon carbide.

In Figure 1, the reactor core is shown within a fabricated steel pressure vessel surrounded by primary heat exchangers and decay heat removal loops. The entire primary circuit is enclosed within a secondary pressure boundary with a protective enclosure.

The coolant used is helium, and the core outlet temperature will be approximately 850°C. A heat exchanger transfers heat to a secondary gas cycle containing a helium-nitrogen mixture, which drives a closed-cycle gas turbine. The waste heat from the gas turbine exhaust is then used to elevate steam in a steam generator for driving a steam turbine. This kind of combined cycle is a common practice in natural gas-fired power plants, so in the case of GFR, it represents the use of established technology with the only difference being the use of a closed-cycle gas turbine (Figure 2).

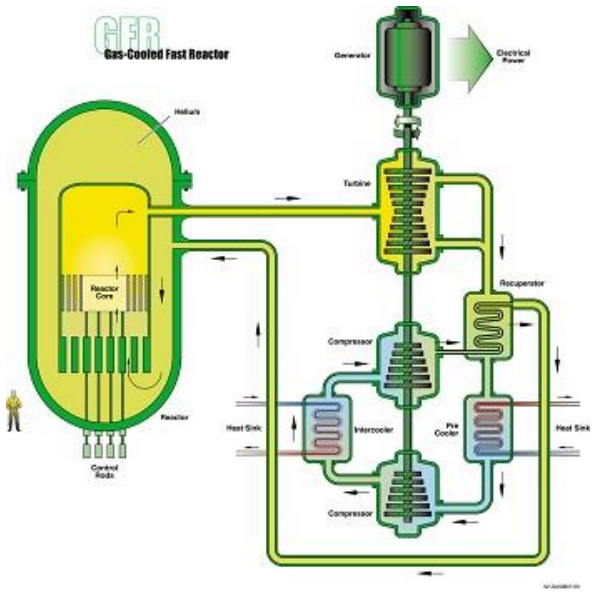

Figure 8 Gas-cooled fast reactor FR system representation (11)

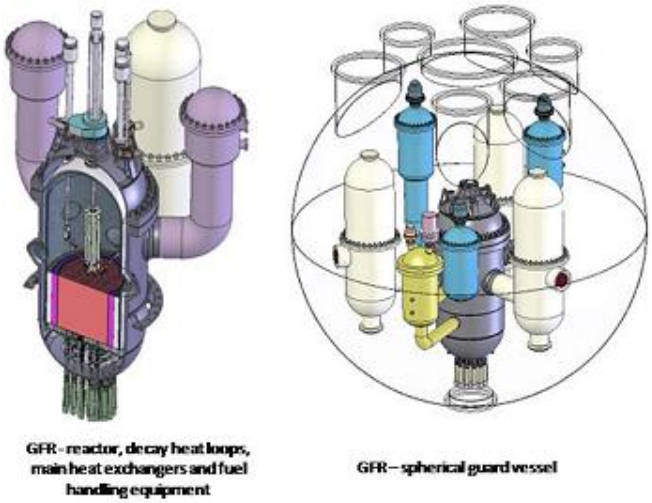

Figure 9 GFR reactor and guard vessel (11)

II. Lead-Cooled Fast Reactor (LFR) (11)

Lead-cooled fast reactors (LFRs) have characteristics that include a fast neutron spectrum, high-temperature operation, and cooling with either molten lead or lead-bismuth eutectic (LBE). Both of these coolants support low-pressure operation, have excellent thermodynamic properties, and are relatively inert when in contact with air or water. LFRs are versatile and can have multiple applications, including electricity generation, hydrogen production, and process heat generation.

The system concepts represented in the System Research Plan (SRP) of the Generation IV International Forum (GIF) are based on various LFR designs. These designs draw from the European Lead-cooled Fast Reactor (ELFR) lead-cooled system, Russia's BREST-OD-300, and the SSTAR system concept designed in the United States (Figure 3). Several additional LFR concepts are also in various stages of development in different countries, including China, Russia, the United States, Sweden, South Korea, and Japan.

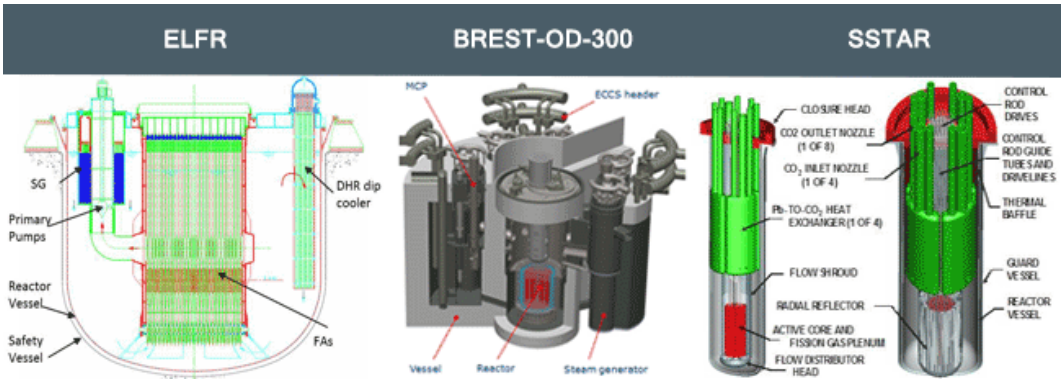

Figure 3 Various LFR tasarımları: ELFR (left-European), BREST (mid-Russia), SSTAR (right-USA) (11)

LFR is known for its excellent material management capabilities because it operates in a fast neutron spectrum and uses a closed fuel cycle for efficient conversion of uranium (Figure 4). It can also be used as a burner to consume actinides from used Light Water Reactor (LWR) fuel and as a burner/breeder in a thorium matrix. One significant feature of LFR is its enhanced safety due to the use of molten lead as a relatively inert and low-pressure coolant. Lead is abundant from a sustainability perspective, even with the deployment of numerous reactors.

Furthermore, fuel sustainability in LFR is significantly improved, mainly through the conversion capabilities of the LFR fuel cycle.

LFR concepts offer significant potential in terms of safety, design simplification, proliferation resistance, and ultimately, economic performance. They contain a liquid coolant with a high margin of boiling, and they interact favorably with air or water. However, there is a need for further development in fuel, material performance, and corrosion control areas. Progress is expected in the next 5 years in materials, system design, and operating parameters. Important testing and demonstration activities are ongoing and planned within this timeframe.

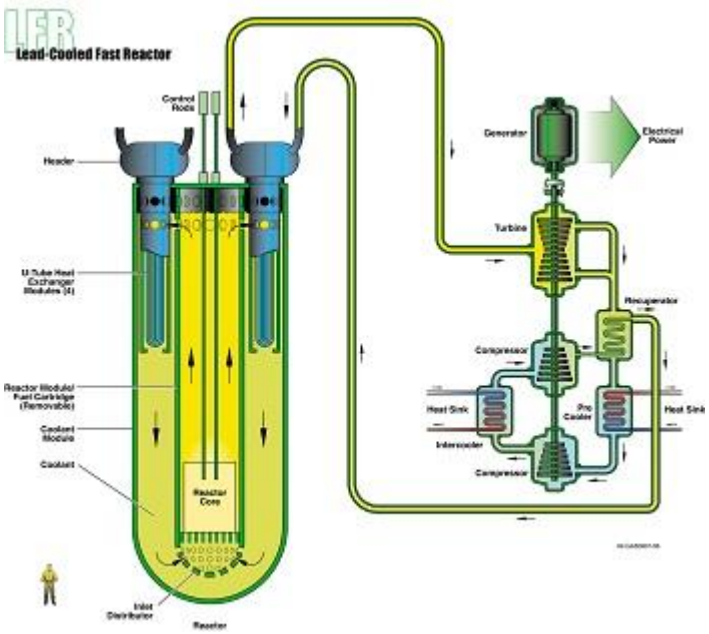

Figure 4 Lead cooled fast reactor LFR cycle (11)

III. Molten Salt Reactor (MSR) (11)

Molten Salt Reactor (MSR) technology was partially developed in the 1950s and 1960s in the United States, including two demonstration reactors at Oak Ridge National Laboratory, which successfully generated power. The demonstration MSRs were thermal-neutron-spectrum graphite-moderated concepts. Research and development have been focused on fast-spectrum MSR concepts (MSFR) since 2005, which combine the generic attributes of fast neutron reactors (enhanced resource utilization, waste minimization) with liquid fuel and molten salt fluorides as a coolant. Several countries, including France (CNRS) and the Netherlands (TU Delft), have led European Union projects (SAMOFAR and SAMOSAFER) in FP6 and Horizon2020. China, Russia, and the United States are also working on their independent designs.

In contrast to many other molten salt reactors previously examined, the MSFR does not contain any solid moderator (usually graphite) in the core. This design choice is motivated by examining parameters such as feedback coefficients, breeding ratio, graphite lifetime, and initial loading of 233U. The MSFR exhibits large negative temperature and void reactivity coefficients, a unique safety feature not found in solid-fueled fast reactors (Figure 5).

Compared to solid fuel reactors, MSFR systems have lower fissile loadings, limitations on radiation damage in available fuel burnup, no need for producing and processing solid fuel, and a homogeneous isotopic fuel composition within the reactor. These and other features

potentially provide unique capabilities for actinide burning and extending fuel resources for MSFRs.

In Russia, MSR developments related to the Molten Salt Actinide Recycler and Transmuter (MOSART) aim to efficiently use transuranic (TRU) waste from used UOX and MOX light water reactor (LWR) fuels as fuel without the support of uranium and thorium. Research is also ongoing on other advanced reactor concepts using liquid salt technology as a primary coolant for encapsulated particle fuels, similar to Fluoride Salt-Cooled High-Temperature Reactors (FHRs) and high-temperature gas-cooled reactors.

More broadly, there has been significant interest in using liquid salts as coolants for both nuclear and non-nuclear applications. These salts can facilitate heat transfer for various applications, including nuclear hydrogen production concepts, concentrated solar power generation, petroleum refineries, and oil shale processing facilities.

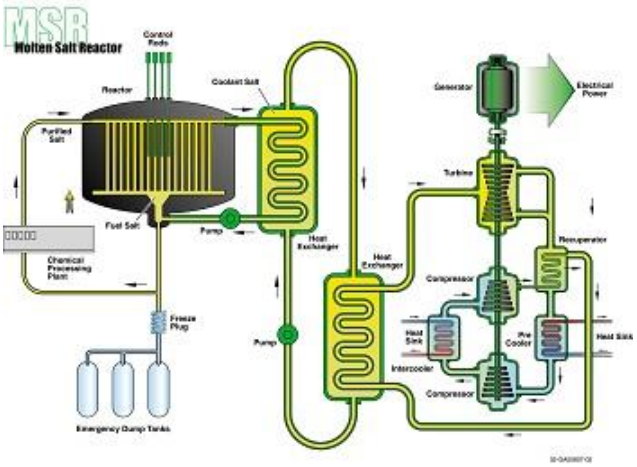

Figure 5 Molten salt reactor (MSR) cycle (11)

TURKISH EFFORTS:

Türkiye's choice of 4th Generation Nuclear Technology and the Status of GIF: As part of the Science and Technology High Council's decision at its 29th Meeting in 2016, efforts have been initiated to introduce nuclear technology into Türkiye's technological infrastructure, focusing on research and development activities aimed at gaining competence in nuclear energy and fuel cycle technologies. With the motivation to be involved in the development of an advanced generation reactor technology that is in line with global nuclear technology research, work has begun on establishing a prototype Molten Salt Reactor (MSR), acquiring its technology, developing special alloy materials for use in the reactor, and obtaining fuel technology. In this context, a "**Molten Salt Reactor Technology Determination Workshop**" was held on December 3-4, 2017, at TÜBİTAK Marmara Research Center, to select the prototype based on parameters such as the type of MSR, the type of salt and fuel, prototype power, and the application areas of heat usage (12). The workshop, moderated by Dr. Murat Makaracı, then VP of TÜBİTAK Marmara Research Center- Strategy and Technology Development, featured seminars by experts in nuclear technology from CNRS-Grenoble in France, including Prof. Dr. Else Merle-Lucotte, Dr. Michel Allibert, and Dr. Axel Laureau, on the types and selection of MSR. The second day, moderated by Dr. Orkun Hasekioğlu, then VP of TÜBİTAK HQ, featured presentations by Turkish participants with expertise in the nuclear field and discussions on the selection of the MSR prototype. At the end of the workshop, the idea of establishing a thorium-based, low-power, breeding, fast-spectrum prototype MSR was accepted, and subsequently, the formal application process for GIF membership was initiated

and is ongoing. In parallel with this international effort, a nationally-funded project has been ongoing for the feasibility studies of a small-scale (13) (less than 300 MW) reactor.

CHINESE STUDIES:

China's Thorium Molten Salt Experimental Reactor Granted Operating License On June 7, 2023, China achieved a significant milestone by obtaining an operating license for its 2MWt thorium-fueled molten salt experimental reactor (14). This achievement followed a comprehensive review of the reactor's operation application and related technical documents. The Shanghai Institute of Applied Physics (SINAP), under the Chinese Academy of Sciences, was granted the license for the experimental TMSR-LF1 thorium-powered molten-salt reactor. Construction of this reactor commenced in Wuwei city, Gansu province, in September 2018.

The decision to issue the 2 MWt liquid fuel thorium-based molten salt experimental reactor with an operating license was based on the determination that the application met stringent safety requirements. The TMSR-LF1 will utilize fuel enriched to less than 20% U-235 and maintain a thorium inventory of approximately 50 kg, with a conversion ratio of about 0.1. A fertile blanket of lithium-beryllium fluoride (FLiBe) with 99.95% Li-7 will be used, along with fuel in the form of UF4.

The successful operation of the TMSR-LF1 is seen as a precursor to China's plans to build a reactor with a capacity of 373 MWt by the year 2030. Notably, in 2022, the Shanghai Institute of Applied Physics (SINAP) received approval from the Ministry of Ecology and Environment to commission an experimental thorium-powered molten-salt reactor. This marked a significant milestone as it was the first molten salt nuclear reactor since the United States closed its test reactor in 1969.

The project is expected to commence with a batch operation involving online refueling and the removal of gaseous fission products. After 5-8 years, all fuel salt will be discharged for reprocessing and the separation of fission products and minor actinides for storage. Subsequently, it will transition to a continuous process of recycling salt, uranium, and thorium, with online separation of fission products and minor actinides. The reactor will increase its thorium fission from approximately 20% to about 80%.

In January 2011, the Chinese Academy of Sciences (CAS) initiated a CNY3 billion (USD444 million) research and development program focused on liquid fluoride thorium reactors (LFTRs), known as the thorium-breeding molten-salt reactor (Th-MSR or TMSR) in China. The goal was to secure full intellectual property rights on this technology, also referred to as the fluoride salt-cooled high-temperature reactor (FHR). The TMSR Centre at SINAP in Jiading, Shanghai, spearheaded these efforts.

Construction of the 2 MWt TMSR-LF1 reactor began in September 2018 and was reportedly completed in August 2021, ahead of the originally planned schedule. The prototype, initially slated for completion in 2024, was accelerated.

Molten salt and thorium reactors offer inherent safety advantages and the potential for reduced nuclear waste, primarily from unused nuclear fuel. These reactors can utilize even-numbered isotopes that are typically harder to split or react. China's developments in waterless nuclear reactors, particularly the molten salt reactor, hold the promise of expanding nuclear energy deployment to desert regions and the plains of central and western China, powered by liquid thorium rather than uranium.

SINAP's TMSR development encompasses two streams: solid fuel (using TRISO in pebbles or prisms/blocks) with a once-through fuel cycle, and liquid fuel (dissolved in fluoride coolant) with reprocessing and recycling. A third stream involving fast reactors to consume

actinides from light water reactors (LWRs) is also in the planning stages. The overarching goal is to advance both the thorium fuel cycle and non-electrical applications within a 20-30-year timeframe (14).

- The TMSR-SF stream utilizes thorium partially, relying on some breeding similar to U-238 and requiring fissile uranium input. It is optimized for high-temperature-based hybrid nuclear energy applications. Initially targeting a 2 MW pilot plant, this has evolved into a simulator (TMSR-SF0). A 100 MWt demonstration pebble bed plant (TMSR-SF2) with an open fuel cycle is projected by around 2025. TRISO particles will contain both low-enriched uranium and thorium, separately.
- The TMSR-LF stream aims for a fully closed Th-U fuel cycle with the breeding of U-233, offering enhanced sustainability with thorium but posing greater technical challenges. It is designed for the efficient use of thorium through electrometallurgical pyroprocessing.

*SINAP envisions a progression that includes a 2 MWt pilot plant (TMSR-LF1) initially, followed by a 10 MWt experimental reactor (TMSR-LF2) by 2025, and a 100 MWt demonstration plant (TMSR-LF3) incorporating full electrometallurgical reprocessing by approximately 2035. Subsequently, a 1 GW demonstration plant is planned. The TMSR-LF timeline is approximately ten years behind the SF stream.

A TMSFR-LF fast reactor, optimized for burning minor actinides, is envisioned to follow. The TMSR-SF0, at one-third scale, generates a 370 kW electric heat source with FLiNaK primary coolant at 650°C and FLiNaK secondary coolant. The 10 MWt TMSR-SF1 employs 17% enriched TRISO fuel in 60mm pebbles, similar to HTR-PM fuel, and features coolant at 630°C and low pressure. The primary coolant is FLiBe (with 99.99% Li-7), and the secondary coolant is FLiNaK. The core dimensions are 3 m in height and 2.85 m in diameter, enclosed in a 7.8 m high and 3 m diameter pressure vessel. Residual heat removal is achieved passively through cavity cooling. Initially envisioned to have a 20-year operating life, the project has since been discontinued.

Construction of the 2 MWt TMSR-LF1 reactor, part of a $3.3 billion program, commenced in September 2018 and was reportedly completed in August 2021. The prototype was initially scheduled for completion in 2024 but saw accelerated progress. Figure 6 depicts a schematic of a Chinese experimental molten salt reactor.

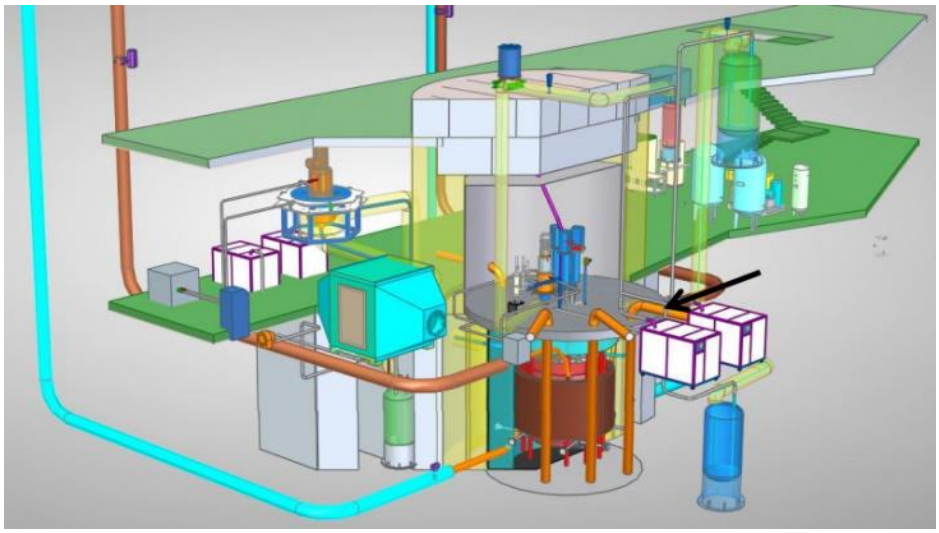

Figure 6 Schematic view of Chinese molten salt reactor (15)

INDONESIAN EFFORTS:

In line with its commitment to reduce climate change and achieve net-zero emissions, the Indonesian government has pledged to undergo an energy transition by promoting research and development in renewable power generation technologies. The government's ambitious target is to have 8 GWe of installed capacity generated by nuclear power plants by 2035, with plans to increase this capacity to 35 GWe by 2060.

PT ThorCon Power Indonesia - a subsidiary of USA-based ThorCon - signed an agreement with Indonesia's Nuclear Energy Regulatory Agency (Bapeten) to officially start a safety, security, and safeguards consultation in preparation for licensing a demonstration 500 MWe floating ThorCon molten salt reactor called TMSR-500 (16).

The consultation's primary aim is to prepare the regulator, applicant, and stakeholders for the formal licensing process. Its objective is to develop a comprehensive roadmap that includes schedules, defines roles and responsibilities, aligns with relevant laws and regulations, outlines the scope and format of technical and administrative documents required for license applications, and assesses the readiness of the design, as explained by ThorCon. The consultation process comprises several key elements. This includes a thorough review of the master plan document for constructing the TMSR500, consultations related to the roadmap for both the TMSR500 prototype and the Non-fission Test Platform (NTP) facility, the creation of essential technical and non-technical documents for the TMSR500 prototype and NTP to support the licensing process, and consultations regarding the approval of the TMSR500's design (16).

The expected duration for the consultation process is approximately 12 months, with ThorCon expressing its intention to proceed with license applications once the consultation concludes. ThorCon views this consultation agreement as a significant milestone, signifying the Indonesian government's commitment to establishing an efficient regulatory framework conducive to the timely and cost-effective licensing of nuclear power. Additionally, ThorCon is actively planning to establish an assembly line for its nuclear power plants in Indonesia. Simultaneously, it is collaborating with multiple universities to develop educational programs focused on molten salt reactor technology. These initiatives are expected to not only stimulate a burgeoning industry within the national economy but also elevate Indonesia's power generation to one of the most environmentally friendly globally (16).

ThorCon's immediate goal is to secure licenses, construct, and operate its inaugural 500 MWe demonstration power plant on Kelasa Island in the Province of Bangka-Belitung by the year 2029. ThorCon emphasizes that it will require only 24 months from the commencement of construction for each plant to be capable of supplying electricity to the grid. Furthermore, this approach allows for the scalability of ThorCon plants, with the potential to produce up to 10 GW of power annually per shipyard or assembly line once production is scaled up. The estimated cost for a two-unit (1 GWe) plant is USD 1.2 billion (16). The following gives milestones:

Indonesia-Thorcon MSR Development Milestones

2015 Concept design completed

2019 Pre-licensing Vendor Design Review in Indonesia

2019 Basic engineering design complete

2021 Start construction of Pre-fission Test Platform

2022 Testing of the Pre-fission Test Platform

2023 Construction of the demonstration power plant

2024 Begin testing of the demonstration power plant

2025 Complete testing of the demonstration power plant; obtain design certification

2026 Begin commercial construction of multiple power plants

2028 Start of commercial operation of multiple power plants

Figure 7 depicts the schematic design of the Thorcon 500 MWe molten salt nuclear power plant for Indonesia, and Figure 8 shows two of the 557 MWth power modules (17).

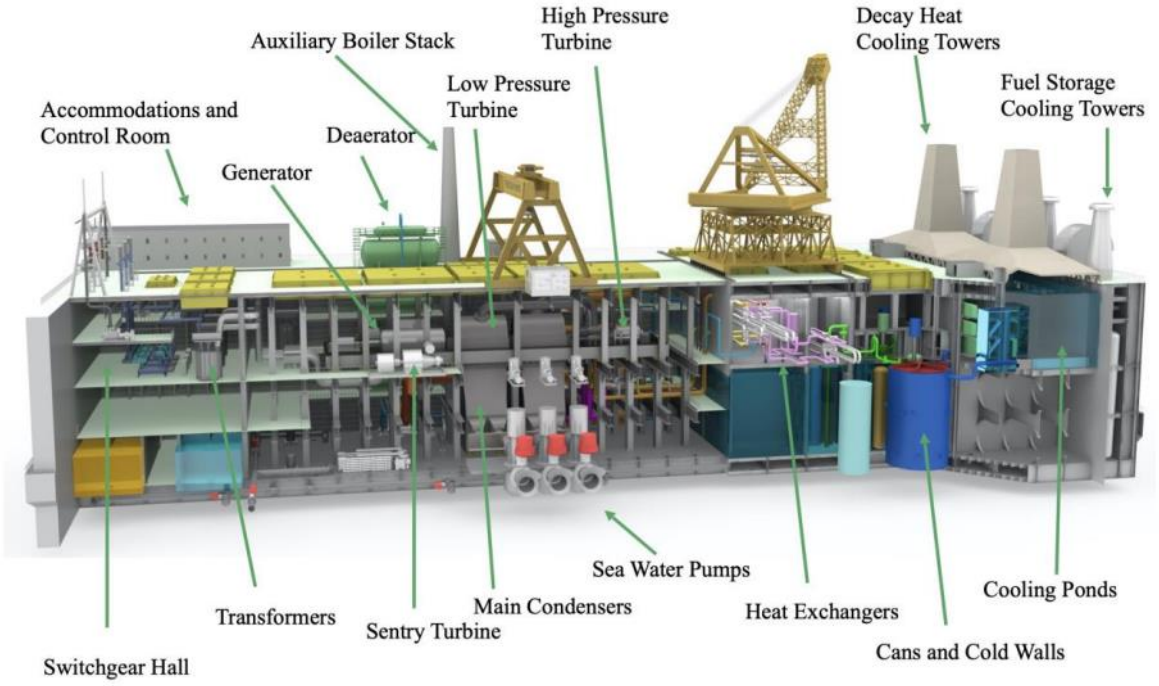

Figure 7 Thorcon 500 MWe molten salt power plant for Indonesia (17)

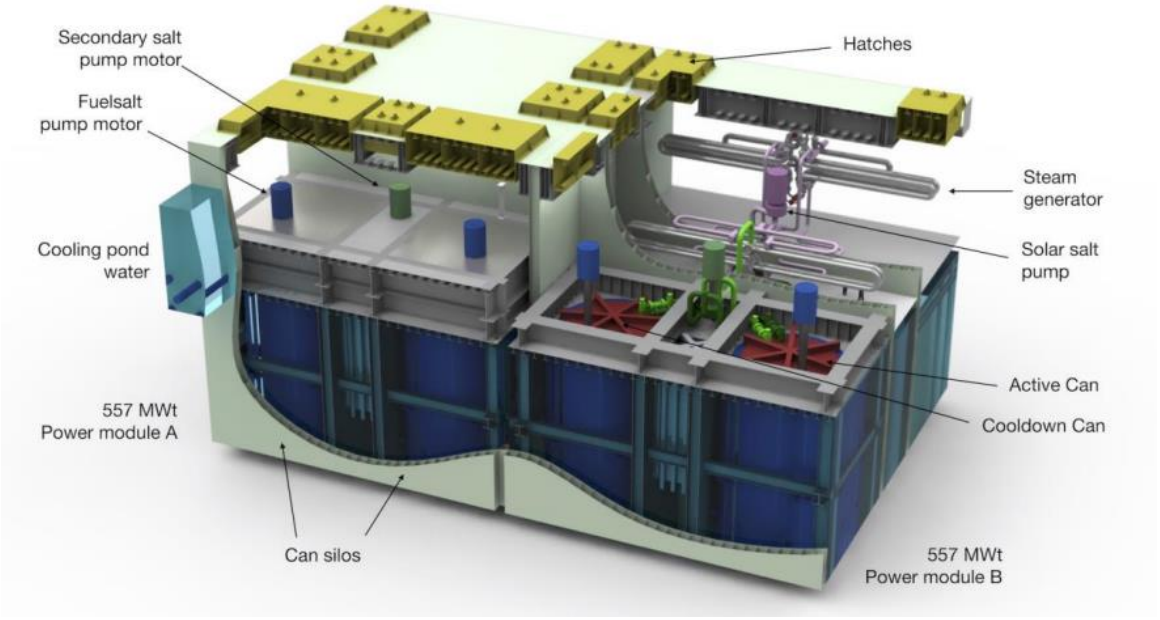

Figure 8 Thorcon Two 557 MWth power modules (17)

IV. Supercritical Water-Cooled Reactor (SCWR) (11)

SCWRs are high-temperature, high-pressure light water-cooled reactors that operate above the thermodynamic critical point of water (374 °C, 22.1 MPa) (Figure 9). Depending on the core design, the reactor can have a thermal or fast neutron spectrum. The concept can be based on existing pressure vessel or pressure tube reactor technologies, using light water or heavy water as the moderator. Unlike existing water-cooled reactors, the coolant in SCWRs will experience a significantly higher enthalpy rise within the core, reducing the core mass flow rate for a given thermal power and raising the core outlet enthalpy to superheated conditions. For both pressure vessel and pressure tube designs, a single-pass steam cycle has been envisaged, neglecting any coolant recirculation within the reactor, similar to a boiling water reactor. As with a boiling water reactor, superheated steam will be fed directly to a high-pressure steam turbine under normal operating conditions, and feedwater from the steam cycle will be returned to the core. Therefore, SCWR concepts combine design and operational experience from hundreds of water-cooled reactors with experience from hundreds of fossil fuel power plants operating with supercritical water (SCW). Unlike some other Generation IV nuclear systems, SCWR can be incrementally developed from existing water-cooled reactors.

Advantages and Challenges

SCWR designs offer unique features that provide several advantages compared to state-of-the-art water-cooled reactors (11):

- SCWRs enhance thermal efficiency compared to existing generation water-cooled reactors. The efficiency of an SCWR can approach or exceed 44%, compared to 34-36% for existing reactors.
- There is no need for reactor coolant pumps in SCWRs. Under normal operating conditions, the only pump that operates the coolant is the one circulating the feedwater, and condensate pumps. Steam generators used in pressurized water reactors and steam separators and dryers used in boiling water reactors are negligible because they overheat within the coolant core. The containment, designed with pressure suppression pools and emergency cooling and residual heat removal systems, can be significantly smaller than those of existing water-cooled reactors. The higher enthalpy of steam allows for downsizing the turbine system and thus reduces the capital costs of the conventional island. These general features offer a lower capital cost for specific electrical power and better fuel utilization potential, thus providing an economic advantage compared to existing light water reactors.

However, there are various technological challenges associated with the development of SCWRs, particularly related to transient heat transfer models (addressing the depressurization from supercritical to subcritical conditions), material qualification (e.g., coating advanced materials and steels), and the demonstration of passive safety systems.

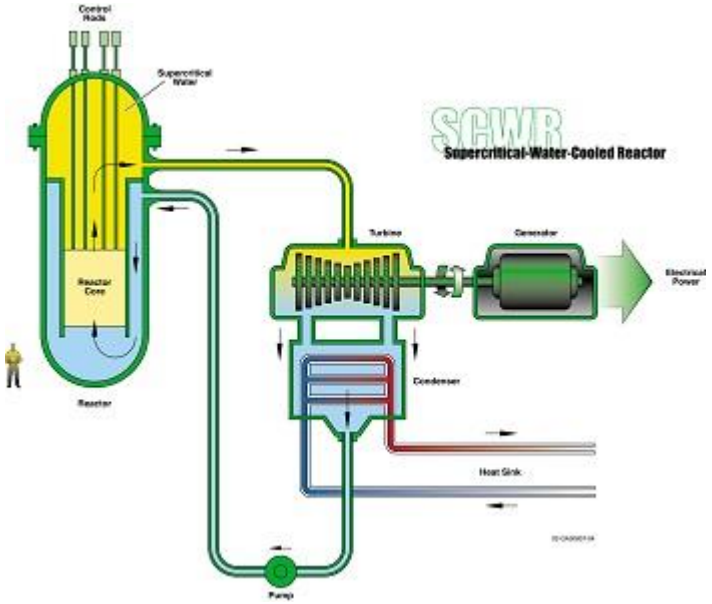

Figure 9 Supercritical-Water-Cooled Reactor (SCWR) cycle (11)

V. Sodium Cooled Fast Reactor (SFR) (11)

SFR uses liquid sodium as the reactor coolant and provides high power density and low-pressure operation with a low coolant volume fraction. It prevents oxygen-related corrosion but requires a sealed cooling system as sodium reacts chemically with air and water. The assessed facility size options vary from small modular reactors, ranging from 50 to 300 MWe, to larger facilities of up to 1500 MWe. The outlet temperature for options allowing the use of previously developed and proven materials is 500-550°C.

SFR employs a closed fuel cycle that enables the regeneration of fissile fuel and simplifies the management of minor actinides (Figure 10). However, this necessitates the development and qualification of recycled fuels. Important safety features of Generation IV systems include a long thermal response time, a reasonable margin for coolant boiling, operation close to atmospheric pressure in the primary system, and an intermediate sodium system separating the radioactive sodium in the primary system from the power conversion system. The working fluids of the power conversion system, such as water/steam, supercritical carbon dioxide, or nitrogen, could be considered for achieving high performance in terms of thermal efficiency, safety, and reliability. Innovations aimed at reducing capital costs are expected to make SFR economically competitive in future electricity markets. Additionally, the fast neutron spectrum significantly extends uranium resources compared to thermal reactors, making SFR an attractive energy source for countries seeking to make the most of limited nuclear fuel resources and manage nuclear waste by closing the fuel cycle.

Much of the fundamental technology for SFR has been created in previous fast reactor programs and has been confirmed through end-of-life tests of the Phenix reactor in France, the restart of Monju in Japan, and the service life extension of BN-600 in Russia. New programs involving SFR technology include the China Experimental Fast Reactor (CEFR), connected to the grid in July 2011, and India's Prototype Fast Breeder Reactor (PFBR), scheduled to go critical in 2021. SFR is considered the most immediate deployment option for actinide management and an attractive energy source for countries seeking to make the most of limited nuclear fuel resources and manage nuclear waste by closing the fuel cycle (11).

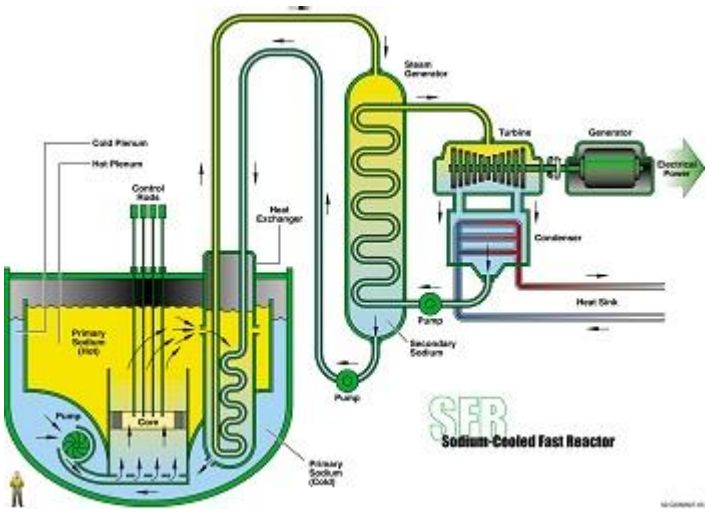

Figure 10 Sodium-Cooled Fast Reactor (SFR) cycle (11)

VI. Very High-Temperature Reactor (VHTR) (11)

The Very High Temperature Reactor (VHTR) is primarily dedicated to the co-generation of electricity and hydrogen. Hydrogen can be produced through thermochemical, electrochemical, or hybrid processes using water as a feedstock.

The high outlet temperature makes VHTR attractive for applications in the chemical, petroleum, and iron industries. The technical basis of VHTR includes the use of TRISO-coated particle fuel, a core structure of graphite, helium coolant, a special core arrangement, and natural decay heat removal, resulting in lower power density. VHTR is characterized by natural safety, high thermal efficiency, the capability for process heat applications, low operating and maintenance costs, and modular potential.

VHTR is the evolutionary step in high-temperature gas-cooled reactor development. It operates with a thermal neutron spectrum, graphite moderation, and helium cooling (Figure 11). It can provide nuclear heat and electricity in the range of outlet temperatures between 700 and 950°C, or potentially over 1000°C in the future. VHTR can have either a prismatic block core design, like the Japanese HTTR, or a pebble bed core design, like the Chinese HTR-10. For electricity production, it can use a helium gas turbine system, operate directly in a primary coolant loop called a direct cycle, or use a traditional Rankine Cycle with a steam generator. For nuclear heat applications such as refineries, petrochemicals, metallurgy, and hydrogen production, the heat application process is typically combined with the reactor through an intermediate heat exchanger (IHX) in what is known as an indirect cycle.

VHTR can produce hydrogen through various methods, including thermochemical processes using heat and water, high-temperature steam electrolysis (HTSE), or steam reformer technology using heat, water, and natural gas.

In the early days of the Generation IV program, the original focus for VHTR was on very high outlet temperatures and efficient hydrogen production. However, market assessments shifted the focus toward electricity production and industrial processes that require modest outlet temperatures (700-850°C) in the next decade. This shift also reduced technical risks associated with higher outlet temperatures. Consequently, over the last decade, the focus has shifted from higher outlet temperature designs like GT-MHR and PBMR to lower outlet temperature designs like the Chinese HTR-PM and the U.S. NGNP.

VHTR can come in two typical reactor configurations: pebble bed and prismatic block. Although the shape of the fuel element differs between the two configurations, the technical basis to achieve high outlet temperatures and maintain fission production within the coated particle is the same for both. VHTR can support alternative fuel cycles such as U-Pu, Pu, MOX, U-Th, and others.

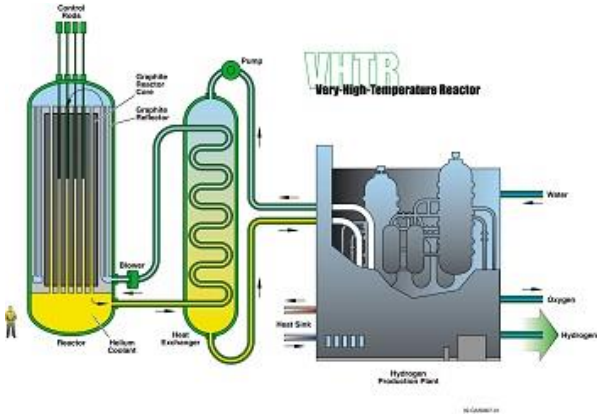

Figure 11 Very-High-Temperature Reactor (VHTR) cycle (11)

REFERENCES

1. SWP Report 2023 | United Nations Population Fund (unfpa.org) https://www.unfpa.org/swp2023 (Retrieved on 7/10/2023)
2. https://www.unfpa.org/data/world-population-dashboard. (Retrieved on 7/10/2023)
3. https://data.worldbank.org/indicator/EG.USE.ELEC.KH.PC?end=2014&start=1960&view=chart. (Retrieved on 7/10/2023)
4. https://www.world-nuclear.org/information-library/facts-and-figures/world-nuclear-power-reactors-and-uranium-requireme.aspx (Retrieved on 7/10/2023)
5. https://pris.iaea.org/PRIS/WorldStatistics/NuclearShareofElectricityGeneration.aspx (Retrieved on 7/10/2023)
6. https://world-nuclear.org/our-association/publications/global-trends-reports/nuclear-fuel-report.aspx (Retrieved on 7/10/2023)
7. https://www.world-nuclear.org/information-library/facts-and-figures/nuclear-generation-by-country.aspx (Retrieved on 7/10/2023)
8. https://www.world-nuclear.org/information-library/facts-and-figures/heat-values-of-various-fuels.aspx (Retrieved on 7/10/2023)
9. https://www.statista.com/statistics/383633/worldwide-consumption-of-electricity-by-country/ (Retrieved on 7/10/2023)
10. https://en.wikipedia.org/wiki/G20#cite_note-6 (Retrieved on 7/10/2023)
11. https://www.gen-4.org/gif/jcms/c_59461/generation-iv-systems (Retrieved on 7/10/2023)
12. https://mam.tubitak.gov.tr/en/duyuru/molten-salt-reactor-technology-determination-workshop (Retrieved on 7/10/2023)
13. INTERNATIONAL ATOMIC ENERGY AGENCY, Innovative Small and Medium Sized Reactors: Design Features, Safety Approaches and R&D Trends, IAEA-TECDOC-1451, IAEA, Vienna (2005). (Retrieved on 7/10/2023)
14. https://www.nextbigfuture.com/2023/06/china-thorium-molten-salt-experimental-reactor-is-licensed-for-operation.html (Retrieved on 7/10/2023)
15. https://neutronbytes.files.wordpress.com/2022/08/china-msr.png (Retrieved on 7/10/2023)
16. https://thorconpower.com/news/ (Retrieved on 7/10/2023)
17. https://aris.iaea.org/PDF/ThorCon_2020.pdf (Retrieved on 7/10/2023)

A Sailfish Optimization Algorithm based Feature Selection to Diagnose Heart Disease

Murat Onur YILDIRIM[1]
Erdal AYDEMIR[2]

1. Introduction

Heart diseases are considerably increasing today and it is not only seen commonly in elderly individuals but also in middle and young age individuals. According to a worldwide study by the World Health Organization in 2016, ischemic heart disease and heart attack cause the most deaths with approximately 15.2 million deaths per year (World Heath Organization, 2018). To diagnose heart disease; nuclear cardiological tests, echocardiography, multi-slice computed tomography, and coronary angiography are commonly used investigations, but they are expensive and time consuming. Unfortunately, these medical investigations are not designed to apply regularly to patients yet early diagnosis of heart disease is extremely important (Saraçoğlu, 2012). Hence, this study aims to provide early diagnosis for patients by using basic features such as gender, age, chest pain level, fasting blood sugar, and serum cholesterol amount. To do that, it is crucial to extract the right set of features rather than providing the whole information (Goodfellow, Bengio, & Courville, 2016), and heuristic algorithms could be utilized for that purpose since they are successful problem-solvers, especially in difficult-to-solve problems.

Heart disease dataset studied in this research has been used in various machine learning applications. Late works in the literature give more attention to feature selection and extraction than earlier works. Therefore, studies that contains feature selection and extraction are considered to present the recent literature and also to make a fair comparison. Bhuvaneswari Amma (NG, 2013) followed an approach based on Principal Component Analysis (PCA) and Adaptive Neuro Fuzzy Inference System (ANFIS) and conclude the study with 92.3% accuracy. In the study of Rajeswari et al. (Rajeswari, Vaithiyanathan, & Pede, 2013), they emphasized and aimed to select correlated features since they are easily accessible and not computationally-expensive and their study returned %87.46 accuracy. Subanya & Rajalaxmi (2014) combined Artificial Bee Colony with KNN in their study and reached 92.4% accuracy. Tomar and Agarwal (2014) selected the features by considering f1-score and conducted Grid Search for hyperparameters optimization and obtained 85.59% accuracy. Long et al. (Long, Meesad, & Unger, 2015) proposed 88.3% accuracy with fuzzy logic with an expensive feature selection method by combining rough sets and chaos firefly algorithm. Vivekandan and Iyengar (Vivekanandan & Iyengar, 2017) employed differential evolution algorithm to select features and their fuzzy neural network found 83% accuracy based on selected features. Shah et al. (2017) conducted a study on feature extraction with probabilistic PCA to select high impact features then they employed support vector machine (SVM) that returned 82.18% accuracy with radial basis function (RBF) kernel. In the study of Uyar and Ilhan (2017), genetic algorithm (GA) with a recurrent fuzzy neural network was implemented and it was able to achieve 96.74%

[1] Res. Asist., Suleyman Demirel University, Faculty of Engineering and Natural Sciences, Dept. of Industrial Engineering, Isparta, Turkiye
[2] Assoc. Prof. Dr., Suleyman Demirel University, Faculty of Engineering and Natural Sciences, Dept. of Industrial Engineering, Isparta, Turkiye

accuracy. Amin et al. (Amin, Chiam, & Varathan, 2019) selected important features from dataset with brute force method and reached the accuracy of 87.41% by Naïve Bayes and Logistic Regression ensemble. Reddy et al. (Reddy, Nee, Min, Ying, & Ying, 2019) applied recursive feature elimination (RFE) and found highest accuracy of %94.96 with random forest (RF). Jayaraman and Sultana (2019) implemented GA, particle swarm optimization (PSO), ant colony optimization (ACO), and cuckoo search for feature selection. According to their results, Evolutionary Particle Bee Optimized Associative Memory Neural Network achieved the highest accuracy score of 99.85%. Khourdifi and Bhaj (2019) used a correlation-based feature selection to filter redundant features and then used these features in PSO. Features selected by PSO used as an input of ACO and decided the final feature set. They concluded the study with %99.63 accuracy. Kannan and Vasanthi (2019) evaluated the machine learning algorithms with the ROC curves for heart disease diagnosis and found 87% accuracy. Alim et al. (2020) adopted an approach based on significant features and ensemble model which acquired 86% accuracy. Escamila et al. (2020) utilized both chi-square and PCA for feature selection and it resulted in 98.7% accuracy. Ali et al. (Ali, et al., 2021) utilized feature importance scores of various machine learning algorithms and random forest algorithm was able to reach 100% accuracy. Table A and B that summarize the literature provided in the Appendix.

The scope of this study is to highlight simple machine learning approaches that perform better with feature selection and hyperparameter optimization since medical decision support systems should be affordable, efficient, and effective to be accessible. Even though there are many applications on the heart disease data set, there is a deficiency in the literature about our specific purpose. Hence, as a feature selector, sailfish optimization algorithm (Shadravan, Naji, & Bardsiri, 2019) that can converge rapidly and avoid local optima has been combined with various machine learning algorithms to achieve better classification results in heart disease prediction. To increase performance of the models, Grid Search was applied for hyperparameter optimization. This chapter tries to answer the following research questions:

(1) Which features are required for proper decision while diagnosing heart disease?
(2) Are similar or better results obtained with simpler machine learning models by feature selection?
(3) Does optimizing hyperparameters improve the performance compared to default hyperparameters?

The rest of this chapter is organized as follows: Proposed methodologies, dataset and solution procedure are given in Section 2. Then, computational findings and discussion are presented in Section 3. Conclusion and future directions are given in Section 4.

2. Methodology

Machine learning can be defined as an AI approach that supports the creation and development of mathematical models to help understand data (VanderPlas, 2017). These models are able to "learn" with parameters that can be updated based on observed data. Hence, they can be used to predict and understand unseen data, after "learning" based on previously seen data. The concept of the machine learning is well-suited to the medical decisions since they require an inductive engine that learns the decision characteristics of the diseases and diagnoses future patients with uncertain disease states (Güler & Übeyli, 2005). In most cases, however, using raw data in machine learning applications will not be conducive (Fink, et al., 2020). That is why pre-processing methods such as standard scaling, and one hot encoding are applied to the datasets before executing machine learning algorithms. Furthermore, datasets may contain many redundant features which generally cost a large number of computational times and deteriorate system performance (Zhu, Hu, Qi, Ma, & Peng, 2015) so that right set of features should be selected.

The workflow of this study is as follows: (i) Data pre-processing was executed after dividing data into train set (80%) and test set (20%). (ii) Machine learning algorithms with default parameters were observed to create a baseline for our study and (iii) SFO was applied to select relevant features with respect to accuracy score. (iv) Finally, hyperparameter optimization were performed on a best-performed model subsequent to feature selection. In all these steps, only train set (80%) was used with 5-fold cross validation. Test set (20%) was exposed to the models for observing their performance only. The pseudocode that describes the flow of study and its logic is given in Table 1. We have used Python 3.8.5, Scikit-learn 0.23.1 and Pandas 1.0.5 in this study.

Table 1. Pseudocode for this study

```
heartDisease = pandas.read_csv('heartDisease.csv')
apply data pre-processing steps
x = heartDisease (FeatureSet)
y = heartDisease (Target)
x_train, x_test, y_train, y_test = train_test_split(x, y, test_size=0.2)
# Basic Classification Approach
for each learner:
        cross_val_score(learner, x_train, y_train, cv=5)
        learner.score(x_test, y_test)
end
# Feature selection with Sailfish Optimizer
For each learner:
        apply SFO
        cross_val_score(learner, x_train, y_train, cv=5)
        learner.score(x_test, y_test)
end
# Hyperparameter optimization
for best learner:
        initialize parameter space
        apply gridsearchCV
end
```

In the following subsections, used dataset and implemented methods were briefly introduced: Standard Scaler and One-Hot encoding as pre-processors, Decision Tree as the best performing machine learning algorithm and rest of the learning algorithms that were tried, Sailfish Optimization algorithm as a feature selector, GridSearchCV as a hyperparameter optimization, k-Fold Cross Validation as a performance evaluator and, accuracy, precision, recall and f1-score as performance evaluation metrics.

2.1. Data Pre-processing

The data was collected from the UCI Machine Learning Repository (1989) which contains a vast and varied number of datasets from various domains. The heart disease dataset which was briefly described in Table 2 consists of 13 features and 303 observations. It had been constructed by collecting data from Hungarian Institute of Cardiology, Zurich University Hospital, Basel University Hospital and V.A. Medical Center.

Table 2. Short description of UCI Heart Disease Dataset

Feature	***Short Description***	***Feature***	***Short Description***
age	Age of the person	thalach	Maximum heart rate achieved
sex	Sex of the person	exang	Exercise-induced angina (0: False, 1: True)
cp	Chest Pain level (0 to 3)	oldpeak	ST depression-induced relative to rest
trestbps	Resting blood pressure	slope	The slope of the peak exercise ST segment
chol	Serum cholesterol in mg/dl	ca	Number of major vessels colored by fluoroscopy (0 to 3)
fbs	Fasting blood sugar (1: >120mg/dl, 0: <120mg/dl)	thal	Thallium radioactive tracer injection (1: fixed defect, 2: normal, 7: reversible defect)
restecg	Resting electrocardiography (0: left ventricular hypertrophy, 1: normal, 2: ST-T wave abnormality)	target	Heart Disease (0: Healthy, 1: Diseased)

As a first step, distribution of the data was investigated to navigate whether further processes such as bootstrapping and SMOTE should be applied or not. Data was found well-scattered and balanced, as in Table 3, therefore no further processes were applied to balance the data. Although it was well-balanced, missing values and outliers that would affect machine learning algorithms were found in the dataset. Therefore, missing values were filled with median value of the respective feature while outliers were removed from the dataset to clean irrelevant or only weakly relevant data points (Christy, Gandhi, & Vaithyasubramanian, 2015).

Table 3. Data Distribution Under Target Variable

Category	Percentage (%)
Healthy	54.3
Heart Disease	45.7

When the numerical attributes or features vary in different scales, machine learning algorithms usually don't perform competently (Géron, 2019). Hence, a pre-processing technique standard scaling which reforms the distribution of each feature as $\mu=0$ and $\sigma=1$ is applied to the dataset. One-hot encoding, on the other hand, is a tool to binarize categorical features which leads machine learning algorithms to perform better. Even the number of features increases in one-hot encoding, it is still the most prevalent strategy due to its simplicity (Rodríguez, Bautista, González, & Escalera, 2018).

Finally, dataset was split into train-test (80% - 20%) sets and 5-fold cross-validation was performed on train dataset to have an objective conclusion. Moreover, a stratified target feature was used while splitting the dataset so that initial distribution was preserved. Feature selection, model creation, validation, and hyperparameter optimization were executed on the training dataset. Final scores are obtained by utilizing the test dataset which was seen by models only in the evaluation.

2.2. Learning Algorithms

This study conducts eight different prediction approaches. Decision Tree, one of these algorithms, is described more in detail under a different section since it performed the best. Logistic Regression (LR) basically a multi variate linear regression with a sigmoid function which creates non-linear relationship between inputs and the prediction. K-nearest neighbour (KNN) algorithm makes the classification based on k number of closest data points. Random Forest (RF), an ensemble learning algorithm, combines multiple decision trees into one model to have an enhanced prediction result by majority voting. Support Vector Machine (SVM) creates a hyperplane to separate different classes for prediction. Naïve Bayes (NB) utilize Bayes' theorem with the "naive" assumption that each pair of features is conditionally independent given the value of the class variable. XGBoost (XGB) is a scalable and highly accurate implementation of a Gradient Boosting Decision Trees (GBDT) which is constructed by a group of shallow decision trees are iteratively trained and with each iteration using the error residuals of the prior model to fit the new model.

2.3. Decision Tree

The decision tree (DT) algorithm, illustrated in Figure 1, divides search space into little subspaces that are not overlapped with others and each region is represented by corresponding nodes (Goodfellow, Bengio, & Courville, 2016). Trees start with a root node and then spread information through internal nodes until getting the final leaf nodes. Each node is divided into two new nodes with basic Yes/No or True/False questions. Deciding which feature should be the root, internal nodes or leaf is crucial to have an eminent decision tree. Thus, “impurity” and “information level” concepts were developed for this deciding process. Gini Index and Entropy which measure impurity and information level are given in equation (1) and (2) respectively where pn is the proportion of the samples that are belong to class c. When initiating the decision tree, a feature with the lowest impurity score is selected as an initial node. Then, impurity is calculated for the newly formed nodes until the model reaches the leaves. The node is decided as a leaf if the impurity of the existing node is better than the nodes that would be generated from that. Decision tree that reached its leaf nodes would be able to predict the data.

$$I_G = 1 - \sum_{n=1}^{c} (p_n) \tag{1}$$

$$I_H = -\sum_{n=1}^{c} p_n log_2^{p_n} \quad when\ p \neq 0 \tag{2}$$

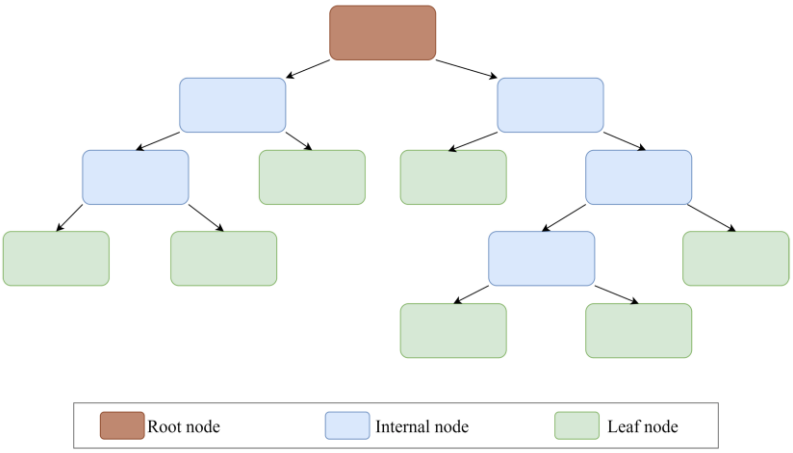

Figure 1. Basic Representation of Decision Tree Algorithm

2.4. Sailfish Optimization Algorithm

The Sailfish Optimization (SFO) Algorithm inspired by a group of hunting sailfish (Shadravan, Naji, & Bardsiri, 2019). There are two different populations in this algorithm: the sardine (Sardinella aurita) population to diversify search space and the sailfish (Istiophorus platypterus) population to intensify search around the best solution. It was claimed that the SFO algorithm outperforms the reputable algorithms in the literature with the avoidance of local optima, and rapid convergence especially on large-scale global optimization (Shadravan, Naji, & Bardsiri, 2019).

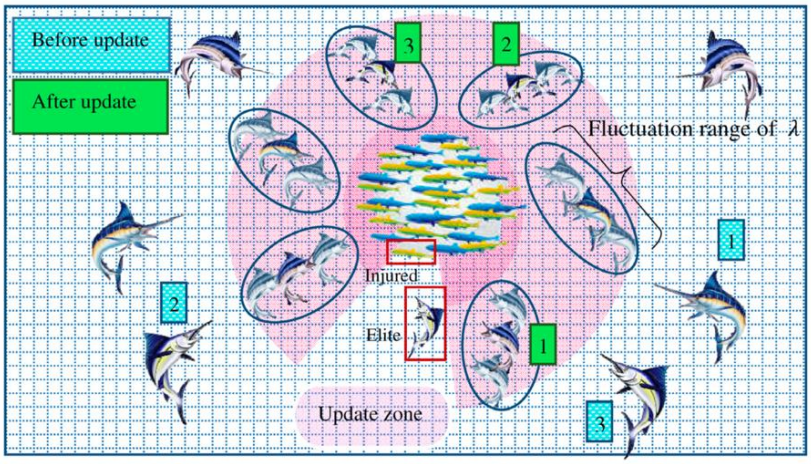

Figure 2. Working principle of Sailfish Optimizer Algorithm (Shadravan, Naji, & Bardsiri, 2019)

In the algorithm, the sailfish and sardine population are generated randomly. Afterwards, parameter that represents attack power of the sailfishes is initialized. The value of this parameter decreases in each iteration. Fitness values of each sailfish and sardine are calculated and stored in matrices. The best sailfish and sardine are known as elite sailfish and injured sardine in the algorithm. Each school of fish updates its positions based on defined parameters until the termination conditions are satisfied. Sailfishes replace their position based on both the elite one and the injured sardine. Sardine school, however, moves depend on the attack power of the sailfishes. All sardines modify their positions if attack power is greater than 0.5, otherwise, the number of sardines that are proportional to attack power just redirect their position. Furthermore, in each iteration, elite sailfish and injured sardine are updated if a better one is observed. The position of a final elite sailfish is returned from the sailfish matrix and concludes the algorithm. The visual representation of the algorithm is also presented in Figure 2.

2.5. Hyperparameter Optimization

Hyperparameters are as significant as the model itself in machine learning since they control the learning level of the model. That is why hyperparameter optimization is quite fascinating not only in overcoming over-fitting and under-fitting problems but also in increasing the accuracy of the model. GridSearchCV was adopted to optimize the hyperparameters in this study. It evaluates all the possible user-defined alternatives with k-fold cross-validation and returns the optimal values for each hyperparameter among defined alternatives.

2.6. K-fold Cross-Validation

K-Fold Cross Validation provides an unbiased classification while overcoming overfitting and underfitting issues (Goodfellow, Bengio, & Courville, 2016). The data set is divided into K pieces while the K-1 piece of training set is created in each iteration, there is only 1 test set to observe the performance. After obtaining performance metrics for each set or iteration, the average of those performance metrics constitutes the final metric of the model.

2.7. Performance Metrics

Accuracy, Recall and Precision given in equation (3), (4) and (5) respectively are the default and well-descriptive performance metrics in both traditional machine learning and deep neural networks (Goodfellow, Bengio, & Courville, 2016). F1-score is basically a harmonic average of recall and precision.

True Positive (TP) result is one in which the model accurately identifies the positive class. Similarly, True Negative (TN) is a result for which the model accurately predicts the negative class. On the other hand, False Positive (FP) indicates where the model incorrectly predicts the positive class and False Negative (FN) is an outcome where the model incorrectly predicts the negative class. Confusion matrices are helpful figures to illustrate TP, TN, FP and FN to understand success of the models.

$$\text{Accuracy:} \quad \frac{TP + TN}{TP + TN + FP + FN} \tag{3}$$

$$\text{Recall:} \quad \frac{TP}{TP + FN} \tag{4}$$

$$\text{Precision:} \quad \frac{TP + TN}{TP + FP} \tag{5}$$

3. Results and Discussion

3.1. Results

Accuracy scores of each algorithm were represented in Table 4. The average accuracy improvement with SFO was found as 18.03%. KNN improved 9.80% and DT received the maximum improvement with 41.93%. Hence, DT reached the best accuracy score after SFO, although it returned the worst result in the beginning. Selected features for DT are presented in Table 5.

Table 4. Accuracy Scores of Test Set with and without SFO

Methods	**Accuracy Scores**		**Improvement (%)**
	Before SFO	**After SFO**	
Logistic Regression (LR)	0.8196	0.9180	12.01
K-Nearest Neighbors (KNN)	0.8361	0.9180	9.80
Decision Tree (DT)	0.6699	0.9508	41.93
Random Forest (RF)	0.7868	0.8852	12.51
Support Vector Classifier (SVC)	0.7869	0.9016	14.58
Naïve Bayes (NB)	0.7869	0.9016	14.58

XGBoost (XGB)	0.7869	0.9180	16.66
		Average	**17.43%**

Hyperparameter tuning was applied on DT to utilize its all potential and improve the accuracy score further. After the hyperparameter optimization with GridSearchCV, accuracy score was raised to 0.9836 from 0.9508 with hyperparameters in Table 6 and we stated that as our proposed model: SFO_HPO_DT. Confusion matrices in Figure 3 were presented to illustrate the improvement over each process. Detailed and comprehensive description of the proposed model was given in the classification report in Table 7(c), in contrast to Table 7(a) and Table 7(b) where DT and SFO_DT models were presented respectively.

Table 5. Selected Features by Sailfish Optimizer for Decision Tree

Selected Features for DT with SFO							
age	sex	cp	chol	restecg	oldpeak	ca	thal

Table 6. Optimized Hyperparameters for Decision Tree after Feature Selection

Optimized Hyperparameter for DT				
criterion	**max_features**	**min_samples_leaf**	**splitter**	**random_state**
"entropy"	"sqrt"	0.02	"random"	42

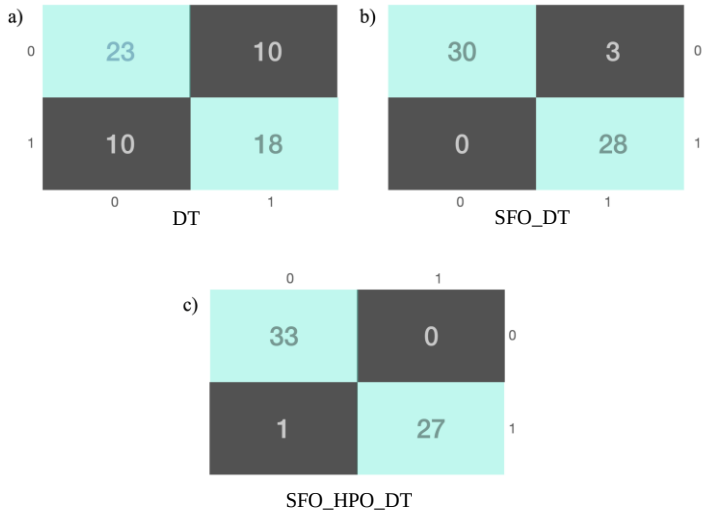

Figure3. Confusion Matrix of (a) Decision Tree, (b) DT with Feature Selection, (c) Proposed Model

Table 7. Classification Performance Results for (a) DT (b) SFO_DT (c) SFO_HPO_DT

a) Classification Results for DT						
dt	**precision**	**recall**	**f1-score**	**accuracy**	**improvement (%)**	
0	0.70	0.70	0.70	0.6699	-	
1	0.64	0.64	0.64			
b) Classification Results for SFO_DT						
0	0.90	1.00	0.95	0.9508	(a)	
1	1.00	0.91	0.95		41.93	
c) Classification Results for SFO_HPO_DT						
0	1.00	0.97	0.99	0.9836	(a)	(b)
1	0.96	1.00	0.98		46.83	3.45

3.2. Discussion

When the proposed model SFO_HPO_DT was compared with the literature in Table 8, it gives promising results even these studies mostly focused on the highest accuracy which leads to larger, complicated, and more expensive models. Our purpose was, however, simplicity and efficiency for explainable early diagnosis of heart disease while attaining worthy performance scores. Especially, simplicity and explainability have significant importance for medical support systems since medical doctors (MDs) want to know the reasons behind the diagnosis which is done by AI before taking an action. That is why ensemble methods, feature extraction and sequential feature selection approaches which are proposed by studies of (Jayaraman & Sultana, 2019), (Khourdifi & Bahaj, 2019) and (Garate-Escamila, Hassani, & Andres, 2020) usually are not adequate and preferable for hospitals and MDs. Although (Ali, et al., 2021) reached a remarkable score, selected features are still vague in their paper and random forest algorithm which they utilized in their study was far more complicated than a single decision tree. Our fast, explainable, efficient, and effective model proves its success by having only one feature selection algorithm and simple yet amplified decision tree algorithm with its optimized hyperparameters.

Table 8. Performance Comparison with Related Works based on UCI Heart Disease Dataset

Author/s	**Accuracy**
Ali et al. (2021)	1.0000
Jayaraman and Sultana (2019)	0.9985
Khourdifi and Bahaj (2019)	0.9963
Garate-Escamila et al. (2020)	0.9870
SFO_HPO_DT (Our study)	**0.9836**
Uyar and İlhan (2017)	0.9778
Reddy et al. (2019)	0.9496
Kanagarathinam el al. (2022)	0.9434
N.G. (2013)	0.9320
Subanya and Rajalaxmi (2014)	0.9240
Long et al. (2015)	0.8830
Amin el al. (2019)	0.8741
Rajeswari et al. (2013)	0.8713
Kannan and Vasanthi (2019)	0.8700
Alim et al. (2020)	0.8694
Tomar and Agarwal (2014)	0.8559
Vivekanandan and Iyengar (2017)	0.8300
Shah et al. (2017)	0.8218

4. Conclusion and Further Research

Coronary heart disease requires high attention in medical practices since it has the most frequent causes of mortality, a wide range of symptoms, and complicated diagnostic processes (Gamberger, Lavrač, & Krstačić, 2003). Common examinations for heart diseases are time-consuming and not budget-friendly. Moreover, these examinations are performed when a patient feels an issue. Therefore, many studies were conducted by researchers on this topic to develop faster and efficient diagnosis methods. However, those studies mostly focused on the highest accuracy result which forces the models to be larger, complicated and expensive. In this paper, our aim was attaining high accuracy while considering simplicity and efficiency for early

diagnosis of heart disease. Based on this motivation, a simple machine learning algorithm DT was employed with SFO algorithm which was utilized to select relevant features in the dataset. After hyperparameter optimization, accuracy score of 98.36% was achieved only with eight selected features from the initial dataset. Even though DT has the lowest score without SFO and hyperparameter tuning, it achieved the highest score at the end due to its simplicity and high flexibility. Further directions for this research would be applying a hyperparameter tuning for heuristic so that same problem could be possibly solved with fewer number of feature or more comprehensive hyperparameter tuning process would be designed to optimize hyperparameters of other ML methods as well.

Conflict of Interest

The authors declare no conflict of interest.

Funding Sources

This research did not receive any specific grant from funding agencies in the public, commercial, or not-for-profit sectors.

References

Ali, M. M., Paul, B. K., Ahmed, K., Bui, F. M., Quinn, J. M., & Moni, M. A. (2021). Heart disease prediction using supervised machine learning algorithms: Performance analysis and comparison. *Computers in Biology and Medicine*, 104672.

Alim, M. A., Habib, S., Farooq, Y., & Rafay, A. (2020). Robust Heart Disease Prediction: A Novel Approach based on Significant Feature and Ensemble learning Model. *2020 3rd International Conference on Computing, Mathematics and Engineering Technologies (iCoMET)*, (pp. 1-5).

Amin, M. S., Chiam, Y. K., & Varathan, K. D. (2019). Identification of significant features and data mining techniques in predicting heart disease. *Telematics and Informatics, 36*, 82-93.

Christy, A., Gandhi, G. M., & Vaithyasubramanian, S. (2015). Cluster Based Outlier Detection Algorithm for Healthcare Data. *Procedia Computer Science, 50*, 209-215.

Detrano, R., Janosi, A., Steinbrunn, W., Pfisterer, M., Schmid, J., Sandhu, S., & Froelicher, V. (1989). International Application of a New Probability Algorithm for the Diagnosis of Coronary Artery Disease. *The American journal of cardiology, 64*(5), 304-310.

Fink, O., Wang, Q., Svensén, M., Dersin, P., Lee, W.-J., & Ducoffe, M. (2020). Potential, challenges and future directions for deep learning in prognostics and health management applications. *Engineering Applications of Artificial Intelligence, 92*, 103678.

Gamberger, D., Lavrač, N., & Krstačić, G. (2003). Active subgroup mining: a case study in coronary heart disease risk group detection. *Artificial Intelligence in Medicine, 28*(1), 27-57.

Garate-Escamila, A. K., Hassani, A. H., & Andres, E. (2020). Classification models for heart disease prediction using feature selection and PCA. *Informatics in Medicine Unlocked, 19*, 1-11.

Géron, A. (2019). Hands-On Machine Learning with Scikit-Learn, Keras, and TensorFlow. Sebastopol, California : O'Reilly Media, Inc.

Goodfellow, I., Bengio, Y., & Courville, A. (2016). *Deep Learning.* Cambridge , Massachusetts: The MIT Press.

Güler, İ., & Übeyli, E. D. (2005). A modified mixture of experts network structure for ECG beats classification with diverse features. *Engineering Applications of Artificial Intelligence, 18*, 845-856.

Jayaraman, V., & Sultana, H. P. (2019). Artificial gravitational cuckoo search algorithm along with particle bee optimized associative memory neural network for feature selection in heart disease classification. *Journal of Ambient Intelligence and Humanized Computing*, 1-10.

Kanagarathinam, K., Sankaran, D., & Manikandan, R. (2022). Machine learning-based risk prediction model for cardiovascular disease using a hybrid dataset. *Data & Knowledge Engineering, 140*, 102042.

Kannan, R., & Vasanthi, V. (2019). Machine Learning Algorithms with ROC Curve for Predicting and Diagnosing the Heart Disease. In *Soft Computing and Medical Bioinformatics* (pp. 63-72). SpringerBriefs in Applied Sciences and Technology.

Khourdifi, Y., & Bahaj, M. (2019). K-Nearest Neighbour Model Optimized by Particle Swarm Optimization and Ant Colony Optimization for Heart Disease Classification. *Studies in Big Data Big Data and Smart Digital Environment, 53*, 215-224.

Long, N. C., Meesad, P., & Unger, H. (2015). A highly accurate firefly based algorithm for heart disease prediction. *Expert Systems with Applications, 42*(21), 1-11.

NG, B. A. (2013). An Intelligent Approach Based on Principal Component Analysis and Adaptive Neuro Fuzzy Inference System for Predicting the Risk of Cardiovascular Diseases. *2013 Fifth International Conference on Advanced Computing (ICoAC)*, (pp. 241-245). Chennai, India.

Rajeswari, K., Vaithiyanathan, V., & Pede, S. V. (2013). Feature Selection for Classification in Medical Data Mining. *International Journal of Emerging Trends & Technology in Computer Science, 2*(2), 492-497.

Reddy, S. C., Nee, S. S., Min, L. Z., Ying, c., & Ying, C. X. (2019). Classification and Feature Selection Approaches by Machine Learning Techniques: Heart Disease Prediction. *International Journal of Innovative Computing, 9*(1), 39-46.

Rodríguez, P., Bautista, M. A., González, J., & Escalera, S. (2018). Beyond one-hot encoding: Lower dimensional target embedding. *Image and Vision Computing, 75*, 21-31.

Saraçoğlu, R. (2012). Hidden Markov model-based classification of heart valve disease with PCA for dimension reduction. *Engineering Applications of Artificial Intelligence, 25*, 1523-1528.

Shadravan, S., Naji, H. R., & Bardsiri, V. K. (2019). The Sailfish Optimizer: A novel nature-inspired metaheuristic algorithm for solving constrained engineering optimization problems. *Engineering Applications of Artificial Intelligence, 80*, 20-34.

Shah, S. M., Batool, S., Khan, I., Ashraf, M. U., Ababs, S. H., & Hussain, S. A. (2017). Feature extraction through parallel Probabilistic Principal Component Analysis for heart disease diagnosis. *Physica A: Statistical Mechanics and its Applications, 482*, 796-807.

Subanya, B., & Rajalaxmi, R. R. (2014). A Novel Feature Selection Algorithm for Heart Disease Classification . *International Journal of Computational Intelligence and Informatics, 4*(2), 117-124.

Tomar, D., & Agarwal, S. (2014). Feature Selection based Least Square Twin Support Vector Machine for Diagnosis of Heart Disease. *International Journal of Bio-Science and Bio-Technology, 6*(2), 69-82.

Uyar, K., & İlhan, A. (2017). Diagnosis of heart disease using genetic algorithm based trained recurrent fuzzy neural networks. *9th International Conference on Theory and Application of Soft Computing, Computing with Words and Perception*, (pp. 588-593). Budapest Hungary.

VanderPlas, J. (2017). *Python Data Science Handbook.* Sebastopol, California : O'Reilly Media Inc.

Vivekanandan, T., & Iyengar, N. C. (2017). Optimal feature selection using a modified differential evolution algorithm and its effectiveness for prediction of heart disease. *Computers in Biology and Medicine*, 125–136.

World Heath Organization. (2018, 05 24). *https://www.who.int*. Retrieved 05 24, 2018, from https://www.who.int/news-room/fact-sheets/detail/the-top-10-causes-of-death

Zhu, G.-N., Hu, J., Qi, J., Ma, J., & Peng, Y.-H. (2015). An integrated feature selection and cluster analysis techniques for case-based reasoning. *Engineering Applications of Artificial Intelligence, 39*, 14-22.

Appendix

Table A: Proposed Feature Selection Approaches from the Literature

Method	Jayaraman, Sultana (2019)	Khourdifi, Bahaj (2019)	Garate-Escamila et al (2020)	SFO_HPO_DT	Uyar,Ilhan (2017)	Malav et al (2017)	Darmawahyuni et al (2019)	Reddy et al (2019)	Satyanandam, Satyanarayana (2019)	N.G. (2013)	Subanya, Rajalaxmi (2014)	Das et al (2009)	Khanna et al (2015)	Bashir et al (2014)
Principal Component Analysis			✓							✓				
Chi-Square			✓											
Correletaion-based Selection		✓						✓						
Min. Redundancy Max. Relevance														
F-score														
Brute Force														
Sailfish Optimizer				✓										
Genetic Algorithm					✓									
Particle Swarm Optimization	✓	✓												
Ant Colony Optimization		✓												
Firefly Optimization														
Artificial Bee Colony Optimization	✓										✓			
Cuckoo Search Optimization	✓													

Method	Long et al (2015)	Amin et al (2019)	Rajeswari et al (2013)	Kannan, Vasanthi (2019)	Alim et al (2020)	Kahramanli, Allahverdi (2008)	Lakshmi et al (2013)	Tomar, Agarwal (2014)	Dwivedi (2018)	Bashir et al (2019)	Revathi, Kavitha (2017)	Shah et al (2017)	Mahmood, Kuppa (2010)	Anooj (2012)
Principal Component Analysis												✓		
Chi-Square														
Correletaion-based Selection			✓		✓									
Min. Redundancy Max. Relevance										✓				
F-score								✓						
Brute Force		✓	✓											
Sailfish Optimizer														
Genetic Algorithm			✓											
Particle Swarm Optimization	✓													
Ant Colony Optimization														
Firefly Optimization														
Artificial Bee Colony Optimization														
Cuckoo Search Optimization	✓													

Table B: Proposed Machine Learning Approaches from the Literature

Method	Jayaraman, Sultana (2019)	Khourdifi, Bahaj (2019)	Garate-Escamila et al (2020)	SFO_HPO_DT	Uyar,Ilhan (2017)	Malav et al (2017)	Darmawahyuni et al (2019)	Reddy et al (2019)	Satyanandam, Satyanarayana (2019)	N.G. (2013)	Subanya, Rajalaxmi (2014)	Das et al (2009)	Khanna et al (2015)	Bashir et al (2014)
Logistik Regression									✓					
K Nearest Neighbors		✓												
Support Vector Machine											✓			✓
Decision Tree				✓										✓
Random Forest			✓					✓						
Naive Bayes														✓
Artificial Neural Network	✓				✓	✓	✓					✓	✓	
Recurrent Neural Network														
K-means						✓								
Linear Discriminant Analysis														
Ensemble Learning												✓		✓
Fuzzy Logic					✓									
ANFIS										✓				
Hyperparameter Optimization				✓										
Cross Validation		✓		✓				✓					✓	✓

Method	Long et al (2015)	Amin et al (2019)	Rajeswari et al (2013)	Kannan, Vasanthi (2019)	Alim et al (2020)	Kahramanli, Allahverdi (2008)	Lakshmi et al (2013)	Tomar, Agarwal (2014)	Dwivedi (2018)	Bashir et al (2019)	Revathi, Kavitha (2017)	Shah et al (2017)	Mahmood, Kuppa (2010)	Anooj (2012)
Logistik Regression				✓					✓	✓				
K Nearest Neighbors														
Support Vector Machine		✓	✓					✓		✓		✓		
Decision Tree													✓	
Random Forest					✓									
Naive Bayes											✓			
Artificial Neural Network						✓								
Recurrent Neural Network														
K-means														
Linear Discriminant Analysis							✓							
Ensemble Learning														
Fuzzy Logic	✓					✓								✓
ANFIS														
Hyperparameter Optimization								✓						
Cross Validation		✓		✓	✓	✓	✓	✓	✓	✓	✓	✓		

Biofuel Production And Ecological Footprint Nexus

Nazlıhan TEKİN[1]
Bilgehan TEKİN[2]

Introduction

The 21st century has witnessed an ever-growing concern for sustainable energy sources and environmental (EN) conservation. In the quest to mitigate climate change, reduce greenhouse gas emissions, and decrease reliance on fossil fuels, biofuel (BF)s have emerged as a promising alternative. These fuels, derived from renewable biological resources such as crops and organic waste, have become a potential solution to our planet's energy and EN challenges. However, the adoption and expansion of BF production have not occurred without consequences, particularly in terms of their ecological footprint (EF). The EF represents a crucial measure of humanity's impact on the environment, quantifying the extent to which human consumption demands natural resources and ecosystem services. It is a metric expressed in global hectares, capturing the ecological space required to support our consumption patterns. The relationship between BF production and EF presents a complex and multifaceted nexus, raising questions about bioenergy systems' sustainability and EN implications. Investigating the relationship between BF production and EF is of paramount importance in the field of EN science and sustainable development. This subject holds significant relevance due to its implications for global energy strategies, climate change mitigation, and the preservation of our planet's ecosystems.

BFs, derived from biomass resources, are positioned as a renewable and sustainable energy source with the potential to mitigate greenhouse gas emissions in a carbon-negative manner (Matsuda & Takeuchi, 2018). Given the increasing demand for energy, especially in the transportation sector, BFs are presented as a viable alternative to fossil fuels (Zahedi et al., 2019; Mizik & Gyarmati, 2021). The transportation sector primarily relies on fossil fuels, significantly contributes to carbon emissions. BFs are proposed to curtail this dependence, enhancing energy security while reducing the EF (Owusu & Asumadu-Sarkodie, 2016). BFs have gained prominence in international trade, with several countries participating in their production. This can help achieve a trade balance by relying more on domestic resources and contributing to global energy security (Takeuchi et al., 2018).

Stoeglehner and Narodoslawsky (2009) suggest that BFs can offer EN benefits compared to fossil fuels. This finding aligns with the potential positive EN impact often associated with BF production, which is a point that your study may also emphasize. The authors emphasized the importance of regional context and EF in assessing BF sustainability. BF sustainability assessments often consider their EF. A study by Hoekman & Broch (2018) discusses the sustainability of BFs and their impact on land use, greenhouse gas emissions, and biodiversity, emphasizing the need for comprehensive analyses to support sustainable BF production. The study by Xue, Pang, and Landis (2014) assesses three agricultural management practices to enhance the EN sustainability of corn-based bioethanol. They employ Life Cycle Assessment (LCA) to compare strategies like no-tillage, manure fertilizer usage, and buffer strips. Findings

[1] PhD, Ankara University
[2] Assoc. Prof., Çankırı Karatekin University

indicate that no-tillage and buffer strips effectively reduce greenhouse gas emissions and nutrient runoff, thereby improving the EN performance of corn-derived ethanol.

Land use change associated with BF production can have profound EN impacts. A research paper by Lapola et al. (2010) examines the EF of different BF feedstocks and underscores the importance of land use choices in mitigating ecological consequences. The study by Phuang et al. (2022) compares the EN impacts of palm biodiesel and large-scale solar systems in Malaysia using life cycle assessment (LCA). It was found that large-scale solar systems outperform palm biodiesel in all damage assessments, with EN hotspots identified in both technologies. The study highlights the importance of considering LCA results in policymaking for Malaysia's energy transition toward renewables, aligning with the national renewable energy implementation roadmap. The study conducted by Canabarro et al. (2023) assessed the production, land use, and EN impacts of ethanol and biodiesel production in developing economies, including Argentina, Brazil, Colombia, and Guatemala. It found that transforming a small percentage of pastures into arable land could significantly increase BF production, while improved raw material productivity could reduce land demand. Ethanol and biodiesel production demonstrated substantial reductions in global warming and energy sustainability compared to gasoline and diesel production, with positive energy ratios. The study also examined the impact of public policies like RenovaBio on the BF supply chain in these countries. Ritu et al. (2023) share several common themes and objectives related to the role of BFs in reducing EFs. They offer a broader discussion of the potential benefits and policy implications of BF adoption. Moreover, in recent years, the use of waste raw materials for biofuel production without the need for land cultivation has come to the fore. These raw materials are non-edible, rich in nutritional content, cheap and sustainable. For this reason, research in the literature has focused on using these materials, called second-generation raw materials, in biofuel production (Singh et al., 2011; Patel et al., 2015).

Lifecycle assessments (LCA) are widely used to evaluate the EF of BFs. The study by Dasan et al. (2019) highlights the potential of microalgae (third-generation raw materials) as a renewable biomass source for BFs due to their rapid growth and high lipid content. However, it emphasizes that sustainable microalgae BF production requires highly optimized systems. The research employs a cradle-to-gate approach to assess different cultivation systems' impact on energy, carbon emissions, and economic factors. Results reveal energy-intensive processes, high capital investments, and negative CO2 balance in traditional microalgae BF production pathways. Sustainable BF production can also be linked to sustainable agricultural practices. A study by Fargione et al. (2008) examines the ecological consequences of BF expansion and suggests strategies for mitigating its impact on ecosystems. BFs have been promoted as a potential solution to reduce greenhouse gas emissions and combat climate change. The study by Reinhard and Zah (2009) evaluates the EN impacts of replacing 1% of Switzerland's diesel consumption with soybean methyl ester (SME) from Brazil or palm methyl ester (PME) from Malaysia. They use a consequential life cycle assessment (LCA) approach to account for future consequences, considering greenhouse gas emissions, land occupation, and various EN indicators. The analysis compares these scenarios to fossil diesel, highlighting the ecological consequences of increased biodiesel consumption in Switzerland.

The expansion of BF production often involves changes in land use, which can lead to deforestation and habitat destruction. A comprehensive review by Koh and Ghazoul (2008) discusses the impacts of BF production on biodiversity, emphasizing the need for research to assess its EF. Understanding these effects is essential for making informed decisions about sustainable land management. BF production competes with food production for agricultural resources. A study by Searchinger et al. (2008) highlights the importance of considering the EF of BFs in the context of food security. Investigating the nexus between BF production and EF

helps policymakers balance energy needs with food production. Sustainable Development Goals (SDGs), such as those set by the United Nations, prioritize EN conservation alongside economic development. Researchers underscore the role of BFs in achieving SDGs and stress the significance of minimizing their EF for long-term sustainability. Policymakers rely on scientific evidence to shape energy and EN policies. A study by Hoogwijk et al. (2003) illustrates the importance of accurate data on BF production and its EN consequences for effective policy formulation. The study by Naqvi et al. (2023) explored the impact of BF and waste energy production on EN degradation (END) in 14 Asia Pacific Economic Cooperation (APEC) nations. Their findings indicate that BF and waste energy production has a negative and significant association with END. Specifically, a 1% increase in BF and waste energy production was associated with a reduction in END by -0.050%. Additionally, their study revealed positive correlations between END and economic development, natural resources, and financial development. They highlighted the need for checks and balances in the financial sector to address END and emphasized the importance of sustainable natural resource use for optimal economic development. Investigating the relationship between BFs and EF provides crucial insights for policy decisions. Research on BFs often involves technological advancements aimed at reducing their EF. For instance, research explores the potential of advanced BFs and emphasises innovation's role in achieving sustainable BF production. Understanding this relationship encourages further research and innovation in the field. These studies highlight various aspects of the relationship between BF production and EF, including sustainability assessments, policy implications, land use change, and the broader context of global energy transition. These studies underscore the importance of conducting comprehensive research in this field to ensure that BF production aligns with EN conservation and sustainability objectives.

In conclusion, the investigation of the nexus between BF production and EF is vital for addressing pressing global challenges, including climate change, biodiversity loss, and sustainable development. Past research has highlighted this relationship's intricate and multifaceted nature, demonstrating the need for comprehensive analysis to inform sound policy decisions, promote sustainability, and advance the bioenergy field. In this study, we embark on a comprehensive exploration of the intricate connection between BF production and EF from 1980 to 2021. To facilitate this investigation, we employ the Autoregressive Distributed Lag (ARDL) Bound test, a robust econometric method suitable for analyzing long-term relationships among variables. The dataset employed for this analysis is sourced from two reputable organizations: the Energy Information Administration (EIA) for world BF production data and the Global Footprint Network for EF statistics. It is essential to note that BF production is measured in million barrels of oil equivalent per day (mb/d), providing a standardized metric for our analysis.

This study aims to uncover the dynamic and evolving relationship between BF production and EF on a global scale, spanning over four decades. By doing so, we intend to contribute to the ongoing discourse on sustainable energy practices, EN conservation, and the imperative to strike a balance between energy security and ecological responsibility. Our investigation seeks to shed light on the dynamic interplay between these two critical factors - BF production and EF - over four decades, with a particular focus on the global context. The findings of this study not only provide valuable insights into the EN consequences of BF production but also offer policymakers and stakeholders a comprehensive understanding of the sustainability challenges and opportunities associated with this industry. This research contributes to the ongoing discourse on sustainable energy practices and the imperative to minimize humanity's EF in the pursuit of a more harmonious coexistence with the natural world. The findings presented herein will deepen our understanding of the BF-ecology nexus and inform policymakers, industry

stakeholders, and researchers on the path towards a more sustainable and environmentally conscious energy future.

Methodology

This study investigates the complex interplay between *BF* production and *EF* over the period from 1980 to 2021. To rigorously examine this relationship, we employed two primary datasets sourced from reputable organizations. World *BF* data were obtained from the Energy Information Administration (EIA), a well-established and authoritative source for global energy statistics. The *EF* data, which quantifies the *EN* demand arising from human consumption, was procured from the Global Footprint Network, recognized for its comprehensive *EF* measurements. The *EF* is expressed in standard units known as global hectares (gha), while *BF* is measured in million barrels of oil equivalent per day (mb/d).

We utilised a two-fold analytical approach to unravel the intricate dynamics between BF production and EF: The Autoregressive Distributed Lag (ARDL) Bound test and the Toda-Yamamoto Granger causality test.

The ARDL Bound test is a robust econometric technique that assesses long-term relationships between variables. In our study, it is employed to examine the existence of cointegration between *BF* and *EF*, which signifies a long-term equilibrium relationship. This test helps to establish whether these two variables are interrelated in the long run. The ARDL Bound test provides critical insights into the direction and strength of the relationship.

To delve deeper into causality, we applied the Toda-Yamamoto Granger causality test. This test is specifically designed to ascertain the direction of causality between two variables. In our case, it aids in determining whether *BF* Granger causes changes in the *EF* or vice versa. This step is essential in deciphering the temporal causality between these two critical factors.

Table 1 shows descriptive statistics. The descriptive statistics for *BF* and *EF* reveal important data characteristics. On average, *BF* production is approximately *6.33* units, with a moderate level of variability as indicated by a standard deviation of approximately *1.08*. The distribution of *BF* data exhibits a slight positive skewness (*0.096*) and relatively light tails (kurtosis of *1.862*), while *the Jarque-Bera* test suggests normality with a probability of *0.312*. In contrast, *EF* has a mean of approximately *0.34*, similar to *BF*, and a lower standard deviation of approximately *0.15*, indicating lower variability. *EF* data display slight negative skewness (*-0.091*) and lighter tails (kurtosis of *1.599*), with a *Jarque-Bera* test probability of *0.174*, also suggesting a normal distribution.

Table 1. Descriptive Statistics

Statistics	**lnBF**	**lnEF**
Mean	6.334337	0.339197
Median	5.856356	0.337617
Maximum	7.927044	0.541291
Minimum	4.168214	0.078635
Std. Dev.	1.075239	0.150186
Skewness	0.095577	-0.090618
Kurtosis	1.861892	1.598545
Jarque-Bera	2.330702	3.494614
Probability	0.311813	0.174243
Observations	42	42

Unit Root Tests

The challenge posed by traditional unit root tests like PP and ADF lies in their inability to detect structural breaks within the data, whether they exist or not. Zivot and Andrews (2002),

however, present a unit root test as a solution to this problem. The Zivot and Andrews test takes into account each data point as a prospective breakpoint (TB) and conducts a regression analysis for each potential breakpoint sequentially. As indicated in Table 2, the results of the Zivot and Andrews unit root test have been displayed. Upon close examination of stationarity with respect to *LNBF* while accounting for structural breaks, it was observed that the test statistics were higher than the critical values. However for *LNEF* series the test statistics were smaller than the critical values. This leads us to the conclusion that while *LNBF* series is stationary at level, *LNEF* exhibits unit roots and is stationary at first differences, I(1).

Table 2. Zivot-Andrews Breakpoint Unit Root

Null Hypothesis: lnBF has a unit root with a structural break in both the intercept and trend		
Chosen lag length: 1 (maximum lags: 4)		
Chosen break point: 2006		
	t-Statistic	Prob. *
Zivot-Andrews test statistic	-5.585630	0.004530
1% critical value:	-5.57	
5% critical value:	-5.08	
10% critical value:	-4.82	
Null Hypothesis: lnEF has a unit root with a structural break in both the intercept and trend		
Chosen lag length: 0 (maximum lags: 4)		
Chosen break point: 2010		
	t-Statistic	Prob. *
Zivot-Andrews test statistic	-4.020904	0.066766
1% critical value:	-5.57	
5% critical value:	-5.08	
10% critical value:	-4.82	
Null Hypothesis: DlnEF has a unit root with a structural break in both the intercept and trend		
Chosen lag length: 1 (maximum lags: 4)		
Chosen break point: 1994		
	t-Statistic	Prob. *
Zivot-Andrews test statistic	-6.460901	0.007845
1% critical value:	-5.57	
5% critical value:	-5.08	
10% critical value:	-4.82	

To determine unit root with structural breaks, we apply also another unit root test called Dickey-Fuller min-t. Null hypothesis in this test is the variable has a unit root. Table 3 reports the results of the Dickey-Fuller min-t breakpoint unit root test. The test results confirm the Zivot and Andrews (2002) test.

Table 3. Dickey-Fuller min-t method Breakpoint Unit Root

Null Hypothesis: lnBF has a unit root			
Break Date: 2005			
	Augmented Dickey-Fuller test statistic	t-Statistic	Prob.*
		-6.292065	< 0.01
	1% level	-5.347598	
Test critical values:	5% level	-4.859812	
	10% level	-4.607324	
Null Hypothesis: lnEF has a unit root			
Break Date: 2003			
	Augmented Dickey-Fuller test statistic	t-Statistic	Prob.*
		-3.920109	0.4230
Test critical values:	1% level	-5.347598	

	5% level	-4.859812
	10% level	-4.607324

Null Hypothesis: D(lnEF) has a unit root
Break Date: 1992

		t-Statistic	Prob.*
Augmented Dickey-Fuller test statistic		-7.054524	< 0.01
Test critical values:	1% level	-5.347598	
	5% level	-4.859812	
	10% level	-4.607324	

Notes: *Trend Specification: Trend and intercept; Break Specification: Intercept only; Break Type: Innovational outlier; Break Selection: Minimize Dickey-Fuller t-statistic; Lag Length: 1; Automatic - based on Schwarz information criterion*

The coefficient of ARDL bound test long-run form represents the estimated long-run relationship or the long-run effect of the ln*EF* variable on the ln*BF* variable. The coefficient value indicates the estimated change in the dependent variable (ln*BF*) for a one-unit change in the independent variable (ln*EF*), holding all other factors constant. Since the coefficient is positive, it implies a positive relationship between ln*EF* and ln*BF* production in the long run. This means that ln*BF* production is also expected to increase as the ln*EF* increases, and vice versa. It's essential to assess whether this coefficient is statistically significant. Low p-values (typically less than *0.05*) indicate statistical significance. The ARDL bound test long-run form represents the estimated long-term effect of the ln*EF* variable on the variable (ln*BF*), indicating a positive relationship between the two variables in the long run.

The results obtained from analysis using the ARDL bound test, Toda-Yamamoto causality test, and Error Correction Model (ECM) have important implications for understanding the relationship between *EF* and *BF* production. Co-integration suggests a long-term relationship between the variables under investigation. In this study, it indicates that there is a stable and enduring relationship between *EF* and *BF* production over the period (1980-2021). This implies that changes in one variable have a lasting impact on the other, and they tend to move together in the long run. Finding causality in analysis means that one of the variables is causing changes in the other. If *BF* production causes changes in *EF*, or vice versa, it suggests a directional relationship. For example, if the Toda-Yamamoto causality test indicates that *BF* causes changes in *EF*, it suggests that as BF production increases or decreases, it influences the *EF*. The Error Correction Model is used to explore the short-term dynamics of the relationship between variables after co-integration has been established. It helps to understand how quickly the system adjusts to long-term equilibrium. The fact that *ECt* is negative and significant at the *1%* level indicates a mechanism exists to correct any deviations from the long-term equilibrium relationship between *EF* and *BF* production. In other words, if there is a short-term disturbance or shock that pushes the system away from its long-term equilibrium, it will be corrected relatively quickly.

Overall, these results suggest that there is a meaningful and statistically significant relationship between *EF* and *BF* production. The co-integration implies a long-term connection, the causality suggests a directional influence between the two variables, and the negative and significant *ECt* in the *ECM* signifies a correction mechanism that brings the system back to its long-term equilibrium. These findings provide valuable insights into how changes in BF production can affect the EF and vice versa, which is crucial for policymakers and stakeholders aiming to balance energy production with *EN* sustainability.

The ARDL Bound Test results with natural logarithmic values provide crucial insights into the long-term relationship between *BF* and *EF*. The F-statistic, standing at *7.7052*, surpasses the critical values at all conventional significance levels. This indicates the presence of a

cointegrating relationship between *BF* and *EF*, implying a long-term equilibrium relationship even when considering the natural logarithmic transformations of the variables.

In the levels equation, the coefficient of the natural logarithm of *EF* is estimated at *6.5111* with a standard error of *0.4315*, yielding a t-statistic of *15.0907*. This coefficient signifies that for every percent increase in the natural logarithm of EF, BF production increases by approximately *6.5111* units of oil equivalent per day. The intercept (C) is estimated at *4.2977* with a standard error of *0.1855*, exhibiting a t-statistic of *23.1649*. This constant term represents the *BF* when the natural logarithm of *EF* is zero. The error correction term (EC) is calculated as the difference between *BF* and its long-term equilibrium value.

Additionally, the error correction model (ECM) provides insights into the short-term dynamics of the relationship. Notably, the coefficient of the first-differenced natural logarithm of *BF* lagged by one period *(D(BF(-1)))* is *0.6410* with a standard error of *0.0853*, resulting in a t-statistic of 7.5142. This coefficient reflects the speed of adjustment toward the long-term equilibrium after deviations. *D(EF)* and *D(EF(-1))* denote the first-differenced natural logarithm of *EF* and its lagged value, respectively. These variables showcase short-term impacts on *BF* production.

The *CointEq(-1)** term represents the lagged value of the error correction term. It carries a coefficient of *-0.1995* with a standard error of *0.0403*, yielding a t-statistic of *-4.9473*. This coefficient signifies the short-term influence of deviations from the long-term equilibrium on *BF* production.

Table 4. ARDL Bound Test Results

Test	**Value**
F-Statistic	7.7052
F-Bounds Test (Critical Values)	
k (Lags)	1
10%	*3.02*
5%	*3.62*
2.5%	*4.18*
1%	*4.94*

Table 5: ARDL Long-term Coefficients

Variable	**Coefficient**	**Std. Error**	**t-Statistic**	**Prob.**
lnEF	6.5111	0.4315	15.0907	0.0000
C	4.2977	0.1855	23.1649	0.0000
EC = BF - (6.5111*EF + 4.2977)				

Table 6. Error Correction Model (ECM) Regression

Variable	**Coefficient**	**Std. Error**	**t-Statistic**	**Prob.**
D(lnBF(-1))	0.6410	0.0853	7.5142	0.0000
D(lnEF)	1.0629	0.4359	2.4384	0.0201
D(lnEF(-1))	-1.6130	0.5058	-3.1890	0.0031
CointEq(-1)*	-0.1995	0.0403	-4.9473	0.0000

Toda-Yamamoto Granger Causality Test

Following the completion of the ARDL Bound Test and the establishment of a cointegrating relationship between *BF* production and *EF*, the next analytical step involves conducting the Toda-Yamamoto Granger Causality Test. This sequential analytical approach is motivated by several key reasons. Firstly, the ARDL Bound Test primarily serves to ascertain the presence of a long-term equilibrium relationship between the variables under investigation, namely *BF* and *EF*. While this test is instrumental in revealing the existence of a stable and integrated relationship, it does not inherently address the issue of causality. Therefore, it becomes imperative to employ a suitable causality test to elucidate the direction and nature of causality between the variables. Secondly, the Toda-Yamamoto Granger Causality Test is particularly well-suited for this analysis due to its ability to accommodate cases where variables exhibit cointegration, as is the case here. The test allows for the examination of both short-term and long-term causal relationships, which is essential for a comprehensive understanding of how changes in one variable influence the other over time. In addition, this causality test provides robustness to potential omitted variable bias, endogeneity issues, and the presence of lagged effects. By rigorously examining the causal linkages between *BF* and *EF*, the Toda-Yamamoto Granger Causality Test ensures that the conclusions drawn from the analysis are grounded in sound statistical methods.

In this section, we will interpret and discuss *the Wald test* results, which assess causality from *EF* to *BF* and from *BF* to *EF* separately. *The Wald test* provides valuable insights into the influence that changes in one variable exert on the other, shedding light on the intricate interplay between *BF* and *EF*. *The Wald test* results for *Toda-Yamamoto Granger causality* analysis reveal important insights into the causal relationship between *BF* and *EF*.

For causality from *EF* to *BF* the test statistic is *14.75487* and the p-value is *0. 000625*.These results indicate that there is strong evidence to suggest that *EF* Granger causes changes in *BF*. In other words, variations in *EF* appear to have a statistically significant influence on the fluctuations in *BF* over time. The low p-value (*0.000625*) suggests a high level of statistical significance, reinforcing the validity of this causal relationship. For causality from *BF* to *EF* the test statistic is *6.313004* and the p-value is *0.042574*. In contrast, the results for causality from *BF* to *EF* indicate a somewhat weaker, but still statistically significant relationship.

The first set of results (*EF to BF*) suggests that *EF* plays a significant role in driving changes in *BF* production. This is of particular significance in the context of *EN* sustainability, as it implies that efforts to reduce *EF*, such as through eco-friendly practices or resource conservation, can influence the production of *BFs*. The second set of results (*BF* to *EF*) suggests that there is also a statistically significant causal relationship in the opposite direction, albeit with a slightly weaker statistical significance compared to the first test. This implies that changes in BF production can influence *EF*. This could be due to factors such as the *EN* impact of *BF* production processes or the use of *BFs* as a more environmentally friendly energy source, leading to changes in *EF*.

Table 7. Toda Yamamoto Granger Causality / Wald Test

	LNEF ⟹ LNBF	
Test Statistic	Value	Probability
Chi-square	14.75487	0,000625
	LNBF ⟹ LNEF	
Test Statistic	Value	Probability
Chi-square	6.313004	0,042574

Diagnostic tests in statistics and econometrics are tools used to assess the validity and assumptions of regression models, helping researchers and analysts identify potential issues or problems with the model's underlying assumptions. In this study the diagnostic test results suggest that our ARDL model has a high *R-squared* value (*0.9948*), indicating strong explanatory power. *The Durbin-Watson* test shows little to no significant autocorrelation in the residuals (*2.0463*), a favorable result. *The Jarque-Bera* test for normality (*0.0650, p=0.9680*) suggests that the residuals may follow a normal distribution. Both *heteroskedasticity* tests, *Breusch-Pagan-Godfrey* (*1.0832, p=0.3872*) and Harvey (*1.3302, p=0.2751*), indicate that we do not have strong evidence to reject the null hypothesis of homoskedasticity, which is a positive finding. *The Breusch-Godfrey LM* test (*0.2066, p=0.8144*) also does not provide evidence of autocorrelation. *The Ramsey Reset Test* (*F-statistic 2.7050, p=0.0625*) suggests that there might be room for improvement in the model's specification, although this result is not statistically significant at the conventional *0.05* significance level.

Table 8. Diagnostic Tests

Tests	**Coeff/prob.**
R^2	0.994806
Durbin–Watson test	2.0463
Jarque–Bera test for normality	0.0650 (0.9680)
Heteroskedasticity Test: Breusch-Pagan-Godfrey	1.083161 (0.3872)
Heteroskedasticity Test: Harvey	1.330151 (0.2751)
Breusch–Godfrey LM test	0.206595 (0.8144)
Ramsey Reset Test (F-İstatistik)	2.705035 (0.0625)

The CUSUM (Cumulative Sum) and CUSUM Square graphs are useful for detecting structural breaks or changes in the relationship between variables. In this study used for monitoring the stability of coefficients in your ARDL model. As seen in Graph 1, both the CUSUM and CUSUM Square lines fall within the *5%* significance limits. It implies that our ARDL model is stable, and there is no strong evidence of significant changes in the relationship between *BF* production and *EF* over the studied time period. This result suggests that the chosen model adequately captures the dynamics of the variables under investigation.

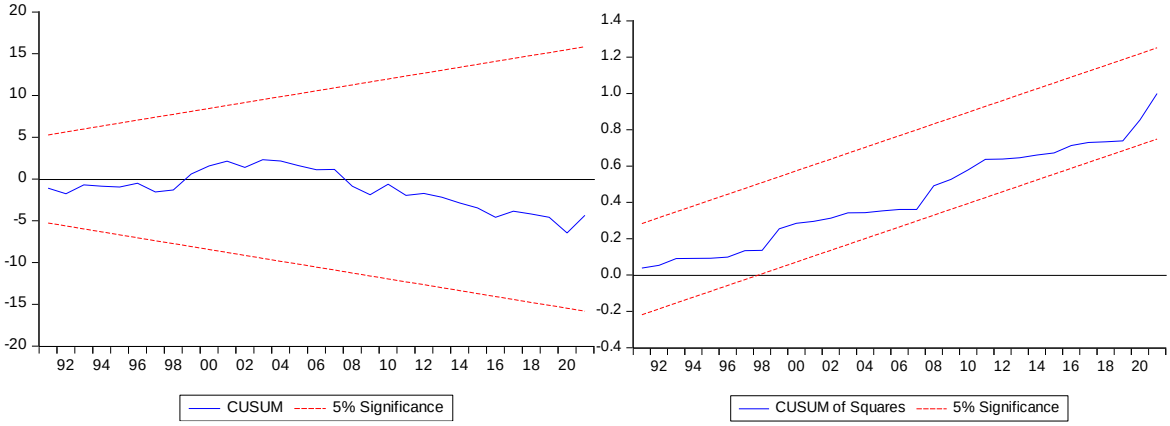

Graph 1. Cusum & Cusum Square Bounds

Conclusion

The results of the ARDL Bound Test with natural logarithmic values confirm the existence of a long-term cointegrating relationship between *BF* production and *EF*. The positive coefficient of the natural logarithm of *EF* in the levels equation underscores the direct and substantial impact of *EF* on *BF* production, even after accounting for logarithmic transformations. This implies that as human demand on natural resources, as indicated by the

EF, increases proportionally, *BF* production also rises, aligning to mitigate ecological impact through sustainable energy sources.

Furthermore, the ECM results reveal the presence of short-term dynamics in the relationship. The positive coefficient of *D(lnBF(-1))* suggests that deviations from the long-term equilibrium are corrected at a rate of *0.6410* in the following period, highlighting the role of feedback mechanisms in maintaining equilibrium. The coefficients of *D(lnEF)* and *D(lnEF(-1))* indicate short-term impacts of changes in the natural logarithm of *EF* on *BF* production, emphasizing the need for timely adjustments.

The negative coefficient of the lagged error correction term (*CointEq(-1)**) underscores the significance of short-term deviations in influencing *BF* production, even when considering natural logarithmic transformations. These deviations may result from various factors such as policy changes, market fluctuations, or *EN* events.

These findings underscore the dynamic and bidirectional relationship between *BF* production and *EF*. Policymakers and researchers should consider both directions of causality when formulating strategies for sustainable bioenergy production and *EN* conservation. Efforts to reduce *EF* may contribute to increased *BF* production, while *BF* production practices can also impact ecological sustainability. It's worth noting that the statistical significance of the second test (*BF* to *EF*) is slightly weaker, but still below conventional significance levels ($p < 0.05$).

Building upon the foundation of co-integration, we further explored the causal dynamics between *BF* and *EF* using the Toda-Yamamoto Granger Causality Test. This rigorous analysis allowed us to unveil causality's direction and statistical significance.

Intriguingly, the Toda-Yamamoto Granger Causality Test results revealed bidirectional causality between *BF* and *EF*, shedding light on the intricate interplay between these variables. This finding underscores the pivotal role of *EF* in influencing *BF* production, emphasizing the importance of ecological sustainability practices in shaping bioenergy production. Conversely, the analysis also unveiled that *BF* Granger causes changes in *EF*, albeit with slightly weaker statistical significance. This result suggests that the dynamics of *BF* production can have a discernible impact on *EF*, potentially through the *EN* implications of *BF* production processes or the adoption of *BFs* as a greener energy source. Wald test results provide valuable insights into the causal dynamics between *BF* production and *EF*, highlighting the interplay between these two crucial aspects of *EN* and energy sustainability.

The co-integration and causality analyses collectively offer a comprehensive view of the relationship between *BF* production and *EF*. The presence of co-integration confirms the existence of a long-term equilibrium, while the bidirectional causality highlights the dynamic nature of this relationship. These findings hold significant implications for sustainable energy and *EN* policies. Efforts to reduce *EF* through eco-friendly practices, resource conservation, and sustainable consumption can influence the production of *BFs*. Conversely, *BF* production practices can also impact ecological sustainability. This bidirectional causality underscores the need for integrated strategies promoting *EN* conservation and renewable bioenergy production.

The findings of this study offer valuable insights into the complex relationship between *BF* production and *EF*. Our study and Ravindranath et al.'s (2011) research converge on the importance of a comprehensive and sustainable approach to *BF* production. While our research provides insights into the bidirectional causality between *BF* production and *EF*, Ravindranath et al. (2011) offer a detailed assessment of the implications of large-scale *BF* production in India. Together, these findings emphasize the need for evidence-based policy formulation that considers the complex interactions between *BF* production, land use, food security, water

resources, biodiversity, rural development, and *EN* sustainability in the pursuit of a greener energy landscape.

Results also align with the broader discussions in the literature, as Sharma et al. (2020) exemplified in their comprehensive review on sustainable *EN* management and *BF* technologies. Both studies share a common thread in recognizing the importance of transitioning towards renewable and environmentally sustainable energy sources to mitigate the challenges posed by rising energy demands and *END*. Our study's findings, which reveal a bidirectional causality between BF production and *EF*, resonate with the broader sustainability discourse exemplified by Sharma et al. (2020). Both studies underscore the vital role of *BFs*, such as bioethanol and biodiesel, as versatile alternatives for sustainable energy needs. While Sharma et al. (2020) primarily focus on sustainability criteria and process improvements, our research uniquely contributes by uncovering the dynamic relationship between *BF* production and *EF*. These shared insights emphasize the significance of holistic approaches to promote both economic and *EN* viability in the *BF* industry, aligning with the global pursuit of clean and sustainable energy solutions.

The recent study by Naqvi, Hussain, and Ali (2023) explored the influence of *BF* and waste energy production on *END* in Asia Pacific Economic Cooperation (APEC) nations. Their findings indicate a negative association between BF and waste energy production and *END*, aligning with our results. They report that a 1% increase in *BF* and waste energy production reduces *END*, thereby highlighting the potential for BFs to mitigate adverse *EN* outcomes. However, there are notable distinctions in the *EN* indicators examined in our study and that of Naqvi et al. (2023). While our study delves into *EF*, Naqvi et al. (2023) focus on END. This variance underscores the multifaceted nature of the *EN* impact of bioenergy production, with both studies providing valuable insights into different dimensions of this relationship. Our study contributes to understanding the dynamic relationship between BF production and *EF*, complementing Naqvi et al.'s (2023) emphasis on *END*. Collectively, these findings emphasize the complex interplay between bioenergy production and *EN*.

This study provides empirical evidence of the intricate interplay between *BF* production and *EF*, offering valuable insights for policymakers, researchers, and stakeholders in the pursuit of a more sustainable and eco-friendly energy landscape. The bidirectional causality underscores the importance of holistic approaches to *EN* and energy sustainability. This analysis provides robust evidence of the interconnectedness between *BF* production and *EF*, considering natural logarithmic transformations of the variables. It underscores the pivotal role of *BFs* in mitigating ecological impact while meeting growing energy demands, even in a logarithmic context. Policymakers and stakeholders should consider this study's long-term and short-term dynamics when formulating strategies for sustainable energy and *EN* management. Further research may be warranted to explore the mechanisms and drivers behind this co-integration and causal relationships to inform targeted interventions and policies.

References

Canabarro, N. I., Silva-Ortiz, P., Nogueira, L. A. H., Cantarella, H., Maciel-Filho, R., & Souza, G. M. (2023). Sustainability assessment of ethanol and biodiesel production in Argentina, Brazil, Colombia, and Guatemala. Renewable and Sustainable Energy Reviews, 171, 113019

Dasan, Y. K., Lam, M. K., Yusup, S., Lim, J. W., & Lee, K. T. (2019). Life cycle evaluation of microalgae biofuels production: Effect of cultivation system on energy, carbon emission and cost balance analysis. Science of the total environment, 688, 112-128.

Fargione, J., et al. (2008). Land clearing and the biofuel carbon debt. Science, 319(5867), 1235-1238.

Hoekman, S. K., & Broch, A. (2018). Environmental implications of higher ethanol production and use in the US: A literature review. Part II–Biodiversity, land use change, GHG emissions, and sustainability. Renewable and Sustainable Energy Reviews, 81, 3159-3177.

Hoogwijk, M., et al. (2003). Exploration of the ranges of the global potential of biomass for energy. Biomass and Bioenergy, 25(2), 119-133.

Koh, L. P., & Ghazoul, J. (2008). Biofuels, biodiversity, and people: Understanding the conflicts and finding opportunities. Biological Conservation, 143(5), 1307-1313.

Lapola, D. M., et al. (2010). Indirect land-use changes can overcome carbon savings from biofuels in Brazil. Proceedings of the National Academy of Sciences, 107(8), 3388-3393.

Matsuda, H., & Takeuchi, K. (2018). Approach to biofuel issues from the perspective of sustainability science studies. Science for Sustainable Societies, 11–15. https://doi.org/10.1007/978-4-431-54895-9_2

Mizik, T., & Gyarmati, G. (2021). Economic and sustainability of biodiesel production—A systematic literature review. Clean Technologies, 3(1), 19–36. https://doi.org/10.3390/cleantechnol3010002

Naqvi, S. A. A., Hussain, B., & Ali, S. (2023). Evaluating the influence of biofuel and waste energy production on environmental degradation in APEC: Role of natural resources and financial development. Journal of Cleaner Production, 386, 135790

Owusu, P. A., & Asumadu-Sarkodie, S. (2016). A review of renewable energy sources, sustainability issues and climate change mitigation. Cogent Engineering, 3(1). https://doi.org/10.1080/23311916.2016.1167990

Patel, A., Sindhu, D. K., Arora, N., Singh, R. P., Pruthi, V., & Pruthi, P. A. (2015). Biodiesel production from non-edible lignocellulosic biomass of Cassia fistula L. fruit pulp using oleaginous yeast Rhodosporidium kratochvilovae HIMPA1. Bioresource Technology, 197, 91-98.

Phuang, Z. X., Lin, Z., Liew, P. Y., Hanafiah, M. M., & Woon, K. S. (2022). The dilemma in energy transition in Malaysia: A comparative life cycle assessment of large scale solar and biodiesel production from palm oil. Journal of Cleaner Production, 350, 131475.

Ravindranath, N. H., Lakshmi, C. S., Manuvie, R., & Balachandra, P. (2011). Biofuel production and implications for land use, food production and environment in India. Energy policy, 39(10), 5737-5745.

Reinhard, J., & Zah, R. (2009). Global environmental consequences of increased biodiesel consumption in Switzerland: consequential life cycle assessment. Journal of Cleaner Production, 17, S46-S56.

Ritu, J. R., Khan, S., Ambati, R. R., & Gokare Aswathanarayana, R. (2023). Biofuels an option for reducing ecological footprint. In Biofuels in circular economy (pp. 89-101). Singapore: Springer Nature Singapore.

Searchinger, T., et al. (2008). Use of U.S. croplands for biofuels increases greenhouse gases through emissions from land-use change. Science, 319(5867), 1238-1240.

Singh, A., Olsen, S. I., & Nigam, P. S. (2011). A viable technology to generate third-generation biofuel. Journal of Chemical Technology & Biotechnology, 86(11), 1349-1353.

Sharma, S., Kundu, A., Basu, S., Shetti, N. P., & Aminabhavi, T. M. (2020). Sustainable environmental management and related biofuel technologies. Journal of Environmental Management, 273, 111096

Stoeglehner, G., & Narodoslawsky, M. (2009). How sustainable are biofuels? Answers and further questions arising from an ecological footprint perspective. Bioresource technology, 100(16), 3825-3830.

Xue, X., Pang, Y., & Landis, A. E. (2014). Evaluating agricultural management practices to improve the environmental footprint of corn-derived ethanol. *Renewable energy*, *66*, 454-460.

Zahedi, S., Batista-Foguet, J. M., & van Wunnik, L. (2019). Exploring the public's willingness to reduce air pollution and greenhouse gas emissions from private road transport in Catalonia. Science of the Total Environment, 646, 850–861. https://doi.org/10.1016/j.scitotenv.2018.07.361

Unlocking Aircraft System Health Management Insights: Data Mining and Digital Twin Technology

Oğuz BEKTAŞ[1]

Introduction

Aircraft System Health Management (ASHM) has become a crucial field in aviation, aiming to enhance the safety, reliability, and efficiency of aircraft operations. This paper explores the collaborative potential of data mining techniques and Digital Twin technology in uncovering valuable insights within ASHM. Data mining methods involve specialized algorithms designed for data analysis, enabling them to extract patterns and categorize data effectively (Elias, 2003). In the aviation context, these datasets comprise sensor data, maintenance records, and flight data, providing profound insights into aircraft system behaviour and performance.

At the same time, Digital Twin technology creates a dynamic, real-time virtual model of an aircraft, facilitating the monitoring and analysis of its physical counterpart (Singh et al., 2021). By combining data mining with Digital Twin technology, a comprehensive ASHM framework can be developed, promoting a proactive approach to aircraft maintenance and operational decision-making. This approach leads to reduced downtime, improved safety, and more efficient operational costs.

This paper demonstrates the potential application of data mining techniques in ASHM, including machine learning algorithms, anomaly detection, and predictive analytics. It also delves into the development of Digital Twins for aircraft systems, outlining their key components and the integration of real-time data streams. Case studies and practical examples illustrate the successful implementation of this integrated approach in the aviation industry.

The paper underscores how data mining and Digital Twin technology can provide new insights into aircraft system behaviour, enabling predictive maintenance, optimizing operations, and ultimately enhancing safety and reliability in aviation. This research sets the stage for the future of ASHM, underscoring the significance of advanced data-driven solutions in an era of increasingly complex and interconnected aviation systems.

Data Mining and Its Role in ASHM

When dealing with data mining, a typical process includes collecting, refining, processing, analysing, and extracting valuable insights from data. In practical scenarios, there's a significant diversity in the aspects of interest, applications, techniques, and data formats encountered. As a result, "data mining" serves as a broad term that covers all these different aspects of working with data (Aggarwal, 2015).

Although the literature may offer diverse classifications for the Data Mining process, the major stages encompass the following (see Figure 1):

- **Data Collection:** In this initial stage, the acquisition and gathering of data from various sources are undertaken. This step is crucial to provide the necessary data set for subsequent analysis.

[1] Öğretim Görevlisi Dr, İstanbul Medeniyet Üniversitesi

- **Data Exploration:** At this phase, a careful examination of the data characteristics of conducted, with a focus on a specific problem statement. This analytical effort may require querying, visualization, and reporting techniques to unravel insights from the data.
- **Feature Selection:** This phase involves intelligently selecting relevant features from the dataset. The process is driven by the goal of improving the efficiency and effectiveness of the modelling process by preserving only those attributes that have significant discriminatory features.
- **Data Modelling**: From now on, it is of great importance to choose appropriate modelling techniques in comparison with the prepared data.
- **Deployment**: The final stage involves evaluating the model results against predefined goals. This evaluation process may lead to the emergence of new requirements that can be attributed to new patterns noticed in the model results or other influencing factors.

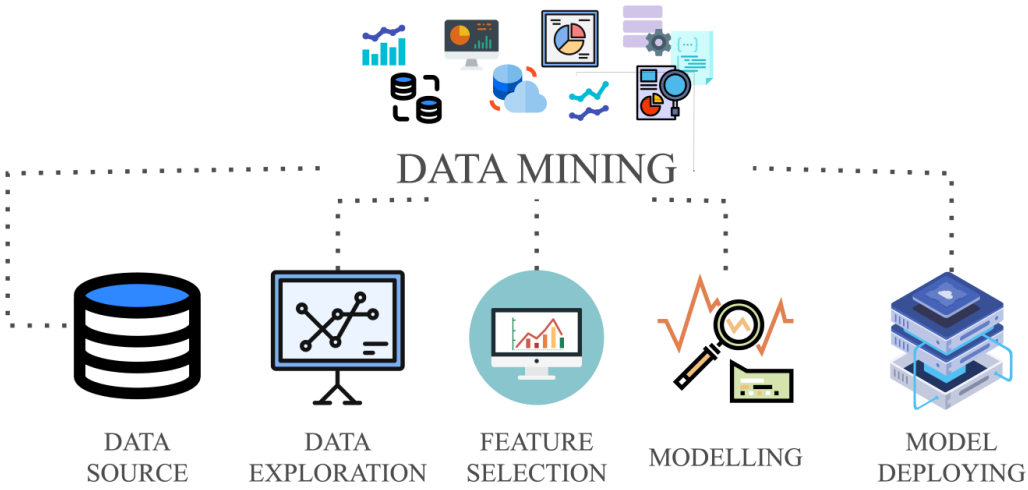

Figure 1. Main Stages of Data Mining

These stages of data mining play a crucial role in ASHM by leveraging a structured approach to extract valuable insights from the vast and diverse data generated by aircraft systems. In the first stage, data is obtained from various sources such as sensors, maintenance records and flight data. These collected data form the basis of subsequent analysis. Next comes Data Exploration, where analysis and interpretation of large amounts of data generated by an aircraft's numerous sensors and tracking systems. By examining this data, next stages can gain valuable information about the health and performance of the systems. This is followed by selecting the most relevant and informative features which is crucial for effective analysis and decision making.

By identifying and prioritizing specific data features, one can streamline the processing of large data sets and focus on indicators that are most indicative of potential problems or anomalies. This process not only reduces the computational burden, but also improves the ability to detect and respond to potential maintenance or safety issues, ultimately contributing to the overall safety and reliability of aircraft operations. Finally, Data Modelling step helps create predictive models and identify potential problems in aircraft systems and its deployment evaluates results of the model against predefined goals. This assessment has the potential to reduce downtime, enhance safety, and optimize operational costs.

The Synergy of Digital Twin Technology

Another transformative technology that has emerged to support ASHM along with data mining is Digital Twin technology. This innovative concept involves creating a dynamic, real-time virtual model of an aircraft. This digital twin mirrors its physical counterpart in nearly every aspect, offering a highly accurate representation of the aircraft's current state.

A Digital Twin is a highly detailed and probabilistic simulation of a real vehicle or system that uses advanced physical models, sensor data, fleet history, and more to closely replicate the performance and characteristics of its real-world counterpart; It covers critical and interconnected systems. airframe, propulsion, energy storage, life support, avionics and thermal protection (Glaessgen, E., & Stargel 2012). The concept of 'digital twins' was introduced in a presentation by Grieves in 2003, according to (Grieves 2014). Since then, it caught the interest of both researchers and businesses, and a lot of work has been done in this field (You et al. 2022). Over time, research has expanded into domains such as predictive maintenance (Aivaliotis et al. 2019, Liu et al. 2018, You et al. 2022) and holds promise for the broader field of system health management, with a particular emphasis on aircraft systems, showcasing significant advancements.

The potential of ASHM (Aircraft System Health Management) performance can be further optimized through the integration of data mining techniques and Digital Twin technology. This collaborative fusion holds paramount significance, offering a comprehensive approach that not only enhances well-being but also ensures the sustainability of aircraft system performance. Consequently, it can establish a holistic ASHM framework by merging data mining methods with Digital Twins. This framework has the potential to enable a proactive approach to aircraft maintenance, operational decision-making, and even crisis management. Its unique capability to detect anomalies and predict potential failures translates into reduced downtime, heightened security, and more cost-efficient operations. The resulting savings, in terms of both time and resources, possess the potential to be substantial, ultimately reshaping the aviation industry.

Case Studies and Practical Examples

To make these concepts more concrete and practical, this article cites two examples of data utilization within the context of a digital twin framework that vividly demonstrate the successful application of this integrated approach in the aviation industry. These case studies provide a window into the tangible benefits that arise from combining data techniques with Digital Twin technology, providing a new perspective on understanding the behaviour of aircraft systems.

These examples can shed light on the capacity to collect, process and analyse significant amounts of data in real time and highlight how the integration of this data into Digital Twins improves our understanding of complex aircraft systems.

By examining these real-world scenarios, readers can gain insight into how this integrated approach supports predictive maintenance, proactive decision-making, and crisis management. As these case studies emerge, they offer a glimpse into the unique potential of digital representation of a physical object, individual, or process embedded in a digital representation of its environment. This digital twin concept facilitates the simulation of systems and their outcomes, enabling decision makers to make more informed and effective choices.

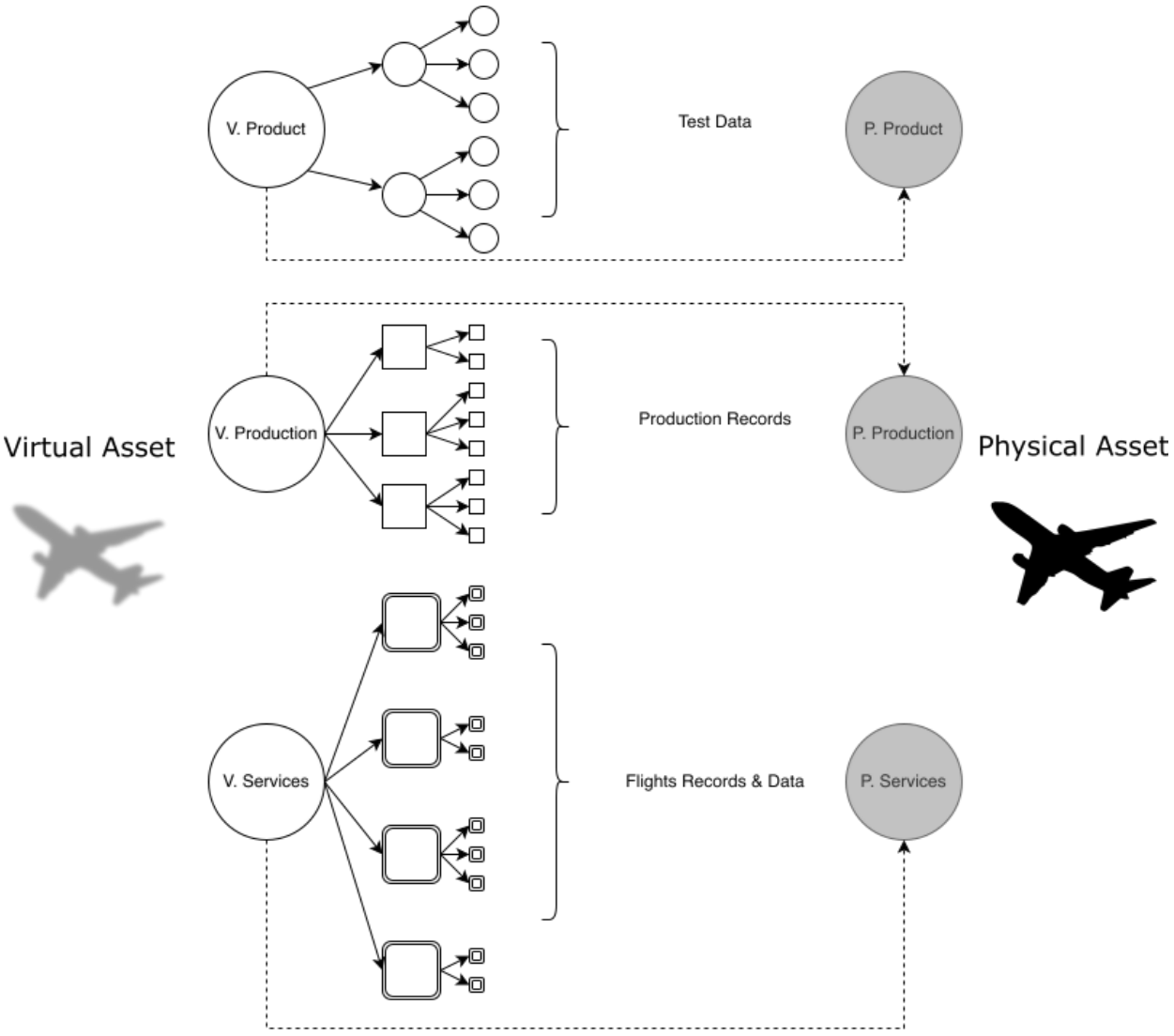

Figure 2. Depiction of the Digital Twin Paradigm in the Aviation Industry (AIAA 2020)

The study presented by AIAA (2020) addresses the DIGITAL TWIN concept and the increasing complexity of aerospace systems that surpass traditional development methods. The article, which claims that this increasing complexity has led to a significant rise in costs associated with traditional aerospace processes maintenance, explores the potential of virtual capabilities that can simulate physical environments with increasing precision and efficiency to overcome these challenges.

The main focus is on the concept of Digital Twin as shown in Figure 2 adapted from the original source. Visually, a Digital Twin represents a connected physical asset throughout its entire lifecycle, enabling the migration of work from physical to virtual space and providing predictive insights into asset conditions AIAA (2020). This transition promises significant resource savings, especially in system health management and its sub-branches.

Developed jointly by academia, industry, and government stakeholders, the document of AIAA (2020) has four goals:

- create a common understanding of the Digital Twin for the Aerospace community
- demonstrate its applications and value by example,
- examine its alignment between Aerospace industry's perspective on Digital Twin and

- identify future priorities and tasks to explore achieving value through the use of Digital Twins

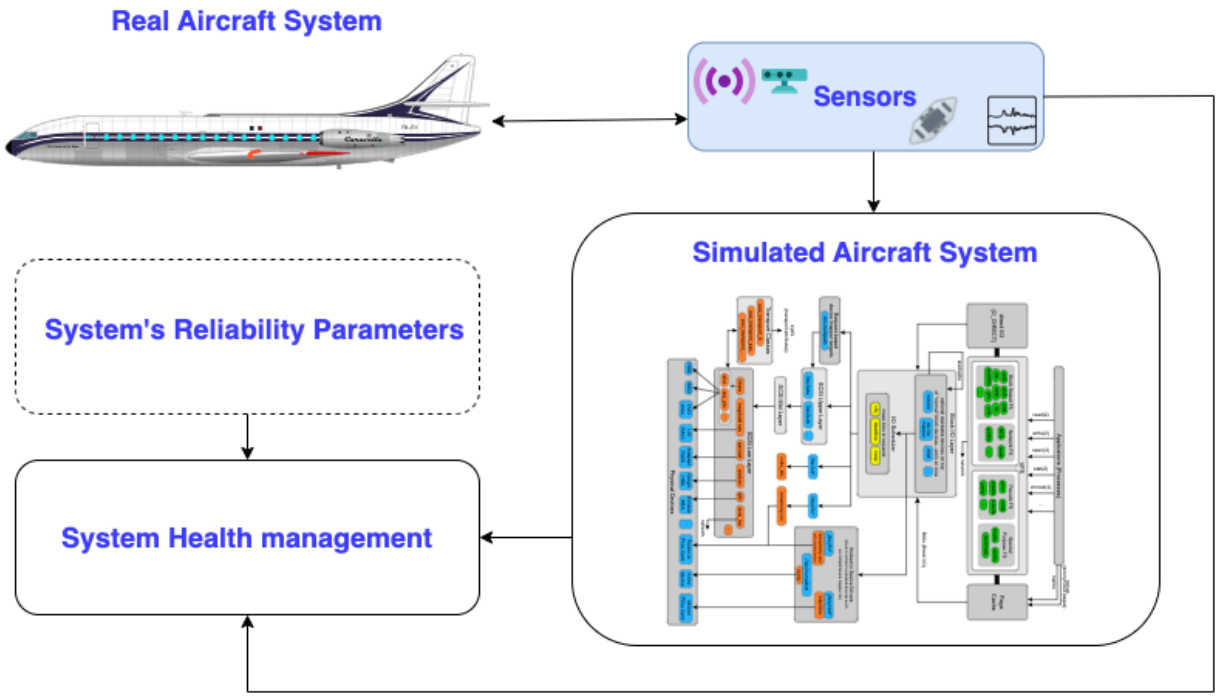

Figure 3. Grafik Adı (Aivaliotis, 2019)

In a similar study, Aivaliotis et al. (2019) suggest that using static digital models to generate the data necessary to estimate the remaining useful life (RUL) of systems, a critical component of system health management, is not recommended due to potential changes in the actual state of the machine. To solve this problem, they suggest that data generated by simulating digital models must be constantly updated with real-world data to ensure accurate RUL prediction. As a solution, they introduced a Digital Twin model for predictive maintenance to calculate the RUL of systems in a manufacturing facility. This calculation is based on the combined analysis of data from the real system and physics-based simulation, as shown in Figure 3 adapted from Aivaliotis et al. (2019).

Their work consists of several basic stages:

- Improved physical modelling of systems.
- Ongoing fine-tuning of simultaneous simulation of physics-based machine models. This continuous adjustment is important as simulation is used for RUL calculations and deviations between actual and simulated functionality need to be minimized.
- Simulation of physics-based models using data collected from sensors and the system.
- In the final stage, integration of simulation results with monitored machine data to estimate the RUL of the machines. The reliability parameters of the machines are integrated into the simulation models.

The Future of ASHM

In closing, this book section highlights the profound impact of combining data mining and Digital Twin technology in shedding light on previously unexplored aspects of aircraft system behaviour. By leveraging the power of these cutting-edge tools, there is not only advancing the

field of aviation, but also revolutionizing the way on how to approach predictive maintenance, operational optimization, and overall safety and reliability in the aviation industry.

This serves as a stepping stone in shaping the future of Aircraft System Health Management (ASHM). It shows the critical importance of using data mining solutions, especially in an era characterized by the increasing complexity and interconnectivity of aviation systems and managing system health. The opportunities that lie ahead are virtually limitless, with the potential to significantly improve both aviation safety and operational efficiency to unprecedented levels.

Drawing on the combination of data mining and Digital Twin technology, ASHM is on the verge of ushering in a transformative era in aviation. With these two innovative approaches working together, the aviation industry is poised to unlock a realm of possibilities that promises to evolve the aviation industry in ways once thought beyond our reach. With the synergy of data mining and Digital Twin technology, the future of aviation is truly bright; redefines the boundaries of what is achievable.

REFERENCES

Aggarwal, C. C. (2015). *Data mining: the textbook* (Vol. 1). New York: springer.

Aivaliotis, P., Georgoulias, K., & Chryssolouris, G. (2019). The use of Digital Twin for predictive maintenance in manufacturing. *International Journal of Computer Integrated Manufacturing*, *32*(11), 1067-1080.

AIAA Digital Engineering Integration Committee. (2020). Digital Twin: Definition & Value—An AIAA and AIA Position Paper. *AIAA: Reston, VA, USA*

Aivaliotis, P., Georgoulias, K., & Chryssolouris, G. (2019). The use of Digital Twin for predictive maintenance in manufacturing. *International Journal of Computer Integrated Manufacturing*, *32*(11), 1067-1080.

Elias, B. (2003, September). Extracting landmarks with data mining methods. In *International conference on spatial information theory* (pp. 375-389). Berlin, Heidelberg: Springer Berlin Heidelberg.

Glaessgen, E., & Stargel, D. (2012, April). The digital twin paradigm for future NASA and US Air Force vehicles. In 53rd AIAA/ASME/ASCE/AHS/ASC structures, structural dynamics and materials conference 20th AIAA/ASME/AHS adaptive structures conference 14th AIAA (p. 1818).

Grieves, M. (2014). Digital twin: manufacturing excellence through virtual factory replication. *White paper*, *1*(2014), 1-7.

You, Y., Chen, C., Hu, F., Liu, Y., & Ji, Z. (2022). Advances of digital twins for predictive maintenance. *Procedia computer science*, *200*, 1471-1480.

Singh, M., Fuenmayor, E., Hinchy, E. P., Qiao, Y., Murray, N., & Devine, D. (2021). Digital twin: Origin to future. *Applied System Innovation*, *4*(2), 36

Liu, Z., Meyendorf, N., & Mrad, N. (2018, April). The role of data fusion in predictive maintenance using digital twin. In *AIP conference proceedings* (Vol. 1949, No. 1). AIP Publishing

Data Analytics and Informatics Usage for Enhanced Academic Achievement

Oğuz ONAT[1]

Introduction

Introduction to Data Analytics and Informatics in Education

Data analytics and informatics in education are powerful tools used to enhance student success, improve the quality of instruction, and guide educational policies (Baker & Yacef, 2009). These fields involve the analysis and interpretation of large data sets, enabling educators and policymakers to make more informed decisions (Picciano, 2012). Data analytics and informatics have various applications in an educational context. For instance, they are used to monitor student performance, optimize learning resources, and adjust teaching strategies (Siemens & Long, 2011). Moreover, these tools have assisted educational institutions in better understanding student needs and serving them more effectively (Daniel, 2015). Data-driven decision-making has a transformative effect in education. For example, educators have identified areas where students struggle using data analytics and informatics and provided additional support in these areas (Ferguson, 2012). These tools have also been used to evaluate the effectiveness of educational policies (Picciano, 2012).

The aim of this chapter is to introduce data analytics and informatics in education and demonstrate how these disciplines can elevate academic achievement. Firstly, the concepts of data analytics and informatics are defined and a discussion on their uses in education is conducted. Subsequently, the potential advantages of data-driven decision-making are examined. Finally, the structure and objectives of this chapter are summarized.

Collecting and Managing Educational Data

In the ever-changing landscape of education, data-informed decision-making has become the cornerstone of personalized instruction and continuous improvement. Educational institutions are now collecting large amounts of data from various sources to gain insights into student performance, instructional effectiveness, and administrative operations. This section examines the fundamental aspects of collecting and managing educational data, highlighting its primary sources, challenges, and strategies to ensure data quality and integrity.

Sources of Educational Data

Educational data originates from various sources within educational institutions. Understanding these sources is of fundamental importance to harness the potential of data-driven insights. The primary sources of educational data include:

Student Records: This encompasses a wide range of information, including demographic data, enrollment history, transcripts, and academic progress. Student records form the basis for understanding individual students and their academic journeys (Baker & Yacef, 2009).

Assessments: Educational assessments provide critical data about student performance. This includes formative assessments, summative assessments, standardized tests, and teacher-

[1] Lecturer, Yalova University

created assessments. Analysis of assessment data helps educators tailor instruction to meet the needs of their students (Pellegrino et al., 2001).

Attendance Records: Tracking attendance data is important for monitoring student engagement and identifying potential issues such as chronic absenteeism. This data can also assist in evaluating the impact of attendance on academic outcomes (Gottfried, 2010).

Learning Management Systems (LMS): LMS platforms generate a wide range of data related to online learning activities. This includes student engagement, completion rates, and interactions with digital learning materials. LMS data plays a key role in understanding the effectiveness of online courses (Gašević et al., 2015).

Administrative Systems: Beyond academic data, educational institutions collect administrative data related to finance, personnel, facilities, and resource allocation. These data sources assist in managing the logistical and financial aspects of educational operations (Bowers et al., 2017).

Surveys and Feedback: Collecting feedback through surveys from students, teachers, and parents provides valuable qualitative data that complements quantitative data. This data can provide information about the learning environment, quality of instruction, and overall satisfaction levels (Hattie & Timperley, 2007).

Addressing Challenges in Data Collection, Storage, and Privacy

While educational data offers great potential, it also presents various challenges that need to be addressed:

Data Collection Challenges: Educational data collection can be fragmented, with different systems and departments independently collecting data. Ensuring data consistency and standardization within the institution can be a significant challenge (Picciano et al., 2014).

Data Storage and Security: Educational institutions should establish robust data storage systems that prioritize compliance with privacy regulations such as the Family Educational Rights and Privacy Act (FERPA). Protecting sensitive student information is of utmost importance (Reidenberg et al., 2013).

Data Privacy: Preserving data privacy is fundamental to building trust among stakeholders. Data anonymization and access controls are critical components in protecting student and staff information (Zeide & Nissenbaum, 2017).

Emphasizing Data Quality and Integrity Considerations

The usefulness of educational data is dependent on its quality and integrity. Low-quality data can lead to incorrect conclusions and ineffective decision-making processes. Key considerations for ensuring data quality and integrity include:

Data Verification: Implementing verification checks at the point of data entry to prevent errors and inconsistencies (Reidenberg et al., 2013).

Data Cleaning: Regularly reviewing the data and correcting errors, eliminating duplicates, and ensuring accuracy (Bowers et al., 2017).

Data Integration: Creating a comprehensive and consistent data set by bringing together data from different sources (Gašević et al., 2015).

Importance of Data Governance and the Role of Data Stewards

Data governance plays a critical role in preserving the quality, security, and privacy of data. This involves defining policies, processes, and responsibilities. Data stewards undertake

significant tasks by conducting quality control, regulating access controls, and ensuring compliance with data policies (Glendinning et al., 2021). In the subsequent sections of this topic, each of these elements is examined in detail, addressing issues of ensuring data quality, strategies for overcoming challenges, and how to establish effective data management practices in educational institutions. Educational institutions can fully benefit from data-driven insights to improve educational and administrative processes. This requires mastery in the collection and management of educational data.

Applying Data Analytics in Education

In today's rapidly evolving educational landscape, the integration of data analytics has emerged as a transformative force, offering educators and institutions unprecedented opportunities to enhance teaching and learning (Baker & Inventado, 2014). This section explores the multifaceted application of data analytics in education, encompassing descriptive, predictive, and prescriptive analytics. We delve into real-world use cases that demonstrate the practicality of data analytics, emphasizing its potential to track student progress, identify at-risk students, evaluate teaching methods, and extend beyond these fundamental functions. Moreover, we underscore the pivotal role of data visualization in extracting valuable insights from educational data. Finally, this section sheds light on the utilization of machine learning and artificial intelligence (AI) techniques offering a glimpse into the future of advanced educational analysis.

Diving into Descriptive, Predictive, and Prescriptive Analytics for Education

The integration of data analytics in education begins with a comprehensive understanding of its three fundamental dimensions: descriptive, predictive, and prescriptive analytics (Ferguson, 2012). Each plays a different but complementary role in shaping educational practices and outcomes.

Descriptive Analytics: At a basic level, descriptive analytics involves the exploration and summarization of historical data (Ferguson, 2012). In education, this means examining the history of student performance, attendance records, and course outcomes. Using data visualization tools and techniques (Few, 2012), educators can identify trends and patterns to pinpoint areas of success and concern. For example, a school district could use descriptive analytics to evaluate standardized test scores over the years (Baker & Inventado, 2014), revealing areas for improvement or attention.

Predictive Analytics: Building on descriptive analytics, predictive analytics uses historical data to predict future events and trends (Ferguson, 2012). In an educational context, this could involve predicting a student's likelihood of success in a particular course or identifying factors contributing to academic failure. Predictive models can help educators provide early intervention and targeted support for at-risk students (Siemens & Long, 2011), ultimately increasing retention rates and student success.

Prescriptive Analytics: The most proactive dimension of data analytics in education (Ferguson, 2012), prescriptive analytics goes beyond predicting outcomes to suggest action steps for improvement. For example, if a predictive model identifies students at risk of dropping out (Siemens & Long, 2011), prescriptive analytics could suggest specific interventions to address the underlying issues and increase the likelihood of student success. These interventions could include tutoring (Baker & Inventado, 2014), mentorship programs, or counseling.

Illustrating Real-World Use Cases

To appreciate the transformative potential of data analytics in education, it is important to examine real-world use scenarios that highlight its practical applications.

Tracking Student Progress: Data analytics allows educators to closely monitor each student's academic journey. By analyzing past performance data, educators can track individual progress, identify areas for improvement, and adapt teaching approaches to meet the specific needs of students (Shabihi & Kim, 2021).

Identifying At-Risk Students: Predictive analytics can assist in identifying students at risk of academic failure or dropping out. Factors such as absenteeism records, participation metrics, and past performance data can be analyzed to provide targeted support and preventive interventions for these students (Soncin & Cannistrà, 2022).

Evaluating Teaching Methods: Data analytics enables institutions to evaluate the effectiveness of various teaching methods and curriculum designs. By analyzing student outcomes and feedback, educators can improve teaching strategies and enhance the overall learning experience through data-driven decisions (Lee, Cheung & Kwok, 2020).

Beyond the Basics: The use of data analytics in education extends far beyond these basic use scenarios. Institutions are exploring innovative applications such as creating personalized learning pathways, optimizing resource allocation, and increasing administrative efficiency with data-driven decisions.

The Pivotal Role of Data Visualization

In the field of education, data visualization serves as a critical bridge between raw data and actionable insights. It transforms complex data sets into visual representations that educators can easily interpret and use to inform decision-making processes (Shahril Khuzairi & Che Cob, 2021). Through graphs, charts, dashboards, and heat maps, data visualization allows educators to identify trends, outliers, and patterns that might remain hidden in large data sets.

Effective data visualization in education requires a combination of artistic design and data literacy. Educators and data analysts should collaborate to create visualizations that convey meaningful information without distorting the underlying data. Well-designed visualizations enable educators to clearly communicate their findings and involve stakeholders in data-driven decisions within educational institutions, fostering a culture of evidence-based decision-making.

Utilizing Machine Learning and AI Techniques

As technology advances, machine learning and artificial intelligence techniques are expected to play an increasingly larger role in educational data analytics (Celik et al., 2022). These techniques offer the potential to automate data analysis, predict student outcomes with greater accuracy, and derive detailed insights from complex data sets.

Machine learning models can be trained to recognize patterns in student behavior and performance, enabling educators to provide personalized recommendations and interventions. Natural language processing (NLP) techniques can be used to analyze student feedback and emotional state, assisting institutions in enhancing the quality of teaching and learning experiences.

In summary, this section emphasizes the multifaceted nature of data analytics applications in education. By adopting descriptive, predictive, and prescriptive analytics, educators and institutions can unlock new opportunities to enhance educational outcomes. While real-world use scenarios demonstrate the tangible benefits of data analytics, data visualization and artificial intelligence techniques further empower educators to make data-driven decisions that positively impact teaching and learning.

Leveraging Informatics for Enhanced Learning

Technology's Transformative Role in Learning Experiences

The integration of technology into educational paradigms has triggered a radical transformation in the landscape of pedagogy (Chaudhry & Kazim, 2021). This chapter examines the multifaceted impact of information sciences on contemporary learning experiences and elucidates its role in revolutionizing pedagogical methodologies and knowledge acquisition across various contexts. Modern pedagogical approaches have been significantly reshaped with the involvement of technology in the learning process. This transformation is manifested in the shift from traditional, teacher-centered models to student-centered and technology-mediated educational environments (Wilichowski & Cobo, 2021). The proliferation of digital tools and resources has not only expanded access to information but also fundamentally altered the dynamics of knowledge transmission. Furthermore, the increasing prevalence of online learning platforms, virtual classrooms, and educational software has sparked discussions on redefining pedagogical roles, learning objectives, and assessment methods (Nguyen et al., 2021).

Adaptive Learning Systems: Personalizing Learning Paths through Data Insights

One of the most noteworthy innovations brought about by information sciences in the field of education is the development of adaptive learning systems (Martin et al., 2020). These systems leverage the power of data analytics to customize learning experiences for individual students and align educational content with personal needs, preferences, and abilities. Adaptive learning systems represent a pedagogical paradigm shift from a one-size-fits-all approach to a student-centered dynamic model (Shemshack et al., 2021). By continuously collecting and analyzing data about students' performance, engagement, and interaction patterns, adaptive learning systems possess the capacity to dynamically adjust the pace, content, and instructional strategies employed in the learning process. Such personalization not only boosts student engagement but also facilitates deeper understanding and retention of knowledge (El-Sabagh, 2021).

Gamification and Interactive Platforms: Enhancing Engagement in Learning

In the pursuit of creating participatory and motivating learning experiences, gamification and interactive platforms have emerged as compelling strategies based on information sciences (Saleem et al., 2022). Gamification involves the integration of game elements, such as rewards, challenges, and competition, into non-game contexts, including education (Sanchez et al., 2019). The aim is to leverage the intrinsic appeal of games to enhance students' motivation, engagement, and resilience in educational tasks.

While exploring the design principles that underpin effective gamified learning experiences, it emphasizes the importance of alignment with learning objectives and pedagogical goals. It also highlights the pivotal role of interactive platforms that offer students opportunities to explore and manipulate educational content. These platforms include simulations, virtual laboratories, and interactive multimedia resources, and they promote active learning, problem-solving skills, and critical thinking.

In summary, this section addresses the evolving landscape of education from the perspective of information sciences. It underscores the transformative potential that technology carries to shape contemporary pedagogical paradigms and illuminates innovative ways of adaptive learning systems, gamification, and interactive platforms to enhance learner engagement and educational outcomes. The in-depth examination of these aspects aims to shed light on the complex interaction between technology and education in this academic exploration

and offers insights informing the design and implementation of effective and inclusive learning environments.

Ethical and Privacy Considerations

In today's data-driven educational environment, the responsible and ethical use of student data is of paramount importance. This chapter delves deeply into the key considerations that educational institutions and stakeholders need to keep in mind as they navigate the complexities of collecting, analyzing, and using student data. Striking a delicate balance between data usage, student privacy, and informed consent lies at the heart of these ethical and privacy concerns (Safarov et al., 2017).

Balancing Data Utilization, Student Privacy, and Informed Consent

The collection and analysis of student data have opened up new possibilities for personalized learning, targeted interventions, and educational research. However, this newfound power brings with it a profound responsibility to protect student privacy and ensure respect for their data usage rights (Marín et al., 2022). Achieving this balance requires a challenging effort but is crucial for maintaining trust between educational institutions and the students and families they serve. The principles that should guide this effort include:

Student Privacy

Student privacy should be held sacred. Educational institutions must implement robust data protection measures to safeguard sensitive information such as academic records, demographic data, and personally identifiable information (Cremer et al., 2021). These measures should include secure data storage, encryption protocols, access controls, and regular audits to identify and mitigate potential vulnerabilities.

Informed Consent

Informed consent is the cornerstone of ethical data usage. Students and their parents or guardians should be informed about the types of data being collected, the purposes for which it will be used, and their rights regarding data usage (O'Sullivan et al., 2021). Obtaining clear and unambiguous consent should be a priority and should include preference mechanisms that offer the opportunity to make informed choices about their data.

Data Security and Regulatory Compliance

Securing student data is not just an ethical obligation but also a legal one. Educational institutions must comply with relevant regulations such as the Family Educational Rights and Privacy Act (FERPA) (U.S. Department of Education) that governs the handling and disclosure of educational records and imposes penalties for non-compliance. To ensure compliance, institutions should:

Data Encryption

Implement end-to-end encryption to protect data both in transit and at rest. Encryption ensures that data remains unreadable and inaccessible even if unauthorized access occurs.

Access Controls

Establish strict access controls to limit who can access student data. Access should be granted only to authorized personnel who have a legitimate need.

Regular Audits and Assessments

Conduct regular security audits and reviews to identify vulnerabilities and ensure that data protection measures remain effective over time.

Transparent Communication

Transparently conveying data usage practices is vital for maintaining trust among all stakeholders involved in education (Hofmann and Strobel, 2020). This includes students, parents, teachers, administrators, and the broader community. Institutions should adopt the following strategies to promote transparency:

Clear Privacy Policies

Develop clear and understandable privacy policies that explain what data is being collected, how it will be used, and what security measures are in place to protect it.

Consent Processes

Ensure that consent processes are simple, accessible, and well-documented (O'Sullivan et al., 2021). Individuals should be aware of their rights and have the ability to choose whether or not to participate in data collection and usage.

Importance of Transparency and Accountability

Transparency and accountability are fundamental principles of responsible data usage. Educational institutions should be prepared to answer questions about their data practices, address concerns, and be held accountable for these practices. This includes:

Accountability Mechanisms

Create mechanisms for individuals to report data misuse or breaches, and ensure that complaints are addressed promptly and appropriately (Brandsma and Schillemans, 2013).

Regular Auditing

Conduct regular audits of data practices to ensure compliance with rules and regulations (Knechel et al., 2013). These audits should be carried out by independent and impartial institutions.

In conclusion, ethical considerations and privacy in the field of student data are complex and multifaceted. Finding the right balance between data usage, student privacy, and informed consent is important for promoting trust and ensuring that data-driven education initiatives benefit all stakeholders (Gaventa and McGee, 2013). Furthermore, transparency and accountability should be prioritized to ensure that educational institutions' data usage strategies uphold the highest ethical standards.

Challenges and Limitations of Data Analytics in Education

Data analytics in education offers a promising avenue for enhancing teaching and learning outcomes. However, like any powerful tool, it is not without challenges and limitations. This section examines the key issues to consider when using data-driven approaches in an educational context.

Discussing Potential Limitations of Data-Driven Approaches

Data-driven approaches in education are dependent on data access and data quality. While the digital age has brought with it many sources of data, there are some limitations that need careful consideration:

Data Availability

Not all educational institutions have equal access to high-quality data. Schools in small or resource-poor areas may struggle to collect sufficient data for meaningful analysis (Baig et al.,

2020). Additionally, data may be dispersed across different systems, complicating efforts to construct a comprehensive view of a student's educational journey.

Data Quality:

The accuracy and completeness of data can vary significantly. Incorrect or incomplete data can generate incorrect results and recommendations (Baig et al., 2020). Data cleaning and verification processes are essential but can be demanding in terms of time and resources.

Privacy Concerns:

The collection and analysis of student data raise significant privacy concerns (Jones, 2019). Striking a balance between the need for data-driven insights and protecting students' personal information is an ongoing challenge (Jones, 2019). Compliance with data privacy regulations such as the Family Educational Rights and Privacy Act (FERPA) in the U.S. is mandatory.

Ethical Considerations:

The use of student data for predictive analyses and interventions raises ethical dilemmas (Murchan and Siddiq, 2021; Atenas et al., 2023). Thoughtful consideration of how data informs decisions about students' educational paths is important to prevent reinforcing biases or unfairly labeling individuals (Atenas et al., 2023).

Addressing Bias in Data Collection and Analysis

Bias is a common concern in data analytics and is particularly important in education (Baker and Hawn, 2022). Bias can emerge at various stages of the data analytics process; this includes the processes of data collection (Tempelaar et al., 2020), model development (Baker and Hawn, 2022), and decision-making (Baldwin et al., 2022). Attention to and proactive measures for addressing bias are necessary to ensure that data-driven approaches uphold fairness and equality in education:

Bias in Data Collection

Bias can seep into the data during the collection process (Tempelaar et al., 2020). For example, if the data primarily originates from certain demographic groups or learning environments, it may not accurately represent the entire student population (Tempelaar et al., 2020). Diligent efforts should be made to collect diverse and representative data.

Algorithmic Bias

Machine learning algorithms can perpetuate and even amplify biases present in educational data (Baker and Hawn, 2022), leading to unfair outcomes such as lower academic achievement predictions for certain student groups (Baker and Hawn, 2022). Regular audits of algorithms and integration of fairness metrics are vital for reducing algorithmic bias.

Interpretation Bias:

Human interpreters of data analytics results can introduce their own biases when making decisions based on the data (Baldwin et al., 2022). Providing training and guidelines to ensure educators and administrators make informed and unbiased decisions when applying data insights is important.

Challenges in Quantifying Complex Human Behaviors and Learning Processes

Quantifying complex human behaviors and learning processes constitutes one of the central challenges in educational data analytics (Baker and Siemens, 2014; Khine and Areepattamannil, 2016). Human learning is multifaceted and influenced by many factors, making its accurate capture and measurement a daunting task:

Non-Cognitive Factors:

Learning encompasses non-cognitive factors that include motivation, self-regulation, and socio-emotional development (Liu et al., 2022). Measuring these factors in an objective and standardized manner presents a significant challenge (Baker and Siemens, 2014).

Context Dependency:

Learning outcomes can vary depending on the context in which they occur (Khine and Areepattamannil, 2016). Variables such as classroom environment, teaching methods, and peer interactions can influence learning (Khine and Areepattamannil, 2016). Quantifying and accounting for these contextual variables in data analysis is complex (Baker and Siemens, 2014).

Long-Term Outcomes:

Educational success is often measured by long-term outcomes such as graduation rates and career successes (Khine and Areepattamannil, 2016). Predicting these outcomes accurately based on short-term data can be difficult and may require advanced predictive models (Baker and Siemens, 2014).

In conclusion, while data analytics has the potential to revolutionize education, it is important to bear in mind the challenges and limitations that come with its implementation (Khine and Areepattamannil, 2016). Data quality, reducing bias, and the complexities of human learning processes are key considerations for those seeking to effectively harness the power of data in education (Khine and Areepattamannil, 2016; Buckingham Shum et al., 2019). These challenges should be addressed with a mindful and ethical approach. This can help create a more equitable educational environment and facilitate data-driven decision-making.

Evaluation of Data-Driven Interventions in Education

The field of education is characterized by a dynamic structure that continually evolves to meet the changing needs of students, educators, and educational institutions. In recent years, the integration of data-driven methods into educational paradigms has gained significant importance. These methods are used to inform and enhance decision-making processes in education through the power of information analytics, machine learning, and artificial intelligence (Bianco, 2015; Wilcox et al., 2021). The potential of data-driven interventions is undeniably appealing; however, a critical imperative arises for them to be effectively evaluated to ensure real benefits for students and educators (Gauthier et al., 2022).

Significance of Assessing the Efficacy of Data-Driven Approaches

The integration of data-driven methods into education is predicated on the belief that they can inform and support decision mechanisms based on the evolution of educational outcomes (Skedsmo & Huber, 2022). However, it is important to emphasize that merely using data does not automatically guarantee positive outcomes (Ozga, 2009). Therefore, measuring the effectiveness of data-driven interventions becomes essential to distinguish their impacts across different aspects of education. These interventions may include personalized learning algorithms, predictive analytics for early intervention, and data-based pedagogical strategies (Coburn & Turner, 2011; Spillane, 2012).

The evaluation of data-driven interventions provides several important functions. These include: "

Informed Decision-Making

Effective evaluation endows education stakeholders, including administrators, educators, and policymakers, with the capacity to make judicious decisions about the adoption,

improvement, or termination of data-driven interventions (Skedsmo and Huber, 2022; Ozga, 2009). This understanding aids in identifying effective strategies and helps allocate resources efficiently to approaches that yield the most benefit (Ozga, 2009).

Fostering Accountability and Transparency

The evaluation process encourages accountability within the education system and holds educators and institutions responsible for the outcomes of data-driven interventions (Smith and Benavot, 2019). Additionally, the element of transparency in the evaluation process promotes external audit and approval of the methodologies used and findings obtained, thereby enhancing trust in both the methods employed and the results achieved (Jongbloed et al., 2018).

Facilitating Continuous Enhancement

The evaluation process serves as a catalyst for continuous improvement (Reimers et al., 2020). By illuminating both strengths and weaknesses, it facilitates the refinement of data-driven interventions over time. This iterative journey is an integral part of ensuring that educational practices remain responsive and adaptable to evolving challenges and needs (Reimers et al., 2020).

Emphasizing Robust Evaluation Methodologies

The use of rigorous evaluation methodologies is crucial for accurately assessing the effectiveness of data-driven interventions in an educational setting (Double et al., 2020). These methodologies go beyond superficial evaluations and attempt to establish causal relationships between interventions and outcomes. In this context, three fundamental methodologies stand out:

Control Groups

Control groups involve comparative analysis between a group exposed to a data-driven intervention and a group not subjected to this intervention (Double et al., 2020). This comparison allows researchers to attribute observed changes to the intervention itself and isolate them from the influence of external variables. Control groups provide a starting point for robustly measuring the effectiveness of an intervention.

Randomized Trials

Random trials, often referred to as randomized controlled trials (RCTs), take the concept of control groups a step further (Chow and Hampton, 2022). In RCTs, participants are randomly assigned to either the intervention group or the control group (Chow and Hampton, 2022). This random assignment ensures that any differences in outcomes are clearly attributed to the effects of the intervention rather than pre-existing differences between groups.

Long-Term Follow-Up

Comprehensive evaluation of long-term outcomes of data-driven interventions is of great importance (Schult et al., 2022). Short-term successes may not always translate into lasting benefits (Schult et al., 2022). Long-term follow-up studies meticulously track the long-term trajectory of student progress or institutional developments, providing researchers with insights into the lasting effects of interventions and whether these effects diminish over time (Schult et al., 2022).

While the importance of evaluation and adoption of rigorous methodologies is indisputable, it is important to acknowledge the challenges that arise when evaluating complex interventions characterized by numerous variables. In the field of data-driven interventions in education, there are several complexities to consider:

Interconnected Variables

Data-driven interventions often simultaneously focus on a range of educational dimensions, including curriculum design, pedagogical methods, and student support systems. The complex dependencies among these variables can pose formidable challenges to isolating the specific impact of individual interventions (Wong and Li, 2020).

Temporal Dynamics

Educational outcomes can exhibit temporal dynamics. Some interventions may yield noticeable improvements in the initial stages but may later be observed to decrease in effectiveness, while others may display their effects with a delay (Grant et al., 2023). Therefore, evaluators should take these temporal subtleties into account when designing their studies.

Ethical Considerations

Data-driven interventions inevitably involve the collection and use of sensitive student data. Ethical considerations related to privacy, consent, and data security require careful resolution throughout the evaluation process to protect students' rights and welfare (Atenas et al., 2023).

In summary, evaluating data-driven interventions in education is crucial for determining whether these methodologies are effective in improving educational outcomes. The use of robust evaluation methodologies, including control groups, random trials, and long-term follow-ups, provides a reliable way to determine the true impact of these interventions (Wilcox et al., 2021). However, the complexity of multi-variable complex interventions requires careful evaluation and a rigorous approach (Petticrew, 2011). Overcoming these challenges is an important step towards developing data-driven educational practices that are as ethically robust as they are effective (Wilcox et al., 2021).

Role of Educators in Data-Driven Decision-Making

In an era characterized by a continually increasing flow of data, educators find themselves at the forefront of a significant transformation in the field of education. This chapter addresses the critical role of educators in improving teaching practices, collaborating with data analysts and information experts, and playing an active role in the design and implementation of data-driven interventions.

How educators can use data to inform teaching practices

Educators bear the primary responsibility for nurturing their students' cognitive development. To do this, they must continually adapt and improve their teaching methods. Data-driven decision-making enables educators to make informed choices about teaching strategies, curriculum development, and individual student support (Ndukwe & Daniel, 2020). By analyzing student performance data, educators can identify patterns, trends, and areas for improvement. This allows them to adapt their teaching to meet students' specific needs, address learning gaps, and optimize classroom experiences (Krishen & Petrescu, 2019).

Moreover, data usage is not limited to formative assessments and can encompass various aspects of the educational process. Educators can examine students' absenteeism records, behavioral data, and even socio-economic information, which can help them gain a comprehensive understanding of their students (Kassarnig et al., 2018). Equipped with this knowledge, educators can implement proactive measures to create a learning environment that promotes academic and personal development.

Collaboration between educators and data analysts/informaticians

Data analysis is a complex field that often requires expertise. Therefore, collaboration between educators and data analysts or information experts is vital for fully leveraging the potential of data-driven decision-making. Data professionals can assist educators in developing robust data collection systems, designing effective data visualization tools, and conducting in-depth statistical analyses (Bowers, 2021). These collaborations not only enhance educators' access to valuable insights but also ensure the effective and ethical use of data.

Effective communication and mutual understanding between educators and data experts are central to these collaborations. Educators should articulate specific data needs, and data experts should translate the data into actions that are compatible with educators' pedagogical goals and effective (Mora-Ruano et al., 2019). When educators and data experts work together, the result is a symbiotic relationship that directs meaningful educational improvements through data.

Educator involvement in the design and implementation of data-driven interventions

While educators benefit from the data analysis conducted by data analysts, their active participation in the design and implementation of data-driven interventions is equally important. This participation ensures that interventions are contextually appropriate, aligned with educational objectives, and responsive to the unique needs of students and classrooms. Educators bring on-the-ground insights, pedagogical expertise, and an understanding of classroom dynamics that can guide the development of effective interventions (Bianco, 2010).

In this collaborative process, educators serve as key stakeholders who provide significant contributions at all stages from inception to evaluation of intervention outcomes. Their contributions can help shape intervention strategies, identify potential challenges, and guide adjustments in real-time (Kochmar et al., 2021). By actively participating in the design and implementation of data-driven interventions, educators become advocates for innovations that promote positive change within educational institutions.

In conclusion, educators are indispensable actors in the changing landscape of data-driven education. Their abilities to use data for informed decision-making, to effectively collaborate with data professionals, and to actively participate in the design and implementation of data-driven interventions enable data to become a powerful tool for improving educational outcomes (Wilcox et al., 2021).

Role of Students in Data-Driven Decision-Making

In the rapidly evolving landscape of education, data-driven decision-making has gained importance as a powerful tool for teachers and administrators to enhance learning outcomes (Afzaal et al., 2021). However, the role of students in this process should not be overlooked. Involving students in the data-driven decision-making process empowers them to take control of their learning journey and fosters a sense of ownership over their educational experiences (Kochmar et al., 2022). This section addresses the multifaceted participation of students in this area, including how students can shape their learning strategies with information, how they can participate in the design and implementation of data-driven interventions, and how they can provide valuable feedback on the effectiveness of these interventions.

How Students Can Use Data to Inform Their Learning Strategies

Data can serve as a guiding compass for students, aiding them in making informed decisions. By gaining access to their own academic performance data, students can acquire valuable insights into their strengths, weaknesses, and areas for improvement (Schifter et al.,

2014). For instance, tracking assessment scores, attendance records, and participation metrics can help students identify patterns and trends in their academic journey.

With access to this data, students can customize their study plans and approaches to suit their learning needs. They can set realistic goals, create personalized study schedules, and prioritize areas to focus on. Additionally, students can utilize various data visualization tools to represent their academic trajectory visually, gaining a deeper understanding of their academic journey (Schifter et al., 2014).

Imparting students with the ability to interpret and use data not only instills a sense of responsibility for their learning but also equips them with critical skills that are applicable beyond the classroom. Encouraging students to actively use data fosters a culture of self-directed learning and data literacy within educational institutions (Afzaal et al., 2021).

Student Participation in Designing and Implementing Data-Driven Interventions

While teachers and administrators play significant roles in designing data-driven interventions, students can offer unique perspectives and insights that contribute to the effectiveness of these strategies. Collaboration between students and educational stakeholders can lead to more targeted and student-centered interventions.

As important stakeholders in the educational process, students can actively participate in the design and implementation of interventions. They can provide input on what types of interventions are most beneficial as well as suggest improvements. Their lived experiences and field knowledge allow them to make valuable contributions in shaping interventions that resonate with the student body (Strydom & Loots, 2020).

Involving student perspectives in decision-making processes can lead to interventions that address not only academic challenges but also social and emotional needs. Student contributions can lead to the development of support systems such as peer mentoring programs or mental health resources, serving the holistic well-being of the student community (Xu & Stefaniak, 2021).

Students' Feedback on the Effectiveness of Data-Driven Interventions

Student feedback is a critical component in the continuous improvement of data-driven interventions. After implementing these strategies, it is important to collect and analyze student feedback to accurately assess their effects. Students are in a unique position to provide insights into the real-world impacts of these interventions, illuminating what works and what needs adjustment (Wisniewski, Zierer & Hattie, 2020).

Feedback mechanisms can take various forms, such as surveys, focus groups, and one-on-one interviews. These channels provide students with opportunities to express their opinions, share their experiences, and suggest changes to existing interventions. Additionally, feedback helps hold educational institutions accountable for fulfilling their promises of data-driven improvements (Ahea et al., 2016).

In conclusion, the role of students in the data-driven decision-making process extends far beyond being mere passive recipients of interventions. Students can use data to inform their own learning strategies (Krishen & Petrescu, 2019), actively participate in the design and implementation of interventions (Li et al., 2019), and provide critical feedback on their effectiveness. By involving students in these processes, educational institutions can develop a more inclusive, student-centered approach to data-driven decision-making, ultimately enhancing the quality of education and overall learning experience.

Collaboration in Advancing Data Analytics and Informatics in Education

In the constantly changing landscape of education, the use of data analytics and information science has emerged as a powerful tool for triggering innovations, enhancing student learning outcomes, and informing pedagogical decision-making processes (Karaoglan Yilmaz, 2022). This section addresses the significant role that collaboration plays in advancing the use of data analytics and information science in education. In particular, it examines the importance of collaboration between institutions, researchers, and technology companies that are shaping the development of tools, methodologies, and best practices in this field. It also highlights the importance of research initiatives aimed at deepening the impact of data analytics on academic achievement.

Importance of Collaboration Between Institutions, Researchers, and Tech Companies

Collaboration has always been the cornerstone of progress, and the field of data analytics and information science in education is no exception (Mohajerzad et al., 2021). Whether it's primary schools, universities, or online learning platforms, educational institutions have begun to recognize the transformative potential of data-driven insights. However, they often lack the expertise and resources necessary to fully exploit these opportunities. This is where collaboration with researchers and technology companies becomes inevitable.

Institutional collaborations can take various forms, from partnerships between universities and local school districts to collaborations between new ventures in educational technology and established educational institutions. These partnerships offer a unique fusion of academic discipline and practical application and allow for the development and testing of innovative data analytics tools and methodologies in real-world educational environments. Additionally, collaboration with technology companies brings the latest advancements in data analytics technology, helping educational institutions stay ahead of innovations (Rienties et al., 2020).

Collaborative efforts have the added advantage of fostering the development of diverse perspectives and skill sets. Researchers bring their theoretical knowledge and methodological skills, institutions offer their knowledge in a specific field, and technology companies provide the latest technological tools and resources. This multidisciplinary approach is crucial for overcoming complex challenges and developing holistic solutions that respond to the diverse needs of educational stakeholders.

Development of Tools, Methodologies, and Best Practices Through Collaboration

The dynamic nature of data analytics and information science requires constant innovation and adaptation. Collaboration serves as a catalyst for developing tools, methodologies, and best practices that effectively harness the potential of educational data. Through collaborative initiatives, institutions and their partners can co-create solutions that are suitable for specific educational contexts (Luxem et al., 2022).

One notable outcome of such collaboration is the development of customized data analytics platforms for educational purposes. These platforms integrate data from various sources such as student performance metrics, demographic information, and learning behavior to generate actionable insights (Moussavi et al., 2020). Researchers and technology companies work together to design user-friendly interfaces that allow educators and administrators to effectively interpret and apply these insights (Lee et al., 2020). Additionally, methodologies for data collection, analysis, and visualization are improved and optimized through feedback loops in collaboration, ensuring their relevance and accuracy (Peersman, 2014).

In addition to technical tools, collaboration also contributes to the development of best practices in data management and ethics. Given the sensitivity of educational data, collaborative efforts often lead to the creation of guidelines and protocols for responsible data handling

(Atenas et al., 2023). These best practices not only protect student privacy but also build trust among stakeholders and facilitate sustainable use of data analytics in education (Hakimi et al., 2021).

Research Initiatives to Deepen the Understanding of Data's Impact on Academic Achievement

While the potential benefits of data analytics in education are apparent, it is vital to continually evaluate and improve these practices through rigorous research. Research initiatives conducted in collaboration advance the foundation of evidence-based decision-making in education. Researchers of diverse backgrounds collaborate with educational institutions and technology companies to investigate the impact of data analytics on academic achievement (Lnenicka et al., 2020).

Such research efforts encompass a wide range, from large-scale quantitative analyses of student outcomes to qualitative examinations of the experiences of educators and students (Carmean et al., 2021). Through collaboration, researchers have the opportunity to investigate nuanced questions about the relationship between data-driven interventions and student success (Soncin & Cannistrà, 2022). These findings inform a continuous improvement process for data analytics tools and interventions, ensuring their effectiveness and alignment with educational goals.

In conclusion, collaboration between institutions, researchers, and technology companies plays a significant role in advancing the field of data analytics and information science in education. It fosters innovation, supports the development of customized solutions, and backs efforts to deepen understanding of the impact of data on academic achievement (Moussavi et al., 2019). As educational stakeholders embrace the power of data analytics, collaboration will continue to serve as the driving force behind the transformation of education in the digital age.

Transforming Education through Data Analytics: Case Studies

This section provides a detailed examination of a series of illuminating case examples that vividly demonstrate the impact of data analytics and information science on academic achievement. These examples span different educational levels and subjects, offering a comprehensive panorama of the transformative potential carried by these technologies.

Predicting Academic Success with Data Analytics

In the field of data analytics, there is a valuable tool for increasing academic success across different educational landscapes. A notable study conducted by Zhang et al. (2021) used machine learning algorithms to predict student performance based on midterm grades. The model achieved an impressive classification accuracy of 70-75%, strongly demonstrating the potential of data analytics to predict academic outcomes and guide teaching strategies (Zhang et al., 2021). This study highlights the indispensable role of data analytics in identifying at-risk students and facilitating timely interventions that elevate academic success.

Illuminating Student Retention with Data Analytics

Data analytics shines a light on increasing student attendance rates. A comprehensive study by Aljohani (2016) provided an extensive review of significant works and theoretical models related to student attendance in higher education. The study emphasized that institutions could achieve high attendance rates by offering customized support and using effective teaching methods (Aljohani, 2016). This study underscores the indispensable role of data analytics in identifying at-risk students and creating customized interventions that increase attendance rates.

Elevating Graduation Rates through Data Analytics

The promising field of data analytics extends to increasing graduation rates. An enlightening study conducted by Picciano (2012) addresses the strategic analysis of student data and its potential to significantly increase return on investment (Picciano, 2012). This study highlights how data analytics can be a game-changer in increasing graduation rates, contributing to the overall success of educational institutions.

Fostering Holistic Student Excellence Across Educational Levels and Subjects

The benefits of data analytics extend beyond traditional academic metrics to include comprehensive evaluations of student performance. For instance, the study titled "Predicting Student Performance Using Data Mining and Learning Analytics Techniques: A Systematic Literature Review" systematically examines student performance prediction (SPP) from the perspective of machine learning and data mining (Zhang et al., 2021). This study is particularly noteworthy for emphasizing data analytics as a catalyst for enhancing student excellence across different educational levels and subjects.

In conclusion, these case studies exemplify the transformative potential of data analytics and information science in education. By leveraging the capabilities of these technologies, educational institutions can promote innovation, improve student outcomes, and make informed decisions in pedagogy.

Future Directions and Challenges

In this section, we embark on an exploratory journey towards the future of data analytics and information science in education. We contemplate the continually evolving landscape of these technologies, foresee potential advancements and impacts (Valverde-Berrocoso, Acevedo-Borrega & Gresham, 2022), and confront ongoing challenges that lie ahead, including formidable issues such as data silos (Brown, 2017), technological infrastructure (Barrett et al., 2020), and faculty and staff training.

Pondering the Evolving Landscape of Data Analytics and Informatics in Education

The journey of data analytics and information science in education is far from over; in fact, it's just beginning. As we stand on the threshold of a new era, it's important to contemplate how these technologies will continue to evolve. How will data analytics tools expand? What new methods and data sources will emerge? How will these developments reshape the educational landscape? By examining these questions, we attempt to predict exciting transformations awaiting in the field of education.

Anticipating Technological Advancements and Potential Impacts

Technological advancements in the field of data analytics and information science have the potential to redefine education. Looking ahead, we examine emerging trends such as artificial intelligence, predictive analytics, and personalized learning platforms. We also consider their potential impacts, which can range from adaptive curriculum design to real-time student support systems. By foreseeing these developments, we gain an understanding of how they could revolutionize educational practices and outcomes (Valverde-Berrocoso et al., 2022).

Addressing Persistent Challenges: Data Silos, Technological Infrastructure, and Faculty/Staff Training

While the future holds promise, we must acknowledge and address ongoing challenges that continue to hinder seamless integration of data analytics and information science in education. Data silos remain a difficult barrier impeding data sharing and collaboration (Brown, 2017). We also acknowledge the importance of robust technological infrastructure to support data

analytics initiatives (Barrett et al., 2020) and recognize the urgent necessity for comprehensive teacher and staff training to effectively use these technologies. In this section, we confront these challenges and explore strategies to overcome them.

Exploring Collaborative Opportunities Between Institutions, Researchers, and Tech Companies

The future of data analytics and information science in education is not a solitary endeavor. Collaboration partnerships between educational institutions, dedicated researchers, and technology companies hold great potential (Payumo et al., 2021). These synergistic alliances can promote innovation, support the development of cutting-edge tools, and ensure that the benefits of data analytics reach every corner of the educational landscape. In this final subsection, we envision collaboration opportunities and thereby identify ways such partnerships could collaboratively shape the future of education.

As we conclude our exploration in education through data analytics and information science, we are reminded that the journey continues and that the potential for transformation is limitless. By actively engaging with future directions and challenges outlined in this chapter, educators, researchers, stakeholders can play a significant role in shaping a more data-driven and technologically supported educational landscape for future generations.

Conclusion

In the conclusion section of this academic book chapter, key insights and thoughts emerging from our exploration into data analytics and information science in education are brought together. As we conclude this chapter, we affirm the transformative potential carried by these technologies while targeting academic success (Valverde-Berrocoso et al., 2022). We also make a strong call encouraging educational institutions to adopt data-driven approaches as a tool for achieving continuous improvement and creating a brighter future for education (Agasisti & Bowers, 2017).

Summarizing Key Insights Discussed in the Chapter

Throughout this chapter, we embarked on a comprehensive journey covering the educational landscape in the field of data analytics and information science. We examined the underlying principles of these technologies, focused on real-world case examples demonstrating their versatile applications and effectiveness across different educational domains. Several key insights emerged:

- Data analytics and information science offer powerful tools for understanding student behavior, personalizing instruction, and predicting academic outcomes (Baig et al., 2020).

- These technologies have the potential to increase not just student performance but also student retention and graduation rates (Luan et al., 2020).

- Despite their great promises, data analytics and information science face ongoing challenges, including data silos (Brown, 2017), limitations in technological infrastructure (Barrett et al., 2015), and the need for comprehensive training.

- Collaboration between institutions, researchers, and technology companies is key to unlocking the full potential of data-driven approaches in education (Payumo et al., 2021).

Reiterating the Transformative Potential of Data Analytics and Informatics

It's important to reemphasize the transformative potential of data analytics and information science. These technologies can reshape the educational landscape by forming the foundation for personalized learning, data-informed decision-making, and improved academic outcomes.

By using insights derived from data analytics, educational institutions can open new possibilities for students, instructors, and administrators (Valverde-Berrocoso et al., 2022).

Issuing a Call to Action for Institutions

In conclusion, we make a call to all educational institutions worldwide. The key to progress is the adoption of data-driven approaches for continuous improvement. It's vital for institutions to invest in necessary infrastructure (Barrett et al., 2020), promote a culture of data literacy (Agasisti & Bowers, 2017), and form collaboration partnerships (Payumo et al., 2021). In doing so, they can harness the full potential of data analytics and information science and ultimately enable more equitable and effective educational experiences. The journey we began in this chapter is not an end but a beginning - the dawn of a new era where data-informed decision-making becomes the foundation for excellence in education.

REFERENCES

Agasisti, T., & Bowers, A. J. (2017). 9. Data analytics and decision making in education: Towards the educational data Scientist as a key actor in schools and higher education institutions. Handbook of contemporary education economics, 184.

Ahea, M. M. A. B., Ahea, M. R. K., & Rahman, I. (2016). The Value and Effectiveness of Feedback in Improving Students' Learning and Professionalizing Teaching in Higher Education. Journal of Education and Practice, 7(16), 38-41.

Afzaal, M., Nouri, J., Zia, A., Papapetrou, P., Fors, U., Wu, Y., ... & Weegar, R. (2021). Explainable AI for data-driven feedback and intelligent action recommendations to support students self-regulation. Frontiers in Artificial Intelligence, 4, 723447.

Ahea, M. M. A. B., Ahea, M. R. K., & Rahman, I. (2016). The Value and Effectiveness of Feedback in Improving Students' Learning and Professionalizing Teaching in Higher Education. Journal of Education and Practice, 7(16), 38-41.

Aljohani, O. (2016). A Comprehensive Review of the Major Studies and Theoretical Models of Student Retention in Higher Education. Higher education studies, 6(2), 1-18.

Atenas, J., Havemann, L., & Timmermann, C. (2023). Reframing data ethics in research methods education: a pathway to critical data literacy. International Journal of Educational Technology in Higher Education, 20(1), 1-27.

Baig, M. I., Shuib, L., & Yadegaridehkordi, E. (2020). Big data in education: a state of the art, limitations, and future research directions. International Journal of Educational Technology in Higher Education, 17(1), 1-23.

Baldwin, J. R., Pingault, J.-B., Schoeler, T., Sallis, H. M., & Munafò, M. R. (2022). Protecting against researcher bias in secondary data analysis: challenges and potential solutions. European Journal of Epidemiology, 37, 1-10.

Baker, R. S., & Hawn, A. (2022). Algorithmic Bias in Education. International Journal of Artificial Intelligence in Education, 32, 1052-1092.

Baker, R. S., Martin, T., & Rossi, L. M. (2016). Educational data mining and learning analytics. The Wiley handbook of cognition and assessment: Frameworks, methodologies, and applications, 379-396.

Baker R., & Inventado P. S. (2014). Educational Data Mining and Learning Analytics. In J. Larusson & B. White (Eds.), Learning Analytics: From Research to Practice (pp. 61-75). Springer.

Baker R.S.J.d., Yacef K. (2009) The State of Educational Data Mining in 2009: A Review and Future Visions. Journal of Educational Data Mining 1(1):3-17.

Barrett, P., Davies, F., Zhang, Y., & Barrett, L. (2015). The impact of classroom design on pupils' learning: Final results of a holistic, multi-level analysis. Building and Environment, 89, 118-133.

Bianco, S. D. (2010). Improving Student Outcomes: Data-Driven Instruction and Fidelity of Implementation in a Response to Intervention (RTI) Model. Teaching Exceptional Children Plus, 6(5), n5.

Bowers A.J., Shoho A.R., Barnett B.G. (2017) Using Data and Inquiry to Build Equity-Focused College-Going Cultures: A Guide for Educators. Routledge.

Bowers, A. J. (2021). Data visualization, dashboards, and evidence use in schools: Data collaborative workshop perspectives of educators, researchers, and data scientists. https://doi.org/10.7916/d8-jj2g-e225

Brandsma, G. J., & Schillemans, T. (2013). The accountability cube: Measuring accountability. Journal of Public Administration Research and Theory, 23(4), 953-975.

Brown, J. T. (2017). The Seven Silos of Accountability in Higher Education: Systematizing Multiple Logics and Fields. Research & Practice in Assessment, 11, 41-58.

Buckingham Shum, S., Ferguson, R., & Martinez-Maldonado, R. (2019). Human-centred learning analytics. Journal of Learning Analytics, 6(2), 1-9.

Carmean, C., Kil, D., & Baer, L. (2021). Why Data Matters for Student Success in a Post-Pandemic World.

Celik, I., Dindar, M., Muukkonen, H., & Järvelä, S. (2022). The promises and challenges of artificial intelligence for teachers: A systematic review of research. TechTrends, 66(4), 616-630.

Chaudhry, M. A., & Kazim, E. (2021). Artificial Intelligence in Education (AIEd): a high-level academic and industry note 2021. AI and Ethics, 2, 157-165.

Chow, J. C., & Hampton, L. H. (2022). A systematic review of sequential multiple-assignment randomized trials in educational research. Educational Psychology Review, 34(3), 1343-1369.

Chudowsky N., Glaser R. (2001) Knowing What Students Know: The Science and Design of Educational Assessment. National Academy Press.

Coburn, C. E., & Turner, E. O. (2011). Research on data use: A framework and analysis. Measurement: Interdisciplinary Research and Perspectives, 9(4), 173–206.

Daniel, B. (2015). Big Data and analytics in higher education: Opportunities and challenges. British Journal of Educational Technology, 46(5), 904-920.

Double, K. S., McGrane, J. A., & Hopfenbeck, T. N. (2020). The impact of peer assessment on academic performance: A meta-analysis of control group studies. Educational Psychology Review, 32, 481-509.

El-Sabagh, H. A. (2021). Adaptive e-learning environment based on learning styles and its impact on development students' engagement. International Journal of Educational Technology in Higher Education, 18(1), 1-24.

Ferguson, R. (2012). Learning analytics: drivers, developments and challenges. International Journal of Technology Enhanced Learning, 4(5/6), 304-317.

Foltýnek, T., & Glendinning, I. (2015). Impact of policies for plagiarism in higher education across Europe: Results of the project. Acta Universitatis Agriculturae et Silviculturae Mendelianae Brunensis, 63(1), 207-216.

Gaventa, J., & McGee, R. (2013). The impact of transparency and accountability initiatives. Development Policy Review, 31, 3-28.

Gašević D., Dawson S., Siemens G. (2015) Let’s not forget: Learning analytics are about learning. TechTrends 59(1):64-71.

Gauthier, A., Rizvi, S., Cukurova, M., & Mavrikis, M. (2022). Is it time we get real? A systematic review of the potential of data-driven technologies to address teachers' implicit biases. Frontiers in Artificial Intelligence, 5, 994967.

Gottfried M.A. (2010) Evaluating the Relationship Between Student Attendance and Achievement in Urban Elementary and Middle Schools: An Instrumental Variables Approach. American Educational Research Journal 47(2):434-465.

Grant, M., Meissel, K., & Exeter, D. (2023). Promoting Temporal Investigations of Development in Context: a Systematic Review of Longitudinal Research Linking Childhood Circumstances and Learning-related Outcomes. Educational Psychology Review, 35(1), 19.

Hakimi, L., Eynon, R., & Murphy, V. A. (2021). The ethics of using digital trace data in education: A thematic review of the research landscape. Review of Educational Research, 91(5), 671-717.

Hattie J., Timperley H. (2007) The Power of Feedback. Review of Educational Research 77(1):81-112.

Hofmann, Y. E., & Strobel, M. (2020). Transparency goes a long way: information transparency and its effect on job satisfaction and turnover intentions of the professoriate. Journal of Business Economics, 90, 713-732.

Jones, K. M. (2019). Learning analytics and higher education: a proposed model for establishing informed consent mechanisms to promote student privacy and autonomy. International Journal of Educational Technology in Higher Education, 16(1), 1-22.

Jongbloed, B., Vossensteyn, H., van Vught, F., & Westerheijden, D. F. (2018). Transparency in higher education: The emergence of a new perspective on higher education governance. European higher education area: The impact of past and future policies, 441-454.

Karaoglan Yilmaz, F. G. (2022). The effect of learning analytics assisted recommendations and guidance feedback on students' metacognitive awareness and academic achievements. Journal of Computing in Higher Education, 34(2), 396-415.

Kassarnig, V., Mones, E., Bjerre-Nielsen, A., Sapiezynski, P., Dreyer Lassen, D., & Lehmann, S. (2018). Academic performance and behavioral patterns. EPJ Data Science, 7, 1-16.

Khine, M. S., & Areepattamannil, S. (Eds.). (2016). Non-cognitive skills and factors in educational attainment. Springer.

Knechel, W. R., Krishnan, G. V., Pevzner, M., Shefchik, L. B., & Velury, U. K. (2013). Audit quality: Insights from the academic literature. Auditing: A journal of practice & theory, 32(Supplement 1), 385-421.

Kochmar, E., Vu, D. D., Belfer, R., Gupta, V., Serban, I. V., & Pineau, J. (2022). Automated data-driven generation of personalized pedagogical interventions in intelligent tutoring systems. International Journal of Artificial Intelligence in Education, 32(2), 323-349.

Krishen, A. S., & Petrescu, M. (2019). Data-driven decision making: Implementing analytics to transform academic culture. Journal of Marketing Analytics, 7, 51-53.

Lee, L. K., Cheung, S. K., & Kwok, L. F. (2020). Learning analytics: current trends and innovative practices. Journal of Computers in Education, 7, 1-6.

Li, Q., Wang, P., Sun, Y., Zhang, Y., & Chen, C. (2019). Data-driven decision making in graduate students' research topic selection: Cognitive processes and challenging factors. Aslib journal of information management, 71(5), 657-676.

Liu, Y., Afari, E., & Khine, M. S. (2022). Effect of non-cognitive factors on academic achievement among students in Suzhou: evidence from OECD SSES data. European Journal of Psychology of Education, 1-15.

Lnenicka, M., Kopackova, H., Machova, R., & Komarkova, J. (2020). Big and open linked data analytics: a study on changing roles and skills in the higher educational process. International Journal of Educational Technology in Higher Education, 17(1), 1-30.

Luan, H., Geczy, P., Lai, H., Gobert, J., Yang, S. J., Ogata, H., ... & Tsai, C. C. (2020). Challenges and future directions of big data and artificial intelligence in education. Frontiers in psychology, 11, 580820.

Luxem, K., Sun, J. J., Bradley, S. P., Krishnan, K., Yttri, E., Zimmermann, J., ... & Laubach, M. (2023). Open-source tools for behavioral video analysis: Setup, methods, and best practices. Elife, 12, e79305.

Marín, V. I., Carpenter, J. P., Tur, G., & Williamson-Leadley, S. (2022). Social media and data privacy in education: an international comparative study of perceptions among pre-service teachers. Journal of Computers in Education, 1-27.

Martin, F., Chen, Y., Moore, R. L., & Westine, C. D. (2020). Systematic review of adaptive learning research designs, context, strategies, and technologies from 2009 to 2018. Educational Technology Research and Development, 68, 1903-1929.

Mohajerzad, H., Martin, A., Christ, J., & Widany, S. (2021). Bridging the gap between science and practice: Research collaboration and the perception of research findings. Frontiers in psychology, 12, 790451.

Mora-Ruano, J. G., Heine, J. H., & Gebhardt, M. (2019, August). Does teacher collaboration improve student achievement? Analysis of the German PISA 2012 sample. In Frontiers in Education,4, 85

Moussavi, M., Amannejad, Y., Moshirpour, M., Marasco, E., & Behjat, L. (2020). Importance of data analytics for improving teaching and learning methods. Data Management and Analysis: Case Studies in Education, Healthcare and Beyond, 91-101.

Murchan, D., & Siddiq, F. (2021). A call to action: a systematic review of ethical and regulatory issues in using process data in educational assessment. Large-scale Assessments in Education, 9(1), 25.

Ndukwe, I. G., & Daniel, B. K. (2020). Teaching analytics, value and tools for teacher data literacy: A systematic and tripartite approach. International Journal of Educational Technology in Higher Education, 17(1), 1-31.

O'Sullivan, L., Feeney, L., Crowley, R. K., Sukumar, P., McAuliffe, E., & Doran, P. (2021). An evaluation of the process of informed consent: views from research participants and staff. Trials, 22, 1-15.

Ozga, J. (2009). Governing education through data in England: From regulation to self-evaluation. Journal of Education Policy, 24(2), 149–162.

Papamitsiou, Z., Pappas, I. O., Sharma, K., & Giannakos, M. N. (2020). Utilizing multimodal data through fsQCA to explain engagement in adaptive learning. IEEE Transactions on Learning Technologies, 13(4), 689-703.

Payumo, J., He, G., Manjunatha, A. C., Higgins, D., & Calvert, S. (2021). Mapping collaborations and partnerships in SDG research. Frontiers in Research Metrics and Analytics, 5, 612442.

Petticrew, M. (2011). When are complex interventions 'complex'? When are simple interventions 'simple'?. The European Journal of Public Health, 21(4), 397-398.

Peersman, G. (2014). Overview: Data collection and analysis methods in impact evaluation. UNICEF Office of Research-Innocent

Pellegrino J.W.,Nguyen, T., Netto, C. L. M., Wilkins, J. F., Bröker, P., Vargas, E. E., Sealfon, C. D., Puthipiroj, P., Li, K. S., Bowler, J. E., Hinson, H. R., Pujar, M., & Stein, G. M. (2021). Insights Into Students' Experiences and Perceptions of Remote Learning Methods: From the COVID-19 Pandemic to Best Practice for the Future. Journal of Educational Technology Systems, 49(4), 569–596.

Picciano, A. G. (2012). The evolution of big data and learning analytics in American higher education. Journal of Asynchronous Learning Networks, 16(3), 9-20.

Picciano A.G., Seaman J., Shea P., Swan K. (2014) Educational Transformation through Online Learning: To Be or Not to Be. Journal of Asynchronous Learning Networks 17(2):17-35.

Reidenberg J.R., Russell N.C., Kovnot J., Norton T.B., Cloutier D., Alvarado D.R. (2013) Privacy and Cloud Computing in Public Schools. Center on Law & Information Policy, Fordham University School of Law.

Reimers, F., Schleicher, A., Saavedra, J., & Tuominen, S. (2020). Supporting the continuation of teaching and learning during the COVID-19 Pandemic. Oecd, 1(1), 1-38.

Rienties, B., Køhler Simonsen, H., & Herodotou, C. (2020). Defining the boundaries between artificial intelligence in education, computer-supported collaborative learning, educational data mining, and learning analytics: A need for coherence. In frontiers in Education, 5, 128).

Safarov, I., Meijer, A., & Grimmelikhuijsen, S. (2017). Utilization of open government data: A systematic literature review of types, conditions, effects and users. Information Polity, 22(1), 1-24.

Sanchez, E., van Oostendorp, H., Fijnheer, J. D., & Lavoué, E. (2019). Gamification. In R. R. Hoffman (Ed.), The Cambridge Handbook of Applied Perception Research (pp. 1-23). Cambridge University Press. https://doi.org/10.1017/9781316676202.002

Saleem, A. N., Noori, N. M., & Ozdamli, F. (2022). Gamification Applications in E-learning: A Literature Review. Technology, Knowledge and Learning, 27(1), 139-159.

Schifter, C., Natarajan, U., Ketelhut, D. J., & Kirchgessner, A. (2014). Data-driven decision-making: Facilitating teacher use of student data to inform classroom instruction. Contemporary Issues in Technology and Teacher Education, 14(4), 419-432.

Schult, J., Mahler, N., Fauth, B., & Lindner, M. A. (2022, April). Long-term consequences of repeated school closures during the COVID-19 pandemic for reading and mathematics competencies. In Frontiers in Education,13, 867316.

Shabihi, N., & Kim, M. S. (2021). Big data analytics in education: a data-driven literature review. In 2021 International Conference on Advanced Learning Technologies (ICALT) (pp. 154-156). IEEE.

Shahril Khuzairi, N. M., & Che Cob, Z. (2021). A Preliminary Model of Learning Analytics to Explore Data Visualization on Educator's Satisfaction and Academic Performance in Higher Education. SpringerLink.

Shemshack, A., Kinshuk, & Spector, J. M. (2021). A comprehensive analysis of personalized learning components. Journal of Computers in Education, 8(4), 485-503.

Siemens, G., & Long, P. (2011). Penetrating the fog: Analytics in learning and education. EDUCAUSE Review, 46(5), 30-32.

Skedsmo, G., & Huber, S. G. (2022). Data-driven approaches to education governance and their implications. Educational Assessment, Evaluation and Accountability, 34(1), 1–4.

Smith, W. C., & Benavot, A. (2019). Improving accountability in education: the importance of structured democratic voice. Asia Pacific Education Review, 20, 193-205.

Soncin, M., & Cannistrà, M. (2022). Data analytics in education: are schools on the long and winding road?. Qualitative Research in Accounting & Management, 19(3), 286-304.

Spillane, J. P. (2012). Data in practice: Conceptualizing the data-based decision-making phenomena. American Journal of Education, 118(2), 113–141.

Strydom, F., & Loots, S. (2020). The student voice as contributor to quality education through institutional design. South African Journal of Higher Education, 34(5), 20-34.

Tempelaar, D., Rienties, B., & Nguyen, Q. (2020). Subjective data, objective data and the role of bias in predictive modelling: Lessons from a dispositional learning analytics application. PLoS One, 15(6), e0233977.

U.S Department of Education.(n.d). Family Educational Rights and Privacy Act (FERPA).

Valverde-Berrocoso, J., Acevedo-Borrega, J., & Cerezo-Pizarro, M. (2022). Educational technology and student performance: A systematic review. In Frontiers in Education, 7, 916502

Wilichowski, T., & Cobo, C. (2021). Transforming how teachers use technology. World Bank Blogs. https://blogs.worldbank.org/education/transforming-how-teachers-use-technology.

Wisniewski, B., Zierer, K., & Hattie, J. (2020). The power of feedback revisited: A meta-analysis of educational feedback research. Frontiers in psychology, 10, 3087.

Wilcox, G., Fernandez Conde, C., & Kowbel, A. (2021). Using evidence-based practice and data-based decision making in inclusive education. Education Sciences, 11(3), 129.

Wong, B.T.M., & Li, K.C. (2020). A review of learning analytics intervention in higher education (2011–2018). Journal of Computers in Education, 7(1), 7-28.

Xu, M., & Stefaniak, J. (2021). Embracing children's voice to support teachers' pedagogical reasoning and decision-making for technology enhanced practices in early childhood classrooms. TechTrends, 65(3), 256-268.

Zhang, Y., Yun, Y., An, R., Cui, J., Dai, H., & Shang, X. (2021). Educational data mining techniques for student performance prediction: method review and comparison analysis. Frontiers in psychology, 12, 698490.

Zeide E., Nissenbaum H. (2017) The Limits of Education Purpose Limitations. University of Colorado Law Review 88(3):571-626.

Experimental Analysis of Selimiye Hammam Mortars

Özlem GÖKÇE KOCABAY[1]

Introduction

Selimiye Hammam is located in the Selimiye neighbourhood of Üsküdar, which has been preferred as a settlement area since ancient times due to its location and topographical features. The aerial photograph of Selimiye Hammam, which is located on Selimiye Hammam Street in Selimiye neighbourhood, Üsküdar district, Istanbul province, is as given in Figure 1.

Figure 1. Aerial photograph of Selimiye Hammam

Selimiye Hammam was built to serve Selimiye Barracks. There is no inscription of the hammam, but an expenditure record dated 20-03-1218 (10 July 1803 AD) is documented in the public records. Selimiye Hammam has 4 facades. The sections of dressing room, hottest room, tepidity room and grate room can be clearly traced as in classical hammam facades (Gür, 2019).

Cultural heritage properties such as historic constructions, archeological sites, and monuments, their contents and collections, besides their intangible aspects are a heritage from our passe which gain a feeling of place, identity, and esthetics welfare to localized inhabitants (Sesana et al., 2021).

Fundamental element of the sustainability of historical constructions is the utilization of practicable, compatible materials at restoration area (Gulbe, Vitina & Setina, 2017).

Throughout the centuries, mortar has been one of the most using construction materials, and it was utilized in conjunction with natural stones, bricks or artificial blocks to raise the complicated constructions of the present day world cultural heritage. The mixture of natural pozzolan and lime has been the fundament of the mortars employed throughout history, and the attention in the area is demonstrated via various empirical researches available in the literature. Well rehabilitation interferences, specially those carried out on cultural heritage buildings,

[1] Dr., T.R. Ministry of Culture and Tourism

should necessitate a deeper knowledge of the physical and mechanical characteristics of both the existing materials and those to be used. Of late years, taken into account the developments in the technology processes, there has been a kind of recovery of conventional technicals in the cultural heritage area. Lime mortars have been reevaluated for restoration work, specially in combination with pozzolanic materials (Monaco et al., 2021).

A study in the literature describes the composition of a lime mortar specimen linked to a loose brick piece from the ruins of an old church from the Spanish Colonial period in Manila, Philippines (Cayme & Asor, 2016). In another study, spectroscopic, petrographic, chemical analyses and luminescence dating of historical mortar from the Western Portic ground mosaics of Northern Sacred Agora (WPNSA) at Laodicea ancient city (Denizli-Turkey) were carried out (Koralay, Kiymaz & Şimşek, 2023). Another study characterised the microstructure and mineral composition tests of mortars collected from the walls of thirteenth century from the tower at Lublin Castle (Klimek, 2023).

The non-existence of a systematical and elaborative base data on historic lime mortar composite at the Selimiye Hammam, an Ottoman Turkish Hammam makes present work original and big deal in time to come conservation study, since it will provide that mortar replacements are more compatible with the original material. The characteristics and problems of the mortar samples were examined by visual analysis, simple spot tests, petrographic analysis, loss on ignition (calcination), acid loss and visual analysis of aggregates which do not react with acid under stereo microscope.

Materials and method

Materials

35.5% hydrochloric acid (HCl) was purchased from Sigma-Aldrich. Nitric acid (HNO_3), silver nitrate ($AgNO_3$) (technical grade), barium chloride ($BaCl_2$), diphenylamine, concentrate sulfuric acid (H_2SO_4) were obtained from Merck. Epoxy resin and hardener set was supplied by RAKU-TOOL.

Sample taking and macro identification of mortar samples by visual analysis

Before starting the chemical and physical analyses, the texture, color, condition (strength), type, color, size and approximate amounts of aggregates, visible organic additives, contamination, etc. of the mortar samples were examined, identified together with the locations where they were taken and the results are given below.

Sample 1: It is a light pink mortar sample taken from the right wall of the tepidity room, containing small sized and medium quantity brick fragments, small sized and a very small amount of grey aggregates and white masses from place to place, with medium sized pores up to 0.5 mm in size, of medium strength. Photograph of mortar sample 1 is presented in Figure 2.

Figure 2. Visual analysis of mortar sample 1 in chemistry laboratory

Sample 2: It is a brown colored mortar sample taken from the original arch and haunching of the tepidity hypocaust, containing a medium amount of aggregates of various colors and sizes, with a small amount of pores up to 0.2 mm in size, and weak. Photograph of mortar sample 2 is presented in Figure 3.

Figure 3. Visual analysis of mortar sample 2 in chemistry laboratory

Sample 3: It is a cream-pink colored, medium strength jointing sample taken from the outer wall of the entrance of the hammam, containing a small amount of small sized brick fragments, a small amount of small sized grey aggregates and white masses from place to place, with medium amount pores up to 0.5 mm in size. Photograph of mortar sample 3 is presented in Figure 4.

Figure 4. Visual analysis of mortar sample 3 in chemistry laboratory

Sample 4: It is a cream-beige colored, solid mortar sample taken from the floor filling of hypocaust, containing medium amount and size of brick fragments and medium amount, size and various colored aggregates, with abundant pores up to 0.5 mm in size, with grey colored pollution on the surface. Photograph of mortar sample 4 is presented in Figure 5.

Figure 5. Visual analysis of mortar sample 4 in chemistry laboratory

Sample 5: It is a pink colored, medium strength plaster sample taken from the tepidity room, containing a medium amount of small sized brick fragments, white masses from place to place, containing a small amount of tow, with a small amount of pores up to 0.5 mm in size, with a plaster layer of approximately 1 cm thick on the surface (Sample 5a). It is a white colored,

aggregate free, medium strength plaster sample with small amount of pores up to 0.2 mm in size, white colored paint layer on the surface, located on Sample 5a (Sample 5b). Photograph of mortar sample 5 is presented in Figure 6.

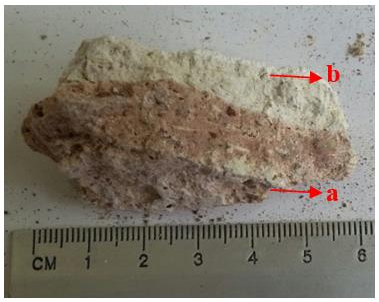

Figure 6. Visual analysis of mortar sample 5 in chemistry laboratory

Sample 6: It is a pink colored, solid mortar sample taken from the dome of the tepidity room, containing a medium amount of brick fragments of various sizes, white masses from place to place, containing a very small amount of tow, with abundant pores up to 0.5 mm in size, with cream colored mortar contamination on it. Photograph of mortar sample 6 is presented in Figure 7.

Figure 7. Visual analysis of mortar sample 6 in chemistry laboratory

Loss on ignition (calcination) analysis

After the dehydrated porcelain crucibles were tared (W_d), approximately 1 g of powdered mortar sample was weighed (SARTORIUS, CP224S model) and the weight data (W_0) was noted. The mortar samples were kept in an oven at 105ºC for 4 h. The porcelain crucibles, which were took away the oven and cooled in the desiccator, were weighed and their weight (W_1) was noted, the realized weight loss was due to the moisture included in the sample. After mentioned process; the mortar samples were hold in the muffle furnace (Protherm, PLF 110/10) at 550ºC for half an hour. The mortar samples placed in the desiccator were weighed after cooling and the weighing value (W_2) were noted. Mortar samples were hold in a muffle furnace at 1050ºC about 5 min. After cooling, it was weighed (W_3) and the values were noted. To compare and control experiment results acquired, two tests were performed for each mortar sample. Employing the conclusions of calcination analysis, the amount of moisture, molecular water and organic materials in the mortar sample, associated with the amount of carbon dioxide (CO_2) moved away the mortar sample and thus the amount of calcium carbonate ($CaCO_3$) were determined.

Calculation of percent moisture:

$$\text{Moisture\%} = \frac{W_0 - W_1}{W_1 - W_d} \times 100 \qquad (1)$$

here:

W_d: Weight of dried crucible

W_0: W_d + Mortar sample

W_1: Weight of mortar sample dehydrated at 105°C

Calculation of molecular water and organic matter content of mortar sample:

$$\%=\frac{W_1-W_2}{W_1-W_d}\times 100 \qquad (2)$$

here:

W_d: Weight of dried crucible

W_1: Weight of mortar sample dehydrated at 105°C

W_2: Weight of mortar sample dried at 550ºC

Calculation of $CaCO_3$ content in mortar sample:

$$CaCO_{3(s)} \xrightarrow{1050°C} CaO_{(s)}+CO_{2(g)} \qquad (3)$$

At 1050ºC, the calcium carbonate ($CaCO_3$) in the mortar sample decomposed and the gas carbon dioxide (CO_2) was removed from its composite. The amount of carbon dioxide (CO_2) was determined employing the difference in the weight of the mortar sample, and the amount of $CaCO_3$ in the mortar sample was calculated utilizing these results and the molar weights of the compounds in the reaction. The amount of $CaCO_3$ in the mortar sample was estimated by the following ratio utilizing mole weights and weighing data in conformity with the above-mentioned reaction:

here;

$CaCO_3$ mole weight: 100 g.mole^{-1}

CO_2 mole weight: 44 g.mole^{-1}

W_d: Weight of dried crucible, g

W_0: W_d + Dried mortar sample weight, g

W_3: Weight of sample dried at 1050ºC, g;

Considering that 100 g $CaCO_3$ contains 44 g CO_2,

How many g of $CaCO_3$ include (W_0- W_3) g of CO_2

$$CaCO_3\%=\frac{\left[\left(W_0-W_3\right)\times 100\right]/44}{W_0-W_d}\times 100 \qquad (4)$$

Acid loss and sieve analysis

The dehydrated beaker was tared (KERN, PFB 600-2M model) with an accuracy of 0.01 g and the indicated weight was noted (W_0). Then, approximately 20-30 g of mortar sample was placed in the beaker, its weight was noted (W_1) and the sample was dried in an oven (Memmert, UM100) at 105ºC. After the mortar sample was cooled in the desiccator, it was weighed once more and its weight (W_2) was noted. After the weighing process was completed, approximately 25 mL of 10% hydrochloric acid (HCl) was put to the mortar sample and kept in a fume hood. The resulting admixture was mixed with a glass rod periodically and HCl was added on it, and

mentioned process was continued until the sample did not react with HCl. The top solution was moved away and the sample was neutralized by distilled water. Afterwards, the mortar sample remaining in the beaker was dried at 105ºC for 4 h. The quantity of W_3 was determined by weighing the dry sample cooled in the desiccator; moisture% and acid loss% were calculated by the below equation.

Percent moisture calculation:

$$\text{Moisture\%} = \frac{W_1 - W_2}{W_1 - W_0} \times 100 \quad (5)$$

here;

W_0: Weight of dried beaker

W_1: W_0 + Sample

W_2: W_0 + Dried Sample

Calculating of percent acid loss:

$$\text{Remainder\%} = \frac{W_3 - W_0}{W_1 - W_0} \times 100 \quad (6)$$

$$\text{Loss\%} = 100 - \text{Remainder\%} \quad (7)$$

here;

W_0: Weight of dried beaker

W_1: W_0 + Sample

W_3: W_0 + Dried sample remaining after acid loss

Immediately after acid loss, the sample was first dried to constant weight at 105ºC and then cooled in a desiccator. The weighed samples were then stored for sieve analysis. Then, sieve analysis was carried out, weight was taken and the samples were individually packed according to the aggregate sizes and kept for microscope examination.

Analysis of water soluble salts

First of all the mortar samples are powderized, then 1 g of powdered sample is got and an admixture is made with 100 mL distilled water (Millipore, elix 10). The conductivity of the mixture, that was mixed with a glass rod at predetermined time intervals and kept for 48 h, was measured with a conductometer (WTW pH/cond 340i SET PORTABLE). After that spot tests are carried out to specify the presence of water soluble chloride (Cl^-), nitrate (NO_3^-), sulfate (SO_4^{2-}) salts.

Petrographic analysis

Thick section analysis

Approximately 2x2 cm mortar specimen was placed in the mould with epoxy and accelerator mixture.

Thin section analysis

The thin section is a piece of the mortar sample (0.030-0.005) mm thick and covered with a lamella, placed on a lame (Gökçe Kocabay & İsmail, 2023).

Results and discussion

Loss on ignition (calcination) analysis

The percentage of ingredients such as moisture, molecular water, organic matter and calcium carbonate ($CaCO_3$) in the mortar sample were determined with the loss on ignition (calcination) analysis performed on the powdered materials by taking advantage of the weight changing at incremental temperatures (Table 1).

Table 1. Loss on ignition (calcination) analysis results

Sample number	Moisture Average (%)	Organic Loss Average (%)	Calcination Average (%)
1	13.04	2.02	61.87
2	31.46	11.98	7.47
3	4.63	4.15	68.66
4	12.72	5.95	54.73
5a	27.20	9.96	30.85
5b	5.45	4.50	78.30
6	23.02	10.76	37.15

Acid loss and sieve analysis

Acid loss and sieve analyses were performed to determine the proportions, qualities and size distributions of silicate aggregates and pozzolanic materials (used as both fillers and additives) other than binders and carbonated aggregates in mortars.

In order to determine the size distribution, aggregates were sieved using <125, 125, 250, 600, 1000, 2500 μ sieve set and weighed separately. Aggregates were examined under a stereo microscope, their visual characteristics were determined and the results are given in Table 2.

Table 2. Results of acid loss and sieve analysis

Sample			Sieve Analysis (%)					
	Loss (%)	**Remaining (%)**	**2500**	**1000**	**600**	**250**	**125**	**<125**
1	71.32	28.68	0.00	36.32	10.85	9.91	13.21	29.72
2	18.18	81.82	27.02	11.36	2.74	4.83	3.52	50.52
3	70.81	29.19	33.25	22.08	6.49	5.71	10.13	22.34
4	67.07	32.93	27.73	16.53	6.44	4.20	10.92	34.17
5a	79.13	20.87	0.00	0.00	0.00	0.00	0.00	100.00
5b	89.85	10.15	0.00	0.00	0.00	0.00	0.00	100.00
6	72.13	27.87	0.00	22.11	3.79	6.95	20.00	47.16

Water soluble salts analyses

This analysis was performed using simple spot tests and conductivity measurements to determine the qualification and quantity of water soluble salts (chloride (Cl^-), nitrate (NO_3^-), and sulfate (SO_4^{2-})) present in the samples (Table 3).

Table 3. Results of water soluble salt analysis

Sample number	Cl^-	$SO_4^=$	NO_3^-	Conductivity (µs)	Salt%
1	-	-	-	99	0.55
2	-	++	-	870	4.84
3	-	-	-	148	0.82
4	-	-	-	97	0.54
5a	-	-	-	1800	10.01
5b	-	-	-	2070	11.51
6	+	-	-	200	1.11

Very-high amount (++++), high amount (+++), medium amount (++), low amount (+), ultralow amount (±).

Visual analysis of aggregates with stereo microscope

The silicate aggregates of the samples whose binders were decomposed by acid treatment, which did not react with acid, were examined under stereo microscope after being separated into sizes by sieve analysis and their visible properties (color, shape, weight ratios) are given below.

Sample 1: Approximately 35% of the remaining 28.68% of the sample after the acid treatment is above 1000 µ and the aggregates are under 4 mm sieve. Aggregates are generally grey, cream and tile red colored. The aggregates of the sample are angular.

Sample 2: Approximately 40% of the remaining 81.82% of the sample after the acid treatment is above 1000 µ, 25% is 10 mm gravel, and the aggregates are under 5 mm sieve. Aggregates are generally brown in color. The aggregates of the sample are angular.

Sample 3: Approximately 55% of the remaining 29.19% of the sample after the acid treatment is above 1000 µ, 30% is 8-10 mm gravel and the aggregates are under 4 mm sieve. Aggregates are generally grey, tile red and cream colored. The aggregates of the sample are angular.

Sample 4: Approximately 45% of the remaining 32.93% of the sample after the acid treatment is above 1000 µ, 30% is 10 mm gravel and the aggregates are under 5 mm sieve. Aggregates are generally tile red and cream colored. The aggregates of the sample are angular.

Sample 5a: The remaining 20.87% of the sample after the acid treatment is all brick dust.

Sample 5b: All of the remaining 10.15% of the sample after the acid treatment is a cream colored powdery particle.

Sample 6: Approximately 20% of the remaining 27.87% of the sample after the acid treatment is above 1000 µ and the aggregates are under 6 mm sieve. A few of the aggregates are transparent and most of them are tile red colored. The aggregates of the sample are angular.

Petrographical analysis results

Thick section analyses of mortar samples

Textural and aggregate properties were determined by examining the thick sections prepared from the mortar samples embedded in epoxy under stereo microscope and the results are given below.

Sample 1: The remainder of the sample, which has a binding area is approximately 30 to 35%, is aggregate and freely dispersed minerals. The binder/binder and binder/aggregate phases of the sample are in good condition and have a medium amount of pores up to 0.5 mm in size. The thick section photograph of specimen 1 is given in Figure 8.

Figure 8. Thick section photograph of Sample 1

Sample 2: The remainder of the sample, which has a binding area is approximately 15 to 20%, is aggregate and freely dispersed minerals. The binder/binder and binder/aggregate phases of the sample are in good condition and have a small amount of pores up to 0.2 mm in size. The thick section photograph of specimen 2 is given in Figure 9.

Figure 9. Thick section photograph of Sample 2

Sample 3: The remainder of the sample, which has a binding area is approximately 30 to 35%, is aggregate and freely dispersed minerals. The binder/binder and binder/aggregate phases of the sample with a medium amount of pores up to 0.5 mm in size are relatively good. The thick section photograph of specimen 3 is given in Figure 10.

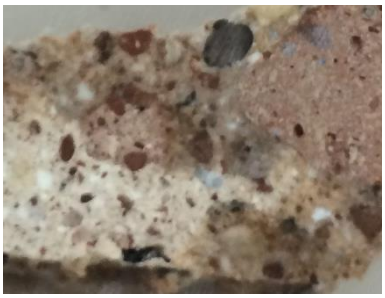

Figure 10. Thick section photograph of Sample 3

Sample 4: The binder area of the sample is around 30%, the rest of the sample is aggregate and freely dispersed minerals. The binder/binder and binder/aggregate phases of the sample are in good condition and have a medium amount of pores up to 0.5 mm in size. The thick section photograph of specimen 4 is given in Figure 11.

Figure 11. Thick section photograph of Sample 4

Sample 5a: The binder area of the sample is around 30%, the rest of the sample is aggregate and freely dispersed minerals. The binder/binder and binder/aggregate phases of the sample with a small amount of pores up to 0.2 mm in size are relatively good.

Sample 5b: Almost all of the sample is binder, the rest is aggregate and freely dispersed minerals. The binder/binder phase of the sample with a small amount of pores up to 0.2 mm in size is in good condition. The thick section photograph of sample 5 is given in Figure 12.

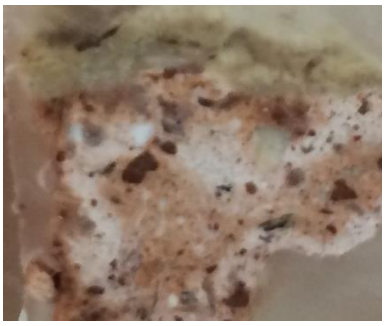

Figure 12. Thick section photograph of Sample 5

Sample 6: The binder area of the sample is around 30%, the rest of the sample is aggregate and freely dispersed minerals. The binder/binder and binder/aggregate phases of the sample are in good condition and have a medium amount of pores up to 0.5 mm in size. The thick section photograph of sample 6 is given in Figure 13.

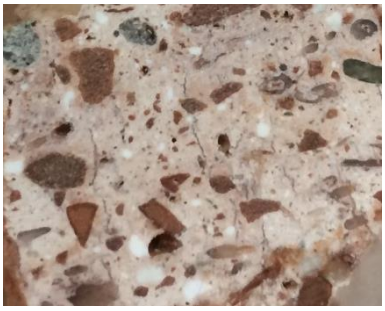

Figure 13. Thick section photograph of Sample 6

Thin section analyses of mortar samples

The most suitable sample for mineralogical-petrographic analyses (sample number 4) was subjected to examination in the Petrography Laboratory. Thin sections of the sample hardened by embedding in epoxy were prepared. Within the scope of the analysis, the aggregate and mineral types, binder-aggregate relationship and void structure of the sample were determined.

Sample 4: Brick fragments, marble fragments, sandstone fragments and freely distributed quartz, feldspar, calcite, iron oxide and opaque minerals were found as aggregate types in the sample (Figure 14). It was stated that sandstone is particularly prominent among the many rock types employed in historical façades (Klimek & Grzegorczyk-Frańczak, 2021). Besides it has been reported that according to the mineralogical data and the thin section analysis, sample KM21 has a great number of marble fragments bigger than 2 mm in size in the aggregate. KM21 additionally involves quartzite rock fragments, calcite and opaque minerals (Miriello et al., 2015). It has been expressed that in the petrographic analysis of Yelli mosque samples, a variety of grain sizes from thin up to large feldspar minerals have been observed (Solak, 2016). In another study, it was stated that black inclusions defined with Raman spectroscopy might be associated with carbonaceous material of an amorphous character and iron oxides and hydroxides (hematite/goethite) (Iordanidis & Garcia-Guinea, 2013). The binder-aggregate relationship is good. Amorphous voids were observed in the binder part. It has been pointed out that the density of the old mortar is less and this was caused by the voids and cracks in the mortar (Talib et al., 2023).

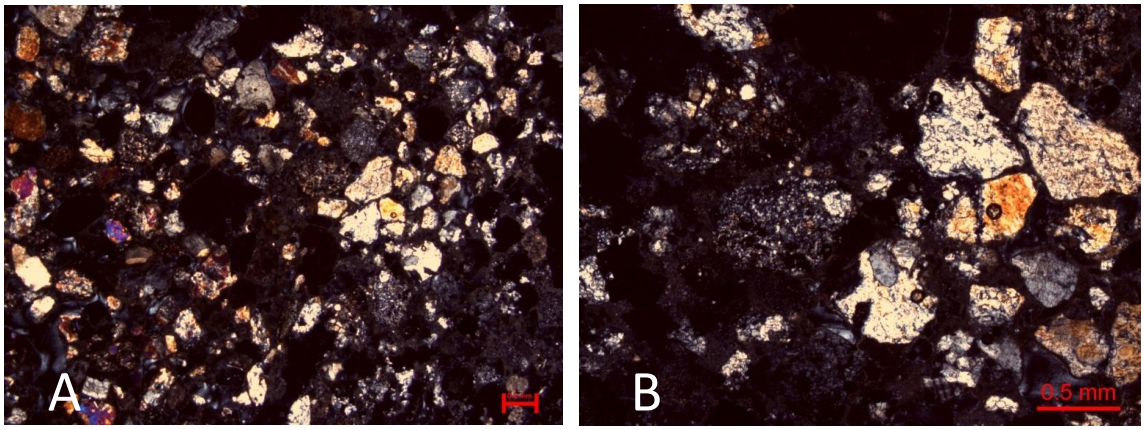

Figure 14. General view of thin section of Sample 4 under polarising microscope. A-B. The general texture of the sample and the aggregate and mineral particles in it (Double Nicol)

Findings of material analyses

The above analyses were performed on the mortar samples of Selimiye Hammam, the binder, aggregate and admixture types and ratios (by weight) of the samples are given below and the material suggestions to be made as a result of the evaluation are given.

Sample 1: The binder of mortar sample number 1 is 30-35% aerial lime (lime putty). Numerous investigators think of aerial lime as the most appropriate material for repair mortars since aerial lime was the most commonly binder in mortar till late in the 19th century and it is chemically compatible with ancient mortars (Silva, Pinto & Gomes, 2014). The aggregates of the sample are under 4 mm sieve. The sample does not contain salt.

Sample 2: The binder of mortar sample number 2 is soil with 10-15% lime added. The aggregates of the sample are under 5 mm sieve. The medium amount of sulfate (SO_4^{2-}) salt detected in the sample is thought to be caused by environmental pollution. It has been expressed that the existence of sulfates could be resulting from a synergism of parameters such as raw materials with sulfate high content (gypsum, brick dust, cement), air-pollution, or even to the foundation ground (Papayianni et al., 2013).

Sample 3: The binder of jointing sample number 3 is 30-35% aerial lime (lime putty). In a study, 47 mosaic mortar specimens, that were collected from the Southern Bath, Macellum (Agora) and Southern Basilica mosaics in the Perge Antique City, were analysed to characterise their characteristics and identifying their problems. The binder of the first subgroup of the mortars in the second group was determined as 1 portion (with the ratio of 30-35%) slaked lime putty (Uğur, 2011). The aggregates of the sample are under 4 mm sieve. The sample does not contain salt.

Sample 4: The binder of mortar sample number 4 is aerial lime (lime putty) around 30% with 5-10% pozzolan added. It has been reported that lime (aerial or hydraulic) is generally employed in combination with pozzolanic admixtures or cement, to accord with both, chemical/mineralogical and mechanical compatibility criteria (Dimou et al., 2022). The aggregates of the sample are under 5 mm sieve. The sample does not contain salt.

Sample 5a: The binder of plaster sample number 5a is about 30% aerial lime (lime putty) with 5-10% pozzolan added. The aggregates of the sample are under 125 μ sieve. The sample contains a very small amount of tow. It was stated that the organic tow (plant, straw, etc.) added to the composition of plaster specimens in order to enhance the adhesion to the surface can be observed in plasters unlike mortars (Karataş, Alptekin & Yakar, 2022). The sample does not contain salt.

Sample 5b: The binder of plaster sample number 5b is 40-45% aerial lime (lime putty). The aggregates of the sample are under 125 μ sieve. The sample does not contain salt.

Sample 6: The binder of mortar sample number 6 is aerial lime (lime putty) around 30% with 5-10% pozzolan added. A great number of works have been performed proving that air lime mortars mixed with pozzolans exhibited quicker setting properties and an increment in their mechanical capacity and durability (Monteiro, Silva & Faria, 2021). The aggregates of the sample are under 6 mm sieve. The sample contains a very small amount of tow. The small amount of chloride (Cl^-) salt detected in the sample is thought to be caused by environmental pollution. It has been reported that the most commonly developed efflorescence involves sulphate or chloride efflorescence (Bochen, Słomka-Słupik & Ślusarek, 2021).

Suggested recipes for repair mortars

The following solution proposals should be practiced in the general repairs to be made by bringing together the evaluations made above.

Sample 1:

1 part aerial lime (lime putty) (50% ± 2 aqueous), which has been hydrated and aged for at least 2 years,

1 part 4 mm sieved aggregate,

2 parts of 4 mm sieved brick fragments and dust.

It was stated that mortars and plasters consisted of a admixture of brick dust and lime have been employed dated from ancient ages by virtue of their hydraulic qualities (Böke et al., 2006).

Sample 2:

1 part aerial lime (lime putty) (50% ± 2 aqueous), which has been hydrated and aged for at least 2 years,

6 parts of sieved (with 5 mm sieved aggregate) soil.

According to the results of the analysis of the mortar of the Büyük Mud-brick Tower of Van Castle, the binder (aerial lime (lime putty)):aggregate (sieved soil) ratio in the formulation

to be applied for the compatible restoration mortar is 1:6 as in this study (Gökçe Kocabay & İsmail, 2022).

Sample 3:

1 part aerial lime (lime putty) (50% ± 2 aqueous), which has been hydrated and aged for at least 2 years,

1 part 4 mm sieved aggregate,

1.5 parts of 4 mm sieved brick fragments and dust,

0.5 part 10 mm sieved gravel.

In Greece, in Akrotiri of Thera (1,700-1,400 BC), gravel was also used to make building mortars (Pachta et al., 2014).

Sample 4:

1 part aerial lime (lime putty) (50% ± 2 aqueous), which has been hydrated and aged for at least 2 years,

0.25 part pozzolan,

1.25 parts of 5 mm sieved aggregate,

1 part 5 mm sieved brick fragments and dust,

0.5 part brick gravel.

It has been stated that properties of Roman lime mortars employed in buildings such as water-related buildings and tomb in Sagalassos were analyzed to produce repair mortars compatible with the available ones. The Roman mortars were consisted of lime and pozzolanic aggregates. Lime/aggregate ratios were between 1/3-2/3 by weight (Taşcı, 2021).

Sample 5a:

1 part aerial lime (lime putty) (50% ± 2 aqueous), which has been hydrated and aged for at least 2 years,

1 part gypsum,

1.75 parts of 1 mm sieved brick fragments and dust,

1.5 parts of 2 mm sieved limestone fracture.

A study examined different kinds of mortar from historical water-related constructions in Sicily and compared both their hydraulic qualities and textural qualities in relation to their status in the building. The lime:aggregate ratios were between 2/3-3/2 by weight (Rizzo et al., 2008). This result was similar to the result obtained with Sample 5a.

In one study, it was expressed that in precast decorations gypsum plaster is the main component, while in those specimens where application was on site, the addition of calcitic lime was widespread, in order to enhance the workability of the material (Freire et al., 2008).

Sample 5b:

It will be appropriate to use a mixture of 1 part of hydrated and aged for at least 2 years aerial lime (lime putty) (50% ± 2 aqueous), 2.25 parts of limestone dust under 1 mm sieve and trowelling of the surface. It is also recommended to add 100-150 g of tow per m^3 of this mixture.

In a study conducted within the scope of the "Nuruosmaniye Mosque Repair Project", the quality and problems of the mortar and plaster samples taken from the sanctum sanctorum,

basement floor and courtyard of the mosque were investigated. In finishing plaster repairs, it was stated that it would be appropriate to use the part stripped from the carbonated surface of the aged lime or 1 part of hydrated aerial lime (lime putty) and 1.75-2 parts of limestone dust ground under 1 mm sieve (Güleç, 2012).

Sample 6:

1 part aerial lime (lime putty) (50% ± 2 aqueous), which has been hydrated and aged for at least 2 years,

1 part 4 mm sieved limestone fracture,

2 parts of 6 mm sieved brick fragments and dust.

It has been stated that the aggregates used in all mortars and plasters taken from Imaret-i Atik Mosque and determined by laboratory tests were brick fragments and dust and limestone fracture and dust. Only in the plaster samples numbered 22 and 40, which were made as finishing plaster, it was determined that limestone fracture and dust were used as aggregate (İş, 2019).

Conclusions

Essential parameter of the sustainability of historical constructions is the use of practicable, compatible materials in restoration.

The principle goal of present work was to define and characterize the binders and aggregates of historical mortars, plasters and jointing used in Selimiye Hammam using chemical and mineralogical data so as to gather data which will be considered for the formulation of restoration mortars compatible with ancient masonry.

As a result of analyses, it can be said that the samples have almost the same binder (aerial lime (lime putty)). Unlike the others, the binder of Sample 2 is lime added soil.

The average binder/aggregate ratios were measured as follows: 1:1.625 for Sample 5a, 1:2.25 for Sample 5b, 1:3 for Samples 1, 3, 4 and 6, and 1:6 for Sample 2.

Brick fragments, pozzolan and limestone fracture were generally used as aggregate. It was observed that the aggregate distribution in the binder was homogeneous and mainly consisted by fine to coarse angular particles.

Salt crystallization within the porous matrix of architectural materials has long been recognized as an important and common reason of decay, but no significant salt content was detected in the analyses performed in this study.

The data acquired in this paper will be beneficial in the explaining in details of compatible repair mortars and, thereby, in the definition of a proper conservation strategy on the Selimiye Hammam.

Acknowledgements

The author would like to thank her esteemed colleagues and institution director at the Ministry of Culture and Tourism, Istanbul Restoration and Conservation Central and Regional Laboratory Directorate for their assistance. The author would also like to acknowledge the support of Prof. Dr. Ahmet Güleç as general scientific advisor. The author also gratefully acknowledges the assistance of the geologists in the petrography laboratory.

REFERENCES

Bochen, J., Słomka-Słupik, B., & Ślusarek, J. (2021). Experimental study on salt crystallization in plasters subjected to simulate groundwater capillary rise. *Construction and Building Materials, 308,* 125039. Doi: 10.1016/j.conbuildmat.2021.125039

Böke, H., Akkurt, S., İpekoğlu, B., & Uğurlu, E. (2006). Characteristics of brick used as aggregate in historic brick-lime mortars and plasters. *Cement and Concrete Research, 36* (6), 1115-1122. Doi: 10.1016/j.cemconres.2006.03.011

Cayme, J.-M. C., & Asor, A. N. J. (2016). Characterization of historical lime mortar from the Spanish Colonial Period in the Philippines. *Conservation Science in Cultural Heritage, 16* (1), 33-57. Doi: 10.6092/issn.1973-9494/7164

Dimou, A. E., Metaxa, Z. S., Kourkoulis, S. K., Karatasios, I., & Alexopoulos, N. D. (2022). Tailoring the binder matrix of lime-based binders for restoration interventions with regard to mechanical compatibility. *Construction and Building Materials*, *315,* 125717. Doi: 10.1016/j.conbuildmat.2021.125717

Freire, T., Silva, A. S., Veiga, M. R., & Brito, J. D. (2008). Characterization of Portuguese Historical Gypsum Mortars. *HMC08 1st Historical Mortars Conference - Characterization, Diagnosis, Conservation, Repair and Compatibility*, 24-26 Sep 2008, Lisbon.

Gökçe Kocabay, Ö., & İsmail, O. (2022). Mortar analysis for Van Castle Restoration. *2. International Congress on Contemporary Scientific Research*, 2-3 Nov 2022, Gaziantep, Turkey, (pp. 129-135).

Gökçe Kocabay, Ö., & İsmail, O. (2023). Characterization of ancient mortars: The case of the Harem Buildings in Topkapi Palace. *Current Debates on Natural and Engineering Sciences 9* (1th ed., pp. 393-409). Ankara: Bilgin Kültür Sanat Yayınları.

Gulbe, L., Vitina, I., & Setina, J. (2017). The influence of cement on properties of lime mortars. *Procedia Engineering, 172,* 325-332. Doi: 10.1016/j.proeng.2017.02.030

Güleç, A. (2012). Nuruosmaniye Camii'ne ait malzemelerin nitelik ve problemlerinin analizi. *Vakıf Restorasyon Yıllığı, 5*, 59-75.

Gür, B. (2019). Selimiye Hamamı'nın Korunması ve Yeniden Kullanılmasına Yönelik Öneriler, Yüksek Lisans Tezi, Yıldız Teknik Üniversitesi Fen Bilimleri Enstitüsü.

Iordanidis, A., & Garcia-Guinea, J. (2013). Mineralogical study of different mortar types from historical monuments of Northern Greece. *2nd International Balkans Conference on Challenges of Civil Engineering, BCCCE*, 23-25 May 2013, Epoka University, Tirana, Albania, (pp. 1010-1018).

İş, M. (2019). İmaret-i Atik Camii'nde Kullanılan Osmanlı-Bizans Dönemi Harç ve Sıvalarının İncelenmesi, Yüksek Lisans Tezi, Fatih Sultan Mehmet Vakıf Üniversitesi Mimarlık Anabilim Dalı.

Karataş, L., Alptekin, A., & Yakar, M. (2022). Detection of materials and material deterioration in historical buildings by spectroscopic and petrographic methods: The example of Mardin Tamir Evi. *Engineering Applications, 1* (2), 170-187.

Klimek, B. (2023). Characteristics of 13th-century mortars from the tower at Lublin Castle. *Archives of Civil Engineering*, *69* (2), 83-95. Doi: 10.24425/ace.2023.145254

Klimek, B., & Grzegorczyk-Frańczak, M. (2021). Properties of mortars with recycled stone aggregate for the reconstruction of sandstone in historic buildings. *Sustainability*, *13* (3), 1386. Doi: 10.3390/su13031386

Koralay, T., Kiymaz, G., & Şimşek, C. (2023). Spectroscopic, petrographic, chemical analyses and luminescence dating of historical mortar from the Western Portic ground mosaics of Northern Sacred Agora (WPNSA) at Laodicea ancient city (Denizli-Turkey). *Periodico di Mineralogia*, *92*, 97-119. Doi: 10.13133/2239-1002/17842

Miriello, D., Antonelli, F., Apollaro, C., Bloise, A., Bruno, N., Catalano, M., Columbu, S., Crisci, G. M., Luca, R. D., Lezzerini, M., Mancuso, S., & Marca, A. L. (2015). A petro-chemical study of ancient mortars from the archaeological site of Kyme (Turkey). *Periodico di Mineralogia*, *84* (3A), 497-517. Doi: 10.2451/2015PM0028

Monaco, M., Aurilio, M., Tafuro, A., & Guadagnuolo, M. (2021). Sustainable mortars for application in the cultural heritage field. *Materials*, *14* (3), 598. Doi: 10.3390/ma14030598

Monteiro, J., Silva, V., & Faria, P. (2021). Effect of type of curing and metakaolin replacement on air lime mortars for the durability of masonries. *Infrastructures*, *6* (10), 143. Doi: 10.3390/infrastructures6100143

Pachta, V., Stefanidou, M., Konopisi, S., & Papayianni, I. (2014). Technological evolution of historic structural mortars. *Journal of Civil Engineering and Architecture*, *8* (7), 846-854. Doi: 10.17265/1934-7359/2014.07.005

Papayianni, I., Stefanidou, M., Pachta, V., & Konopisi, S. (2013). Content and topography of salts in historic mortars. *3rd Historic Mortars Conference*, 11-14 Sep 2013, Glasgow, Scotland.

Rizzo, G., Ercoli, L., Megna, B., & Parlapiano, M. (2008). Characterization of mortars from ancient and traditional water supply systems in Sicily. *Journal of Thermal Analysis and Calorimetry*, *92*, 323-330. Doi: 10.1007/s10973-007-8758-4

Sesana, E., Gagnon, A. S., Ciantelli, C., Cassar, J., & Hughes, J. J. (2021). Climate change impacts on cultural heritage: A literature review. *WIREs Climate Change*, *12* (4), e710. Doi: 10.1002/wcc.710

Silva, B. A., Pinto, F., & Gomes, A. (2014). Influence of natural hydraulic lime content on the properties of aerial lime-based mortars. *Construction and Building Materials*, *72*, 208-218. Doi: 10.1016/j.conbuildmat.2014.09.010

Solak, A. (2016). Experimental investigation of lime mortar used in historical buildings in Becin, Turkey. *Materials Science*, *22* (1), 105-112. Doi: 10.5755/j01.ms.22.1.9022

Talib, H., Khan, R. B. N., Khitab, A., Benjeddou, O., & Khan, R. A. (2023). Scanning through multidisciplinary techniques and recreation of historic mortar: Case study of Rohtas Fort. *Case Studies in Construction Materials*, *18*, e02052. Doi: 10.1016/j.cscm.2023.e02052

Taşcı, B. (2021). Properties of Lime Binders and Aggregates of Roman Mortars in Western Anatolia, Ph.D. dissertation, Graduate School of Engineering and Sciences of İzmir Institute of Technology.

Uğur, T. (2011). Perge Antik Kentine Ait Mozaik Harçlarının Karakterizasyonu, Yüksek Lisans Tezi, İstanbul Üniversitesi Sosyal Bilimler Enstitüsü.

Digital Transformation and Distance Education Systems of Universities in Türkiye During the Pandemic

Ali DURDU[1]
Özkan CANAY[2]

Introduction

The COVID-19 pandemic has significantly impacted various fields worldwide, from healthcare systems to economies. One of these impacts was observed in the education sector, leading to profound changes in the functioning of universities and student-teacher interactions. The limitations of face-to-face education and the measures taken to prevent the spread of the pandemic rapidly pushed universities into the realm of digital transformation. The pandemic has become a period where many universities had to suspend their long-standing face-to-face education models. However, this challenging period necessitated universities to swiftly adapting to new technologies and online learning platforms. With the acceleration of digital transformation, fundamental elements such as interaction between students and teachers, examination systems, and teaching materials underwent radical changes.

The COVID-19 pandemic, which began in early 2020, substantially changed the education sector. Particularly during the spring semester of the 2019-2020 academic year, the closure of educational institutions and the implementation of quarantine measures almost worldwide led to the rapid rise and normalization of distance education. During this period, educational institutions had to resort to distance education methods to ensure students did not fall behind in their studies. This transition posed a significant adaptation process for educators and students alike. Many individuals without experience in distance education suddenly had to transition to digital learning platforms. This situation created a necessity for educators to learn how to deliver their courses effectively in online environments and for students to learn effectively in this new system.

Educational institutions began to use various online tools and platforms to overcome this challenging period and succeed in distance education. Online education tools such as Zoom, Google Classroom, and Moodle, among others, have assisted educators and students in organizing interactive lessons and facilitating learning. However, distance education also brought forth some challenges. Issues like unequal access among students, lack of motivation, and social isolation made the successful implementation of this new education model more challenging.

The COVID-19 pandemic significantly impacted universities in Türkiye and was directed by essential decisions made by the Council of Higher Education (YÖK). At the onset of the pandemic, universities decided to suspend in-person education for three weeks to safeguard the health of students and teachers. Subsequently, YÖK instructed universities to transition to remote education, making it clear that face-to-face education would not occur under pandemic conditions (YÖK, 2020a). The remote education process began with live lessons for universities equipped with digital resources, while others were supported by creating a repository of open

[1] Asst. Prof. Dr., Management Information Systems, Ankara Social Sciences University, ali.durdu@asbu.edu.tr
[2] Lecturer, Computer Technologies, Sakarya University of Applied Sciences, canay@subu.edu.tr

course materials. The President of YÖK stated that theoretical courses would be delivered through digital methods and practical courses would be conducted with a suitable schedule. Universities made efforts to manage the pandemic period by offering flexibility to students through synchronous and asynchronous remote education methods.

The evolution of remote education is a result of the process of adapting to contemporary technological advancements. As technology advanced, societal structures underwent a significant transformation, impacting the education system, evolving traditional learning methods. Education has transcended the mere process of memorizing information from books; it now aims to teach students crucial skills such as critical thinking, data analysis, and access to information. These processes consider education not only as the transmission of knowledge but also as a process aimed at developing students' abilities to understand and solve the world. Education must continually renew itself by adapting to changing societal dynamics. The new societal structure has necessitated the education system to construct a new framework (Parlar, 2012, p.194-195).

Rapid advances in science and technology have profoundly affected the relationship between education and society. The world requires a similar development in the field of education in order to keep up with this rapid change. Individuals have to develop and adopt new ways of thinking, behavior and learning methods required by an ever-changing society. In this context, the education system also needs a radical transformation. The new approach brings education and technology together and suggests the integrated use of these two fields (Alkan, 2005, p.11). As a result of these developments, the concept of "distance education", which emerged from the combination of education and technology, has gained importance. In the most basic terms, the concept of distance education is characterized as education and learning carried out in a situation where the teacher and the learner are located in different places. Although the teacher and the learner are in different locations, they can engage in learning-teaching activities with each other through information technology. This situation is defined as "distance education" (Uslusoy, 2017, p.4-5).

Alkan (1987, p.37) defines distance education as the communication and interaction of the instructor and the learner through technological tools in different environments in cases where traditional learning methods cannot be applied due to their limitations. Kaya (2002, p.22) is of the opinion that distance education and technology are inseparable parts: "a form of education that uses electronic media or customized learning tools and equipment". Simonson et al. (2012, p.32) discuss the definition of distance education based on its basic elements. Accordingly, distance education is defined as a method that provides institution-based, interactive communication, where learners and teachers are in different locations, and provides a learning experience by sharing information through tools such as data, audio, video.

One of the main reasons why distance education plays an important role in many countries is that it has the ability to bring together individuals with different personal characteristics and provide services at an international level. Furthermore, distance education programs allow students and teachers to benefit from independent, individual and group study environments. Individuals living in different parts of the world have the opportunity to communicate effectively through this educational model (İşman, 2011, p.3). Distance education has shown a significant development at national and international level since the early 1980s. Among the aims of this education model are to eliminate the limitations of traditional education and to increase the literacy rate, even to make it completely widespread (Kesim, 2009, p.82).

Distance education has a history of more than two centuries, during which time it has witnessed significant changes in learning processes and information communication. These changes range from the times when basic correspondence was done through mail to modern

education methods using various tools offered through online platforms (Özüçelik, 2019, p.20). With this historical evolution, distance education stands out as a dynamic education model that constantly renews itself and adapts to different forms of communication. Distance education is an interdisciplinary field that aims to eliminate the limitations between students, teachers and learning resources and focuses on using existing technologies effectively to achieve this. Looking at the history of the field of distance education, it is seen that the most common information and communication technologies of the period were used in learning and teaching processes and that these technologies shaped the periods and phases of distance education.

In addition, the examination of distance education processes shows that it has evolved towards concepts such as learning, ease of access and flexibility (Bozkurt, 2017, p.87). It is clearly seen that technology plays a decisive role in the classification of distance education. Based on these classifications, it can be said that each period includes the previous period and contributes to the development (Moore & Kearsley, 2011). In other words, it is observed that the periods and phases of distance education are not independent from each other, each period includes the previous one and progress is achieved in this way (Rodriguez, 2012).

In this study, the effects of the COVID-19 pandemic on universities will be examined, how universities overcame this challenging period and their digital transformation, and the systems used in distance education systems will be examined. It investigates how there has been an adaptation process against the challenges brought by the pandemic, how educational institutions have developed their digital infrastructures and which methods they prefer in distance education. It will also emphasize the importance of digital transformation in the field of education by addressing the effects of this transformation on the future of education and the student-teacher experience. In the second part of the study, the development of distance education in the world, in the third part, the development of distance education in Turkey, in the fourth part, distance education systems, in the fifth part, digital transformation and distance education infrastructures of universities in Turkey during the pandemic period, and in the sixth part, conclusions are given.

The development of distance education around the world

In literature, the beginning of distance education in the world is widely recognized to have started in 1728 when a newspaper in Boston announced that it would offer shorthand, or fast writing, lessons through correspondence. Following this announcement, in 1833, the announcement of shorthand lessons via correspondence in Sweden is considered one of the first practical applications of distance education. In 1840, Isaac Pitman, working in the field of shorthand in Bath, England, began to provide shorthand lessons to students through letters and would evaluate their work by providing feedback. This is widely accepted as the true initiation of early distance education practices (Kaya, 2002, p.28).

In the early years of distance education initiatives, the courses offered often focused on shorthand skills and were predominantly conducted through continuous correspondence. The majority of participants in these courses were women. The institutionalization of distance education occurred in 1873 with the establishment of the "Society to Encourage Home Studies" by Anna Ticknor. A visual representation of the historical periods and phases of distance education in a global context is presented in Figure 1 (Bozkurt, 2017, s.87).

One of the prominent figures in distance education via correspondence was William Rainey Harper, the founder of the University of Chicago. Harper, in 1883, at the Chautauqua Institute in New York and later in 1891 at the University of Chicago, developed correspondence courses, thereby ensuring that education became a democratic environment accessible to every

individual. Harper is considered an important educator who, like contemporaries Pitman and Ticknor, advocated for the right to education for every individual (Akçay, 2014, p.27).

Advancements in technology have made information more accessible, thereby facilitating learning. However, during this period, education was still provided via postal mail, leading to delays, issues such as lost mail, and increased costs. The invention of radio and television helped overcome these issues and created a more effective and faster education network. During this time, the number of universities providing education through radio and television increased (WEB 1, 2007).

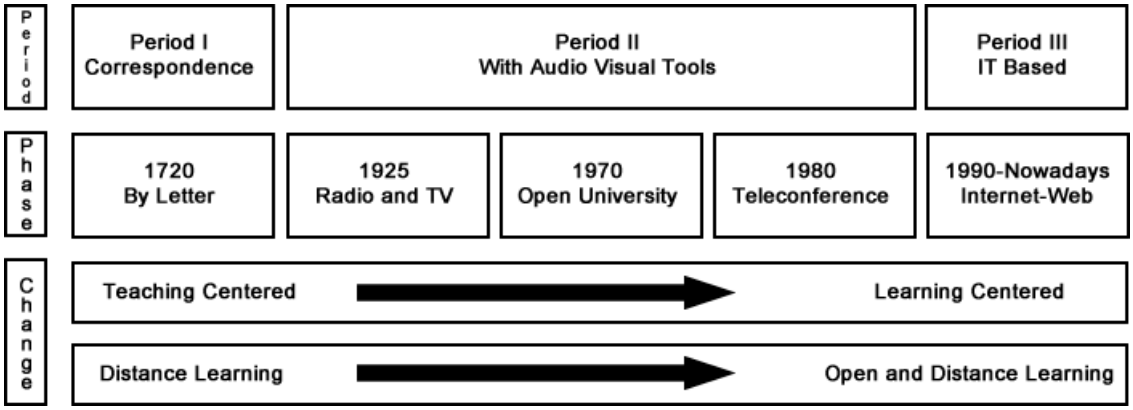

Figure 1. *The development of distance education around the world.*

In 1921, Brigham Young University in the United States became the first university to grant a bachelor's degree through radio broadcasts (Saettler, 2004, p.201). Following that, in 1922, the universities of Wisconsin and Minnesota in the US used the same method to offer undergraduate programs. While radio-based distance education made significant advancements in its early stages, it did not receive the expected attention. Consequently, universities made efforts to find a more effective method of distance education (Akçay, 2014, p.29). The invention of television excited universities in the field of distance education, and they quickly integrated this new communication medium into their educational purposes. By the late 1930s, the number of lessons offered through television increased. By the 1950s, many universities offered their courses through television; however, the continuity between radio and television technologies was not maintained (Moore and Kearsley, 2005, p.31).

The early 1970s marked a significant turning point in distance education. Advancing technology, growing learning needs, and the experiences gained from previous years laid the foundations for a different model in distance education. During this period, Charles Wedemeyer, a faculty member at the University of Wisconsin in the United States, developed an education project called AIM (Articulated Instructional Media Project) (Moore and Kearsley, 2005, p.33). The main goal of the AIM (Articulated Instructional Media Project) was to combine different technologies to provide high-quality and cost-effective education to students outside the campus. In 1965, Wedemeyer provided information about the AIM project in 1967, and he made a significant contribution to the establishment of The Open University in the United Kingdom.

While the periods of correspondence and radio-television represent times when distance education methods were used, traditional education processes continued to exist. During these periods, concerns related to the content of the courses and their delivery made it difficult for distance education processes to go beyond traditional education. Even with the establishment of open universities, it was observed that distance education processes did not achieve the expected efficiency. Heydenrych and Prinsloo (2010, p.15) explained this by the lack of content

development and the inadequacy of effective communication and interaction environments. Anderson and Dron (2011, p.85) defined these periods as distance education eras that emphasize personalized learning, are teacher-centered, and focus on cognitive or behavioral characteristics related to content creation.

Advancements in technology and increased interaction significantly changed the distance education model, particularly in the 1980s. This period is defined as the teleconferencing era, where students take on a more active role, feedback is provided more rapidly, and two-way interaction becomes crucial. Within this era, three different categories of teleconferencing are examined based on the technology used: non-video teleconferencing, visual-textual teleconferencing, and video teleconferencing. Non-video teleconferencing is a method used to provide educational opportunities to students. This method allows live audio conversations among students located in different geographical regions and offers a quick response to immediate educational needs. Subsequently, a video conferencing system was developed, enabling face-to-face education opportunities. Students and instructors can communicate in real time through video conferencing.

With the widespread adoption of the internet and advancements in internet technology in the 1990s, distance education underwent a significant transformation. Teleconferencing systems carried out via desktop computers empowered students to participate more actively, making the learning experience more effective (Moore, 2007, p.15). The development of the internet, its increasing usage, and the emergence of web-based applications presented significant opportunities for distance education. The internet put an end to one-way communication between students and teachers and introduced features that encouraged interactive learning. Innovations offered by the internet, such as smart boards, chat rooms, and file sharing, paved the way for creating a real time, efficient, and interactive learning environment (Newman, Callahan, and Gallagher, 2002, p.13).

As the internet continued to evolve and gain broader usage, the opportunities in the field of distance education became more widely recognized. As a result of these developments, universities, colleges, and institutes began organizing their educational programs in an internet-based format and started offering online learning opportunities to students. Especially in the 1990s, pioneering initiatives were undertaken, such as Regent University's online doctoral program in communication and Stanford University's asynchronous distance education project. Additionally, Duke University initiated online MBA programs that covered Europe, Asia, and Latin America in 1996 (Beldarrain, 2006, p.142). This era is considered one of the periods that significantly boosted distance education.

The development of distance education in Türkiye

When expressing the developmental periods and phases of distance education in Türkiye, attention has been given to the technologies used in distance education processes and significant developments affecting distance education. Based on this, it can be said that Türkiye has gone through four distinct periods in terms of distance education. The relevant periods are illustrated in the figure below (Bozkurt, 2017, p.87).

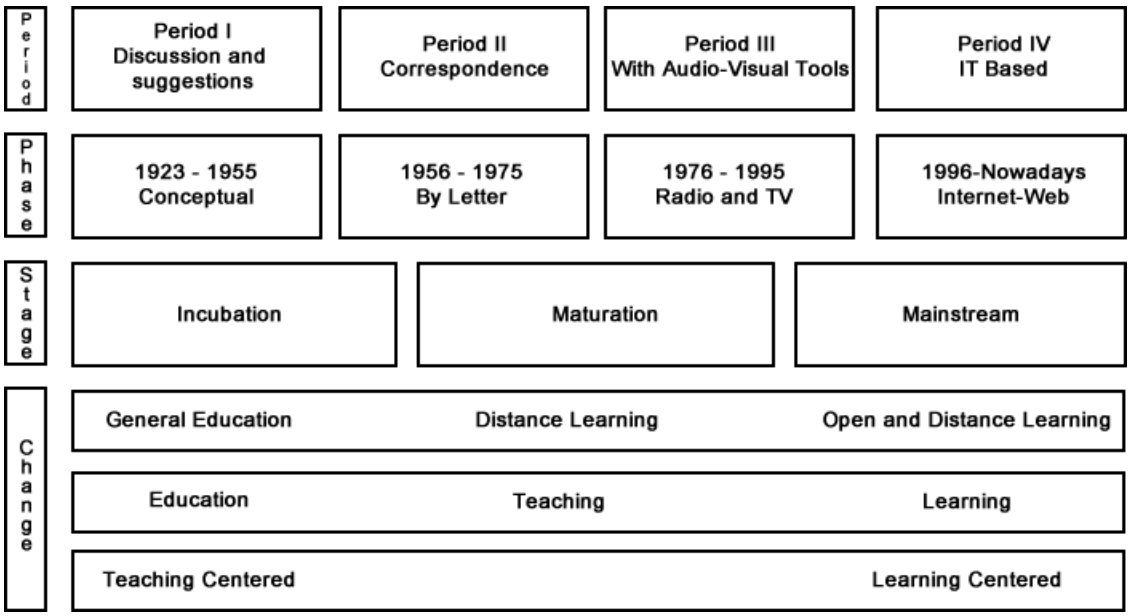

Figure 2. *The development of distance education in Türkiye.*

After the proclamation of the Republic, distance education in Türkiye made significant progress through foreign expert educators. This process initially started with recommendations focusing on teacher training and increasing literacy rates. Renowned educational theorist John Dewey recommended the use of distance education in Türkiye to train teachers, which introduced Türkiye to distance education. In the 1930s, educators from various countries prepared reports on education through various commissions. These reports recommended the widespread expansion of educational institutions and emphasized the need to deliver technical knowledge and general education via mail to some regions due to economic difficulties. In 1939, scientific committee meetings were held, emphasizing the necessity of bringing education to every corner of Anatolia (Uygun, 2008, p.297).

During these years, as the groundwork for the distance education system was being laid, initiatives were made, such as universities collaborating with community centers and organizing university weeks in various regions. During the IVth National Education Summit, studies and applications related to distance education gained momentum, with various innovations being introduced. However, until this period, distance education efforts remained largely conceptual (Alkan, 1987, p.25). By the mid-1900s, the demand for education increased, and existing schools couldn't meet these demands. As a result, correspondence education practices began. These practices were developed by taking examples from correspondence education systems in other developed countries. After the initial attempts, significant decisions were made during the 1982 National Education Summit, leading to the creation of the "Open Higher Education Regulation."

The groups benefiting from correspondence education included children who could not access formal education, individuals looking to improve their general knowledge and vocational skills, and those seeking to participate in exams for higher degrees. During this period, correspondence education centers were institutionalized and achieved the status of the general directorate. By proving its success, correspondence education became an important part of other education methods (Özüçelik, 2019, p.24). In 1975, the distance education system became more institutionalized, leading to the establishment of the Directorate of Distance Higher Education (YAYKUR). This institution allowed for a more planned approach to distance education and provided higher education opportunities in various fields, such as

teaching, social sciences, and foreign languages. Anadolu University Open Education Faculty, founded in 1982 with Law No. 2547, is still actively providing distance education today (Kırık, 2014, p.82).

As radio and television broadcasting advanced in Türkiye, radio and television broadcasts were organized under the Türkiye Radio and Television Corporation (TRT), an autonomous entity. With the start of TRT's broadcasts in 1968, educational programs were also made available to viewers. The use of television and radio broadcasts for educational purposes became more widespread in the following years. Educational programs developed by the Film Radio Television and Education Center (FRTEM) under the Ministry of National Education were presented to viewers in the form of 15-minute short programs (Uşun, 2006, p.28). In 1982, Anadolu University's Open Education Faculty, established, holds the distinction of being the first university-based institution for distance education in Türkiye. During its early years, the faculty supported its courses through radio and television broadcasts. Programs were especially broadcast on TRT for associate degree students. By 1989, Middle East Technical University (METU) started offering certification programs in engineering using distance education methods. At this time, internet connectivity was available in only eight universities, and METU began sending distance education materials to students via email (Özüçelik, 2019, p.26).

In 1997, universities in Türkiye initiated web-based distance education endeavors. The "Inter-University Communication and Technology-Based Distance Higher Education" studies initiated by the Higher Education Council (YÖK) in 1999 accelerated web-based distance education applications in universities. This process was further shaped in 2000 with the establishment of the "National Informatics Committee (EMK)" under YÖK. The "Regulation on Distance Education Based on Information and Communication Technologies" aimed to share educational opportunities between universities and encouraged the use of interactive and multimedia elements in distance education (Akçay, 2014, p.42). Sakarya University began developing and implementing its distance education system in the 2000s. As a result of these efforts, Sakarya Vocational School started offering Computer Programming and Information Management programs through distance education in the 2001-2002 academic year. Later, the Business program was added to these programs. Until 2003, these programs were offered under Sakarya Vocational School, and then they were transferred to Adapazari Vocational School. Various new programs have been added over time (SAU Uzem, 2023).

Today, distance education practices are widely used by many universities in Türkiye, public institutions, and private Distance Education Centers (UZEM). These units offer certificate programs in various fields and support lifelong learning for students. Moreover, many higher education institutions offer various education options through distance education, including associate degrees, undergraduate degree completion programs, bachelor's degrees, master's degrees, and certificate programs. Students can easily access exams, lecture videos, and digital course materials through web platforms thanks to advancing technology (Kaçan and Gelen, 2020, p. 4-5). The Ministry of National Education has also made significant progress in distance education and has contributed to teachers' professional development and providing distance education to students through the "Educational Informatics Network (EBA)" (Gelişli, 2015, p.316).

Distance education

Distance education is a method of learning that allows students to receive education without the necessity of being physically present in a classroom. This type of education is facilitated through the use of digital technologies such as online platforms, video conferencing tools, educational software, and internet-based resources. Distance education provides students with the opportunity to receive education from geographically distant locations and offers a

flexible learning experience. In distance education, students can access course materials through online platforms, which may include text documents, audio recordings, videos, interactive learning activities, and exams. Students have the flexibility to work through these materials at their own pace and can complete a significant portion of their coursework from their homes or any location of their choice.

Distance education is commonly utilized, especially during extraordinary circumstances like pandemics, and it is also preferred by adult learners and professionals who need to continue their professional development. This method not only provides students with increased flexibility and accessibility but also allows educational providers to reach a broader student audience. With the advancement of digital technologies, distance education has become more prevalent and has triggered significant transformations in the field of education.

Synchronous distance education

Synchronous remote education is an instructional model where students and instructors come together online from different geographical locations at the same time. In this form of education, teachers conduct live classes, and students participate in these classes within a specified time frame. Synchronous remote education offers students a real time interactive experience, allowing them to ask questions and communicate with instructors instantly (Biroğul et al., 2010). Synchronous remote education typically employs video conferencing tools or dedicated education platforms. Students join live classes at specific times, watch instructors' presentations, and engage in interactions. This method ensures that students follow a set schedule and participate in live discussions related to the lessons.

Synchronous remote education is especially preferred during extraordinary situations like a pandemic when face-to-face educational opportunities are limited. However, it can pose challenges related to time zone differences for students living in different geographic regions, as it requires them to be online simultaneously. To mitigate this issue, educational providers may offer access to recorded lesson videos or other asynchronous educational resources. Synchronous systems allow remote learners to draw energy from the learning group, reducing the feeling of isolation. Feedback plays a crucial role in remote language learning. Real-time communication provides immediate feedback. However, synchronous communication results in some loss of flexibility as not all learners can engage at the same time. Some students may prefer having a fixed time to attend a class, while others might find this restrictive.

In the synchronous (real time) model, traditional learning methods also encompass e-learning. In this model, instructors (or mentors) and participants work together in pairs, typically involving face-to-face interaction and sharing experiences. Online synchronous learning also offers the opportunity for participants to be in different locations simultaneously. It includes elements such as traditional classroom settings, virtual classrooms, live practical applications (labs), interactive discussions, and mentorship. Within the current technology infrastructure, all users need to have adequate technical hardware, infrastructure, and technological literacy. Moreover, this type of learning always requires a stable and high-bandwidth Internet connection. Synchronous remote education comes with both advantages and disadvantages.

Table 1. *Advantages and disadvantages of synchronous distance education*.

Advantages	**Disadvantages**
Interaction and Communication	Internet Access Problems
Instant Feedback	Time Zone Issues
Similarity to Face-to-Face Experience	Equipment and Technology Issues
A Specific Program	Student Participation Issues
Instructor Capacity	Teacher Capacity
Motivation and Discipline	One Way Communication
Geographic Flexibility	Motivation Issues

Based on the advantages presented in Table 1, synchronous remote education provides live interaction and communication between students and teachers. Teachers can provide live feedback, answer questions, and make immediate corrections. Synchronous remote education offers live lessons similar to traditional classroom experiences. The class schedules are well-defined and structured, providing students with a consistent program. Teachers have more control and resources to organize live lessons and interact with students. Additionally, it can enhance motivation and discipline among students. It allows students from geographically distant areas to access education.

As for the disadvantages presented in Table 1, in synchronous education, some students may lack a reliable internet connection, which can negatively affect their participation in classes. Students from different geographical regions might struggle to attend classes at suitable times due to time zone differences. Some students may not have access to suitable technology or may face difficulties in using it. Student participation in synchronous education can be low, and students may struggle with distractions or lack of engagement. Synchronous remote education may also require teachers to invest more time and effort in preparation. Students might have limited access to in-class discussions and group work, which can result in a lack of interaction that negatively affects the learning experience. Lastly, students may experience a lack of motivation when attending live classes and focusing on an online environment.

Asynchronous distance education

According to the advantages presented in Table 2, asynchronous remote education offers students the freedom to review and study educational materials at their own pace. Students can manage their learning processes to align with work, family, or other commitments. They have the flexibility to tailor their learning to their individual schedules. Students from different geographical regions can access education without geographical barriers, allowing for a broader student reach. Each student can work at their own learning speed and based on their unique needs. It provides students with the opportunity to personalize their learning to fit their preferences. Asynchronous education can encourage students to engage in more written communication through text-based discussion forums, emails, or other communication tools, which can help improve their written communication skills. Moreover, there are no time zone issues for students in different zones; each student can access educational materials according to their own time zone.

As for the disadvantages presented in Table 2, students may experience a lack of interaction due to not being able to see instructors or other students in real time. This lack of interaction can be attributed to the absence of instant feedback and instructor guidance as in live classes. Additionally, asynchronous remote education requires students to be disciplined and self-motivated because there is no instant feedback or teacher guidance as in live classes.

In summary, asynchronous remote education provides a learning model that can be tailored to the individual needs and preferences of both students and education providers. It is preferred when traditional classroom education is challenging or when students need to receive education in a manner that aligns with their personal schedules.

Table 2. *Advantages and disadvantages of asynchronous distance education*.

Advantages	**Disadvantages**
Flexibility	Technological Problems
No Time Zone Problem	Social Isolation
More Collaboration	Monitoring and Evaluation Challenges
Geographic Flexibility	Motivation Challenge
Customized Learning	Lack of Interaction

According to the disadvantages presented in Table 2, in asynchronous remote education, students cannot see their instructors or other students in real time. This communication issue can lead to a lack of interaction and may result in students not receiving immediate answers to their questions. Asynchronous education requires students to be disciplined and self-motivated since they do not receive instant feedback as in live classes. Students cannot receive instant feedback as they would in live classes. Instructors cannot monitor students' progress or participation in real-time. The assessment and feedback process may take longer.

Students need to have access to a suitable computer and internet connection. Students who face difficulties in accessing technology may encounter challenges in participating in education. Furthermore, asynchronous education may lead to students not physically interacting with other students in a classroom, which can contribute to social isolation. In summary, while asynchronous remote education offers flexibility, it also presents challenges related to interaction, discipline, motivation, and technology access. These challenges should be considered when implementing asynchronous education models.

Distance education systems

Distance education systems include online platforms and software that enable students to receive education when they are geographically remote or unable to attend physical classes. These systems allow teachers to deliver educational materials online and students to attend classes, submit assignments, and take exams online. Distance education systems have played an important role in providing education to students and professionals from different geographical regions, especially in extraordinary situations such as pandemics. When establishing distance education systems at universities, they must use two different tools together: the learning management system and the live lesson system. This is because the learning management system is used to plan and present both synchronous and asynchronous training to students, while the live lesson system is required to provide synchronous training.

Learning management systems

Learning Management Systems, or LMS, are online platforms or software used to manage, monitor, and facilitate the processes of education and teaching. These systems are designed to assist educators in creating course content, managing participants, and tracking student performance. Key features include content management, communication tools, exam and assessment capabilities, reporting, and analytics. LMS is widely used in educational institutions, businesses, the healthcare sector, online education providers, military organizations, and many other industries. These systems make the learning process more

accessible, customizable, and traceable, thus enhancing the efficiency and effectiveness of educational processes.

With LMS, educators can upload, edit, and share course materials, which can take various forms, such as text, video, audio, presentations, and quizzes. They can create courses, add participants, and organize course content. LMS facilitates the tracking and management of courses. It allows for monitoring of course progress, exam results, and participation, providing educators with data on student performance. Communication tools within LMS systems facilitate interaction between students and teachers. Educators and students can communicate through messaging, forums, or email. Educators can create exams, edit quizzes, and automatically calculate exam results. Additionally, LMS systems offer reports and analyses on student performance. This feedback assists in improving courses and instructional materials. LMS systems are available as both open-source software and paid proprietary software solutions.

Open-source learning management system software

Open source refers to an approach where the source code of software, hardware, or other information and technology products is available and accessible to the public. Open-source represents a model in which these source codes are publicly available, modifiable, and redistributable. This creates a framework for contributing, collaborating, and sharing knowledge in software and technology development processes. Open-source learning management systems software are learning platforms that are freely available and often supported by community developers. There are many open-source LMS systems widely used in the market. These are Moodle, Canvas, Sakai, Chamilo, ILIAS, ATutor, Claroline, and Open edX open-source systems.

Moodle

Moodle is an open-source learning management system used for education and training. Designed for educational institutions, teachers, and students, Moodle is used as an online learning and course management platform. Its main features include creating and managing courses, creating course materials containing various content types, offering communication and interaction tools, and providing automatic examination and evaluation opportunities. Moodle also stands out for its customizability; It offers user-customizable themes, plugins, and extensible features. Although Moodle is used predominantly by educational institutions, teachers, and students, it is also widely used in businesses, healthcare, and many other sectors. Being an open-source project, it ensures support from many developers and communities around the world, resulting in regular updates and improvements.

One of the advantages of Moodle is that it is flexible and customizable so that instructors can provide students with authentic learning experiences, and it keeps costs low. Moodle is one of the most widely used open-source LMS platforms. It has a flexible and customizable structure and is preferred by many educational institutions around the world. Moodle is one of the most popular LMS systems with support for 77 different languages and 75000 registered users in 138 countries. Moodle is coded based on PHP. Since it is open-source, the source codes are accessible. Developers can add additional features using source code. Courses are created in modules. It supports Linux, Unix, Windows and Mac OSX operating systems. The trial version and help system are instantly accessible over the internet. It is used under GPL license and managed with portal logic. GPL (General Public License) is a type of open-source software license that regulates the use, distribution and modification of free software (Elmas et al., 2008).

Canvas

Canvas LMS is an online learning and course management platform developed for educational institutions, businesses and teachers. Canvas is designed to enable students and instructors to have an interactive and flexible learning experience. This platform offers users the capabilities to create courses, share content, track student progress, communicate, and provide assessments and feedback to students. Canvas features include customizable course structures, rich content creation tools, interactive class discussions and communication tools, online quiz and assignment management, automated assessment, and student progress tracking and reporting options. Additionally, in addition to being an open-source platform, Canvas has a user-friendly interface and is compatible with mobile devices, offering broader access to students and instructors. Canvas LMS enables educational institutions and businesses to manage educational programs online and deliver interactive learning experiences to students. For this reason, it is preferred by many organizations that need a learning management system. Canvas is designed to meet modern education needs, with updated features and a constantly evolving platform.

Sakai

Sakai stands out as a learning management system designed specifically for higher education institutions. Sakai is an open-source platform and is used by many universities and educational institutions. This LMS was developed to enable students and instructors to have an interactive learning experience. Sakai's key features include the ability to create and manage courses, share content, and track and evaluate students. Instructors can share a variety of materials, create online quizzes and tasks, and track student progress. Students can access course content, upload their homework and interact in the classroom through this platform. One of the advantages of Sakai is that it is open-source. This allows organizations to customize the platform according to their needs and access the source code. Additionally, Sakai is a community-developed project, making it easy to add regular updates and new features. Sakai is one of the popular LMS systems used by over 350 educational institutions worldwide, with the number of users varying from 200 to 200,000 for each system (Kantar et al., 2023).

Google classroom

Google Classroom is a user-friendly online learning platform designed for teachers and students. Teachers can create virtual classrooms and create customized content for each class. These contents can be created with text documents, presentations, videos, web links, and even Google Workspace tools such as Google Docs, Spreadsheets, and Presentations. Google Classroom offers teachers the ability to assign tasks and assignments. Teachers can set due dates for assignments and additional explanations if necessary. Students respond to these tasks, submit them within the specified time, and teachers can provide feedback. The platform also provides convenience in tracking student progress and grading. Teachers can view, evaluate and provide feedback on assignments submitted by students. This helps students instantly track their course performance and see their progress.

Google Classroom is an online learning platform that combines Google products such as Google Drive, Google Docs, Gmail, and Google Calendar. It offers students the ability to create, distribute, communicate, and plan course materials. Students can join classes via special invitation codes or automatic data integration. Each class creates a separate folder in the corresponding user's Google Drive; Here students can submit their assignments. Additionally, mobile apps available for iOS and Android devices offer students the ability to take photos, share files, and access offline. Teachers can monitor students' progress and give students

feedback after their assignments are graded. Students can add comments to revise and improve their assignments.

Additionally, teachers can post postings to a class stream to communicate information to students. Google Classroom is a powerful learning management system that facilitates student-teacher interaction and makes it simpler for students to access course materials and for teachers to track student progress. (Magid, 2014). Google Classroom offers communication tools such as in-class chats and comments to facilitate communication between students and teachers. Students can use these tools to ask questions or participate in course-related discussions. Google Classroom serves as a powerful tool to accelerate digital transformation in education and increase student-teacher interaction. Its integration with Google Workspace increases the productivity of educators and students and makes the online learning experience more effective.

Closed source paid learning management system software

Blackboard learn

Blackboard Learn is a platform used as a learning management system for higher education institutions and businesses. This platform allows teachers to create digital classrooms, interact with students online, share course content, and track student progress. Blackboard Learn stands out for its ability to host a variety of educational materials. Teachers can upload various content to the system, such as text documents, presentations, videos, assignments and exams. These enable students to access classroom content and complete their work online. The platform also includes communication and collaboration tools. Students can communicate with their teachers and classmates through classroom chats, forums, and posting. This increases student-teacher interaction and allows students to ask questions, participate in discussions, and work together. Teachers can monitor students' progress, evaluate tasks and quizzes, and provide feedback when necessary. This is an important tool for assessing student performance and providing support where necessary.

Moodle workplace

Moodle Workplace stands out as a powerful learning management system (LMS) specifically designed for corporate training needs. This platform offers flexibility, customization and scalability for large-scale organizations and businesses. Moodle Workplace allows organizations to customize the platform to reflect their corporate identity and also offers comprehensive capabilities for user management. Reporting and tracking tools make it easy to track student progress and increase engagement, while integration capabilities ensure it can work seamlessly with other business processes and systems. Moodle Workplace makes corporate training more efficient by enabling organizations to manage, customize and deliver training content to students effectively.

Microsoft teams

Microsoft Teams is a powerful collaboration and communication platform developed by Microsoft for business and education. This platform offers its users a variety of communication tools such as text chats, voice and video calls, file sharing and online meetings. It also works integrated with Microsoft 365 (Office 365), providing users with the convenience of editing and sharing documents. Microsoft Teams is an ideal solution, especially for projects that require remote work, distance learning and collaboration. Users can seamlessly communicate, collaborate and work efficiently with team members located in different locations.

Microsoft Teams is a platform used to improve communication and collaboration in workplaces. Videoconferencing combines collaboration tools such as videotelephony, instant messaging, file sharing, notes, and attachments. It is also a very useful tool for remote working and distance education. Microsoft developed this platform specifically as a rival to Slack and officially introduced it in November 2016. Microsoft Teams integrates with companies' Office 365 subscription suite and also offers plugins that are compatible with non-Microsoft products. In this way, users can create an experience that suits their business needs. While Teams is available as a web-based desktop application, it is built on the Electron framework. It uses the Chromium rendering engine and the Node.js JavaScript platform. Microsoft Teams has replaced legacy platforms such as Skype for Business and Microsoft Classroom among enterprise messaging and collaboration platforms (Ankush, 2022).

Advancity LMS

Advancity LMS stands out as a learning management system that serves in the field of corporate training and talent development. This platform makes it easy for organizations to create, edit and manage training content, while also offering the ability to personalize the user experience with customizable course design. It provides comprehensive reporting tools for monitoring and evaluating student progress, and can work seamlessly with other business processes and systems thanks to its integration capabilities. With its mobile support, it makes learning accessible anywhere and anytime. Advancity LMS offers a powerful solution to meet the needs of organizations to train their employees and develop their skills. It meets all communication and sharing needs of faculty members and students for formal and distance education. It works easily on any mobile device without requiring any extra software. It provides a solution to the complex and intense workload problem that exams create on institutions. It is a completely domestic academic education management system developed by Advancity that meets all communication and sharing needs of faculty members and students for formal and distance education. Preferred by 120 institutions, including nearly 60 distinguished higher education institutions of Türkiye, ALMS is the preferred academic learning management system in Türkiye with an active user base of 800,000 (ALMS, 2023).

Toltek LMS

It is an educational management system that can be adapted to any institution with its modular structure. It is a system that has a hierarchy that can be adapted to the corporate structure, can manage training within certain date ranges, can integrate many third party software that is desired to be used together, and can instantly monitor the status of all virtual classes. Toltek LMS was developed by a domestic software company (ToltekLMS, 2023).

University Information Management System (ÜBYS) LMS

University Information Management System is an e-university project consisting of integrated modules covering all administrative and academic processes of universities. It was designed in accordance with the multi-layered and Service-Oriented Architecture (SOA) in which mandatory changes arising from legislation such as the Constitution, Law, Regulation, Directive, Communiqué, Circular, and official instructions from the Upper Institutions can be easily adapted on the software, and its analysis was carried out by the administrative and academic staff of Izmir Kâtip Çelebi University. ÜBYS LMS system is offered as a module of this integrated software. The LMS system is a system that brings together students, teachers and educational resources regardless of location, and works fully integrated with the Student Information System. The primary purpose of the LMS system is to ensure that the management of administration, student affairs, faculty members, and student processes can be carried out

easily and quickly. For this reason, it is aimed to be easily accessible from all mobile devices and tablets, as well as computers of all resolutions. This system, which is designed to be platform independent, provides great flexibility to its users (ÜBYS, 2023)

Open-source free live course software

BigBlueButton

BigBlue Button is a free and open-source web conferencing software developed for educational institutions. It works via WebRTC protocol. BigBlueButton, an HTML5-based web application with an infrastructure written in Ruby and JavaScript languages, is a platform independent application (BigBlueButton, 2023). Supporting LTI 1.0 standards, BigBlueButton has integration with many different LMS infrastructures such as Open edX, Moodle, Canvas LMS. BigBlueButton offers the following basic features to its users, in addition to the additional features that may come with the plugin infrastructure:

- Creating classes, rooms, groups
- Teacher/student interaction via whiteboard
- User (Teacher/Current/Student) rights management
- Screen sharing management
- Publishing PDFs and presentations via Whiteboard
- Watching educational videos on the whiteboard
- Chat tool (public/private)
- Raise your hand (no words)
- Note sharing and export (PDF, OpenDocument, HTML)
- Post-survey question, open-ended questions
- Video/Lecture recording feature

Closed source paid live course software

Zoom

Zoom is a videoconference platform that uses end-to-end encryption developed by Zoom Video Communications. Provides video chat service. It allows joining meetings for free on up to 100 devices simultaneously, with a 40-minute time limit for free accounts with three or more participants (Weiner, 2017). Users have the option to upgrade by subscribing to one of their plans, with the largest allowing up to 1,000 people at once with no time restrictions. In addition to voice or video calls, content sharing can also be made. Video conferencing or training can be provided in the institution. Zoom meetings can be used to make presentations, lectures or give seminars. Thanks to Zoom's meetings feature, you can easily share your screen with participants during the meeting. It is also possible to hold virtual events live on Zoom. A virtual event can be held for a moderate crowd, provided that it is not too crowded (Zoom, 2023).

During the COVID-19 pandemic, Zoom has seen a huge increase in usage for remote work, webinars, distance learning, and online social engagements. In the new normal, individuals have begun to spend most of their daily lives online, in front of technological devices. It has been determined that individuals who carry out all kinds of activities through online platforms frequently use the Zoom application during this period and that Zoom is an

important component of individuals' lives. Individuals spending most of the day on Zoom for different reasons has caused physical, cognitive, and psychological problems to arise. All problems experienced because of excessive, unconscious and uncontrolled Zoom use are expressed as Zoom fatigue in the literature (Turgut and Okur, 2022).

Adobe connect

Adobe Connect is a platform that enables virtual meetings and distance education regardless of location. It is preferred by many companies and educational institutions as the most used virtual classroom application in the world, especially with the possibility of access from mobile devices. Adobe Connect includes all the basic components required for virtual meetings and distance education. Adobe Connect meetings and virtual classes can be easily accessed, monitored, and managed from different mobile devices. Content can be loaded from devices with Android operating system (Adobe, 2023). In addition to audio and video communication, illustrated expressions can be made with Flash animations (swf), software simulations, visual elements, video files (.flv, .mp4), PDF documents and desktop sharing, messaging, and whiteboard applications (İBUZEM, 2023).

Google meeting

Google Meet is an application that provides video conferencing service. Thanks to Google Meet, you can easily organize video meetings and conferences. The free version of Google Meet has some limitations. In the free version, users can hold meetings with a maximum of 100 participants and limited to 1 hour. For one-on-one meetings, the duration is 24 hours. Google Meet is designed primarily to host video meetings. However, you can activate the camera and microphone independently, so you can use them only for voice calls if you wish.

One of the best things about Google Meet is that you don't need to install any software on the desktop. Everyone on the call (organizer and participants) just needs to use a modern web browser. Google Meet provides the opportunity to meet with up to 100 members per call for G Suite Basic users, up to 150 members for G Suite Business users, and up to 250 members for G Suite Enterprise users. It can be integrated with Google Calendar for one-click meeting calls. It offers features such as screen sharing to present documents, spreadsheets or presentations, encrypted calls between all users, real time captions based on speech recognition. Google Meet usage increased 30-fold during the pandemic period, with 100 million users per day between January and April 2020 (Johnston, 2017).

Cisco webex

Cisco Webex offers the opportunity to make video conference calls with its cloud-based video platform service. You can plan your trainings or meetings with Cisco Webex, which offers effective and easy use, especially for people working remotely or studying remotely. Cisco Webex provides quality audio, video, and content transfer because it uses cloud-based connection. In addition, Cisco Webex is frequently preferred by many corporate companies for video conferences because it is very secure. In addition to its secure and cloud-based nature, Cisco Webex offers numerous advantages to users. Participation in conferences through Cisco Webex is possible from various devices, thereby providing ease of access. In addition to scheduled meetings, you can hold instant video conference calls with Cisco Webex. As with almost all video conferencing applications, Cisco Webex offers paid and free services to its users. In the free version of Cisco Webex, a meeting can be created with a maximum of 100 participants and a maximum duration of 50 minutes. Meetings can be started instantly in the personal meeting room. Meetings can only be recorded on the computer's hard disk. There are many extended features in the paid Cisco Webex version (Webex, 2023).

Perculus

Perculus offers a unique online dating experience with a multitude of features. You can share images and sounds, work on your documents and make presentations using your device's camera and microphone in online training with your colleagues, students, customers or dealers via the Perculus system. Many more features like this are offered to you with standard modules in Perculus. Perculus offers you the convenience of starting a live session, inviting participants and user management thanks to its easy management interfaces. It is a tool offered by Advancity (Perculus, 2023).

The whiteboard, an indispensable part of training, is offered to you as a standard feature in Perculus. You will experience the convenience and comfort of expressing your ideas by drawing and writing. Thanks to this feature, other participants will be able to easily see your writings and drawings and take an active role in this process. Its most important feature compared to normal wood is; It allows you to draw and write on the picture or presentation by placing any file, presentation or picture you want on it. You can also draw shapes and rotate and move those shapes. Participants who do not have a camera or microphone can express themselves by writing Perculus. They can even have private correspondence with other participants thanks to the private message sending feature. They also have the following characteristics.

- Provides an educational environment in accordance with YÖK virtual classroom regulations.
- When you want to watch the sessions again, it makes them watchable on every video platform.
- Provides the opportunity to create attendance reports.
- Integrates with education systems.
- You can easily use it from the browser installed on your computer or mobile device.

Distance education in universities during the pandemic period

The COVID-19 pandemic, which started at the beginning of 2020 and affected the whole world, has profoundly affected many sectors, and has also radically changed the field of education. Due to the pandemic, universities had to close campuses and suspend face-to-face education to protect the health of students and educators. This situation has rapidly directed educational institutions to distance education systems (Turk-internet, 2020). Universities had to quickly prepare their infrastructure for distance education and ensure that instructors could teach effectively in this new environment. However, many instructors have not used distance education tools before and were caught unprepared for this new era. The lack of experience in distance education led to some initial difficulties.

Distance education must be based on a pedagogical foundation and courses must be designed effectively. However, since there was not enough time to do such preparatory work during the pandemic period, educational institutions had to quickly direct instructors to use distance education tools and transfer existing materials online. During the pandemic period, universities tried to provide education to students using synchronous (simultaneous) and asynchronous (non-simultaneous) distance education methods. While synchronous education requires students to attend live classes at a certain time, asynchronous education gives students more flexibility and gives them the opportunity to review course materials at their own pace.

The pandemic period also stood out as a period in which universities accelerated their digital transformation processes. Infrastructures for distance education have been strengthened, online learning platforms have been used more, and instructors have been trained on digital

education tools. This process has paved the way for distance education to be used more widely in the future. The distance education systems used by universities during the pandemic period were examined in the study by Durak et al., and the learning management systems used by universities and their frequency of use are given in Table 3 (Durak et al., 2020).

Table 3: *Learning management systems used in universities and their frequencies.*

Learning management system	**Frequency**
Moodle	13
Advancity LMS	10
Microsoft Teams	6
ÜBYS	3
Toltek	3
Google Classroom	2
Sakai	2
BlackBoard	1
Canvas	1

The distance education process, which accelerated with the pandemic period, is not only specific to this period but is used by many universities in all periods. However, during the pandemic period, many universities were caught unprepared for this process and made efforts to establish the system they could as an emergency solution as soon as possible. As seen in Table 1, the most used learning management systems in universities are Moodle and ALMS. The reason for this is that although more universities prefer the free open-source system, the first and most convenient system used is Moodle.

It seems that universities that choose a paid solution make similar choices because the ALMS system is widespread and known. It is seen that universities that have established a paid system prefer Microsoft Teams, UBYS and Toltek LMS system in the next ranking. As can be seen from here, domestic companies such as UBYS and Toltek are preferred by universities for their domestic software as well as foreign purchases. The distance education systems used by universities during the pandemic period were examined in the study by Durak et al., and the live course software used by universities and their frequency of use are given in Table 4 (Durak et al., 2020).

Table 4: *Live course software used in universities and their frequencies*.

Live course software	**Frequency**
BigBlueButton	12
Perculus	11
Microsoft Teams	9
Zoom	9
Adobe Connect	6
Blackboard	4
Google Meet	3
Cisco Webex	1

Upon reviewing Table 4, it becomes evident that the predominant live course software utilized is BigBlueButton, an open-source software that is freely available. Budget inadequacies and purchasing difficulties of universities, which had to urgently switch to distance education during the pandemic, have a large share in this. Domestic and foreign companies demand high fees for live lesson systems, which makes it difficult for universities to purchase them. Especially during the pandemic period, many local and foreign companies made high increases

in their wages. This is a result of the sales strategy of turning the crisis into an opportunity. Many universities have turned to free open-source systems with their own staff qualifications.

BigBlueButton, one of the popular solutions offered as a live lesson system, is an important part of its popularity because it is free. It seems that universities that go for a paid solution prefer Perculus, a local software that has become widespread with the pandemic, preferred by many universities. Perculus Advancity is the live course software of the ALMS system developed by the local company. Microsoft Teams and Zoom commercial software were the third most preferred applications. The distance education systems used by universities during the pandemic period were examined in the study by Durak et al., and the methods and frequencies of universities' courses are given in Table 5 (Durak et al., 2020).

Table 5: *Universities' course offer methods and frequencies.*

Course offer method	**Frequency**
Most courses are taught asynchronously	9
Most courses are taught synchronously	9
All courses are taught asynchronously	7
All courses are taught synchronously	6
Half of the courses are taught synchronously and half asynchronously	1

As seen in Table 5, as a result of the emergency distance education during the pandemic, many universities were not prepared for synchronous education and due to insufficient infrastructure, universities preferred to teach their courses asynchronously. This is significantly confirmed by the fact that 7 universities offer all their courses asynchronously. Although 9 universities teach most of the courses asynchronously, they teach some courses synchronously. In this case, it can be said that the infrastructure of most universities is inadequate. Many universities have tried to manage this crisis situation by updating their existing systems and reaching more capacity. Current distance education systems have strengthened their infrastructure to accommodate more students and faculty members. They did not choose to switch to a completely new system, but instead preferred to continue with their existing systems.

The biggest factor here is the difficulty of establishing a new system during the emergency crisis period and the failure to change usage habits. Ease of use and being free can be listed as other factors in choosing learning management systems. It can be said that universities tend to pay a little more for live course software. One of the reasons for this is that the university that wants to use open-source free software such as BigBlueButton needs to set up a server with a capacity of approximately 500 users. In this case, the total cost of purchasing a server may be very high depending on the number of students. Free live course software can be seen as an ideal solution for universities with a small number of students.

The most important factor here is the university's current employment of IT competent personnel and the adequacy of the server systems. Both adequate server systems and competent personnel to install and run open-source systems are important for the use of open-source systems. Many universities have turned to paid ready-made software due to both lack of infrastructure and competent personnel. In the research conducted by Durak and his colleagues, it was seen that the most used learning management systems in universities during the pandemic period were Moodle in the free option and Advancity LMS in the paid option. The live course software most used by universities is BigBlueButton in the free option, and Perculus, the live course software of the Advancity LMS system, in the paid option (Durak et al., 2020).

Conclusion

The COVID-19 pandemic has been a significant turning point that accelerated the digital transformation processes of universities and made remote education systems a top priority. This article examines the challenges universities face during the pandemic, the measures taken to overcome these challenges, and the impact of digital transformation on education. The widespread adoption of remote education systems has enabled students and teachers to enhance their digital skills and enrich their online learning experiences. However, the technical and pedagogical challenges encountered during this process should not be overlooked.

The impact of the COVID-19 pandemic on universities in Türkiye was guided by significant decisions made by the Council of Higher Education (YÖK, 2020b). At the beginning of the pandemic, universities were granted a 3-week break to ensure the safety of students and teachers. Subsequently, YÖK instructed universities to conduct remote education, stating that face-to-face education would not be feasible under pandemic conditions. Many universities attempted to manage this crisis by updating their existing systems to increase their capacity. They strengthened their infrastructure to accommodate more students and faculty members within their current remote education systems. Instead of transitioning to an entirely new system, they preferred to continue using their existing platforms. The major factors contributing to this choice were the difficulty of implementing a new system during a crisis and the reluctance to change established usage patterns. Ease of use and cost-effectiveness were among the other factors for the preference of learning management systems.

It can be noted that universities tended to allocate more resources to live class software during the pandemic. Free live class software could be an ideal solution for universities with few students. However, the most crucial factors are the adequacy of the university's information technology personnel and server systems. Adequate server systems and competent personnel to implement and maintain open-source systems are essential for their usage. Many universities turned to paid ready-made software due to a lack of both infrastructure and competent personnel for open-source systems. In conclusion, the pandemic has made the digital transformation of universities an inevitable reality and will continue to shape future education models. Educational institutions need to strengthen their digital infrastructure, support teachers in developing digital skills, and adopt flexible approaches to integrate various learning methods. This will be a significant step towards enhancing the quality of education and supporting student success.

REFERENCES

Adobe, (2023). Adobe Connect Release Notes of all releases. https://helpx.adobe.com/nz/adobe-connect/connect-releasenotes.html, 13/09/2023.

Akçay, S. (2014). An Application for the Use of Simultaneous Virtual Classroom Environment in Graphic Design Course and Student Perceptions (Gazi University Example). (Master's Thesis). Gazi University Institute of Educational Sciences, Ankara.

Akıncı, S. (1988). A Perspective on Violin Education from the Perspective of "Conditions that Ensure the Development of Learning". M. Ü. Atatürk Faculty of Education Journal of Educational Sciences, Vol. 7, pp. 1-10.

Alkan, C. (1987). Comparative Examination of Open Education Distance Education Systems. Ankara: Ankara University Faculty of Educational Sciences Publications.

Alkan, C. (2005). Education Technology. Ankara: Anı Publishing.

ALMS, (2023), ALMS - Formal and distance education management system for universities. https://yardim.kampus365.com/aym/alms/alms-nedir-18089171.html, 18/09/2023.

Anderson, T. and Dron, J. (2011). Three Generations of Distance Education Pedagogy. International Review of Research in Open and Distance Learning, Vol. 12, No. 3, pp. 80-97.

Ankush, D. (2022). Microsoft Decides to Drop the Linux App for Teams to Replace it as a Progressive Web App Instead. https://news.itsfoss.com/microsoft-linux-app-retire/, 2/09/2022.

Barış, M. F. (2014). Investigation of University Students' Attitudes Towards Distance Education: The Case of Namık Kemal University, Sakarya University Journal of Education, Vol. 5, No. 2, pp. 36-46.

Beldarrain, Y. (2006). Distance Education Trends: Integrating New Technologies To Foster Student Interaction and Collaboration. Distance Education, Vol. 27, No. 2, pp. 139-153.

BigBlueButton, (2023). BigBlueButton Foundation. https://bigbluebutton.org/2010/07/12/bigbluebutton-foundation/, 10/09/2023.

Biroğul, S., Özkaraca, O, Işık, AH., Karacı, A. (2010). Comparative Analysis of Web-Based Synchronous Distance Education Systems. Academic Informatics 10, Muğla.

Bozkurt, A. (2017). The Past, Present and Future of Distance Education in Turkey. Journal of Open Education Applications and Research, Vol. 3, No.2, pp. 85-124.

Burnet, J. (2008). On Education (Translated by Ahmet Aydoğan). Istanbul: Say Publications.

Deveci, M. (2019). The Use of New Communication Technologies in Distance Education in Higher Education Institutions in Turkey. (Doctoral dissertation). Marmara University Institute of Social Sciences, Istanbul.

Dinçer, M. (2003). The Power of Education in the Process of Social Change. Ege Education Journal, Vol. 3, No.1, pp. 102-112.

Durak, G., Çankaya, S., İzmirli, S. (2020). Examining the Turkish Universities' Distance Education Systems During the COVID-19 Pandemic. Necatibey Faculty of Education Electronic Journal of Science and Mathematics Education, Vol. 14, No. 1, pp. 787-809.

Elmas, Ç., Doğan, N., Biroğul, S., Koç, MS.(2008). Distance Education Application of a Sample Course with Moodle Learning Management System. Journal of Information Technologies, Vol. 1, No. 2, pp. 53-62.

Gelişli, Y. (2015). Teacher Training Practices in Distance Education: History and Development, Journal of Research in Education and Teaching, Vol. 4, No. 3, pp. 313-321.

Heydenrych, J.F. ve Prinsloo, P. (2010). Revisiting The Five Generations Of Distance Education:Quo Vadis?. *Progressio*, Vol. 32, No. 1, pp. 5-26.

IBUZEM, (2023) Adobe Connect. http://ibuzem.ibu.edu.tr/connect/adobeconnect.html, 19/09/2023.

İşman, A. (2011). Distance Education. Ankara: Pegem Publishing.

Johnston, S. (2023), Meet the new Hangouts. https://blog.google/products/g-suite/meet-the-new-enterprise-focused-hangouts/, 09/03/2017.

Kaçan, A. and Gelen, İ. (2020). An Overview of Distance Education Programs in Turkey. International Journal of Education Science and Technology, Vol. 6, No. 1, pp. 1-21.

Kaya, Z. (2002). Distance Education. Ankara: Pegem Publishing.

Kantar et al., (2023). Open Source Education Management Systems: Comparison of Sakai and Moodle. https://ab.org.tr/ab13/sunum/246.pptx, 23/09/2023.

Keleş, Ö. (2007). Implementation and Evaluation of Ecological Footprint as an Environmental Education Tool for Sustainable Living. (Doctoral dissertation). Gazi University Institute of Educational Sciences, Ankara.

Kesim, M. (2009). Creativity and Innovation in Learning: The Changing Roles of ICT. Turkish Online Journal of Distance Education-TOJDE, Vol. 10, No. 3, pp. 80-88.

Kırık, A. M. (2014). Historical Development of Distance Education and its Status in Turkey. Marmara Journal of Communication, Vol. 21, pp. 73-94.

Krishnamurti J. (2008). In the Problem is the Solution: Question and Answer Meetings in India. Chennai: Krishnamurti Foundation.

Magid, L. (2014). Google Classroom Offers Assignment Center for Students and Teachers. https://www.forbes.com/sites/larrymagid/2014/05/06/google-classroom-offers-control-center-for-students-and-teachers/, 6/05/2014.

Moore, M. (2007). Handbook of Distance Education. New York: Routledge.

Moore, M. G. and Kearsley, G. (2005). Distance Education: A Systems View. Canada: Thomson Wadsworth.

Newman, A., Callahan, A. and Gallagher, S. (2002). Strategies for Supporting Off-Campus

Growth. Educase Center for Applied Research, Vol. 3, pp. 13-21.

Özüçelik, E. (2019). Usage of Distance Education Systems Uludağ University Example. (Master's thesis). Bursa Uludag University Institute of Social Sciences, Bursa.

Parlar, H. (2012). Information Society, Change and New Education Paradigm. Yalova Journal of Social Sciences, Vol. 4, pp. 193-210.

Perculus, (2023), Online Learning: Activity Based Live Sessions | Perculus. https://advancity.com.tr/urunlerimiz/perculus-cevrimici-sanal-sinif, 09/10/2023.

Russell, B. (1999). On Education. (Translated by Nail Bezel). Ankara: Say Publications.

SAU Uzem, (2020). Sakarya University Distance Education Center. https://uzem.sakarya.edu.tr/tr/icerik/12039/50471/tarihce, 30/09/2023.

Simonson, M., Smaldino, S., Albright, M., & Zvacek, S. (2012). Teaching And Learning At A Distance: Foundations Of Distance Education. Boston, MA: Pearson Education.

Tekeli, İ. (2003). Thinking on Education. Ankara: TÜBA Publications.

Tezcan, M. (1996). Sociology of Education. Ankara: Feryal Matbaası.

ToltekLMS, (2023). Toltek LMS - Toltek. https://www.toltek.com.tr/Products/Tolteklms, 18/09/2023.

Turgut, T., Okur, S. (2022). A New Concept Emerging in the COVID-19 Pandemic Process: Zoom Fatigue. İnsan ve Toplum, Vol. 12, No. 3, pp. 47-71.

Turk-internet, (2020). A 'Remote' Look at the Distance Education System Infrastructures Used by Universities during the Pandemic Period. https://turk-internet.com/pandemi-doneminde-universitelerin-kullandiklari-uzaktan-egitim-sistemi-altyapilarina-uzaktan-bakis/, 28/03/2020

Uslusoy, B. (2017). A Comparative Study on Student Attitudes Towards Distance Education: USA/Turkey Example. (Master's thesis). Beykent University Institute of Social Sciences, Istanbul.

Uşun, S. (2006). Distance Education. Ankara: Nobel Publication Distribution.

Uygun, S. (2008). The Impact of John Dewey on the Teacher Education System in Turkey. Asia-Pacific Journal of Teacher Education, Vol. 36, No. 4, pp. 291-307.

ÜBYS, (2023). İKÇÜ University Information Management System. https://ubs.ikc.edu.tr/ubys, 18/09/2023.

WEB 1, (2020). A Brief History of Distance Education. http://webberm.wordpress.com/com-546-papers/history-of-distance-education/, 18/07/2020.

Webex, (2023). Use the Webex Meetings desktop app. https://help.webex.com/en-us/article/nqx2ohdb/Webex-Meetings-masa%C3%BCst%C3%BC-uygulamas%C4%B1n%C4%B1-kullan%C4%B1n, 19/09/2023.

Weiner, Y. (2017). The Inspiring Backstory of Eric S. Yuan, Founder and CEO of Zoom. https://medium.com/thrive-global/the-inspiring-backstory-of-eric-s-yuan-founder-and-ceo-of-zoom-98b7fab8cacc, 2/10/2017.

YÖK, (2020a). "Press Release". Council of Higher Education. https://basin.yok.gov.tr/KonusmaMetinleriBelgeleri/2020/04-yok-baskani-saracuzaktan-egitime-iliskin-basin-toplantisi.pdf, 29/04/2020.

YÖK, (2020b). YÖK Statement on Distance Education to be Implemented in Universities. https://www.yok.gov.tr/Sayfalar/Haberler/2020/universitelerde-uygulanacak-uzaktan-egitime-iliskin-aciklama.aspx, 18/03/2020.

Zoom, (2023). What is Zoom? How to use Zoom? https://manpower.com.tr/blog/zoom-nedir-zoom-nasil-kullanilir, 19/09/2023.

Utilization of Information Systems to Enhance the Efficiency of Internal Audit Activity Management and Audit Testing Processes

Ali DURDU[1]
İbrahim ÇINAR[2]
Özkan CANAY[3]

Introduction

The evolution of information systems (IS) has led to an increase in the utilization rate of these systems in corporations for executing business processes, transforming data into information, and utilizing and reporting this information in daily operations (Menna et al., 2016). Today, companies leverage information systems in crucial business processes such as customer relationship management, logistics, procurement, and accounting. Previously paper-based and archived processes have now been digitalized using information technology. This transition saves time by reducing or eliminating manual tasks and enhances the quality of work outputs by minimizing error rates. Due to the significant benefits derived from information technology (IT) resources, many firms make substantial investments in IT. For instance, according to a report by Information Week that tracked the top 500 information systems followers, investments in IT in the banking and finance sectors constituted 8.7% and 9% of companies' annual revenues in 2011 and 2012, respectively. These investments can reach up to 40% of firms' total capital expenditures (Menna et al., 2016).

Increasing the effectiveness of internal audit activity management and audit testing processes can be achieved by using information systems. Information systems play an essential role in improving the internal audit function by strengthening the control environment, reviewing the internal control structure, and monitoring information system operations and control procedures on behalf of management (Goodwin-Stewart & Kent, 2006). By leveraging information systems, internal audit functions can increase their effectiveness by addressing key stakeholders' different perceptions of the effectiveness of internal audits (Erasmus & Coetzee, 2018). This understanding allows internal audit functions to manage relationships with stakeholders more effectively. Companies' adoption and characteristics of internal audit departments also contribute to their effectiveness. Companies that prioritize internal audit activities allocate sufficient resources, and develop the necessary competencies show increasing interest in internal audit activities (Arena & Azzone, 2007). In a digitalized business environment, the agility of internal audit planning and knowledge of information technology (IT) risks, including cybersecurity threats, become essential factors in improving the effectiveness of internal audits (Betti & Sarens, 2020).

The relationship between internal audit and senior management is another critical consideration. Internal auditing can be essential to monitor a company's risk profile and identify areas to improve risk management processes (Sarens & Beelde, 2006). The effectiveness of internal audits is affected by the audit's adequacy, objectivity, and quality. These factors positively impact the effectiveness of internal controls (Novranggi & Sunardi, 2019). To ensure

[1] Asst. Prof. Dr., Management Information Systems, Ankara Social Sciences University, ali.durdu@asbu.edu.tr
[2] Science Expert, Audit and Risk Management, Ankara Social Sciences University, ibrahimcinar@gmail.com
[3] Lecturer, Computer Technologies, Sakarya University of Applied Sciences, canay@subu.edu.tr

the effectiveness of internal audit activities, organizations must focus on the determinants that actively contribute to their effectiveness. This includes elements such as management support critical to the effectiveness of internal audit activities (Gökoğlan, 2022). Information management is vital in improving the effectiveness and efficiency of organizations' internal controls, governance, and risk management processes (Nighia & Nguyen, 2022).

The importance of IT in modern business operations cannot be underestimated. Its role in digitizing traditional paper-based processes realizes cost and time efficiencies and improves data accuracy and reliability. The capability to swiftly analyze and report on large datasets enables firms to make more informed decisions, thereby gaining a competitive advantage. These benefits explain the significant proportion of revenue firms are willing to allocate to IT investments, particularly in sectors like banking and finance, where data integrity and process efficiency are paramount. Internal audit departments within companies are also benefiting from the ongoing digital transformation. As firms transition to paperless systems and develop auditing software, paperless audits are becoming more prevalent. Advancements in information technology are significantly altering the nature of the auditing process, which traditionally relied on paper-based source documents (Bierstaker et al., 2001). Thanks to the utilization of information technologies in various business processes within the company, internal audit departments can quickly and easily obtain the data they need for conducting audit tests from the relevant information systems. Furthermore, they employ various IT tools while testing the data gathered.

In addition, internal audit departments leverage information technology to manage general audit activities such as planning, documentation, reporting of audit results, and follow-up. They may utilize packaged audit software obtained through procurement or develop customized software tailored to their needs. The use of information technology in both data gathering and testing processes, as well as in the management of audit activities, frees auditors from many mundane tasks, allowing them to devote their time to understanding audit subject processes and evaluating various risks (Bierstaker et al., 2001). According to a 2006 survey by The Institute of Internal Auditors (IIA), which involved internal audit departments in different sectors like public, financial services, manufacturing, and insurance, 78% of participants indicated they use audit management software, 74% use risk management software, 69% use data analytics software, 50% use fraud detection software, and 32% use continuous auditing software (Gray, 2006). Thus, internal audit departments globally utilize one or multiple software for various purposes while conducting auditing activities.

This study initially examines information technology's benefits to internal audit departments in managing their business processes. Subsequently, the impact of the advantages of information systems on internal audit departments' audit test processes is scrutinized. This scrutiny provides insight into the effects of the changes information systems have brought to the routine business processes and audit testing activities of internal audit departments and, consequently, the benefits realized in terms of the ultimate objective of internal audit—adding value to the company.

Utilization of IS in managing internal audit activities

It is crucial to recognize the evolving landscape of internal auditing to set the stage for the ensuing discussion on the role of information systems in internal audit activity management. Historically considered a function isolated to compliance and financial reporting, internal auditing has transcended its traditional boundaries to play a more strategic role in organizational risk management. Advances in information systems have been instrumental in catalyzing this transformation. Information systems serve as the backbone that empowers internal audit departments to execute complex tasks ranging from planning to audit documentation and

reporting. These systems address the challenges of handling vast data sets, multiple business processes, and ever-changing regulatory environments. The synergy between internal auditing and information systems has created avenues for more informed decision-making, enhanced risk assessment capabilities, and, ultimately, better alignment with organizational objectives.

This section explores the critical role of information systems in internal audit management, mainly focusing on the planning, documentation, and reporting stages. The review is based on scholarly works, incorporating findings from multiple surveys and guidelines established by The Institute of Internal Auditors (IIA). This approach offers an exhaustive analysis of contemporary methods and technologies employed in internal auditing. Following this preamble, proceed to a detailed examination of how information systems aid in the planning stage of internal audits.

Planning

Audit activities start with the determination of the annual audit plan. Considering the size of the existing audit universe inventory, the priority of audits and the limited audit resources require strategic action in audit planning (Krishna et al., 2011). A risk-focused audit planning approach is used in audit processes to ensure the effective use of resources. Moreover, the internal audit's function includes assessing the effectiveness of internal controls and conducting fraud investigations, identifying organizational risks, and making process improvement recommendations to manage risks appropriately (Krishna et al., 2011). Auditors must clearly understand whether and how risks are being addressed and managed, which requires them to identify and assess all risks related to the company's business processes (Menna et al., 2016). Accordingly, while planning the audit for the relevant audit period, the risks associated with the company's business processes are identified and evaluated, and the company's risk map is prepared. Then, according to the risk assessment results, the mid and low-risk level operations are included in that year's audit plan, starting with the processes identified as high-risk, considering the time and human resources (number of audit teams).

Information systems provide significant benefits to internal audit departments in determining company risks. To identify risks, it is first necessary to determine the company's business processes and risk inventory. Then, the processes and risks in the inventory are matched so that the factors specific to the relevant process are considered when making a risk assessment, and the process-risk matching turns into an integrally traceable structure. Especially in large companies, there are many processes and sub-processes. For example, 1590 business processes are defined in the eTOM (enhanced Telecom Operations Map) process map created by TMForum, which models the business processes of companies in the telecommunications sector (TMForum, 2021). It is almost impossible to manually archive, update, and track the process map and related risk inventory in a structure of this size. At this point, information systems facilitate internal audit departments in dealing with big data such as this.

According to a 2006 survey by The Institute of Internal Auditors (IIA) among internal audit departments, 74% of respondents indicated they use risk management software for risk analysis (Gray, 2006). Utilizing Enterprise Risk Management (ERM) software allows for the digital storage of the company's process map and simultaneously enables the alignment of identified risks with the corresponding processes. Risk magnitudes are then determined through risk assessment studies. Thanks to the technological opportunities offered by these systems, processes can be easily monitored and evaluated by coloring them according to the level of risk they carry in terms of probability and impact - for example, the high-risk group is red, the medium-risk group is yellow, the low-risk group is green - with heat maps, a type of risk map that graphically shows the probability and impact of risks (Rao, 2009). Based on this, the

internal audit manager can create the annual audit plan by directing resources to audit the right processes. This is where audit management systems come into play. According to a survey of internal audit departments conducted by The Institute of Internal Auditors (IIA), 80% of respondents who said they use audit management software to manage their activities said they use it for audit planning, and 65% said they use it to create the audit calendar (Gray, 2006).

Audit documentation

Documentation of the actions taken by the auditor during the audit process is of immense importance. One of the most well-known mottoes regarding internal audit is "if it is not documented, it is not done." According to Standard No. 2330 of the IIA (The Institute of Internal Auditors), which sets the standards for internal auditing globally, "Internal auditors are required to document sufficient, relevant, reliable, and useful information that serves as the basis for their audit conclusions." (TIDE, 2017). The test performed by the relevant auditor is expected to be repeatable by another auditor and, when repeated, to reach the same conclusion as the relevant auditor. In this respect, an essential reason for proper audit documentation is to transcribe and archive the activities performed to prove the auditor's objectivity. Accordingly, in addition to the imprint information of the audit, such as the audit team, schedule, and scope, the auditor should document and archive the working papers that include how the auditor performed the audit tests, how he reached the conclusions because of these tests, and the supporting information and documents he used to reach these conclusions.

This documentation can be done in digital environments using information technologies. According to a survey conducted by The Institute of Internal Auditors (IIA) among internal audit departments, 55% of respondents who said they use audit management software to manage their activities indicated that they use it to create automated working papers (Gray, 2006). With audit software, working papers from previous years can be easily integrated into the current year's working papers when necessary, and even data kept on paper can be converted into an electronic format with the help of a scanner and made available in a digital environment (Bierstaker et al., 2001). An essential advantage of electronic working papers that increase efficiency is that information in a common database can be shared among auditors in different locations thanks to remote access (Bierstaker et al., 2001).

By Standard No. 2330 set by the IIA (The Institute of Internal Auditors), "The Internal Audit Manager must determine the principles for retaining engagement records, regardless of the medium in which each record is stored." (TIDE, 2017). Keeping the data in digital environments on information systems significantly reduces the storage space and cost of past and current working papers. Multiple backup copies of audit documentation can be stored electronically in various locations for security purposes (Bierstaker et al., 2001). Utilizing information systems in audit documentation provides the conveniences mentioned above and saves time for audit departments. Effortless updates can be made on the works in the digital environment, and review and approval processes can be completed quickly. In addition, information technologies enable secure data access management according to predetermined rules so that each auditor can access only the data they need for their work.

Reporting and monitoring of audit results

Information systems can also be used to effectively communicate the outputs of the audit process both within the department and across the company. Thanks to audit management software, the results of audit work can be categorized based on risk levels and related department management and shared digitally with the audit manager and associated department managers. Thus, audit results can be made available only to the relevant persons by ensuring the confidentiality and integrity of the data. The reporting made with this software can include

the presentation of the results in tables or dashboards with summary graphical representations. The same software can also obtain corrective action plans from the relevant management unit for the findings obtained because of the audit and monitor whether these action plans are fulfilled on time. Thanks to the audit management software, the action plan follow-up process for hundreds of findings from previous periods and those identified during the current audit year can be carried out in an accessible and reportable manner at any time.

Impact of IS usage on audit testing processes

In parallel with the development of information technologies, significant changes have occurred in how companies do business. Companies have started to use information technologies extensively in their daily business processes, and today, many business lines have moved into the era of "paperless" business processes. Almost all large corporations now employ enterprise information systems like SAP or Oracle, where business processes are integrated, and analysis and reporting are conducted from a singular data source (Bierstaker et al., 2001). These platforms consolidate disparate data sources and facilitate more efficient and robust analytics, enabling more effective and streamlined internal auditing processes.

Developments in information technologies have also greatly affected the internal audit profession. With the widespread use of enterprise computing platforms, audit evidence and control points that were once in paper format are now electronic (Bierstaker et al., 2001). As a result of the use of information technologies in the execution of daily activities in companies, auditors are now required to collect and assess evidence electronically (Boydaş, 2013). Therefore, in addition to traditional audit procedures, audit methods based on the use of technology have also begun to be employed today (Menna et al., 2016).

Technological tools that can be used in audits may include the following:

Electronic working paper. These are the most easily accessible and least costly software options. Today, audit tests can be conducted by preparing electronic working papers through MS Excel, a tool available on almost all computers. With MS Excel, the auditor can import and format data as desired. The auditor can then utilize the functions in MS Excel to create tables, employ formulas to verify the accuracy of calculations performed by the business unit, and use pivot tables to summarize the data, making it more easily analyzable.

Computer-aided audit software (generalized audit software). These programs enable access to company data files, retrieval of relevant data, and performing audit tests with various analysis methods. These may be package programs that include pre-designed test functions for relatively standardized tests such as accounting audits, or they may consist of software developed by auditors according to their needs.

System-integrated audit modules. These programs are embedded in advanced enterprise resource programs (such as SAP). They can be used to automatically detect control weaknesses or conflicting authorizations in the configurations of the relevant program, such as user access authorizations and approval strategies defined for work steps in the system.

Data analysis software. These applications operate through custom algorithms developed by auditors using a programming language tailored to business processes or through pre-embedded algorithms to detect abnormal data movements in large datasets. These tools are used for conducting tests based on the analysis of data that covers the entire population. Standard procedures can be automated to run continuously (e.g., daily), enabling real-time alerts to auditors when unexpected patterns emerge within the large dataset.

This software can be used separately or in combination, enabling the following analysis techniques to be utilized in audit tests (Boydaş, 2019):

Filtering. A specific attribute of the data under review is determined, and the software scans the entire record to select only those entries that meet the filtering criteria. The software also allows filtering based on multiple criteria in a single operation. This enables the exclusion of irrelevant data, narrowing the dataset under investigation. Utilizing software with advanced functionalities is particularly beneficial when the dataset originates from an extensive database, as it enhances the audit test's effectiveness.

Identification and equation. This generally involves the auditor re-performing calculations based on arithmetic operations. In this technique, the auditor defines a set of mathematical formulas in relevant software, re-calculates, and compares the obtained results with the values in the dataset. This serves to test the completeness and accuracy of values in calculation-involved fields.

Gap detection. This method applies to series records like invoice numbers or procurement requests that follow a sequential or specific pattern. It effectively identifies irregularities in the sequence or missing records that should be present (e.g., deleted entries). Appropriate software algorithms assist the auditor in identifying inconsistencies that might not be manually detectable, mainly when working with massive datasets containing various combinations.

Statistical analysis. Statistical analyses are mathematical modeling that detect anomalies in data containing numerical values. Statistical analysis models defined in the relevant software give a general idea of the data set through the records. The analysis creates a vision for the auditor in which data field the error should be searched.

Detection of duplicate records. Information technologies provide great convenience in detecting records repeated in specific periods or according to a pattern by analyzing data that should be singular or expected to contain random values under normal conditions. Especially in accounting audits, it significantly contributes to the auditor in identifying records that repeat in specific periods in small amounts but contain fraud.

Summarization. In its raw form, data may appear vast and complex. However, appropriate auditing software enables categorizing this data into more meaningful and analytically digestible units. As a result, it becomes straightforward to determine totals, counts, or the presence or absence of specific content within each category.

Layering. Similar to summarization, auditing software can divide data into layers based on specific numerical ranges. Following this division, totals and percentage values can be calculated within each layer. This functionality allows auditors to more easily analyze the data and quickly pinpoint ranges that may contain outliers or necessitate further detailed scrutiny.

Merging and association. Information technologies can be utilized to combine large amounts of data that are related to but obtained from different databases or systems. The auditor can establish a connection between datasets using an essential piece of data, merging different data lists by their relationships to form a single dataset. Auditing tests can then be performed on this newly created list.

In traditional audit methods, auditors conduct audit tests on a sample selected from data based on the results of a risk assessment that identifies processes as high-risk. They then generalize the conclusions drawn from this sample to the entire population, assuring the overall effectiveness of the process. However, significant risks may not always be detected in traditional testing methods. When engaging with advanced information systems, auditors may find it challenging to reduce the audit risk to an acceptable level by relying solely on tests of material accuracy (Bierstaker et al., 2001). Accurate decision-making is contingent upon the quality and timeliness of information; therefore, efficiently analyzing larger volumes of data in shorter periods has become important (Boydaş, 2013).

It can be argued that information technologies catalyze terms of the impact they have on the efficiency of audit methods (Önce & İşgüden, 2012). With the automation of business processes, auditors are no longer solely reliant on samples to evaluate controls or detect fraud and abuse. Instead, auditors can easily collect and analyze large volumes of electronically available data in databases, thanks to the advantages provided by information technology (Menna et al., 2016). Furthermore, information technologies can facilitate the automation of audit testing processes, thereby strengthening a company's overall approach and methodology to auditing (Ertaş & Güven, 2008).

Continuous audit and its contribution to the effectiveness of audit testing processes

Although common elements exist, it is observed that varying definitions for continuous auditing are present in the literature. While these definitions often emphasize its use predominantly in financial audits, broader characterizations are also found. Global organizations in accounting, such as the American Institute of Certified Public Accountants (AICPA) and the Canadian Institute of Chartered Accountants (CICA), define continuous auditing as "a methodology that enables an independent auditor to provide written assurance on the subject matter using a set of auditor reports prepared either simultaneously with, or a short period after, the occurrence of an audit-relevant event" (Boydaş, 2013).

ISACA (Information Systems Audit and Control Association), an international professional association focusing on IT governance and auditing, describes continuous auditing as a method that allows for the receipt of written reports relating to audit-relevant transactions almost instantly or shortly after they occur (Boydaş, 2013). The Institute of Internal Auditors (IIA), an organization that sets standards and provides guidance for the internal auditing profession, describes continuous auditing in the Global Technology Audit Guide (GTAG) as "a method commonly used by internal auditors for frequent automated control and risk assessment" (Boydaş, 2013).

Drawing on the common thread among all these definitions, the term "continuous auditing" refers to the method whereby data in a computerized environment is analyzed using information systems, such as analysis software, in real-time (or near real-time) and automatically, and assurance is provided based on the results obtained (Boydaş, 2013). With the advent of advanced information systems based on emerging technologies in business processes, it has become increasingly important to align audit processes with these technologies, integrate information technology into audit processes for automation, and improve audit quality and effectiveness.

Sufficiency is a measure of the quantity of evidence (e.g., sample size), while appropriateness is a measure of the quality of the evidence (Barr, 2019). Data analysis tools like continuous auditing allow for examining the entire transaction population in real-time or near real-time, proportionally increasing sufficiency (Barr, 2019). The more qualitative, sufficient, and appropriate the audit evidence, the more convincing the auditor's conclusions will be. Compared to traditional periodic sampling-based audits, adequately designed data analysis tools increase the appropriateness of the evidence as they allow access to up-to-date data that auditors can independently obtain from relevant systems (Barr, 2019).

Utilizing information technology for continuous auditing enhances the quality of audit evidence and the auditor's inclination to report findings assured by the credibility of the collected evidence (Barr, 2019). Additionally, external auditors reviewing the company will have increased confidence in the work conducted by internal auditors when the internal audit report is based on evidence gathered through automation methods (Barr, 2019).

Conclusion

The advent of information technologies has significantly transformed corporate operational methods. Previously, paper-based processes have been digitized, catalyzing changes in audit methods and increasing the efficiency of audit activities. As companies transition to paperless systems and audit software becomes more advanced, the use of information systems in managing audit processes and conducting audit tests becomes widespread. These evolving technologies have substantially altered the traditional nature of the audit process, which was previously reliant on paper-based source documents.

Internal audit managers can use audit management software to construct an annual plan based on risk assessment outcomes, thus allocating resources to audit the correct processes. Leveraging information systems in audit documentation saves time for audit departments. Effortless documentation and updating of digital work and speedy review and approval processes can be realized. Additionally, information technologies enable secure data access management based on pre-defined rules, further enhancing audit outcomes. Audit results can be shared digitally among audit managers and relevant department heads, maintaining data confidentiality and integrity, thanks to audit management software. The same software allows for straightforward and reportable action plan tracking processes for hundreds of findings identified in past and current audit years.

Adopting advanced information systems in business processes has led to integrating information technologies into audit processes, providing automation, and increasing audit quality and effectiveness. Auditors no longer rely solely on samples to evaluate controls or detect fraud. Instead, data analysis software enables collecting and analyzing large volumes of electronically available data in databases. Data analytics tools like Continuous Auditing allow for the examination of the entire transaction population in real-time or near-real-time, proportionally increasing the sufficiency and quality of audit evidence. The more the quality, adequacy, and appropriateness of audit evidence, the more convincing and valuable the auditor's results will be.

In conclusion, using information technologies in managing audit activities and the data collection and testing process liberates the auditor from many routine audit tasks. It allows the auditor to allocate time to more sophisticated duties like understanding the subject processes and evaluating various risks. Automation in audit testing processes further fortifies the company's audit approach and methodology.

REFERENCES

Arena, M. & Azzone, G. (2007). Internal audit departments: adoption and characteristics in Italian companies. *International Journal of Auditing*, Vol. 11, No. 2, pp. 91-114). https://doi.org/10.1111/j.1099-1123.2007.00357.x

Barr-Pulliam, D. (2019). Continuous auditing and role duality affect the incidence and likelihood of reporting management opportunism. In Management Accounting Research (Vol. 44, pp. 44–56). Elsevier BV. https://doi.org/10.1016/j.mar.2018.10.001

Betti, N. & Sarens, G. (2020). Understanding the internal audit function in a digitalised business environment. *Journal of Accounting & Organizational Change*, Vol. 17, No. 2, pp. 197-216. https://doi.org/10.1108/jaoc-11-2019-0114

Bierstaker, J.L., Burnaby, P. & Thibodeau, J. (2001). "The impact of information technology on the audit process: an assessment of the state of the art and implications for the future," *Managerial Auditing Journal*, Vol. 16 No. 3, pp. 159–164. https://doi.org/10.1108/02686900110385489

Boydaş, H. H. (2013). Using Digital Analysis Techniques in Continuous Audit and an Application, *PhD Thesis*, Marmara University Institute of Social Sciences, Department of Business Administration, Istanbul.

Hazar, Ü. H. B. (2019). Application of computer-aided auditing tools and techniques *Financial Analysis/Mali Çözüm Dergisi*, 29(156).

Erasmus, L. & Coetzee, P. (2018). Drivers of stakeholders' view of internal audit effectiveness. *Managerial Auditing Journal*, Vol. 33, No. 1, pp. 90-114. https://doi.org/10.1108/maj-05-2017-1558

Ertaş, F. C., & Güven, P. (2008). The Effects of Information Technologies on Auditing Process, *Journal of Accounting and Finance/Muhasebe ve Finansman Dergisi*, 37, 50 - 59.

Goodwin-Stewart, J. & Kent, P. (2006). The use of internal audit by Australian companies. *Managerial Auditing Journal*, Vol. 21, No. 1, pp. 81–101. https://doi.org/10.1108/02686900610634775

Gökoğlan, K. (2022). Research on the determinants of internal audit effectiveness in business. *Odü Sosyal Bilimler Araştırmaları Dergisi (Odüsobiad)*. https://doi.org/10.48146/odusobiad.1100666

Gray, G. L. (2006). An array of technology tools: a broad mix of spreadsheet and audit-specific products enables auditors to take on many different tasks, according to the 2006 Internal Auditor Software Survey. *Internal Auditor*, 63(4), 56–62.

Önce, S. & İşgüden, B. (2012). Evaluation of internal auditing activity for growing and changing information technology environment: ISE-100 example. *Journal of Management and Economics Research*, 10 (17), 38-70. https://doi.org/10.11611/JMER3

Krishna M., Seetharaman, A. Mohamed, Z., & Gopalan, M. (2011). The impact of information technology on internal Auditing, *South African Journal of Business Management*, January 2011, https://doi.org/10.5897/AJBM10.1047

Menna, T., Mohamed, E. K., Hussain, M., & Mohamed, B. (2016). The implication of information technology on the audit profession in developing country, *International Journal of Accounting & Information Management*, *25*(2), 2017, 237–255, https://doi.org/10.1108/IJAIM-03-2016-0022

Nighia, D. & Nguyen, H. (2022). Knowledge management model for internal auditing. *European Conference on Knowledge Management*, Vol. 23, No. 2, pp. 768–776. https://doi.org/10.34190/eckm.23.2.523

Novranggi, E. (2019). The effect of competence, objectivity and internal audit quality the effectiveness of internal audit with senior management support as variable moderation. *Kne Social Sciences*. https://doi.org/10.18502/kss.v3i26.5359

Rao, A. (2009). Implementation of Enterprise Risk Management (ERM) Tools-A Case Study. *Academy of Accounting and Financial Studies Journal*, pp. 13, 87.

Sarens, G. & Beelde, I. (2006). The relationship between internal audit and senior management: a qualitative analysis of expectations and perceptions. *International Journal of Auditing*, Vol. 10, No. 3, pp. 219-241. https://doi.org/10.1111/j.1099-1123.2006.00351.x

TIDE-Internal Audit Institute of Turkey, (2017). International Standards on Internal Auditing (Standards) within the Scope of Professional Practice Framework, https://www.tide.org.tr/file/documents/pdf/UMUC-2017-updated.pdf, 13/05/2023.

TMForum, (2021). Business Process Framework (eTOM), https://www.tmforum.org/business-process-framework/, 13/05/2023.

Similarity Analysis on Mobile Game Play Videos

İsmail İŞERİ[1]

Introduction

Design suitability is a crucial factor for a mobile game to achieve a high download rate Design suitability is a crucial factor for a mobile game to achieve a high download rate and be deemed successful. Companies strive to maximize the time users spend playing the game after downloading it, ensuring that the game remains engaging and profitable through methods such as in-game advertising, in-game sales, and more. This helps prevent unnecessary expenses and time loss in the design analysis process. Research has shown that games with high download rates excel in aspects like color harmony, object placement, mechanics, and overall user experience, while games with low download and retention rates often fall short in these areas. Analyzing successful games for design inspiration can be a valuable guide to improving a game's design and increasing its chances of becoming a hit quickly.

To determine the design similarity of games, it is essential to analyze the visual similarities within game videos. Visual similarity does not have a clear definition because it is a relative concept connected to human perception (Unzicker *et al.*,1998). Therefore, no similarity metrics allow us to arrive at the correct measurements for the similarity value. When the researches are examined, it is stated that people generally adhere to visual features such as color, texture, shape, etc. in video similarity and colors have an important place in human perception, especially in these similarity measurements (Farag and Abdel-Wahab, 2003). In one of the earliest studies involving the definition of visual similarity, it was emphasized that similar videos should be similar in visual characteristics such as color and texture (Liu *et al.*, 1999).

While there are numerous studies in the literature on video similarity, research on similarity assessments for game videos has been notably absent. Seshadrinathan K. and Bovik A. C. developed a Video Structural Similarity index known as V-SSIM, which incorporates motion modeling with optical flow for assessing video sequence quality. Experimental studies conducted on the VQEG database have demonstrated that their proposed index outperforms other video quality evaluation systems (Seshadrinathan and Bovik, 2007).

Bekhet C. and Ahmed A. provided a systematic analysis of various video similarity/distance metrics, including Euclid, Manhattan, Chi Sqr, Histogram intersection, Bhattacharyya, Cosine, EMD, and Chebyshev. Their experiments on several standard video datasets revealed that the most effective measurements are the Manhattan and Euclidean distances (Bekhet and Ahmed, 2020).

Wolf L. and Levy N. introduced a new similarity score aimed at reducing false similarity due to pose similarity. Their video recognition study, using the YouTube Faces DB dataset, incorporated a newly introduced classifier called SVMminus. The study demonstrated that the proposed classifier produced superior results compared to other models (Wolf and Levy, 2013).

Zeng Z. et al. introduced the Tencent-MVSE dataset, a benchmark dataset, to enhance multimodal video similarity evaluation and contribute to video recommendation systems. This

[1]Unvan, Ondokuz Mayıs University

dataset is unique in its capacity to consider video text, elucidate similarity between elements, and its larger structure compared to existing datasets (Zeng *et al.*, 2022).

Liu Y. et al. proposed a novel feature extraction module and similarity measurement method in their video-based person identification study. Through experiments on three challenging datasets, iLIDS-VID, PRID-2011, and MARS, they achieved an average performance of 71% accuracy on the iLIDS-VID dataset, 81% accuracy on the PRID-2011 dataset, and 61% accuracy on the MARS dataset, outperforming other methods (Liu *et al.*, 2018).

Ma C. et al. introduced a machine learning-based method using radiomic analysis on SSIM subindex maps for feature inference to aid traditional gamma analysis in error detection within intensity-modulated radiotherapy (IMRT) quality assurance (QA) processes. They achieved the highest performance with the Linear-SVM model, boasting an accuracy rate of 86% (Ma *et al.*, 2021).

Han Z. et al. proposed the Video Similarity and Alignment Learning (VSAL) approach, aiming to model spatial similarity, temporal similarity, and partial alignment simultaneously. Experiments conducted on the VCDB core dataset and the FIVR-200k dataset indicated that the VSAL approach outperformed other models, producing higher F1 scores (Han *et al.*, 2021).

In a separate study, Liu R. explored the effects of three image enhancement techniques (Gaussian blur, blunt masking, and grayscale) on various videos to enhance video similarity search. Experimental results revealed that Gaussian blur was the most effective image filter, making similar frames more similar and different frames more distinguishable compared to the other two image enhancement techniques (Liu, 2021).

The ability to predict whether a mobile game will achieve a high download rate remains uncertain. Game studios and individual developers strive to attain the highest standards of design to ensure their games stand out in the competitive gaming industry. To conduct a design analysis of a game, it must be launched in the market, incurring certain expenses. Therefore, one approach to predict the design suitability of a game involves making inferences by assessing its similarity to successful games within the same category.

This study focuses on analyzing the similarity of a mobile game to popular games of the same category based on gameplay videos, utilizing the SSIM (Structural Similarity Index) and cosine similarity methods. Furthermore, to validate the study's effectiveness, we also obtained similarity values between the game and games from different categories and compared the differences in visual similarity values.

The primary contributions of this study are as follows:

- The first application of similarity analysis to game videos.
- The first investigation into identifying design shortcomings of a game by assessing its proximity to successful games.
- Determination of the most effective video similarity algorithms for detecting game video similarity.
- Conducting similarity analysis of game videos with feature extraction based on deep learning techniques.

The remainder of this paper is structured as follows: Section 2 provides definitions for the materials and methods employed in the study. Section 3 presents the experimental part and its results. Finally, Section 4 concludes the article, offering insights into potential future research directions.

Materials and Methods

Data Set

Within the framework of this study, our game expert selected 10 popular games belonging to the Hypercasual-Runner category from the Google Play Store. To conduct a similarity analysis with these successful games, our game expert also identified three different games that are not considered hits. Among these three games, one has not achieved hit status but garnered a high score from our game expert and exhibits significant similarity to hit games. The second game is characterized by a low hit game similarity score and a poor design rating. The third game was selected from a different category, distinct from the category of the 10 hit games identified on the Play Store.

The reason for this diverse game selection for comparison is to assess the performance of the similarity algorithms effectively. Gameplay videos for all selected games were obtained from YouTube, consisting of screenshots capturing the gameplay. Given that the foundation of this study lies in assessing the similarity of these images, the videos were segmented into individual frames.

Pre-Processing

In the event that the game videos downloaded from YouTube included multiple games, the video associated with the game chosen for similarity analysis was isolated by trimming, thus obtaining the specific game videos for analysis. These videos were resized to match the dimensions of the game's screenshots, and extraneous components, such as intros, logos, and any black screens appearing at the video's outset and conclusion, were systematically removed to enhance the dataset's quality by eliminating irrelevant data.

Frame Parsing

To extract frames from the videos, they were named according to their respective game titles and organized within a dedicated folder. Subsequently, frames were stored in automatically generated folders, each bearing the name of the corresponding video. Throughout the frame extraction process, no frame skipping was implemented; all frames from the videos were meticulously collected. As a result, each video encompassed a minimum of 5,000 frames.

Feature Extraction

Feature extraction serves as a dimension reduction technique that partitions high-dimensional input data into lower-dimensional representations, simplifying subsequent data processing. This technique finds extensive application in various domains, including image processing, pattern recognition, and natural language processing. Extracted image features typically encompass attributes such as color, texture, shape, and pixel values (Choras, 2007). Deep learning models are frequently employed for the extraction of features from images.

In the study, feature extraction was performed on individual frames using pre-trained deep learning models, specifically ResNet50 and VGG16. ResNet50 is a 50-layer neural network model trained on the ImageNet dataset, while the VGG16 model, also trained on ImageNet, consists of 21 primary layers.

Similarity Calculation Methods

Image similarity, a subfield of image processing, focuses on quantifying the degree of similarity between two images. Various methods for calculating image similarity are employed to assess this likeness. To determine the similarity ratio between videos, the images extracted from video frames are input into the chosen similarity algorithm. The accurate selection of a similarity algorithm is pivotal in generating the most precise similarity score. In this study, two

specific similarity algorithms, cosine similarity, and the structural similarity index, were employed.

Cosine Similarity

Cosine similarity stands out as one of the most favored methods for measuring similarity distances. This metric calculates the cosine of the angle formed between two non-zero vectors within an inner product space (DeepAI, n.d.). The calculation for cosine similarity (Lahitani *et al.*, 2016):

$$cos\alpha = \frac{A \times B}{|A| \times |B|} = \frac{\sum_{i=1}^{n} A_i \times B_i}{\sqrt{\sum_{i=1}^{n}(A_i)^2} \times \sqrt{\sum_{i=1}^{n}(B_i)^2}}$$

In this equation:

- A represents the weights of each property in vector A.
- B represents the weights of each property in vector B.

A cosine similarity value of 1 indicates that the two vectors are perfectly similar. The diagram depicting the study conducted using the cosine similarity algorithm is illustrated in Figure 1.

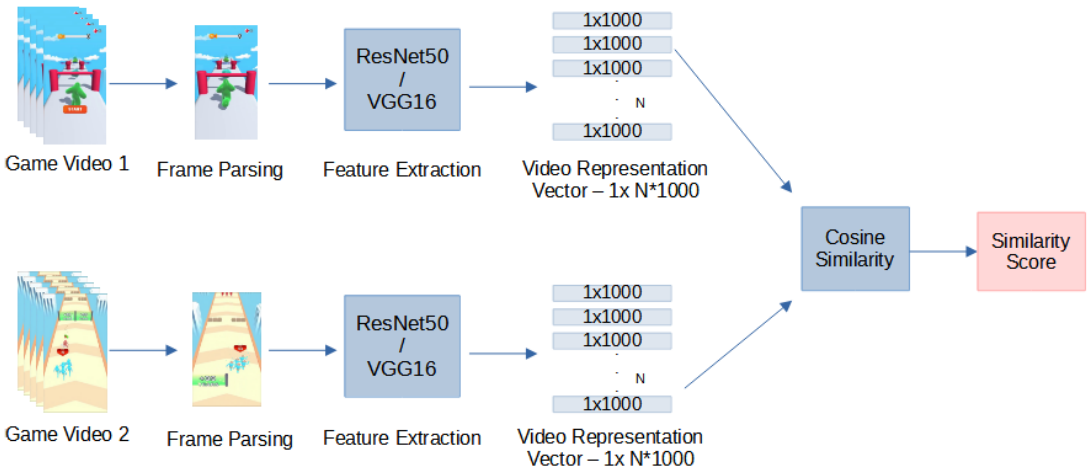

Figure 1. Diagram of Video Similarity Pipeline Using Cosine Similarity

Structural Similarity Index (SSIM)

SSIM, developed by Wang et al., is a quality metric employed to assess the similarity between two images (Wang *et al.*, 2004). The SSIM index is closely linked to the quality perception of the human visual system (HVS), making it a valuable tool in visual simulation studies. It involves calculations based on the similarities in brightness l(f,g), contrast c(f,g), and structure s(f,g) to measure the dissimilarity between SSIM indices of K × K image patches, denoted as f and g (Bergmann et al., 2018). The specific definition of SSIM is:

$$SSIM(f,g) = l(f,g)^{\alpha} c(f,g)^{\beta} s(f,g)^{\gamma}$$

The α, β, and γ values mentioned here are user-defined constant coefficients used to assign weights to the three provided terms.

$$l(f,g) = \frac{2\mu_f\mu_g + c_1}{\mu_f^2 + \mu_g^2 + c_1}$$

$$c(f,g) = \frac{2\sigma_f\sigma_g + c_2}{\sigma_f^2 + \sigma_g^2 + c_2}$$

$$s(f,g) = \frac{\sigma_{fg} + c_3}{\sigma_f\sigma_g + c_3}$$

In this context:

- l(f,g) measures the proximity of the average brightness of two images.
- c(f,g) measures the proximity of the contrast between two images.
- s(f,g) calculates the correlation coefficient between images f and g.

The positive constants c1, c2, and c3 are introduced to ensure numerical stability and prevent division by zero. The SSIM index yields values within the range of [0,1], with a value of 0 indicating no correlation between the images, and a result of 1 when comparing images f and g (Hore and Ziou, 2010). The diagram illustrating the study conducted using the SSIM algorithm is provided in Figure 2.

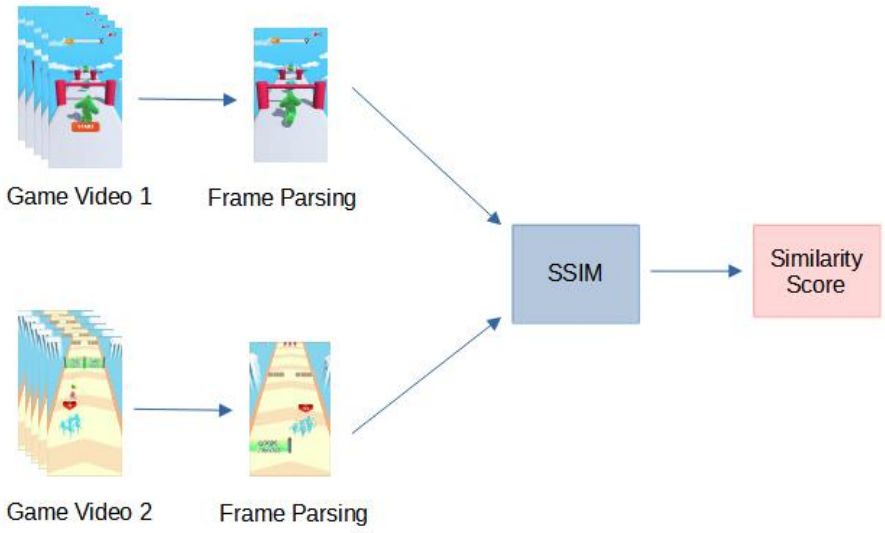

Figure 2. Diagram of Video Similarity Pipeline Using SSIM

Experimental Results

In the experimental results, frame extraction was conducted on the videos within the dataset employed. Subsequently, various methods were employed to determine different similarity scores for each. Within these experiments, our gaming expert compared ten popular games in the Runner game category with a highly-rated Runner game and a poorly-rated Runner game.

To assess the likelihood that these games exhibited the least visual similarity, a comparison of the visual similarity between the popular Runner games and a game from a different category was carried out using both the cosine similarity and SSIM index. The comparative results are presented. The frames extracted from the videos used in the study are provided in Figure 3.

Figure 3. Random Selected Frame Examples of The Compared Videos

Results Obtained by Cosine Similarity Method

The frames were converted into vector representations through feature inference for cosine similarity, utilizing pre-trained deep learning models ResNet50 and VGG16. Prior to input to the deep learning models, frames were resized to dimensions of (224,224,3), and feature extraction was performed, resulting in each frame being represented as a 1x1000 vector.

A total of 300 frames were extracted from the videos with 15-frame intervals, and these 1x1000 size frames were concatenated to create a single 1x300,000 size vector representation for the video. Subsequently, the cosine similarity between the video representations of the games was computed.

The video similarity scores derived from the application of ResNet50 and the cosine similarity method to a high-rated runner game, a low-rated runner game, a game from a different category, and the popular games are presented in Table 1. Furthermore, the similarity scores obtained from the video similarity analysis conducted using VGG16 and the cosine similarity method are detailed in Table 2.

Table 1. Similarity Scores Using ResNet50 and Cosine Similarity (%)

Game Videos	Hit Game 1	Hit Game 2	Hit Game 3	Hit Game 4	Hit Game 5	Hit Game 6	Hit Game 7	Hit Game 8	Hit Game 9	Hit Game 10
High Score Runner Game	24.31	18.98	28.11	26.21	22.59	22.92	14.84	15.97	21.1	18.39
Low Score Runner Game	26.08	20.45	28.67	29.01	23.49	27.73	11.72	14.47	22.39	17.52
The Game in a different category	45.5	29.88	31.71	25.59	13.6	38.31	15.88	10.56	31.12	23.66

Table 2. Similarity Scores Using VGG16 and Cosine Similarity (%)

Game Videos	Hit Game 1	Hit Game 2	Hit Game 3	Hit Game 4	Hit Game 5	Hit Game 6	Hit Game 7	Hit Game 8	Hit Game 9	Hit Game 10
High Score Runner Game	8.59	9.26	12.44	12.28	11.65	9.36	6.46	8.41	8.38	7.18
Low Score Runner Game	20.29	16.52	21.61	24.11	16.45	19.74	9.31	11.99	16.46	13.63
The Game in a different category	42.23	28.2	30.7	22.95	11.47	36.39	13.99	8.55	30.68	21.7

The bar graphs depicting the similarity scores obtained using ResNet50 and the cosine similarity method are displayed in Figure 4. Additionally, the bar graphs illustrating the similarity scores obtained with VGG16 and cosine similarity can be found in Figure 5.

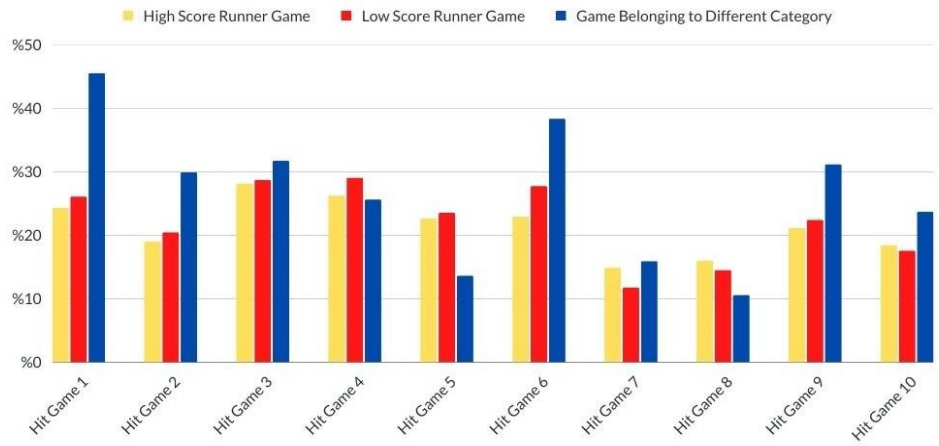

Figure 4. Bar Graph of Similarity Scores Obtained Using ResNet50 and Cosine Similarity

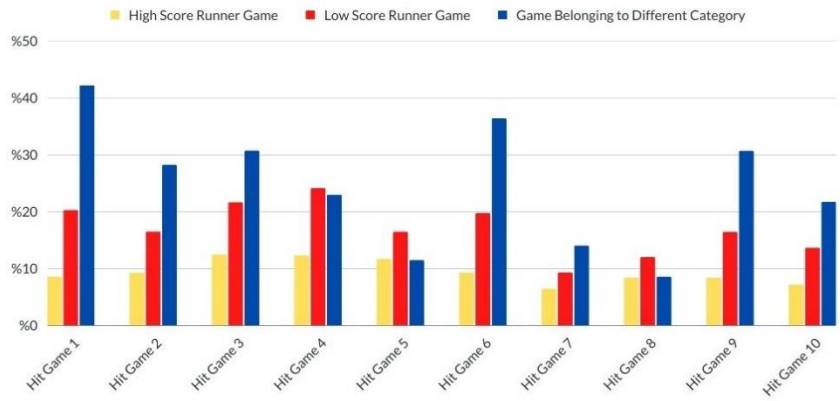

Figure 5. Bar Graph of Similarity Scores Obtained Using VGG16 and Cosine Similarity

In the experimental results, the average similarity of the highly-rated game to the hit games was computed as 21% using ResNet50 and 9% using VGG16. The average similarity score of the poorly-rated game to the hit games was determined as 22% with ResNet50 and 17% with VGG16. Furthermore, the similarity between the game from a different category and the hit games was assessed as 26% using the ResNet50 model and 24% with the VGG16 model.

Results Obtained with the SSIM Method

In the computation of similarity using the SSIM method, the frames recorded in the files were read into an array. Prior to input into the similarity algorithm, these frames were resized to dimensions of (224, 224, 3) to ensure color consistency.

The frames from two videos were sequentially processed through the similarity algorithm, with the resulting similarity scores compiled into a sequence. From these scores, both the average similarity score and the individual similarity scores of the videos were computed. The obtained similarity scores from the video similarity analysis using the SSIM method are presented in Table 3, and the bar graphs illustrating these SSIM-based similarity scores are displayed in Figure 6.

Table 3. Similarity Scores Obtained Using SSIM Index (%)

Game Videos	Hit Game 1	Hit Game 2	Hit Game 3	Hit Game 4	Hit Game 5	Hit Game 6	Hit Game 7	Hit Game 8	Hit Game 9	Hit Game 10
High Score Runner Game	7.12	22.54	37.32	19.06	14.85	5.74	11.23	14.11	38.22	15.42
Low Score Runner Game	5.81	9.42	14.62	10.05	7.43	4.45	6.25	7.07	15.5	6.82
The Game in a different category	5.55	9.28	12.11	9.49	6.9	3.74	6.25	7.53	13.75	5.87

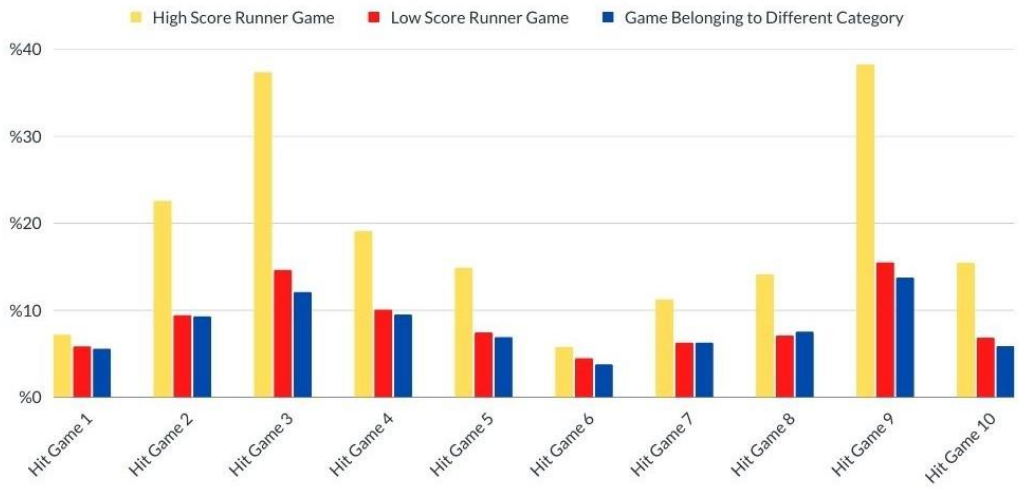

Figure 6. Bar Graph of Similarity Scores Obtained Using SSIM Index

In the experimental results, the average similarity between the highly-rated game and the hit games was computed as 18%, while the average similarity score between the poorly-rated game and the hit games was determined to be 8%. Moreover, the similarity between the game from a different category and the hit games yielded a score of 8%.

Conclusion

This study aimed to assess the similarity between two videos using the cosine similarity and the SSIM index. Inferences were drawn by comparing the similarities of game videos to popular hit games. Upon analyzing the experimental results, notable trends emerged. For instance, it was observed that a high-scoring runner game exhibited relatively low similarity to the hit games when measured by the cosine similarity. Conversely, a lower-rated game displayed a higher similarity score when employing the cosine similarity metric. This contrast was intriguing and raised questions about the effectiveness of the design score in relation to similarity. Moreover, when a different game, unrelated to the runner category, was expected to be less similar in terms of design to runner games, it surprisingly exhibited the highest degree of similarity according to the cosine algorithm.

In the video similarity study conducted using the SSIM index, a different pattern emerged. The runner game with a high design score demonstrated higher similarity to the hit games than the other games. Conversely, games with low design scores and those from different categories exhibited lower similarity to the hit games, aligning with the expected results based on design similarity. Consequently, it was determined that assessing video similarity in terms of design using the SSIM index, as opposed to vector similarity, yielded more accurate results.

Subsequent studies will aim to identify the optimal values for design similarity in game videos and evaluate video similarities based on this optimal value, with a focus on detecting copy games.

REFERENCES

Bekhet, S., & Ahmed, A. (2020). Evaluation of similarity measures for video retrieval. *Multimedia Tools and Applications, 79*(9), 6265-6278.

Bergmann, P., Löwe, S., Fauser, M., Sattlegger, D., & Steger, C. (2018). Improving unsupervised defect segmentation by applying structural similarity to autoencoders. *arXiv preprint arXiv:1807.02011*.

Choras, R. S. (2007). Image feature extraction techniques and their applications for CBIR and biometrics systems. *International journal of biology and biomedical engineering*, *1*(1), 6-16.

DeepAI. (T.Y.). *Cosine similarity*. Erişim tarihi: 10 Ekim 2022, https://deepai.org/machine-learning-glossary-and-terms/cosine-similarity

Farag, W. E., & Abdel-Wahab, H. (2003, July). A human-based technique for measuring video data similarity. In *Proceedings of the Eighth IEEE Symposium on Computers and Communications. ISCC 2003* (pp. 769-774). IEEE.

Han, Z., He, X., Tang, M., & Lv, Y. (2021, October). Video similarity and alignment learning on partial video copy detection. In *Proceedings of the 29th ACM International Conference on Multimedia* (pp. 4165-4173).

Hore, A., & Ziou, D. (2010, August). Image quality metrics: PSNR vs. SSIM. In *2010 20th international conference on pattern recognition* (pp. 2366-2369). IEEE.

Lahitani, A. R., Permanasari, A. E., & Setiawan, N. A. (2016, April). Cosine similarity to determine similarity measure: Study case in online essay assessment. In *2016 4th International Conference on Cyber and IT Service Management* (pp. 1-6). IEEE.

Liu, R. (2021). Effects of Image Filters on Video Similarity Search. *choice*, *2*, 3.

Liu, X., Zhuang, Y., & Pan, Y. (1999, October). A new approach to retrieve video by example video clip. In *Proceedings of the seventh ACM international conference on Multimedia (Part 2)* (pp. 41-44).

Liu, Y., Xie, C., Zhou, W., & Li, H. (2018, December). Effective Similarity Measurement for Video-based Person Re-identification. In *2018 IEEE Visual Communications and Image Processing (VCIP)* (pp. 1-4). IEEE.

Ma, C., Wang, R., Zhou, S., Wang, M., Yue, H., Zhang, Y., & Wu, H. (2021). The structural similarity index for IMRT quality assurance: radiomics-based error classification. *Medical Physics*, *48*(1), 80-93.

Seshadrinathan, K., & Bovik, A. C. (2007, April). A structural similarity metric for video based on motion models. In *2007 IEEE International Conference on Acoustics, Speech and Signal Processing-ICASSP'07* (Vol. 1, pp. I-869). IEEE.

Unzicker, A., Jüttner, M., & Rentschler, I. (1998). Similarity-based models of human visual recognition. *Vision Research*, *38*(15-16), 2289-2305.

Wang, Z., Bovik, A. C., Sheikh, H. R., & Simoncelli, E. P. (2004). Image quality assessment: from error visibility to structural similarity. *IEEE transactions on image processing*, *13*(4), 600-612.

Wolf, L., & Levy, N. (2013). The svm-minus similarity score for video face recognition. In *Proceedings of the IEEE conference on computer vision and pattern recognition* (pp. 3523-3530).

Zeng, Z., Luo, Y., Liu, Z., Rao, F., Li, D., Guo, W., & Wen, Z. (2022). Tencent-MVSE: A Large-Scale Benchmark Dataset for Multi-Modal Video Similarity Evaluation. In *Proceedings of the IEEE/CVF Conference on Computer Vision and Pattern Recognition* (pp. 3138-3147).

Application Of Fruit Recognition Systems

M. Barış Eminoğlu[1]
Uğur Yegül[2]

Introduction

Fruit production is important for human nutrition and the country's economy, both for table consumption and in the food industry. Fruit harvest accounts for the largest share of fruit growing in terms of labor and production costs. The results obtained from the research conducted on this subject (Gezer, 2001; Ünal, 2005; Burks et al.; 2005) support this situation.

Fruit harvesting is generally done by three main methods. In manual harvesting of fruits, the ripe fruits are held by hand and rotated around the stem to separate them from the main plant. This method is especially used in the harvest of table and easily damaged fruits. In the harvesting of fruits by mechanical methods, the fruits on the tree crown are harvested mechanically. In this method, fruit damage is high due to mechanical effects. This method is used to harvest fruits used for industrial purposes. In fruit harvesting using semi-mechanical methods, the process of separating the fruit from the main plant is done manually; all other operations are carried out mechanically. From this perspective, the equipment used in semi-mechanical methods combines manual labor and mechanical harvesting.

High fruit harvest labor and harvest costs, lack of availability of qualified harvest labor, epidemics and wars around the world; causes the development of automation applications instead of human labor in fruit harvesting.

When automation applications in fruit harvesting are mentioned, harvesting fruits with robots comes to mind. These automation applications can be done with unmanned land or air vehicles, as seen in Figure 1.

Figure 1 Unmanned ground vehicle (a) (Silwal et al., 2017), unmanned aerial vehicle (b) (Anonymous a, 2022)

[1] Dr. Öğr. Üyesi, Ankara Üniversitesi Ziraat Fakültesi Tarım Makinaları ve Teknolojileri Mühendisliği Bölümü, (sorumlu yazar)
[2] Dr., Ankara Üniversitesi Ziraat Fakültesi Tarım Makinaları ve Teknolojileri Mühendisliği Bölümü

These robotic applications used in fruit harvest automation can be generally examined in three main sections shown in Figure 2.

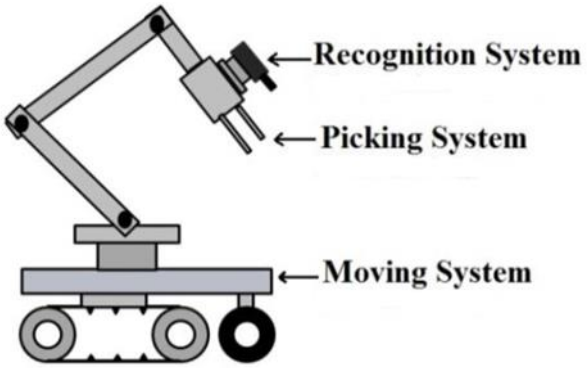

Figure 2 Components of the fruit harvesting robot (Bachche, S. 2015)

These main components are the recognition system in which the identification and location of the fruits are verified, the picking system in which they are held and separated from the branch, and the movement system that enables movement during work in greenhouses or gardens.

In this section, information will be given about the hardware and software that enable the recognition of fruits, and fruit identification systems that have been used in academic studies will be included.

Fruit recognition systems

Robots harvesting fruit must first separate the fruit from other objects. This process is done with image processing technique. This process has two main components: software and hardware.

The hardware component may consist of one or more cameras. The most commonly used cameras in fruit harvest automation studies are; monocular, stereo cameras, spectral and thermal cameras. The most used algorithms are color, shape and texture based analysis and neural network approaches.

Gongal et al. (2015) used different camera types in fruit harvest automation according to fruit characteristics and their evaluations based on image classification methods. Although black/white cameras are not affected by different lighting conditions, the lack of color information has been stated as a negative aspect. In the literature studies they emphasized that when used in evaluations based on geometric features, fruit identification accuracy of 68-75% was achieved. They also emphasized that although color cameras provide color texture and geometric information, they are affected by lighting conditions. In the literature studies they mentioned, that when color was used in evaluations based on characteristics, fruit identification accuracy of 80-85% was achieved for apples and citrus fruits. Artificial intelligence algorithms used with color cameras vary. Although spectral cameras provide different wavelengths and color information, it has been stated that they are negative in that the evaluations take time. Thermal cameras can be used if the colors of the fruit and other objects in the picture are the same, but the negative aspects are that they are affected by the size of the plant and cannot be applied at all hours of the day.

Grand D'Esnon et al. used three color CCD (Charge Coupled Device) cameras to identify fruits in the system of the project named "MAGALLI", which was one of the first examples of robotic harvest applications they developed for apple harvest in 1987 (Figure 3).

With the 950, 650 and 550 nm wavelength filters they used with these cameras, they tried to determine which pixel belonged to the fruit and which pixel belonged to other objects such as leaves and branches.

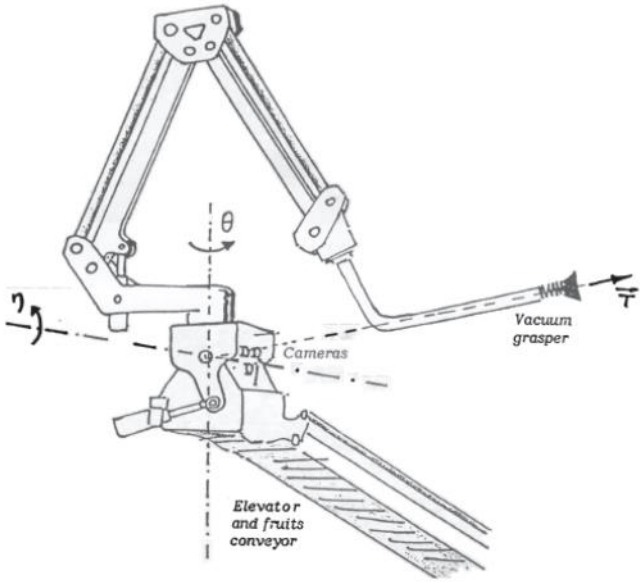

Figure 3 Robot arm developed for apple harvesting (Grand D'Esnon et al. 1987)

Yang et al. (2007) developed a system to identify ripe tomatoes in tomato clusters located at different distances in their study in a tomato greenhouse. The developed system used a color stereo camera and the CLG (Color Layer Growing) method to separate fruits from other objects and parasites. It was stated that the image resolution used was 600x480. In this study, the distance of the camera to the fruits was tried to be determined by placing the camera at a distance of 32~35cm, 50~53cm and 65~68cm on the fruit bunches.

Figure 4 Raw image (left), identified fruit clusters (right) (Yang et al., 2007)

As seen in Figure 4, after the image taken with the camera was processed with software, clusters containing ripe fruits could be detected. As a result of the tests carried out to determine the distance of the fruit bunches to the camera, it was stated that the maximum measured distances of the fruit bunches and the calculated distance values were very close to each other.

Thendral et al. (2014) compared color and edge detection-based methods in their study to identify orange images from photographs taken under natural light randomly selected from the internet.

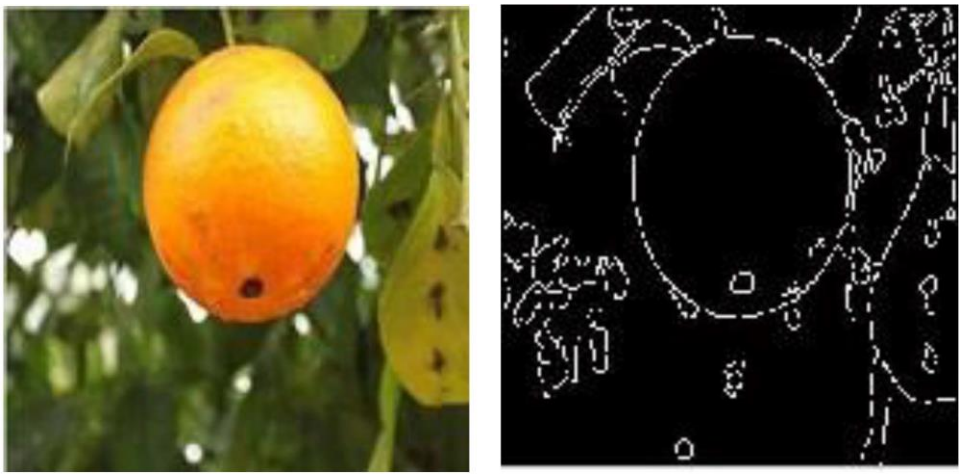

Figure 5 Original image (left) and image obtained from edge detection based method (right) (Thendral et al. 2014)

The image on the left in Figure 5 was converted into the image on the right using threshold values obtained with an edge detection algorithm.

In the color determination-based algorithm, the image is first processed using a filter and then converted to L*a*b color space. Pixels belonging to the “a” color plane were used for rough determination of the fruit region. Detectable pixels were defined as “1” and those that could not be detected were defined as “0”. Thus, those identified as "1" in the picture were converted to white, and those identified as "0" were converted to black, to the form shown in Figure 6.

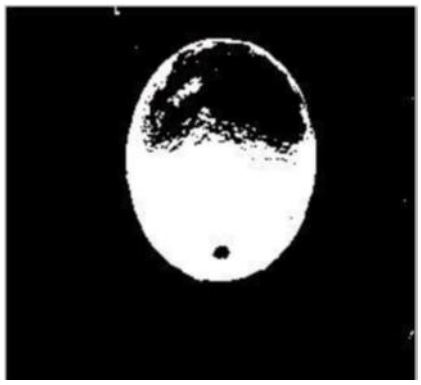

Figure 6 Fruit image expressed with binary coding (Thendral et al. 2014)

In the picture in Figure 6, the small images that did not represent the fruit were eliminated, the gaps were filled, and the picture showing the geometric structure of the fruit was obtained in Figure 7.

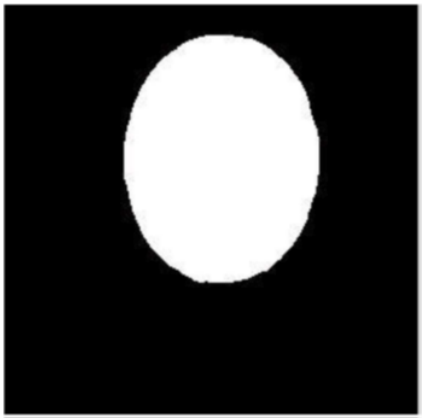

Figure 7 Final output of color detection based algorithm (Thendral et al. 2014)

Thendral et al. (2014) evaluated twenty randomly selected orange fruit images with two different image processing algorithms in their study. They stated that while they achieved 85% success with the color detection-based algorithm, they could not achieve success in fruit identification with the edge-based algorithm.

Wang et al. (2009) compared the SVM (support vector machine) approach with methods based on color and shape determination in the identification of fruits. 640×480 pixel 24-bit RGB color images were used in the study. In the study, the success of three different functions of the SVM approach was evaluated. The highest fruit identification percentage, with a value of 93.3%, was determined for the RBF function where the color and shape identification basis were used together.

Bulanon et al. (2002) compared three different color models for four different lighting conditions in their study for the identification of Fuji apples by robotic harvesting systems. A color CCD camera was used in the study. The image taken from the camera is 320x240 pixels 24-bit RGB color data. As the illumination factor, fruit images were taken under front lighting, back lighting, shading of the fruit and cloudy conditions. In the front lighting condition, the camera was positioned so that the sunlight came from behind the camera, and in the back lighting condition, pictures were taken when the sun came from behind the fruit.

In the RGB color model applied to analyze pixels in images, red (R), green (G), blue (B) pixel intensities are defined between 0-255.

In the second analysis method, the rg-chromaticity method, three chromatic coefficients and color intensity are found with the help of a diagram. These coefficients can be shown simply as follows.

$$r=R/(R+G+B)$$

$$g=G/(R+G+B)$$

$$b=B/(R+G+B)$$ (Bulanon vd., 2002)

In this method, only “r” and “g” coefficients are used.

In the third method, the LRCD model, RGB values are converted into brightness and color signals. By calculating the brightness (Y) value with the help of the equation below, the brightness difference values (CR, CG, Cb) of red, green and blue pixel intensities were obtained.

$Y = 0.299xR + 0.587xG + 0.114xB$

$CR = R - Y$

$CG = G - Y$

$CB = B - Y$ (Bulanon vd., 2002)

The images obtained with this method are given in Figure 8.

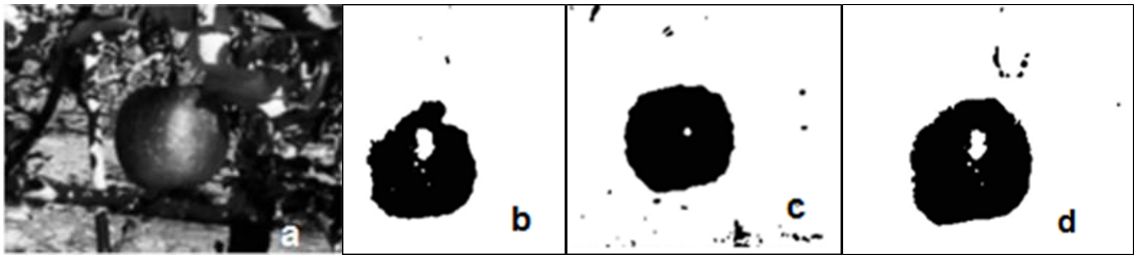

Figure 8 Apple image (a); RGB(b); r-g chromaticity (c) and LRCD (d) images obtained with models (Bulanon et al., 2002)

When the results of the study were evaluated, it was stated that the decision function created with the r-g chromaticity model among the three methods was successful with high identification rate and low signal distortion, especially in the backlight condition. It was stated that the identification success of the three models was at an acceptable level in front lighting, shading and cloudy conditions. It has been stated that RGB and LCRD models are affected by lighting conditions. In the rg-chromaticity model, since the brightness value is separated from the color values, only hue and saturation are focused on. For this reason, it has been stated that it is useful in different illumination conditions for an average decision function.

In the studies, different cameras, sensors and different algorithms were used to identify different fruits. In fruit parcels, there are many different objects such as leaves, branches, support cables, and immature products near the product to be collected. These objects other than ripe fruit make it difficult to recognize the fruit. However, texture and color changes caused by diseases make it difficult to identify the fruit. Some fruits can be found in clusters on the branches. This makes it difficult to recognize the fruit. One of the most important factors that reduce the success of fruit identification systems is the cultivation methods of fruit trees. In studies conducted on this subject, it is recommended to carry out operations such as fruit tree training systems and thinning pruning (Silwal et al., 2017). It would be beneficial to switch to cultivation systems called fruit walls (Saeys and Nguyen, 2012), to create narrow crowns instead of wide crowns, and to prune the fruits so that they are on the outside of the crown.

REFERENCES

Anonim a, 2022. Web adresi: https://ndion.de/en/flying-autonomous-robots-an-autonomous-drone- as-a-harvest-helper/Bachche, S. (2015). Deliberation on design strategies of automatic harvesting systems: A survey. Robotics, 4(2), 194-222.

Bulanon, D. M., Kataoka, T., Ota, Y., Hıroma, T., 2002. A Color Model for Recognition of Apples by a Robotic Harvesting System, Journal Of The Japanese Socıety Of Agrıcultural Machınery, 2002, Volume 64, Issue 5, Pages123-133,

Burks, T., Villegas, F., Hannan, M., Flood, S., Sivaraman, B.,Subramanian, V. And Sikes, J.

2005..Engineering and Horticultural Aspects of Robotic Fruit Harvesting: opportunities and Constraints. HortTechnology January-March 2005 15(1)

Gezer, İ., 2001. The situation of mechanical fruit harvesting in Turkey. 20th National Congress of Agricultural Mechanization, Şanlıurfa, p. 251-256.

Gongal, A., Amatya, S., Karkee, M., Zhang, Q., Lewis, K., 2015. Sensors and systems for fruit detection and localization: A review, Computers and Electronics in Agriculture, Volume 116,

Pages 8-19, ISSN 0168-1699, https://doi.org/10.1016/j.compag.2015.05.021.

Grand D'Esnon, A, Rabatel, G., Pellenc, R., Journeau, A and Aldon, M.J. 1987."MAGALI": a self-propelled robot to pick apples ASAE Paper 87-1037, St. Joseph, MI 49085 Saeys, W., & Nguyen, T. T. (2012). CROPS project deliverable 6.3: Report on the plantation and pruningmethods to have fruit readily suited for automated harvesting. Leuven, Belgium: KU Leuven.

Silwal, A, Davidson, JR, Karkee, M, Mo, C, Zhang, Q, Lewis, K. Design, integration, and field evaluation of a robotic apple harvester. J Field Robotics. 2017; 34: 1140–1159. https://doi.org/10.1002/rob.21715

Thendral, R., A. Suhasini A. and Senthil, N., 2014. "A comparative analysis of edge and color based segmentation for orange fruit recognition," 2014 International Conference on Communication and Signal Processing, 2014, pp. 463-466, doi: 10.1109/ICCSP.2014.6949884.

Ünal, H. 2005. Ceviz Yetiştiriciliğinde Hasat ve Hasat Sonrası Mekanizasyon Uygulamaları. Bahçe Ceviz 34 (1): 193– 203

Wang, J. -j., Zhao, D. -a., Ji, W., Tu, J-j., and Zhang, Y., 2009. "Application of support vector machine to apple recognition using in apple harvesting robot," 2009 International Conference on Information and Automation, 2009, pp. 1110-1115, doi: 10.1109/ICINFA.2009.5205083.

Yang, L., Dickinson, J., Wu, Q. M. J. and Lang, S., 2007. "A fruit recognition method for automatic harvesting," 2007 14th International Conference on Mechatronics and Machine Vision in Practice, 2007, pp. 152-157, doi: 10.1109/MMVIP.2007.4430734.

Molecular Markers for Sex Determination in Dioic Plants and Their Use for Figs

Nurdan MISMIL[1]
Gülsüm Ebru ÖZER UYAR[2]

Introduction

It is difficult to determine the sex in the early period before flowering in dioic plants. Sex determination from the beginning of life, particularly in agricultural product cultivation and manufacturing, is critical for product quality, diversity, and continuity. In dioic plants, male and female organs are not found on the same individual. Therefore, it is very difficult to determine the sex of the dioic species in the early stages of breeding and breeding studies. Studies use both traditional and molecular methods to determine sex. However, considering the concepts of time and cost, molecular marker systems and new biotechnological methods should be alternatives that support and complement traditional programs. The developing biotechnology and genetic approaches receive support from DNA and PCR-based molecular marker systems. The molecular markers are used in many subjects, such as defining any gene region in the genome, labeling, gene mapping, and genetic analysis of complex characters. Dioic plants such as figs can be identified and characterized by molecular approaches in certain sex-linked genes. One of the earliest known cultivated plants, the fig (*Ficus carica*), is a member of the Moraceae family. It is a dioecious plant and an important plant in the world and in our country. It stands out for human health with its mineral, vitamin, antioxidant, and fiber content.

Asexual reproduction in plants occurs when a plant cell or part of it separates from the parent plant. It develops vegetatively and through spores. Sexual reproduction occurs with the union of two sex cells, that is, as a result of fertilization. Flowers are the first sexual reproductive agents, and seeds are the next. If male and female flowers are found on the same plant, such plants are monoecious. The dioecious plant is in a situation where male and female flower organs are on different plant individuals. Dioecy is a rather uncommon occurrence among angiosperms. In recent years, studies on dioecious plants have begun to gain momentum in terms of covering plant species with agricultural and economic value (Grewal & Goyat, 2015). Dioecy can also be advantageous for producers since female plants only produce fruit from their female flowers and do not use energy to produce male flowers. The existence of female plants is particularly significant in dioecious plants whose fruits are consumed. Male plants generally only need to be present in a limited amount of growing space for pollination. The distinction between male and female plants is frequently not determined until flowering during production from seeds, breeding research, and materials of unknown origin. Therefore, it is very important to determine the sex of the plant in the early stages. Separating the genotypes of superior races among species that have been crossed with classical breeding by phenotypic selection is a very laborious and expensive practice. Likewise, it is very difficult to determine sex in dioecious plants in the early period. Differences at the DNA level can be assessed with molecular markers, the desired gene or characteristic may be monitored, sex determination analyses can be performed, and maximum yield can be reached by starting production with the

[1] MSc, Kocaeli University, Institute of Natural and Applied Sciences, Department of Horticultural Sciences
[2] Assist. Prof. Dr., Kocaeli University, Faculty of Agriculture, Department of Plant Protection

least margin of error in the early stages of cultivation. The development of sex-associated molecular markers, which is crucial for agricultural plants with a long-term juvenile stage, may be influenced by the accumulation of repetitive DNA sequences in sex chromosomes. The importance of molecular markers has begun to be understood in recent years and has created a new field for academic studies. Although there is not yet a molecular marker that will meet all needs, analyses can be made by selecting one or more marker systems suitable for the study to be carried out (Semagn et al., 2006). Depending on the cultivation goal, plant cultivators can assign various values to male and female plants in a flower. Because they may yield seeds and fruits, female flowers are valued higher in agricultural production. Kiwi (*Actinidia deliciosa*), papaya (*Carica papaya*), pistachio (*Pistacia vera*), date (*Phoenix dactylifera*), and sea buckthorn (*Hippophae rhamnoides*) are examples of the most preferred species in cultivation, especially due to their female flowers (Grewal & Goyat, 2015).

Sex determination is an important developmental event in the life cycle of all living and reproducing plants, and it is the process that involves the differentiation and separation of structures responsible for the production of male and female gametes in a plant (Chuck, 2010). Dioetyny provides insight into the evolutionary, developmental, and molecular processes that lead to different mechanisms for sex expression. Genetic control of sex determination is mediated by chromosomes and sex-determining genes in dioecious plants (Heikrujam et al., 2015). Molecular markers have been used for early sex identification in dioecious plants to increase economic potential and better understand the causes of sexual dimorphism. Instead of morphological indicators, molecular markers are more advantageous for sex identification in many plant species (Ince et al., 2010).

Dioecious Plants and Sex Determination

Dioecious forms can be found in 65% of plant orders and about 5% of higher plant species (Fak, 2002). All individuals in many sexually reproducing plant species are basically of the same sex. Many species are hermaphrodites. A wide range of sex determination systems, from primitive to highly structured species, have evolved many times (Charlesworth, 2002). Dioecious plants typically have three types of sex systems, or male-heterogametic system, female-heterogametic system, and haploid sex system, which correspond to XX/XY, ZW/ZZ, and U/V sex chromosomes, respectively (Zhang et al, 2022). It is well-recognized that both genetic and epigenetic variables play a role in identifying the sex of a flower or individual (Ainsworth et al., 1997). Sex determination in plants is one of the essential aspects that should be investigated regarding economic values. Early detection of sexual characteristics in commercially important species grown for fruit or seed serves as a reference in selecting how to culture these species. This situation is more important from an economic point of view, especially for plants that stay in the generative phase for many years. However, in dioecious plants, it can be very challenging to identify the sex of the plant before flowering. Biochemical and cytological analyses performed for detection are not always achievable for determining sex (Grewal & Goyat, 2015). In adult plants, sex determination may be more problematic or even impossible (Milewicz & Sawicki, 2013). In determining sex in flowering plants, sex-determining genes, sex chromosomes, DNA methylation with small RNAs, epigenetic control, and physiological regulations with phytohormones are used (Aryal & Ming, 2014). Traditional propagation methods and breeding strategies can be used to determine the sex of plants. However, this can be a time-consuming and costly process that depends on environmental conditions. The use of traditional methods in sex determination studies, which require a lot of time and effort, does not guarantee that every variety developed in this way will be sold on the market as a commercial product. It is vital to employ both conventional techniques and new-generation biotechnology procedures to reduce any potential drawbacks that may arise during the production process. It is suggested that the varieties to be developed thanks to molecular

markers will be able to reach criteria in a shorter time, such as being resistant to diseases and pests, having high adaptability, and having better quality and higher productivity in the selections made (Usage & Breed, 2015). After the first germination, molecular markers can be used in genetic research to identify the genes of the species that are resilient to all types of stress. Moreover, after the early sex determination of these species is made, the yield and quality can be increased quickly with varieties selected to suit the desired conditions.

Molecular Markers

The limitations of phenotype-based genetic markers have led to the development of more general and useful direct DNA-based markers known as molecular markers (Agarwal et al., 2008). DNA fragments, known as molecular markers, can be found in the genome near any gene region. Molecular markers are also known as DNA markers because they constitute the DNA-based type of genetic markers. The emergence of marker systems in the last 30 years has also closely followed developments in the fields of molecular biology and biochemistry. In plants, the utilization of markers to determine genetic links between phenotypes comes before genetics. Many discoveries have been made throughout history to examine the genetic structures of plant traits and today, serious progress has been made with the addition of new markers to these discoveries (Schulman, 2007). Studies used the number and arrangement of germ cells in plants to determine systematic relationships between species (Charlesworth, 2021; Razumova et al., 2022; Li et al., 2022; Zhang et al., 2022).

Molecular Marker Types

Molecular markers used in studies are grouped into two groups: hybridization-based markers and Polymerase Chain Reaction (PCR)-based markers. Hybridization-based markers: RFLP (Restriction Fragment Length Polymorphism), PCR-based markers: SSR (Simple Sequence Repeat or Microsatellites), RAPD (Random Amplified Polymorphic DNA), AFLP (Amplified Fragment Length Polymorphism), and ISSR (Inter Simple Sequence Repeat). Apart from these, some molecular markers are given in Table 1.

Table 1. *Types of molecular markers*

Molecular markers		**Reference**
SRAP	Sequence Related Amplified Polymorphism	(Jones et al., 2009)
SCAR	Sequence Characterized Amplified Regions	(Xu et al., 2004)
STS	Sequence Tagged Site	(Jones et al., 2009)
CAPS	Cleaved Amplified Polymorphic	(Barth et al., 2002)
ALP	Amplicon Length Polymorphism	(Thakur et al., 2019)
SNP	Single Nucleotide Polymorphism	(Al-Samarai et al., 2015)
MP-PCR	Microsatellite Primed Polymerase Chain Reaction	(Sharma et al., 1995)
AP-PCR	Arbitrarily Primed Polymerase Chain Reaction	(Li & Caufield, 1998)
AS-PCR	Allele Specific Polymerase Chain Reaction	(Ugozzoli & Wallace, 1991)
DAF	DNA Amplification Fingerprinting	(Caetano-Anollés et al., 1991)

Today, molecular markers are used in the construction of genetic maps, gene discovery and labeling, evolutionary genetics, genetic diversity, QTL (Quantitative Trait Loci) analyses, protection of newly developed varieties, determination of parents to be used in breeding studies, and purity analysis in seed production (Usage and Breed, 2015). In addition, molecular markers are used in paternity tests, detection of mutant genes associated with hereditary diseases, genotype determination, variety registration of plants, identification of breeding lines, variety purity tests in hybrids, genetic origins of gene resources, determination of performance and adaptation abilities in agricultural studies, marker-assisted breeding of products, population history, and epidemiology. They are also used in many different areas, such as food safety and

population studies (Idrees & Irshad, 2014). Molecular markers, with the help of modern computational capabilities, are most suitable for assessing genetic diversity, which is vital for the survival of species, as they provide rapid, inexpensive, and highly distinguishing features between species or within varieties (Agarwal et al., 2019).

A molecular marker should have the following qualities to be considered ideal: a) It should be polymorphic and used throughout the genome; b) It should be sufficient to reveal genetic differences; c) It should produce a large number of independent and reliable markers; d) It should be simple, fast, and inexpensive; e) It should only require a small amount of DNA or tissue; and f) It should be able to be listed as having a connection with various phenotypes. The preferred molecular marker should display the broadest possible coverage of the trait being analyzed. An effective marker should guarantee reproducibility and be easy to detect. Molecular markers facilitate the analysis of variation between individuals regardless of their developmental stage, which is particularly useful in sex determination.

In dioecious plants, levels of genetic variation between the sexes are different because male and female reproductive organs occur in separate plants (Kumar & Agrawal, 2019). Environmental and genetic factors play a role in determining sex in dioecious plants, and a very small portion of these plants have developed sex chromosomes. Since early sex determination in dioecious plants is a problem in classical fruit breeding studies, the fact that molecular markers are not affected by environmental conditions and are reliable provides an advantage in sex determination (Ağır, 2020). For this reason, molecular markers are used to determine differences between genders in dioecious plants (Sarmah et al., 2017; Heikrujam et al., 2015).

Studies Conducted Using Molecular Markers in Dioecious Plants

Economically significant dioecious plants have molecular marker systems that aid in understanding stress mechanisms and provide a different viewpoint on all issues (Francia et al., 2004). Species whose sex is determined using molecular markers are used in breeding studies. Since the use of molecular markers, obtaining the results of studies such as sex determination, detection of genetic mutations, genetic diversity determinations, breeding studies, resistance to diseases and pests, and increasing product quality in a shorter time and faster has a positive impact on the quality and efficiency of the products studied. The sex-related molecular markers discovered in previous studies were reviewed in detail in two different articles (Heikrujam et al., 2015; Milewicz & Sawicki, 2013). Table 2 summarizes the plant species employed and the molecular markers used after the date that these review articles were published. Numerous dioecious plants have been successfully sex-identified using molecular markers (Xu et al., 2004).

Table 2. *Plant species studied with molecular markers*

Plant species	Molecular marker	Reference
Actinidia arguta		
Actinidia kolomikta	SNP	(Gustafson, 2016)
Ailanthus excelsa Roxb	RAPD, ISSR, SCoT	(Bano et al., 2020)
Asparagus officinalis	RFLP	(Kanno et al., 2014)
Borassus flabellifer L.	RAPD, AFLP, SCoT, ILP, SSR	(Pipatchartlearnwong et al., 2019)
Cannabis sativa L.	RAPD-SCAR	(Punja et al., 2017)
Carica papaya	SCAR	(Chaturvedi et al., 2014)
Coccinia grandis L.	RAPD	(Bhowmick et al., 2014)
	RAPD	(Hossain et al., 2016)
Dovyalis caffra	SRAP	(Hajari et al., 2019)
Eucommia ulmoides Oliver	SNP	(Wang & Zhang, 2017)
Momordica charantia	RAD- seq	(Matsumura et al., 2014)
	RAPD	(Baratakke et al., 2013)
Phoenix dactylifera	RAPD-SCoT	(Adawy et al., 2014)
	RAPD-ISSR	(Dhawan et al., 2013)
Piper betel	SCAR	(Sheeja et al., 2013)
	RAPD	(Kamiab et al., 2014)
Pistacia vera L.	SNP	(Kafkas et al., 2015)
Simarouba glauca	RAPD	(Vaidya & Naik,2014)
Trichosanthes dioica Roxb.	ISSR	(Adhikari et al., 2014)

One hundred decamer primers of randomly amplified polymorphic DNA in dioecious Asparagus (*Asparagus officinalis*) were tested to identify sex-linked molecular markers, and one primer (S368) was found to produce two markers (S368-928 and S368-1178) in female plants. This DNA marker was identified in male and female plants, respectively, and the S368-928 marker was found to be linked to the female sex locus (Gao et al., 2007). ISSR markers were used for the early detection of male and female individuals in jojoba (*Simmondsia chinensis*), and the UBC-807 primer was accepted as the putative sex-linked marker (Sharma et al., 2008). In a study conducted using RAPD and SCAR markers, it was observed that the genotypes of Pistacia species in the used seedling phenophase gave more reliable results in determining sex determination (Esfandiyari et al., 2012). *Encephalartos natalensis* (Cycad) seedlings' sexes were identified using a RAPD marker in the early stages of their development, and it was discovered that this marker could help farmers save time and money by identifying the sex of their plants (Prakash & Van Staden, 2006).

Use of Molecular Markers for Sex Determination in Figs

Fig (*Ficus carica* L.) is a dioecious plant belonging to the Moraceae (Mulberry) family. It is divided into approximately 60 genera and has more than 1400 species. It is the only member of the genus grown for its fruit (Figure 1), *F. carica* (Ferguson et al., 2011). This economically significant plant is grown using conventional breeding and culture techniques. The fig is a resilient fruit that is high in vitamins and minerals and has a high demand for both dried and fresh fruit. Thanks to developing technology and new biotechnological approaches, rapid sex determination at an early stage will increase the fig supply by allowing producers to choose more figs among the species to be grown.

Figure 1. The fruit of F. carica (https://www.britannica.com/plant/fig)

All cultures, from the east to the west, regard it as a sacred tree. It occurs in numerous cultures, as well as in religious, mythical, and folklore tales (Günal, 2008). Fig, with its fruit, leaves, tree, and milk, has represented many symbols such as life, power, productivity, abundance, wisdom, and brightness in all cultures from mythology to today (Koçak, 2011). Figs, which are seen as a fruit from heaven, have also been the subject of sacred books (Saçlı, 2020).

The total cultivated area of fig worldwide is over 290,000 hectares, and its annual production is 1,332,813 tons (FAO, 2019). With a production of 310,000 tons over an area of roughly 52,000 hectares, our country is a global leader (FAO, 2019). As with many other dioecious species, the fruits of the fig plant are economically valuable (Ağır, 2020). Fig is a fruit that contains E, C, A, and B-group vitamins, calcium, potassium, iron, and magnesium minerals. It has a protective effect against some diseases with its fiber content and antioxidant properties. In addition, benzaldehyde and coumarins in its structure are compounds with anti-carcinogenic properties and are used for treatment purposes (Duman & Yazıcı, 2018). Its high nutritional content compared to many other fruits, its rich fiber, mineral, and polyphenol content, its absence of fat and cholesterol, and its being a commercial fruit with different evaluation methods make fig a highly preferred fruit (Duman & Yazıcı, 2018). Its fruit is consumed fresh and dried. In addition to many fig varieties that stand out with their different aspects in our country, the 'Sarılop' variety is preferred especially for dried consumption, while the Bursa Black fig is one of our varieties that is ideal for fresh consumption with its size and hard-shelled structure (Cąkan, 2020). The origin of figs is Anatolia, but they are also widespread in the Arabian Peninsula and the Eastern Mediterranean. It can spread in tropical and subtropical climates and is a plant with high adaptability.

The flowering and fertilization biology of figs is unique. The trees can be separated into female figs and caprifigs (sometimes referred to as male figs). Although pollination occurs by wind, pollination is difficult because the male and female flowers of the fig plant are closed in the flower sheath (Özrenk & Gül, 2019). Fruit that can be eaten grows on female figs. The majority of the fruit's edible portion is formed when the long-styled female flowers (pistils) that grow inside the syconium reach maturity (Stover et al., 2007). The female fig fruit's quality and storability increase after pollination, and although caprifigs are often not edible, they do generate pollen due to the stamens growing inside the syconia (Lama et al., 2020; Marcotuli et al., 2020). Fig-wasp (*Blastophaga psenes* L.) larvae may also be found in the short-styled female flowers (galls) in the syconia of caprifigs (Gu & Yang, 2013; Zhang et al., 2020; Wang et al., 2021).

According to Storey (1975), two genes on the same chromosome determine sex: G stands for the female flower with a long stigma tube (dominant allele), while g stands for the female flower with a short stigma tube (recessive allele), A is the dominant allele for male flower production, and a is the recessive allele that suppresses male flower production. Genotypes of female figs are ga/ga, while male figs can be either GA/ga or rarely GA/GA. It is noted that all male fig genotypes have at least one dominant G or A allele (Storey, 1975).

Determinations regarding the genetic control of sex in figs are based on breeding studies in *F. carica*, and this species is a rather exceptional species with a long breeding history and growing in temperate climates (Parrish et al., 2004). This process is quite costly, especially since fruit breeding programs take a long time. In fig trees, the sex of the trees cannot be determined by morphological markers until they bear fruit. For this reason, it is easier and faster to determine sex in the early period after germination in breeding studies with the help of molecular markers, saving time and effort (Fang et al., 2007). Recent research suggests that more than one gene or transcription factor is involved in determining the sex of plants. Consequently, it makes sense to suggest that genes involved in determining plant sex may include numerous sex-identification markers (Leite Montalvão et al., 2021). The sex of plants is clearly seen in floral organs. The C-type functional AGAMOUS (AG) of the MADS-box family participates in the development and differentiation of carpels, stamens, and floral meristems in the ABCDE model of plant floral organ production (Dreni & Kater, 2014). In plants, MADS-box genes have a role in the regulation of all key developmental processes, including the production of male and female gametophytes, embryos and seeds, as well as roots, flowers, and fruits.

It has been reported that molecular markers such as RFLP, RAPD, ISSR, and SSR have been used successfully for the characterization of fig varieties, and it is known that molecular markers give positive results in improving factors such as disease resistance, yield, quality, and abiotic stress tolerance (Aljane et al., 2018). In a study using the SNP (single nucleotide polymorphism) marker for fig, the first draft genome sequence of the fig was created and analyzed. Initial mapping based on genome-wide SNPs was done, followed by DNA sequencing (RAD-sequence) analysis. As a result, a key candidate gene was identified, as well as the Responsive-To-Antagonist1 (*RAN1*) area (Mori et al., 2017). The Turkish fig germplasm collection and the F1 population derived from the hybrid between the female genotype "Bursa Black" and the male genotype "Ak Ilek" were used to validate an ortholog of the *RAN1* loci known to be linked with sex determination in fig (Ikten & Yilmaz, 2019). In another study, AG and *RAN1* genes were investigated for their potential role in differentiating between male and female fig trees. While their exact biological functions in sex determination had not been confirmed, the study identified one AG gene in female fig trees, specifically expressed in the pistil, and three AG genes in male fig trees. These male genes were expressed in different parts, with one in the gall, and the other two in both the gall and stamen. The study successfully established a highly efficient AG-Marker-based method for fig sex identification and improved the previously reported RAN1-Marker method. These findings introduce new markers and insights into the sex determination system of *F. carica* (Wang et al., 2021).

In a sex determination study using SCAR, RAPD, and SRAP markers in figs, Ağır (2020) screened five registered male and five female dioecious fig genotypes, and while he was able to obtain monomorphic bands with RAPD and SRAP primers, he could not obtain polymorphic bands for male and female genotypes. Clones were created with 23 male figs (*F. carica caprificus*) varieties, and using the RAPD method, a total of 195 bands were obtained using 10-base sequence primers, and 51 of them showed polymorphism and 144 showed monomorphism. Similarity rates of the clones created were determined (Mestav & Dalkılıç, 2007). Polymorphism was detected with the AFLP marker in the *F. fulva* variety, and a total of 89 polymorphic fragments were produced from three primer combinations. Then, base sequences

characterizing male individuals were marked using SCAR, and equal-sized pieces were produced for male and female individuals, which showed that the sequence difference between male and female-specific chromosomal regions was low (Parrish et al., 2004). PCR-based marker systems (SRAP, MS-SRAP, ISSR) were used to analyze the genetic relationships between male and female fig populations (İkten et al, 2023). These markers revealed genetic differences and partial separation between male and female populations, though no clear-cut genetic structure differences were found. The study employed association mapping in natural fig populations to identify gene-specific markers, with the potential to develop markers for fruit quality-related horticultural traits. The study involved 47 male and 49 female fig genotypes from various geographic regions, using the mentioned marker systems for PCR amplification and suggested the need for a sex-specific marker in fig breeding programs. Another study focuses on differentiating between male and female compartments of *F. carica* L. in Tunisia using "Conserved DNA-derived polymorphism (CDDP)". This marks the first exploration of the *F. carica* L. genome with a gene target marker, uncovering genetic diversity associated with plant gene functional domains. CDDP proves to be an effective tool for investigating genetic diversity and distinguishing between groups. The results from CDDPs suggest classifications based on sex and type, aligning with the geographic origin. The study recommends using CDDP-based QTL mapping in future research to identify traits related to flowers, sex, or resistance in *F. carica* species. This can provide molecular mapping information for marker-assisted selection programs aimed at improving multiple desirable traits. Additionally, the study highlights the value of wild *F. carica* populations as a biological resource that can be harnessed for scientific and breeding purposes. Establishing a comprehensive molecular database with markers specific to the species is crucial for defining a core collection that represents local diversity and identifies potential gene reservoirs for resistance to both biotic and abiotic stress (Haffar et al., 2022). Studies on sex determination using molecular markers are given in Table 3.

Table 3. *Studies on gender analysis using molecular markers in fig (F. carica)*

Feature	**Markers Used**	**References**
Analysis of genetic differences of 21 female figs	RAPD	(Khadari et al., 1995)
Analysis of genetic differences in 55 female fig plants	RAPD, İzoenzim	(Elisiário et al., 1998)
Determination of morphological and phenological differences in six female fig plants	RAPD	(Galderisi et al., 1999)
Genotype analysis in *'Sarılop'* and *'Sarı zeybek'* species	RAPD, İzoenzim, AFLP	(Cabrita et al., 2001)
F.carica and 17 different *F. spp.* identification of types	SSR	(Khadari et al., 2001)
Genotype analysis of 63 female and three male fig species	RAPD	(Papadopoulou et al., 2002)
Genotype analysis of eight male and 64 female fig species	ISSR, SSR	(Khadari et al., 2003)
Similarity analysis between *F. carica 'Bianco del Cilento'* and *'Dottato'* varieties	RAPD	(De Masi et al., 2003)
Male-specific trait analysis in *F. fulva*	AFLP	(Parrish et al., 2004)
Similarity analysis between genotypes in 23 male figs	RAPD	(Mestav, 2005)
Genotype similarity analysis in 20 different local figs	RAPD	(Sadder, 2006)
Detection of male/female phylogenetic analysis among 192 genotypes	RAPD, SSR, ISSR, SRAP	(İkten, 2007)
Analysis of 43 different seed genotypes	RAPD	(Dalkılıç et al., 2011)
Sex determination analysis in *F. carica, 'Horaishi'* cultivar	CAPS, SNP	(Mori et al., 2017)
Gender determination analysis of five female and five male fig varieties	RAPD, SRAP, SCAR	(Ağır, 2020)

Conclusion

Molecular markers are new-generation markers used to easily identify sex in plants at any stage of growth and development. In addition to classical breeding studies, using molecular markers in genetic determinations will help make studies faster, easier, and less economically costly. Although the applicability of markers to every plant is limited, more reliable and faster methods may begin to be developed for early sex determination in dioecious plants. Utilizing molecular markers using biotechnological approaches in the development of existing species and the detection and development of new species will also guide future studies. The fig plant should not be thought of as just its fruit. In addition to increasing the genetic diversity of figs, more fig varieties need to be evaluated in the ornamental plant industry, and when carrying out such studies, being able to characterize existing varieties morphologically and genetically using genetic characterization analyses based on molecular markers may be the best alternative. Closely following genetic technological approaches will increase the speed and quality of similar studies.

References

Adawy, S.S., Jiang, J. Atia, M.A.M. (2014) Identification of Novel Sex-specific PCR-Based Markers to Distinguish the Genders in Egyptian Date Palm Trees, International Journal of AgriculturalScience and Research (IJASR) 4, (5), 45-54.

Adhikari, S., Saha, S., Bandyopadhyay, T.K. & Ghosh, P. (2014). Identification and Validation of a New Male Sex-Specific ISSR Marker in Pointed Gourd *(Trichosanthes dioica Roxb.)*. The Scientific World Journal. 2014:216896.

Agarwal, M., Shrivastava, N. & Padh, H. (2008). Advances in Molecular Marker Techniques and Their Applications in Plant Sciences. Plant Cell Reports, 27(4): 617–631.

Ağır, A. (2020). İncirde *(Ficus carica L.)* RAPD, SRAP ve SCAR Belirteçleri ile Cinsiyetin belirlenmesi, Adnan Menderes Üniversitesi Fen Bilimleri Enstitüsü, MSc Thesis.

Ainsworth, C. P. & Buchanan-Wollaston, J.V. (1997). 5 Sex Determination in Plants. Current Topics in Developmental Biology, 38: 167–180.

Aljane, F., Essid, A. & Nahdi, S. 2018. Improvement of fig (*Ficus carica* L.) by conventional breeding and biotechnology. In "Advances in Plant Breeding Strategies: Fruits". J. Al-Khayri, S. Jain and D. Johnson (Ed), p. 343. Springer International Publishing AG, Cham.

Al-Samarai, F.R. & Al-Kazaz, A.A. (2015). Molecular Markers: An Introduction and Applications. European Journal of Molecular Biotechnology, 9(3): 118–130.

Aryal, R. & Ming, R. (2014). Sex Determination in Flowering Plants: Papaya as a Model System. Plant Science, 217–218, 56–62.

Bano, S., Ansari, S., Choudhary, M. & Tomar, U.K. (2020). Gender-Based Genetic Variability of *Ailanthus excelsa Roxb*, Populations Using, RAPD, ISSR and SCoT Markers. Current Journal of Applied Science and Technology, 39(45): 75-83.

Baratakke, R.C., Patil, C.G., Poornima, B. & Sankannavar, S.H. (2013). Molecular Tool for Sex Identification (female) in *Momordica dioica Roxb.* with Reference to Medicinal Values. International Journal of Research in Ayurveda and Pharmacy (IJRAP), 4(4): 487-490.

Barth, S., Melchinger, A.E. & Lübberstedt, T.H. (2002). Genetic Diversity in Arabidopsis thaliana L. Heynh. Investigated by Cleaved Amplified Polymorphic Sequence (CAPS) and Inter-Simple Sequence Repeat (ISSR) Markers. Molecular Ecology, 11(3): 495–505.

Bhowmick, B.K., Nanda, S., Nayak, S., Jha, S. & Joshi, R.K. (2014). An APETALA3 MADS-Box Linked SCAR Marker Associated with Male Specific Sex Expression in *Coccinia grandis (L).* Voigt. *Scientia Horticulturae*, *176*: 85-90.

Cabrita, LF., Aksoy, U., Hepaksoy, S. & Leitão, J.M. (2001). Suitability of Isozyme, RAPD and AFLP Markers to Assess Genetic Differences and Relatedness Among Fig *(Ficus carica L.)* clones. Scientia horticulturae, 87(4): 261-273.

Caetano-Anollés, G., Bassam, B.J. & Gresshoff, P.M. (1991). DNA Amplification Fingerprinting: A Strategy for Genome Analysis. Plant Molecular Biology Reporter, 9(4): 294–307.

Cąkan, V.A. (2020). Forecasts for Turkey Fresh Fig Production and Dried Fig Export: Arima Model Approach. Journal of Tekirdag Agricultural Faculty, 17(3): 357–368.

Charlesworth, D. (2002). Plant Sex Determination and Sex Chromosomes. Heredity, 88(2): 94–101.

Charlesworth, D. (2021). When and how do sex-linked regions become sex chromosomes?. Evolution 75-3: 569–581

Chaturvedi, K., Bommisetty, P., Pattanaik, A., Chinnaiyan, V., Ramachandra, D.M. & Chennareddy, A., 2014. PCR Detection Assay for Sex Determination in Papaya Using SCAR Marker. Acta Botanica Croatica, 73(2): 291-298.

Chuck, G. (2010). Molecular Mechanisms of Sex Determination in Monoecious and Dioecious Plants. Advances in Botanical Research (54).

Dalkılıç, Z., Mestav, H.O., Günver-Dalkılıç, G. & Kocataş, H. (2011). Genetic Diversity of Male Fig (*Ficus carica caprificus* L.) Genotypes With Random Amplified Polymorphic DNA (RAPD) Markers. African Journal of Biotechnology, 10(4): 519-526.

De Masi, L., Vella, F.M., Laratta, B., Volpe, M.G., Tiseo, M. & La Cara, F. (2015). Biochemical and Genetic Characterization of a Red Fig Cultivar *(Ficus carica)* from Southern Italy. In V International Symposium on Fig 1173 pp. 81-86.

Dhawan, C., Kharb, P., Sharma, R., Uppal, S. & Aggarwal, R.K. (2013). Development of Male-Specific SCAR Marker in Date Palm *(Phoenix dactylifera L.)*. Tree Genetics & Genomes, 9(5): 1143-1150.

Dreni, L., & Kater, M. M. (2014). MADS reloaded: evolution of the AGAMOUS subfamily genes. New Phytol. 201, 717–732. doi: 10.1111/nph.12555

Duman, E. & Yazıcı, A. (2018). Yaş İncir (Mor Güz - Sarı Lop) Çekirdek ve Çekirdek Yağlarının Fiziko-Kimyasal Özellikleri.Anadolu Ege Tarımsal Araştırma Enstitüsü Dergisi, *24*(2): 69–76.

Elisiário, P.J., Neto, M.C., Cabrita, L.F. & Leitão, J.M. (1998). Isozyme and RAPDs Characterisation of a Collection of Fig *(Ficus carica L.)* Traditional Varieties. Acta Horticulturae, 480: 149-154.

Esfandiyari, B., Davarynejad, G.H., Shahriari, F,. Kiani, M. & Mathe, A. (2012). Data to the Sex Determination in Pistacia Species Using Molecular Markers. Euphytica, 185(2): 227–231.

Fak, Z. (2002). Çiçekli Bitkilerde Tozlanma Ve Çiçektozu Taşıyıcıları. Ege Üniversitesi Ziraat Fakültesi Dergisi, 39(2): 151–158.

Fang, J., Chen, J., Henny, R.J. & Chao, C.C.T. (2007). Genetic Relatedness of Ornamental Ficus Species and Cultivars Analyzed by Amplified Fragment Length Polymorphism Markers. *J*ournal of the American Society for Horticultural Science, 132(6): 807–815.

Ferguson, L., Michailides, T.J. & Shorey, H.H. (2011). The California Fig Industry. Horticultural Reviews, 12: 409–490.

Francia, E., Rizza, F., Cattivelli, L., Stanca, A.M., Galiba, G., Tóth, B. & Pecchioni, N. (2004). Two Loci on Chromosome 5H Determine Low-Temperature Tolerance in a "Nure" (winter) x Tremois' (spring) Barley Map. Theoretical and Applied Genetics, 108(4): 670–680.

Galderisi, U., Cipollaro, M., Di Bernardo, G., De Masi, L., Galano, G. & Cascino, A. (1999). Identification of the Edible FigBianco del Cilento'by Random Amplified Polymorphic DNA Analysis. HortScience, 34(7): 1263-1265.

Gao, J.S., Sun, X.W. & Liang, L.Q. (2007). Conversion of RAPD Markers Linked to Cold Tolerance to SCAR Markers in Common carp. J Dalian Fish Univ, 22(3): 194-197.

Grewal, A. & Goyat, S. (2015). Marker Assisted Sex Differentiation in Dioecious Plants. Journal of Pharmacy Research, 9(8): 531–549.

Gu, D. & Yang, D. R. (2013). Utilisation of chemical signals by inquiline wasps in entering their host figs. J. Insect Physiol. 59, 1065–1068. doi: 10.1016/j.jinsphys.2013.08.005

Gustafson, H. (2016). Marker Assisted Selection of Sex Determination in *Kiwiberry (Actinidia arguta and Actinidia kolomikta)*. Doctoral dissertation, University of New Hampshire (Printed).

Günal, N. (2008). Türk Dünyasında İncir Kültürü.Electronic Turkish Studies, 3:5.

Haffar, S., Baraket, G., Usai, G., Aounallah, A., Mustapha, S.B., Abdelkrim, A.B. & Hannachi, H.S. (2022) Conserved DNA-derived polymorphism as a useful molecular marker to explore genetic diversity and relationships of wild and cultivated Tunisian figs (*Ficus carica* L.) Trees, 36:723–735 https://doi.org/10.1007/s00468-021-02244-2

Hajari, E., Hannweg, K., Nonyane, D., Shezi, Z., de Jager, K. & du Preez, R. (2019). Sex Determination in Kei-apple *(Dovyalis caffra)* Using Molecular Markers and Flow Cytometry. South African Journal of Botany, (127): 278-283.

Heikrujam, M., Sharma, K., Prasad, M. & Agrawal, V. (2015). Review on Different Mechanisms of Sex Determination and Sex-Linked Molecular Markers in Dioecious Crops: A Current Update. Euphytica, 201(2): 161–194.

Hossain, M.U., Islam, M., Afroz, M., Sultana, S.S. & Alam, S.S. (2016). Karyotype and RAPD Analysis of Male and Female *Coccinia grandis L*. from Bangladesh. Cytologia, 81(3): 349-355.

Idrees, M. & Irshad, M. (2014). Molecular Markers in Plants for Analysis of Genetic Diversity: A Review. European Academic Research, 2(1): 1513–1540.

İkten, H. (2007) İncir genotiplerinin karakterizasyonu ile cinsiyet ve bazı meyve özellikleri için ilişkilendirme haritalaması yöntemi ile moleküler işaretleyicilerin belirlenmesi, Ege University, PhD Thesis.

Ikten, H. & Yilmaz, Y. (2019). Validation of Gender Specific CAPS Marker in Turkish Fig *(Ficus carica L.)* Collection and F1 Progenies. Notulae Botanicae Horti Agrobotanici Cluj-Napoca, 47(3): 867–871.

İkten, H., Gülşen, O., Mutlu, N., Polat, İ. & Aksoy, U. (2023) Genetic Diversity, Population Structure, and Association Analysis of Female and Male Fig Genotypes (*Ficus carica* L.) Erwerbs-Obstbau, 65:1603–1616

Ince, A.G., Karaca, M. & Onus, A.N. (2010). A Reliable Gender Diagnostic PCR Assay for Jojoba *(Simmondsia chinensis (Link)* Schneider.Genetic Resources and Crop Evolution,57(5):773-779.

Jones, N., Ougham, H., Thomas, H. & Pasakinskien, I. (2009). Markers and Mapping Revisited: Finding Your Gene. New Phytologist, 183(4): 935–966.

Kafkas, S., Khodaeiaminjan, M., Güney, M. & Kafkas, E. (2015). Identification of Sex-linked SNP Markers Using RAD Sequencing Suggests ZW/ZZ Sex Determination in *Pistacia vera L.* BMC genomics, 16(1): 1-11.

Kamiab, F., Ebadi, A., Panahi, B. & Tajabadi, A. (2014). RAPD Analysis for Sex Determination in Pistacia vera L. Journal of Nuts, 5(01): 51-55.

Kanno, A., Kubota, S. & Ishino, K. (2014). Conversion of a Male-Specific RAPD Marker into an STS Marker in *Asparagus officinalis L.* Euphytica, 197(1): 39-46.

Khadari, B., Hochu, I., Santoni, S., Kjellberg, F. (2001) Identification and characterization of microsatellite loci in the common fig (*Ficus carica* L.) and representative species of the genus Ficus. Mol Ecol Notes. https://doi.org/10.1046/j.1471-8278.2001.00072.x

Khadari, B., Lashermes, P. & Kjellberg, F. (1995). RAPD Fingerprints for Identification and Genetic Characterization of Fig *(Ficus carica L.)* Genotypes. Journal of Genetics and Breeding, 49: 77-77.

Khadari, B., Hochu, I., Santoni, S., Oukabli, A., Ater, M., Roger, J.P. & Kjellberg, F. (2003). Which Molecular Markers are Best Suited to Identify Fig Cultivars: A Comparison of RAPD, ISSR and Microsatellite Markers. Acta Horticulturae, 605: 69-75.

Koçak, A. (2011). "Bilgelik" Varlık Bereket Sembolü İncirin Serüveni. Bilge Seyidoğlu Kitap, Dergah Yayınları, s. 1–14. İstanbul.

Kumar, J. & Agrawal, V. (2019). Assessment of Genetic Diversity, Population Structure and Sex Identification in Dioecious Crop, *Trichosanthes dioica* Employing ISSR, SCoT and SRAP Markers. Heliyon, 5(3): e01346.

Lama, K., Peer, R., Shlizerman, L., Meir, S., Doron-Faigenboim, A., Sadka, A., Aharoni, A. & Flaishman, M.A. (2020). Tissue-specific organic acid metabolism in reproductive and nonreproductive parts of the fig fruit is partially induced by pollination. Physiol. Planta 168, 133–147. doi: 10.1111/ppl.12941

Leite Montalvão, A. P., Kersten, B., Fladung, M., & Müller, N. A. (2021). The diversity and dynamics of sex determination in dioecious plants. Front. Plant Sci. 11:580488. doi: 10.3389/fpls.2020.58048

Li, Y. & Caufield, P.W. (1998). Arbitrarily Primed Polymerase Chain Reaction Fingerprinting for the Genotypic Identification of Mutans Streptococci From Humans. Oral Microbiology and Immunology, 13(1): 17–22.

Li, N., Wang, Y., Wang, J., Zhang, W., Meng, Z., Wang, Y., Zhang, Y., Li, S., Gao, W. & Deng, C. Identification of Sex Differentiation-Related microRNAs in Spinach Female and Male Flower. Int. J. Mol. Sci. 2022, 23, 4090. https://doi.org/10.3390/ijms23084090

Marcotuli, I., Mazzeo, A., Colasuonno, P., Terzano, R., Nigro, D., Porfido, C., Tarantino, A., Aiese Cigliano, R., Sanseverino, W., Gadaleta, A. & Ferrara, G. (2020). Fruit development in *Ficus carica* L.: morphological and genetic approaches to fig buds for an evolution from monoecy toward dioecy. Front. Plant Sci. 11:1208. doi: 10.3389/fpls.2020.01208

Matsumura, H., Miyagi, N., Taniai, N., Fukushima, M., Tarora, K., Shudo, A. & Urasaki, N. (2014). Mapping of the Gynoecy in Bitter gourd *(Momordica charantia)* Using RAD-seq Analysis. PloS one, 9(1): e87138.

Mestav, H.O. (2005) Identification of some male fig cultivars with RAPD markers, Çanakkale Onsekiz Mart University, MSc Thesis.

Mestav, H.O. & Dalkılıç, Z. (2007). Bazı Erkek İncir Çeşitlerinin RAPD Belirteçleri İle Tanımlanması. Adnan Menderes Üniversitesi Ziraat Fakültesi Dergisi, 4(1/2): 49–58.

Milewicz, M. & Sawicki, J. (2013). Sex-linked Markers in Dioecious Plants. Plant OMICS, 6(2): 144–149.

Mori, K., Shirasawa, K., Nogata, H., Hirata, C., Tashiro, K., Habu, T., Kim, S., Himeno, S., Kuhara, S. & Ikegami, H. (2017). Identification of RAN1 Orthologue Associated with Sex

Determination Through Whole Genome Sequencing Analysis in Fig *(Ficus carica L.).* Nature Scientific Reports, 7(1): 1-15.

Özrenk, K. & Gül, Y. (2019). İncir *(Ficus carica L.)* Genetik Kaynaklarının Belirlenmesine Yönelik Bir Çalışma: Türkiye, Siirt Yöresi. Türkiye Tarımsal Araştırmalar Dergisi, 6(3): 328–335.

Papadopoulou, K., Ehaliotis, C., Tourna, M., Kastanis, P., Karydis, I. & Zervakis, G. (2002). Genetic Relatedness Among Dioecious *Ficus carica* L. Cultivars by Random Amplified Polymorphic DNA Analysis, and Evaluation of Agronomic and Morphological Characters. Genetica, 114(2): 183-194.

Parrish, T.L., Koelewijn, H.P. & Van Dijk P.J. (2004). Identification of a Male-Specific AFLP Marker in a Functionally Dioecious Fig, *Ficus fulva Reinw. ex Bl.* (Moraceae). Sexual Plant Reproduction, 17(1): 17–22.

Pipatchartlearnwong, K., Juntawong, P., Wonnapinij, P., Apisitwanich, S. & Vuttipongchaikij, S. (2019). Towards Sex Identification of Asian Palmyra palm *(Borassus flabellifer L.)* by DNA Fingerprinting, Suppression Subtractive Hybridization and *de novo* Transcriptome Sequencing. PeerJ, 7: e7268.

Prakash, S. & Van Staden, J. (2006). Sex identification in Encephalartos natalensis (Dyer and Verdoorn) Using RAPD Markers. Euphytica, 152(2): 197–200.

Punja, Z.K., Rodriguez, G. & Chen, S. (2017). Assessing Genetic Diversity in *Cannabis sativa* Using Molecular Approaches. In: Chandra, S., Lata, H., ElSohly, M. (eds) *Cannabis sativa* L. - Botany and Biotechnology. Springer, Cham. https://doi.org/10.1007/978-3-319-54564-6_19

Razumova, O.V., Alexandrov, O.S., Bone, K.D., Karlov, G.I. & Divashuk, M.G. (2023) Sex Chromosomes and Sex Determination in Dioecious Agricultural Plants. Agronomy, 13, 540. https://doi.org/10.3390/agronomy13020540

Saçlı, M. (2020). İncir ve Zeytin: Tin Suresi Bağlamında Kur'an'ın Teşrifine Mazhar olmuş iki nimet. Mecmua, (10): 216-239.

Sarmah, P., Barua, V.J., Nath, J., Sarma, R.N., Kurian, B., Hemanthkumar, A.S. & Sabu, K.K. (2017). ISSR and SSR Markers Reveal Sex-specific DNA Sequences in three Calamus Species from India. Agroforestry Systems, 91(3): 509–513.

Schulman, A.H. (2007). Molecular Markers to Assess Genetic Diversity. Euphytica, 158(3): 313–321.

Semagn, K., Bjørnstad, A. & Ndjiondjop, M.N. (2006). An Overview of Molecular Marker Methods for Plants. African Journal of Biotechnology, 5(25): 2540–2568.

Sharma, P.C., Hüttel, B., Winter, P., Kahl, G., Gardner, R.C. & Weising, K. (1995). The Potential of Microsatellites for Hybridization- and Polymerase Chain Reaction-Based DNA Fingerprinting of Chickpea (*Cicer arietinum* L.) and Related Species. Electrophoresis, 16(1): 1755–1761.

Sheeja, T.E., Bindu, K.H., Anto, P., Dhanya, K., Siju, S. & Kumar, T.V. (2013). A SCAR Marker Based Method for Sex Determination in Dioecious Betel vine *(Piper betle).* Ind J Agri Sci, 83: 1409-1410.

Storey, W. B. (1975) Figs in Advances in Fruit Breeding (eds. Janick, J. & Moore, J. N.) 568–589 (Purdue University Press.

Stover, E., Aradhya, M., Ferguson, L. & Crisosto, C. H. (2007). The fig: ov erviewof an ancient fruit. HortScience 42, 1083–1087. doi: 10.21273/HORTSCI.42.5.1083

Thakur, V.V., Tiwari, S., Tripathi, N. & Tiwari, G. (2019). Molecular Identification of Medicinal Plants With Amplicon Length Polymorphism Using Universal DNA Barcodes of the atpF–atpH, trnL and trnH–psbA Regions. 3 Biotech, 9(5): 1–10.

Ugozzoli, L. & Wallace, R.B. (1991). Allele-specific Polymerase Chain Reaction. Methods, 2(1): 42–48.

Usage, T. & Breed, M.M. (2015). Moleküler Markörlerin Bitki Islahında Kullanımı.Bahri Dağdaş Bitkisel Araştırma Dergisi, 4(2): 1–12.

Vaidya, G. & Naik, G.R. (2014). Molecular Identification of Sex in Simarouba glauca by RAPD Markers for Crop Improvement Strategies. Biotechnology Reports, 4: 56-59.

Wang, W. & Zhang, X. (2017). Identification of the Sex-Biased Gene Expression and Putative Sex-Associated Genes in Eucommia ulmoides Oliver Using Comparative Transcriptome Analyses. Molecules, 22(12): 2255.

Wang, Y., Jia, H. M., Shen, Y. T., Zhao, H. B., Yang, Q. S. & Zhu, C. Q. (2020). Construction of an anchoring SSR marker genetic linkage map and detection of a sex-linked region in two dioecious populations of red bayberry. Hortic. Res. 7:53. doi: 10.1038/s41438-020-0276-6

Wang, R., Yang, Y., Jing, Y., Segar, S. T., Zhang, Y., Wang, G., Chen, J., Liu, Q.F., Chen, S., Chen, Y., Cruaud, A., Ding, Y.Y., Dunn, D.W., Gao, Q., Gilmartin, P.M., Jiang, K., Kjellberg, F., Li, H.Q., Li, Y.Y., Liu, J.Q., Liu, M., Machado, C.A., Ming, R., Rasplus, J.Y., Tong, X., Wen, P., Yang, H.M., Yang, J.J., Yin, Y., Zhang, X.T., Zhang, Y.Y., Yu, H., Yue, Z., Compton, S.G. & Chen, X.Y. (2021). Molecular mechanisms of mutualistic and antagonistic interactions in a plant-pollinator association. Nat. Ecol. Evol. 5, 974–986. doi: 10.1038/s41559-021-01469-1

Xu, W.J., Wang, BW. & Cui, K.M. (2004). RAPD and SCAR Markers Linked to Sex Determination in Eucommia ulmoides Oliv. Euphytica, 136(3): 233–238.

Zhang, X., Wang, G., Zhang, S., Chen, S., Wang, Y., Wen, P., Ma, X., Shi, Y., Qi, R., Yang, Y., Liao, Z., Lin, J., Lin, J., Xu, X., Chen, X., Xu, X., Deng, F., Zhao, L., Lee, Y.L., Wang, R., Chen, X.Y., Lin, Y.R., Zhang, J., Tang, H., Chen, J. & Ming, R. (2020). Genomes of the banyan tree and pollinator wasp provide insights into fig-wasp coevolution. Cell 183, 875.E–889.E. doi: 10.1016/j.cell.2020.09.043

Zhang, X., Pan, L., Guo, W., Li, Y. & Wang, W. (2022) A convergent mechanism of sex determination in dioecious plants: Distinct sex-determining genes display converged regulation on floral B-class genes. Frontiers in Plant Science, 13: 953445. doi: 10.3389/fpls.2022.953445

An Approach Based on Ecological Planning Ecological Risk (Sensitivity) Assessment: The Example of Fethiye-Göcek Special Environmental Protection Area

Zeynep R. ARDAHANLIOĞLU[1]
Yahya BULUT[2]

INTRUDUCTION

Decisions regarding future land use form the basis of planning studies. It is very important that the planning process is carried out correctly to ensure the sustainable use of protected areas for the future. Ecological planning approaches should be taken into account when planning land use in protected areas. With ecological planning, it is aimed to create a spatial plan for society by ensuring the sustainability of the living systems of living organisms and improving their conditions (Meier 2003). The basis of ecological planning is to ensure sustainable land use and appropriate use of natural resources (Forman 1995). Land use planning, defined as a part of ecological planning, determines the most appropriate land use in the future (Collins et al. 2001). Planning for this purpose takes into account the economic, social, cultural and ecological aspects of land use (Mc Donald and Brown 1995; Leitao and Ahern 2002). Ecological planning is also a method of examining optimal biophysical and sociocultural land use systems that are specifically applicable to a particular region. In the last 40-50 years, many studies have been conducted on planning methods for ecological approaches (Yin et al. 2006; Rossi et al., 2008; Yihua et al. 2009; Cao and Liu, 2010; Zhang et al, 2010; Özhancı, 2014; Düzgüneş and Demirel, 2016; Kurdoğlu et al., 2018). However, in general, the evaluation criteria are based on McHarg's method (Ayaşlıgil 2011). While ecological planning meets people's needs, it also protects the ecological balance, which is sensitive with limited natural resources (Özügül 2006). In recent years, research examining the processes occurring within the landscape and planning decisions based on them, rather than mathematical modeling of natural and cultural landscape elements, has become more important. In this context, as a condition for the development of world landscape ecology, landscape planning reveals the structure, function and changes of landscapes and reveals natural and cultural data such as landscape, water and erosion (Uzun et al. 2010). The ecological approach is now a generally accepted approach in making land use decisions. The basis of the ecological approach in planning is the developments and changes that emerged in the 1960s, bringing to the fore the concepts of "environmental concern" until the 1980s, and "quality of life" and "sustainability" after 1980 (Şahin 2003).

With this study, in which the ecological risk (sensitivity) assessment of the Fethiye-Göcek Special Environmental Protection Area was made within the scope of ecological planning, the importance of ecological planning was emphasized and it was stated that all plans made without taking ecological factors into consideration would be insufficient to ensure the sustainability of land uses.

[1] Dr.Öğr.Üyesi Zeynep R. ARDAHANLIOĞLU, Muğla Sıtkı Koçman Üniversitesi, Fethiye A.S.M.K Meslek Yüksekokulu, Peyzaj ve Süs Bitkileri Yetiştiriciliği Programı, 48300, Muğla (Fethiye), Türkiye.
[2] Prof. Dr. Yahya BULUT, Atatürk Üniversitesi, Mimarlık ve Tasarım Fakültesi, Peyzaj Mimarlığı Bölümü, Erzurum, Türkiye.

MATERIAL and METHOD

Material

The research area is Fethiye-Göcek Special Environmental Protection Area. Fethiye, a district of Muğla province, has been a settlement since the earliest known times. Covering an area of 3055 km2, 816.02 km2 of the district borders were declared as a Special Environmental Protection Area in 1988 in terms of the natural resource values of the district. Its coastal length is 235 km, its sea area is 345 km², and its terrestrial area is 471 km². Many areas within the borders of the region are protected with different protection statuses. The region's coastline has enabled the formation of beautiful bays. The plain base of the Region, which is surrounded by high mountains, consists of fertile agricultural lands.

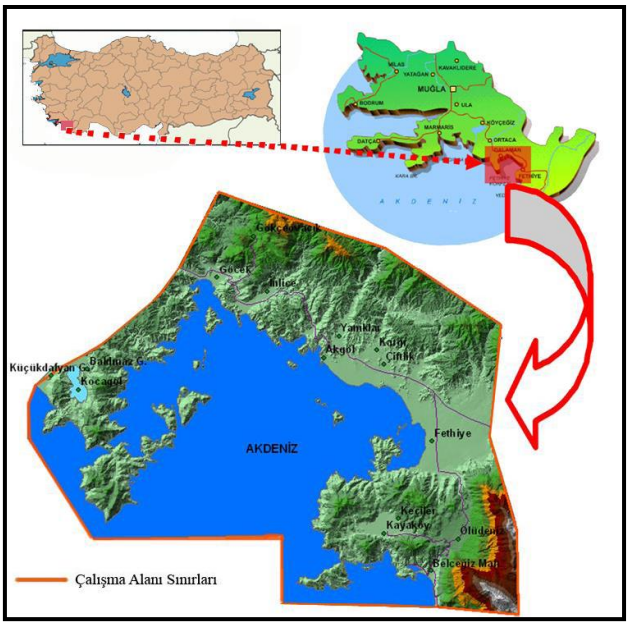

Figure 1. Research area (Ardahanlıoğlu, 2014)

Method

In the method developed for the ecological sensivity assessment of the Fethiye-Göcek Special Environmental Protection Area, different methods used for similar purposes in domestic and international studies were interpreted to suit the research area [Mc Harg (1992), Lyle (1985), Huali et al., (2005). Yıldız (2006), Alkan (2006), Yin et al., (2006), Zengin (2007), Özyurt (2009), Cengiz (2011), Aksu (2012)]. Geographic Information Systems were used for the applicability of the method. As a method;

- In the first stage, data collection and literature review were carried out. The factors that will participate in the ecological sensivity assessment were determined and the necessary base maps were obtained. Factors involved in ecological sensivity assessment; topography, soil, current land use status and hydrology. In addition, sub-factors of each factor were also included in the sensivity assessment. The factors and sub-factors involved in ecological sensivity assessment are listed in Table 1.

Table 1. Factors and sub-factors involved in ecological sensivity assessment

Factors	Sub-Factors
Topography	Elevation
	Slope
	Aspect
Soil	Land Use Ability Class
	Major Soil Groups
	Soil depth
	Erosion
Current Land Use	Forest
	Maquis
	Agriculture
	Residential areas
	Bare surfaces
Hydrology	Sea
	Lake
	Stream

- For the purpose of ecological sensivity assessment, an expert group consisting of different professional disciplines has been established on the subject. Expert group; It consists of 4 landscape architects, 1 agricultural engineer, 1 soil expert, 1 biologist and 1 geological engineer. After the expert group was formed, the scores to be given to the factors that would participate in the ecological sensivity assessment were determined using the multi-criteria decision-making technique. Considering that each factor to be included in the ecological sensivity assessment will not be of equal importance, the impact and contribution levels have been determined for each factor. Effect levels were evaluated in three groups: 3=very effective, 2=effective, 1=less effective. Risk levels were scored in four groups: 3=high, 2=medium, 1=low, 0=ineffective. When calculating risk scores, impact levels were multiplied by risk levels.

- For ecological sensivity assessment, all base maps were first converted to raster format and the research area was Arcgis 9.3. In the program, it is divided into 10x10m grid squares. The result obtained by multiplying the impact and risk values of each factor determines the result that each grid square will receive. After collecting the scores of the grid squares, separate risk maps were created for each factor. Sub-factor maps were used as a base when creating risk maps. The maps used for topography risk map are elevation, slope and aspect maps. These maps are Arcgis 9.3. The topographic risk map was obtained by overlapping the program. For the soil risk map, sub-factor maps of the soil factor were used as a base. These maps; They are large soil groups map, Erosion map, Land use ability class map and Soil depth maps. These maps are Arcgis 9.3. Soil risk map was obtained by superimposing in the program.

- The difference between the minimum value and the maximum value obtained from the total risk scores of these maps created separately for each factor was found and divided by three, the resulting value was added to the minimum value and the risk level was grouped as low, medium and high.

In topography sensitivity assessment, the degree of impact of the topography factor and the risk degrees of the sub-factors used are shown in Table 2, and the degree of impact of the current land use situation and the risk degrees of the sub-factors used are shown in Table 3. The impact level of the topography factor was determined as 2, and the impact level of the current land use situation was determined as 3.

Table 2. Impact and risk levels of the topography factor

	Evaluation Factors and Subunits (Impact Degree = 2)	Risk Degree
Topography	**Elevation**	3
	0-200 m	2
	200-400 m	2
	400-600 m	1
	600-800 m	1
	00 m +	
	Slope	3
	%0-2	3
	%2-6	2
	%6-12	2
	%12-20	2
	%20-30	1
	%30 +	
	Aspect	
	South	3
	North	1
	NW, SW, NE, SE,	2

Table 3. Impact and risk levels of the current land use situation factor

	Evaluation Factors and Subunits (Impact Degree = 2)	Risk Degree
Current Land Use	Forest	3
	Maquis	2
	Agriculture	3
	Residential areas	0
	Bare surfaces	1

In soil sensitivity assessment, the degree of influence of the soil factor and the risk degrees of the sub-factors used are shown in Table 4. The effect level of the soil factor was determined as 3.

Table 4. Effect and risk levels of soil factor

	Evaluation Factors and Subunits (Impact Degree = 2)	Risk Degree
Soil	**Land Use Ability Class**	
	I.Class	3
	II. Class	3
	III. Class	3
	IV. Class	2
	V. Class	2
	VI. Class	2
	VII. Class	1
	VIII. Class	1
	Major Soil Groups	
	Alluvial soil	3
	Colluvial soil	3
	Alluvial coast	2
	Hydromorphic alluvial soil	2
	Rural forest	2
	Limeless brown forest	2
	Limeless brown soil	2
	Red Mediterranean	2
	Traditional Mediterranean	2

	High mountain-meadow	1
	Bare rock	1
	Soil depth	
	Shallow (20-50cm)	1
	Very shallow (0-20 cm)	2
	Erosion	
	Light	1
	Middle	2
	Severe	2
	Very severe	3

The degree of impact of the hydrology factor and the risk degrees of the sub-factors used are shown in Table 5. The impact level of the hydrology factor was determined as 3.

Table 5. Impact and risk levels of hydrology factor

Hydrology	**Evaluation Factors and Subunits (Impact Degree = 2)**	**Risk Degree**
	Sea	
	0-100 m	3
	>100 m	2
	Lake	
	0-100 m	3
	>100 m	2
	Stream	
	0-100 m	3
	>100 m	2

- In the last stage of the study, the current land use status and ecological sensitivity assessment map of Fethiye-Göcek Special Environmental Protection Area was compared. Area use changes were evaluated within the scope of ecological planning and various solutions were proposed to ensure sustainable use in the Region.

RESEARCH FINDINGS

As a result of the evaluation made by the ecological sensitivity assessment expert group for the Fethiye-Göcek Special Environmental Protection Area, firstly the sensitivity assessment of each factor was made separately, and then the risk maps of all the factors obtained were superimposed in the Arcgis 9.3 program and a total risk map was created. The sensitivity assessment of each sub-factor according to the results obtained is stated below.

Topography sensivity situation

From an ecological point of view, its ecological value depending on the topographic structure features has a guiding effect in planning. The main effective factors in the effect of topography on planning are; elevation, relief, slope and aspect (Tozar 2006). Plans made by taking the topography factor into consideration will ensure that future land uses are shaped more accurately (Kasapoğlu 2012). While Fethiye-Göcek Special Environmental Protection Area has risky areas in terms of topography, slope, aspect and elevation were included in the evaluation as sub-factors. The impact level of the topography factor was determined as 2 by taking the common opinions of the experts. Arcgis 9.3. The topography risk map was obtained by overlapping the slope, aspect and elevation maps converted to raster format in the program. In determining the topography sensivity status, the areas with the highest risk degree in terms of elevation are areas with a height between 0-200 m, the areas with the highest risk degree in terms of slope are areas with a slope between 0-6%, and the areas with the highest risk degree in terms of aspect are areas facing south. As a result of the evaluation, the topographically risky

areas of Fethiye-Göcek Special Environmental Protection Area and the areas they cover are shown in Table 6.

Table 6. Topography sensivity status and areas covered

Risk Degree	Area (ha)	Ratio (%)
Low	7875	16,72
Middle	26 471	56,20
High	12 754	27,08
Total	47 100	100,00

According to Table 6, 7875 ha (16.72%) of the Fethiye-Göcek Special Environmental Protection Area has a low risk in terms of topography, 26472 ha (56.20%) has a medium risk, and 12754 ha (27.08%) has a moderate risk. has a high degree of risk. When we look at the topographically risky areas in the Fethiye-Göcek Special Environmental Protection Area, the plain floors of Fethiye-Göcek-Ölüdeniz and Kayaköy settlements have a high risk level in terms of topography. In these areas, the risk levels are high in terms of topography because the altitude is 0-200 m, the slope is between 0-6% and they are generally south-facing areas (Figure 2).

Soil sensivity situation

In the ecological sensitivity assessment, the impact level of the soil factor was determined as 3. The sub-factors selected to determine the soil risk status were determined as land use ability class, large soil groups, soil depth and erosion.

According to the ecological sensitivity assessment made for the Fethiye-Göcek Special Environmental Protection Area, the areas covered by the risk levels of the soil factor are shown in Table 7. According to Table 7, in terms of soil factor of Fethiye-Göcek Special Environmental Protection Area, 9966 ha (21.16%) is at high risk, 31192 ha (66.23%) is at medium risk, 5942 ha (12%) is at moderate risk. .61) has a low degree of risk. When we look at the risky areas in terms of soil in the Fethiye-Göcek Special Environmental Protection Area, it is seen that the areas used as residential areas today, especially in all three settlement units, have a high level of risk in terms of soil (Figure 3).

Table 7. Soil risk status and areas covered

Risk Degree	Area (ha)	Ratio (%)
Low	5942	12,61
Middle	31 192	66,23
High	9966	21,16
Total	47 100	100,00

Risk (sensivity) situation in terms of area use

Another factor included in the ecological risk assessment in the Fethiye-Göcek Special Environmental Protection Area is the land use situation. Since the ecological structure is deteriorated in areas used as residential areas today, the ecological risk in these areas is given as "0". Other land uses that are included in the risk assessment in case of land use are forest, maquis, agriculture, settlement and land uses containing bare surfaces. The current land use situation has been included in the ecological sensitivity assessment to guide future planning. Today, the ecological risk value of areas used as forest and agricultural areas has been determined to be at the highest level, the risk level of maquis areas to be at a medium level, and the risk level of areas with bare surfaces to be low. As a result of the evaluation in which risky areas in terms of land use were determined, the map of risky areas of Fethiye-Göcek Special

Environmental Protection Zone in terms of land use is shown in Figure 4. Areas with forest areas and agricultural areas have a high level of risk.

Hydrology sensivity situation

In the assessment of the hydrological risk status of the Fethiye-Göcek Special Environmental Protection Area, Arcgis 9.3 for distances of 100 m to the rivers, lakes and sea shores within the borders of the region. In the program, a buffer zone was created and points were evaluated by experts to indicate a high ecological risk level for these areas. In areas other than 100 meters from water sources, the degree of risk in terms of hydrology is low. The hydrological status map of Fethiye-Göcek Special Environmental Protection Area is shown in Figure 5.

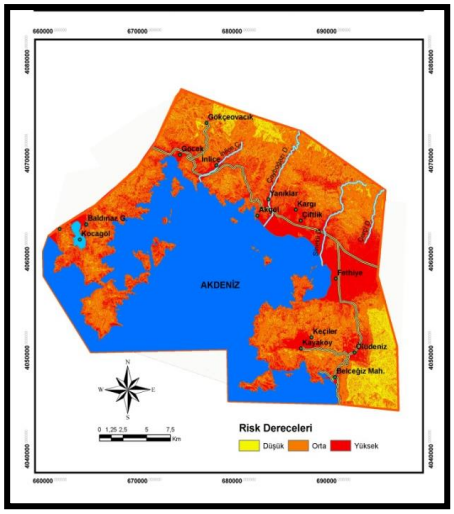

Figure 2. Fethiye-Göcek Special Environment
Protection Zone topography risk map (Ardahanlıoğlu, 2014)

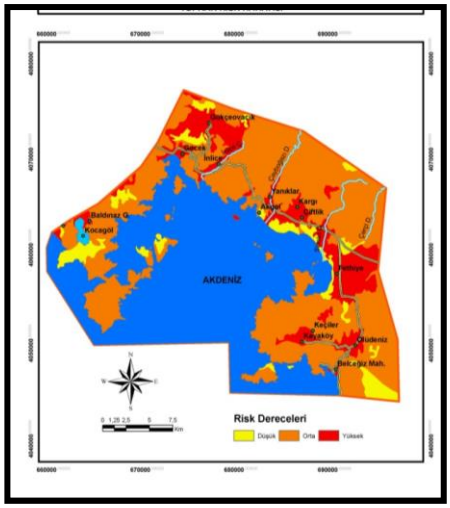

Figure 3. Fethiye-Göcek Special Environmental Protection Area soil risk map (Ardahanlıoğlu, 2014)

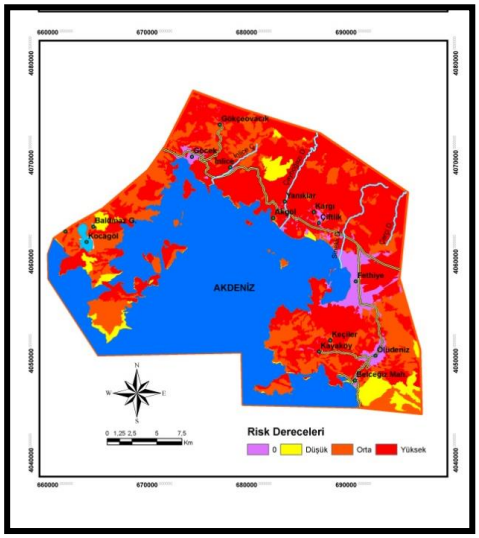

Figure 4. In terms of current space usage
risk map (Ardahanlıoğlu, 2014)

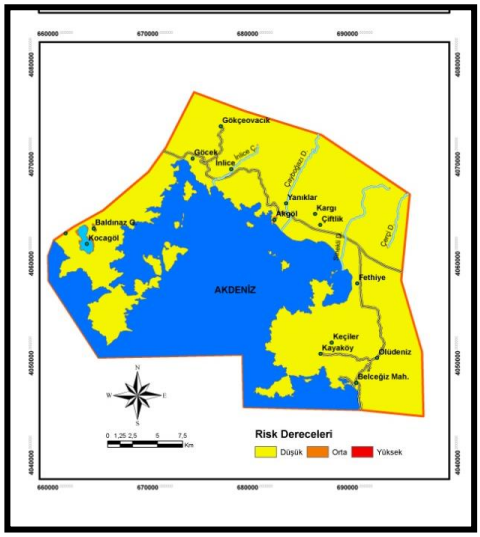

Figure 5. Hydrology risk map (Ardahanlıoğlu, 2014)

Ecological risk (sensitivity) Result Map

A map of areas with high ecological value was obtained by superimposing the soil, topography, hydrology and current land use factors included in the ecological risk assessment (Figure 6). According to the ecological risk assessment made for the Fethiye-Göcek Special Environmental Protection Area, the areas covered by the risk levels are shown in Table 8, and the map of the areas with high ecological value is shown in Figure 6. According to the results obtained, 17510 ha (37.18%) of the Fethiye-Göcek Special Environmental Protection Area is at high risk, 22315 ha (47.38%) is at medium risk, and 7275 ha (15.45%) is at medium risk. i has a low degree of risk.

Table 8. Total risk status and areas covered

Risk Degree	Area (ha)	Ratio (%)
Low	7275	15,45
Middle	22 315	47,37
High	17 510	37,18
Total	47 100	100

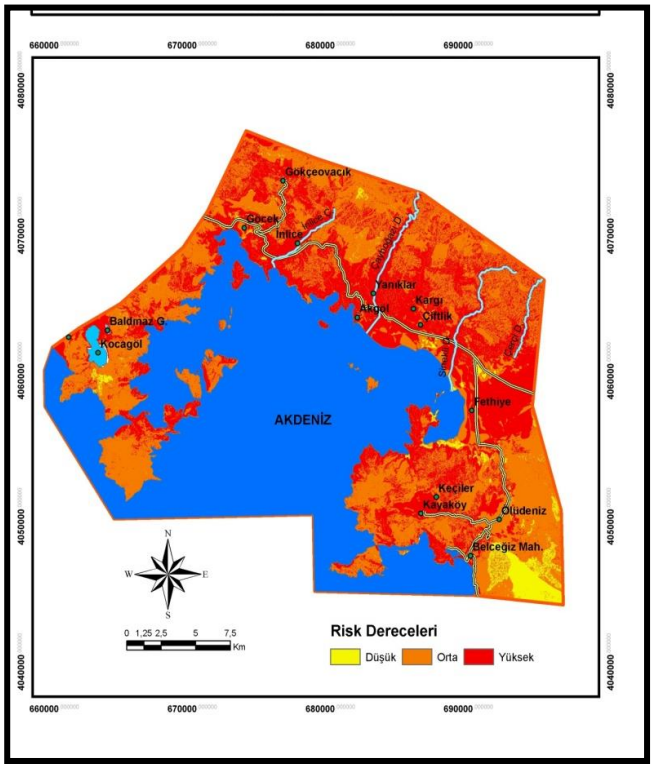

Figure 6. Total ecological sensitivity map of Fethiye-Göcek Special Environmental Protection Area (Ardahanlıoğlu, 2014)

CONCLUSION

Fethiye-Göcek Special Environmental Protection Area, located on the coast of the Mediterranean Region, has been under the pressure of tourism and urbanization, especially in the last decade. According to the results obtained in this study, which was conducted to determine areas with high ecological sensitivity within the scope of ecological planning in the Fethiye-Göcek Special Environmental Protection Area; 7275 ha (15.45%) of the region has a low risk level, 22315 ha (47.38%) has a medium risk level, and 17510 ha (37.18%) has a high risk level. When we look at the topographically sensitive areas in the Fethiye-Göcek Special Environmental Protection Area; It has been determined that the plain floors of Fethiye-Göcek-

Ölüdeniz and Kayaköy settlements have high sensitivity in terms of topography. In these residential areas, the sensitivity levels were high in terms of topography in areas where the altitude was 0-200 m, the slope was between 0-6%, and the aspect was south facing. When we look at the risky areas in terms of soil in the Fethiye-Göcek Special Environmental Protection Area; It has been revealed that there is a high level of sensitivity in terms of soil in these areas, especially since there are Class I and II agricultural soils in the regions used as settlement areas today and these soils are generally composed of alluvial and colluvial soils. Today, the ecological risk value of areas used as forest and agricultural areas is found to be at the highest level, the risk level of maquis areas is found to be at a medium level, and the risk level of areas with bare surfaces is found to be low. In areas other than 100 meters from the hydrological water resources of the Fethiye-Göcek Special Environmental Protection Area, the degree of hydrological sensitivity is low.

According to the results of ecological risk assessment; It is seen that the areas with high risk in the Fethiye-Göcek Special Environmental Protection Area are generally areas where there are fertile agricultural lands and the topographic slope is close to flat. These areas are the areas around Fethiye Plain, Kayaköy and Yanıklar village, where the urban settlement is located today. In addition, the plain floor in Göcek and the plain floor of Belcekız District, located within the borders of Ölüdeniz Nature Park, are mostly high-risk areas. Fethiye, Göcek, Belcekız District and Kayaköy, which feature a plain base in the region, consist of fertile agricultural lands. While there should be no construction activities in areas with high ecological risk, the ecological cycle in these areas has changed with the construction of these areas in the historical process. Kayaköy settlement has not been subject to much change yet. The ecological risk is moderate in the area where Hisarönü and Ovacık neighborhoods are located within the borders of Ölüdeniz town. Areas with low ecological risk levels are generally areas with bare surfaces.

As a result, in line with the findings obtained, it has been determined that the protection status of the Region should be re-evaluated within the scope of ecological planning, especially in areas where the natural texture is damaged, and in areas where the natural texture is not damaged and has a high ecological risk value, it should be protected with an absolute protection zone. Taking ecological planning into account in the plans to be made in the Fethiye-Göcek Special Environmental Protection Area will help to ensure sustainable use in the region. The protection of areas with high ecological value should be prioritized. Healthy shaping of future land uses depends on the effective implementation of ecological planning.

Acknowledgements: This study was produced from the doctoral thesis titled "Evaluation of Land Use Changes in the Fethiye-Göcek Special Environmental Protection Area within the Scope of Ecological Planning".

REFERENCES

Aksu, G. (2012). Peyzaj değişimlerinin analizi: İstanbul, Sarıyer örneği. Doktora tezi, Fen Bilimleri Enstitüsü, Peyzaj Mimarlığı Anabilim Dalı, İstanbul.

Alkan, Y. (2006). Erdemli kenti mücavir alanı içinde ekolojik kapsamlı alan kullanımı üzerine bir araştırma. Yüksek Lisans Tezi, Fen Bilimleri Enstitüsü, Adana.

Ardahanlıoğlu, Z.R. (2014). Fethiye-Göcek özel çevre koruma bölgesindeki alan kullanım değişimlerinin ekolojik planlama kapsamında değerlendirilmesi. Atatürk Üniversitesi, Fen Bilimleri Enstitüsü, Doktora Tezi.

Ayaşlıgil, T. (2011). Sarıyer örneğinde ekolojik mekan ayrımı. *İstanbul Ticaret Üniversitesi Fen Bilimleri Dergisi,* Sayı: 20, 55-79.

Cengiz Özel, E. (2011). Ekolojik açıdan kentsel alan kullanımları: Çanakkale kent merkezi örneği. Doktora Tezi, Fen Bilimleri Enstitüsü, Biyoloji Anabilim Dalı, Çanakkale.

Collins, M.G., Steiner, F.R., & Rushman, M.J. (2001). Land-use suitability analysis in the united states: Historical development and promising technological achievements. *Environmental Management* 28 (5), 611–621.

Dai, X., Li, Z., Lin, S., & Xu, W. (2012). Assessment and zoning of eco-environmental sensitivity for a typical developing province in China. *Stoch Environ Res Risk Assess*, 26, 1095–1107.

Düzgüneş, E., & Demirel, Ö. (2016). Milli parkların koruma yapısının ekolojik duyarlılık analizi ile ortaya konması: Altındere vadisi milli parkı (Trabzon/Türkiye) örneği. *Kastamonu University Journal of Forestry Faculty*, 16(1).

Forman, T.R. (1995). *The ecology of landscapes and regions*. Cambridge University Pres.

Huali, C., Wang, Y., Ding, G., & Jlang H. (2005). Ecological sensitivity analysis on landscape ecological planning in tourist resorts a case of nanhuashan national forest park, Hunan province.

Kurdoğlu, B. Ç., Yeniçırak, P. Ö., & Bayramoğlu, E. (2018). Ekolojik duyarlılık analizi: Kaçkar dağları milli parkı örneği. *Journal of ınternational social research*, 11(61).

Leitao, A., & Ahern, J. (2002). Applying landscape ecological metrics in sustainable landscape planning. *Landscape and Urban planning*, Vol 59, pp 65-93.

Lyle, T.J. (1985). Design for ecosystems. *Van Nostrand Reinhold*, 115 Fifth Avenue, New York, 100003, pp:265.

McDonald, G., & Brown, L. (1995). Going beyond environmental impact assessment: Environmental input to planning and design, *Environmental Impact Assessment Review* Vol 15, Issue 6, 483-495.

Mc Harg, I. L. (1969). *Design with nature*. Natural History Book Pres. New York, USA

Meier, R. L. (2003). *Ecological planning, management and design*. University of California, College of Environmental Design, Berkeley.

Mingwu, Z., Haijiang, J., Desuo, C., & Chunbo, J. 2010. The comparative study on the ecological sensitivity analysis in Huixian Wetland, China. *Procedia Environmental Science*, 2, 386-398.

Özhancı, E. (2014). Kırsal alanlarda ekolojik temelli görsel peyzaj karakter analizi; Bayburt örneği. Fen Bilimleri Enstitüsü, Peyzaj Mimarlığı Anabilim Dalı, Doktora Tezi. Erzurum.

Özügül, M. (2006). Ekolojik planlamada kullanılabilecek analitik bir model önerisi; Ömerli içme suyu havzası örneği. Yıldız Teknik Üniversitesi, Mimarlık Fakültesi E-dergisi. 1(4). 201-217.

Özyurt, S.,S. (2009). Kentsel gelişme planlarının doğal yapı üzerindeki etkisinin adana kenti imar planı örneğinde irdelenmesi. Yüksek Lisans Tezi, Fen Bilimleri Enstitüsü, Peyzaj Mimarlığı Anabilim Dalı, Adana.

Rossi, P., Pecci, A., Amadio, V., Rossi, O., & Soliani, L. (2008). Coupling indicators of ecological value and ecological sensitivity with indicators of demographic pressure in the demarcation of new areas to be protected: The case of the Oltrepo Pavese and the Ligurian-Emilian Apennine Area (Italy). *Landscape Urban Planning*, 85, 1, 12–26.

Şahin, Ş. (2013). Ekolojik planlama. Uluslararası Türk Dünyası Çevre Sorunları Sempozyumu Bildiriler Kitabı, Eskişehir.

Yin Hai-Wei, Xu J., Chen, C., & Kong, F., H. (2006). Gis-based ecological sensitivity analysis in the east of wujiang city. *Scıentıa Geographıca Sınıca*, (1) 64-69, ISSN: 1000-0690 CN: 22-1124/P.

Yıldız, N. (2006). tortum çayı havzasının uygun alan kullanımlarının cbs ile belirlenmesi. Doktora tezi, Fen Bilimleri Enstitüsü, Peyzaj Mimarlığı Anabilim Dalı, Erzurum.

Uzun, O., Karadağ, A., & Gültekin, P. (2010). Coğrafi bilgi sistemlerinin ve uzaktan algılama'nın peyzaj planlamada kullanımı. III. Uzaktan Algılama ve Coğrafi Bilgi Sistemleri Sempozyumu.

Zengin, M. (2007). Ardahan kura nehri ve yakın çevresi alan kullanımlarının belirlenmesi ve optimal alan kullanım önerileri. Doktora Tezi, Fen Bilimleri Enstitüsü, Peyzaj Mimarlığı Anabilim Dalı, Erzurum.

Zhang, M., Jin, H., Caı, D., & Jiang, C. (2010). The comparative study on the ecological sensitivity analysis in Huixian karst wetland, China. *Procedia Environmental Sciences* 2, 386–398.

Decision Systems for Urban Underground Space Excavations

Mehmet Kemal GOKAY[1]

Introduction

Natural and man-made spaces are the main concern in urbanisation. Increase in population, and climatic features (hot & cold temperature cases) force engineers to rethink opportunities of underground spaces in urban developments. When the spaces in the rock masses are considered with their individual volume, micro and macro scale spaces should be evaluated. Exploration of groundwater, oil, and natural gasses facilitate micro scale spaces in rock masses. These micro spaces also provide favourable underground options for discarded gasses in the carbon-zero economies. Rock porosities have currently researched for safe CO^2 depositions. Macro-scale underground spaces are caves, mine openings, tunnels, historic underground shelters & cities, and urban underground spaces (UUSs). Recent urban underground space (UUS), developments in crowded cities have gradually pushed the government authorities to introduce new understanding in urban master plans. UUSs' stability & safety considerations have parameters which are different from the other underground openings like in mining operations. When they would like to be evaluated systematically for their predefined failure risk potentials, decision environments and related parameters should also be considered in detail. In this paper, complexity of the decision parameters required to have stable and safe UUS are aimed to be presented together with offering decision clustering.

Underground space developments

Requirements of UUS have been related to human settlement necessities. Protection parameters provided through underground and surface spaces have changed through the time starting from early human history. In fact, underground spaces are also used by animals/insects and some of them have the habit of using caves/cavities. There are also animals/insects which dig their protected subterranean living spaces with their bare teeth and legs. Complexity and ordered underground nests of ants for example have enough enthusiasm for humans about their underground space usages. Caves were early used underground spaces which have still supplied protection for harmful outside influences like; sun radiations, wild animals, climatic features (rain, snow, hot/cold temperatures, etc.), enemies, etc. For different requirements of humans, earth crust provides enough opportunities through its underground energy, material, mineral, micro&macro spaces, etc. resources. Volchko, etal., (2020) wrote these opportunities in summary. In civilisation history, surface urban structures have been built through main load bearing materials like; stones, woods, wood&stone combinations, bricks, concrete, steel, brick&concrete combinations, steel&concrete combinations, steel&brick&concrete combinations, etc. Each load bearing material mentioned here has its conditions of usage (limitations) in applications; i.e; wooden materials have their weakness in case of fires for example. When the human settlements have getting crowded, localities in cities have discriminated as district of; businesses, offices, industrial facilities, residential houses&apartments, entertainments, etc. Number of houses and apartments have gradually increased at certain localities of urban areas which cause also the raise in the land costs to build

[1] Prof. Dr., Konya Technical University, Mining Engineering Department, Konya-Turkey.

surface structures. Eventually, high rise apartments in the centre of the cities have progressively been constructed as the demands for them have improved. Adding a basement level for required small depot spaces for householders was an early usage of urban underground spaces until the 2000s in Turkey. In later years, basements of residential apartments started to be used as either for car parks or additional flat layers in Turkey. Basement levels at the apartments have also gradually been increasing as the land cost of housing has risen in certain localities of cities. Currently, there are shopping centres in different cities which have several basement levels for car parks under their surface facilities. With a new trend, some commercial buildings (residential & commercial complexes) have begun to be designed in such a way that their surface structures are generally for residential purposes. They additionally have several basement levels which could be designed for shopping centres, carparks, etc. One of the similar constructions is located in Istanbul (Turkey) and it has 3 basement floors for a shopping mall and 3 additional basement floors for car parks for example. Besides historical underground settlements all around the world, usages of apartment basement levels which are directly connected to surface constructions have been starting points for realising the opportunities of modern underground facilities. UUSs excavated specially for sheltering or depository purposes are widespread in the world. As the UUS usage increased, "underground engineering" concept was also introduced due to the requirements of engineering decisions (including engineering duties and responsibilities) for regulated urban settlements. Researching in the scientific fields related to rock formations & mechanical rock behaviours are the areas of concerns in underground engineering. Providing engineering judgements (decisions) with professional responsibilities is also covered by this engineering branch.

Governing bodies in the world have supplied Legislative Acts and Rules for different aspects including safety precautions related to UUSs. These Acts generally define the concept of decisions, decision-makers, rights, duties and responsibilities. Defined ranges of responsibilities are usually beyond the actual predefined (formulated) decision reasoning environments which require additionally careful evaluation of experts' knowledge and experiences. For instance; decisions related to mechanical behaviours of the rock masses which would be host rocks of the planned UUSs are usually determined conferring to laboratory&field tests. Predefined test procedures are supplied by international standards in these activities. However, it is also known that there are accepted uncertainties related to these test results due to the inhomogeneity characteristics observed in rock masses. Mining engineers and rock engineers are well aware of these concepts, and they handle "decisions" related to earth crust (soils, mainly rock masses) with more comprehensive manners. Relevant decisions of the UUSs should then be evaluated in multidisciplinary decision procedures. At this point, supplying logical approaches through decision-tree based judgements (decision-support system) for selective concepts of underground engineering might be helpful in UUS development stages. Engineered preferences lead the phases of project-connected decisions. Therefore, preferred selections in engineering decisions should be taken according to predefined knowledge bases, (Gokay, 1994). Actually, UUS related decision parameters could be clustered and then they can be analysed on the basis of laboratory&field test data and professionals' experiences to comprehend limits of decision environments. UUSs construction steps could essentially be studied by dividing them into two main categories; i) UUS utilisation cases through already available underground spaces, and ii) UUS development&utilisation cases with excavating new underground spaces. Decision parameters in these two categories have some differentiations due to the characteristics of the underground spaces and rock masses surrounding themselves.

Conditions related to UUS

Underground spaces have many dynamic design variables which should be engineered appropriately. These design parameters must be considered with their internal interactions to provide reasoning steps in UUS planning stages. The decision-systems involved in UUS development&utilisation can be evaluated under; a) USS related decision issues: *[designs, excavations, supports, ventilation, construction, stability, flooding, fire dangers, gas explosions, etc.],* b) Decision issues expected to be arose due to USS influences: *[social and natural environments, ownerships rights&responsibilities, businesses, stability of surrounding structures in/on earth surface, etc.],* c) Other decision factors: *[auxiliary works involved at the UUS realisation stages (before-during-after the projects; Governing procedural features for firms related with UUS operations; Monitoring, maintenance, rescue, and quality of service checking options and their implementation; etc.]*. Actually, the stages of UUS developments&utilisations are also key factors in these active decision-systems which should be emphasized to be followed. UUS developments could be handled in 3 main stages, these are; "Before-Excavation", "Excavation", and "After-Excavation" stages. When the intact state (primary stress&strain distribution state) of underground rock masses are disturbed and UUS excavation is started, induced stress&strain distributions (secondary stages of stress&strain distributions) are formed around them. These changes in the rock masses cannot be eliminated (withdrawn) anymore. Backfilling of the excavated underground spaces could not disregard induced secondary level stress&strain distributions. In reality, backfilling of the opened underground spaces pushes the induced stress&strain distribution cases into a new position which is called tertiary stage. This means that once the underground excavation is done, there is no way for the stress&strain distribution state to return back to their initial (primary) state. Therefore, opening a "space" in the rock masses is a major (important) step to be considered carefully and implemented in "engineered" manners. Stability of the surface structures and underground spaces has first priority in underground engineering operations. Total cost of underground space is directly influenced by its excavation related operations and its stability concerns. Mechanical properties of earth crust which are alternating through its soil&rock mass types, *(even the same rock mass can produce different mechanical properties due to its weakness zones and discontinuities)* influence the stabilities of engineered structures in/on earth crust. In reality, natural caves and archaeological remnants of the ancient underground spaces have provided enough indications of their stability conditions. Stable ancient UUSs (which are still safe enough after years of extended usage) have their design parameters which should also be evaluated for modern UUS excavations. Engineers working on UUS projects supply decisions regarding the locations, depths, dimensions and orientations of these spaces. They also command excavations and related activities in the UUS developments. Their on-site operational decisions should also be taken according to UUS plans which are products of multi-professional team-work. Decision-support systems would be helpful here to raise the confidences level of engineers who have to supply decisions under complex input-data which contain uncertainties as well.

Mining engineering history has covered many design and operational experiences related to underground mining activities in different rock masses (together with their success/failure circumstances). Collapses of mine openings (galleries, stopes, raises, shafts, etc.) and related rescue operations in underground mining operations have comprehended valuable experiences. Design features of mine openings, operational conditions in mines, rock masses' related input data, and performed engineered analyses before and after these failures are all vital assets for the future considerations of underground spaces. For instance, the stability of stopes and rooms in underground mining operations handling "open-stope mining method" and "room&pillar mining method" have similarities with UUS stability conditions, (except the dimensions and

shapes of stopes and rooms). Due to these resemblances, stability analyses performed for "open-stope" and "room&pillar" mining methods are valuable. Stability and risk of failure evaluations for mine galleries, rooms and stopes provide research areas of interest for UUS cases as well. At this point, the study performed by Qi, etal., (2018) could be forwarded as an example, this work was about a random-forest artificial intelligent algorithm. They wrote that this algorithm "*can model the nonlinear relationship between inputs and output without no statistical assumptions was found useful in predicting hangingwall stability*" for open stope mining operations. Stability conditions of UUSs, and induced stress&strain distributions features in surrounding rocks of UUSs have forced the engineers reconsider all underground spaces and surface constructions in the urban areas through urban master planning concepts (Tann, etal., 2020). Thus, design and operational UUS parameters influencing the engineering decisions have to be collected as detail as possible. However, there are too many parameters to be considered, but mining engineers working at underground mines have been working in similar decision environments for years. They have classified decision contents into interrelated and interactive decision-groups concentrating on various issues of underground mining activities. Similar classification could also be offered for UUS excavations. Decision-groups for UUS operations could then be organised according to UUS related aspects like; excavations, operation control, space stability&safety, social&environmental impacts, and economic circumstances. Due to the huge number of parameters related to development&utilisation of UUS, organised decision environment is considered like a decision-forest consisting of many sub-groups of decision-trees (Fig. 1). Decision-tree concepts and subject classifications were studied by Breiman, etal., (1984). Decision-tree and random-forest works have usually been under considerations for complex input-data structure cases like; image processing & computer graphics (Criminisi, etal., 2011); random-forests (Breiman, 2001), machine learning techniques (Blakely, etal., 2018); rock engineering applications (Matin, etal., 2018); underground mine stabilities (Qi, etal., 2018; Erten, etal., 2021; Zhou, etal., 2022).

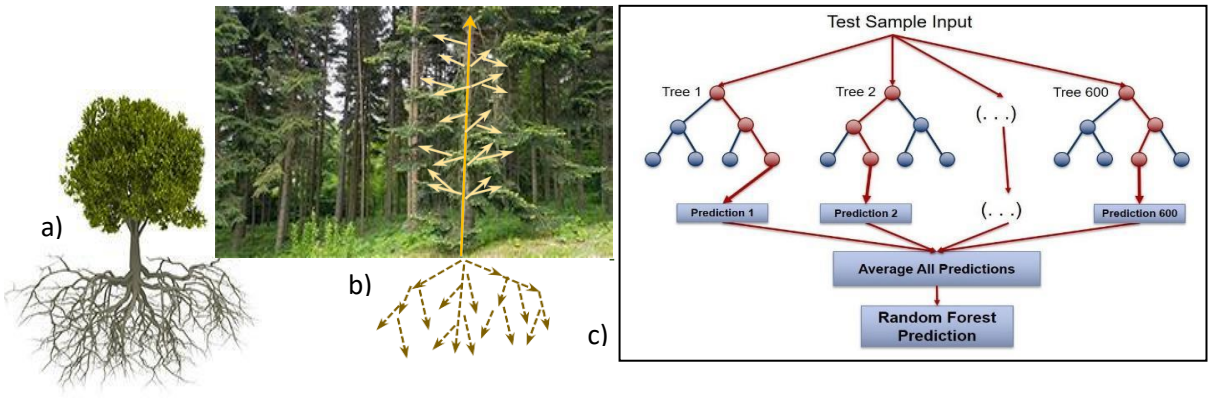

Figure 1. a) Consideration of a) individual tree, (Embark, 2023), and b) forest, might be the base concept of decision-systems here, c) random-forest decision reasoning is also applicable for the cases including complex and large numbered data conditions (Blakely, etal., 2018).

Modern urban life styles have city limits extending to cover large surface areas. There are all features of urbanisation (houses, apartments, roads, streets, pedestrian areas, playgrounds, natural parks, carparks, countryside, industrial areas, etc.) in these areas including possibly one of the members of underground spaces, (caves, historical shelters, abandoned underground mine galleries, sinkholes, archaeological underground cities, etc.) as well. Common urban areas in the modern world seldom have one or more of the underground spaces listed above. But, they have definitely underground features like; apartments' basement layers, car parks, metro tunnels & stations, road tunnels (Sturk, etal., 1996), shopping centres & pedestrian walkways (PATH, 2023). All these underground constructions need to be designed and developed in the

first step. Then, they have to be equipped (utilised) for their usage. After that, they must be monitored closely for their stabilities and safety cases. Beside these activities, UUS developments should also have considerations related to their impact on environments, social & economic welfare, and legal registration concern related to 3D land ownership procedures, (Zaini, etal., 2013).

Development in computer systems and software which supply 3D digital graphics has been the starting point to develop 3D digital maps (including surface and underground area & volume presentations, 3D modelling), (Saeidian, etal., 2021). New trends in this field of software applications cover 3D registry (positioning) systems for surface and underground constructions. Certain projects have already been commissioned for the pioneering cities for their underground features. The progresses which have been achieved for Singapore's 3D mappings (ETH, 2022) are needed to be mentioned here. These developments have initiated new enthusiasm for the digitalisation works performed for; regional&city planning, civil&mining engineering projects, and architectural applications (which all cover surface/underground structures). Additionally, Building Information Modelling (BIM) based programmes, Land Administration Systems (LAS), and Land Administration Domain Models (LADM), have also application examples in 3D coordinate and feature registries (Ramlakhan, etal., 2021; Yan, etal., 2021; Guler & Yomralioglu, 2022; Ramlakhan, etal., 2023). BIM usage for instance, in the presentation of information related to underground stations (Huang, 2022) helps to understand further UUS related risk analyses.

Systems required to have safe UUS

Any space planned to be excavated for surface/underground constructions should be regulated through regional & urban master plans. All the features of excavation location in regional and local level are better to be analysed for unexpected natural influences. There should be legal perspective and permission also for the excavation procedures. All the operations are going to be followed according to applicable work&workplace safety and health procedures, that means all the stages of excavations include the required operational and control units. If there is an available abandoned underground mine *(or possibly: caves, part of underground mine galleries & stopes, archaeological tunnels & underground city galleries, historic underground shelters, etc.)*, and if there is a possibility to use it for its secondary utilisation as a UUS purposes, underground excavation stage and required engineering works have to be differentiated into evaluation and controlling of the abandoned mine spaces for their secondary usage stabilities. Responsible engineers should ensure about their decision reasoning steps to provide deduction if the abandoned mine spaces supply engineering standard qualities for safe UUS specifications. On the contrary, the decision parameters defined in the following content are aimed to provide safe UUS cases with a new excavation in the earth crust. Engineering decision procedures are required here to handle complex input-data for UUS designing, excavation, utilisation and monitoring stages in separate decision layers. UUS operations including similar stages are better to follow predefined design procedures. These procedures must categorise the duties of government bodies, investors (who require to have UUS through single and/or group-projects), consultants, and contractors (who realise the engineering operations according to pre-described sub-contracts' procedures). Parameters listed below (Table 1) include realisation steps of UUS through underground excavation operations. These steps could be improved in time for further details as the requirements appeared. Decision parameters related to having stable & safe UUS cases can be grouped firstly according to defined 3 main stages. Then rule-based decision reasoning steps are combined as "decision-systems" for their specific (classified) subjects (Table 1).

Table 1. Decision-systems which could be applicable in UUS development cases.

a) Pre-excavation stage:

- Government body issues (Systems a1 to a10);

i) System-a1 (Social circumstances);
ii) System-a2 (Impact on businesses, supply & demand cases);
iii) System-a3 (Natural environment cases);
iv) System-a4 (Rock&soil formations, local geology);
v) System-a5 (Urban master planning);
vi) System-a6 (Definitions of "2D land ownerships" and "3D space ownerships rights & responsibilities);
vii) System-a7 (Imaging underground rock masses);
viii) System-a8 (Regional rock mechanics & rock behaviour evaluation);
ix) System-a9 (Regional stability analyses, quake influences);
x) System-a10 (Regulating surface & UUS structures with accepting responsibilities);

- Issues related to investors (Systems a11 to a20);

xi) System-a11 (Local stability analyses for selected surface parcels and UUS case);
xii) System-a12 (Imaging local (parcels related) underground rock masses);
xiii) System-a13 (Local (parcels related) rock mechanics & rock behaviour evaluation);
xiv) System-a14 (Definition of UUS dimensions, depth and shape);
xv) System-a15 (USS design with operational options);
-System-a15-1 (Excavation types and procedure design);
-System-a15-2 (Supporting types and procedure design);
xvi) System-a16 (Defining UUS influences on other structures in/on earth surface);
xvii) System-a17 (Defining influences of structures in/on earth surface on UUS);
xviii) System-a18 (Defining UUS safety precautions and related design options);
ixx) System-a19 (Evaluations of design by following latest standards' options);
xx) System-a20 (Accepting the design / Repeating the procedure starting from System-a11);

b) Excavation stage:

- Government body issues (Systems b1 to b5);

i) System-b1 (Regulating work&workplace safety and health, control);
ii) System-b2 (Evaluating stabilities of UUS and surroundings);
iii) System-b3 (Monitoring excavation steps; reporting including images);
iv) System-b4 (Organising regular work-parties & meetings with investors' engineers & directors to exchange project data and evaluation);
v) System-b5 (Define improvements of excavation steps if required);

- Issues related to investors (Systems b6 to b15);

vi) System-b6 (Work&workplace safety and health procedures, control engineering);
vii) System-b7 (Rock fracturing procedures);
-System-b7-1 (Blasting design and controls);
-System-b7-2 (Rock cutting properties & machine selection steps);
viii) System-b8 (Hauling of fractured rock materials, optimisation);
ix) System-b19 (Ventilation design & air quality controls including gasses & dusts);

x) System-b10 (Auxiliary requirements & optimisation; compressed air, power lines, etc.);
xi) System-b11 (Water pumping design for groundwater discharges & flooding options);
xii) System-b12 (Evaluating rescue options for excavation and after excavation stages);
xiii) System-b13 (Monitoring environmental and social influences);
xiv) System-b14 (Keeping moral of employee, good relation with surrounding societies);
xv) System-b15 (Formal reporting by following underground engineering concepts);

c) After excavation stage:

- Government body issues (Systems c1 to c10);

i) System-c1 (Regulating work&workplace safety and health, control);
ii) System-c2 (Evaluating stabilities of UUS and surroundings);
iii) System-c3 (Monitoring UUS and surroundings through installed instrumentations);
iv) System-c4 (Monitoring UUS and surroundings through surface measurements);
v) System-c5 (Monitoring UUS safety and stabilities in regular bases);
vi) System-c6 (Organising regular work-parties & meetings with researchers, and investors' engineers & directors; to exchange project data and evaluation);
vii) System-c7 (Organising monitoring projects);
viii) System-c8 (Evaluating any additional reinforcement projects if necessary);
ix) System-c9 (Regulating safety-rescue and after disaster circumstances);
x) System-c10 (Regulating safety usages of the UUS);

- Issues related to investors (Systems c11 to c12);

xi) System-c11 (Keeping the project data as long as possible for further discussions case);
xii) System-c12 (Attending the meetings defined at System-c6);

The decision-systems described above interrelated & interacted among themselves and they should be organised to produce semi-decisions and concluding decisions related to their group subjects. These outcomes are then re-ruled to reach the final conclusion about the UUS development stages. These decisions, semi-decisions, and final conclusions (which could be supplied through a software program) help engineers & directors of UUS projects. Human history has success and failure stories in engineering activities. There have always been acting counterparts in these activities and they have been proud of the project when there have been successful outcomes. However, for the cases of project failure circumstances, outcomes are usually different. The counterparts in the project usually do not want to take their full and moral responsibilities, they generally prefer to stay behind on their written contracted responsibilities. Therefore, defining all the influencing decision-systems (minor and major ones) in UUS development & utilisation is vital to define necessary UUS project-related legal contracts. However, engineering practices have also revealed experiences that, there are always some subjects staying in "black-zones", which had not been thought about during the projects' contracting periods (at the beginning). Therefore, modern engineering UUS projects should always be ready for those black-zone type events/situations during their operations. This events/situations should be reported in writing forms whenever these out-off-contract case is experienced to define legal duties&responsibilities with additional sub-contracts. Therefore, the definition of decision- systems *(each system can be diagnosed as a "decision-group")* should cover the entire decision environment based on the identified group of issues. Since there are a

large number of decision parameters, their interrelated interactions have also formed numerous decision factors. Organisation of all these parameters either with rule-based decision-tree groups or decision-forest type reasoning steps have resulted in semi-conclusions and then conclusions which are very helpful for decision-makers and engineers in UUS development projects.

Final decision which would like to be reached through defined decision-systems (Table 1) combines decision-trees in their specific subject. Therefore, each decision-system includes several subject related decision-trees like tree-groups in a forest. Example supplied in Table 1 has a "Pre-excavation stage" which has 10 individual decision-systems for government bodies and 10 others for "investors", (as counterparts of UUS projects). These two sub-groups are defined in the 3 stages of UUS project *(representing duties which should be realised by i) government bodies, and ii) investors).* In the given UUS development&utilisation sample case; there are; *a) 20 decision-systems (10+10) for "Pre-excavation stage";* b) *15 decision-systems (5+10) for "Excavation stage";* and c) *12 decision-systems (10+2) for "After excavation stage"*. In the UUS related decisions described here have totally 6 sub-groups examples. These decision-systems consist of separate decision-trees for their detached intellectual target arrangements. Moreover, the systems sampled in Table 1 *(those systems are most probably going to be enhanced as the underground engineering cases improved for UUS projects)* have to be organised in a manner that they should share their input data sets through pre-described decision-tree protocols. These decision-systems could also be arranged to share their semi-decisions whenever required to facilitate their reasoning.

When the engineers in different branches, city planners, architects, archaeologists, art historians, real estate employees etc. are concentrated on UUS development&utilisation projects, decision parameters required and listed by these professionals form large numbered data sets. Therefore, input-data related to UUS projects could be collected as detail as possible to help these professionals' decision reasoning steps (according to predefined decision-systems procedures). For instance; when the "Excavation stage" is under concern for the decision environment described in Table 1, systems related to "investors" are listed from Systems-b6 to System-b15. These are actually the main "underground engineering" subjects in the mining context. Considering mining operations in separate interconnected "systems" was also the manner used by Gokay&Shahriari (2017) for mine safety issues. When the excavation activities for a new UUS project is started, the decision-systems forwarded in the content of System-b6 to System-b15 are also started to be considered individually one by one in detail. These activities are briefly related to; Work&workplace safety and health procedures; Rock fracturing procedures; Hauling of fractured rock materials; Ventilation design & air quality controls; Auxiliary requirements & optimisation; Water pumping; Rock support design and implementations; Evaluating rescue options; Monitoring environmental and social influences; etc.

Decision precautions for dynamic data sets

The decision environment considered in Table 1 is aimed to provide decisions through its decision-systems for a UUS project selected. However, the decisions supplied through the decision-systems here have tendency to be changed according to the differentiation realised in two main regulating environments; "time" and "enclosed-space". When the "time" is under focus, UUS projects' "life cycles", *(starting from its first idea of consideration, which is the time periods before the pre-excavation stage)* ought to be considered cautiously. In point of fact, decision-trees in each decision-system have their reasoning through rule-based decisions. Input-data for these systems have their confines representing a time period of data collection. As the UUS project time continues to advance, input parameters features for pre-described

decision environments have also gradually differentiated. These changes are natural characteristics of climate and earth crust materials' properties. For this reason, the input parameters provided for these decision-systems must be collected sequentially at certain time intervals. These re-evaluation activities reveal the need for a continuous effort to keep the input-data conditions of decision-systems up-to-date. The second regulating decision concept is related to the underground "enclosed-space" variable. Work&workplace environments for the employees of underground excavations are not similar to the other working groups. As the underground excavation operations continues, work&workplace environments are gradually changed also. This is commonly experienced by mining employees working underground, therefore their experiences are the general base of the UUS excavation works. As the excavation operations are advanced, dimensions of underground openings are also expanded. Thus, decision parameters related to UUS stabilities and UUS safety related input-data have gradually changed also. As a result, these dynamic working conditions are then surveyed (researched) orderly in certain time intervals to protect input-data up-to-date fitness. The time interval here should be defined purposely for selected UUS projects. If revised input-data have not been introduced into the related ongoing UUS project' decision-systems, all the decision outputs of these systems are outdated because they facilitate their decision-trees with out-of-date character input-data (which represented one step earlier "operation-period"). In other words, the decision-systems are evaluating their reasoning steps with the data representing one step earlier UUS excavation conditions. This also means one step earlier dimensions of "enclosed-space". That means, out-of-date type decisions might not be suited with the decisions taken through up-to-date input-data. Basically, changing time (no controls over it) and changing dimensions of UUS (engineers have access to control the rates) have influenced the data contents collected and natural results of decision-systems offered. When the main three stages of UUS realisation is

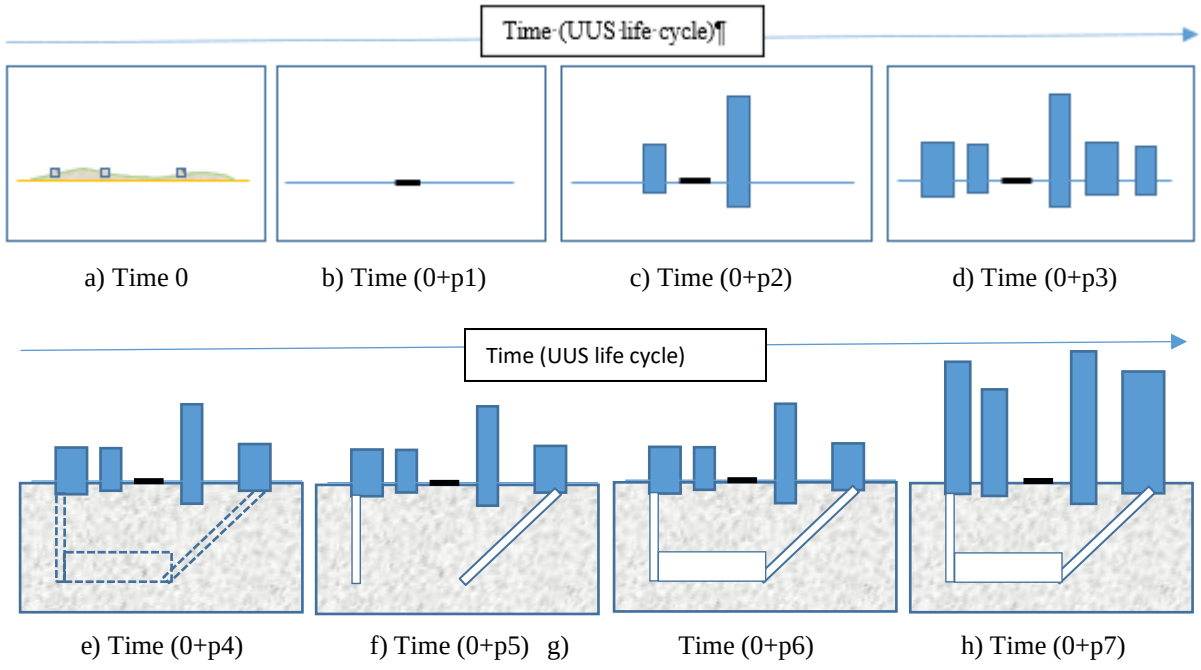

*Figure 2. Urbanisation on the base of urban master plans through periods of time including additive living spaces on the surface then underground; (**Pre-excavation stage**; a) Countryside conditions, b) Levelling the "Land", roads&infrastructures, c) Surface structures, d) Additional surface structures, e) Plan of the UUS), (**Excavation stage**; f) Opening vertical/inclined shafts for UUS development, g) Excavating UUS), (**After excavation stage**; h) UUS in service, extra surface structures).*

under concern, the sketched status-quos presented in Fig. 2 have visualised the "time" and "enclosed- space" differentiation concept more clearly. As the sketches illustrated, time, *(as an independent influencer on the proposed decision systems),* represents also all the physical, chemical, and mechanical characteristic differentiations (weathering) of the earth crust. Another important differentiation that happened in the illustrated urbanisation works include addition of "enclosed-spaces" (in/on earth crust) to the available ones. Numbers and dimensions' of spaces have prime importance on influences on the structures' wellbeing. Therefore, stability&safety of the surface and underground construction should be monitored simultaneously. New decision conditions have appeared in time as new surface/underground structures have been added to the available urban structures. Decision conditions and input-data environments have gradually changed and they should be analysed by engineers to reach stable&safe UUSs. Decision procedures described through neuro-rule based conceptdescribed by Gokay (1993) could also be utilised here to arrange decision-systems' data handling procedures. Urbanisation in new settlement areas (Fig. 2a) should be started according to urban master plans. Surface morphology of the selected areas are then re-arranged *(surface excavations, cut-fills trenches, flattening and stabilising roads, infrastructures, etc.),* accordingly (Fig. 2b). These activities have their procedures in civil engineering and cover numerous factors to follow. Surface urban structures are then constructed as the urbanisation has developed, (Fig. 2c to Fig. 2d), for the selected settlement area. Reshaping the original surface morphology, and applying loads on the foundations of roads, houses, apartments have induced new order of stress&strain distributions in rock/soil masses. These differentiations have to be monitored together with surface morphology 3D coordinates to control any influences of subsidence and slope movements which affects all the decision-systems' input-data and conclusions accordingly. Logical decision-systems (*decision-tree groups for the cases Fig. 2e to Fig. 2h)* supplied for UUS development steps have also their periodical input-data collection procedures. These procedures keep the decision-systems' outputs up-to-date. It is important to note here that each surface/underground structure which redistributes actual stress&strain fields around itself should be carefully monitored also for its neighbourhood stability&safety cases.

Decision parameter complexity in UUS realisation

In order to perform engineering activities numbers of decisions should be handled to site-workers, foreman, engineers, and directors. Some decisions are even written forms in official reports. Therefore, decision-systems in the final decision environment (target of specially articulated decision forest type reasoning, possibly decision-support system) have to be methodically in good order. Selective decision-systems should handle UUS decision conditions and background knowledge adequately to support (assist) engineers. Decision parameters collected for the design of UUS' pre-excavation stage should be wide enough to cover all the possibilities related to UUS associated variables. The levels of analyses are complicated as the detail of the parametric analyses are getting deeper. Engineering firms offering their service should then be valued according to their analyses, and depth of their decision reasoning steps for a UUS project. Supplying input parameters for underground excavation stabilities cover tests results and experiences. Uncertainties arose due to natural characteristics of rock/soil masses hindering the comparability of the test results with the actual values representing the whole masses of rocks/soils. Thus, rock engineering decision works (Einstein & Baecher, 2023) in proper decision conditions had better then cover input-data analyses including criteria, statistical methods, and experience catching procedures. Interaction matrix concept offered by Hudson (1992) is logical evaluation of expert's rates for parametric interactions. By defining criticality&dominance levels of each decision parameter in selected decision groups helps decision-makers. Including these levels into decision-systems improves their results'

acceptability. There are other approaches to overcome input-data complexity in earth crust related engineering projects like random-forest solutions (Breiman, 2001; Matin, etal., 2018; Qi, etal., 2018; Zhou, etal., 2022) and rock mass classification systems (Bieniawski, 1989). The classification systems can actually also be accepted as experts' decision reasoning to categorise the rock masses. The existence of different rock mass classification systems shows that different decision-rules could be formulated (based on experts' knowledge&expertises) to reach different conclusions by selecting particular input values among the same input-data. Thus, each rock mass classification system can be considered one decision-tree reasoning concept in a particular decision-system which groups whole rock classification systems and evaluates their results accordingly.

Conclusions

Decisions followed through input parameters are offered also through the decision support systems in logical approaches. In earlier times, these procedures were supplied by knowledge-based decision systems. Statistical methodologies, rating classifications, expert systems, fuzzy decisions, random-forests, etc. applications are approaches to attempt supplying decision procedures in complex input-data cases. Developing and utilisation of urban underground spaces have issues to be clarified in; 3D graphical modelling through 3D land registration procedures; Design efforts and required decision parameter identification for the stages of UUS realisation; Procedure supply for input-data differentiations in "time" and "enclosed-space" dimension changes; Input-data evaluation in rule-based reasoning according to selected data&expertise analyses; etc. When the engineering applications concerning UUS projects are divided into multiple decision-systems, the common benefit to be achieved through these systems is their up-to-date knowledge and experts' expertise contents. In this form of logical decision supporting programmes would be useful to handle for engineers & directors in UUS projects for supporting them in their decisions. Decision environment and related restrictions & limitations in decision-systems are samples here to present importance of the up-to-date input-data and their evaluation procedures. Stability and safety analyses of UUS are required to be performed through all possible input-data evaluation methodologies. Thus, handling systems covering mathematical analyses and systems including human expertise reasoning (expert systems) is valuable in UUS engineering application.

REFERENCES

Bieniawski, Z.T. (1989) *Engineering rock mass classifications*. Wiley, Chichester, p251.

Blakely, L., Reno, M.J. and Broderick, R.J. (2018) Evaluation and comparison of machine learning techniques for rapid QSTS simulations, *Sandia Report*, SAND2018-8018, Sandia National Laboratories, California, US, p61.

Breiman, L., Friedman, J.H., Olshen, R.A. and Stone, C.J. (1984) *Classification and regression trees*. Wadsworlh Statistics/Probability series, Chapman&Hall/ CRC, ISBN 0-412-04841-8, London, UK, p358.

Breiman, L. (2001) Random forests. *Machine learning*, 45, 1, pp5-32.

Criminisi, A., Shotton, J., and Konukoglu, E. (2011) Decision forests for classification, regression, density estimation, manifold learning and semi-supervised learning, *Microsoft research technical report*, TR-2011-114, p146.

Einstein, H.H. and Baecher, G.B. (2023) Decision making in rock engineering and engineering geology, *Geostrata magazine*, · Feb. 2023, Doi:10.1061/geosek.0000466.

Embark, (2023) *The importance of protecting tree roots*, Embark Tree Care, Webpages; The Importance of Protecting Tree Roots - Embark Services, Retrieved in Sep. 2023.

Erten, G.E., Keser, S.B. and Yavuz, M. (2021) Grid search optimised artificial neural network for open stope stability prediction, *Int. journal of mining, reclamation and environment*. Doi; 10.1080/17480930.2021.1899404.

ETH, (2022) *Digital underground*, Singapore-ETH Centre, Webpages; https://sec.ethz.ch/ research/digital-underground.html, Retrieved in Aug. 2023.

Gokay, M.K. (1993) Developing computer methodologies for rock engineering decisions. *PhD Thesis*, Mineral resources engineering department, Imperial college of science technology and medicine, University of London, UK, p396.

Gokay, M.K. (1994) A knowledge-based decision support system development for geomechanical applications. *Third international symposium on mine planning and equipment selection.* 18-20 Oct. 1994, Istanbul, Balkema Press, pp615-618.

Gokay, M.K. & Shahriari, M. (2017) Mine design evaluation for safe mine workplaces, *International symposium on occupational safety and hygiene*, (ISBN 978-989-98203-7-1, (Eds. Arezes,P. etal), 10-11 April 2017, Guimaraes, Portugal, pp13-15.

Guler, D. and Yomralioglu, T. (2022) Reviewing the literature on the tripartite cycle containing digital building permit, 3D city modeling, and 3D property ownership, *Land use policy*, 121, 106337.

Huang, M. (2022) BIM for underground stations: Supporting decision making on lifesycle stages, *PhD thesis*, Department of civil engineering, Monash University, p155.

Hudson, J.A. (1992) *Rock engineering systems:Theory and practice*. Ellis-Honvood, UK, p185.

Matin, S.S., Farahzadi, L., Makaremi, S., Chelgani, S.C., and Sattari, G. (2018) Variable selection and prediction of uniaxial compressive strength and modulus of elasticity by random forest, *Applied soft computing*, 70, pp980-967.

Qi, C., Fourie, A., Du, X., and Tang, X. (2018) Prediction of open stope hangingwall stability using random forests. *Natural hazards*, 92, 2, pp1179-1197.

PATH, (2023) *PATH Master plan study*, City of Toronto, Webpages; PATH Master Plan Study- Transportation Planning-City Planning | City of Toronto (archive.org), Retrieved in Sep.2023.

Ramlakhan, R.J.K., Kalogianni, E., and Van Oosterom, P.J.M. (2021) Modelling 3D underground legal spaces in 3D land administration systems, *Proceedings of the 7th international FIG workshop on 3D cadastres*, (Virtual/online event), pp37-52.

Ramlakhan, R.J.K., Kalogianni, E., Van Oosterom, P.J.M. and Atazadeh, B. (2023) Modelling the legal spaces of 3D underground objects in 3D land administration systems, *Land use policy*, 127, 106537.

Saeidian, B., Rajabifard, A., Atazadeh, B., Kalantari, M. (2021) Underground land administration from 2D to 3D: Critical challenges and future research directions, *Land*, 10, 1101.

Sturk, R., Olsson, L. and Johansson, J. (1996) Risk and decision analysis for large underground projects, as applied to the Stockholm Ring Road tunnels, *Tunnelling and underground space technology*, 11, 2, pp157-164.

Tann, L.V.D., Sterling, R., Zhou, Y. and Metje, N. (2020) Systems approaches to urban underground space planning and management - A review, *Underground space*, 5, pp144-166.

Volchko, Y., Norrman, J., Ericsson, L.O., Nilsson, K.L., Markstedt, A., Oberg, M., Mossmark, F., Bobylev, N., and Tengborg, P. (2020) Subsurface planning: Towards a common understanding of the subsurface as a multifunctional resource, *Land use policy*, 90, 104316.

Yan, J., Van Son, R. and Soon, K.H. (2021) From underground utility survey to land administration: An underground utility 3D data model, *Land use policy*, 102, 105267.

Zaini, F., Hussin, K., Suratman, R., and Rasid, K.A. (2013) Review of the underground land ownership in Malaysia, *Jurnal Pentadbrian Tanah*, 3, 1, pp39-52, ISSN 2231-9190.

Zhou, J., Huang, S. and Qiu, Y. (2022) Optimization of random forest through the use of MVO, GWO and MFO in evaluating the stability of underground entry-type excavations, *Tunnelling and underground space technology*, 124, 104494.

Optıcal And Structural Propertıes Of Schottky Dıodes

İlhan CANDAN[1]
Sezai ASUBAY[2]

1. INTRODUCTION

Schottky diodes, also known as Schottky barrier diodes, are semiconductor devices that have gained significant importance in modern electronics due to their unique electrical, optical, and structural properties (Singh, Dwivedi, Chakrabarti, & Prakash, 2009; Von Wenckstern et al., 2015; Yadav & Sannakashappanavar, 2021). In this chapter, we will delve into the intricate details of Schottky diodes, exploring their fundamental principles, optical characteristics, and structural aspects.

2. BASICS OF SCHOTTKY DIODES

2.1. Schottky Barrier Formation

Unlike conventional p-n junction diodes(Hueting, Rajasekharan, Salm, & Schmitz, 2008; Nishiwaki, Kushida, & Kawahashi, 2001), Schottky diodes consist of a metal-semiconductor junction, known as the Schottky barrier shown in Figures 1 and 2 (Tung, 2001, 2014). The formation of this barrier is essential to understand their properties. When a metal contacts a semiconductor, a potential barrier is created at the interface due to the difference in work functions between the metal and the semiconductor material (Sharma, 2013).

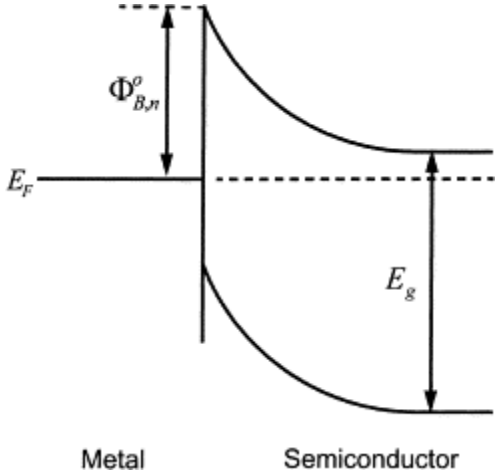

Figure 1. *A metal–semiconductor interface and basic energy band diagram (Tung, 2001).*

[1] Dr., Dicle Üniversitesi, Fen Fakültesi, Fizik Bölümü, 21280 Diyarbakır
[2] Prof. Dr., Dicle Üniversitesi, Fen Fakültesi, Fizik Bölümü, 21280 Diyarbakır

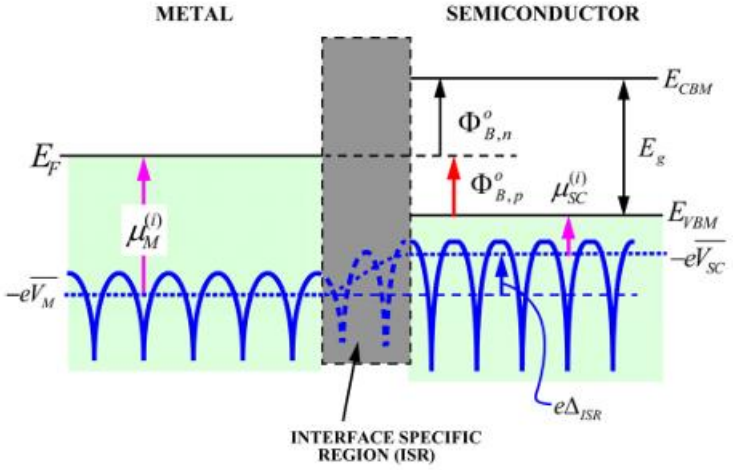

Figure 2. *Energy band diagram at the interface of metal semiconductor interface. The dotted lines represents the average electrostatic potential energy (Tung, 2014).*

2.2. Thermionic Emission

The operation of Schottky diodes relies on thermionic emission (Appenzeller, Radosavljević, Knoch, & Avouris, 2004; Wong, Troadec, Wee, & Goh, 2020), where electrons in the semiconductor overcome the Schottky barrier when a forward voltage is applied. This flow of charge carriers creates a forward current, allowing the diode to conduct. The absence of a p-n junction reduces the charge storage time, enabling fast switching (Kiziroglou et al., 2006).

3. OPTICAL PROPERTIES OF SCHOTTKY DIODES

3.1. Energy Band Structure

The energy band structure of the semiconductor material used in a Schottky diode plays a pivotal role in its optical properties. The energy bandgap determines the range of photon energies that can be absorbed and the corresponding wavelengths of light (Clark & Robertson, 2007; Tersoff, 1986).

3.2. Optical Absorption

Schottky diodes exhibit optical absorption characteristics influenced by their energy bandgap (Haciismailoglu, Ahmetoglu, Haciismailoglu, Alper, & Batmaz, 2022). Incident photons with energies greater than the bandgap can excite electrons across the Schottky barrier, contributing to the photocurrent. This property makes Schottky diodes suitable for photodetectors (Ezhilmaran et al., 2021).

3.3. Responsivity

Responsivity measures a photodetector's ability to convert incident optical power into an electrical signal(Hesler & Crowe, 2007). Schottky diodes often exhibit high responsivity due to their efficient photon-to-electron conversion process(Kamruzzaman & Zapien, 2017; Pristavu, Brezeanu, Pascu, Drăghici, & Bădilă, 2019). This attribute is valuable in applications like optical communication systems and sensors.

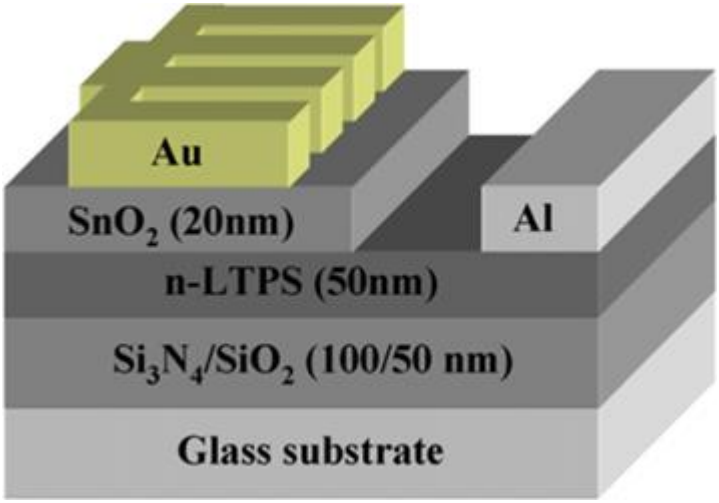

Figure 3. *Schematic of Schottky diode with Au/SnO2/n-LTPS MOS cross-section (Al-Ahmadi, 2020).*

4. STRUCTURAL PROPERTIES OF SCHOTTKY DIODES

4.1. Metal-Semiconductor Interface

The metal-semiconductor interface is a critical aspect of Schottky diodes' structural properties. The choice of both the metal and semiconductor materials greatly influences the device's performance as shown in Figure 3 (Al-Ahmadi, 2020; Grüb, Krozer, Simon, & Hartnagel, 1994). A well-engineered interface results in lower Schottky barrier heights and improved electrical characteristics(Ahmed et al., 2018).

4.2. Schottky Contact Quality

The quality of the Schottky contact significantly impacts the diode's structural properties (Von Wenckstern et al., 2015; Zhao, Jie, Wang, Castellanos-Gomez, & Frisenda, 2020). A high-quality contact ensures good electrical conductivity and minimal series resistance (Chen et al., 2009). Techniques such as surface passivation and interface engineering are employed to enhance contact quality.

4.3. Fabrication Techniques

Schottky diodes can be fabricated using various techniques, including vacuum evaporation, sputtering, and chemical vapor deposition (CVD) (Giovine et al., 2011; Güllü, Aydoğan, & Türüt, 2008; Liang, Cui, & Varahramyan, 2003). The choice of fabrication method affects the uniformity and quality of the metal-semiconductor junction, influencing the diode's structural properties and performance.

5. APPLICATIONS OF SCHOTTKY DIODES

5.1. Photovoltaic Cells

Schottky diodes are integral components in photovoltaic cells, where they serve as energy-conversion devices (Lee, Lee, & Park, 2014; Yi et al., 2016). When exposed to light, the absorbed photons generate electron-hole pairs in the semiconductor, contributing to the photocurrent (Luther et al., 2008). Schottky diodes are widely used in solar panels to efficiently convert sunlight into electricity.

5.2. Mixers and Detectors

The fast-switching speed and excellent high-frequency performance of Schottky diodes make them ideal for use in microwave mixers and detectors (Goy, 1982; Hesler, Xu, Brissette, & Bishop, 2008). These applications are critical in radar systems, communication equipment, and wireless technology, where high-frequency signal processing is required.

5.3. Power Rectification

Schottky diodes are employed as rectifiers in power supply circuits (Ao et al., 2010; Takahashi et al., 2009). Their low forward voltage drop and minimal reverse recovery time result in reduced power loss and improved efficiency. They are commonly used in DC power supplies and voltage converters.

6. CONCLUSION

Schottky diodes, with their unique optical and structural properties, find widespread use in modern electronics. Their ability to efficiently absorb light and exhibit high responsivity makes them invaluable in photodetectors, photovoltaic cells, and optical communication systems. Understanding the intricacies of their metal-semiconductor interface and fabrication techniques is crucial for optimizing their performance in various electronic applications.

This chapter provides an in-depth exploration of the optical and structural properties of Schottky diodes. It covers their fundamental principles, optical characteristics, structural aspects, and key applications. For a more comprehensive understanding, additional research and experimentation are recommended.

References

Ahmed, M. A. M., Mwankemwa, B. S., Carleschi, E., Doyle, B., Meyer, W. E., & Nel, J. M. (2018). Effect of Sm doping ZnO nanorods on structural optical and electrical properties of Schottky diodes prepared by chemical bath deposition. *Materials Science in Semiconductor Processing, 79*, 53-60.

Al-Ahmadi, N. A. (2020). Metal oxide semiconductor-based Schottky diodes: a review of recent advances. *Materials Research Express, 7*(3), 032001.

Ao, J.-P., Takahashi, K., Shinohara, N., Niwa, N., Fujiwara, T., & Ohno, Y. (2010). *S-parameter analysis of GaN Schottky diodes for microwave power rectification.* Paper presented at the 2010 IEEE Compound Semiconductor Integrated Circuit Symposium (CSICS).

Appenzeller, J., Radosavljević, M., Knoch, J., & Avouris, P. (2004). Tunneling versus thermionic emission in one-dimensional semiconductors. *Physical review letters, 92*(4), 048301.

Chen, D., Huang, Y., Liu, B., Xie, Z., Zhang, R., Zheng, Y., . . . Narayanamurti, V. (2009). High-quality Schottky contacts to n-InGaN alloys prepared for photovoltaic devices. *Journal of Applied Physics, 105*(6).

Clark, S., & Robertson, J. (2007). Band gap and Schottky barrier heights of multiferroic BiFeO3. *Applied physics letters, 90*(13).

Ezhilmaran, B., Patra, A., Benny, S., Sreelakshmi, M., Akshay, V., Bhat, S. V., & Rout, C. S. (2021). Recent developments in the photodetector applications of Schottky diodes based on 2D materials. *Journal of Materials Chemistry C, 9*(19), 6122-6150.

Giovine, E., Casini, R., Dominijanni, D., Notargiacomo, A., Ortolani, M., & Foglietti, V. (2011). Fabrication of Schottky diodes for terahertz imaging. *Microelectronic Engineering, 88*(8), 2544-2546.

Goy, P. (1982). A packaged Schottky diode as detector, harmonic mixer, and harmonic generator in the 25–500 GHz range. *International Journal of Infrared and Millimeter Waves, 3*, 221-234.

Grüb, A., Krozer, V., Simon, A., & Hartnagel, H. (1994). Reliability and micro-structural properties of GaAs Schottky diodes for submillimeter-wave applications. *Solid-state electronics, 37*(12), 1925-1931.

Güllü, Ö., Aydoğan, Ş., & Türüt, A. (2008). Fabrication and electrical characteristics of Schottky diode based on organic material. *Microelectronic Engineering, 85*(7), 1647-1651.

Haciismailoglu, M. C., Ahmetoglu, M., Haciismailoglu, M., Alper, M., & Batmaz, T. (2022). Electrical and optical properties of Schottky diodes fabricated by electrodeposition of Ni films on n-GaAs. *Sensors and Actuators A: Physical, 347*, 113931.

Hesler, J. L., & Crowe, T. W. (2007). Responsivity and noise measurements of zero-bias Schottky diode detectors. *Proc. ISSTT*, 89-92.

Hesler, J. L., Xu, H., Brissette, A., & Bishop, W. L. (2008). *Development and characterization of THz planar Schottky diode mixers and detectors.* Paper presented at the Proc. 19th Int. Symp. on Space Terahertz Technology.

Hueting, R. J., Rajasekharan, B., Salm, C., & Schmitz, J. (2008). The charge plasma PN diode. *IEEE electron device letters, 29*(12), 1367-1369.

Kamruzzaman, M., & Zapien, J. (2017). Reduction of schottky barrier height, turn on voltage, leakage current and high responsivity of li doped ZnO nanorod arrays based schottky diode. *Journal of Nanoscience and Nanotechnology, 17*(7), 5061-5072.

Kiziroglou, M., Zhukov, A., Li, X., Gonzalez, D., De Groot, P., Bartlett, P. N., & de Groot, C. (2006). Analysis of thermionic emission from electrodeposited Ni–Si Schottky barriers. *Solid state communications, 140*(11-12), 508-513.

Lee, Y. K., Lee, H., & Park, J. Y. (2014). Tandem-structured, hot electron based photovoltaic cell with double Schottky barriers. *Scientific Reports, 4*(1), 4580.

Liang, G., Cui, T., & Varahramyan, K. (2003). Fabrication and electrical characteristics of polymer-based Schottky diode. *Solid-State Electronics, 47*(4), 691-694.

Luther, J. M., Law, M., Beard, M. C., Song, Q., Reese, M. O., Ellingson, R. J., & Nozik, A. J. (2008). Schottky solar cells based on colloidal nanocrystal films. *Nano letters, 8*(10), 3488-3492.

Nishiwaki, K., Kushida, T., & Kawahashi, A. (2001). *A fast and soft recovery diode with ultra small Qrr (USQ-Diode) using local lifetime control by He ion irradiation.* Paper presented at the Proceedings of the 13th International Symposium on Power Semiconductor Devices & ICs. IPSD'01 (IEEE Cat. No. 01CH37216).

Pristavu, G., Brezeanu, G., Pascu, R., Drăghici, F., & Bădilă, M. (2019). Characterization of non-uniform Ni/4H-SiC Schottky diodes for improved responsivity in high-temperature sensing. *Materials Science in Semiconductor Processing, 94*, 64-69.

Sharma, B. (2013). *Metal-semiconductor Schottky barrier junctions and their applications*: Springer Science & Business Media.

Singh, A. K., Dwivedi, A., Chakrabarti, P., & Prakash, R. (2009). Electronic and optical properties of electrochemically polymerized polycarbazole/aluminum Schottky diodes. *Journal of Applied Physics, 105*(11).

Takahashi, K., Ao, J.-P., Ikawa, Y., Hu, C.-Y., Kawai, H., Shinohara, N., . . . Ohno, Y. (2009). GaN Schottky diodes for microwave power rectification. *Japanese Journal of Applied Physics, 48*(4S), 04C095.

Tersoff, J. (1986). Calculation of Schottky barrier heights from semiconductor band structures. *Surface Science, 168*(1-3), 275-284.

Tung, R. T. (2001). Recent advances in Schottky barrier concepts. *Materials Science and Engineering: R: Reports, 35*(1-3), 1-138.

Tung, R. T. (2014). The physics and chemistry of the Schottky barrier height. *Applied Physics Reviews, 1*(1).

Von Wenckstern, H., Splith, D., Purfürst, M., Zhang, Z., Kranert, C., Müller, S., . . . Grundmann, M. (2015). Structural and optical properties of (In, Ga) 2O3 thin films and characteristics of Schottky contacts thereon. *Semiconductor Science and Technology, 30*(2), 024005.

Wong, C. P. Y., Troadec, C., Wee, A. T., & Goh, K. E. J. (2020). Gaussian Thermionic Emission Model for Analysis of Au/Mo S 2 Schottky-Barrier Devices. *Physical Review Applied, 14*(5), 054027.

Yadav, A. B., & Sannakashappanavar, B. S. (2021). Investigation of Schottky barrier height using area as parameter: effect of hydrogen peroxide treatment on electrical optical properties of Schottky diode. *Optical Materials, 119*, 111341.

Yi, S.-G., Kim, S. H., Park, S., Oh, D., Choi, H. Y., Lee, N., . . . Yoo, K.-H. (2016). Mo1–x W x Se2-Based Schottky Junction Photovoltaic Cells. *ACS applied materials & interfaces, 8*(49), 33811-33820.

Zhao, Q., Jie, W., Wang, T., Castellanos-Gomez, A., & Frisenda, R. (2020). InSe Schottky diodes based on van der Waals contacts. *Advanced Functional Materials, 30*(24), 2001307.

Investigation of Ferroresonance in Transformers Connected to a Power Transmission Line

Hilmi ZENK[1]

1. Introductıon

In the transformers connected to this energy system, ferroresonance is affected during loaded operation. As it is known that transformers, which are the basic elements of energy carrying capacity, the quality of the energy that provides the ferroresonance effect may deteriorate. These effects will be examined through a transformer modeled in the Matlab/Simulink environment.

2. Transformers

One of the most important advantages of electrical energy compared to other types of energy is that it can be easily transmitted to areas of use at geographically distant distances. In order to benefit more from the unit energy produced at the point of consumption, it is important that energy transmission is carried out with the highest efficiency and minimum loss. In order to achieve this, it is desired that the basic electrical parameters in the transmission system undergo some transformations, that is, the voltage should be at very high values and the current at very low values.

With developing technology, a large number of semiconductor electronic control circuit elements are used in electrically powered devices. The electrical parameters required by these elements can be at very different levels. In order to meet the needs at these different levels, transformers are used in the supply units of many electrical devices both to change the voltage level and for electrical insulation.

Internal Structure of Transformers

Transformers are made of thin sheets and consist of two windings placed on the iron body, wrapped with insulated conductors with a closed magnetic circuit called the iron body. Except for auto transformers, these two windings are completely electrically isolated from each other. The first of these windings is called the primary winding and the other is called the secondary winding. The primary winding is the input winding of the transformer and is connected to the network. The secondary winding is also the output winding and is connected to the load. Copper conductors are generally used in the windings of transformers. However, aluminum conductor can be used in transformers used for some special applications [1].

[1] Assoc. Dr., Department of Electrical and Electronics Engineering, Giresun University, Turkey

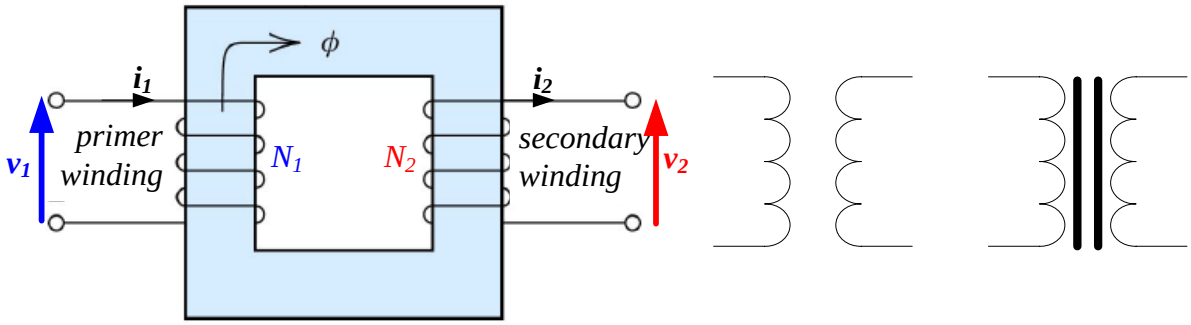

(a) (b) (c)

Figure 1. A transformer core and its symbols

In transformers, the closed magnetic body on which the windings are wound is called the core. Soft iron, steel and air are used in core construction. Soft iron and steel cores are used in transformers operating in low-frequency networks. Air core is used in transformers operating in very high frequency networks. As stated in Figure 1. (a), the part on which the windings of the core are wound is called the yoke, and the lower and upper parts of the legs are called yokes. When transformers are drawn in electrical circuits, symbols are used instead of core shapes. Figure 1. (b) shows the symbol of an air-core transformer, and Figure 1. (c) shows the shape of an iron-core transformer.

Working Principle of Transformers

As is known, Lenz's law explains that in order to induce any voltage in a conductor, the conductor must either be in a variable magnetic field or move in a constant magnetic field. Since transformers are static electrical machines and have no moving parts, the magnetic field created must be mobile. When an alternating current is applied to the primary winding of a transformer whose secondary winding ends are free, a small current flows through the primary winding. This current circulating through the primary winding creates a variable flux in the primary winding. This flux completes its circuit through the core of the same transformer. The magnetic flux occurring in the core lags 90° behind the voltage applied to the primary winding. The change of primary winding voltage and flux can be seen in Figure 3. Since the flux that completes its circuit on the core also cuts the secondary winding, a voltage is induced in the secondary winding.

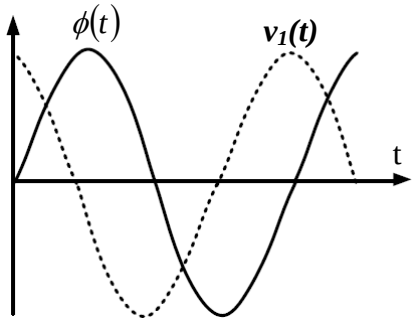

Figure 2. Variation of magnetic flux with voltage.

When an alternating voltage is applied to the primary of the transformer, a time-varying magnetic field is created. The magnetic field reaches its maximum value in one quarter of the period. The average value of the electromotive force induced in a conductor in time T/4;

$$E_{1ort} = \frac{\phi_{\max}}{T/4} \text{(V)} \quad (1)$$

where E1avg is defined as the average value of the induced voltage (Volts), $\phi_{\max}$, is the largest magnetic flux (Weber), T is defined as the period (Seconds) and f is defined as the Frequency (Hertz). The equation for a winding with N_1 number of turns in the primary;

$$E_{1ort} = \phi_{\max} f 4\mathrm{N}_1 \text{ (V)} \quad (2)$$

It takes the form.

Ideal Transformer

It is a term used for lossless transformers having one input and one output winding. For a transformer to be considered ideal,

1. Hysteresis and eddy current losses, which constitute core losses, are neglected.

2. Leakage fluxes are neglected. That is, all the flux flows through the core and cuts the windings.

3. The excitation current required to create the flux has been neglected. In other words, the core magnetic permeability is assumed to be infinite.

4. Winding resistances are neglected.

The ratio of the voltage induced in the primary winding to the voltage induced in the secondary winding is equal to the number of turns in the primary winding and the number of turns in the secondary winding. This ratio is called the transformation ratio of the transformer and is indicated by the coefficient "α".

$$\frac{V_1}{V_2} = \frac{4{,}44\phi_{\max} f\mathrm{N}_1}{4{,}44\phi_{\max} f\mathrm{N}_2} = \frac{N_1}{N_2} = a \quad (7)$$

If the losses of the transformer are accepted as zero, all the power applied to the primary winding is transferred to the secondary winding. Primary winding and secondary winding apparent powers,

$$S_1 = V_1 I_1 \text{ (V)} \quad (8)$$

$$S_2 = V_2 I_2 \text{ (V)} \quad (9)$$

can be written as . Primary winding power is equal to secondary winding power.

$$S_1 = S_2 = V_1 I_1 = V_2 I_2 \text{ (VA)} \quad (10)$$

If equations (7) and (10) are combined, the transformation ratio of the transformer can be written as in equation (11):

$$\frac{V_1}{V_1} = \frac{N_1}{N_2} = \frac{I_2}{I_1} = a \quad (11)$$

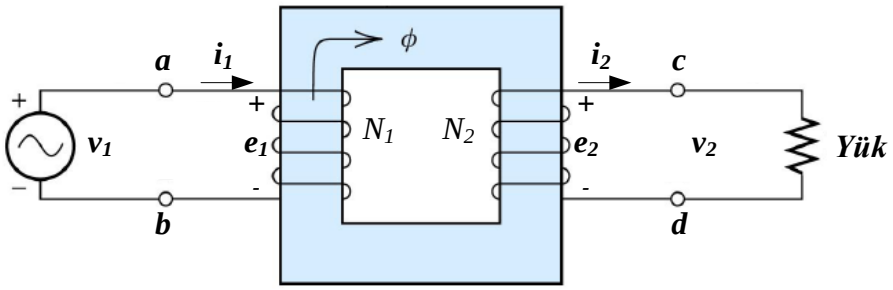

Figure 3. Load-Connected Ideal Transformer.

Let's assume that a load as in Figure 4 is connected to an ideal transformer, with winding resistances, leakage inductances and excitation losses neglected. For sinusoidal steady-state operation, the input impedance is

$$\frac{V_1}{I_1} = Z_1 \tag{12}$$

load impedance,

$$\frac{V_2}{I_2} = Z_2 \tag{13}$$

From here,

$$\frac{V_1}{I_1} = \left(\frac{N_1}{N_2}\right)^2 Z_2 \tag{14}$$

It is possible. Considering the effect of impedance Z_2 on the primary, if an equivalent impedance Z_2' is shown in the primary circuit instead of Z_2,

$$Z_2^{'} = \left(\frac{N_1}{N_2}\right)^2 Z_2 \tag{15}$$

This situation is shown in Figure 5. impedance is the value of $Z_2^{'}$ impedance transferred to the primary side.

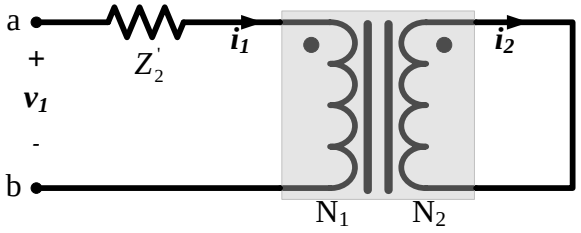

Figure 4. Ideal transformer with load impedance reduced to the primary.

Figure 6 shows the equivalent circuit of the secondary with respect to a load-connected transformer and the primary.

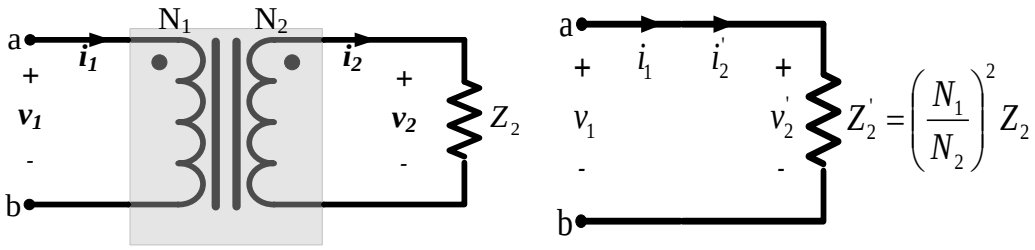

(a) **(b)**

Figure 5. (a) An ideal transformer with a load connected to its secondary. (b) Equivalent electrical circuit.

1.1. Leakage Fluxes in Transformers

The conductors forming the primary and secondary windings of the transformer have a resistance value, albeit small. Among these resistors, which are connected in series to the windings, R1 represents the primary winding resistance and R_2 represents the secondary winding resistance.[2]

If an alternating voltage is applied to the primary winding of the transformer, current I_1 passes through the primary winding and ϕ_1 magnetic flux occurs. A small part of this flux, ϕ_{l1} completes its circuit from air and does not interrupt the secondary winding. It can be represented by L_1 leakage inductance or X_1 leakage reactance. The remaining part of the ϕ_1 flow ϕ_m ,completes its circuit through the core. In that case;

$$\phi_1 = \phi_{l1} + \phi_m \tag{16}$$

When Figure 6 is examined, for the electrical circuit of the transformer,

$$v_1(t) = v_{1a}(t) + R_1 i_1(t) \tag{17}$$

can be written, according to Faraday's law,

$$v_{1a}(t) = N_1 \frac{\partial \phi_1}{\partial t} \tag{18}$$

When a load is connected to the secondary winding side, current I_2 flows through the secondary winding and magnetic flux ϕ_2 occurs. It completes the circuit ϕ_{l2}, which is a small part of the magnetic flux ϕ_2, through air. This flux is represented in the equivalent circuit by the leakage inductance L_2 or the leakage reactance X_2. The remaining part completes its circuit through the core in the opposite direction to the ϕ_m flux. fm is the common magnetic flux crossing both the primary winding and the secondary winding. The flux fl1, produced by the primary winding and completing its circuit with air, and ϕ_{l2} flux, produced by the secondary winding and completing its circuit with air, are called leakage flux. While ϕ_{l1} flux occurs in both unloaded and loaded operation, ϕ_{l2} flux occurs only in loaded operation. The efficiency of transformers decreases due to leakage fluxes. In other words, the amount of power transferred from the primary winding to the secondary winding decreases. In ideal transformers, since there

are no leakage fluxes, all of the primary winding power is transferred to the secondary winding [3].

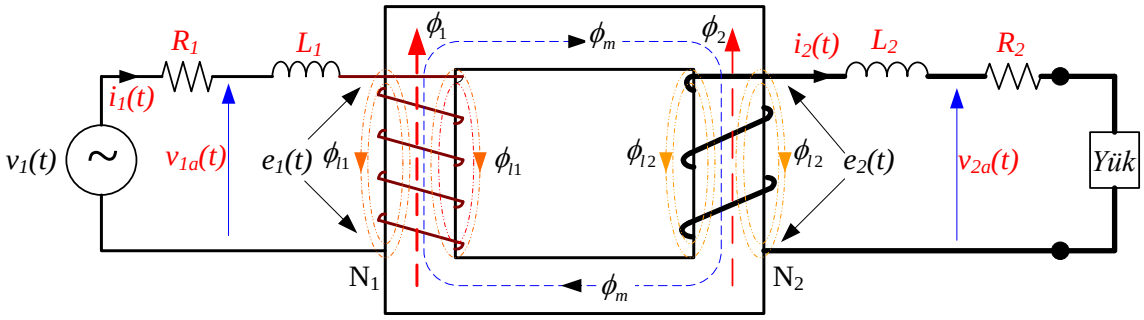

Figure 6. Model of a Transformer

When a load is connected to the secondary winding of the transformer, current I_2 flows through the secondary winding. The magnetic flux ϕ_2 produced by I_2 is in the opposite direction to the magnetic flux ϕ_1 produced from the primary winding according to the right-hand rule. The common magnetic flux ϕ_m crossing both windings is the difference between the magnetic fluxes produced by the primary and secondary windings,

$$\phi_m = \phi_1 - \phi_2 \tag{19}$$

equal. As the transformer is loaded, the current I_2 increases, and as a result, the magnetic flux ϕ_2 also increases. Increasing the magnetic flux ϕ_2 reduces the common magnetic flux ϕ_m . The transformer needs to increase the ϕ_1 flux to meet the decreasing ϕ_m common magnetic flux and draws more current I_1 from the primary. For this reason, as transformers are loaded, they draw more current from the circuit. Excessive I_1 current drawn must not exceed the label value to prevent damage to the transformer. The magnetic equivalent circuit of a transformer is shown in Figure 7.

$$v_1(t) = R_1 i_1(t) + N_1 \frac{\partial \phi_{l1}}{\partial t} + N_1 \frac{\partial \phi_m}{\partial t} \tag{20}$$

obtained. Leakage flux of primary winding,

$$L_1 \frac{\partial i_1}{\partial t} = N_1 \frac{\partial \phi_{l1}}{\partial t} \tag{21}$$

The emf induced in the primary winding,

$$e_1 = N_1 \frac{\partial \phi_m}{\partial t} \tag{22}$$

It is defined as. If Kirchhoff's voltage law is applied to the primary circuit given in Equation 16,

$$v_1(t) = R_1 i_1(t) + L_1 \frac{\partial i_1}{\partial t} + e_1(t) \tag{23}$$

can be written.

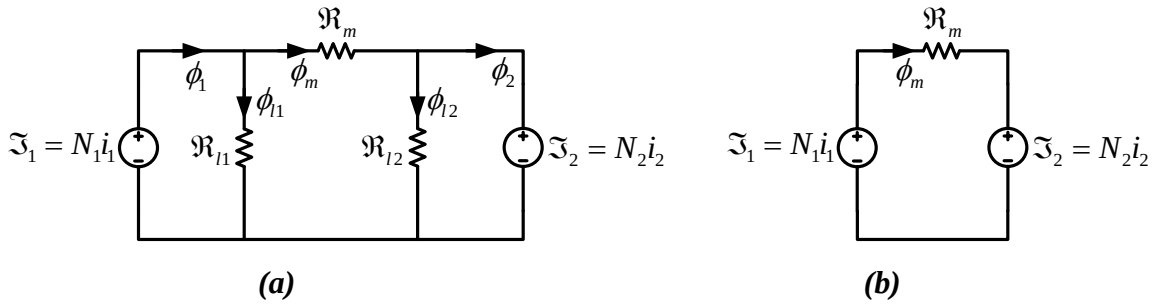

Figure 7. (a) Detailed magnetic equivalent circuit of a transformer (b) Equivalent electrical circuit

Looking at the magnetic equivalent circuit in Figure 9, it can be seen that ϕ_m flux is produced in the magnetic circuit as a result of the difference between $\Im_1$ and $\Im_2$.

$$\phi_m \Re_m = N_1 i_1 - N_2 i_2 \tag{24}$$

obtained. The above definitions are based on the assumption of linear B-H characteristic. A new trend can be identified here. i_ϕ excitation current. This current in the primary is necessary to produce the ϕ_m flux.

$$\phi_m \Re_m = N_1 i_\phi \tag{25}$$

$$N_1 i_\phi = N_1 i_1 - N_2 i_2 \tag{26}$$

When this definition is used, the linear acceptance limitation is removed.

$$i_1 = i_\phi + \frac{N_1}{N_2} i_2 \tag{27}$$

$$i_1 = i_\phi + i_2' \tag{28}$$

As can be seen from the equation, the primary current can be expressed as the sum of the excitation current and the secondary current transferred to the primary. The excitation current is not in sinusoidal format due to the hysteresis curve of the magnetic material used in the core. However, only the fundamental wave component of the excitation current will be taken into account here.

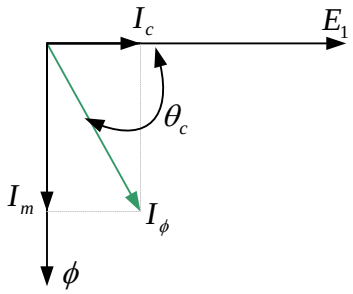

Figure 8. Phasor diagram of excitation current

The excitation current can be divided into and components as shown in Figure 10. Its component is the magnetizing current and is in phase with the magnetic flux. The component

represents the core losses and is in phase with. The presence of excitation current is indicated here by the parallel combination of a resistance and a reactance.

1.2. Transformer Equivalent Circuit

In circuit analysis and simulation of transformers, equivalent circuits are used instead of the real model. An equivalent circuit should reflect all the parameters of the real transformer as much as possible, that is, it should have all the features. All parameters of the transformer must be taken into account when creating the equivalent circuit. The equivalent circuit must have all the features of the transformer. In the equivalent circuit of the transformer, copper losses, core losses (eddy current losses and hysteresis losses) and leakage flux losses must be taken into account. Figure 11 shows the equivalent circuit of a real transformer. The primary winding leakage flux ϕ_{l1}, is expressed as reactance X_1. Secondary winding leakage flux ϕ_{l2} is expressed as reactance X_2. Since the leakage flux value is zero in an ideal transformer, the leakage flux reactances X_1 and X_2 are also equal to zero. The voltage drop occurring due to primary winding leakage fluxes is expressed as $V_{1leakage}=I_1.X_1$. The voltage drop that occurs due to the leakage flux in the secondary winding is expressed as $V_{2leakage}=I_2.X_2$. Resistors R_1 and R_2 in the equivalent circuit are the resistances of the primary and secondary windings. The "α" coefficient in the equivalent circuit is the transformation ratio of the transformer.

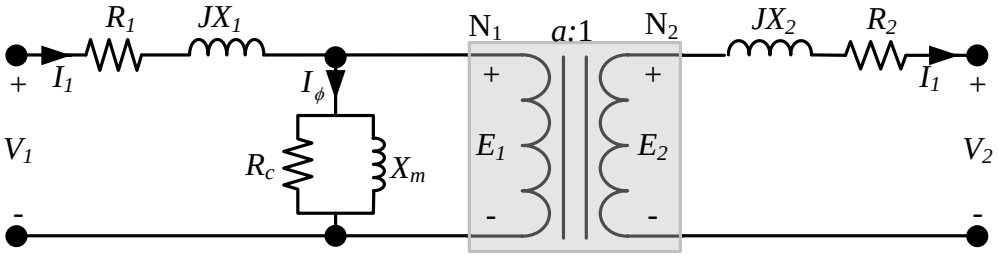

Figure 9. Equivalent circuit of a real transformer

3. Ferroresonance

Ferroresonance literally means a special type of resonance that occurs between inductive and capacitive elements in systems with iron core inductive elements. The most common type of ferroresonance is the ferroresonance phenomena that occur when trying to provide the required magnetic flux in transformers. This particular type of resonance can sometimes be used usefully under necessary controls. Ferroresonance is different from resonances that occur in linear systems. Resonance in linear systems causes high-amplitude sinusoidal current and voltage waveforms. In addition, ferroresonance generally causes irregular or chaotic waveforms at high current and voltage values [4].

In terms of the formation of ferroresonance phenomenon, which is different from linear resonance with its dependence on voltage as well as frequency; It depends on factors such as small changes in the source or operating voltage that occur for any reason, switching angle, residual magnetism of the iron cores in the system, load status of the capacities, circuit parameters (R,X.C). Once introduced, it depends on the circuit parameters (R, L, C) and the iron losses of the iron cores [5-6].

Ferroresonance is a complex electrical phenomenon. It has been known since the beginning of the 1920s and is among the least known phenomena in power systems research, and it has long been known that ferroresonance occurs as a result of various accidents in

electrical power systems [7]. Ferroresonance phenomenon is the nonlinear inductance of the saturated transformer core and the oscillation it creates in the same circuit with the capacitor [8-9]. In a power system, ferroresonance may occur when some of the load groups are disabled or very lightly loaded on the transmission line where transformers are located [10].

Simple ferroresonance circuit

The circuit given in Figure 10, which is assumed to have no resistance to bring the magnetic core to saturation, consists of a voltage source V_s, a capacitor C and an inductance L wrapped around a closed magnetic circuit.

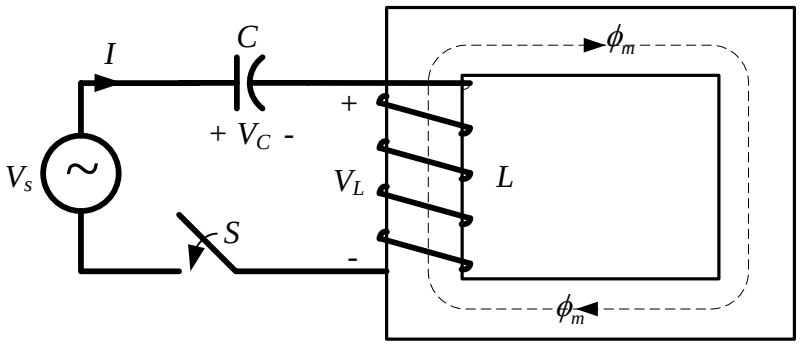

Figure 10. Connecting a coil wound to a closed magnetic circuit.

In the circuit in Figure 10, when the switch *S* is closed at time t_0, current begins to flow in the circuit and oscillation occurs. Angular frequency of the system,

$$\omega_1 = \frac{1}{\sqrt{LC}} \tag{29}$$

magnetic flux expression of inductance,

$$\phi = \left(\frac{V_0}{\omega_1}\right) \sin \omega_1 t_1 \tag{30}$$

It is found in the form.

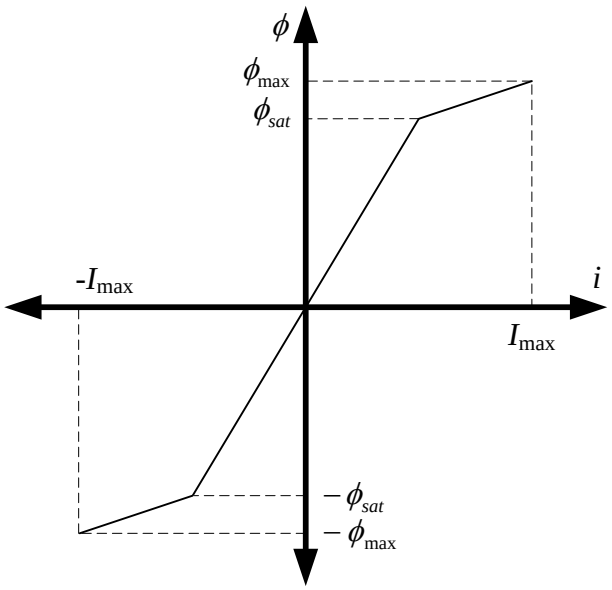

Figure 11. Simplified magnetic flux-current characteristic of a coil wound in a closed magnetic circuit

After neglecting the losses of the iron core inductance, the simplified fi magnetization curve is given in Figure 10. Expression of V_C voltage at the capacitance ends;

$$V_C = V_0 \cos \omega_1 t \tag{31}$$

is calculated.

$$\left(\frac{V_0}{\omega_1} \right) > \phi_{sat} \tag{32}$$

When Figure 11 is examined, under the conditions given in the expression (32), the magnetic flux fi reaches the saturation flux value fisat at time t_1. The capacitor terminal voltage becomes equal to the V_a value and at this moment the inductance reaches saturation, the L_S saturation inductance is much smaller than the initial L value. The energy in the capacitor C is suddenly discharged and the current waveform in the inductance L changes.

$$\omega_2 = \frac{1}{\sqrt{LC}} \tag{33}$$

When the electromagnetic energy stored in the E_L inductance is equal to the electrostatic energy formed in the E_C capacitor, the current and flux reach their maximum values.

$$E_C = \frac{1}{2CV_a} \tag{34}$$

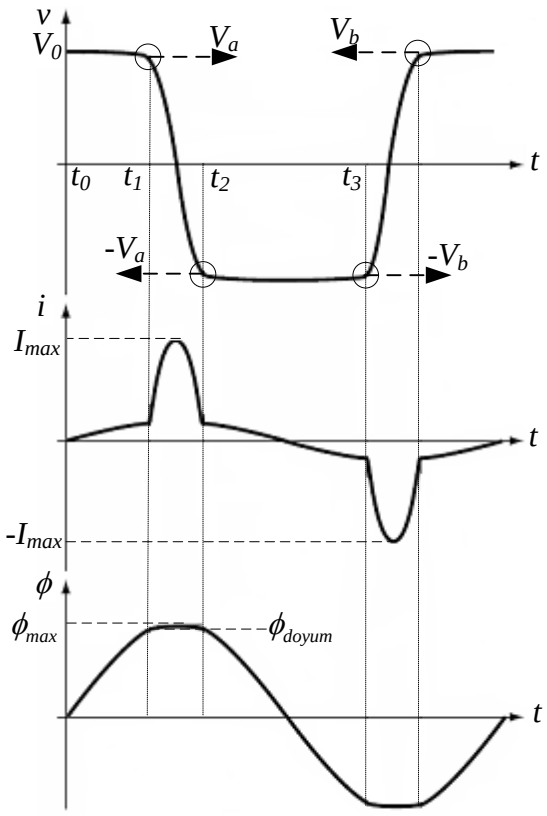

Figure 12. Time variation curves of capacitor voltage, series circuit current and magnetic flux in iron core inductance.

When the time change curves of voltage, current and magnetic flux in Figure 12 are examined, the following comments can be made;

1. At t_2, the magnetic flux φ returns from the φ_{max} value to the φ_{sat} saturation flux value.

2. The inductance reaches the value L and the voltage V becomes equal to $-V_a$ due to neglect of losses. At t_3, the φ flux reaches the φ_{sat} saturation value.

3. Voltage is equal to $-V_b$. Since ω_1 is used very little, it can be taken as $V_1 \cong V_2 \cong V_0$.

In this case, period T is unsaturated, including the oscillation range.

$$T = 2\pi\sqrt{LC} \tag{35}$$

In case of saturation time interval,

$$t_3 - t_2 \cong \frac{2\phi_{sat}}{V_0} \tag{36}$$

$$T = 2\pi\sqrt{L_S C} + 2(t_3 - t_2) \tag{37}$$

is calculated. for frequency,

$$\frac{1}{2\pi\sqrt{LC}} \langle f \langle \frac{1}{2\pi\sqrt{L_{sat}C}} \tag{38}$$

The expression is reached. In the nonlinear case, this frequency expression depends on the φ_{sat} value and the initial state of the voltage V_0. In real applications, the amplitude of the V voltage decreases due to losses due to the resistance R present with the inductance ($V_b<V_a<V_0$). The magnetic flux change $\Delta\varphi$ occurring during the t_3-t_2 period in which there is no saturation is expressed as follows [11]

$$\Delta\phi = 2\phi_{sat} = \int_{t_2}^{t_3} V dt \tag{39}$$

The decrease in the amplitude of the capacitor terminal voltage due to core and joule losses causes the frequency to decrease. If the energy losses are covered by the voltage source V_s feeding the system, the decrease in the frequency value can create resonance conditions for the source frequency feeding the system (if the leading frequency is greater than the source frequency) or many sub-frequencies of the source frequency (if the leading frequency is lower than the source frequency). This situation distinguishes the ferroresonance phenomenon from the linear resonance phenomenon. This new situation shows that, unlike linear resonance, resonance will occur in a very wide range of C values for a given inductance value.

Characteristic Features of Ferroresonance

There are some basic features that make the ferroresonance phenomenon different from other energy system phenomena. These; Extreme sensitivities to system parameters and initial conditions can be expressed as the presence of more than one stable operating point.

Sensitivity of Ferroresonance to Changing System Parameters

A ferroresonance circuit with non-linear inductors and capacitors to create the ferroresonance phenomenon can be seen in Figure 13.

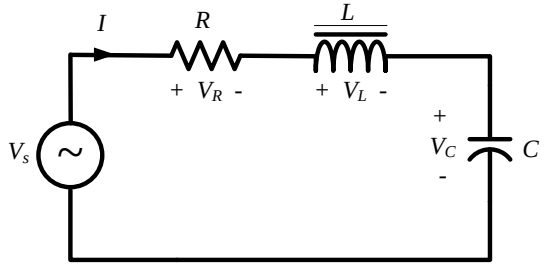

Figure 13. A ferroresonance circuit

The change of V_L voltage and C capacitance values of the L inductance in this circuit is given in Figure 14.

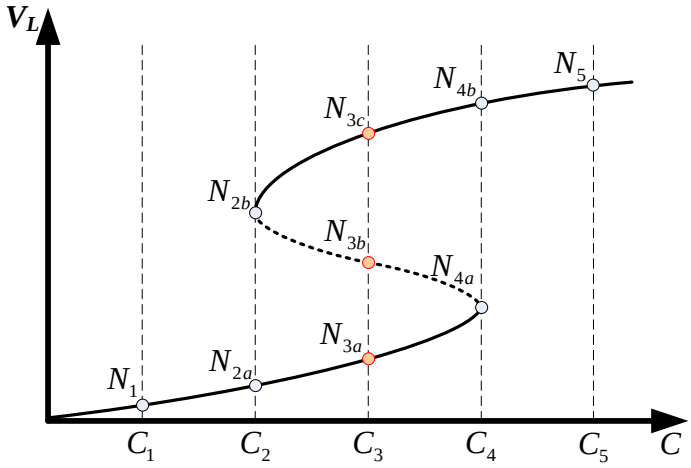

Figure 14. Sensitivity to splash phenomenon and system parameters.

When the graph given in Figure 14 is examined;

1. When the value of the capacity is C_1, the system solution is at a single point and this value is N_1. This solution corresponds to the normal operating condition that can be obtained with the linear assumption.

2. While the value of the capacity is C_2, it jumps from point N_{2a}, which is the stable operating point of the system, to point N_{2b}. Point N_{2a} is a limit value.

3. While the value of the capacity is C_3, the system has three solution points: N_{3a}, N_{3b} and N_{3c}. While N_{3a} at these points occurs in normal operating state, N_{3c} corresponds to the state in which the system is in ferroresonance. The answer in the part between these two points, shown as dotted lines, is point N_{3b}, which is a situation that cannot be reached in practice.

4. While the value of the capacity is C_4, the second limit point jumps from N_{4b} to N_{4a}.

5. When the capacitance value is C_5, there is only a single operating point N_5, which is the ferroresonance state.

Jumping (jumping or bouncing phenomenon), which is one of the distinguishing features of the ferroresonance phenomenon, causes the system to operate in a complex manner as described above. The reason for the jumping phenomenon seen in Figure 14 is the change of capacitance, one of the system parameters. Jumping can occur with changes in other parameters such as capacitance change. Changing values of the source voltage of the system and the resistance that is responsible for suppressing unusual current and voltage components caused by ferroresonance in the system will also cause great changes in the reaction response of the system. Ultimately, the source of these changes is the extreme sensitivity of the ferroresonance phenomenon to the system parameters. A small change in system parameters or one of the transient events can produce sudden jumps from one stable operating point to a very different stable operating point [12].

Sensitivity of Ferroresonance to Changes in System Initial Conditions

Initial conditions for the occurrence of ferroresonance in electrical energy transmission and distribution systems are very important. Initial conditions are important for understanding the state of the system at the moment immediately before this transient event occurs. The most important parameters are the amplitude of the system voltage, the value of the capacitive elements in the system and the resistance values that can provide damping in the system. The

size of the source voltage, system capacitances and resistances determine which type of ferroresonance the response of the system in ferroresonance will be [13]. The amount of energy contained in the capacitive elements in the system, when a part of the system is isolated for any reason, will be discharged through the inductive components on the system and drags the system into the situations explained above. Another initial condition of great importance is the amount of flux in the transformer core. The density of the flux in the core depends on the structure of the transformer core [14]. The magnitude of the residual flux in the core will create a driving force in driving the transformer to saturation or deepening saturation [15].

4. Review of The System

The Matlab / Simulink circuit shown in Figure 15 was established to examine the ferroresonance effect of a transformer connected to an energy system in the loaded operating state. In the system, the ferroresonance effect occurring during the entry and exit of 3 different loads connected to the secondary circuit of a 150 MVA transformer in a 500 kV - 60 Hz single-phase energy transportation system was observed. There are 3 secondary circuit loads parallel to each other, Inductive reactive power (Q_L) 30 MVAR, Active power (P) 15 MW. These loads are activated at 0.25s, 0.5s and 0.666 seconds, respectively. The circuit breaker connected to the primary of the transformer also opens in the 6th cycle of a total of 60 cycles for 1 second within the scope of 60 Hz frequency, within 1 second from the moment it is connected to the source, remains open for 3 cycles and closes in the 9th cycle. Figure 16 shows the 1-second Flux, I_{mag} - I_{exc} and U_1 -U_2 voltages and $I_{Breaker}$ currents of the system in pu.

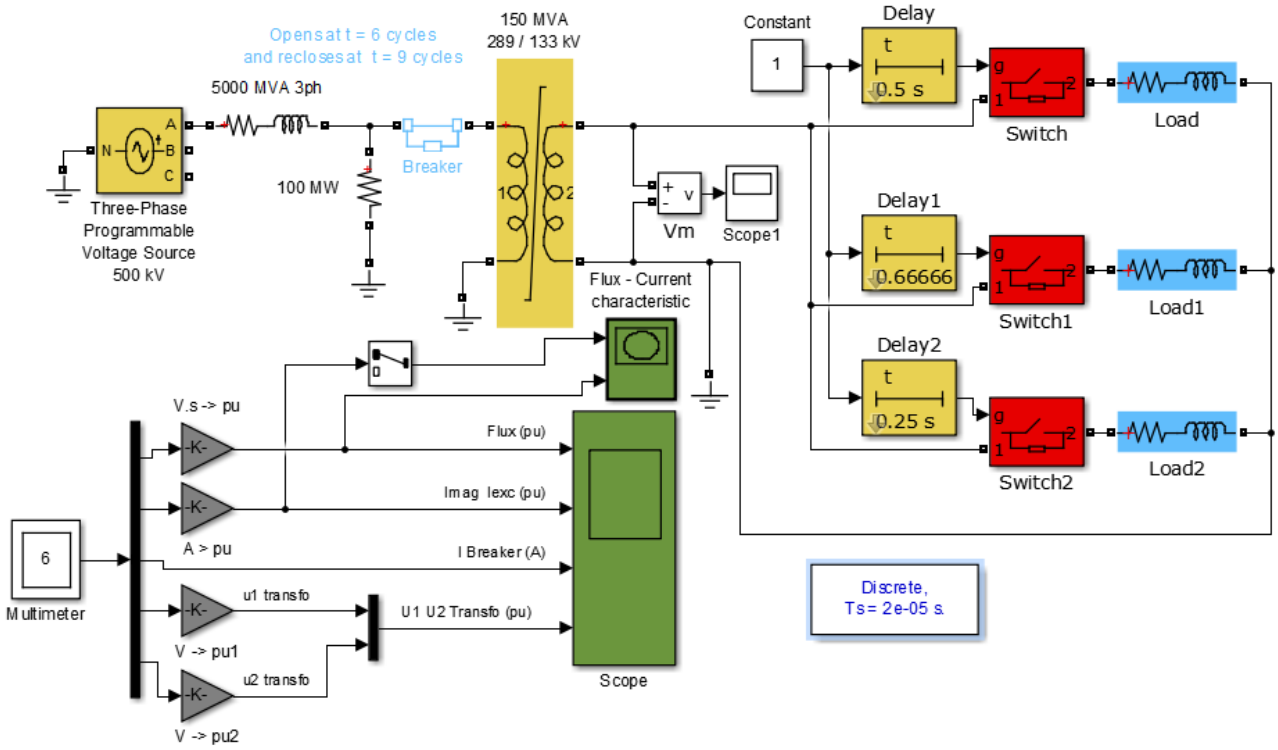

Figure 15.Block diagram of the installed system.

The switch connected to the primary of the transformer opens at the beginning of the 6th period of the source signal and closes at the beginning of the 9th period.

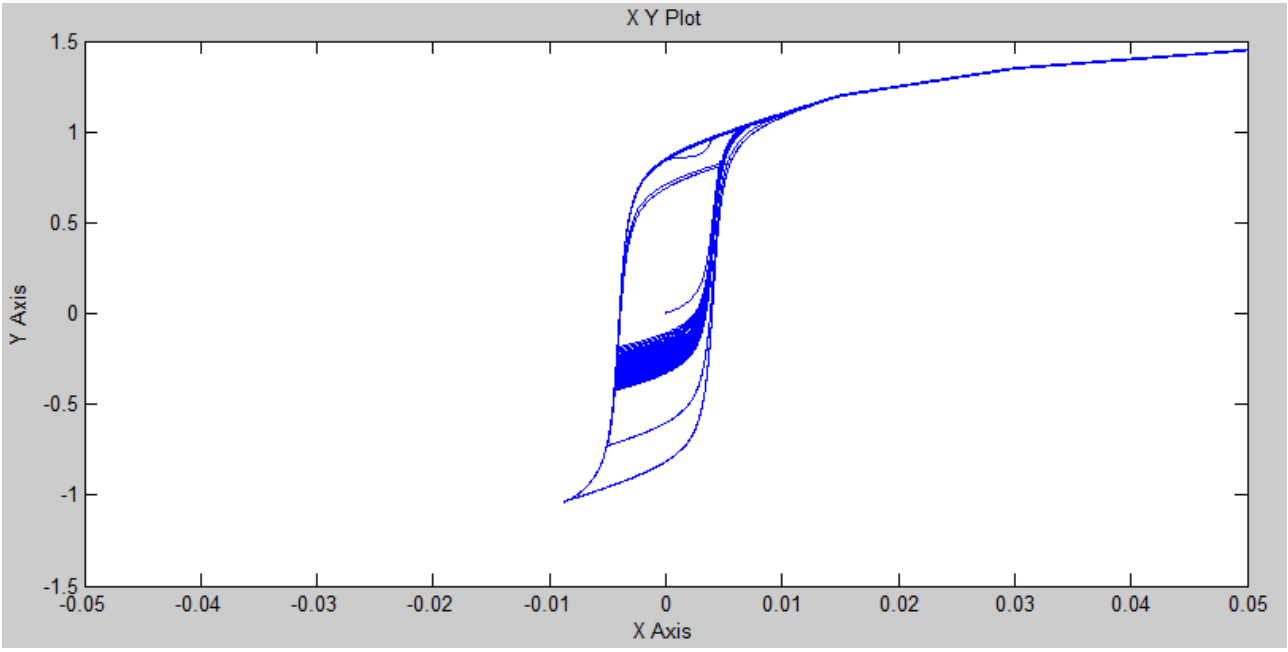

Figure 16. Hysteresis loop of the transformer under specified load and operating conditions.

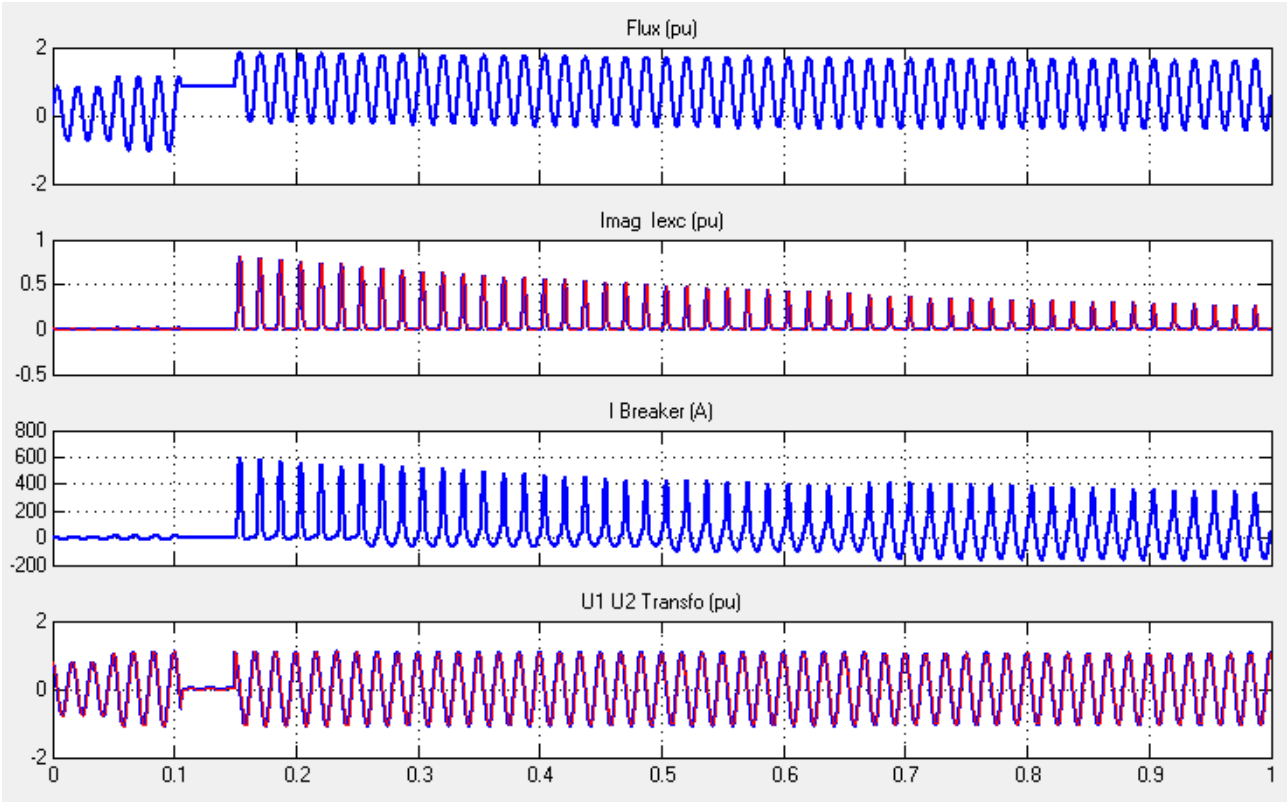

Figure 17. Some electrical parameters of the transformer under specified load and 1-second operating conditions.

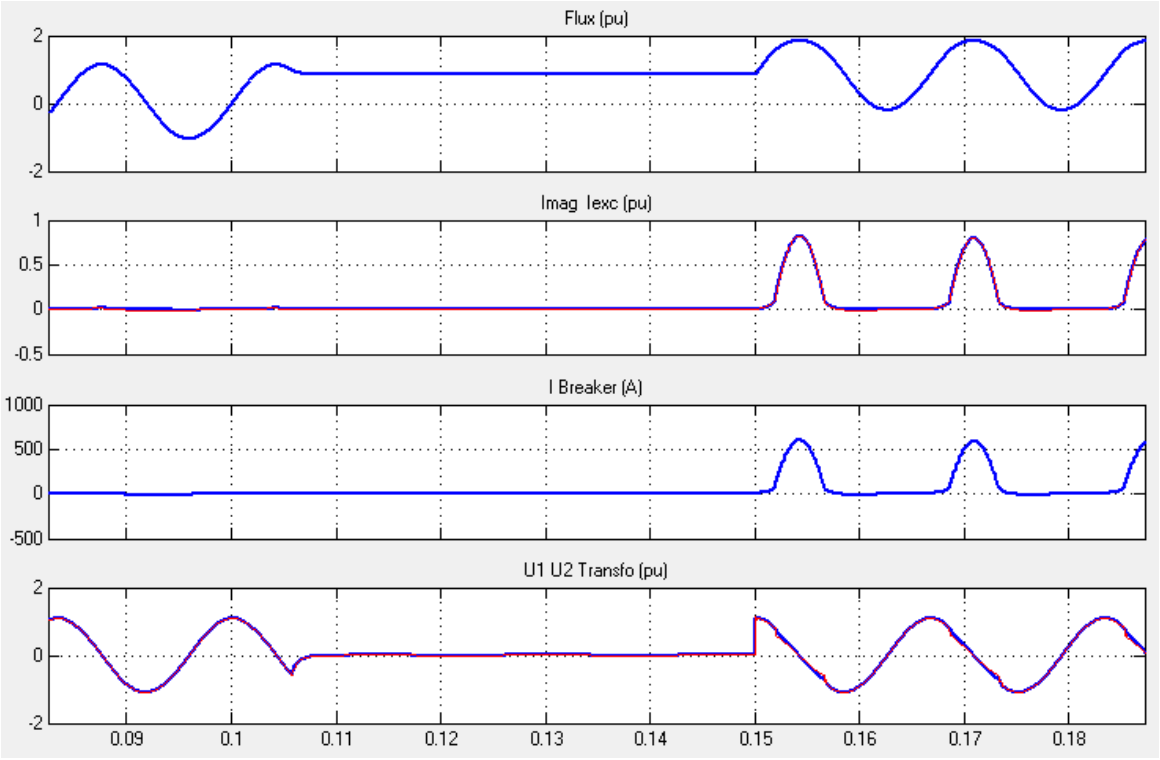

Figure 18. Detailed examination of the changes in electrical parameters during operation when the position of the switch changes

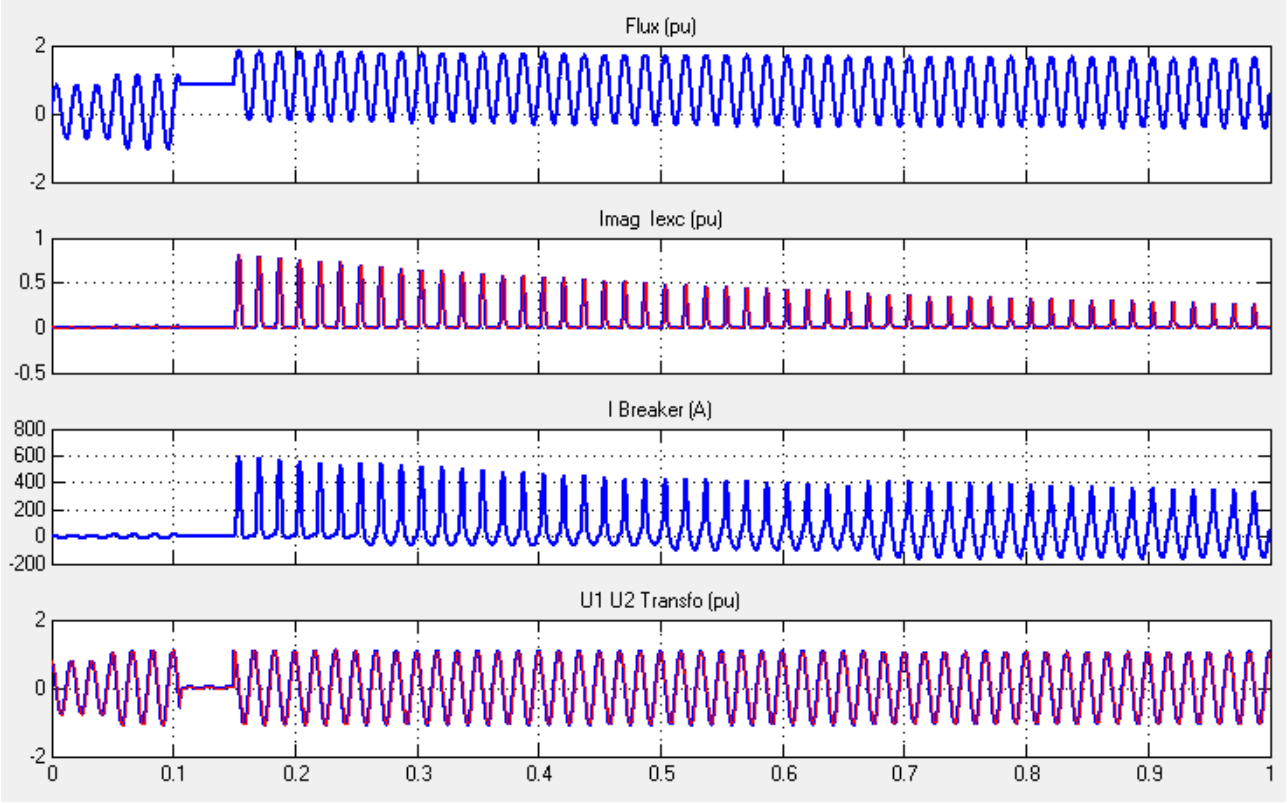

Figure 19. Change of electrical parameters during the process when the switch in the transformer primary changes position

5. Results

Improving power quality has been effective in bringing the issue of increasing the efficiency of the elements that undertake basic duties in the energy system back to the agenda. In this study, the phenomenon of ferroresonance, which may occur from time to time when transformers commonly used in energy systems are converting energy, was studied. The studies were carried out through both simulation and theoretical investigations. In order to understand the events occurring in a high voltage system, a transformer used in high voltage energy systems was used.

In the studies, the ferroresonance state of the transformer was established. In order to understand the relationship between the ferroresonance state and the system voltage, the loads were transferred and removed from the circuit via switches whose time was previously set. The effects of this switch on the hysteresis loop were examined by measuring the electrical parameters of the phase to which it was connected.

References

1. Zenk H., Akpinar A. S., High Voltage Instrument Transformers Ferroresonance Events Occurring in the Investigation of the Circuit Breaker Switch Positions, Electrical and Electronic Engineering, Vol. 4 No. 1, 2014, pp. 10-19. doi: 10.5923/j.eee.20140401.02.
2. Akıncı, T.Ç.; Gökmen, G., Mokryani, G.; Ekren, N.; Seker, S.: "Bir Fazlı İletim Sistemlerinde Ferrorezonans Olayının İncelenmesi, 5.Uluslararası İleri Teknolojiler Sempozyumu, Karabük, Türkiye, 13-15 Mayıs (2009).
3. Sen, P. S., Principles of Electric Machines and Power Electronics, Toronto:John Wiley & Sons, 1997.
4. Yiğit E., Güç Trafolarında Ferrorezonans Olayların Kaotik Analizi, Yüksek Lisans Tezi, Fen Bilimleri Enstitüsü, Sakarya Üniversitesi, Haziran 2009.
5. Akıncı, T. Ç., Güç Sistemlerinde Ferrorezonans Olayının Spektral ve Dalgacık Analizi Yöntemleriyle Belirlenmesi, Yüksek Lisans Tezi, Marmara Üniversitesi, Fen Bilimleri Enstitüsü, İSTANBUL, 2009.
6. Akpınar S., An Approach To The Analysıs of Fundamental Frequency Ferroresonance , Electnc Machines and Power Systems , No: 18 , 1990.
7. Jacobson, D.A.N.; Swatek, D.R.; Mazur, R.W.: "Mitigating Potential Transformer Ferroresonance in a 230kV Converter Station", Transmission and Distribution Conference, Canada, 15-20 September (1996) 269-275.
8. Al-Anbarri, K., Ramanujam, R., Keerthiga, T., Kuppusamy, K., Analysis of Nonlinear Phenomena in MOV Connected Transformer, IEE Proc.- Gener.Transform Distribution, Vol.148, No.6, November (2001) 562-566.
9. Van Craenenbroeck, T., Van Dommelen, D., Stuckens, C.; Janssens, N.;A.Monfis, P., Harmonic Balance Based Bifurcation Analysis of Three-Phase Ferroresonance with Full Scale Experimental Validation, IEEE Transmission and Distribution Conference, Vol.2, 772-777, New Orleans, USA, ISBN:0-7803-5515-6, 11-16 April 1999.
10. Sanaye Pasand, M., Aghazadeh, R., Capacitive Voltage Substations Ferroresonance Prevention Using Power Electronic Devices, International Conference on Power Systems Transients-IPST'03, New Orleans, USA, 2003.
11. Ferracci, P., Ferroresonance, Cahier Technique, No. 190, Schneider Electric, Mart 1998.
12. S. Mozaffari; M. Sameti; A. C. Soudack, Effect of initial conditions on chaotic ferroresonancein power transformers, IEE Proc.-Cener. Transm. Distrib., Vol. 144, No. 5, September 1997.
13. Smith, K., n.d.: Wind Farm Transformer Inrush Studies. PSCAD Application Notes.https://pscad.com/resource/File/Library/Application_Note_Wind_Farm_Transformer_Inrush_Studies.
14. Zenk, Hilmi. (2017). Design of an Intelligent Control System to Prevent the Ferroresonance Effect in Current Transformers.
15. Zenk, Hilmi. (2014). The Effect of Turnıng-Off Angle on Ferroresonance Event, PhD. Dissertation KTÜ.

Current Debates on Natural and Engineering Sciences

11